

# Sheffield Hallam University

*Real-time analysis and feedback of performance indicators in elite diving*

SOTHERAN, Adam William

Available from the Sheffield Hallam University Research Archive (SHURA) at:

<http://shura.shu.ac.uk/29237/>

## A Sheffield Hallam University thesis

This thesis is protected by copyright which belongs to the author.

The content must not be changed in any way or sold commercially in any format or medium without the formal permission of the author.

When referring to this work, full bibliographic details including the author, title, awarding institution and date of the thesis must be given.

Please visit <http://shura.shu.ac.uk/29237/> and <http://shura.shu.ac.uk/information.html> for further details about copyright and re-use permissions.

# **Real-time Analysis and Feedback of Performance Indicators in Elite Diving**

Adam William Sotheran

A thesis submitted in partial fulfilment of the requirements of  
Sheffield Hallam University  
for the degree of Doctor of Philosophy

Collaborating Organisation: British Diving

November 2019

## Candidate Declaration

I hereby declare that:

I have not been enrolled for another award of the University, or other academic or professional organisation, whilst undertaking my research degree.

None of the material contained in the thesis has been used in any other submission for an academic award.

I am aware of and understand the University's policy on plagiarism and certify that this thesis is my own work. The use of all published or other sources of material consulted have been properly and fully acknowledged.

The work undertaken towards the thesis has been conducted in accordance with the SHU Principles of Integrity in Research and the SHU Research Ethics Policy.

The word count of the thesis is 48,200.

Name	Adam William Sotheran
Date	November 2019
Award	PhD
Faculty	Health and Wellbeing
Director(s) of Studies	Dr Simon Goodwill

## Abstract

The difficulty and quality of dives required to win medals in Olympic springboard diving has increased throughout the modern era. A greater understanding of optimal diving technique, increased training opportunity and support from disciplines of sports science and medicine have influenced this trend.

Progress towards world class standards is enhanced by objective measurement of performance in a training and competition context from which an assessment of the effect of training interventions can be made, leading to a programme individualised for each diver.

A description of kinematic parameters representing high quality performance of the world's hardest dives did not exist. Standards were therefore defined following analysis of dives performed over five years of springboard competition. This new knowledge contributes to a model called 'What It Takes To Win' (WITTW).

A practical method to calculate kinematic metrics from dives in training also did not exist, limiting comparison between training and WITTW standards. To bridge this gap, a flexible method for analysing dives in training and competition was developed and a bespoke tool created to calculate and feedback performance data with a greater level of sensitivity than in related studies in the sport. Automatic tracking was designed and implemented to facilitate 'real-time' measurement of kinematic data, providing a new training process where objective data added to subjective interpretation of quality throughout training.

Four World Class Programme divers were tracked through a season's preparatory phase. Change in performance was measured and an analysis conducted to compare progress towards WITTW standards and assess the influence of strength and conditioning training in performance outcomes.

Statistical analysis of longitudinal training data showed that independent variables relating to 'best' performances were not common to all divers and that an individualised set of critical variables could be identified for each diver as strengths around which to focus training.

## Acknowledgements

Thank you to:

- Simon Goodwill and John Kelley for the continued guidance, patience and flexibility of time
- Alexei Evangulov and British Diving for supporting the work and welcoming the results
- The divers, coaches and staff at Sheffield Diving and Ponds Forge for facilitating the study
- Hayley, Kira and Taylor – this took a long time and you helped me loads, never minded my typing time and always made it more fun

## Table of Contents

1	Introduction .....	1
1.1	Olympic Diving .....	1
1.2	Development of performance .....	1
1.3	Motivation for research .....	2
1.4	Aim and objectives .....	3
2	Literature review .....	4
2.1	Diving rules of competition .....	4
2.1.1	Competition format .....	4
2.1.2	Groups, shapes and degree of difficulty .....	5
2.1.3	Judging and scoring .....	7
2.1.4	Conclusion .....	8
2.2	Successful diving nations .....	8
2.3	What It Takes to Win.....	9
2.3.1	Scores.....	10
2.3.2	Difficulty.....	11
2.3.3	The increasing success of the World Class Programme.....	11
2.3.4	Conclusion .....	12
2.4	Performance Science.....	13
2.4.1	Injury prevention .....	13
2.4.2	Development of physical qualities.....	14
2.4.3	Conclusion .....	15
2.5	Biomechanical and kinematic research in diving.....	16
2.5.1	Jumping from a springboard.....	17
2.5.2	Hurdle step .....	18
2.5.3	Take-off parameters .....	19
2.5.4	Flight .....	21
2.5.5	Simulation.....	22
2.5.6	Conclusion .....	23
2.6	Tracking and measurement .....	24
2.6.1	Electromagnetic motion tracking .....	24
2.6.2	Inertial sensors .....	25
2.6.3	Video analysis .....	26
2.6.4	Conclusion .....	31
2.7	Camera Calibration.....	32
2.7.1	Camera model .....	32
2.7.2	Multiple cameras .....	33
2.7.3	Calibration method.....	34

2.7.4	Conclusion .....	37
2.8	Body segment models – representation of a human .....	37
2.8.1	Models .....	38
2.8.2	Segment mass and position of COM.....	39
2.8.3	Conclusion .....	40
2.9	Software tools for kinematic and biomechanical analysis.....	40
2.9.1	System needs.....	40
2.9.2	Existing tools.....	41
2.9.3	Conclusion .....	43
2.10	Summary .....	43
2.11	Objectives of the study .....	45
3	Camera calibration – Intrinsic parameters .....	46
3.1	Introduction .....	46
3.2	Hardware requirements.....	46
3.3	Intrinsic parameters .....	49
3.2.1	Calibration object and pattern .....	49
3.2.2	Method for collecting images.....	51
3.2.3	Identification of a suitable number of images for calibration .....	53
3.2.4	Calibration parameters.....	57
3.2.5	Consistency of intrinsic parameter calculation.....	62
3.3	Summary .....	63
4	Extrinsic parameters .....	65
4.1	Introduction .....	65
4.2	Considerations for placing a camera in a scene.....	65
4.3	Control points.....	66
4.4	The effect of restricted control points on extrinsic parameters in a simulated setting.....	69
4.4.1	Introduction.....	69
4.4.2	Method .....	70
4.4.3	Results .....	74
4.4.4	Implementing the extrinsic-parameter calibration method in the pool environment.....	76
4.5	Assessment of the accuracy of angle calculation .....	81
4.6	Summary .....	83
5	Body segment model .....	85
5.1	Introduction.....	85
5.2	Identification and adaptation of existing body-segment models .....	86
5.2.1	Modifications to existing models – lower arm and lower leg.....	86
5.3	Location of segment landmarks .....	88

5.4	Calculation of centre of mass .....	90
5.4.1	Reduction of the body to stick-figure.....	90
5.4.2	Consideration of hands and feet.....	91
5.5	Variation in COM location and influence on performance data.....	92
5.5.1	Introduction.....	92
5.5.2	Method.....	93
5.5.3	Results.....	95
5.5.4	Discussion.....	96
5.6	A study to assess the effect of intra-user error in manual digitisation.....	97
5.6.1	Introduction.....	97
5.6.2	Method.....	97
5.6.3	Results.....	99
5.6.4	Discussion.....	101
5.7	A method to determine the most appropriate body-segment model for a diver and dive.....	102
5.7.1	Introduction.....	102
5.7.2	Selection of skills to calculate the best body-segment model.....	105
5.7.3	Method.....	108
5.7.4	Results.....	110
5.7.5	Measurement of error.....	112
5.7.6	Discussion.....	113
5.8	Summary.....	114
6	Markers.....	116
6.1	Introduction.....	116
6.2	A study to identify a suitable tape for markers.....	117
6.2.1	Introduction.....	117
6.2.2	Method.....	117
6.2.3	Results.....	121
6.2.4	Discussion.....	127
6.3	Application of markers.....	127
6.3.1	Method.....	128
6.3.2	Results.....	129
6.3.3	Discussion.....	129
6.4	Lighting the scene.....	130
6.4.1	Introduction.....	130
6.4.2	Method.....	132
6.4.3	Results.....	132
6.4.4	Discussion.....	134
6.5	A study into the effect on COM of segment-end approximation using retro-reflective tape markers.....	135
6.5.1	Introduction.....	135



6.5.2	Method .....	136
6.5.3	Results .....	137
6.5.4	Discussion .....	137
6.6	A study into the comparability of COM-position using six and three-segment models to represent the diver. ....	138
6.6.1	Introduction.....	138
6.6.2	Method .....	139
6.6.3	Results .....	143
6.6.4	Discussion .....	144
6.7	Summary .....	144
7	Marker tracking .....	147
7.1	Introduction .....	147
7.2	Methods .....	148
7.2.1	Introduction.....	148
7.2.2	Camera exposure.....	149
7.2.3	Background subtraction.....	149
7.2.4	Conversion to grayscale.....	150
7.2.5	Thresholding .....	151
7.2.6	Starting frame and pose estimation .....	154
7.2.7	Tracking movement .....	155
7.2.8	Correspondence .....	157
7.2.9	Occlusion and landmark prediction .....	159
7.2.10	Tracking termination .....	162
7.3	Examples .....	163
7.4	A study to assess the performance of the automated tracking process .....	164
7.4.1	Introduction.....	164
7.4.2	Method .....	165
7.4.3	Results .....	165
7.4.4	Discussion .....	167
7.5	Summary .....	168
8	'diveTracker' software tool.....	170
8.1	Introduction .....	170
8.2	Implementation of methods.....	171
8.2.1	Calibration files .....	171
8.2.2	Landmarks .....	172
8.2.3	Body segment models .....	173
8.2.4	Automated marker tracking .....	173
8.2.5	Key-frames.....	175
8.3	Output from tool.....	177
8.3.1	Key frame images and image-strips.....	177

8.3.2	Annotated replay .....	178
8.3.3	Key performance information .....	179
8.3.4	Marker positions and joint angles .....	180
8.4	Developing understanding of World Class performance.....	181
8.5	Summary .....	181
9	What It Takes to Win – kinematic performance data .....	183
9.1	Introduction .....	183
9.2	Method.....	184
9.2.1	Athletes.....	184
9.2.2	Competitions .....	185
9.2.3	Performance metrics .....	185
9.3	Results .....	189
9.3.1	Comparison of results using different data collection measures .....	193
9.3.2	Flight time .....	194
9.3.3	Take-off velocity .....	195
9.3.4	Somersault speed and opening height .....	195
9.3.5	Drop and preparation for entry .....	197
9.4	Discussion.....	197
9.5	Summary .....	198
10	The effect of preparatory-phase training .....	199
10.1	Introduction .....	199
10.1.1	Training programme.....	200
10.2	Methods .....	201
10.2.1	Profiling and agreement of goals .....	201
10.2.2	Dives measured in the study .....	203
10.2.3	Selection of divers .....	204
10.2.4	Environment.....	204
10.2.5	Production of kinematic data .....	205
10.3	Results .....	205
10.3.1	Changes in strength measured in profiling sessions .....	205
10.3.2	Performance metrics – data tables .....	207
10.3.3	Board deflection .....	208
10.3.4	Vertical take-off velocity .....	213
10.3.5	Relationship between board deflection and vertical take-off velocity .....	218
10.4	A study investigating influential components for take-off performance .....	219
10.4.1	Hurdle step and forward jump (100a).....	219
10.4.2	Back jump 200a .....	222
10.5	Performance metrics and WITTW values .....	224
10.6	Discussion.....	227

10.7	Summary .....	228
11	Summary and next steps.....	230
11.1	Introduction .....	230
11.2	New process .....	230
11.3	New knowledge.....	231
11.4	New practice .....	231
11.5	Benefits to the diver.....	232
11.6	Future development .....	233
11.6.1	Longitudinal tracking and prediction of WITW kinematic parameters .....	233
11.6.2	Identification of critical take-off parameters .....	233
11.6.3	Projects.....	234
11.6.4	Enhance automated marker tracking.....	235
11.6.5	Extend the tool to analyse platform diving .....	235
11.7	Summary .....	236
	References.....	237
	Appendix A - Automated marker tracking examples.....	247
	Appendix B - Athlete data .....	254
	Diver 1 .....	254
	Diver 2 .....	263
	Diver 3 .....	274
	Diver 4 .....	284
	Appendix C - CSV Output.....	295
	Appendix D - Health and Safety documentation .....	297
D.1	Health team involvement and support of profiling .....	297
D.2	Risk assessment for diving squad pool training .....	298
D.3	Athlete letter of consent.....	303
D.4	Letter of support from facility.....	305
	Appendix E - What It Takes to Win competencies.....	306
	Appendix F – Annual review feedback.....	312
	Appendix G – Results of regression analyses.....	317



## List of Figures

<i>Figure 2-1. Athletes perform dives in a range of shapes. The shape influences the difficulty of a dive. __</i>	<i>5</i>
<i>Figure 2-2. Scores to achieve a gold medal (gold band), silver or bronze medal (bronze band) and top-8 (green band) in Olympic springboard events. Scores are taken from the major event of the year or are a prediction of score for future years. Adapted from A Sotheran et al., (2016). _____</i>	<i>10</i>
<i>Figure 2-3. The highest degree-of-difficulty list used by a World or Olympic medallist each year in springboard events. Reproduced from Sotheran et al (2016)._____</i>	<i>11</i>
<i>Figure 2-4. UK Sport funding for Diving’s World Class Programme. Reproduced from <a href="http://www.uksport.gov.uk/sports/olympic/diving">http://www.uksport.gov.uk/sports/olympic/diving</a>._____</i>	<i>12</i>
<i>Figure 2-5. Examples of exercises used to build absolute and explosive strength in athletes. Reproduced from <a href="https://stronglifts.com">https://stronglifts.com</a> and <a href="http://crossfitzonex.com">http://crossfitzonex.com</a>._____</i>	<i>15</i>
<i>Figure 2-6. A hurdle step is used to increase springboard deflection and increase take-off speed. Reproduced from <a href="https://www.pinterest.co.uk/zonetotalsports/plongeon-springboard-diving-techniques">https://www.pinterest.co.uk/zonetotalsports/plongeon-springboard-diving-techniques</a>. _____</i>	<i>18</i>
<i>Figure 2-7. Factors influencing production of height (Sanders, 2003). _____</i>	<i>20</i>
<i>Figure 2-8. Factors influencing creation and optimisation of rotation (Sanders, 2003). _____</i>	<i>21</i>
<i>Figure 2-9. A tight shape (right) spins faster than an open shape (left) due to reduction of moment of inertia. Reproduced from <a href="http://cbraccio.pbworks.com">cbraccio.pbworks.com</a> and <a href="http://robmacca.blogspot.com">robmacca.blogspot.com</a>. _____</i>	<i>22</i>
<i>Figure 2-10. Computer models have been created using digitisations of real performances. _____</i>	<i>22</i>
<i>Figure 2-11. Digitised technique (upper sequence) compared to simulation (lower sequence). _____</i>	<i>23</i>
<i>Figure 2-12. The Polhemus motion tracker is a phone-sized sensor transmitting movement data to a hub for future analysis. Image reproduced from <a href="https://polhemus.com/case-study/detail/case-study-bull-3d-system-using-the-polhemus-g4">https://polhemus.com/case-study/detail/case-study-bull-3d-system-using-the-polhemus-g4</a>._____</i>	<i>25</i>
<i>Figure 2-13. The small, waterproof IMeasureU inertial measurement unit. Reproduced from <a href="http://ImeasureU.com">ImeasureU.com</a>. _____</i>	<i>26</i>
<i>Figure 2-14. Manual digitisation of landmarks allows the calculation of performance data. Reproduced from <a href="http://en.triatlonoticas.com">en.triatlonoticas.com</a>. _____</i>	<i>27</i>
<i>Figure 2-15. Hawk-eye uses multiple cameras to track a single-unit object and both track and predict motion with reference to fixed landmarks in the arena (tramlines, stumps etc.)._____</i>	<i>28</i>
<i>Figure 2-16. A calibrated scene and an example of marker-tracking. This method suits constrained movement in a known field of view. _____</i>	<i>30</i>
<i>Figure 2-17. LED markers, combined with image-processing techniques to remove the background from the image, leave clear white pixels in an image. Reproduced from <a href="http://phasespace.com">phasespace.com</a>. _____</i>	<i>30</i>
<i>Figure 2-18. Passive markers are used to locate physical landmarks for motion tracking. _____</i>	<i>31</i>
<i>Figure 2-19. A pinhole camera mode. Reproduced from Bouget (2015). _____</i>	<i>32</i>
<i>Figure 2-20. A calibration cube used in DLT calibration (Boutros et al., 2015). _____</i>	<i>35</i>
<i>Figure 2-21. A checkerboard, used for planar calibration (CSER, 2013). Red arrows indicate the local coordinate system. _____</i>	<i>36</i>

Figure 2-22. The body can be represented by three models – the particle model (a), the stick figure model (b) and the rigid segment model (c). Reproduced from <a href="http://cw.routledge.com">http://cw.routledge.com</a> .	38
Figure 2-23. Examples of tools for motion analysis (clockwise from top left): Dartfish, Kinova, SIMImotion, Quintic.	42
Figure 3-1. The camera, lens and PC used for the study.	47
Figure 3-2. View of selected images of the position of the diver. Clockwise from top left: (1) During recoil, (2) maximum height, (3) opening and (4) preparation for entry. The quality of the image must enable the coach and athlete to make subjective assessment of the quality of the dive.	48
Figure 3-3. Square intersections detected in the image; pixel-distances between intersections are used to calculate intrinsic parameters.	50
Figure 3-4. Check2D uses a checkerboard pattern printed on a flat surface as its calibration object	50
Figure 3-5. Images collected by moving a camera around a fixed calibration object.	52
Figure 3-6. Check2D and Matlab used to show square-intersection coverage and range of camera positions relative to the checkerboard.	53
Figure 3-7. Intrinsic parameters were calculated using an excessively high number of images.	54
Figure 3-8. Example coverage of square-intersections for image-sets of different sizes.	55
Figure 3-9. Barrel (left) and pincushion (right) distortion can be corrected by calculating radial distortion coefficients.	58
Figure 3-10. Check2D allows the user to select the calibration parameters to be calculated.	58
Figure 3-11. Representation of intrinsic parameters and projection error in Check2D.	59
Figure 3-12. Visualisation of the effect of different assumptions in the calibration process. The blue circle shows the position of the centre of the image and the red cross shows the calculated principal point.	61
Figure 4-1. Extrinsic parameters (a rotation matrix and translation matrix) are calculated to define the relationship between the camera and the scene.	65
Figure 4-2. A scale model of the diving pool. The horizontal checkerboard represents the water, the vertical checkerboard represents the movement plane. Four or more control points are identified in Check2D to calculate $R$ and $T$ . This example uses a checkerboard due to the high number of control points whose $(x,y)$ position can be precisely measured.	67
Figure 4-3. Square intersections (identified inside the yellow circles in the images above) are used to calculate extrinsic parameters and to compare results using a small number of points (8, left) and a larger number of points (15, right).	68
Figure 4-4. The diving pool is limited by a small number of control points in the movement plane used by a diver. The diving board (highlighted in red, above) provides measurable points but does not cover the extremes of the image.	69
Figure 4-5. A scale-model (right) simulates the view of the diving board (left). Square-intersections were identified which corresponded with the position of the diving board and origin-positions were matched.	70

Figure 4-6. Control points in the simulated view (centre) were used to calculate R and T. Square intersections were reconstructed and compared to actual positions. Percentage reconstruction error is represented by a heat-map (right). In each position, a lower value indicates a more accurate reconstruction.	70
Figure 4-7. Superimposing the checkerboard from the scale-model over the view of the diving pool identifies control points for use in the scale-model trial.	71
Figure 4-8. Control points for Trial 1, located using the diving board and calibration checkerboard (left). The superimposed checkerboard over the image (centre) allows identification of control points in the scale-model (right). A control point is close to the right edge of the image.	72
Figure 4-9. Control points for Trial 2, located using the diving board, checkerboard and plumb line to reach the lower edge of the view. Control points are now close to two edges (right and bottom) of the image.	72
Figure 4-10. Control points for Trial 3, located using the diving board, checkerboard, plumb-line and extending pole. Control points are now close to three edges of the image: right, bottom and left.	73
Figure 4-11. A representation of error when reconstructing points around the image in a scale-model of the scene. Figures in the heat-map are percentage-error of the distance of each point from the origin (the tip of the diving board). Areas in green represent the lowest reconstruction errors, areas in orange the highest.	74
Figure 4-12. The camera's view of the scene in the diving pool at Ponds Forge International Sports Centre, Sheffield.	76
Figure 4-13. Rotating the camera changed the view from the pool (with no capacity for identifying varied points for reconstruction) to a flat wall on which landmarks could be measured, reconstructed and compared for accuracy.	77
Figure 4-14. Control points used for extrinsic parameters (left); landmarks were identified for point reconstruction(right).	78
Figure 4-15. A simulation of the diving view with a shape placed in multiple positions and orientations to compare known and measured angles.	82
Figure 4-16. A heat-map distribution of error (measured in degrees) between known and calculated angles in different parts of the image	83
Figure 5-1. A body segment model (BSM) represents a human using an approximation based on linked, rigid rods (left) or linked geometric shapes (right).	85
Figure 5-2. The diver's body is symmetrical and in profile on take-off in all diving groups.	87
Figure 5-3. Wrists and ankles should be extended at the points of take-off.	88
Figure 5-4. Landmarks on body digitised to calculate COM.	89
Figure 5-5. Diver's landmarks used to create stick-man model.	91
Figure 5-6. COM calculated using a Clauser model, modified to simplify the illustration. COM-positions (in red) have been re-located to the longitudinal mid-point of each segment).	91
Figure 5-7. COM location varies depending on the body segment model used.	93

Figure 5-8. Dives were digitised to calculate COM-position using a six-segment BSM. The rate of change of COM during take-off was used to calculate take-off velocity. _____	94
Figure 5-9. Take-off velocity was used to calculate COM displacement. _____	94
Figure 5-10. One image was manually digitised multiple times. _____	98
Figure 5-11. Miller (2013) asserts that an assumption of similar displacement of the COM above the board at take-off and the water at entry allows the inference of take-off velocity to a known level of accuracy if flight time is known. Reproduced from 1 <sup>st</sup> Symposium for Researchers in Diving (2013). __	102
Figure 5-12. The diver's COM follows a parabola whose height depends on initial vertical velocity. __	103
Figure 5-13. A very short or over entry makes Miller's method unsuitable due to the mismatch of COM distance from board at take-off and water at entry. Images from <a href="http://www.phoenixhsc.co.uk">www.phoenixhsc.co.uk</a> and <a href="http://ok.co.uk">ok.co.uk</a> . _____	104
Figure 5-14. Vertical take-off velocity (left) can be used to calculate COM displacement at the top of the flight path. Discrepancy between predicted and observed displacement (right) implies an inaccurate BSM. _____	104
Figure 5-15. COM traces for all body-segment models for 100a. _____	106
Figure 5-16. COM traces for 107c. _____	107
Figure 5-17. Examples of Inward 2½ somersaults with tuck (405c), Forward 3½ somersaults with tuck (107c) and reverse 2½ somersaults with tuck (305c), performed by diver RH, were digitised – best model calculations were conducted for each. _____	109
Figure 5-18. Calculations for each model were made for comparison and identification of the best. __	110
Figure 5-19. COM traces (shown in yellow dots) for 107c (top) and 405c (bottom). The best-fit parabola for each dive is shown in white. _____	111
Figure 6-1. Markers facilitate the creation of a stick-figure from blobs to represent the diver. _____	116
Figure 6-2. Coloured tape was used in a trial based on the potential for colour-based image processing. _____	118
Figure 6-3. High-contrast tape was trialled with the aim of isolating markers using contrast-based image-processing. _____	118
Figure 6-4. Retro-reflective tape (left) produces a bright reflection when a light is shined on it (right). _____	119
Figure 6-5. An example of manipulation of colour levels via image processing. Removal of Red and Green and an increase in Blue increases the brightness of pixels containing higher quantities of Blue. Unlit reflective markers are visible on landmark locations on the diver. _____	119
Figure 6-6. A thresholding filter turns all pixels black or white depending on their brightness compared to a threshold value _____	120
Figure 6-7. An inversion function turns dark pixels light and vice versa. _____	120
Figure 6-8. Coloured markers attached to a diver's ankle, leg and rib. _____	121
Figure 6-9. Colour manipulation to enhance blue markers (left), green markers (centre) and red markers (right). _____	122
Figure 6-10. Application of a grayscale and contrast threshold function following colour manipulation to isolate blue (left), green (centre) and red (right) markers in the image. _____	122



Figure 6-11. Black and white zinc oxide tape was used to make markers. The high contrast was selected to maximise the effect of contrast-threshold image-processing.	123
Figure 6-12. Image processing to isolate a white marker (top) and a black marker (bottom) in an image.	124
Figure 6-13. The view of the training environment with successive stages image-processing applied.	124
Figure 6-14. Retro-reflective tape is used to create markers and can be used with and without additional lighting.	125
Figure 6-15. Colour removal is used to isolate the reflective markers in the image. Unlit (no directed lighting) markers are shown left, lit markers right.	125
Figure 6-16. Colour removal and thresholding use to isolate reflective (but unlit) markers.	126
Figure 6-17. Colour removal and thresholding used to isolate lit retro-reflective markers.	126
Figure 6-18. A retro-reflective marker. Edges are trimmed to ensure the divers' comfort.	127
Figure 6-19. Both spray adhesive and surgical tape were used to lengthen the time for which markers stuck to the skin.	128
Figure 6-20. Leukotape was used to increase adhesion time.	128
Figure 6-21. 400w Halogen lights were used to illuminate the scene.	130
Figure 6-22. A theoretically ideal (but impractical) lighting configuration, with halogen lights illuminating the whole flight path of the diver.	131
Figure 6-23. Halogen lights are mounted on handrails to ensure illumination from a range of heights.	131
Figure 6-24. Lighting configurations used in filming tests.	132
Figure 6-25. A two-light setup (left) producing reflections on uncovered markers (right) which were not bright enough for effective image-processing.	133
Figure 6-26. Top – markers visible on the diver in flight. Bottom – markers isolated in the image using image-processing techniques.	134
Figure 6-27. The required arrangement of environmental lighting.	134
Figure 6-28. Top-left – a diver in flight. Top-right, digitised landmarks shown. Bottom-left – anatomical landmarks on lower leg digitised. Bottom-right – retro-reflective marker-centres digitised. Lower leg markers are close to, but not on the desired anatomical locations due to the shape and movement of bone and joint.	136
Figure 6-29. Take-off shapes for dives rotating for different diving groups. The yellow line approximates a segment that goes from the hip landmark and extends through and beyond the neck marker.	139
Figure 6-30. Head and arms can be assumed to be in one of a series of diving-specific postures for the purposes of merging upper-body segments for the three-segment model.	140
Figure 6-31. A process for coalescing Head, Upper-Arm, Lower-Arm and Trunk segments into an Upper-Body segment with re-calculated segment-COM position.	141
Figure 6-32. COM position (shown in white), calculated using three and six segment models.	142
Figure 7-1. The paths of markers tracked through a dive.	148
Figure 7-2. Reducing exposure time darkens the image and provides a different contrast between background and marker reflection.	149

Figure 7-3. Background removal leaves the diver and minimal additional detail in the image for processing. Subsequent processing is required to isolate blobs as foreground detail. _____	150
Figure 7-4. The grayscale filter converts a 24-bit RGB image to an 8-bit grayscale image. _____	151
Figure 7-5. Background subtraction and a grayscale filter produces the image (left). A threshold filter leaves only blobs as foreground features. _____	152
Figure 7-6. A thresholding function applied using manually-specified threshold vales and a threshold value calculated using an Otsu filter. The Otsu filter effectively removes all features but blobs. _____	152
Figure 7-7. The series of processing filters reduces the image to markers against a black background as required. _____	153
Figure 7-8. Markers reduced to a list of white-pixel groups ('blobs'). The red rectangle is the window defines the area to be searched for blobs and can be set by the user. _____	153
Figure 7-9. Knowing the initial pose of the diver allows the identification of landmark by ranking blob-height. _____	154
Figure 7-10. Each image is processed until five markers are detected in the image; this frame is designated the 'start of tracking' frame'. _____	155
Figure 7-11. Crop-windows are created to reduce image-processing time and to simplify the assignment of landmarks to markers. _____	156
Figure 7-12. A crop-window is created around each landmark – this window reduces the area in the successive frame in which the corresponding marker is searched. The white circle below the ribs is the calculated position of COM. _____	157
Figure 7-13. Elements of two markers may appear as blobs in one crop window. This requires a method for identifying the correct blob/marker which represents the landmark. _____	158
Figure 7-14. A marker can become occluded between one frame and the next, requiring a prediction of position. _____	160
Figure 7-15. Segment lengths and interior angle are required for marker prediction. _____	161
Figure 7-16. Two locations are calculated as potential marker positions _____	161
Figure 7-17. Marker location is predicted for the calculation of COM and kinematics. _____	162
Figure 7-18. Key frames in a dive showing tracked markers. _____	163
Figure 7-19. The dots show the position of specific landmarks in all frames of automated tracking. _____	164
Figure 7-20. The path of the COM during take-off and flight calculated with automated tracking. _____	165
Figure 8-1. The diveTracker tool implements the methods used to produce kinematic data describing diving performance. _____	171
Figure 8-2. Calibration files selected to represent movement planes on all boards in the scene. The red box illustrates the plane in which the diver will perform a skill. _____	171
Figure 8-3. Segments are defined by landmarks digitised by the user or from automated marker tracking. The panel highlighted yellow displays the (u,v) and (x,y) coordinates of each landmark digitised. _____	172
Figure 8-4. The most appropriate model for the diver can be calculated or manually selected by the user. The panel highlighted in yellow contains the range of models from which a choice can be made. _____	173

<i>Figure 8-5. Automated tracking can be set-up by the user to optimise the performance of the algorithm. The white dots in the red square show the result of the image-processing algorithm, reducing the image of the diver to the markers designating each landmark.</i>	174
<i>Figure 8-6. Key-frame buttons select points of interest in the dive, consistent with the British Diving Single System technical resource.</i>	175
<i>Figure 8-7. The yellow-highlighted control allows the user to show the posture of the diver in the positions of interest defined in Table 8-1. This provides an opportunity to subjectively compare to ideal positions defined in the Single System technical manual used by the British Diving WCP.</i>	177
<i>Figure 8-8. Image-strips are a stitched sequence of images, selected by the user, showing posture (and kinematic data) at key points in the dive. The yellow highlighted box presents the key-frames available for inclusion in the image strip.</i>	178
<i>Figure 8-9. Performance data superimposed on image during playback and review. The yellow-highlighted box offers kinematic data, selectable by the user, for display alongside the image of the diver.</i>	179
<i>Figure 9-1. 30 Hz video could imprecisely identify key frames – in this example, the point of last contact (where the springboard is level) is not visible. Noting the time-stamps (highlighted in yellow), an intermediate position (in this example, 00:00:14:02.5) was used as the estimate of the timing of the desired position. This process was also used for start/end of somersault and entry frames.</i>	186
<i>Figure 9-2. A vertical trunk position is used to mark the end of each somersault (s/s). For the first somersault, the take-off frame is used as the body does not leave the board with a vertical trunk on skills with rotation.</i>	188
<i>Figure 9-3. The diver opening from a tight somersaulting shape to a right angle defines the point where the ‘drop’ (the preparation for entry) begins.</i>	189
<i>Figure 10-1 – Board deflection with trendline (dotted) – Diver 1.</i>	209
<i>Figure 10-2 – Board deflection with trendline (dotted) – Diver 2.</i>	210
<i>Figure 10-3 – Board deflection with trendline (dotted) – Diver 3.</i>	211
<i>Figure 10-4 – Board deflection with trendline (dotted) – Diver 4.</i>	212
<i>Figure 10-5 – Vertical take-off velocity with trendline (dotted) – Diver 1.</i>	214
<i>Figure 10-6 – Vertical take-off velocity with trendline (dotted) – Diver 2.</i>	215
<i>Figure 10-7 – Vertical take-off velocity with trendline (dotted) – Diver 3.</i>	216
<i>Figure 10-8 – Vertical take-off velocity with trendline (dotted) – Diver 4.</i>	217

## List of Tables

<i>Table 2-1. The diving groups described by the world governing body, FINA.</i>	5
<i>Table 2-2 – Shapes are defined by FINA; breaking the rules of the shape results in deductions from judges.</i>	6
<i>Table 2-3 – construction of degree of difficulty for a series of dives. The dive number (left column) uses FINA’s code for describing dives; each dive has a unique identifying code – for example 636 represents the dive ‘armstand, reverse triple somersault’. From FINA Officials’ manual.</i>	7
<i>Table 2-4. Judges give a score, based on an overall impression of the dive, according to overall impression. Reprinted from the FINA Officials’ manual.</i>	7
<i>Table 2-5. The medal table from the Rio Olympic Games.</i>	9
<i>Table 2-6. Common assumptions made relating to movement and appearance of motion-capture systems using markers.</i>	29
<i>Table 2-7. A comparison of single versus multiple-camera systems.</i>	34
<i>Table 3-1. Subsets of images are constructed by regularly sampling the total set of images. In this example, to keep the same number of images in each set, image0163 and image0164 were unused.</i>	55
<i>Table 3-2. The total set of images were broken up into multiple subsets.</i>	55
<i>Table 3-3. Focal length (expressed in pixel units) calculated from image-sets of a decreasing size. Outlier values are shown in red.</i>	56
<i>Table 3-4. Principal point calculated from image-sets of a decreasing size. Outlier values are shown in red.</i>	57
<i>Table 3-5. Radial and distortion and projection error calculated for image-sets of decreasing size.</i>	57
<i>Table 3-6. Different parameters were calculated in each calibration process.</i>	60
<i>Table 3-7. The effect on model values when the calibration is run selecting different parameters to be estimated. Outlier values are represented in red.</i>	60
<i>Table 3-8. Variation in intrinsic parameters and projection error from ten calibrations of the same camera and lens.</i>	62
<i>Table 4-1. Differences in R, T and reconstruction error using different number of control points.</i>	68
<i>Table 4-2. Point reconstruction error using extrinsic parameters calculated using different available control points.</i>	74
<i>Table 4-3. Reconstruction accuracy of landmarks in an unsimulated view.</i>	79
<i>Table 4-4. The effect of reconstruction error on inferred vertical take-off velocity. u indicates take-off velocity in metres per second.</i>	80
<i>Table 4-5 – Summary of angle calculation in 28 different positions and orientations</i>	82
<i>Table 5-1. Body segment models implemented in the study.</i>	86
<i>Table 5-2. Anatomical landmarks defined by Hinrichs (1990). * indicates additional segments and landmarks defined by author.</i>	89
<i>Table 5-3. Clauser’s distribution of mass and location of segment-COM.</i>	90

<i>Table 5-4. Distribution of COM location for three divers at take-off, as calculated using three different body-segment models.</i>	95
<i>Table 5-5. Variation in take-off velocity, calculated by the rate of change in COM during take-off using three BSM for each diver.</i>	95
<i>Table 5-6. COM displacement for three different BSM per diver.</i>	96
<i>Table 5-7. Standard deviations of coordinates for body landmarks from ten digitisations of the same image. Values are in pixels (image resolution 488x656px). The mean SD value was 0.7, any SD greater than that is highlighted in red.</i>	99
<i>Table 5-8. The effect on COM-position as a result of imprecisely digitising one landmark. Values are in pixels (image resolution 488x656px), outlier values are highlighted in red.</i>	100
<i>Table 5-9. The effect on COM-position resulting from imprecisely digitising both ends of a segment. Values are in pixels (image resolution 488x656px); outlier values are highlighted in red.</i>	101
<i>Table 5-10. RMSE values for reconstructed COM-positions during a forward jump straight (100a) to a best-fit second order polynomial curve for each model. A lower RMSE indicates a better fit.</i>	106
<i>Table 5-11. RMSE values for reconstructed COM-positions during the flight in a forward three and a half somersaults (107c) to a best-fit second order polynomial curve for each model. A lower RMSE indicates a better fit.</i>	108
<i>Table 5-12. 'Best' models for each example of each dive, calculated using all methods.</i>	111
<i>Table 5-13. The difference in maximum COM height calculated as the difference between the highest reported value in the divers' flight path and the peak of the best-fit parabola fitting the COM points across the flight path.</i>	112
<i>Table 5-14. The effect of flight-path and maximum height error on calculated take-off velocity.</i>	113
<i>Table 6-1. A range of strategies were used to fix markers to the divers. The success of each strategy was measured by the number of dives completed before markers became detached.</i>	129
<i>Table 6-2. Segment-end landmarks and retro-reflective markers do not always occupy the same position on the body due to limb shape or skin-stretch.</i>	135
<i>Table 6-3. Comparisons of COM calculation using manual digitisation via observed and marker-based landmarks.</i>	137
<i>Table 6-4. Comparison of horizontal and vertical take-off velocity data calculated using a 3 and 6-segment model. Highlighted cells represent values of 0.1 ° or greater.</i>	143
<i>Table 6-5. Displacement of COM between take-off and the top of the flight path based on initial velocities.</i>	143
<i>Table 7-1. Each landmark can be predicted if a pair of markers have been detected in the image.</i>	160
<i>Table 7-2. The results of running the automated tracking method on a range of dives. The maximum number of frames in one video was 400. 'Post-TOF?' refers to frames after the top of the flight path. Highlighted rows indicate dives in which some success-measures were not achieved.</i>	166
<i>Table 8-1. Positions of interest in a take-off and dive.</i>	176

<i>Table 8-2. Performance data produced for each dive. These data are calculated to increase insight and understanding of the influences on other kinematic variables, for example comparing the knee angle at maximum squat and the speed at which the legs extended to board deflection and take-off velocity.</i>	<i>180</i>
<i>Table 9-1. Divers meeting the standard required for WITTW analysis had won medals in World and/or Olympic competition.</i>	<i>184</i>
<i>Table 9-2. Diving competitions from which kinematic analyses were made. Semi-finals and finals were used for analysis (as Semi-finals aren't run at National Championships, the Preliminary round was used).</i>	<i>185</i>
<i>Table 9-3. Women's 3 m Data collection metrics separated by method of collection. More samples of broadcast video were sampled than from the diveTracker tool.</i>	<i>190</i>
<i>Table 9-4. WITTW Performance indicators – Women's 3 m springboard. Dive numbers are described below the data tables</i>	<i>191</i>
<i>Table 9-5. Men's 3 m data collection metrics separated by method of collection. More samples of broadcast video were sampled than from the diveTracker tool.</i>	<i>192</i>
<i>Table 9-6. WITTW performance indicators – Men's 3 m springboard. Dive numbers are explained below the data tables.</i>	<i>193</i>
<i>Table 9-7. Comparison of flight times for male divers performing dives from different groups between the 1999 World Championships and 2015-2019 WITTW values.</i>	<i>194</i>
<i>Table 9-8. Comparison of flight times for female divers performing dives from different groups between the 1999 World Championships and 2015-2019 WITTW values.</i>	<i>194</i>
<i>Table 9-9. Mean take off (vertical) velocity in optional dives performed by divers in the 1996 Olympic games and 2015-2019 WITTW values.</i>	<i>195</i>
<i>Table 9-10. Correlation (<math>r^2</math>) between kinematic metrics in the dataset of men's dives.</i>	<i>196</i>
<i>Table 9-11. Correlations (<math>r^2</math>) between kinematic metrics in the dataset of women's dives. Only the forward group has 3.5 somersaults and therefore has more than one somersault's speed measured.</i>	<i>196</i>
<i>Table 10-1. The training programme followed by the divers in the study. An 'x' indicates a component of training that would be completed in the day.</i>	<i>200</i>
<i>Table 10-2. Performance goals agreed between diver, coach and diving's Senior Leadership team at annual review (21/9/2018).</i>	<i>202</i>
<i>Table 10-3. Selected profiling results for Sheffield divers relevant to agreed preparatory-phase goals. All testing was performed on ForceDecks force plates and the English Institute of Sport, Sheffield.</i>	<i>203</i>
<i>Table 10-4. Optional dives with their equivalent lead-up skills. The time of the season dictated that lead-up skills would be measured and compared to World Class optional dives in the same group.</i>	<i>203</i>
<i>Table 10-5. Change in jump-testing results pre and post intervention.</i>	<i>206</i>
<i>Table 10-6. Description of dives classified by dive number (defined by FINA).</i>	<i>207</i>
<i>Table 10-7. Dates of data collection.</i>	<i>208</i>
<i>Table 10-8 – Mean board deflection values – Diver 1.</i>	<i>209</i>
<i>Table 10-9 – Mean board deflection values – Diver 2.</i>	<i>210</i>
<i>Table 10-10 – Mean board deflection values – Diver 3.</i>	<i>211</i>

<i>Table 10-11 – Mean board deflection values – Diver 4.</i>	212
<i>Table 10-12 – Mean take-off vertical velocity values – Diver 1.</i>	214
<i>Table 10-13 – Mean take-off vertical velocity values – Diver 2.</i>	215
<i>Table 10-14 – Mean take-off vertical velocity values – Diver 3.</i>	216
<i>Table 10-15 – Mean take-off vertical velocity values – Diver 4.</i>	217
<i>Table 10-16. The relationship between change in board-deflection and vertical take-off velocity. A blue, upward arrow indicates positive change in a metric. A red, downward arrow indicates negative change in a metric. Shaded pairs of arrows indicate a mismatch between direction of change in metrics.</i>	218
<i>Table 10-17. Regression analysis of the dependent variable ‘vertical take-off velocity’ and the independent variable ‘board deflection’. Significance was set at <math>p &lt; 0.05</math>.</i>	220
<i>Table 10-18. Regression analysis of the dependent variable ‘vertical take-off velocity’ and the independent variables ‘maximum board deflection’ and ‘% impulse after maximum deflection’. Significance was set at <math>p &lt; 0.05</math>.</i>	220
<i>Table 10-19. Regression analysis of the dependent variable ‘vertical take-off velocity’ and the independent variables ‘1<sup>st</sup> contact landing velocity’ and ‘1<sup>st</sup> contact knee angle’. Significance was set at <math>p &lt; 0.05</math>.</i>	221
<i>Table 10-20. Regression analysis of the dependent variable ‘vertical take-off velocity’ and the independent variables ‘trunk angle at 1<sup>st</sup> contact’ and ‘1<sup>st</sup> contact knee angle’. Significance was set at <math>p &lt; 0.05</math>.</i>	222
<i>Table 10-21. Regression analysis of the dependent variable ‘vertical take-off velocity’ and the independent variable ‘board deflection’. Significance was set at <math>p &lt; 0.05</math>.</i>	222
<i>Table 10-22. Regression analysis of the dependent variable ‘vertical take-off velocity’ and the independent variables ‘speed of armswing to maximum deflection’ and ‘maximum deflection’. Significance was set at <math>p &lt; 0.05</math>.</i>	223
<i>Table 10-23. Regression analysis of the dependent variable ‘vertical take-off velocity’ and the independent variables ‘% impulse by maximum deflection’ and ‘maximum deflection’. Significance was set at <math>p &lt; 0.05</math>.</i>	223
<i>Table 10-24. The gap between mean vertical take-off velocity achieved by Divers 1-4 in training (of lead-up skills) and the average corresponding WITTW standards. The highlighted cell reflects where the diver exceeded the corresponding WITTW standard. All units are metres per second.</i>	225
<i>Table 10-25. The gap between somersault speed (revs, or ‘somersaults per second’) by Divers 1-4 in each group of lead-ups and the corresponding WITTW standard. Highlighted cells show where WITTW standards have been exceeded. All units are somersaults per second.</i>	225

# 1 Introduction

## 1.1 Olympic Diving

Diving has been an Olympic sport since 1904, when it was known as 'plain diving' for men. The 1908 Games added 'fancy diving' and women's competition was included from 1912. From 1928, one discipline 'Highboard Diving' was the Olympic event and from 1948, diving was split into Springboard Diving and Platform Diving. In Atlanta in 1996, synchronised diving (pair of divers of the same sex performing at the same time) was demonstrated and synchronised Springboard and Platform events were introduced from 2000.

Athletes ('divers') perform a series of somersaulting and twisting skills, each earning scores from judges. Competitions are contested from either 3 m springboard or 10 m platform (FINA, 2013). At the conclusion of the competition, divers are ranked by the total score of their dives, and the highest scoring diver is the winner.

In post-war years, Great Britain won two medals in 1960, one medal in 2004 and 2012 and three medals in 2016.

## 1.2 Development of performance

While the equipment used in Olympic competition has barely changed in thirty years, the complexity of dives has become greater and the artistry and consistency with which divers have had to perform these dives to win medals has also had to raise. Many factors have contributed to this increase in performance standards, from more athletes and coaches making their living from the sport to the enhancement of training and performance-science support.

Diving training is organised to maximise the scoring potential of the diver in competition. Their physical and technical preparation is programmed to both facilitate the completion of the most difficult dives, and to produce consistent, effective and beautiful technique.

Divers receive continuous feedback from their coach and support team. This feedback is intended to give information about the performance of a skill with the aim of



increasing quality and consistency. The standard for feedback to divers is video replay, providing an opportunity to develop divers' proprioceptive skill (enhancing their understanding of the relationship between what they did and what they felt) and to give coaches and support staff an opportunity to look at a skill in fine detail to identify strengths in performance and corrections needed.

### 1.3 Motivation for research

British Diving has a stated aim of being the top diving nation in Europe and in the top two teams in the world by 2020. This aim supported by British sport's funding agency (UK Sport). To achieve this goal and maintain support for the World Class Programme, progression of a pipeline of athletes, coaches and support staff must be enhanced to increase the potential to win World and Olympic medals.

Diving performance is inherently hard to measure. Athletes perform their skills in free space and don't land on a marked court or pitch. Furthermore, the skills and practices developed and enhanced by support staff (strength and conditioning coaches, physiotherapists etc.) are not the skills performed in competition, creating a disconnection between what can be measured out of the pool and what is performed in it.

Research in acrobatic sport is limited to groups of sub-elite athletes, or studies where physical development is measured in a non-diving context. Kinematic analysis of diving has been conducted away from the coach/diver unit and has taken weeks or months of data-processing before results can be shared. Work has been observational but not directly focused on improving the diver being analysed.

There is therefore a gap for a novel solution where the filming of a diver is immediately followed by kinematic analysis and feedback to the diver, coach and support team. These data would add knowledge to the development of key performance indicators (for example height, speed of rotation, body angle at take-off) towards an ideal model of technique.

## 1.4 Aim and objectives

The aim of the work described is to benchmark world class performance and to define and implement a novel method to calculate and feedback kinematic performance data to the athlete, coach and performance support team. The identification of objectives requires a review of relevant research and practice.

## 2 Literature review

The aim of this chapter is to develop the objectives necessary to achieve the aim stated in the introduction. This will be achieved by a review of relevant research in

- Diving rules of competition
- Application of performance science in diving and related acrobatic sports
- Kinematic analysis of diving
- Motion tracking
- Camera systems and calibration
- Representation of a human
- Existing software tools

The chapter concludes with a summary of key insights and which inform and shape the objectives for the study that follows.

### 2.1 Diving rules of competition

An understanding of the rules of competitive diving is required in order to appropriately focus attention on which areas of physical and technical development can lead to most successful competition performance.

#### 2.1.1 Competition format

Diving's world governing body (FINA - Federation Internationale de Natation) defines competition rules. In Olympic Individual competition (Fina, 2010), females and males perform a list of five and six dives respectively from 3 m (the Springboard event) or 10 m (the Platform event). Each dive must be from a different group as described in Table 2-1 (with one group repeated by men on Springboard). The complexity of each dive is at the discretion of the diver.

Olympic Synchronised competitions are contested from 3 m and 10 m Platform. Pairs perform two dives of limited difficulty and either three (women's events) or four (men's events) dives of unlimited difficulty, covering five diving groups.

Each dive is awarded a score; the finishing order is determined by the total score over all dives in the list, with the winner having the highest total.

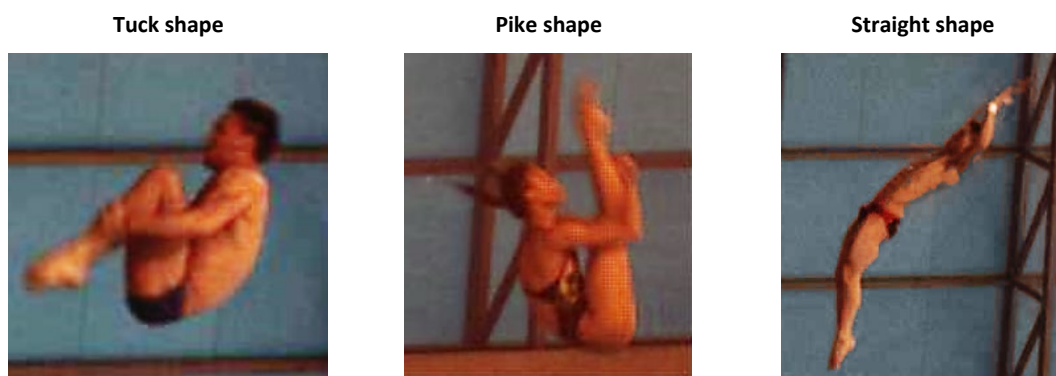
### 2.1.2 Groups, shapes and degree of difficulty

Diving groups (Fina, 2010) are defined by the direction in which the diver faces, the direction in which the diver rotates and whether the diver begins the skill on their feet or on their hands. Table 2-1 describes the six diving groups.

*Table 2-1. The diving groups described by the world governing body, FINA.*

Group	Starting from	Facing	Rotating
1 - Forwards	Feet	Forwards	Forwards
2 – Backwards	Feet	Backwards	Backwards
3 – Reverse	Feet	Forwards	Backwards
4 – Inwards	Feet	Backwards	Forwards
5 – Twist	Feet or hands	Forwards or backwards	Forwards or backwards
6 – Armstand	Hands	Forwards or backwards	Forwards or backwards <sup>1</sup>
<sup>1</sup> - Armstand-inwards (facing backwards, rotating forwards) is not permitted for safety reasons			

Dives can be performed in one of four shapes. Figure 2-1 shows the shapes in which dives may be performed and Table 2-2 describes these shapes by a definition stipulated by the governing body (Fina, 2010). Deductions are applied by judges (and/or the competition referee) should a diver fail to demonstrate the shape as defined, according to the severity of the rule infringement.



*Figure 2-1. Athletes perform dives in a range of shapes. The shape influences the difficulty of a dive.*

Table 2-2 – Shapes are defined by FINA; breaking the rules of the shape results in deductions from judges.

Shape	Definition
Tuck (Letter 'C')	The body is held in a tight, compact shape. There will be a bend ('angle') in the knees and hips. The hands will grab the lower-leg. The feet will be together and pointed.
Pike (Letter 'B')	The body has a bend ('angle') at the hips. The legs will be straight and together, the feet pointed. The position of the arms is optional.
Straight (Letter 'A')	The body is extended at the knees and hips. The feet will be together and pointed. The position of the arms is optional.
Free (Letter 'D')	The diver will make more than one of the shapes ('A', 'B' or 'C' as defined above) during the performance of the dive.

Each dive has an associated 'degree of difficulty' (also known as 'DD' or 'tariff'). The degree of difficulty is calculated by a formula (Fina, 2010) adding components of difficulty for:

- A. Number of somersaults (more somersaults increases component A. Board-height is also considered as flight time from different boards influences the difficulty in completion of a given number of somersaults)
- B. Flight position (more difficulty is earned by performing dives straight, next piked, lowest in the tuck position. This is due to somersaults being more difficult to complete with an increasingly extended body and correspondingly greater moment of inertia)
- C. Number of twists (more twists increases the value of component C)
- D. Approach (the direction the diver faces to make forward or backward rotation; for example, inwards (forward rotation from a back-facing start) gets a higher 'D' component than forwards (forward rotation from a forward-facing start). This reflects the greater mechanical challenge of producing inwards rotation compared to forwards)
- E. Unnatural entry (depending on the direction and number of somersaults being performed, divers cannot see the water for the whole opening and preparation for entry in some dives, leading to a higher value 'E' component where this is shown)
- F. Table 2-3 shows examples of the application of the formula to calculate the degree of difficulty for a dive.

Table 2-3 – construction of degree of difficulty for a series of dives. The dive number (left column) uses FINA’s code for describing dives; each dive has a unique identifying code – for example 636 represents the dive ‘armstand, reverse triple somersault’. From FINA Officials’ manual.

### Examples

Dive	Pos	Hght	A	B	C	D	E	D.D.
636	C	10	2.5	0.2	0.0	0.3	0.4	3.4
5253	B	3	2.2	0.3	0.6	0.2	0.0	3.3
6241	B	10	1.9	0.3	0.5	0	0	2.7
5255	B	10	2.1	0.3	1.0	0.2	0.0	3.6

#### 2.1.3 Judging and scoring

A panel of seven or eleven judges (for individual and synchronised competitions respectively) award a score (Table 2-4) based on the subjective determination of successfully meeting criteria defined in the Official’s manual (Fina, 2010, Chapter 4). Consideration is given to height attained in the dive, distance from the board, the extent to which the diver’s body is vertical at the point of entry (the moment when the diver breaks the surface of the water) and the overall beauty of performance.

Table 2-4. Judges give a score, based on an overall impression of the dive, according to overall impression. Reprinted from the FINA Officials’ manual.

Excellent	10	points
Very Good	8.5 – 9.5	points
Good	7.0 – 8.0	points
Satisfactory	5.0 – 6.5	points
Deficient	2.5 – 4.5	points
Unsatisfactory	0.5 – 2.0	points
Completely failed	0	points

For example, a diver may perform a reverse 3½ somersaults with tuck from 3 m, which has a DD of 3.5. If the judge scores were 6.0, 6.5, 6.0, 6.5, 7.5, 6.0, 7.0 then:

Removing the two highest and lowest scores to leave the three median scores:

6.0, 6.5, 6.0, 6.5, 7.5, 6.0, 7.0

would leave a ‘raw score’ (the sum of counting judge scores before DD is considered) of 19.0. Multiplying 19.0 by 3.5 (the dive’s DD) gives a dive score of 66.50.

#### 2.1.4 Conclusion








The rules of a diving competition limit the ways in which a diver can improve their individual dive score. They can either increase the DD of a dive (by adding somersaults, twists or by changing the shape in which the dive is performed) while maintaining a similar judge-award, or they can increase the quality of the dive so that judge scores are higher with the same difficulty. A definition of performance characteristics of high scoring dives is required to create benchmarks against which divers' performances can be compared.

## 2.2 Successful diving nations

Until 1984, Olympic diving was dominated by the United States of America, the USSR and Italy. From the Los Angeles Olympics onwards, China became a dominant nation, winning the majority of gold medals in each successive Games (recently winning 7 out of 8 gold medals in Beijing, 6 out of 8 gold medals in London and 7 out of 8 gold medals in Rio).

At the 2016 Rio Olympics, China finished top of the medal table followed by Great Britain (1 Gold, 1 Silver and 1 Bronze medal). The medal-table for diving is shown in Table 2-5 (A Sotheran, et al., 2016).

Table 2-5. The medal table from the Rio Olympic Games.

Place	Country	Gold	Silver	Bronze	4 <sup>th</sup>	5 <sup>th</sup>	6 <sup>th</sup>	7 <sup>th</sup>	8 <sup>th</sup>	9 <sup>th</sup>	10 <sup>th</sup>	11 <sup>th</sup>	12 <sup>th</sup>	Total
1	 China	7	2	1			1							10
2	 Great Britain	1	1	1	1	1		1					1	3
3	 USA		2	1	1		1				1	1	1	3
4	 Italy		1	1			1							2
5	 Mexico		1		1	2	1	1			1			1
5	 Malaysia		1			1				1	2			1
7	 Canada			2	2		1	1					1	2
8	 Germany			1	2	1		1		2				1
8	 Australia			1		2	1						1	1
10	 Russia				1			2	1					
11	 PRK				1			1						
12	 France				1									
13	 Ukraine						2						1	
14	 Puerto Rico							1						
15	 Brazil								4	1				
16	 Japan								1					
16	 Ireland								1					
18	 Korea (South)												1	
19	 Columbia												1	

British Diving has aspirations to increasing its medal-success in 2020 and 2024 (A Sotheran et al., 2016) stating as its vision for 2024 “British Diving will become a multi-medal sport, capable of winning medals in every Olympic discipline.”

### 2.3 What It Takes to Win

Sports are required to provide a strategic plan and budget to UK Sport (A Sotheran et al., 2016) to justify an award. Funding submissions require the inclusion of a What It Takes To Win (WITTW) model (A Sotheran et al., 2016). A WITTW model classifies physical, technical, behavioural and environmental requirements for world class success. In some cases, the standards are defined within the WCP while in others, standards are defined by world class competition. WITTW states expected medal-winning scores, levels of difficulty, expected competition experience, timing of peak performances and translation of round-by-round performance to medals by examining trends from scores in historic Olympic Games, World Championships and World Cup



competition. It does not include standards of performance for key metrics (flight time, height, speed of rotation, opening height etc.) or the kinematic influences on these standards (rate of change in joint angles and segment positions etc.) as these have not been determined for contemporary, world class diving.

British Diving (A Sotheran et al., 2016) states as its vision for 2024: “British Diving will become a multi-medal sport, capable of winning medals in every Olympic discipline.” WITTW elucidates the challenge facing the team to achieve this aim.

### 2.3.1 Scores

Figure 2-2 depicts scores from 2012 for the Gold medal (gold scoring band), silver and bronze medals (bronze band) and top-8 (a performance level that qualifies divers to be nominated for a specific level of funding, green band). Scores are taken from the major World or Olympic competition that year and show projected scores the next two Olympic cycles. Projected scores were estimated based on linear trendline from historical data once outlier events had been discounted. As a general trend, scores required to gain medals and win the competition have increased and are projected to continue. Nonetheless, in some years scores required have reduced; generally, scores are suppressed in the post-Olympic year. This can be explained by athletes retiring or taking extended time off after the Games. This consequently has a negative impact on medal winning scores. Furthermore, outdoor competitions typically score lower, due to external factors such as wind, rain and inconsistent lighting compared to indoors.

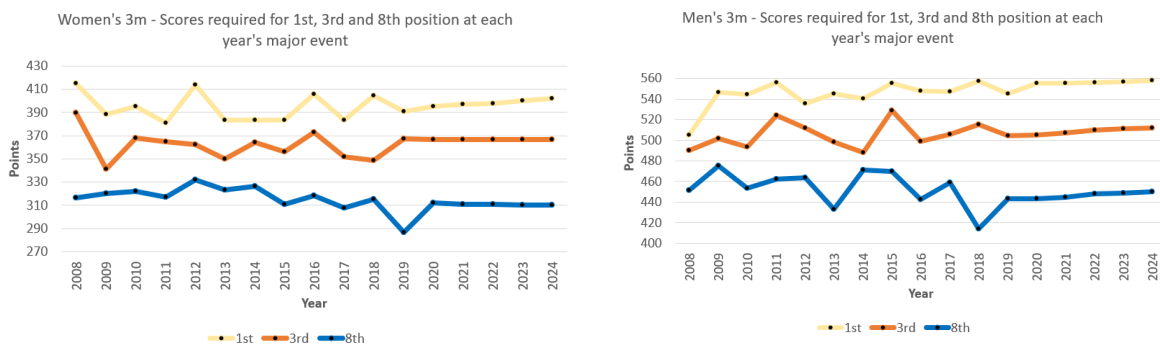


Figure 2-2. Scores to achieve a gold medal (gold band), silver or bronze medal (bronze band) and top-8 (green band) in Olympic springboard events. Scores are taken from the major event of the year or are a prediction of score for future years. Adapted from A Sotheran et al., (2016).

### 2.3.2 Difficulty

Figure 2-3 depicts the highest DD demonstrated by World and Olympic medallists in springboard events since 2008. It can be observed that the difficulty required to win major medals increases over time.

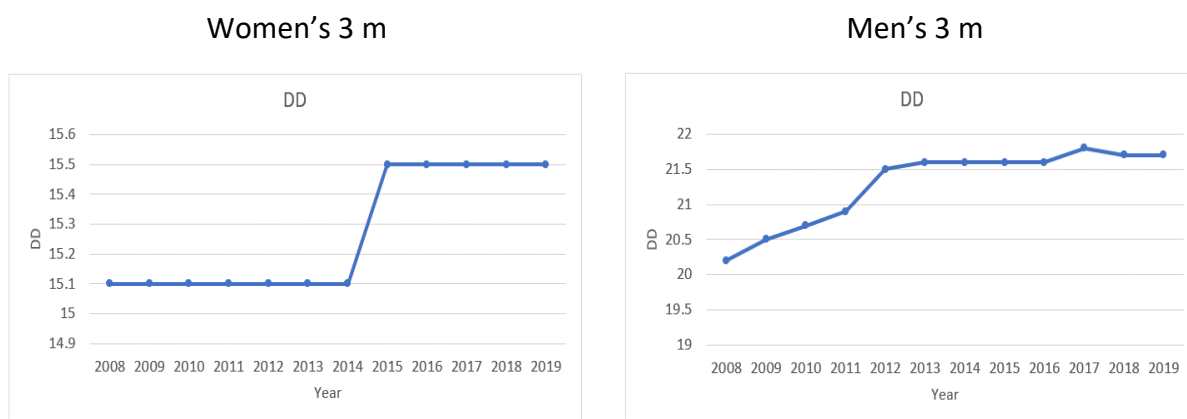


Figure 2-3. The highest degree-of-difficulty list used by a World or Olympic medallist each year in springboard events. Reproduced from Sotheran et al (2016).

The increase of DD and score is not influenced by changes to competition equipment; the Maxiflex B (Duraflex, 2016) springboard has not changed in performance since the 1980-1984 Olympic cycle, likewise the specification of the platform remains the same.

### 2.3.3 The increasing success of the World Class Programme

DD, quality of performance, results and cohort-depth have increased in British Diving (BOA, 2016). Key influences on this improvement include:

- Lottery funding which began following the 1996 Olympic Games (Gibson, 2012) provided Athlete Performance Awards (APA) that allowed divers to be full-time athletes; APA covers both living expenses and sporting costs.
- Successive attainment of UK Sport goals with evidence of talent in the athlete-pipeline resulting in increased funding (Figure 2-4) from £0.9m (1997) to £8.8m (2017) per Olympic cycle (UKSport, 2017). It is recognised (Hogan & Norton, 2000; "Pay up, Pay up and Win the Game," 2006) that increased investment in elite sport results in an "almost linear" increase in medal-performance.

- The employment of more full-time elite coaches in the WCP (from 0 in 2000 to 6 in 2016) (A Sotheran et al., 2016)
- Increased exposure to international competition, from 5-10 starts (preliminary, semi-final and final rounds) prior to the 1996 Olympics to 15+ starts prior to the Rio Games in 2016 (Adam Sotheran, 2017) thereby matching or exceeding competitors
- Access to performance science support through the English Institute of Sport (EIS) and SportScotland Institute of Sport since 1998. The aim of performance-science is to increase athletes' ability to train and compete, and provide innovative solutions to performance questions (EIS, 2018a)
- A focus on a standardised technical model of performance – British Diving's Single System (Evangelov et al., 2016) describes characteristics of diving technique considered optimal for high-DD dives. The distribution of this resource to all coaches on National Programmes, and its adoption as the technical syllabus for coaching courses has clarified expectation of coaching practise in the sport

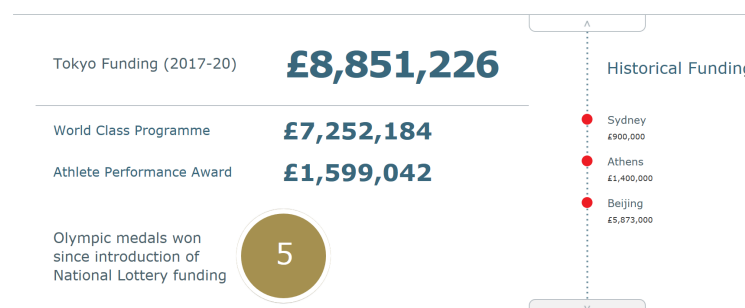


Figure 2-4. UK Sport funding for Diving's World Class Programme. Reproduced from <http://www.uk sport.gov.uk/sports/olympic/diving>.

#### 2.3.4 Conclusion

Development of scoring potential requires the refinement of technique to control take-off direction from the board, optimising height, quality of shape and control of a near-vertical entry. Development of DD depends on increased physical potential to produce more height and more rotation from the board on take-off. Continued investment from UK Sport depends on refining these characteristics to increase

potential for competition success and from providing evidence of an athlete cohort which has the potential to achieve greater success in future. Performance metrics describing physical performance in world class dives have not been established and represents a gap in knowledge. Another gap is the ability to track and evidence these qualities in divers. A method to determine metrics of world class diving and another to measure athletes' performance and progress to these standards would create a competitive advantage in a World Class Programme.

## 2.4 Performance Science

Divers may access performance support in services including:

- Medical (Sports Physician)
- Physiotherapy
- Soft-tissue therapy
- Strength and Conditioning
- Performance Nutrition
- Performance-analysis
- Biomechanics and kinematics
- Performance Psychology
- Performance Lifestyle

As indicated, science and medicine support has been recognised as a driver towards high performance – The English Institute of Sport worked with 93% of Team GB medallists in the Rio Olympics (EIS, 2018b). Practitioners work with coaches and athletes to maximise 'availability' (the divers' ability to train and compete unaffected by illness, injury or mental ill-health), physical capacity and the ability to perform under pressure.

### 2.4.1 Injury prevention

An injury survey (UKSport, 2012) identified that for Team GB athletes, "67% of interruptions to training for British athletes from Olympic sports have been due to injury." Each injury instigated "on average 17 days lost to training and 1 competition

to be missed.” Additionally, injuries were more likely to occur during training than competition. However, this data cannot be seen to be fully representative of the athletes’ state into the London Olympics – due to some sports’ (Diving included) lack of adherence to the monitoring system from which the statistics were derived.

Furthermore, measuring the duration of injury is contingent on the accuracy of record-keeping, notably when the athlete is considered ‘returned to training’. Nevertheless, an ability to measure change in physical qualities (to be correlated with load and compared to historical injury patterns) and variation in technical performance (compared with results obtained in physiological profiling, where physical areas of risk may be identified) would be advantageous in maximising the training opportunity of elite athletes.

A strength of EIS practitioners is their experience across a range of Olympic and Paralympic sports; however, this high-level understanding of multiple domains limits their knowledge of a specific sport. World Class programmes and the Institute work together to enhance the practitioners’ sport specific knowledge, consequently maximising the effect of their interactions. Multiple resources exist to ‘skill-up’ support staff and a tool quantifying performance and comparing it to world-leading standards would add further opportunity for improvement.

#### 2.4.2 Development of physical qualities

There has long been recognition that development of physical qualities (Figure 2-5) is required to progress sporting performance (Makaruk & Porter, 2014a), (Cormie et al., 2011). Physical conditioning “has developed into a vital component and determinant of success for today’s competitive athlete” (Peterson et al., 2004). The implementation of supplementary strength and conditioning training to advance capacity (both upper and lower body) has been investigated by many in both a non-diving context (Makaruk & Porter, 2014b) and with divers (Huber, 1987), (Huber, 1990).

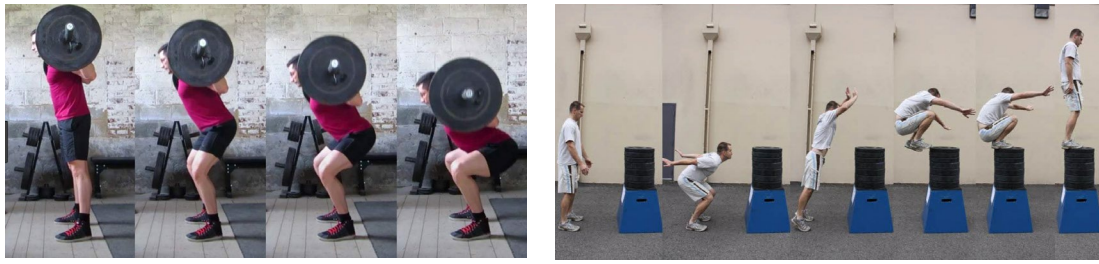


Figure 2-5. Examples of exercises used to build absolute and explosive strength in athletes. Reproduced from <https://stronglifts.com> and <http://crossfitzone.com>.

In acrobatic sport (Hraski, 2015), “from the judges and coaches’ point of view, the flight height is the most interesting parameter of the CG [Centre of Gravity] trajectory is height.” Rotation is optimised by the development of take-off technique and shape in flight (Haering et al., 2017). Diving’s focus is directed at physical development intended to improve take-off speed and production of rotation to allow athletes to ultimately achieve the targets set in WITTW.

The development of lower-limb and posterior-chain (hamstrings, gluteals, erector spinae) function has been modelled (Wong et al., 2016) with the aim of producing a specific goal: jump as high as possible. Muscles were considered in terms of cross-sectional area and muscle-fibre length. Although an optimal proportion of structures was identified, demonstrating that focus on specific development can optimise jumping performance, no attempt to replicate via strength training in athletes was documented. Electrostimulation, combined with plyometric training (Maffioletti et al., 2002) resulted in an increase of 8-10% in a counter-movement jump and up to 21% in a squat jump. Vibration training (Dallas et al., 2015) – a priming process where exercises were performed on a vibrating surface - was undertaken by sub-elite divers and produced a short-term gain in explosive power as well as flexibility. However, neither study investigated the duration of effect, and the change in acrobatic performance.

#### 2.4.3 Conclusion

Performance science interventions have the potential to enhance physical qualities that coincide with the ability to produce height and rotation (key performance indicators of a dive). Existing studies have limitations in the context of world class

diving: there is little measurement of the impact of training on acrobatic performance; conclusions have been drawn based on work with sub-elite athletes and rarely with divers. A process is not presently available to monitor the changes in performance during, and as a consequence of these interventions. Greatest understanding of individual responses to training would be enhanced by development of a system that provides these data in a form helpful to the diver, coach and support staff.

## 2.5 Biomechanical and kinematic research in diving

Biomechanics “uses the tools of mechanics... to study the anatomical and functional aspects of living organisms” (Hall, 2012). The object of biomechanical and kinematic in diving is to understand the contributing factors in:

- Maximising the height of the dive in order both to subjectively impress judges and to complete the dive before entry (D. I. Miller & Sprigings, 2001), (Sayyah et al., 2016), (P. W. Kong et al., 2006). In springboard diving, this is achieved by a combination of application of muscular force and the elastic behaviour of the springboard from which the take-off is made.
- Creating rotation around the transverse and longitudinal axis to complete the desired number of somersaults and twists (K. B. Cheng & Hubbard, 2008), (Frohlich, 1980) with enough time to prepare the body for an aesthetically pleasing entry
- Minimising splash on entry in order to maximise the score from judges in competition (Driscoll et al., 2014), (Qian et al., 2005)

Understanding the contributing factors in enhancing these characteristics is important to develop a performance with maximum effect and efficiency. The complexity of the human system means that enhancement of performance can be achieved in a range of ways; Hall (2012) describes how a gymnast’s double-somersault could be improved by increased armswing speed, increased height or a more compact shape. A clear understanding of biomechanical principles and their effect on performance allows the athlete and supporting team to modify technique or physicality in the most appropriate way.

Biomechanical modelling can also be used to explore potential for new, harder dives with greater scoring potential (Tong & Dullin, 2017).

Kinematic analysis has been performed in the context of Olympic diving since the 1970s (Hebbelinck & Ross, 1974). Since then, research has been focused by theme.

### 2.5.1 Jumping from a springboard

As with gymnastics, springboard divers take off a compliant surface (K. B. Cheng & Hubbard, 2005). The behaviour of a springboard in terms of the change in mass and stiffness depending on the fulcrum setting and the diver's movements on it (K. B. Cheng & Hubbard, 2008), (Haake et al., 2010) has been investigated. Cheng and Hubbard simulated the pattern of activation of musculature around the knee joint, in time with the oscillation of the board, to produce maximum jump height.

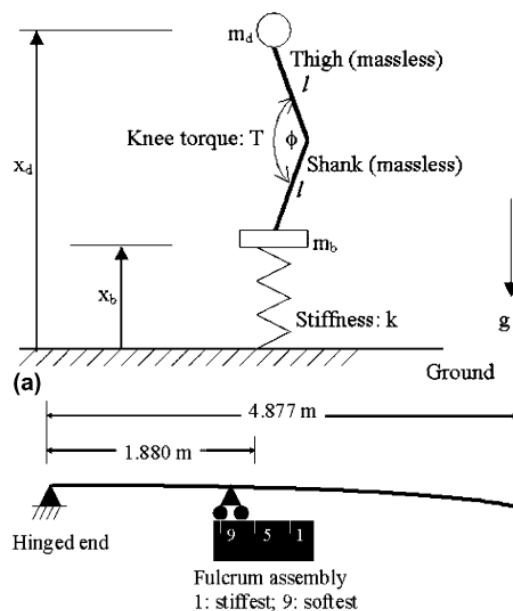


Figure 2-6. A simulation to model the relationship between board mass ( $m_b$ ), fulcrum setting, stiffness ( $k$ ), knee torque ( $T(\phi)$ ) and jump height. Reproduced from Cheng and Hubbard (2008).

It was shown that simulation closely matched data calculated from video analysis, and that optimal joint activation differed from that used to maximise jump height from a rigid surface. It also allowed the calculation of jumping potential using a fulcrum setting that is not that generally used by the diver. Haake et al.'s study measured performance by an elite athlete, whereas Cheng and Hubbard measured sub-elite



athletes, using assumptions (such as a minimum internal knee angle of 90° during the crouch, and a preferred fulcrum setting of 3.5/4) which do not hold for elite athletes. Understanding the two phases of knee flexion, and the timing at which this flexion happens related to the deflection and recoil of the board can, however, inform physical and technical development to optimise the use of the springboard and maximise height.

### 2.5.2 Hurdle step

The hurdle step (Figure 2-7) is the approach used with dives from forwards and reverse groups (and forward/reverse twist dives). The hop from one foot (before landing on the end of the board with both feet and subsequently taking off) increases the diver's potential energy and ability to deflect the springboard, with the aim of increasing take-off speed and height.

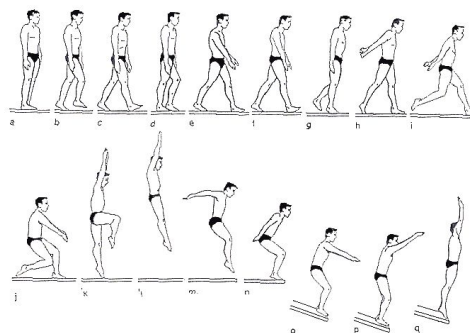


Figure 2-7. A hurdle step is used to increase springboard deflection and increase take-off speed. Reproduced from <https://www.pinterest.co.uk/zonetotalsports/plongeon-springboard-diving-techniques>.

The hurdle of individual world class divers has been examined and described. Liu (Liu, 2013) investigated the characteristics of a hurdle step of a multiple Olympic medallist. Step length, distance from the end of the board at first contact (the initial landing from the hurdle step), maximum deflection (the distance the tip of the board is pressed down) and take-off velocity (both horizontal and vertical) were presented, showing both objective values and subjective interpretation of factors that influence the consistency of take-off (length of the first two steps). These data describe that hurdles

by male divers maximise potential energy by using a long and fast last step followed by a powerful leg drive which both acts a brake (reducing horizontal velocity) and as a force to drive the board down. The consequently greater deflection of the board (compared to that from a slower approach) provides the opportunity of a higher hurdle.

Female divers maximise their potential energy by using a jump-hurdle (where a jump precedes the hop to produce a higher hurdle and greater potential energy). Studies (Doris I Miller et al., 2002), (Sultvedt & Hinrichs, 2005) investigated the increase (and consistency) of take-off velocity through this technique. It was shown that a higher hop provided a higher hurdle, greater potential energy and increased velocity on take-off to a point; technical inconsistency and inability to control the additional force through during the springboard's (stronger) recoil phase limited the gain in height using this approach. The study was conducted shortly after the introduction of the rule-change allowing a hop hurdle – necessitating a change to ingrained technique in senior divers – accordingly this may not reflect the experiences of divers who have grown up with the hop-hurdle. Sultvedt and Hinrichs' study was conducted utilising high-school level divers. Consequently, such conclusions may not be applicable to divers training with the volume and focus required to achieve world class performance.

### 2.5.3 Take-off parameters

A diver produces rotation by generating angular momentum by the point of take-off. This can be achieved by a combination of leaning (not a wholly desirable approach as judges penalise surplus distance from the board, a side-effect of excess lean), transferring momentum (rotation of the trunk and arms in the direction of the desired somersault during contact with the board transfers to rotation of the whole body in flight) and eccentric leg thrust (the reaction force resulting from directional leg-press occurring in a line outside the diver's centre of mass (COM)). Lean and the effect of greater transfer of momentum (reflected by the angle of hip flexion) increase as more rotation is produced (Golden, 1981).

Understanding the requirements of dives of increasing difficulty is important to infer physical and technical requirements of a diver. Despite the compromise to vertical

velocity as more rotation is created, Miller (D. I. Miller & Sprigings, 2001) observed a requirement for increased vertical velocity as the number of somersaults increased. The study measured world class (in 1996) athletes, analysing dives performed at the Olympic Games, thereby observing skills performed by divers in peak condition. Limitations of the study include a small number of examples from each diver (each round only allowed one performance of each measured dive, which may be negatively affected by the pressure of Olympic competition), there was no ability to compare divers of the same sex performing dives with different degrees of rotation (number of somersaults) but the same shape. Additionally, the frame rate used (29 frames per second) and no camera calibration limited the sensitivity and accuracy of measurement.

Comparison of dives performed in the same shape, but with different amounts of rotation and dives with the same number amount of rotation but performed in a different shape, was undertaken (R. Sanders et al., 2002; R. Sanders & Gibson, 2003; R. H. Sanders & Gibson, 2000); using athletes at the 1999 World Championships. The study reinforced Miller's variables of interest during take-off and flight (shown in Figure 2-8 and Figure 2-9) whilst providing an increased sample size and quantity of dives assessed.

- i. Hip angle at the instants of maximum flexion during depression.
- ii. Knee angle at the instants of maximum flexion during depression.
- iii. Hip angle at the instant of takeoff.
- iv. Angle of lean at the instant of takeoff (angle of line from ankle joint axis to shoulder joint axis).
- v. Flight time.
- vi. Peak height of flight (calculated from flight time).
- vii. Work done to gain height (calculated from peak height of flight).

*Figure 2-8. Factors influencing production of height (Sanders, 2003).*

- i. Hip angle at the instant of takeoff from the springboard.
- ii. The angle of lean at takeoff.
- iii. Time of attaining maximum hip flexion with respect to the instant of takeoff.
- iv. Hip angle at maximum flexion.
- v. Time of initiating extension.
- vi. Hip angle at entry.
- vii. Angle of the whole body to vertical at entry (angle of line from shoulder joint axis to ankle joint axis).

*Figure 2-9. Factors influencing creation and optimisation of rotation (Sanders, 2003).*

Conclusions drawn were analogous; divers using higher-DD skills jumped higher, despite requiring increased angular momentum to complete the dive to a satisfactory standard and extended the investigation to changes in joint angles and shape over time to describe the expression of greater physical performance. As with Miller's work, the camera system was limited by measuring a small quantity of skills under the pressure of world class competition, low frame rates (25 FPS) and low resolution (640 x 480 pixels) limiting the sensitivity of landmark location.

#### 2.5.4 Flight

Height and rotation are key characteristics of a dive. Height (Hraski, 2015) and angular momentum must be "properly [utilised] during the airborne phase" to achieve high-scoring dives (Kwon, 1996). Miller (D. I. Miller & Sprigings, 2001) identified that the ability to hold a tight tuck shape was vital for high-difficulty dives, and that specific physical preparation was advantageous to meet that aim.

The relationship between body shape and moment of inertia (and resulting somersault speed) has been investigated. Changing shape from straight to piked reduced moment of inertia by approximately 70% and by a further 35% when changing from piked to tucked (Frohlich, 1980). Until the shape is perfect (knee/hip angles minimised as far as possible), increasing somersault speed is easier by the refinement of shape (Figure 2-10) than it is by changing physical characteristics to be more powerful.



Figure 2-10. A tight shape (right) spins faster than an open shape (left) due to reduction of moment of inertia.  
 Reproduced from [cbraccio.pbworks.com](http://cbraccio.pbworks.com) and [robmacca.blogspot.com](http://robmacca.blogspot.com).

### 2.5.5 Simulation

Yeadon (Maurice R. Yeadon et al., 2006) digitised filmed dives in the forward and reverse groups and inferred take-off forces with the aim of creating a mathematical model that could describe movement (Figure 2-11). The model became less accurate as angular momentum increased and considered two groups out of five on springboard.

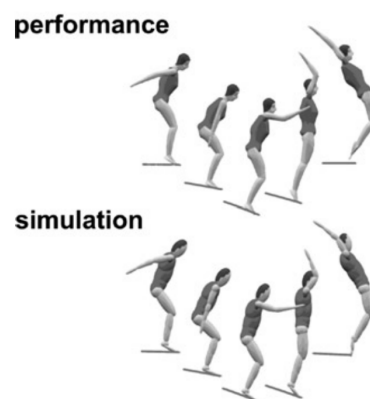


Figure 2-11. Computer models have been created using digitisations of real performances.

Kong (P. Kong, 2005) created a simulation based on an eight-segment model matched against digitisation of a diver (Figure 2-12). Optimal performance characteristics were then established, showing the potential to increase dive height by modifying technique.



Figure 2-12. Digitised technique (upper sequence) compared to simulation (lower sequence).

Optimisation algorithms have been used with models of bodies under take-off forces (Koschorreck & Mombaur, 2012) to produce smooth movement which closely resembles divers in flight. A model of this type was created (Dapena, 1981) with the aim of helping athletes understand the cause (and potential remedies) of errors in performance by comparing take-off parameters causing observed movement with those leading to technically proficient actions. A limitation of this research is its application to dives of all groups and of world class difficulty.

#### 2.5.6 Conclusion

Increasing expectations of DD and quality of performance require a hurdle step developed to increase potential energy, and the physical and technical proficiency to control the increased recoil of the springboard. Athletes must produce greater vertical velocity and greater angular momentum in order to add a more difficult shape or another somersault to an existing skill. Control of flight path and muscular coordination is needed to maximise angular velocity by holding a tight shape.

Where optimal technical performance has been described through simulation, selected skills have been of dives not used in world class competition and are limited by incomplete group coverage. The sensitivity and accuracy of *in natura* studies have been limited by uncalibrated camera systems, low frame-rates and the observation of skills with little relationship to contemporary world class diving; more recent and relevant studies have measured sub-elite athletes or individual athletes making

comparisons to standards across world elite diving inappropriate. A system to describe the performance of contemporary high-difficulty dives across all groups in a natural training setting and with greater accuracy would create new knowledge and should be developed.

## 2.6 Tracking and measurement

Manual methods of tracking (for example, hand-digitising video) are prohibitively slow, labour intensive and necessitate anatomical expertise (Supej, 2010). Consequently, motion tracking (an automated method for describing movement in a subject) is an important consideration to mitigate these drawbacks. Any system used in a diving analysis context must satisfy several requirements:

- Survive repeated immersion in water and the resulting pressure change
- Be comfortably worn by athletes who train in trunks or a swimsuit depending on sex
- Provide data about individual body-segments for kinematic analysis

A review of methods of tracking motion was conducted with the aim of establishing the method best suited to tracking divers in a training environment.

### 2.6.1 Electromagnetic motion tracking

Wireless sensors such as the Polhemus G4 tracker (Polhemus, 2010) provide six degrees of freedom movement data via a unit typically worn on the belt (Figure 2-13). Sensors of this type provide high accuracy and update rate (2 millimetres and 120Hz, respectively).



Figure 2-13. The Polhemus motion tracker is a phone-sized sensor transmitting movement data to a hub for future analysis. Image reproduced from <https://polhemus.com/case-study/detail/case-study-bull-3d-system-using-the-polhemus-q4>.

The requirement for multiple sensors to measure individual body-segments, the size of the sensor and the unsuitability for immersion in water rule out trackers of this type.

#### 2.6.2 Inertial sensors

Inertial sensors offer a method of performance analysis, reporting G-force and angular velocity in three dimensions via a combination of accelerometers and rate gyroscopes contained in a wearable sensor (an example of which is shown in Figure 2-14). Walker *et al* (Walker et al., 2016) described that inertial measurement units (IMUs) offered a method of collecting data for kinematic analysis that improved over historical data collection methods by reducing manual input and processing time expended in manual video digitisation. The use of IMU (IMeasureU sensor – Figure 2-14) was validated to an accuracy of approximately 1% when comparing IMU data with an optical tracking system of a rotating object. Moreover, they demonstrated how an IMU has the capacity to be attached to a diver, enabling the kinematic analysis of rotation speed in forward-facing dives.





Figure 2-14. The small, waterproof IMeasureU inertial measurement unit. Reproduced from ImeasureU.com.

IMU presents data on the athlete as a single unit and does not distinguish between the behaviour of specific body-segments, reducing the ability to quantify technical detail for inference of overall kinematic performance. Two units needed to be attached to each diver to provide redundancy (increasing the cost of measuring a team of divers in training). Therefore, IMUs were excluded as a solution for this study.

### 2.6.3 Video analysis

Obtaining kinematic data from video is achieved by measuring the change in position of objects of interest in relation to time. Video data is desirable as it provides feedback in a familiar format to athletes and coaches who have video-replay systems installed in their training venues. Several methods exist to obtain these data.

Video capture and analysis requires a camera, a method of recording and storing video data and a process for reconstructing real-world coordinates from coordinates on an image.

#### Manual digitisation

Manual digitisation is a process where a user identifies objects of interest (landmarks) in an image. Screen coordinates are converted to world-coordinates and the change in position over time of these landmarks provides data for kinematic analysis (Figure 2-15).

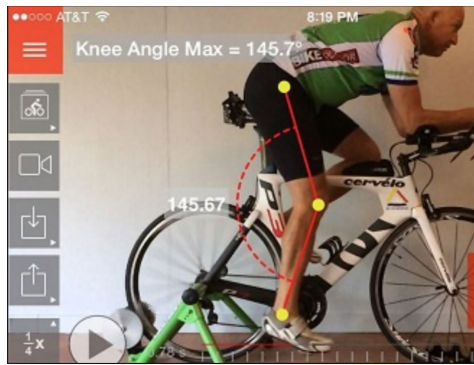


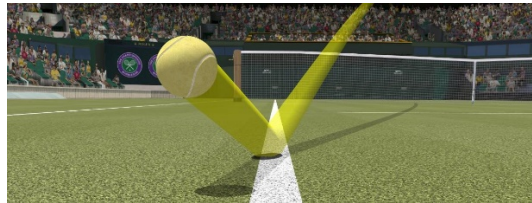
Figure 2-15. Manual digitisation of landmarks allows the calculation of performance data. Reproduced from [en.triatlonoticas.com](http://en.triatlonoticas.com).

Although time-intensive, equipment for manual digitisation is low-cost, and portable camera systems permit setup in any environment. Limitations of manual digitisation include variation in intra-user and inter-user accuracy (consistently locating landmarks in the image) reducing the value in comparison of dives from different venues and dates, although Sayyah *et al* (Sayyah et al., 2016) increased potential for digitising accuracy (increasing resolution to 1280x1024 pixels) and capacity for key-frame identification (250Hz filming allows more sensitivity for determining frames such as maximum deflection, point of take-off and entry) The most accurate conversion of screen coordinates to world coordinates requires a calibrated camera. Finally, manual digitisation takes a considerable amount of time; feedback is typically presented to athletes and support team hours or days after performance (Doris I Miller, 2013), reducing the immediacy and value to decision-making.

### Object tracking

Considering the object to be tracked to be one unit and increasing the number of cameras used to infer world position from multiples images would allow motion tracking to occur. Hawk-eye technology (Duggal, 2014) allows an object of a known size to be tracked using multiple cameras and is most frequently used to augment video of ball movement in cricket and tennis (Figure 2-16) providing information regarding the position of the ball in relation to the court or stumps to support and inform officials' decisions. The system calculates the position of the object by triangulation of positions relative to multiple cameras, showing "an average error of

only 3.6 mm” – well within the level of accuracy required for tracking a diver. The technology has been applied in other domains, both sporting (snooker, football) and non-sporting (industrial and military applications). Limitations of Hawk-eye for use in diving include the assumption of the body as a single segment, the costs and set-up challenges of installation and the need for the tracked object to be of a known size. For these reasons, this method is not appropriate for use in this study.



*Figure 2-16. Hawk-eye uses multiple cameras to track a single-unit object and both track and predict motion with reference to fixed landmarks in the arena (tramlines, stumps etc.).*

### Marker systems

Markers (objects fixed to and identifying specific positions on a body) can be tracked by a camera system; their relative positions and change in location over time allow a body to be represented as a multi-segment model with inferred kinematic behaviour.

Moseland and Granum’s (2001) meta-review of vision-based motion tracking systems identified their benefit (the ‘non-intrusive’ aspect of no instrumentation) and defined characteristics of environments in which vision-based motion tracking was applicable that were common across the literature. These characteristics are shown in Table 2-6.

Table 2-6. Common assumptions made relating to movement and appearance of motion-capture systems using markers.

**The Typical Assumptions Made by Motion Capture Systems Listed  
in Ranked Order According to Frequency**

Assumptions related to movements	Assumptions related to appearance
1. The subject remains inside the workspace	Environment
2. None or constant camera motion	1. Constant lighting
3. Only one person in the workspace at the time	2. Static background
4. The subject faces the camera at all time	3. Uniform background
5. Movements parallel to the camera-plane	4. Known camera parameters
6. No occlusion	5. Special hardware
7. Slow and continuous movements	Subject
8. Only move one or a few limbs	1. Known start pose
9. The motion pattern of the subject is known	2. Known subject
10. Subject moves on a flat ground plane	3. Markers placed on the subject
	4. Special coloured clothes
	5. Tight-fitting clothes

The study summarised that separating the subject from the background was a difficult problem to solve; simple thresholding (separating foreground pixels from background pixels based on value) did not leave the subject alone in the image. The use of a stick-figure representation, coupled with known initial poses and predictable, constrained movement was identified as an effective method for capturing motion.

A stick-figure can be constructed by delineating each end of a segment with markers. Motion analysis can be conducted by tracking the change in position of markers located on known positions on a person's body (Figure 2-17). Kinematic analysis can be performed by considering the change in position, speed and angle of segments whose end-points are identified by the position of these markers.

Kolahi *et al* (Kolahi et al., 2007) defined a method for tracking markers using a DLT-calibrated volume, high-speed cameras and Matlab to perform image processing and kinematic analysis. They further recognised the benefits of low cost, scalability (more cameras provide the potential to increase the range of movements tracked), accuracy (1-1.5%) and low-cost hardware when considering the merits of the method.

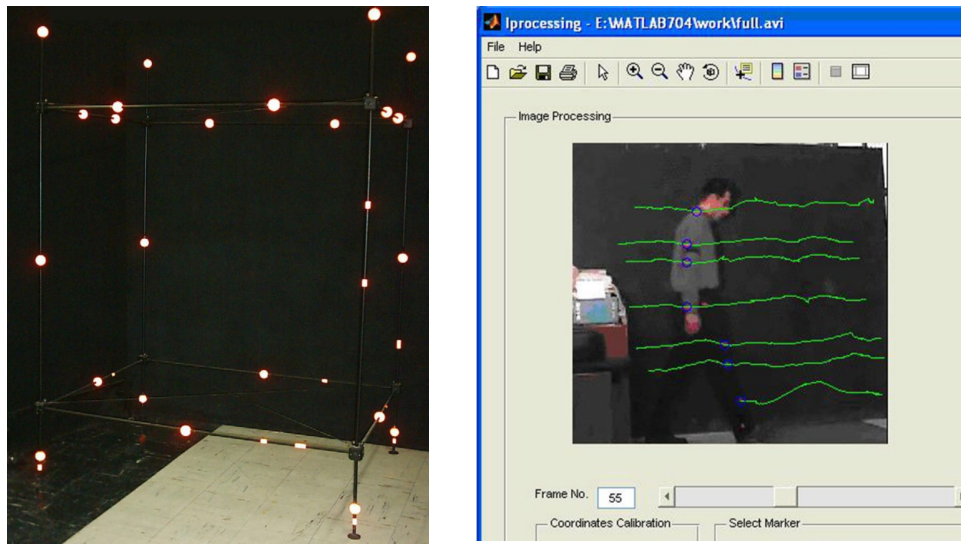


Figure 2-17. A calibrated scene and an example of marker-tracking. This method suits constrained movement in a known field of view.

Systems can use active markers, for example infra-red or LED (Maletsky et al., 2007) (Panjkota et al., 2013) (Phasespace, 2017). Markers attached to the body transmit energy or light which is identified and tracked by a camera system (Figure 2-18).

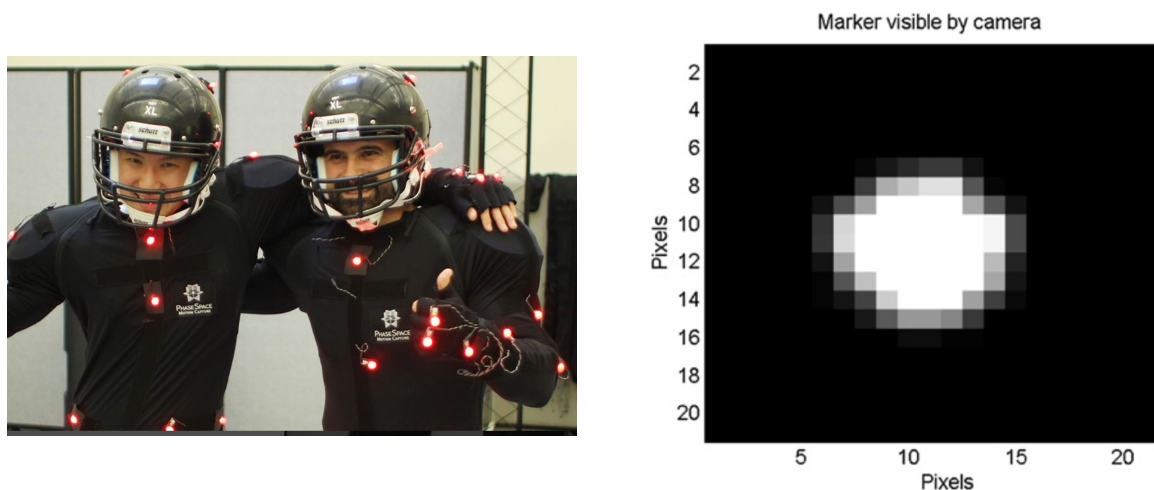


Figure 2-18. LED markers, combined with image-processing techniques to remove the background from the image, leave clear white pixels in an image. Reproduced from phasespace.com.

The benefits of this system are a high degree of accuracy (the study found that tracked LED markers produced reconstructed positions with an RMS-error of less than 0.5 mm in both X and Y axes) and the ease with which markers can be identified. The

risk of correspondence (two markers being so close together as to risk misidentification) can be mitigated by cycling the activation of individual markers so that only one lights per frame.

The restrictions of an active-markers system are that they require power (a limiting factor both considering the performance impact of wearing a battery-pack and the need to mitigate against submersion in water) and that they are typically worn on a suit and protrude from the body (Figure 2-18). Adopting the use of cameras with integrated infrared lights would illuminate the subjects, thus removing the power consideration. However, this would limit the selection of camera used.

Passive-marker (for example, coloured tape shapes, Figure 2-19) systems have benefits over active-marker systems. Markers are low cost; they have no power needs and do not need to be made waterproof. They can be attached directly to the skin or to the clothing (swimsuit or trunks) or supporting leukotape that is worn in training. The disadvantages of a passive marker system are the potential need for additional lighting (if reflective markers are used), and that more image-processing may be needed to remove the background. Finally, with markers that do not switch on and off to a time signal, a solution is required for the correspondence problem.



*Figure 2-19. Passive markers are used to locate physical landmarks for motion tracking.*

#### 2.6.4 Conclusion

Motion tracking is required to quantify and measure movement in a dive. The most appropriate method to track a diver's motion must consider that the athlete wears

little clothing during training and will submerge up to seventy-five times per session. They perform in a known, constrained space and perform in one plane, parallel to the edge of the board, with no longitudinal rotation during take-off. For these reasons the method selected for tracking is a camera system filming passive markers attached to the skin of the diver.

## 2.7 Camera Calibration

The simplest camera model is that of a pinhole camera (Figure 2-20) where light passes from the object in a straight line through the aperture (pinhole) to the image-plane. The pinhole camera has no lens and therefore the only conversion required to reconstruct world coordinates from image coordinates is the application of a scaling function.

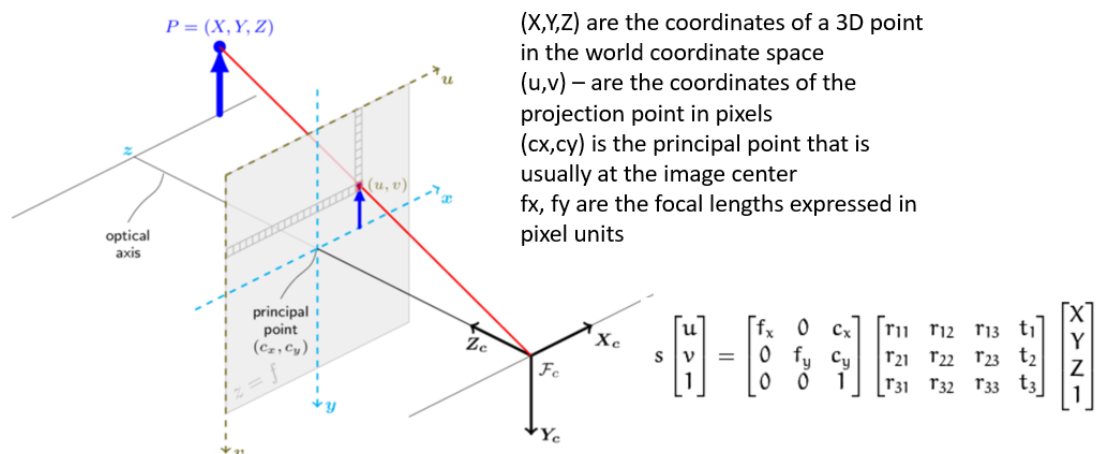


Figure 2-20. A pinhole camera mode. Reproduced from Bouget (2015).

A camera calibration is a method whose goal is to create a model, the use of which facilitates accurate conversion from screen coordinates to world coordinates. The type of calibration process depends on the camera system used.

### 2.7.1 Camera model

For any application where a pinhole camera is unsuitable (including video analysis), a lens is utilised to place the subject in focus. Modelling a lens and image-sensor

requires a camera model (Bouget, 2015), whose parameters are estimated by a calibration. Intrinsic parameters model the camera and lens' geometry and extrinsic parameters describe the position of the camera relative to the filmed scene.

Intrinsic calibration parameters calculated include:

- Principal point – the point on the image-sensor hit by light passing through the centre of the lens. In a perfectly shaped lens (perfectly mounted on the camera), the principal point would be at the centre of the image sensor
- Focal length – the distance between the sensor and the virtual image-plane. In a simple pinhole model, the focal length would be the distance from the aperture to the back of the camera; the position of a lens applied in the system changes focal length
- Radial distortion – the effect of refraction as light passes from less dense air through more-dense glass and then less-dense air to the sensor. On a curved lens, radial distortion is more pronounced towards the edge of the lens
- Tangential distortion – the effect of the lens being imperfectly fitted to the camera and not being parallel to the image sensor

For all models, a reprojection error (the difference in pixels between computed points and their identified location via a calibration pattern) is reported – a lower projection error is preferred for world-coordinate reconstruction accuracy.

Extrinsic parameters calculated in the model are:

- Rotation – the amount of rotation in three dimensions required to align the world coordinate system (where the origin is defined within the scene) to the camera coordinate system (where the origin is within the camera)
- Translation – the amount of linear movement in three dimensions to align the coordinate systems as described above

### 2.7.2 Multiple cameras

The camera model is used to convert a pixel-position in a two-dimensional space (the captured image) to its position in three-dimensions in the world.



Calibrated camera systems have been demonstrated using multiple cameras from a single camera (Suliman et al., 2009), a pair (Song et al., 2007) to six (*Hawk-Eye Innovations*, 2015), (Duggal, 2014). The advantages and disadvantages of single and multiple camera systems in the context of filming diving are identified in Table 2-7.

Table 2-7. A comparison of single versus multiple-camera systems.

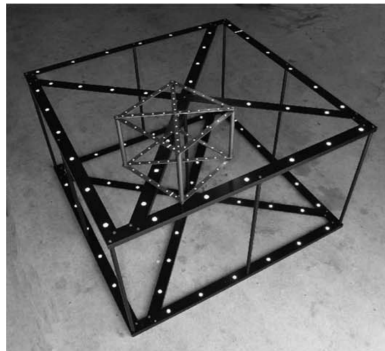
Camera system	Advantages	Disadvantages
Single camera	<p>Practicality - can be set up in any training environment</p> <p>Cheap – a small amount of equipment is needed</p> <p>Matches nature of sport – a diver performs a dive in one plane</p>	<p>Not all landmarks on the body are on the same plane</p> <p>Dives which travel off-plane (towards or away from the plane where <math>z=0</math> will result in greater landmark reconstruction error)</p>
Multiple camera	<p>Could reconstruct landmarks with more accuracy</p> <p>Could reconstruct divers in synchro pairs without occlusion</p>	<p>More complex set-up and calibration</p> <p>Multiple camera positions for stereo reconstruction not always available in diving pools</p> <p>Greater cost of hardware</p>

A single-camera system can be installed in all pools, has a lower cost and provides an acceptable level of reconstruction accuracy given a rigorous calibration process; dives which move sufficiently out-of-plane to cause reconstruction error can be ignored as they are infrequent and do not reflect optimum technique. For the stated reasons, a single-camera system will be used in this study.

### 2.7.3 Calibration method

Performing a camera calibration of a single-camera system can be achieved using different methods. Calibration methods are generally classified as linear (using control points from the scene and where radial distortion is typically not modelled) or non-linear (where a calibration object is used to generate intrinsic model-parameters). A review of methods (Salvi et al., 2002) shows that error is lower when lens distortion is modelled. Two popular calibration methods used in sports applications are Direct Linear Transformation (DLT) and planar methods.

A DLT calibration, (Abdel-Aziz & Karara, 1971) uses the relationship between control points (positions in the scene with known three-dimensional positions relative to an origin, Figure 2-21) and image coordinates of the same landmarks to estimate both the intrinsic and extrinsic parameters of the camera. This method assumes the condition of collinearity (that light travels in a straight line from the control point to the image sensor without being refracted due to the shape of the lens). Without modifying the process, a DLT calibration cannot model lens distortion and therefore risks the introduction of reconstruction error when applied to a system where convex lenses are used to create a large field of view.



*Figure 2-21. A calibration cube used in DLT calibration (Boutros et al., 2015).*

Zhang (Zhang, 2002) describes a non-linear process for generating the intrinsic parameters of the camera without using control points in the scene, known as a planar calibration. A calibration object (Figure 2-22, typically a checkerboard pattern printed on paper and fixed to a flat, rigid base) is used to provide multiple images of known positions on a plane (a corner of one square is designated the origin in each image).

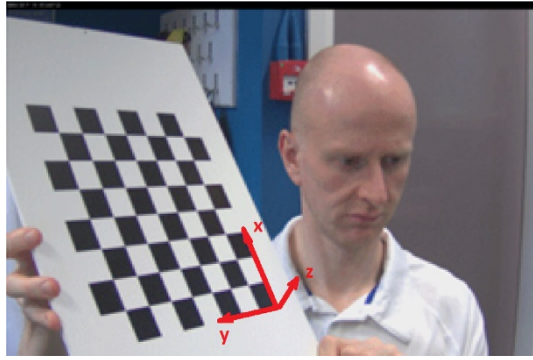


Figure 2-22. A checkerboard, used for planar calibration (CSER, 2013). Red arrows indicate the local coordinate system.

Feature points (the intersections of black and white squares) are located and calibration parameters are recovered using a closed-form solution (Zhang, 2000). A non-linear minimisation process refines the parameters until a stated number of iterations has been performed or until a point of convergence (the change between parameters values becomes lower than a defined limit) is reached.

In relation to the present study the advantages of adopting planar calibration over DLT calibration are:

- A planar calibration can be implemented by moving a calibration object (typically a checkerboard) around the image. This is more practical than identifying enough control points in the diving pool environment (necessary for a DLT calibration)
- The calibration object required for a planar calibration is low-cost and easy to manufacture (typically a chessboard pattern printed on plain paper fixed to a flat, rigid surface (Bouget, 2015), (CSER, 2013). The calibration object required for a DLT calibration (in the absence of sufficient control points) is a larger, more cumbersome object that requires careful alignment in the scene and is impractical.
- A planar calibration models lens distortion. The potentially wide field of view afforded by low-cost camera/lens combinations (and the flexibility required to set the lens to capture dives at different distances from the board in different pools) means that the default DLT calibration (which assumes no lens distortion) would produce greater reconstruction error as the diver moves from

the centre of the image. A DLT calibration can model radial distortion when a larger number of control points (a minimum of 30 ideally even distributed across the boundaries of the volume (Hatze, 1988) can be identified. This is impractical in a pool setting where the movement plane contains only the diving board as a reference point against which control points can be defined

- Both Matlab (Bouget, 2015) and Check2D (software (CSER, 2013) developed by researchers at Sheffield Hallam University to calculate camera models), using the OpenCV library (*Camera Calibration with OpenCV*, 2017), provide tools to perform a planar calibration.

#### 2.7.4 Conclusion

For reasons of flexibility, cost and the assumption that a diver performs in a fixed plane, a single camera will be used for the tracking system. DLT calibration is impractical and inaccurate and therefore planar calibration is the selected method.

## 2.8 Body segment models – representation of a human

McGinnis (2013) states “When we are interpreting and applying Newton’s laws of motion, it is the centre of gravity of a body whose motions are ruled by these laws”. In order to calculate kinematic data about a dive with greatest precision, their centre of mass (COM, an interchangeable term with ‘centre of gravity’ for objects close to the Earth) should be accurately calculated throughout the dive, regardless of the posture or orientation adopted by the subject.

An understanding of the physical characteristics of the human body has been sought using scientific methods since the 17<sup>th</sup> century, where Borelli (Borelli, 1680) and later the Weber brothers established the body’s COM by placing a body on a platform which was then adjusted on a knife-edge fulcrum until it balanced, finding an approximation of COM location. The study was repeated (Harless, 1860) using body segments, creating a more detailed understanding of physical composition. Models have subsequently been defined using a range of techniques including magnetic resonance scanning (Cheng et al., 2000), mathematical models (Nikolova & Toshev, 2007) and the use of force plates and video analysis (Chen et al, 2011).

### 2.8.1 Models

Biomechanical and kinematic understanding of human movement requires an abstraction of the human form to simplify analysis (Figure 2-23). The simplest representation is a particle model where the body is represented by a single point (the centre of mass). This is suitable for describing aspects of flight (assuming the centre of mass is accurately calculated) but does not allow understanding of movement of individual parts of the body. Stick figure models allow segment-specific movement to be measured and provides a simple method for describing movement that is two-dimensional. The rigid segment model offers the most complexity and detail; segments are constructed from geometric shapes which more accurately reflect dimensions of human body segments.

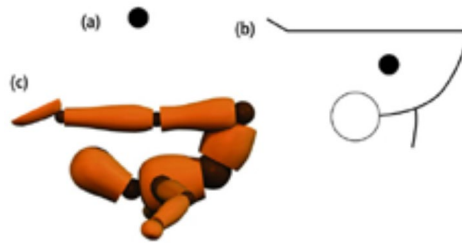


Figure 2-23. The body can be represented by three models – the particle model (a), the stick figure model (b) and the rigid segment model (c). Reproduced from <http://cw.routledge.com>.

The stick-figure model is easily implemented by digitisation of a small number of anatomical landmarks and has been shown (Chan et al., 2016) to be a suitable model to represent movement including jumping when observing human movement where the view is perpendicular to the direction of movement (as for a dive). Representing the athlete using a rigid-segment model adds complexity due to the number of segments typically used – Yeadon’s model (M. R. Yeadon, 2000) uses 11 segments and considers the body in three dimensions which is unnecessary for diving take-off and most aerial behaviour.

### 2.8.2 Segment mass and position of COM

Twentieth Century models were established by dissection of cadavers. Dempster (1955) dismembered individuals to establish segment mass, segment COM, density and moments of inertia. These data were used to understand physical space requirements for a specific task (sitting in a cockpit and controlling an aircraft), introducing the concept of modelling humans to generalise across a larger population. This detailed work (including ranges of motion for each joint for both living and cadaver samples) did not measure subjects of the age and physical condition of elite athletes, they “represented individuals of the older segment of the population” and therefore segment mass-proportions are unlikely to match athletes in a sporting context. Clauser (Clauser, 1969) recognised the value of such models in physical education and conducted a study where thirteen male cadavers were dismembered and analysed using similar dissection and measurement techniques as Dempster. Again, the single-sex cohort whose average age of 48 (and minimum age of 28) does not match characteristics of a world class cohort of divers. Another investigation (Braune & Fischer, 1889) measured more males, and produced what were considered to be the most accurately-measured parameters of the time.

Supplementary models have been defined considering different populations and of subjects of varied ages. Models using subjects from China (Cheng, 2000), Japan (Fujikawa, 1963), Bulgaria (Nicolova *et al*, 2007) and Korea (Ma, 2011). Fujikawa defined both female and male models, furthermore definitions for children (age 6-15) have been calculated (Jensen, 1994).

Divers whose data is contained in the WITTW model represent a range of countries and continents, including China, Korea, Australia, Russia, Germany, Mexico, Canada and Great Britain. This implies the need to recognise variation in morphology due to racial characteristics. There is a difference in age and weight between divers - British World Class divers range between 47 kg and 73 kg as of March 2018 (Diving, 2018), the age-range of British World Class divers has spanned 14 to 32 years of age. Divers have a different mass distribution between springboard-focus and platform (lower-limb development is generally greater in springboard divers, upper-limb development is generally greater in platform divers) (A Sotheran *et al.*, 2016). For these reasons,

approximating COM location using only one model places limits on the accuracy of kinematic parameters of performance.

### 2.8.3 Conclusion

The position of the COM of a diver should be accurately calculated throughout the dive to facilitate the calculation of kinematic data. A stick-figure is the best method for this study due to its ability to represent a diver with a small number of passive markers while allowing body segment models from the literature to be fitted to it.

A range of body-segment models are available for implementation with the aim of calculating the centre of mass of a diver through a dive. The parameters of all models (mass as percentage of total, segment COM, moment of inertia of each segment) are all applicable in the proposed study.

No single model, however, can be an effective representation of all divers given the range of age, sex and racial characteristics exhibited in world class competition. For this reason, the analysis tool should contain a range of models and an algorithm should select the model that most closely represents the athlete being analysed.

## 2.9 Software tools for kinematic and biomechanical analysis

A software tool is required to process positional information and infer kinematic metrics. These data must then be supplied to the diver, coach and support team in a format that meets the requirements of the team.

### 2.9.1 System needs

The feature set of the software tool should include:

- The capacity for feeding back data to the user with enough speed that it fits the dive-feedback cycle (where the diver performs the dive, surfaces, gets feedback from the coach and then sees a replay)

- Data should be presented in the same image as the video replay to minimise the number of sources of feedback to the diver and team
- The functionality to use the calibration model produced by Check2D as this tool is selected as the best solution to calculating a camera model for the single camera system to be used.
- The ability to identify and mark key-frames in a dive so that important positions (maximum deflection, point of last contact etc.) can be quickly compared between dives
- The use of machine-vision cameras (selected due to their ability to be permanently installed and continually stream at a known frame rate)
- A user interface with which users are familiar to minimise learning time.

### 2.9.2 Existing tools

Several tools exist (Figure 2-24) to analyse movement and have individual strengths and limitations. Dartfish (Dartfish, 1999) is a tool that can take a video source from IP cameras and allows the user to annotate video, overlay clips to show differences in performance and track markers. Angles between marked positions can be measured and both key-frames and aspects of performance can be tagged. The tool has been shown to track markers (Eltoukhy et al., 2012) with a closeness of approximately 5 mm to positions returned by a Vicon infra-red camera system. The movement space was calibrated using two points in a plane (linear calibration). Dartfish is limited by its requirement that, should calibration be required to measure movement, the camera must be perpendicular to the plane of movement and linear calibration is used. These tools are limited by their lack of support for a planar calibration process (the method chosen for this study).



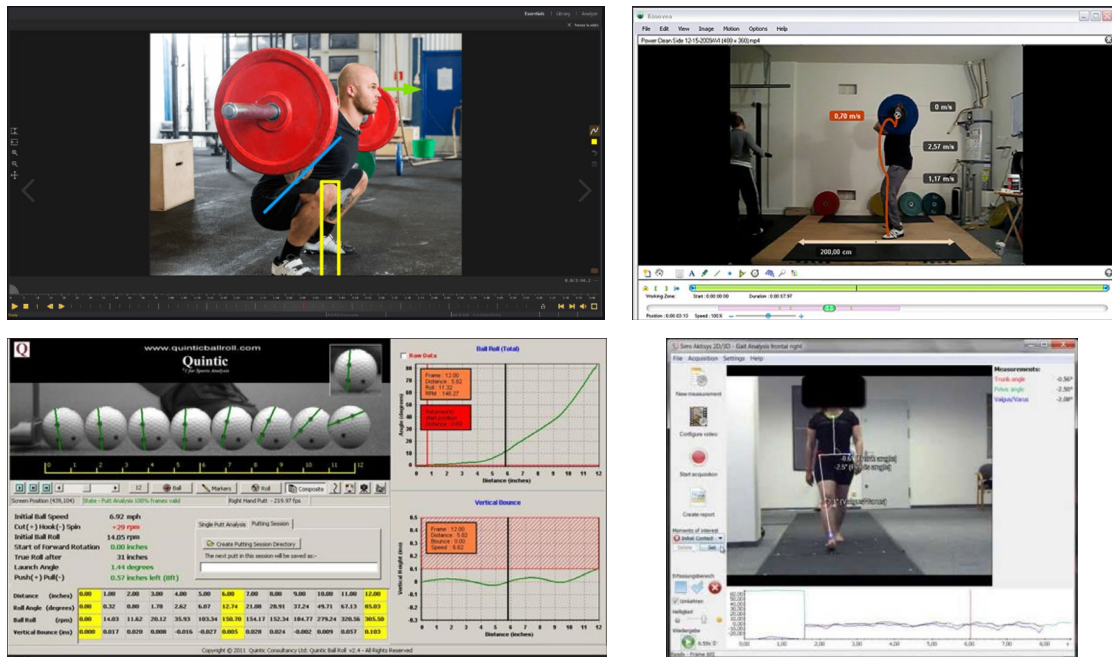


Figure 2-24. Examples of tools for motion analysis (clockwise from top left): Dartfish, Kinova, SIMmotion, Quintic.

Kinovea (T. K. Organisation, 2009) is another tool which can track markers and can overlay data on top of a video, providing contextualised feedback to the user. Its guide for calibrating the scene (K. Organisation, 2009) however, states that measurements on any lines other than those used to calibrate the scene “should be considered a *reasonable approximation* rather than *very accurate*.” It further expresses that no consideration is made for lens distortion, in line with its lack of compatibility with a planar calibration model. These limitations consequently exclude Kinovea as an option, despite its zero cost.

Quintic (Quintic Consultancy Ltd, n.d.-a) have a suite of tools that have been used in a range of sports since 1997, including diving in Great British. Quintic matches other tools in overlaying biomechanical and kinematic data and can output data synced to video for processing by other users. As with the other tools described, Quintic’s biomechanical analysis tool (Quintic Consultancy Ltd, n.d.-b) calibrates without considering lens distortion or a planar calibration model. It calibrates vertically, horizontally or diagonally on screen and so is only applicable when the movement plane is perpendicular to the camera. This limitation coupled with its inability to take data from an IP camera rule its use out for this study.

ProAnalyst is a similar tool with shared functionality and has been used in the biomechanical analysis of gymnastics (Xcitex, 1999) with the aim of maximising performance and minimising risk of injury by understanding the movement and stresses placed on gymnasts at landing. The same limitations exist regarding scene calibration and so ProAnalyst is not appropriate for the environment.

SIMImotion is a tool used in education and provides similar functionality to the tools described above. It has the capacity to use a DLT calibration model which can provide greater accuracy than simple linear calibration. It does not support planar calibration and therefore is not a suitable tool.

Check2D facilitates an analysis of video using a camera model derived from a planar calibration process. This fact makes the tool more viable than the software described above. It was not designed with the sport in mind and has no tagging or automated tracking functionality, nor does it accept streaming data from cameras.

None of the tools described were developed with the aim of analysing diving. A bespoke tool can be developed that meets the needs of the sport and produces appropriate data in a manner that meets the needs of coach, diver and team.

### 2.9.3 Conclusion

No existing tools meet all the requirements of compatibility with planar calibration, support of IP cameras and an interface designed for the analysis of diving. A bespoke tool should be developed that combines the hardware and methods defined in each section above and is designed specifically for the sport, providing a workflow meeting the needs of all users and producing output for identified stakeholders.

## 2.10 Summary

The review of literature presented in this chapter identifies that:

- Maximising score by enhancing judge award and degree of difficulty is required to maintain or exceed the pace of development shown by the rest of the world

in order to win Olympic medals, meet or exceed the sport's target set by UK Sport and continue to be funded for greater long-term success

- Competition results must be matched by an understanding of “What It Takes to Win” which includes a deterministic model of the development of physical capacity and technical skill in order to produce world class medal winning performances. A WITTW model is underpinned by biomechanical and kinematic understanding of the sport
- Analysis in this study is best achieved by measurement of markers in a scene calibrated for a single camera. This reduces the time taken to produce inferred performance metrics and allows comparison of data to previously published work
- A method for calibrating the diving environment should be developed and validated so that it can be replicated in any training environment
- A body segment model should be developed that allows COM-position to be calculated and performance metrics to be inferred from change in marker position.
- A method for attaching markers to divers should be developed to implement the body-segment model in a way that allows normal training by athletes
- A method for extracting marker position from video data should be designed to use the change in marker position to infer kinematic measures and technical performance
- A software tool should be developed to produce these data and present them to diver, coach and team in a way that meets the needs of a multi-disciplinary approach to athlete development.

A study should be conducted to implement the methods detailed above and describe any change in performance based on feedback of these data to a diver, coach and multi-disciplinary team (MDT).

## 2.11 Objectives of the study

This summary has guided the objectives required to meet the aim described at the end of Chapter 1. They are defined as follows:

- To develop an accurate planar calibration method;
- To create an accurate COM model of a diver;
- To validate a stick-figure model from passive markers;
- To design and validate a real-time passive marker tracking system for diving;
- To design a software graphical user interface;
- To define world class diving kinematically;
- To use the system.

## 3 Camera calibration – Intrinsic parameters

### 3.1 Introduction

Tracking a diver's movement in space will be achieved by the calculation of the position of landmarks on the body through time. Precisely calculating the position of these landmarks requires a method of reconstructing world coordinates from the position of the corresponding landmark in the image for each frame of video.

A camera calibration models the parameters (intrinsic, extrinsic and distortion coefficients) of a camera's lens and image-sensor. These parameters, collectively known as a camera model are used to calculate world coordinates from screen coordinates.

Chapter 2 concluded that a planar calibration was the preferred method due to ease and flexibility of implementation and the ability to model lens distortion in all areas of the image, providing greater precision than in other studies of divers' motion (where linear calibration was used).

The aim of this chapter is to define a method to calculate intrinsic parameters of a camera with an acceptable projection error (an indication of the quality of parameter estimation). These data are required before calculating extrinsic parameters which define the relationship between the position of the camera and the scene being filmed.

### 3.2 Hardware requirements

Section 2.7.4 specified a single-camera system and the use of Matlab and Check2D to produce the camera model using a planar calibration process. The preferred solution is one that can be installed, powered and left in the environment but should also support portable, temporary installation when needed, for example when gathering performance data in competition as part of refining performance standards for What It Takes To Win. The range of potential pool configurations, affecting the distance of the camera from the diving boards requires the flexibility of lens choice and the ability to fit a zoom lens to the camera.

The Prosilica GC660c (Technologies, n.d.) (Figure 3-1, left) camera was selected for use in the system; the machine vision device satisfies the following criteria:

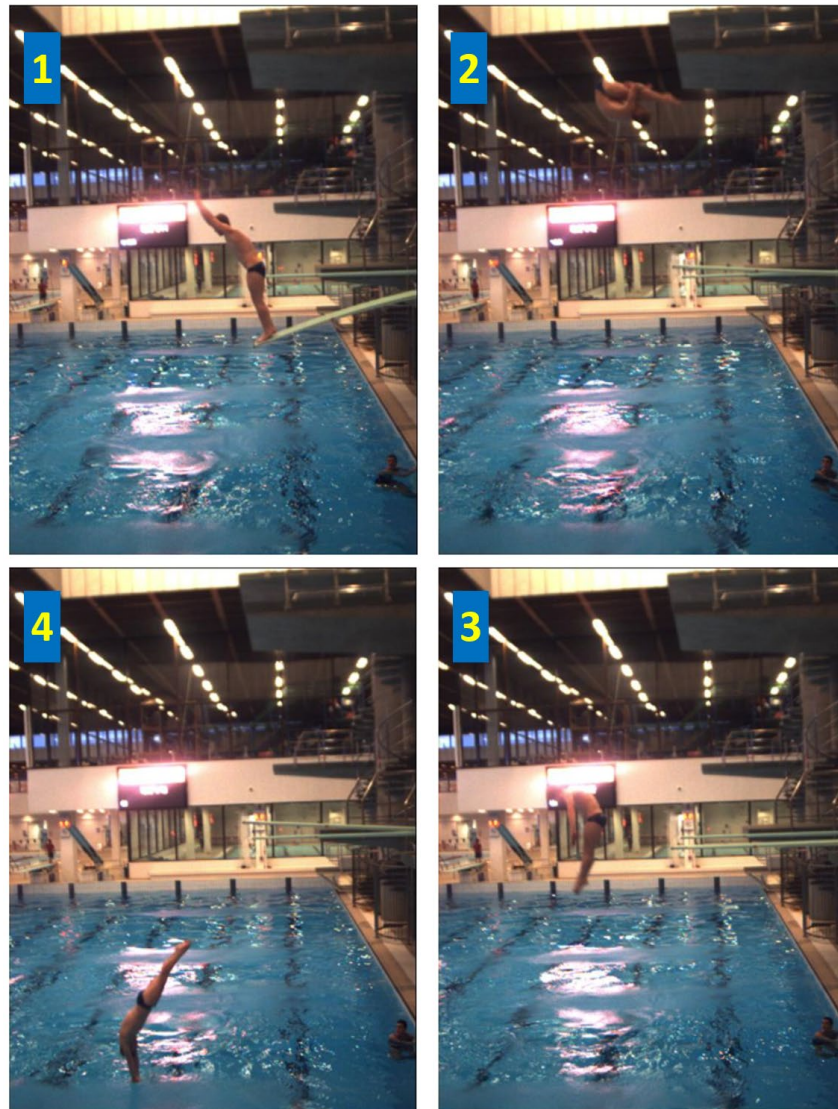
- It can be both mains-powered and powered from a battery, satisfying the demands of permanent and temporary installations
- It streams with a constant framerate (up to 90 frames per second) allowing kinematic analysis at higher framerates than in the studies referenced in Section 2.5
- It streams data over ethernet, supporting cable-lengths of up to 100 metres – allowing for cameras to be mounted on either side of a diving pool and connected to a single PC. This provides immediate access to the captured data; cameras capturing on tape or memory card would require user intervention to retrieve data
- Its operating temperature ranges exceeds the range found in a diving pool
- Its dimensions and weight are suitable for mounting in CCTV housing for permanent installations
- It fits a range of lenses allowing lens choice to be made according to the environment



Figure 3-1. The camera, lens and PC used for the study.

A Varifocal 6-12 mm Manual Iris 1/2" CCD/CMOS Industrial C-mount Lens (Figure 3-1, centre) was chosen as, when used in all GB High Performance Centres, the range of manual zoom allowed the user to frame a view that showed the diver and complete dive

flight-path with the athlete large enough in the image to satisfy the needs of the coach and diver for replay and feedback (Figure 3-2)



*Figure 3-2. View of selected images of the position of the diver. Clockwise from top left: (1) During recoil, (2) maximum height, (3) opening and (4) preparation for entry. The quality of the image must enable the coach and athlete to make subjective assessment of the quality of the dive.*

High humidity and air temperature in the indoor training environment - between 30°C in Sheffield, the pool with the lowest air temperature, to 33°C in Southend, the pool with the highest air-temperature and humidity of between 55% and 65% (SPATA, 2013) – demands a computer that runs in high ambient temperature and with limited airflow. The network interface should support data transfer at a rate as high or higher as the camera records (80 Hz), and the processor should deliver feedback to the diver

and coach within twelve to twenty seconds of the performance of the dive (the observed time used for the diver to surface and receive feedback from the coach); a small form-factor computer with gigabit ethernet and a 2GHz processor satisfies this requirement. The Windows operating system is required as the tracking tool and related tools (Check2D, SimpleCapture) are Windows applications. A small form-factor PC as shown in Figure 3-1 (right) meets the needs for a permanent installation and contemporary laptop computers are suitable for portable setups.

### 3.3 Intrinsic parameters

The calibration process calculates the parameters of the lens and image-sensor of a camera. Parameters which may be calculated are principal point (' $c_c$ '), focal length (' $f_c$ '), radial and tangential distortion (' $k_c$ ') as described in Section 2.7.1.

A series of images of a pattern (a checkerboard is commonly used and is chosen for this study) provide feature point (square intersections) from which parameters are calculated. A software tool (for example Matlab or Check2D) detects these features in the images and calculates parameters accordingly.

#### 3.2.1 Calibration object and pattern

Zhang's planar calibration method (Zhang, 2002) uses regular patterns such as a checkerboard mounted on a perfectly flat surface. The feature points are at a known distance from their neighbours (the length of the side of the square); the pixel-distances between adjacent feature points across the image are used to calculate intrinsic parameters (Figure 3-3).



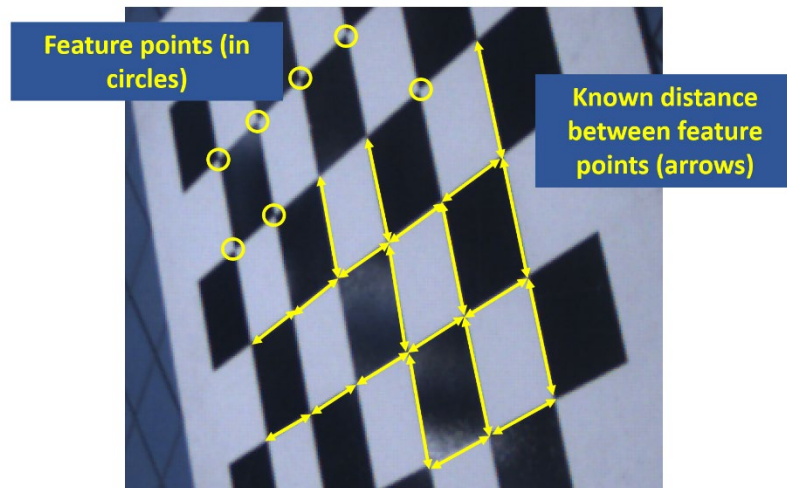


Figure 3-3. Square intersections detected in the image; pixel-distances between intersections are used to calculate intrinsic parameters.

Calibration checkerboards are typically produced by adhering a printout of a pattern on a flat, rigid object or by being printed directly to a flat surface (Figure 3-4). Images for calibration should show a range of positions in the image and a range of angles relative to the camera (Goodwill, 2013).

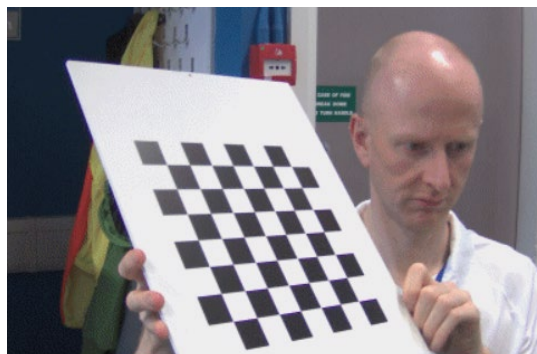


Figure 3-4. Check2D uses a checkerboard pattern printed on a flat surface as its calibration object

Where the object plane is close to the camera, a checkerboard fixed to a small, rigid board is sufficient – the calibration object is light and easy to move and a small area of squares (approximately 300 mm<sup>2</sup>) covers enough of the view that a small number of images can provide complete coverage (square intersections are detected in all areas of the view). For an environment where the object plane is further away (typically 9 to 12 metres in a diving pool), such a checkerboard is unsuitable due to the number of images required to cover the view. Different approaches were used to provide

suitable images for a calibration process and identify a preferred method, described below.

### 3.2.2 Method for collecting images

Zhang's method states that it is acceptable to either 1) fix the camera and move the calibration object or 2) fix the calibration object and move the camera to collect a series of images (Zhang, 2000). In either case, images should be collected whose square-intersections cover the whole of the image (to calculate  $k_c$  and correct for lens distortion) and number is great enough to provide a range of angles of pattern - images should be presented to the camera at between  $30^\circ$  and  $70^\circ$ ) (Sturm & Maybank, 2015).

Moving a calibration object around a fixed camera was discounted as a method due to the difficulty of providing a suitable range of images and the need for a second person to capture images as the first moves the checkerboard.

A light, printed-plastic checkerboard (707 mm<sup>2</sup>) was placed flat on the ground in front of the camera. Images of the calibration object were collected by positioning the camera in a range of distances and orientations to the checkerboard (Figure 3-5).

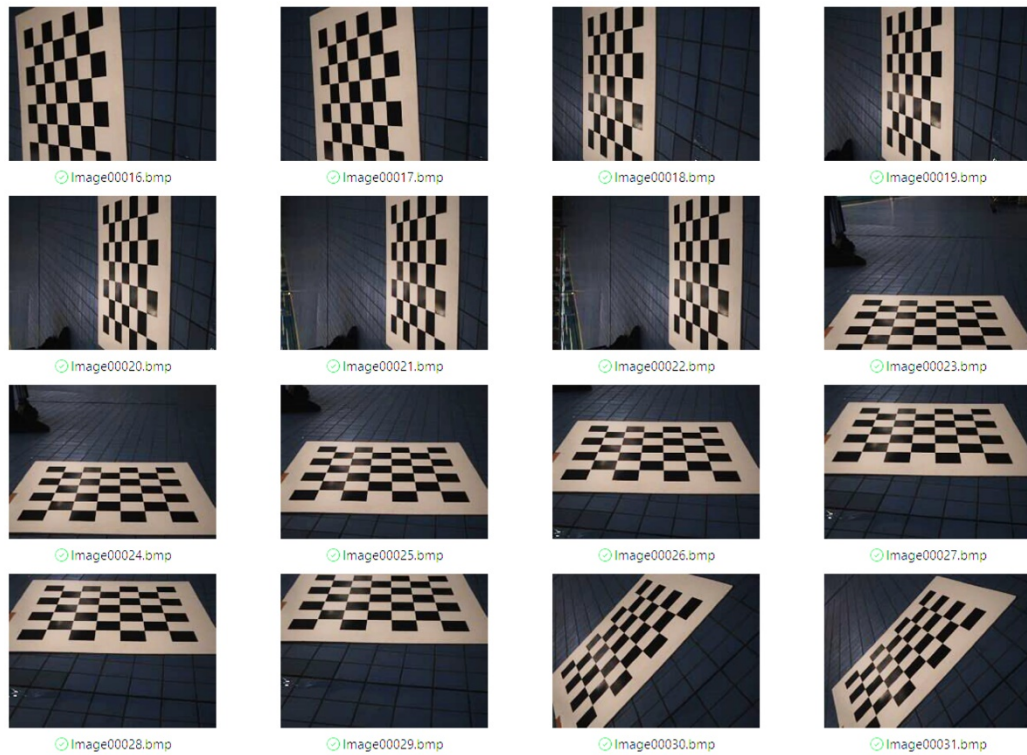
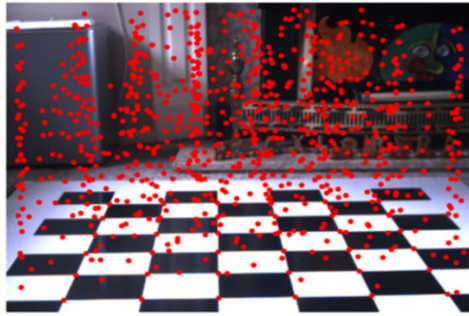


Figure 3-5. Images collected by moving a camera around a fixed calibration object.

The advantages of this method are the ease with which complete coverage can be achieved, and images at a range of angles to the camera. The disadvantage is that the camera must be repositioned in the environment following the collection of images; any manipulation of the camera risks changing lens settings and having a model no longer representing the sensor and lens.

Figure 3-6 shows the results of images captured using the methods described above. Check2D can show coverage – the positions of feature points for all collected images – on an sample image. Matlab produces a visualisation of the checkerboard with virtual camera positions representing the range of poses of the board in relation to the camera.

Red dots indicate positions of square-intersections



Numbers show position of camera relative to calibration object (grey square)

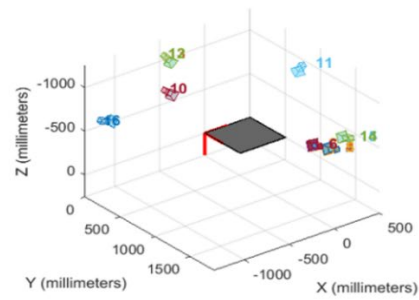


Figure 3-6. Check2D and Matlab used to show square-intersection coverage and range of camera positions relative to the checkerboard.

The coverage and range of camera angles visible in the images illustrates that a suitable set of images can be acquired using this method.

### 3.2.3 Identification of a suitable number of images for calibration

#### Introduction

Zhang (2000) states that a calibration can be performed with a minimum of two images. Matlab's camera calibration tool instructs the user to provide 10-15 images (Bouget, 2015). The risk of too few images is a compromise to the range of orientations of the pattern and restricted coverage of feature points. The practical consequence of too many images is the time taken collect the images and the time taken to reach a solution. The number of variables (size of calibration object, number of features in the pattern, resolution of the sensor, variety in the images) makes general advice for the number of images in any given situation of limited applicability. The number and quality of images needed for the study should be defined for the purposes of efficiency, consistency and repeatability.

A study was conducted to identify the minimum number of images that should be captured from which to calculate intrinsic parameters.

## Method

Many checkerboard images ( $n=164$ ) were captured. For each of four starting positions of the camera (ensuring a range of angles at which the checkerboard was viewed), the camera was moved by a small amount, minimising change between images to ensure that smaller image-sets contained similar views.

The number was considered high enough that extra images would not improve the quality of the calibration and that the set could be split into several image subsets of different sizes, each of which contained images from which parameters could be calculated. The image-set provided good coverage and was used to calculate intrinsic parameters (Figure 3-7).

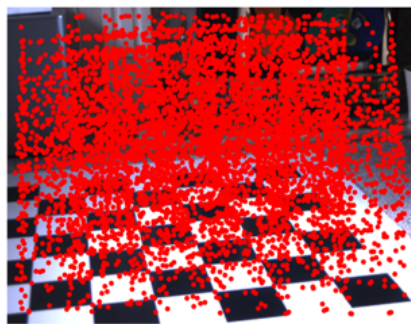


Image set size  $n=164$

Intrinsic parameters:

Focal point (fc), pixel units: 1243.8, 1207.2

Principal point (cc), px: 332.8, 229.7

Radial distortion (kc) : -0.02, 0.08

Projection error, px: 0.2

Figure 3-7. Intrinsic parameters were calculated using an excessively high number of images.

These intrinsic parameters were considered benchmark standards against which those from other, smaller image sets would be compared. Subsets of images were constructed from selecting every  $n^{\text{th}}$  image from the total set used above. For example, 3 subsets would have been constructed as shown in Table 3-1. Images were sampled at regular frequency as (since the camera made small movements between each image's capture) this made each subset as similar as possible, giving similar intersection coverage as shown in Figure 3-8. Any 'remainder' images were unused to keep sub-sets the same size. A subjective assessment of the suitability of that image-set based on coverage was made before running the calibration process.

Table 3-1. Subsets of images are constructed by regularly sampling the total set of images. In this example, to keep the same number of images in each set, image0163 and image0164 were unused.

Set 1	Image0001, image0004, image0007..., image0160
Set 2	Image0002, image0005, image0008..., image0161
Set 3	Image0003, image0006, image0009..., image0162

Subsets were constructed with image-set size as shown in Table 3-2.

Table 3-2. The total set of images were broken up into multiple subsets.

Number of sub-sets	Number of images per sub-set
4	41
5	33
6	27
7	23
8	20
10	16

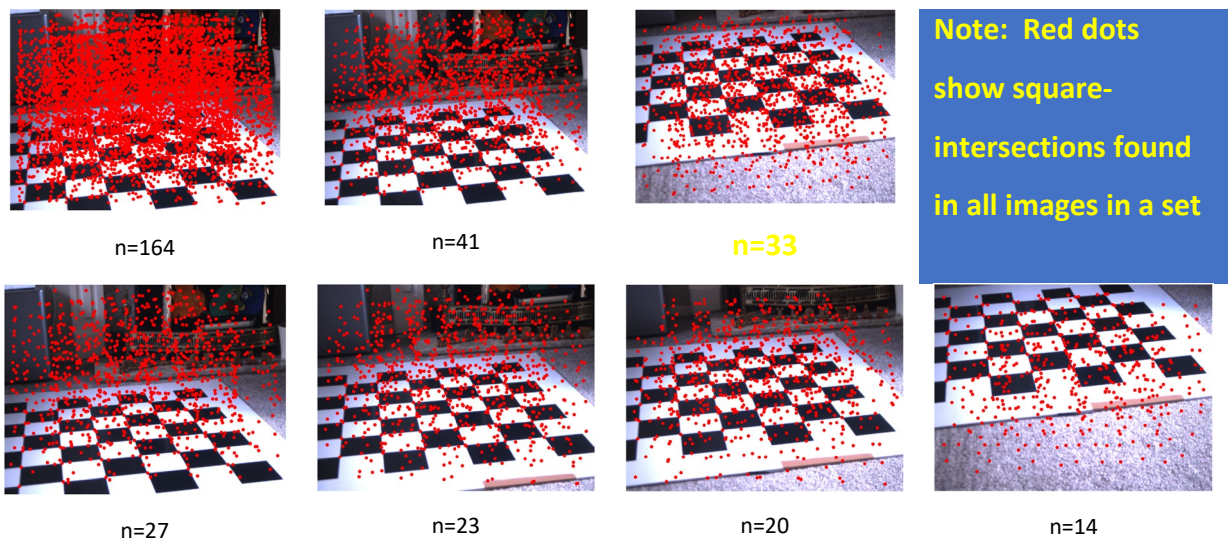


Figure 3-8. Example coverage of square-intersections for image-sets of different sizes.

Each set of images was used to calculate intrinsic parameters. The maximum number of iterations in which to minimise reprojection error, reported as root-mean-square error (RMSE) to below a defined threshold was set at 30, the same number as used by default in Check2D for a small number of images. Mean and standard deviation were calculated for  $cc$ ,  $fc$  and  $kc$  for sets of the same size.

## Results

The results of this study are shown in Table 3-3. The values  $fc_1$  and  $fc_2$  are the values for focal length in the x and y axes respectively.

Table 3-3. Focal length (expressed in pixel units) calculated from image-sets of a decreasing size. Outlier values are shown in red.

Images		Focal length (px)					
# Images	# Sets	$fc(x)_{\text{mean}}$	$fc(x)_{\text{SD}}$	Max difference from mean	$fc(y)_{\text{mean}}$	$fc(y)_{\text{SD}}$	Max difference from mean
164	1	1243.8	0		1207.2		
41	4	1243.8	0.6	0.9	1207.2	1.5	2.4
33	5	1243.9	0.4	0.8	1206.9	1.3	2.2
27	6	1243.8	0.3	0.5	1207.4	1.2	2.6
23	7	1243.8	0.4	0.7	1207.1	2.3	3.2
20	8	1243.8	0.8	1.3	1207.0	2.7	4.4
16	10	1243.8	0.7	1.1	1205.3	6.0	13.5

Mean values for focal length were consistent to within 0.02% regardless of the number of images used, although standard deviation values increased as the image-set size decreased, with the largest increase shown when sets had 20 or fewer images.

Mean values for principal point ( $cc_1$  and  $cc_2$  are x and y coordinates in pixels) were calculated and compared (Table 3-4).

Table 3-4. Principal point calculated from image-sets of a decreasing size. Outlier values are shown in red.

Images		Principal point (px)					
# Images	# Sets	$cc(x)_{mean}$	$cc(x)_{SD}$	Max difference from mean	$cc(y)_{mean}$	$cc(y)_{SD}$	Max difference from mean
164	1	332.8			229.7		
41	4	332.8	0.1	0.1	229.8	0.7	1.1
33	5	332.8	0.1	0.1	229.4	0.6	1
27	6	332.8	0.2	0.2	229.9	0.5	1
23	7	332.8	0.2	0.2	229.5	1.6	3
20	8	332.8	0.2	0.2	227.2	5.4	13.8
16	10	332.8	0.3	0.3	228.9	3.9	8.7

Mean values for principal point were similarly consistent and – mirroring those for focal length – values had a large increase in standard deviation with fewer than 23 images per set (and an increase from 0.5 to 1.6 between 27 and 23 images). Maximum difference from the mean became larger (compared to sets of different sizes) in the two lowest image-set sizes (where n=16 and n=20 images per set).

Table 3-5. Radial and distortion and projection error calculated for image-sets of decreasing size.

Images		Radial distortion						Projection error (px)		
# Images	# Sets	$kc(x)_{mean}$	$kc(x)_{SD}$	max difference from mean	$kc(y)_{mean}$	$kc(y)_{SD}$	max difference from mean	$ProjError_{r_{mean}}$	$ProjError_{r_{SD}}$	max difference from mean
164	1	-0.02			0.08			0.20		
41	4	-0.02	0.00	0.00	0.08	0.00	0.00	0.20	0.00	0.00
33	5	-0.02	0.00	0.00	0.10	0.10	0.10	0.19	0.00	0.00
27	6	-0.02	0.00	0.00	0.09	0.00	0.10	0.19	0.00	0.00
23	7	-0.02	0.00	0.00	0.08	0.00	0.00	0.19	0.00	0.00
20	8	-0.02	0.00	0.00	0.09	0.00	0.10	0.19	0.00	0.00
16	10	-0.02	0.00	0.00	0.13	0.10	0.30	0.19	0.00	0.00

Radial distortion values for mean and standard deviation were similar regardless of the number of images used to create intrinsic parameters. Projection error (an indicator of the accuracy of the model) was consistent to within 0.01 pixels across all image-sets.

These results show that a minimum threshold number of images (greater than 20) should be used to calculate intrinsic parameters.

### 3.2.4 Calibration parameters

Focal length and projection error are calculated in Check2D during every calibration process. Projection error (the difference in distance between observed and calculated



square intersections) is an indication of the quality of the calibration - with a low RMSE value indicating a more accurate model.

At the user's discretion, the calibration process can also calculate:

- The principal point (' $cc'$ ', with  $x$  and  $y$  coefficients) representing the calculated position on the image sensor perpendicularly below the centre of the lens.
- Radial distortion (' $kc'$ ') – parameters to correct the appearance of straight lines as curves (Figure 3-9)
- Tangential distortion – correction for uneven alignment of sensor and lens.

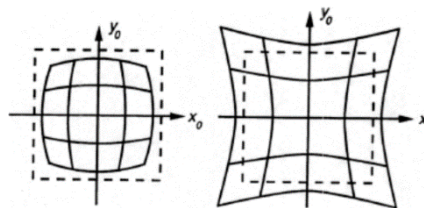


Figure 3-9. Barrel (left) and pincushion (right) distortion can be corrected by calculating radial distortion coefficients.

The user can select (Figure 3-10) which combinations of these parameters should be calculated in the calibration process.

Select	Calculate Principal Point	Calculate Radial Distortions	Calculate Tangential Distortions	Proj Error
<input type="checkbox"/>	<input type="checkbox"/>	<input type="checkbox"/>	<input type="checkbox"/>	n/a
<input type="checkbox"/>	<input checked="" type="checkbox"/>	<input type="checkbox"/>	<input type="checkbox"/>	n/a
<input type="checkbox"/>	<input type="checkbox"/>	<input checked="" type="checkbox"/>	<input type="checkbox"/>	0.582
<input type="checkbox"/>	<input checked="" type="checkbox"/>	<input checked="" type="checkbox"/>	<input type="checkbox"/>	0.565
<input type="checkbox"/>	<input type="checkbox"/>	<input type="checkbox"/>	<input checked="" type="checkbox"/>	n/a
<input type="checkbox"/>	<input checked="" type="checkbox"/>	<input type="checkbox"/>	<input checked="" type="checkbox"/>	n/a
<input type="checkbox"/>	<input type="checkbox"/>	<input checked="" type="checkbox"/>	<input checked="" type="checkbox"/>	n/a
<input type="checkbox"/>	<input checked="" type="checkbox"/>	<input checked="" type="checkbox"/>	<input checked="" type="checkbox"/>	n/a

Figure 3-10. Check2D allows the user to select the calibration parameters to be calculated.

Check2D provides both numerical values for intrinsic parameters and a visualisation of the effect of these values (Figure 3-11) to allow the user to decide if the assumptions made for the model are the right ones.

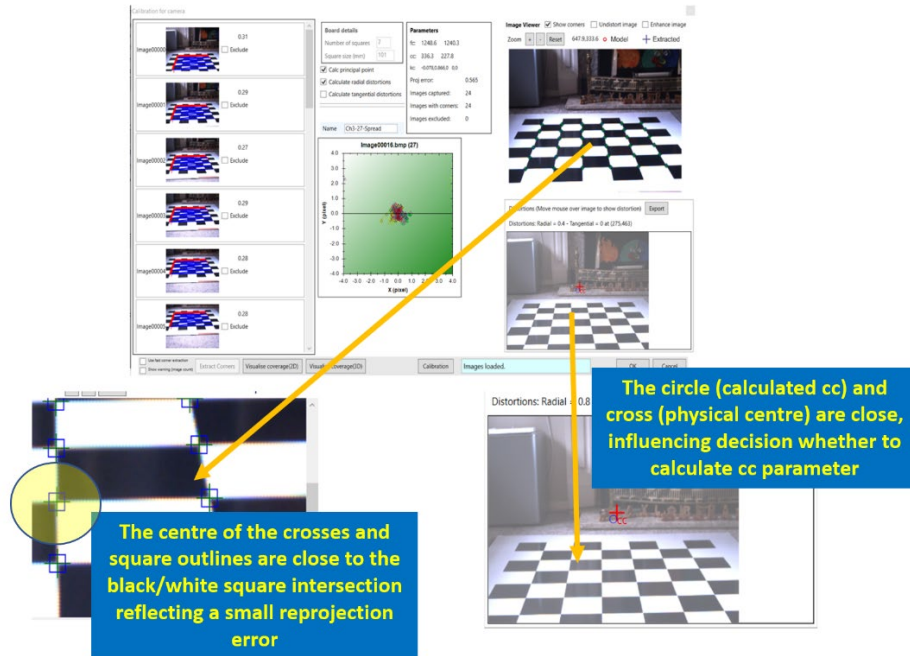


Figure 3-11. Representation of intrinsic parameters and projection error in Check2D.

A study was carried out to identify which parameters should be modelled for this study.

## Method

As described in section 3.3.2 above, a set of 28 images was captured. A calibration was repeated four times, calculating different combinations of parameters in each Table 3-6 :

Table 3-6. Different parameters were calculated in each calibration process.

Calibration	Calculated parameters
1	Focal length only ( $f_c$ )
2	Focal length and principal point ( $f_c, cc$ )
3	Focal length, principal point, radial distortion ( $f_c, cc, kc$ )
4	Focal length, principal point, radial and tangential distortion ( $f_c, cc, kc$ )

The results of each calibration were compared.

## Results

The results of the study are shown in Table 3-7 and the effect of different parameter-estimation on the principal point (' $cc$ ') in  $x$  and  $y$  axes is shown in Figure 3-12.

Table 3-7. The effect on model values when the calibration is run selecting different parameters to be estimated. Outlier values are represented in red.

Parameters estimated	Focal length		Principal point		Radial distortion		Tangential distortion		Error RMSE
	$f_c(x)$	$f_c(y)$	$cc(x)$	$cc(y)$	$kc1$	$kc2$	$kc3$	$kc4$	
None	1241.4	1221.7	327.5	243.5					0.21
$cc$	1246.8	1209.1	332.8	223.2					0.20
$cc, kc$	1247.1	1200.3	332.2	217.6	-0.02	0.12			0.20
$cc, kc(td)$	1245.1	1209.2	<b>346.5</b>	217.2	-0.02	0.14	-0.004	0.004	0.19
Mean	1245.10	1210.08	334.75	225.38	-0.02	0.13			0.20
Max difference	3.7	11.6	11.8	18.1	0.02	0.13			0.01

Values for focal length change little, regardless of the other parameters being estimated. Principal point positions are similar when ' $cc$ ' is the only parameter estimate and when both ' $cc$ ' and ' $kc$ ' (radial distortion) are also estimated. Principal point changes considerably in  $x$  when tangential distortion is calculated, however. RMSE decreases as more parameters are estimated.

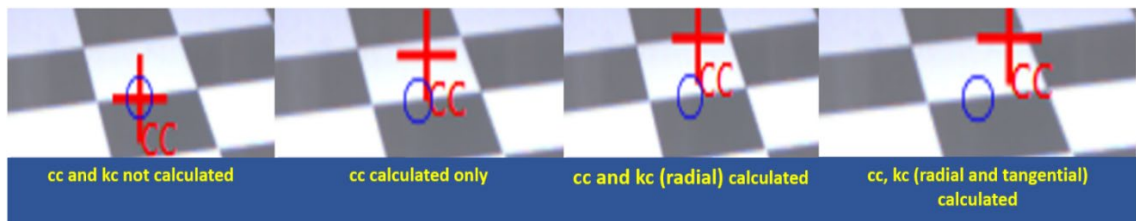


Figure 3-12. Visualisation of the effect of different assumptions in the calibration process. The blue circle shows the position of the centre of the image and the red cross shows the calculated principal point.

The effect on the position of 'cc' is evident when tangential distortion parameters are calculated, moving significantly in x (the crosshair in the rightmost image now intersects the black square to the right).

### Discussion

Projection error decreases with the increase in parameters calculated and is to be expected; a more complex model can fit the points used to create the model more closely.

Focal length is similar for all sets of assumptions, but the principal point moves further from the centre of the image as more coefficients are modelled. When tangential distortion values are calculated, there is a considerable effect on the calculated cc position. The change suggests either misalignment between sensor and lens (which would be visible when setting up the camera) or an over-fitted model. Bouget states, "the tangential component of distortion can often be discarded (justified by the fact that most lenses currently manufactured do not have imperfection in centering)" and Zhang states that calculating tangential distortion can lead to instability in the model. For these reasons, tangential distortion should not be calculated.

It was specified that the camera and lens setting should maximise the size of the diver in the image, while allowing the full flight path of the diver to be in frame. Since the diver will appear in the outer limits of the image, where any radial distortion will be greatest; a model which accounts for radial distortion is therefore required.

### 3.2.5 Consistency of intrinsic parameter calculation

#### Introduction

A study was conducted to establish the variation in calibration parameters using a method which follows the process established so far:

- 23-30 images per set
- A range of angles and good coverage of square intersections
- Images obtained by moving the camera around the checkerboard

#### Method

A series of images was collected as described above on ten separate occasions and subjectively assessed for good coverage. Intrinsic parameters were calculated, modelling  $cc$ ,  $fc$  and  $kc$ . The calibration process was limited to a maximum of 30 iterations to find convergence (the default setting in Check2D). Consistency of the models was measured by comparing mean and standard deviation of parameters in each model.

#### Results

The results of the study are shown in Table 3-8.

Table 3-8. Variation in intrinsic parameters and projection error from ten calibrations of the same camera and lens.

	Focal length (px)		Principal point (px)		Radial distortion		Projection Error (px)
	fc(x)	fc(y)	cc(x)	cc(y)	kc1	kc2	
Min	1242.1	1244.3	329.3	252.3	-0.06	0.011	0.12
Max	1253.6	1251.1	334.6	260.9	-0.003	0.2	0.16
Mean	1247.2	1246.8	332.35	255.31	-0.01	0.12	0.15
SD	3.68	2.37	1.56	2.65	0.02	0.05	0.01
Max difference from mean	6.42	4.31	2.25	5.59	0.05	0.11	0.03

Parameters for focal length and principal point were consistent in each calculation of parameters. Standard deviations were 0.5% of the mean or lower, with minimum and maximum values close to the mean (differences of under 0.5% for focal length and 1% for principal point).

Standard deviation in projection error was close to zero, demonstrating consistency in calculation of model parameters.

## Discussion

The method used to calculate intrinsic parameters has been shown to produce consistent results with any variation in parameter-values a small percentage of their mean. The key features of the method provide a suitable image-set:

- 23 to 30 images
- good coverage
- a range of angles at which the checkerboard is orientated to the camera

### 3.3 Summary

Calculation of intrinsic parameters is one step of the process from which world coordinates can be accurately reconstructed from screen positions. A planar calibration method was selected due to its flexibility and modelling of radial distortion.

It has been shown that an image set of 23-30 checkerboard images, showing good feature point coverage and a range of angles of presentation to the camera can be used to estimate intrinsic parameters with consistency and low RMSE. Larger image sets with similar coverage do not reduce projection error but add time both in image-collection and running the calibration. Although the number of images is greater than that suggested by Zhang or Bouget, this number achieves the above criteria in the context of filming a training environment. For ease of image collection and to allow the method to be completed by a single user, the camera should be moved around the checkerboard pattern to provide a range of angles and feature-points at the edges of view.

The calibration should be performed in Check2D (while other tools such as Matlab can be used to calculate intrinsic parameters, complementary library functions for point reconstruction have been written for a .NET programming language with a Check2D camera model file). Estimation of principal point and radial distortion parameters gives lowest projection error and models distortion at the edges of the image. This is required as an ideal lens setting maximises the size of the diver in the image and fits

their flight path to the edges of the view. Tangential distortion parameters should not be estimated.

The method for calculating intrinsic parameters is therefore:

- Use a calibration object with large squares (approximately 100 mm<sup>2</sup>) in order to minimise the number of images necessary to achieve coverage in a large view
- Collect 23 – 30 images showing good coverage and a range of orientations
- Use Check2D to calibrate, calculating principal point and radial distortion

A projection error (the difference in pixels between the observed and calculated position of each square intersection and an indicator of the accuracy of the calibration) of less than 0.2 px can reliably be achieved using this method.

Following the calculation of intrinsic parameters, extrinsic parameters (defining the relationship between the camera and the origin of the scene) need to be calculated in order to reconstruct world position from image-position.

## 4 Extrinsic parameters

### 4.1 Introduction

Intrinsic parameters model the lens and image sensor of the camera. Intrinsic parameters are independent of the relationship between the camera and the world.

Extrinsic parameters define the position of the camera in relation to the scene being filmed; a rotation ( $R$ ) matrix and translation ( $T$ ) matrix describe the relationship between the camera coordinate system and the world coordinate system. In the context of diving, this is illustrated in Figure 4-1.

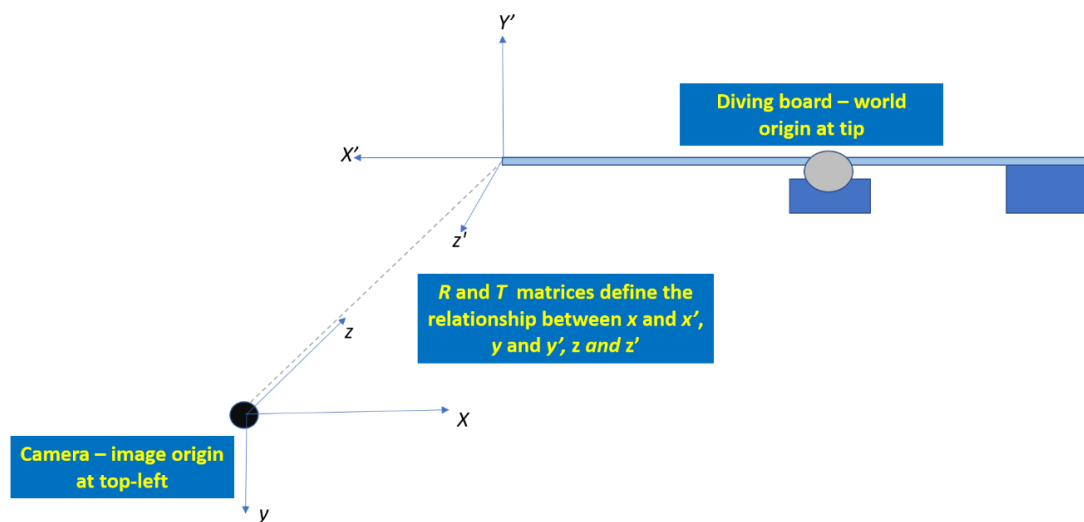


Figure 4-1. Extrinsic parameters (a rotation matrix and translation matrix) are calculated to define the relationship between the camera and the scene.

The aim of this chapter is to define a method by which extrinsic parameters are calculated for filming in a diving environment such that screen coordinates are converted to world coordinates with a known and acceptable level of accuracy.

### 4.2 Considerations for placing a camera in a scene

To successfully create extrinsic parameters, and to film dives such that performance data can be consistently calculated, the camera must be placed in the scene with consideration of several factors:



- The positioning of the camera should allow for an unobstructed view of the whole of the scene including any points used as control points for extrinsic calibration
- The mounting of the camera should be rigid to eliminate any movement of the camera after the calibration process
- The camera should be protected from disturbance and potential movement (for example from objects or people)
- The camera and its power source should meet the facility's requirements for electrical safety
- The camera should be positioned close to perpendicular to the board-tip as possible; if this is not achievable, the view should provide clear location of control points for calibration (such as square-intersections on the calibration checkerboard)
- Any cables used in the system should be managed to eliminate risk of representing a trip hazard

### 4.3 Control points

Control points are positions in a scene whose world coordinates relative to the origin are known. Check2D requires a minimum of four control points to define a plane. A scale model of the diving pool view was created to recreate the view found in the training environment and position control points on a known vertical surface to simulate the plane of movement. An example of control points defined to define a plane is shown in Figure 4-2. A checkerboard pattern is used in the image as the distance from the origin to the square-intersections can be precisely measured.

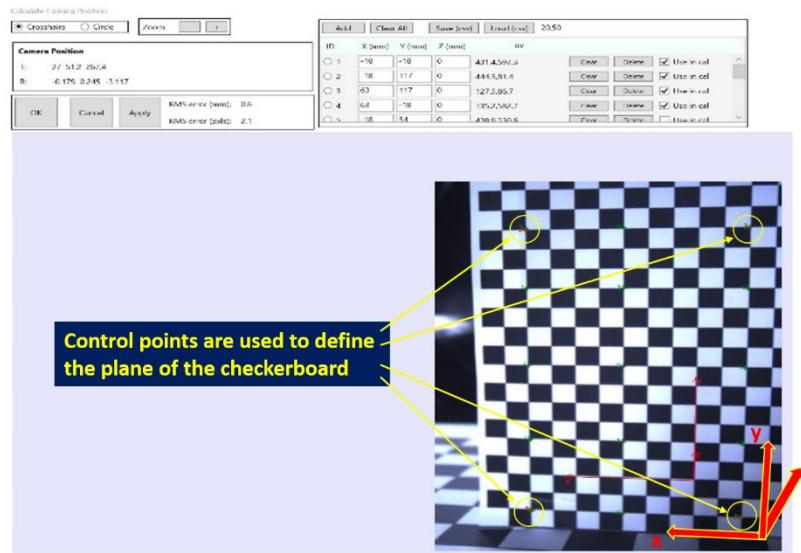


Figure 4-2. A scale model of the diving pool. The horizontal checkerboard represents the water, the vertical checkerboard represents the movement plane. Four or more control points are identified in Check2D to calculate  $R$  and  $T$ . This example uses a checkerboard due to the high number of control points whose  $(x,y)$  position can be precisely measured.

Check2D requires a minimum of four points to define a plane. A greater number of points should (subject to meeting certain conditions) result in  $R$  and  $T$  matrices leading to more accurate point reconstructions in the desired plane. The accuracy of extrinsic parameters is indicated by a root-mean-squared error (RMSE) value reported by Check2D, a measure of the difference between the physical and calculated position of control points

A small number of control points can result in a poorly fitted plane if one point (or more) is imprecisely measured. Fitting a plane to a greater number of control points reduces the impact of one ill-defined control point. Furthermore, should a single control point (out of a large number) be identified as inaccurately measured, it can be excluded from the calculation of  $R$  and  $T$  without negative consequence. This is shown in Figure 4-3 and Table 4-1.

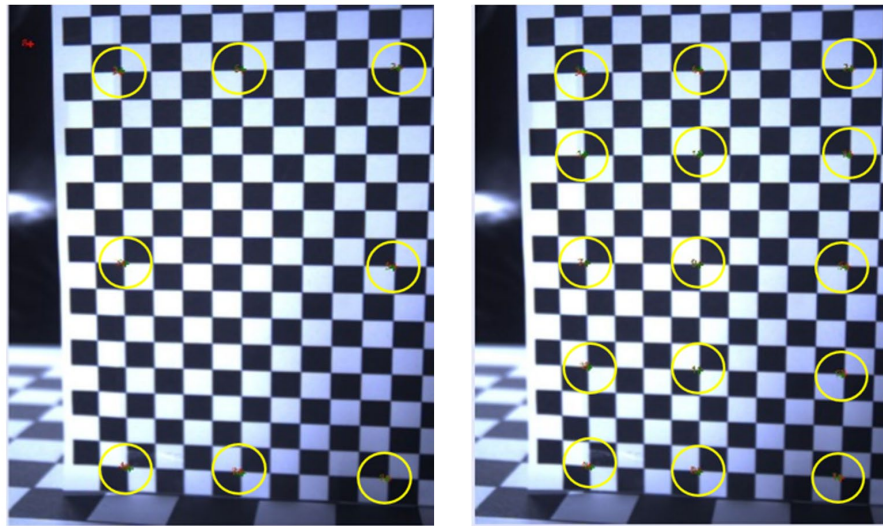


Figure 4-3. Square intersections (identified inside the yellow circles in the images above) are used to calculate extrinsic parameters and to compare results using a small number of points (8, left) and a larger number of points (15, right).

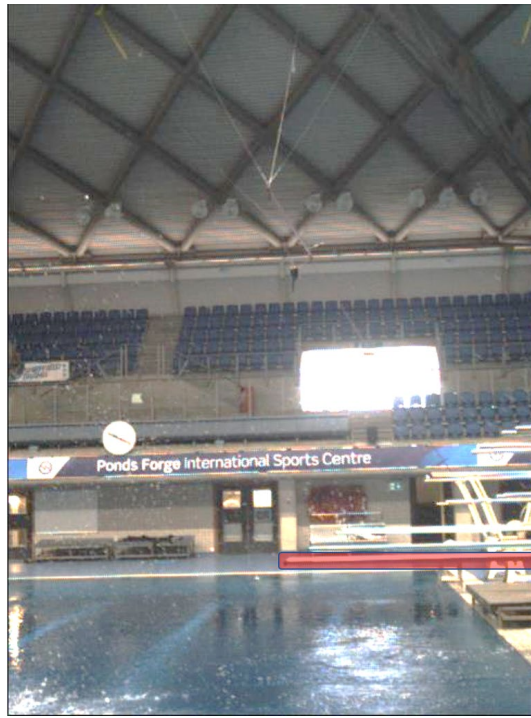
Table 4-1. Differences in  $R$ ,  $T$  and reconstruction error using different number of control points.

Control points	Rotation matrix			Translation matrix			Reconstruction error	
	$R_1$	$R_2$	$R_3$	$T_1$	$T_2$	$T_3$	RMS error (mm)	RMS error (pixels)
8	11.10	11.98	3.12	27.1	51.0	267.4	11.5	2.0
15	10.16	12.23	3.12	27.0	50.9	267.5	0.5	1.8

Adding control points made a small difference in  $R$  and  $T$  but reduced reconstruction error significantly, from 11.5 mm to 0.5 mm.

Control points should be chosen from different parts of the image, particularly if the intrinsic calibration showed a high degree of lens distortion. Control points selected in areas of high distortion (typically towards the edge of the image) allow  $R$  and  $T$  to be calculated with greater accuracy than if distorted areas were modelled without physical points being used to create  $R$  and  $T$ .

A local coordinate system is easily defined using a checkerboard in a scale model where many control points are available. The aim of this chapter is to define a method resulting in accurately-reconstructed world-coordinates in a diving-pool scene where few control points can be used (Figure 4-4).



*Figure 4-4. The diving pool is limited by a small number of control points in the movement plane used by a diver. The diving board (highlighted in red, above) provides measurable points but does not cover the extremes of the image.*

## 4.4 The effect of restricted control points on extrinsic parameters in a simulated setting

### 4.4.1 Introduction

The view of the diving environment differs from the simulation in the previous section; control points are available in fewer areas of the image, and distances between them are smaller. A method is required that will consistently locate enough control points towards edges of the image to provide a high degree of point-reconstruction accuracy in areas of the image inhabited by the diver in take-off and flight.

To assess reconstruction accuracy under these constraints, the scale-model of the scene was used, with the vertical plane represented by a checkerboard, to provide many control points for testing. A view of the diving pool was used for comparison (Figure 4-5); control points on the scale model were identified that corresponded with potential control points in the training environment.

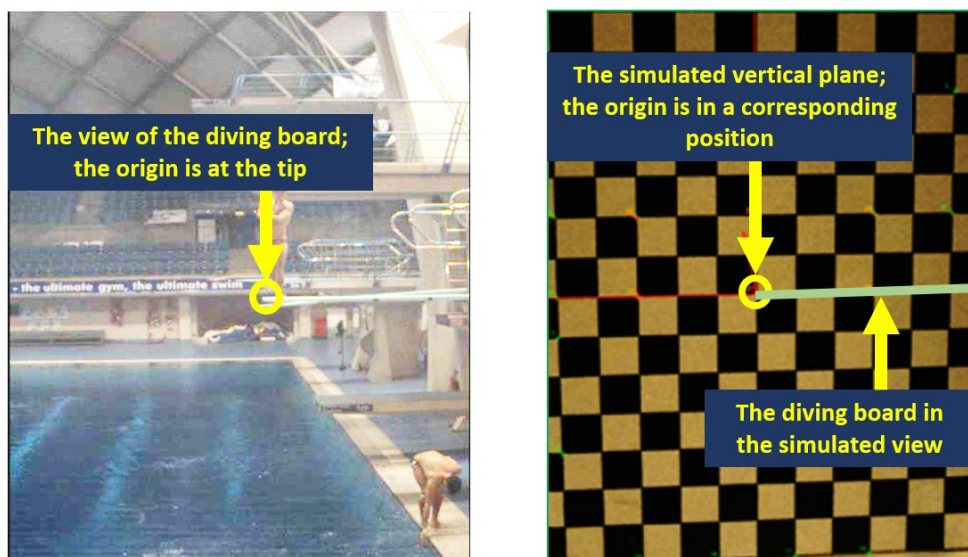


Figure 4-5. A scale-model (right) simulates the view of the diving board (left). Square-intersections were identified which corresponded with the position of the diving board and origin-positions were matched.

#### 4.4.2 Method

For each iteration of the test, a series of control points was identified and used to calculate extrinsic parameters. Landmarks in the image were then reconstructed and distance from the origin to each point was calculated. The difference between calculated distance and actual distance in the model was represented as a percentage-error and these errors across the image were used to create a heat-map of reconstruction error (Figure 4-6).

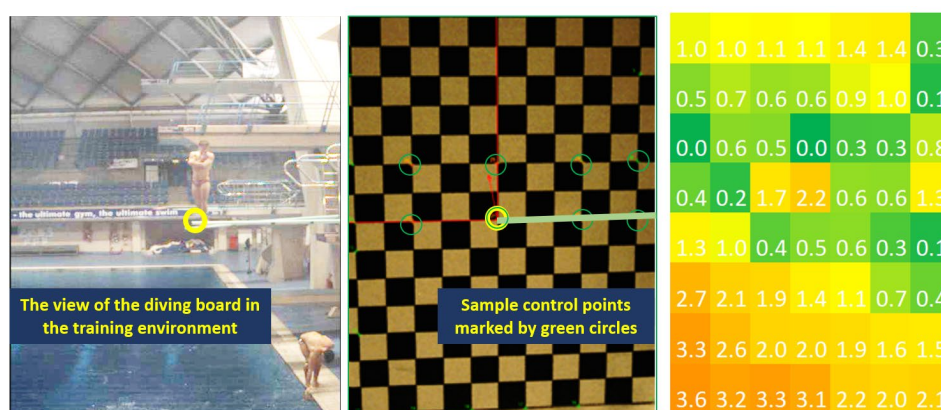


Figure 4-6. Control points in the simulated view (centre) were used to calculate  $R$  and  $T$ . Square intersections were reconstructed and compared to actual positions. Percentage reconstruction error is represented by a heat-map (right). In each position, a lower value indicates a more accurate reconstruction.

It can be seen that the lowest reconstruction error (indicated by the green squares in the heat-map) surrounds the control points, with greater error (represented by yellow and orange colours) evident at the edges of the image, most notably close to the bottom of the image, corresponding to the surface of the water.

The view of the scale model was superimposed on the view of the diving pool to identify where control points could be used which matched possible locations in the training environment (Figure 4-7).

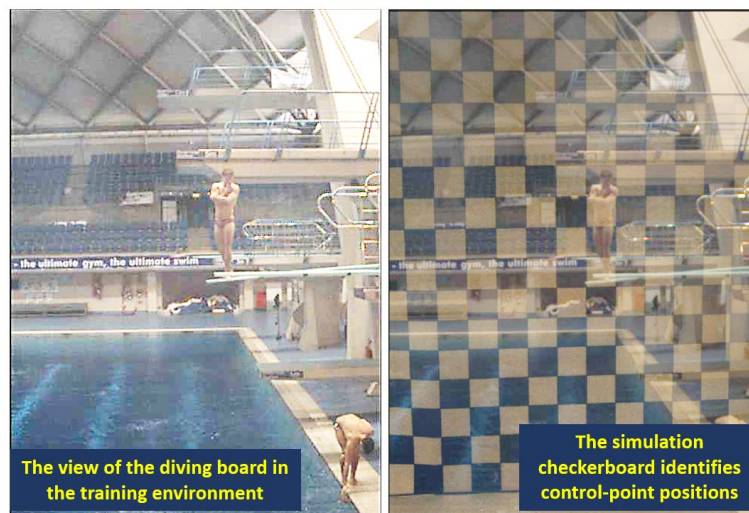


Figure 4-7. Superimposing the checkerboard from the scale-model over the view of the diving pool identifies control points for use in the scale-model trial.

Three trials were conducted, using different equipment to augment the number and position of available control points in the image.

### **Trial 1**

Control points were identified that could be measured using the top edge of the diving board and the checkerboard used to collect sample images for intrinsic-parameter calibration (Figure 4-8).

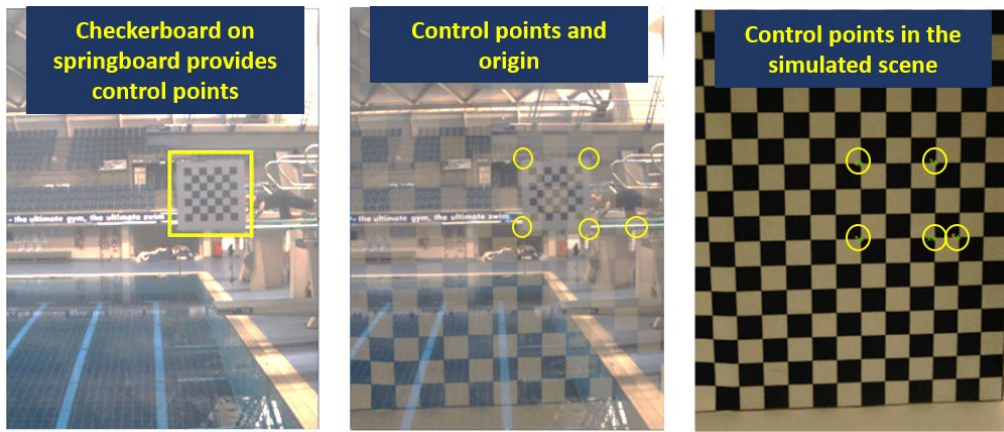


Figure 4-8. Control points for Trial 1, located using the diving board and calibration checkerboard (left). The superimposed checkerboard over the image (centre) allows identification of control points in the scale-model (right). A control point is close to the right edge of the image.

## Trial 2

Control points were defined using the diving board, calibration checkerboard and a plumb line to provide a point vertically below the board towards the edge of the image (Figure 4-9). The length of the plumb-line was known.

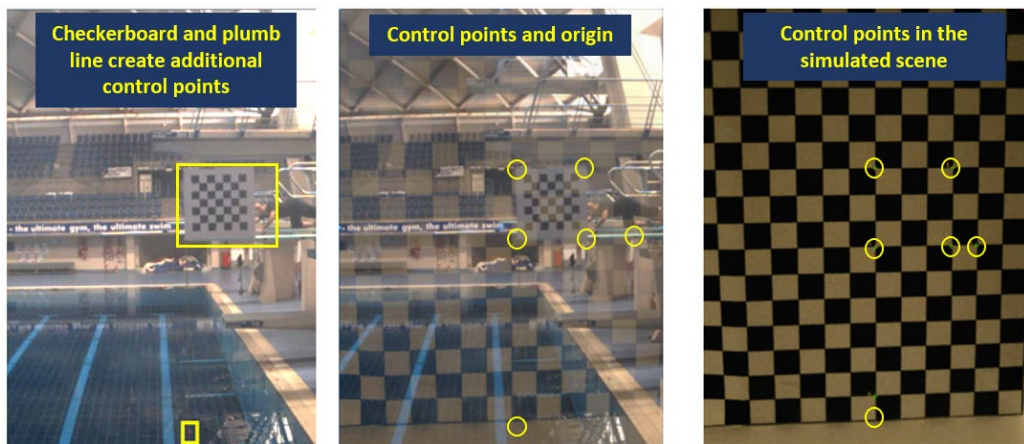


Figure 4-9. Control points for Trial 2, located using the diving board, checkerboard and plumb line to reach the lower edge of the view. Control points are now close to two edges (right and bottom) of the image.

## Trial 3

An additional control point was added towards the left edge of the view, utilising an extending pole to provide an additional known point level with the surface of the board (Figure 4-10). The lengths of the plumb-line and of the pole were known.

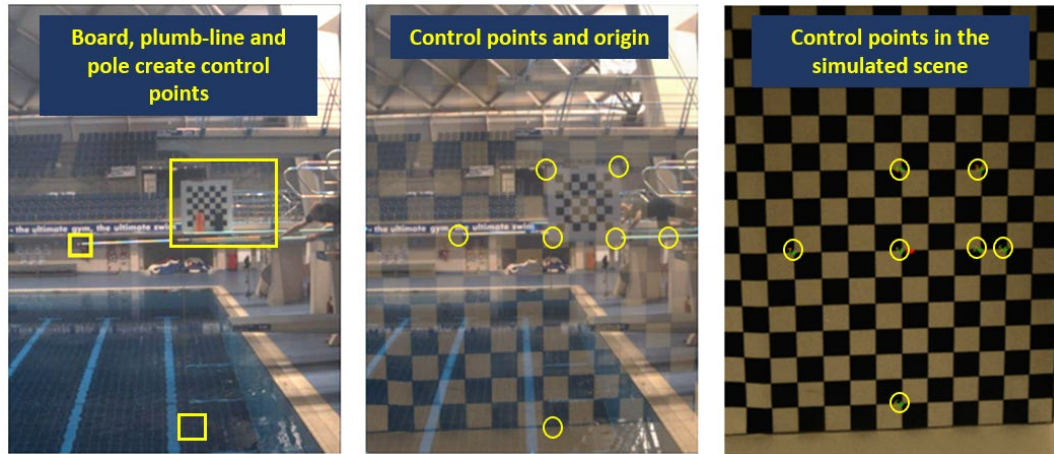


Figure 4-10. Control points for Trial 3, located using the diving board, checkerboard, plumb-line and extending pole. Control points are now close to three edges of the image: right, bottom and left.



#### 4.4.3 Results

Reconstruction error is shown graphically in Figure 4-11 and in Table 4-2 below.

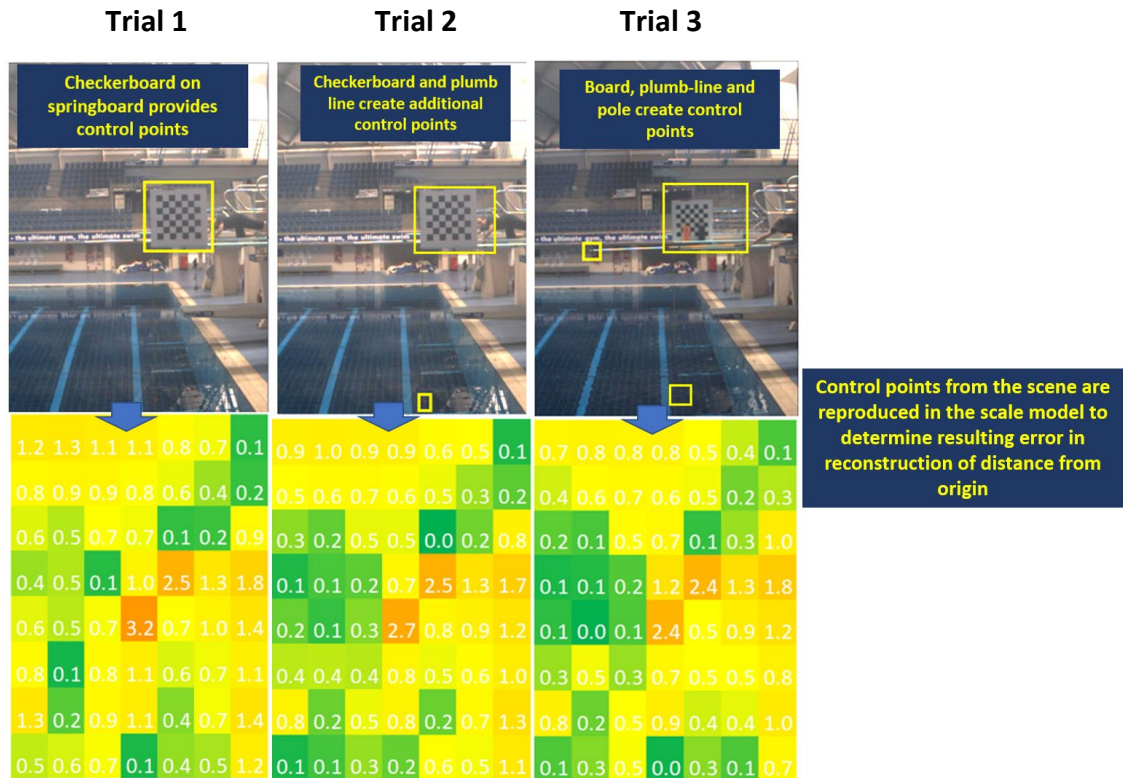


Figure 4-11. A representation of error when reconstructing points around the image in a scale-model of the scene. Figures in the heat-map are percentage-error of the distance of each point from the origin (the tip of the diving board). Areas in green represent the lowest reconstruction errors, areas in orange the highest.

Table 4-2. Point reconstruction error using extrinsic parameters calculated using different available control points.

Control points used	Error (% of measured distance from origin)	
	Range	Mean
Diving board, checkerboard	0.1-3.2	0.81
Diving board, checkerboard, plumbline	0.1-2.7	0.64
Diving board, checkerboard, plumbline, pole	0.0-2.4	0.58

These results confirm that reconstruction accuracy is improved when the number of control points is increased and the distribution of points around the image becomes greater, with maximum and mean error reducing when five control points are increased to seven and control point coverage extends to two more edges.

Using the checkerboard and springboard for control points creates low reconstruction error in the part of the dive where the hurdle begins and the first part of flight. Adding

the control point near the surface of the water reduces reconstruction error in the part of the image where the diver hits the water. This both improves the accuracy of results in the 'opening' to 'entry' phase of the dive (the last metre of flight) and also reduces reconstruction error in the part of the image (close to the centre) where take-off parameters are calculated. Adding the control point to the left-edge of the image reduces reconstruction error in the simulation still further across the image and particularly in the part of view where the diver drops from maximum height. Overall, the percentage error average is lower than 1% when seven control points are used.

It should be noted that, although the highest reconstruction error values occur close to the origin, the absolute error is small in this part of the image. Distances from the origin are small and so any error represents a larger percentage of the true distance than it would towards the edges of the view.

## **Discussion**

The diving pool provides a challenge in the search for an appropriate number of control points from which to calculate intrinsic parameters. The diving board is the sole physical object in the performance-plane and occupies an extremely small part of the scene. Using three props (checkerboard, plumb-line and extending pole) adds control points to the scene which – in a scale model simulation – show that average error in reconstructed distances is small across the image. These additional control points are available regardless of the training environment and the cost of the implements is small; they constitute a reasonable and practical solution to the restrictions in the scene.

The logical next step was to reproduce the experiment in a diving pool to establish reconstruction error in a live environment and assess the suitability of the method for the study.

#### 4.4.4 Implementing the extrinsic-parameter calibration method in the pool environment

##### **Introduction**

An investigation was carried out to measure reconstruction error in a live diving setting and compare results to those above in the simulated (checkerboard-based) view in earlier experiments.

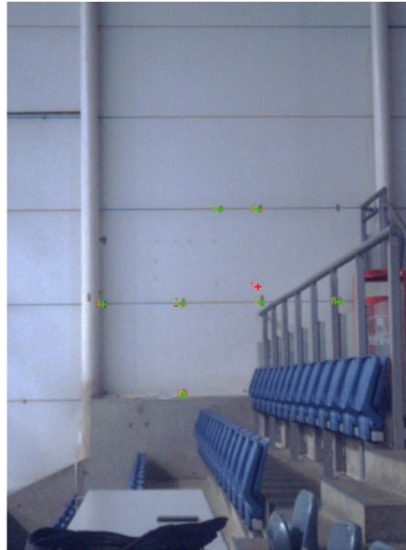
##### **Method**

A camera placed in position to view the diving board and flight path (Figure 4-12); intrinsic parameters were calculated as described in Section 3.3.



*Figure 4-12. The camera's view of the scene in the diving pool at Ponds Forge International Sports Centre, Sheffield.*

Although control points could be created in the scene as described above, the view was limited by the lack of points on the performance plane whose locations could be reconstructed to assess the accuracy of the camera model. Rotating the camera 90° to the right changed the view to a vertical wall (Figure 4-13).



*Figure 4-13. Rotating the camera changed the view from the pool (with no capacity for identifying varied points for reconstruction) to a flat wall on which landmarks could be measured, reconstructed and compared for accuracy.*

The distance of the wall from the camera closely matched the distance to the near springboard in the original view (approximately 9 metres).

Extrinsic parameters were calculated using 5, 6 and 7 control points (Figure 4-14, left) mirroring the process in the simulation and locating points reflecting the size and position of the checkerboard, plumb-line and extending pole (Figure 4-14, left). Landmarks were positioned on the wall and positions measured relative to the origin in the scene (Figure 4-14, right).

Some limitations were evident in the identification of landmarks; health and safety restrictions in the pool environment meant that for some of the higher landmarks, only y-coordinates could be established (height could be calculated based on the size of panels on the wall, but horizontal distance could not be measured due to access restrictions). These landmarks were still considered reasonable for use; consistent measurement of height across the view is important there was no practical solution that offered more points for assessment.

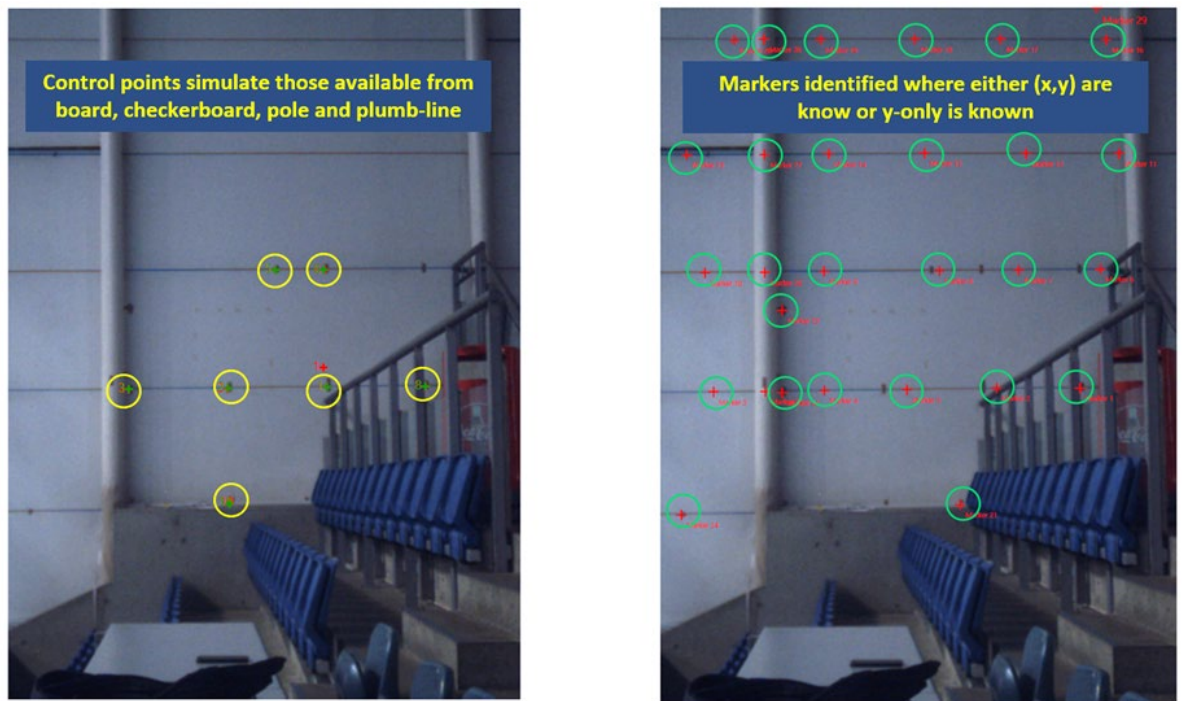


Figure 4-14. Control points used for extrinsic parameters (left); landmarks were identified for point reconstruction(right).

Landmark positions were reconstructed and assessed for accuracy compared to their actual positions. Landmarks were classified into two sets:

### Set 1

Points whose x and y coordinates were known. These points were found in the image where measurement of both coordinates was possible (satisfying safety requirements in the environment)

### Set 2

Points at the extremes of the view where the y-value (height above origin) was known (using the size of the panels on the wall) but x could not be calculated for safety reasons. These points were used to measure the reconstruction in y (reflecting height, the more important component of position in dive tracking) and because they were positioned in areas of the image where the effects of radial distortion would be greatest.

Marker positions were reconstructed and error (calculated as percentage difference in distance from the known and reconstructed position relative to the origin) was calculated for both sets.

## Results

The results of the investigation are shown in Table 4-3.

*Table 4-3. Reconstruction accuracy of landmarks in an unsimulated view.*

# Control points	Landmark set 1, %reconstruction error				Landmark set 2, % reconstruction error			
	Min	Mean	Max	SD	Min	Mean	Max	SD
5	0.5	1.3	2.5	0.8	0.2	1.5	2.5	0.8
6	0.3	1.1	2.3	0.8	0.1	1.3	2.3	0.7
7	0.4	1.1	2.4	0.7	0.2	1.3	2.3	0.8

As seen in the simulation, reconstruction error reduced with the increase in control points used to calculate extrinsic parameters. Landmarks in Set 1 had a mean reconstruction error of 1.1% when control points towards the edges of the image were used. Landmarks from Set 2 had a mean reconstruction error of 1.3%, reflecting their position towards the edge of the view where the effect of radial distortion is greatest.

Since there is not a linear decrease in reconstruction error in all variables as more control points are added, there is no indication that adding more would greatly improve the camera model.

These errors in this investigation are greater than those calculated in the scale-model simulation. Two considerations could contribute to this fact:

1. A pixel represents a greater physical distance in the live environment where the object plane is approximately 9 metres away, compared to the simulation where the object plane is under 0.5 metres from the camera. Any digitisation inaccuracy by the user would consequently have a greater effect on error.
2. The shape of the building (including staircases and seating) restricted the distance of the 'plumb-line' control point from the origin compared to where it would be positioned in the diving pool. This limits the improvement in

reconstruction accuracy that was shown in the simulation where the control point was closer to the edge of the image.

This reconstruction error relates to the accuracy of metrics calculated based on reconstructed positions in the image. A key metric will be vertical take-off velocity, calculated using Equation 4.1:

[4.1]

therefore 
$$u = \sqrt{2as}$$

where  $v$  = finishing velocity (0 at the top of the flight path),  $u$  = starting velocity (the metric to be determined),  $a$  = acceleration due to gravity and  $s$  = displacement of centre of mass (COM).

Using the equation above, COM displacement of 2000 mm implies a vertical take-off velocity of 6.26 metres per second. A 1.1% reconstruction error of COM-position at the top of the flight path (both over-estimate and under-estimate) implies take-off velocities as shown in Table 4-4.

*Table 4-4. The effect of reconstruction error on inferred vertical take-off velocity.  $u$  indicates take-off velocity in metres per second.*

Error (%)	COM displacement (mm)	$u$ (m/s)
-1.1	1980	6.23
0	2000	6.26
1.1	2020	6.29

These results indicate that calculated vertical take-off velocity can be considered to be accurate to within 0.03 metres per second. This actual level of reconstruction accuracy could be greater due to the following points:

- The reconstruction error likely falls between the  $\pm 1.1\%$  and so produces a smaller difference from the actual value
- Positioning the lower control point closer to the edge of the view improves reconstruction accuracy and, in the pool environment, can be placed closer to the edge of the view than in the simulation against the wall as shown above
- The reconstruction error shown close to the top of the image (where the body will be at the top of the flight path) was measured at 0.7% to 0.8%, not the 1.1% average over the image.

## **Discussion**

The investigation into the number and distribution of control points follows the same trend as with the scale-model investigation; more and more widely distributed control points improves reconstruction accuracy. Seven well-positioned control points gives low levels of reconstruction error in parts of the view in which the dive will be performed. Although more control points could be located using the props (for example the square intersections on the checkerboard, a mid-point along the extending pole), an acceptable level of accuracy can be achieved with a small number of points that are readily identified.

## [4.5 Assessment of the accuracy of angle calculation](#)

### **Introduction**

Measurement of angles is a key requirement of the calculation of some performance metrics, including depth of squat, proportion of leg extension before and after maximum deflection, tightness of tuck and pike shapes and opening height. There is therefore a requirement to assess the accuracy of angle measurement.

### **Method**

A camera calibration was performed on a scale-model of the diving environment as described in Section 4.3. A shape with a known size of interior angle ( $28.5^\circ$ ) was



positioned in many positions (n=28) across the view at a range of orientations, simulating a joint angle throughout a rotating dive (Figure 4-15).

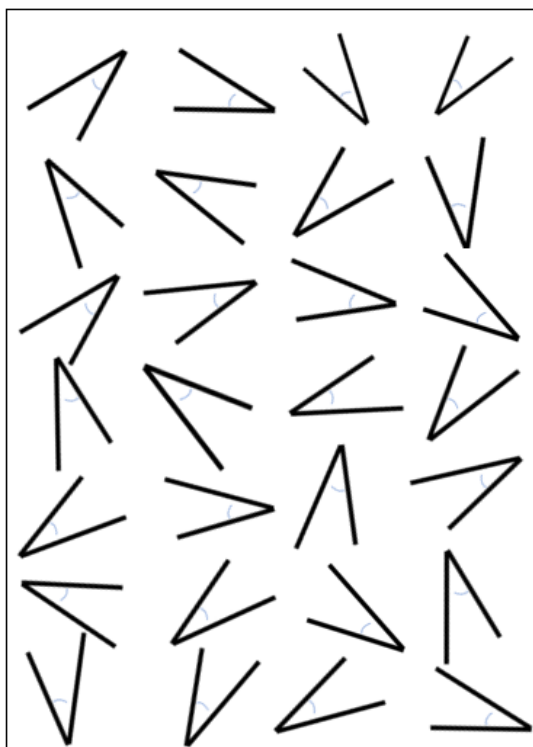


Figure 4-15. A simulation of the diving view with a shape placed in multiple positions and orientations to compare known and measured angles.

The vertices of the shape were digitised in each position and the interior angle calculated. Mean, standard deviation and maximum difference was calculated from the set of results.

## Results

Results are shown in in Table 4-5 and Figure 4-16.

Table 4-5 – Summary of angle calculation in 28 different positions and orientations

Measured angle (°)	28.5
Mean angle digitisations (°)	28.4
Standard deviation (°)	0.9
Maximum error (°)	1.7

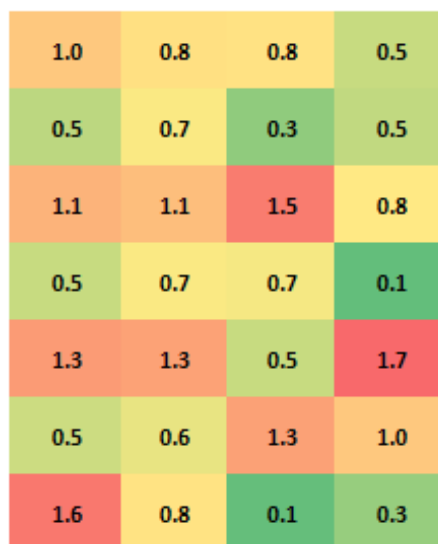


Figure 4-16. A heat-map distribution of error (measured in degrees) between known and calculated angles in different parts of the image

## Discussion

It can be seen that angles are measured with close level of accuracy in the simulation, with a mean angle within  $0.1^\circ$  of the measured value, and with standard deviation of less than  $1^\circ$ .

The heat map shows that the areas of highest error are distributed around the image with no large local collections of inaccurate values, implying that human error is as likely to cause inaccurate results as calibration error.

The coronavirus pandemic restricted access to the diving pool to repeat the experiment in a full-sized environment; repeating the experiment when access to indoor training facilities is allowed would be prudent to compare results found in a simulation with those in the real world.

## 4.6 Summary

It has been shown that extrinsic parameters calculated using many control points distributed over the whole view leads to reconstructions of greater accuracy than when a small number of points collected in one area of the image are used.

A diving pool presents significant challenge in the search for control points. The movement plane has one physical structure (the diving board) in it, and the diving

board provides no great variation in height of control points. Additional control points were required to effectively estimate  $R$  and  $T$  matrices and the points should extend to as many edges of the view as possible and should be able to be created by a single operator to maintain flexibility. Furthermore, the points should be able to be consistently located in any training or competition environment.

The use of three low-cost and portable props (checkerboard, plumb-line and extending pole) has been shown to provide control points which – along with the use of the near, top edge of the diving board – extend to three edges of the view and can be positioned and then digitised by a single operator. Although efforts could be made to define additional control points, a balance of practicality, flexibility and accuracy has been found.

The mean error in this method (1.1% error in reconstructed distance from the origin) implies an error of approximately 0.03 m/s when calculating take-off velocity from COM displacement in flight, compared to a 0.1 m/s level of sensitivity in existing studies. The mean error in angle calculation is smaller ( $0.1^\circ$  in a scale-model environment).

A planar calibration method has been shown to be suitable and fit for purpose; an implementation of the method has been described in Chapter 3 and that has overcome the challenges presented by the environment and has demonstrated that a camera model calculated in this way can be used to reconstruct coordinates in a movement plane with a known and acceptable level of accuracy.

## 5 Body segment model

### 5.1 Introduction

Section 2.8 described that a body-segment model (BSM) simplifies the human body into a small number of segments (Figure 5-1). A segment is defined by the location of its endpoints, its mass (as a proportion of total body mass) and the position of its local centre of mass (COM).

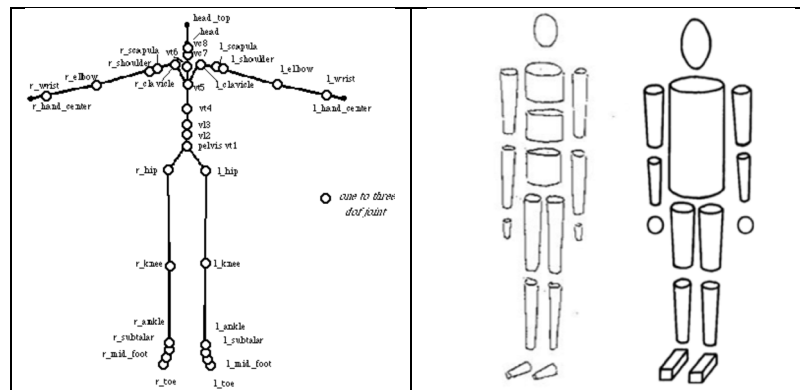


Figure 5-1. A body segment model (BSM) represents a human using an approximation based on linked, rigid rods (left) or linked geometric shapes (right).

Chapters 3 and 4 described a method to reconstruct world coordinates from screen coordinates. Reconstructing segment-end landmarks and measuring the change in position of each segment over time allows movement to be described and kinematic parameters to be calculated.

Section 2.8 concluded that a diver should be represented as a stick figure and that there was a need to have multiple models to reflect a variety of morphologies in an athlete-cohort. This aim of this chapter is to describe a method for representing the diver accordingly and will consider the need to attribute a specific BSM to a diver with the method for objectively evaluating the best model.

A method will be defined that will calculate the position of centre of mass (COM) from either manual digitisation or automated marker tracking on any frame of video, having identified the body segment model most appropriate to the diver.

## 5.2 Identification and adaptation of existing body-segment models

As discussed in Chapter 2, a single generic body segment model will not be able to represent the variation in divers' morphology. Divers in the British World Class Programme are diverse in race and show variation in age, height, mass and bodyfat percentage. These variations are reflected in World and Olympic medal-winning athletes and the use of a generic model would produce COM-positions of variable accuracy. A selection of models was selected for comparison and use; suitability of a model was based on its similar number of segments and the provision of segment COM-position in addition to segment mass. The models used in this study are listed in Table 5-1.

*Table 5-1. Body segment models implemented in the study.*

<b>Model ID</b>	<b>Model</b>	<b>Highlighted details</b>
1	Clauser (Clauser, 1969)	A standard model widely referenced in the literature.
2	Dempster (Dempster, 1955)	A standard model widely referenced in the literature.
3	Zatsiorsky (male) (Zatsiorsky, 2002)	A modification of the Clauser model created by a researcher in sports biomechanics and kinematics
4	Zatsiorsky (female) (Zatsiorsky, 2002)	A modification of the male model
5	Braune/Fischer (Siegel, 1985)	A modification of Clauser
6	Chen (Chen et al., 2011)(Chen et al., 2011)	A kinematic method
7	Cheng (C. Cheng et al., 2000)	A model derived from study of the Chinese population
8	Nikolova (Male) (Nikolova & Toshev, 2007)	Data generated from a geometric method
9	Nikolova (Female) (Nikolova & Toshev, 2007)	Data generated from a geometric method

Parameters for each body segment model were taken from an online repository on GitHub (Robertson, 2015).

### 5.2.1 Modifications to existing models – lower arm and lower leg

The diver is visible in profile on take-off (Figure 5-2) for all diving groups. Although asymmetric movement is shown in the steps and drive into the hurdle step, from the

top of the hurdle step, the diver is symmetrical and moves symmetrically about the longitudinal axis in all take-offs.

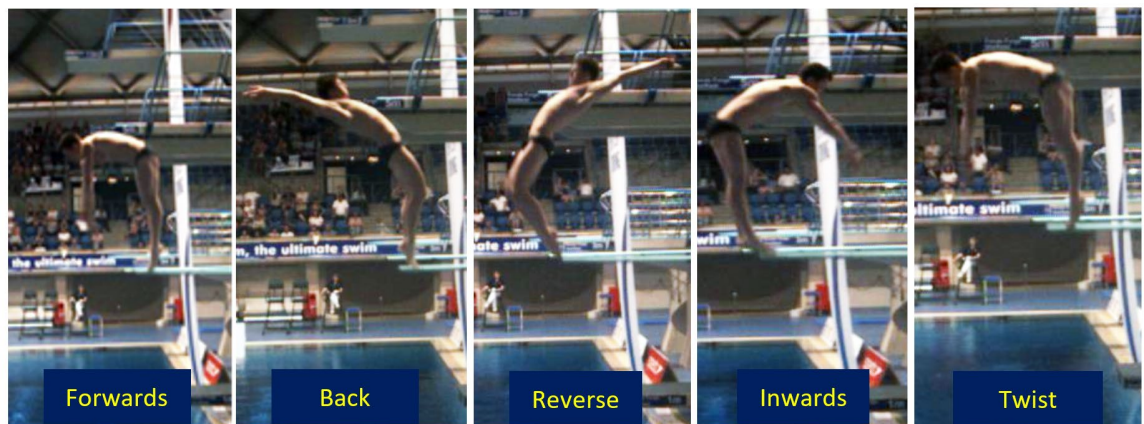


Figure 5-2. The diver's body is symmetrical and in profile on take-off in all diving groups.

This study considers the forearm and hand as one segment (with the mass equal to the sum of the segments) and lower leg and foot similarly. This is an appropriate simplification since:

- Fixing a reflective marker to fingers would limit their flexibility, compromise the ability to grasp the legs in shape and would result in an unnatural sensation for the diver
- The fingers are typically not visible when a diver makes a tuck or pike shape, as they are flexed and grabbing the leg, obscuring a marker for much of the flight time
- Reflective markers on the feet produced a sensation of discomfort to the divers during trials and impeded the feeling of the non-slip diving board surface. This compromised the diver's confidence to take-off as they would naturally

The effect of this assumption on the generation of performance data is mitigated by the diver's posture at take-off. During the last phase of take-off, ankles and wrists are extended (Figure 5-3) to maximise force-production and lever-length respectively.

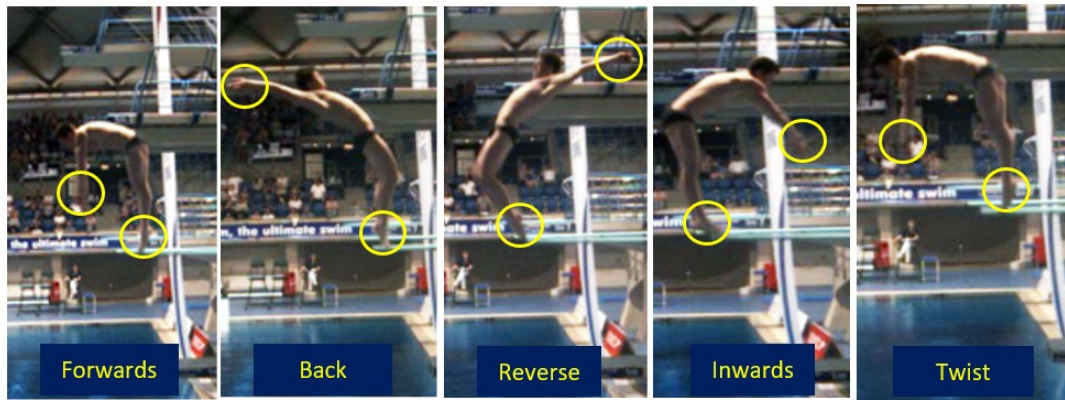


Figure 5-3. Wrists and ankles should be extended at the points of take-off.

FINA defines all shapes have pointed toes (Fina, 2010) to avoid a deduction, therefore the simplification reflects a consistent leg and foot posture throughout the dive. During the take-off, the diver aims to extend the arms to produce the longest possible lever for either creating rotation or to provide an aesthetically pleasing line. This implies that the wrist will be extended for the part of the dive (take-off and start of flight) where the change in the position of the body's COM will be used to infer much of the subsequent performance indicators (Table 4-1).

For times when ankles and wrists are not extended, an assumption is made that the small mass of hands and feet compared to the rest of the body makes a negligible difference to the location of the body's centre of mass.

### 5.3 Location of segment landmarks

When performing manual digitisation, users must identify and digitise the ends of each segment (joint centres). If markers are to be used to facilitate automated tracking, they are applied to specific parts of the body. Segment ends should be precisely defined to ensure consistency of digitisation and calculation of kinematic parameters. Table 5-2 defines the endpoints of each segment.

Table 5-2. Anatomical landmarks defined by Hinrichs (1990). \* indicates additional segments and landmarks defined by author.

Segment	Landmarks	Proximal end of segment	Distal end of segment
Foot*	Toe - ankle	Ankle joint centre	Big toe end
Lower leg	Ankle - knee	Knee joint centre	Ankle joint centre
Upper leg	Knee - hip	Hip joint centre	Knee joint centre
Trunk	Hip - neck	Chin-neck intersect	Hip joint centre
Head*	Neck - top-of-head	Top of head above ear	Chin-neck intersect
Upper arm	Shoulder - elbow	Shoulder joint centre	Elbow joint centre
Lower arm	Elbow - wrist	Elbow joint centre	Wrist joint centre
Hand*	Wrist - finger	Wrist joint centre	Middle finger end

Figure 5-4 shows the diver with these landmarks located and identified. An additional landmark (ribs – along the trunk-profile midline and level with the mid-point of the sternum) is also marked, for prediction of the location of the chin-neck intersect when that landmark is blocked by the arms. Should such a prediction be necessary, the chin-neck intersect is placed in line with the hip and rib landmark at a distance consistent with the ratios calculated when all markers are visible.

Landmarks are identifiable by visual inspection of the image; joint centres are easily identifiable when there is an angle in the joint and location is often indicated by a change in lighting with highlights or shadow occurring around the joint centre.

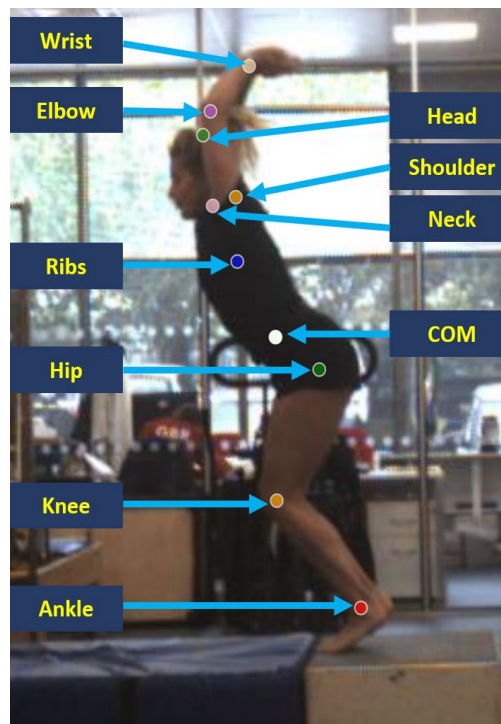


Figure 5-4. Landmarks on body digitised to calculate COM.



## 5.4 Calculation of centre of mass

Centre of mass is calculated using the mass of each segment (as a percentage of the whole body) and the position of the centre of mass between the defining segment-ends as in Equation 5.1:

$$COM_{(x)} = \sum_{i=1}^n M_i D_{i(x)}$$

$$COM_{(y)} = \sum_{i=1}^n M_i D_{i(y)}$$
[5.1]

where M = segment mass proportion, D = distance of segment COM from origin and n=number of segments.

### 5.4.1 Reduction of the body to stick-figure

An example of a six-segment model is shown in Table 5-3.

*Table 5-3. Clauser's distribution of mass and location of segment-COM.*

Segment number	Body segment	Mass (% of total)	COM location from proximal end of segment (%)
1	Lower leg (ankle & foot)	5.55	42.0
2	Upper leg	14.8	36.1
3	Trunk	42.6	37.8
4	Head and neck	6.7	58.9
5	Upper arm (from elbow to shoulder)	2.8	43.6
6	Lower arm and hand	2.2	44.0

Landmark positions reduce the image of the diver to a series of linked segments as shown in Figure 5-5.

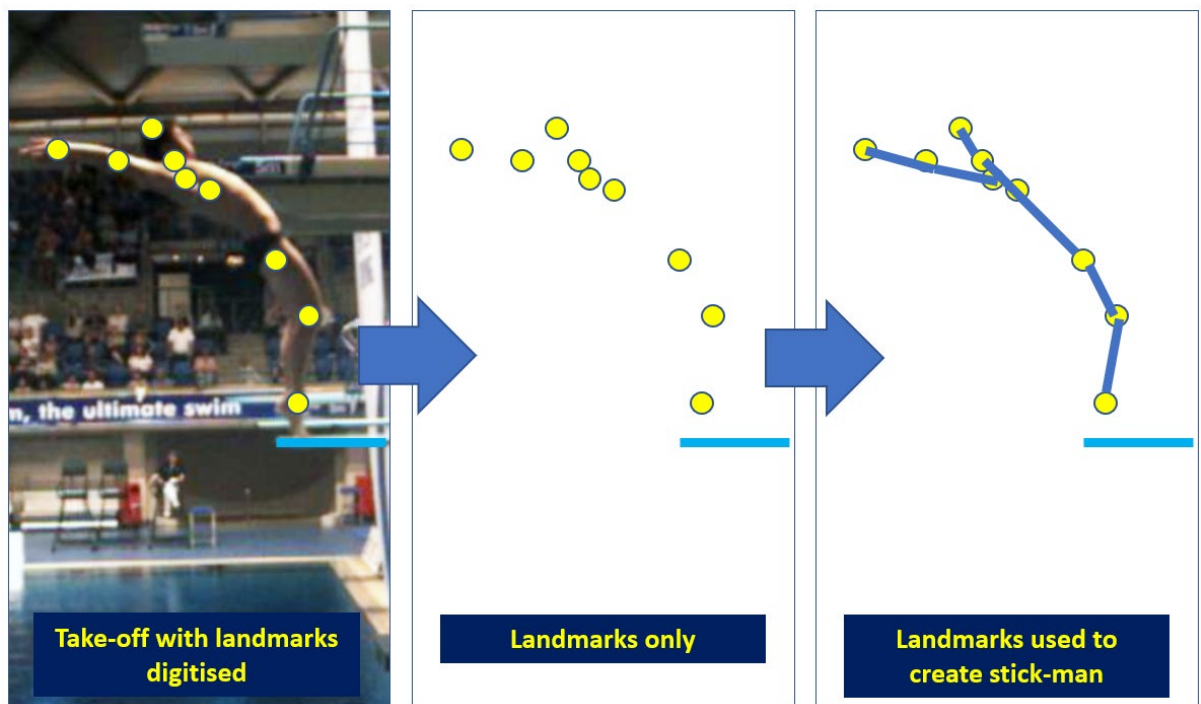


Figure 5-5. Diver's landmarks used to create stick-man model.

An example of segment data being used to calculate COM is shown in Figure 5-6.

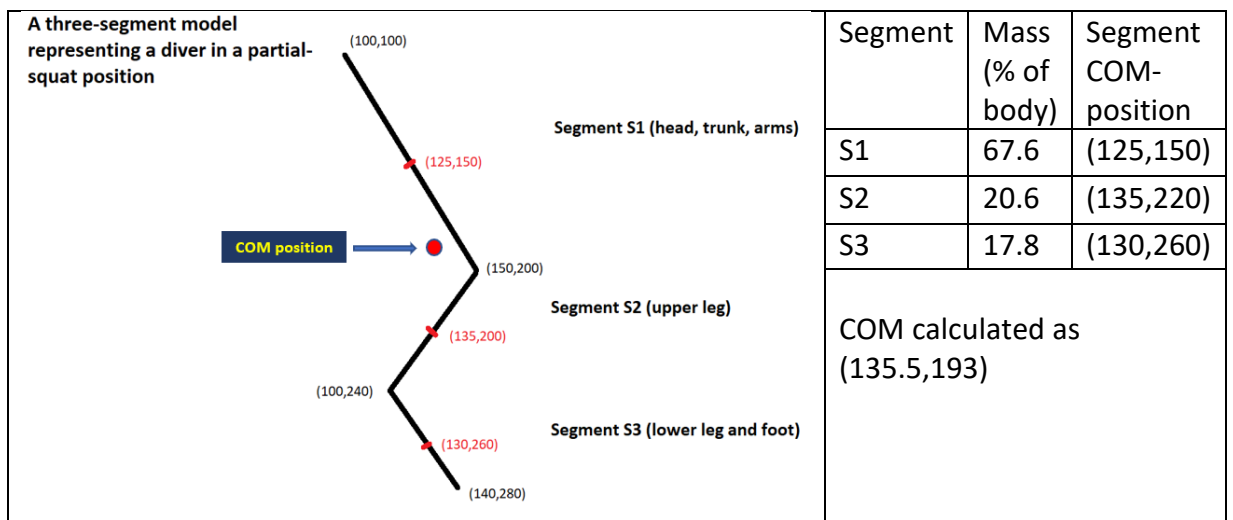


Figure 5-6. COM calculated using a Clauser model, modified to simplify the illustration. COM-positions (in red) have been re-located to the longitudinal mid-point of each segment.

#### 5.4.2 Consideration of hands and feet

The assumption of a single segment comprising lower-arm and hand, and a single segment representing lower-leg and foot, requires a calculation to locate the COM of

the single segment. An investigation of the divers used in the study concluded that the hand was a mean length of 68% of lower arm length, with the foot having a mean length of 44% of lower-leg length.

Assuming extended joints (locating segment-end landmarks on the same line), the COM of the single segment can be calculated. The new combined segment has a mass ( $m_c$ ) as a proportion of the whole body calculated using Equation 5.2:

$$m_c = (m_{s1} + m_{s2}) \quad [5.2]$$

where  $m_{s1}$  and  $m_{s2}$  are the mass proportions of the whole of each segment.

Having established the combined-segment mass proportion, the centre of mass location ( $COM_{cx}$ ,  $COM_{cy}$ ) of the combined segment ( $COM_c$ ) can be calculated using Equation 5.3:

$$COM_{cx} = (m_c m_1 COM_{1x}) + (m_c m_2 \left( 1 + \left( \frac{l_p}{COM_{2x} * 100} \right) \right)) \quad [5.3]$$

$$COM_{cy} = (m_c m_1 COM_{1y}) + (m_c m_2 \left( 1 + \left( \frac{l_p}{COM_{2y} * 100} \right) \right))$$

where  $m_1$  and  $m_2$  are the masses of the two segments (lower arm and hand or lower leg and foot),  $COM_1$  and  $COM_2$  are the position of the COM of each segment and  $l_p$  is the length of the shorter segment (hand or foot) as a percentage of the longer segment (lower arm or lower leg) length.

## 5.5 Variation in COM location and influence on performance data

### 5.5.1 Introduction

Each body segment model may position the COM in different locations (Figure 5-7).



Figure 5-7. COM location varies depending on the body segment model used.

It is necessary to understand the difference in COM location calculated using different body-segment models. A study was conducted to measure this variation on COM-position using a range of models in order to establish the need to pick a best model for different divers.

#### 5.5.2 Method

Dives by divers (both sexes, both springboard and platform and a range of ages) were manually digitised to implement a six-segment body-segment model as described above.

A series of frames around the point of take-off were digitised to calculate the location of COM (Figure 5-8) using three different three body segment models - Dempster (1955) and Zatsiorsky male and female models (Zatsiorsky, 2002). Three calculations were made:

1. Variation in COM-position at the point of take-off
2. Variation in take-off velocity, calculated from the rate of change of COM at take-off.

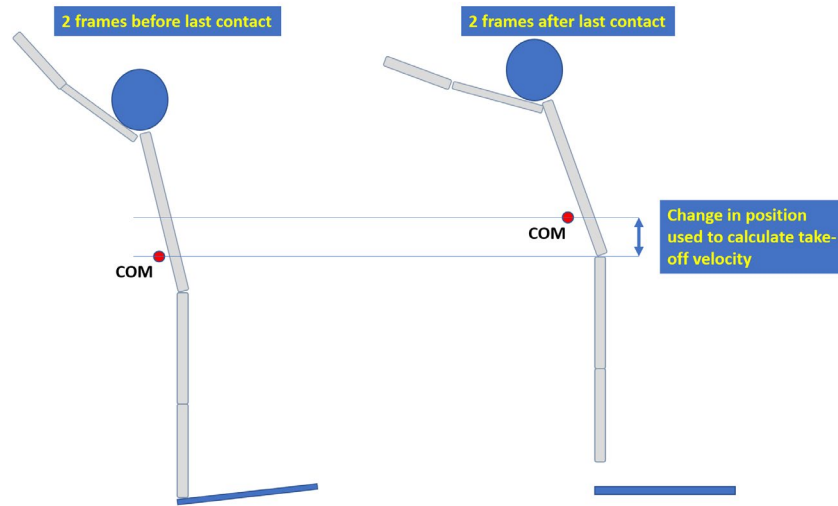


Figure 5-8. Dives were digitised to calculate COM-position using a six-segment BSM. The rate of change of COM during take-off was used to calculate take-off velocity.

3. Variation in COM displacement to the top of the flight path of the dive. Having calculated vertical take-off velocity (above), the COM displacement to the top of the flight path (where vertical velocity = 0, Figure 5-9) was calculated. Equation 5.4 was used

$$v^2 = u^2 + 2as \quad [5.4]$$

where  $u$  = starting velocity,  $a$  = acceleration due to gravity,  $s$  = displacement and  $v$  is finishing velocity.

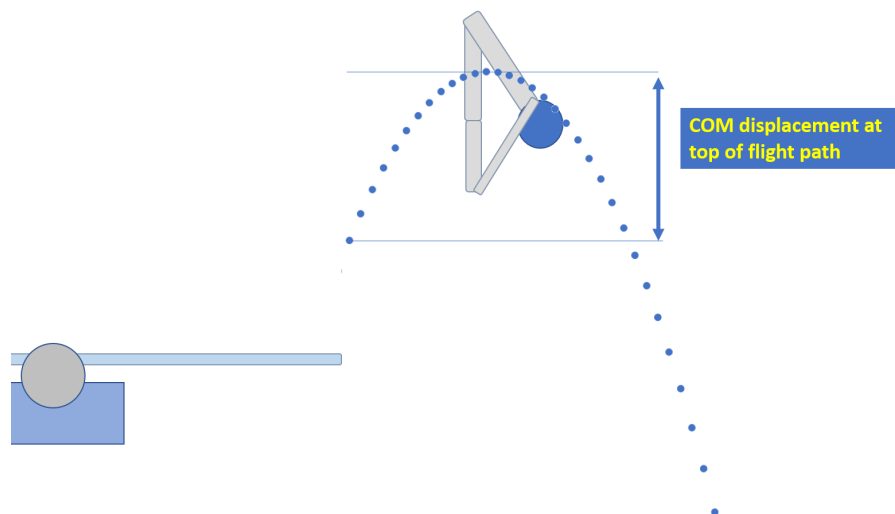


Figure 5-9. Take-off velocity was used to calculate COM displacement.

The results were analysed to test the hypothesis of a need for a specific BSM to represent different divers.

### 5.5.3 Results

#### Variation in COM location at the point of take-off

Variation in COM-locations, calculated using three BSM for each diver are shown in Table 5-4.

Table 5-4. Distribution of COM location for three divers at take-off, as calculated using three different body-segment models.

Diver	COM (mm)			SD % of mean	
	Mean	SD <sub>x</sub>	SD <sub>y</sub>	X	Y
1	322.8, 984.0	21.3	28.0	6.5	2.8
2	22.3, 960.7	12.0	45.7	53.0	4.7
3	-34.0, 880.0	19.7	38.8	57.9	4.4

Standard deviations in all coordinates were high, particularly when considered as a percentage of the mean - between 6.5% and 58% of the mean in x and between 2.8% and 4.7% of the mean in y. These variations imply that the flightpath by the COM for each model would be different.

#### Variation in take-off velocity

Take-off velocities for each diver, calculated using the change in COM during the 0.05 seconds at the point of take-off are shown in Table 5-5.

Table 5-5. Variation in take-off velocity, calculated by the rate of change in COM during take-off using three BSM for each diver.

Diver	Vertical take-off velocity (m/s)					
	Model 1	Model 2	Model 3	Mean	SD	Max difference from mean
1	2.16	2.21	2.06	2.14	0.06	0.08
2	5.04	4.89	4.96	4.96	0.06	0.08
3	4.43	4.55	4.51	4.50	0.05	0.07

Take-off velocities show a standard deviation of 0.05 to 0.06 metres per second. The maximum difference in take-off velocity from the mean are 0.07 and 0.08 metres per second. The low to high range of take-off velocities was between 0.15 and 0.18 metres per second. All values are greater than the variation implied from the investigation into reconstruction accuracy (Section 4.3) and indicate that a BSM selected specifically for the diver would improve the accuracy of performance data.

### Variation in COM displacement to the top of the flight path

COM displacement values for different divers and BSM are shown in Table 5-6.

*Table 5-6. COM displacement for three different BSM per diver.*

Diver	COM displacement (mm)					
	Model 1	Model 2	Model 3	Mean	SD	Max difference from mean
1	238	249	216	234	13.8	18
2	1296	1217	1256	1256	32.7	40
3	998	1054	1037	1029	23.4	31

COM displacement values reflected the range in take-off velocities discussed earlier. Standard deviations and maximum difference from mean values were high. The low to high range in COM displacement for each diver were between 18 mm and 79 mm. This range is too high to suggest that any one BSM can be used for all divers.

#### 5.5.4 Discussion

If one generic BSM was suitable for a range of divers, the variation in results when using different models would be small and calculated performance data would be consistent. The study has shown that this is not the case. Different models used to represent divers produce varying kinematic data; up to 6.4% difference is calculated in height achieved on springboard and 14% difference of the same measure on platform. The variation in performance metrics is much larger than the variation implied by potential point-reconstruction error and is therefore attributed to the characteristics

of the models. For this reason, it is concluded that most accurate kinematic data will be calculated using the most appropriate model for each diver and that the identification of such is a priority.

## 5.6 A study to assess the effect of intra-user error in manual digitisation

### 5.6.1 Introduction

COM-position is calculated based on the position of the COM of each segment. In turn, segment-COM is determined by the location of segment-ends. Any inaccuracy in the digitisation of segment-ends affects segment and whole-body COM-position. Depending on inaccurate digitisation and on the orientation and shape of the diver, any error causes the path of the COM during flight to not follow a parabola (the shape followed by the COM of a body moving under gravity) leading to inaccuracies calculating kinematic data where COM-position (or its change from frame to frame). Examples of kinematic variables dependent on accurate calculation of COM include displacement and velocity.

A study was conducted to assess the size of variation in COM location due to inconsistent digitisation, and the subsequent effect on the accuracy of inferred performance metrics.

### 5.6.2 Method

A frame of video, taken from the performance of a dive was selected (Figure 5-10) to be repeatedly digitised.





*Figure 5-10. One image was manually digitised multiple times.*

### **Study 1 - Variation in landmark locations**

The same user manually digitised the frame ten times. Manual digitisation of ankle, knee, hip, rib, neck, head, shoulder, elbow and wrist landmarks were performed on different days to minimise the effect of image-familiarity on the results. The mean and standard deviation of each marker position was calculated and assessed for consistency.

### **Study 2 - Variation in COM location with inconsistent single-landmark digitisation**

Having established mean and standard deviation for landmark positions in the image (above), a calculation was carried out to establish the effect of imprecise digitisation of any single landmark. COM location was calculated when any single landmark (excluding ribs, as this marker is unused for calculating COM-position in manual digitisations) was modified by changing  $x$  and  $y$  coordinates by  $\pm 2$  standard deviations and calculating COM for each combination. This resulted in 16 COM-positions when considering each landmark. Mean and standard deviation values were then calculated to assess variability.

### **Study 3 - Variation in COM location with inconsistent segment digitisation**

The same calculations for COM variation were made, but two landmarks – representing the ends of each segment - were adjusted by up to  $\pm 2$  standard deviations. Mean and standard deviations were found for the 625 COM locations calculated using this method.

Results were analysed to understand the effect of imprecise manual digitisation on the calculation of COM location.

Screen coordinates were used in all cases and results are presented with values in pixels. Chapter 3 identified that radial distortion away from the edges of the image was zero and therefore segment lengths would be unaffected by the use of  $(u,v)$  coordinates.

### 5.6.3 Results

#### Study 1 - Variation in landmark locations

Results are shown in Table 5-7.

*Table 5-7. Standard deviations of coordinates for body landmarks from ten digitisations of the same image. Values are in pixels (image resolution 488x656px). The mean SD value was 0.7, any SD greater than that is highlighted in red.*

Marker	Mean <sub>x</sub> (px)	SD <sub>x</sub> (px)	Mean <sub>y</sub> (px)	SD <sub>y</sub> (px)
Ankle	141.4	0.3	154.0	0.7
Knee	152.2	0.3	117.7	1.3
Hip	166.8	0.5	58.6	0.8
Ribs	127.0	0.8	82.3	1.1
Neck	126.2	0.7	96.2	0.7
Head	110.1	0.8	117.0	0.7
Shoulder	119.9	0.7	94.4	0.9
Elbow	144.5	0.6	117.2	0.7
Wrist	164.1	0.4	112.5	0.4

Wrist, elbow, neck and ankle landmarks were located and digitised with sub-pixel variation. Ribs were digitised with the greatest variation in both axes but is not used in the calculation of COM (the Ribs landmark exists to predict a neck landmark when reflective markers are used for automated tracking and the arms obstruct the neck marker). The top of the head had variation in digitised-location, possibly due to the line of the head being obstructed by hair. The joint centre of the knee was hard to locate when the legs were straight, and the arms covered the knees.

### Variation in COM location with single-landmark digitisation variation

Results are shown in Table 5-8.

Table 5-8. The effect on COM-position as a result of imprecisely digitising one landmark. Values are in pixels (image resolution 488x656px), outlier values are highlighted in red.

Landmarks adjusted	COM <sub>x</sub>	COM <sub>y</sub>	SD <sub>x</sub>	SD <sub>y</sub>
None	144.7	92.1		
Ankle	144.5	92.0	0.1	.04
Knee	144.2	91.7	0.2	0.2
Hip	143.1	91.4	0.8	0.3
Neck	142.2	91.6	1.1	0.3
Head	144.3	92.0	0.2	0.0
Shoulder	144.5	92.0	0.1	0.0
Elbow	144.4	92.0	0.2	0.1
Wrist	144.6	92.0	0.0	0.0

Inconsistently identifying a single landmark has a very small (sub-pixel) effect on COM coordinates except in the case of either marker defining the trunk segment (hip or neck). This is due to the trunk being the longest and most massive single segment. The risk of variation is relatively small, however, as the standard deviation of neck landmark position (Table 5-7) was small at 0.7 pixels in both axes and low in one axis for hip (the midline of the upper-leg is consistently identified with small variation in position from the proximal end of the femur).

### Variation in COM location with inconsistent segment digitisation

Results are shown in Table 5-9.

Table 5-9. The effect on COM-position resulting from imprecisely digitising both ends of a segment. Values are in pixels (image resolution 488x656px); outlier values are highlighted in red.

+2SD adjustment in	COM <sub>x</sub>	COM <sub>y</sub>	SD <sub>x</sub>	SD <sub>y</sub>
None	144.7	92.1		
Lower leg	140.9	90.1	1.6	0.8
Upper leg	104.0	78.8	18.7	6.0
Trunk	102.0	78.7	18.8	0.6
Head	134.4	90.2	3.8	0.7
Upper arm	139.0	90.8	2.1	0.5
Lower arm	142.6	91.6	0.8	0.2

There is significant variation in COM location when either the upper-leg or trunk is inaccurately digitised. These are the two longest segments and the segments with greatest mass and so there is an importance on accurate digitisation of knee, hip and neck. The results above show that the neck is consistently digitised but there is some inconsistency with knee (when it is straight and covered) and hip accuracy. This finding highlights the need for clear understanding of the positions of each landmark and the use of changes in light and shade on the skin where landmarks are located.

#### 5.6.4 Discussion

That some landmarks are easier to consistently locate is understandable; prominent shadow helps identify the ankle joint centre, the wrist joint centre is clearly visible where it bends to allow the hands to grasp the legs in shape or is marked by tape if the diver uses it for support. The elbow is often shaded along the midline and the joint centre is clear where the arm bends. The knee-joint centre is similarly easy to locate if there is an angle in the leg and has shadow to help identification if the joint isn't occluded (as in Figure 5-10). Conversely, the hip-joint centre has no shadow, tape or (in the case of female divers) swimsuit-line to guide the user. Hair impedes clear and consistent view of the top of the head and hair colour can be hard to distinguish from

the colour of the background. In a fast-spinning dive, image-blur increases difficulty of consistent landmark-location.

While accurate digitisation of light segments (lower leg, arms) has little effect on the consistency of COM calculation, it is clearly important that knee, hip and neck are consistently identified. While location of the greater trochanter (hip landmark) requires training on behalf of the user, knee and neck are consistently digitised. While reflective markers facilitating automated tracking are easy to attach to knee, hip and neck (creating greater consistency with the automated process), consistency in digitisation of the hip marker can be increased with a combination of clear anatomical guidance, repeated palpation and examples of accurate digitisation.

## 5.7 A method to determine the most appropriate body-segment model for a diver and dive.

### 5.7.1 Introduction

Three methods are identified which will determine the best model to represent a diver:

#### 1. Inference of take-off velocity from flight time

Miller (2013) established that if the height of the diver's COM at the point of take-off is similar to the height of the COM above the water at the point of entry (Figure 5-11), take-off velocity can be estimated within 0.1 m/s compared to that calculated by measuring the translation of COM at take-off.

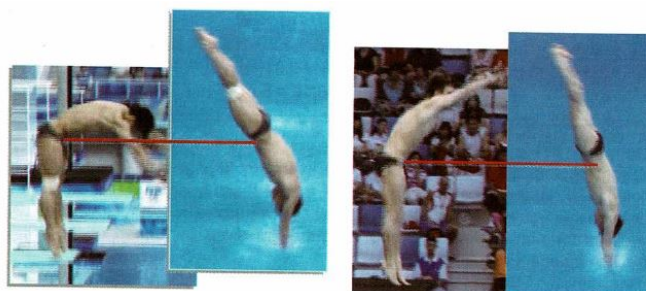


Figure 5-11. Miller (2013) asserts that an assumption of similar displacement of the COM above the board at take-off and the water at entry allows the inference of take-off velocity to a known level of accuracy if flight time is known. Reproduced from 1<sup>st</sup> Symposium for Researchers in Diving (2013).

An object taking off with a known velocity will behave under gravity in a predictable fashion. By using Equation 5.5:

$$s = ut + \frac{1}{2}at^2 \quad [5.5]$$

where  $s$  represents vertical displacement,  $u$ ,  $a$  and  $t$  represent initial vertical velocity, acceleration due to gravity and time of flight respectively, the motion of the object's COM can be predicted, assuming negligible air resistance (Figure 5-12).

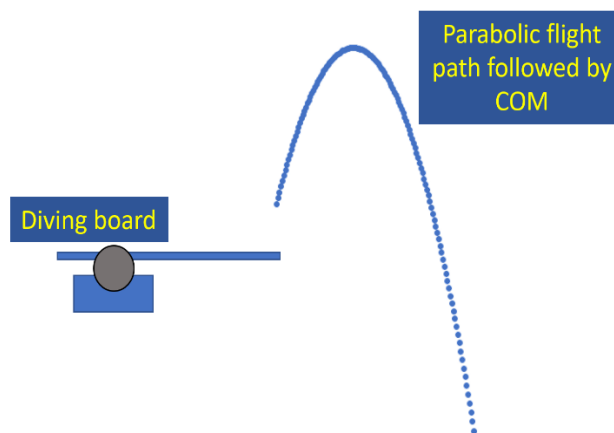


Figure 5-12. The diver's COM follows a parabola whose height depends on initial vertical velocity.

The body-segment model whose take-off velocity matches that inferred from flight time can be identified as the most appropriate for that diver. The reliability of this method is lessened when the entry angle of the diver shortens the distance from COM to water-surface (Figure 5-13).



Figure 5-13. A very short or over entry makes Miller's method unsuitable due to the mismatch of COM distance from board at take-off and water at entry. Images from www.phoenixsc.co.uk and ok.co.uk.

## 2. Comparison of COM-displacement values

Displacement can be determined in two ways. The difference in COM-position between the point of take-off and the top of the flight path is one method. Another is to infer displacement by calculating take-off vertical velocity (by rate of change of COM) and using equations of motion to calculate subsequent movement of the COM (Figure 5-14).

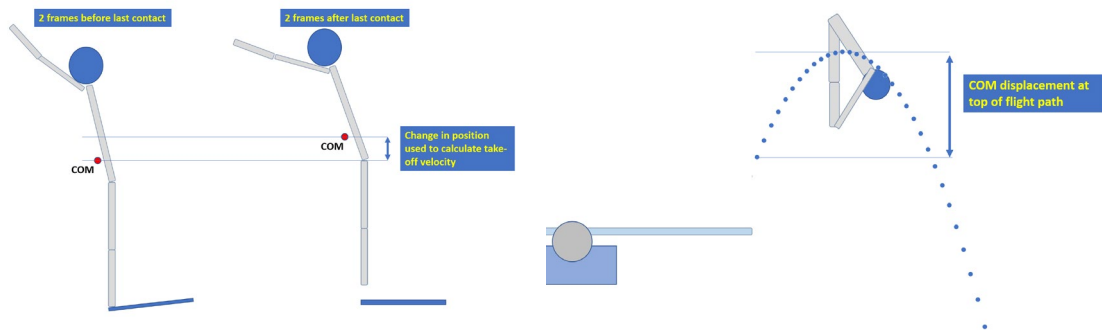


Figure 5-14. Vertical take-off velocity (left) can be used to calculate COM displacement at the top of the flight path. Discrepancy between predicted and observed displacement (right) implies an inaccurate BSM.

An accurate body-segment model will result in similarity in both displacement values. An unsuitable model, however, may appear to be a good fit due to errors contributing to 1) estimation of COM height at take-off, 2) vertical take-off velocity based on rate of change of COM and 3) the calculated position of the COM at the top of the flight path.

In order to mitigate the risk of these simultaneous errors implying a good fit for a BSM, take-off velocity was calculated for all models and an average value used to calculate COM displacement in flight.

This approach is most effective when there is a low variance in take-off velocities across the range of body-segment models. This case is more likely when dives with less rotation (and consequently smaller change in segment position through take-off) are performed.

### **3. Comparison of COM locations during flight to a parabola**

As shown in Figure 5-12 and Figure 5-14, a diver's COM during flight follows a parabola, consistent with any object's projectile motion under the action of gravity. Inaccuracy of body-segment model causes the COM locations during flight to deviate from a parabola. A second order polynomial curve can be fitted to the reconstructed (x,y) points of the COM during flight for each model and root-mean-squared error (RMSE) of the reconstructed points can be calculated for each model. A smaller RMSE indicates COM points closer to a parabola and therefore a better model.

This method is most effective when a greater number of COM points are reconstructed, reflecting the diver in a range of positions and along the flight path and a range of angles of rotation.

#### **Prioritisation of methods**

A model producing a flight path closest to that of a parabola is the method with greatest priority; this is the only method which considers reconstruction in x as well as y and reflects the model's closeness to the COM flight path throughout the dive. COM displacement is the method with next greatest priority as the comparison of one model to the average of all is not influenced by the difference of position of the body on take-off (as with the 'velocity inferred from flight-time' method). Assessing a model's accuracy based on inferred take-off velocity from flight time is the weakest method as there are a small number of combinations of postures possible at take-off and entry with equal COM-displacement from board and water.

#### 5.7.2 Selection of skills to calculate the best body-segment model

A determination must be made regarding the choice of dive used to identify the best model. The most simple skill that can be performed, a straight jump (100a), with COM traces for each body-segment model is shown in Figure 5-15.





Figure 5-15. COM traces for all body-segment models for 100a.

The shape of each trace is similar; no flight paths exclude themselves as obvious outliers compared to the shape of a parabola. RMSE values for each model are shown in Table 5-10.

Table 5-10. RMSE values for reconstructed COM-positions during a forward jump straight (100a) to a best-fit second order polynomial curve for each model. A lower RMSE indicates a better fit.

ID	Model	RMSE (mm)
1	Clouser	33.7
2	Dempster	32.6
3	Zatsiorsky (male)	32.0
4	Zatsiorsky (female)	42.4
5	Braune/Fischer	29.8
6	Chen	31.6
7	Cheng	34.0
8	Nikolova (male)	32.5
9	Nikolova (female)	31.2
Mean		33.5
SD		3.3

The range of RMSE values is small (a standard deviation of 3.3 mm); the difference between models based on this calculation is not enough to select a best model with confidence. By comparison, traces for a high-DD dive - forward three and a half somersaults (107c) are shown in Figure 5-16.

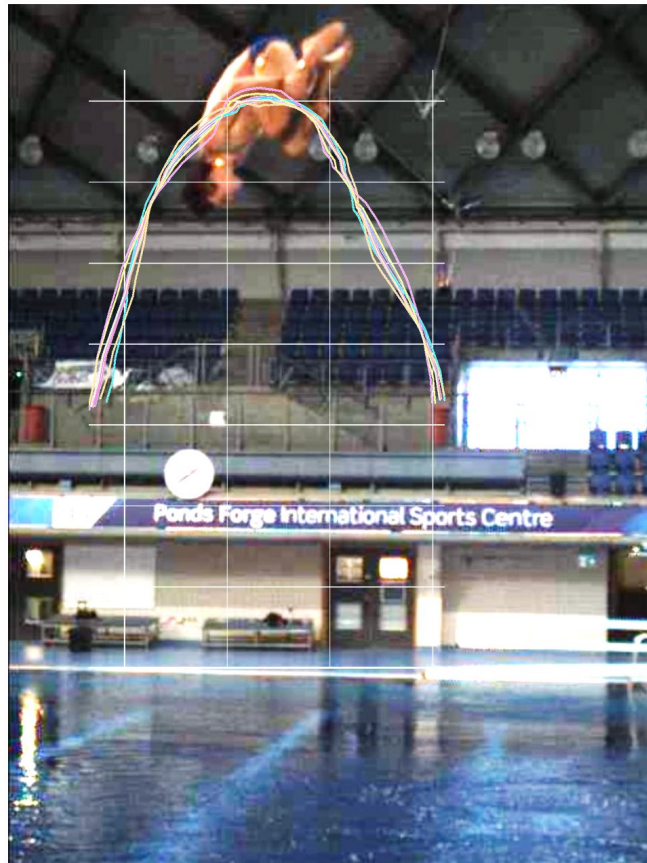


Figure 5-16. COM traces for 107c.

Traces in the jump (100a) had similar shape with varying displacement. In a dive with three and a half somersaults of rotation, the traces are not all similarly shaped and intersect with each other. RMSE values for each model are shown in Table 5-11.

Table 5-11. RMSE values for reconstructed COM-positions during the flight in a forward three and a half somersaults (107c) to a best-fit second order polynomial curve for each model. A lower RMSE indicates a better fit.

ID	Model	RMSE (mm)
1	Clouser	66.8
2	Dempster	60.6
3	Zatsiorsky (male)	67.0
4	Zatsiorsky (female)	112.9
5	Braune/Fischer	63.7
6	Chen	45.1
7	Cheng	110.7
8	Nikolova (male)	72.6
9	Nikolova (female)	61
Mean		72.8
SD		20.9

The variation in RMSE values is much greater than for the simple skill, with a standard deviation approximately six times greater.

The difference in RMSE between skills is explained by:

- The take-off position for a high-DD dive includes an angle at the hips and an angle at the shoulders (required to create rotation). This means that there will be more lateral change in COM-position compared to a jump, where all segments remain as close to vertical (with an unchanging position) as possible.
- A jump has no rotation, the COM is calculated from a similar body-position in all frames. A high-DD dive has shape change (from an open posture to a tight tuck shape) and COM-positions calculated with the body at all orientations.

For these reasons, dives with maximum shape-change and with frames covering multiple rotational positions are preferable skills from which to identify the best model for a diver. A range of dives, covering different directions of take-off and rotation gives a more complete dataset from which to make an assessment.

### 5.7.3 Method

Multiple repetitions of each dive (examples shown in Figure 5-17 ) were digitised for each diver and calculation of the best-model was made for each.

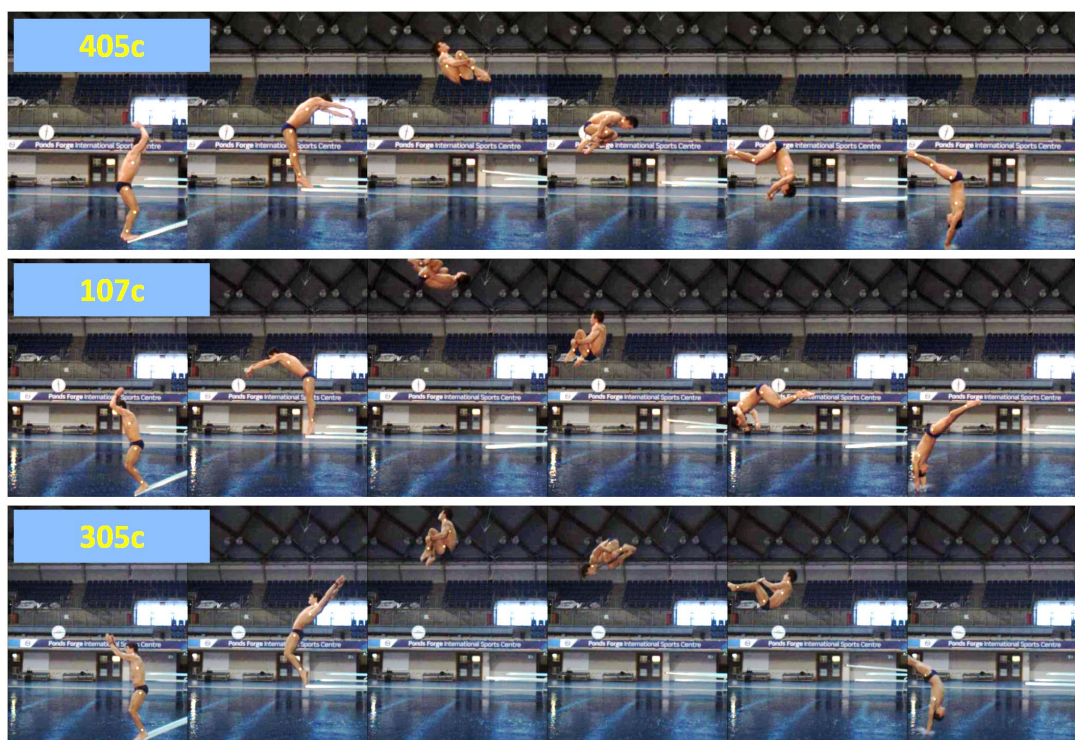


Figure 5-17. Examples of Inward  $2\frac{1}{2}$  somersaults with tuck (405c), Forward  $3\frac{1}{2}$  somersaults with tuck (107c) and reverse  $2\frac{1}{2}$  somersaults with tuck (305c), performed by diver RH, were digitised – best model calculations were conducted for each.

Each model returned a series of calculations used for comparison to determine the best body segment model. ‘Best’ is defined as follows:

#### **Best model by flight time**

The model which has the smallest difference in calculated take-off velocity between values calculated by flight time and COM-position change at take-off.

#### **Best model by COM displacement**

The model which has the smallest difference in calculated take-off velocity between values calculated from maximum COM displacement and from COM change at take-off.

#### **Best model by RMSE**

The model whose flight path is closest (by a calculation of RMSE) compared to a second-order polynomial representing a parabola fitted to that flight path.

In the example shown in Figure 5-18, flight time calculated using take-off velocity from COM change was 0.08 m/s different to that inferred from flight time (calculated using

the number of frames difference between last-contact and entry). The maximum displacement difference between the measured highest COM-position and the average of all models was 2.1 mm and the root mean squared error between the reconstructed COM-positions and a best-fit parabola was 44.9 mm.

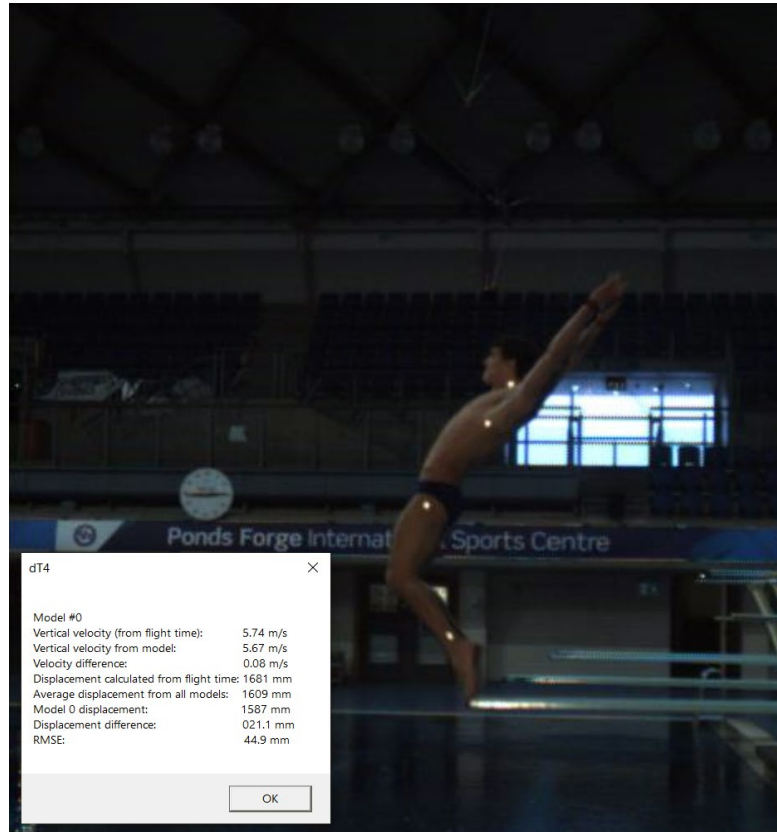


Figure 5-18. Calculations for each model were made for comparison and identification of the best.

#### 5.7.4 Results

For Diver 1, best-model calculations for each method are shown in Table 5-12.

Table 5-12. 'Best' models for each example of each dive, calculated using all methods.

Dive	Best model by flight time	Best model by COM displacement	Best model by RMSE
405c	6	9	6
405c	6	9	6
107c	5	9	1
107c	9	9	6
107c	9	9	6
305c	6	9	1
305c	6	9	1
305c	6	9	9

Model 6 is calculated as best the highest number (4) of times by lowest RMSE, although Model 1 is only rated highest one-time fewer (3). Model 9 is the model most rated over all calculations as the best. Choosing the best model from these results requires additional information. A subjective assessment of the models can be made by observation of the shape of the COM trace for each (Figure 5-19).

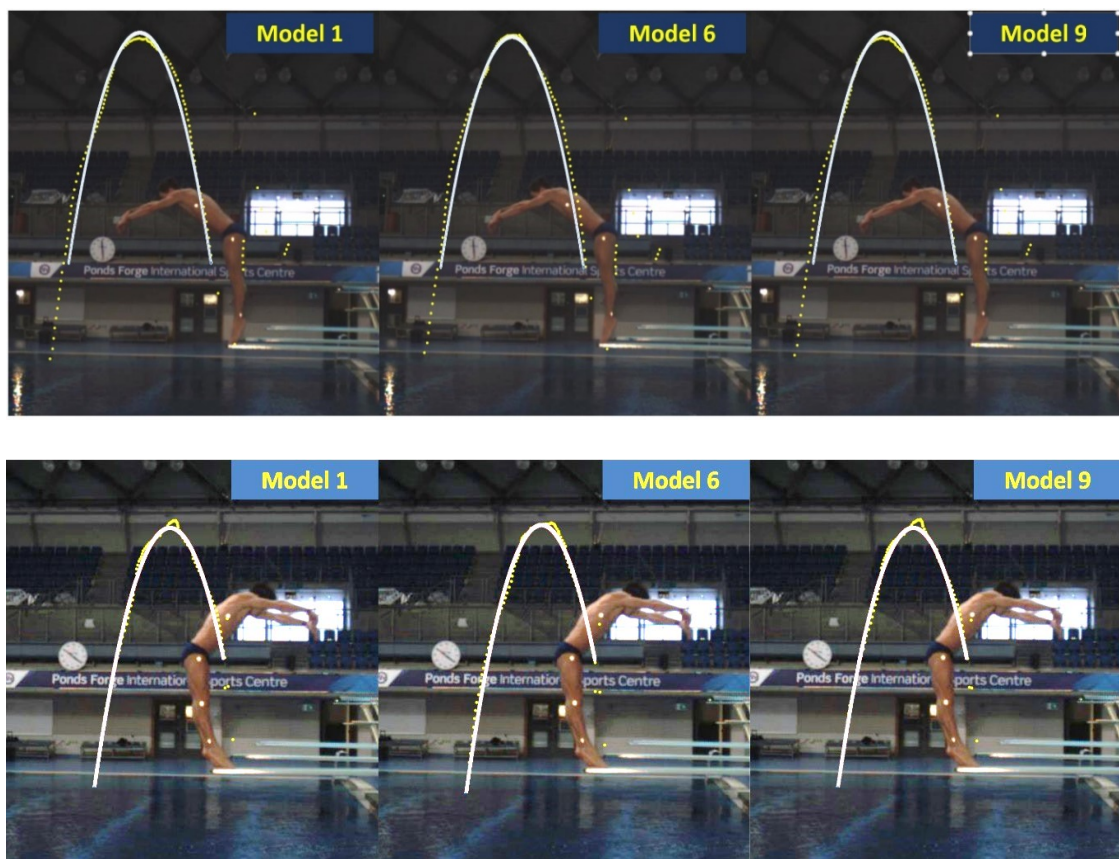


Figure 5-19. COM traces (shown in yellow dots) for 107c (top) and 405c (bottom). The best-fit parabola for each dive is shown in white.

In both cases, model 6 (Chen) is the curve which most closely matches the shape of the best-fit parabola throughout flight. In both dives, the peak of the reconstructed flight path more closely matches the best-fit curve. This subjective assessment is also appropriate if values of error are close for multiple models.

A combination of objective and subjective assessment shows that the Cheng model is most appropriate for Diver 1 and should be used for all dives by that diver.

#### 5.7.5 Measurement of error

##### **Introduction**

Having determined the best model using the RMSE model, error can be calculated by comparing the maximum height measures of both the best-fit parabola and the position of the COM at the same point.

##### **Method**

As described earlier, dives with a high number of rotations (minimum 1.5 somersaults for the female diver, minimum 2 somersaults for male divers) were used, with 124 dives satisfying these criteria. The greatest COM height and the highest point of the parabola best fitting the COM-positions through the flight of the dive were compared for each dive.

##### **Results**

Results are shown in Table 5-13.

*Table 5-13. The difference in maximum COM height calculated as the difference between the highest reported value in the divers' flight path and the peak of the best-fit parabola fitting the COM points across the flight path.*

<b>Group of skills</b>	<b>Total difference in COM height (mm)</b>	<b># Dives</b>	<b>Mean (mm)</b>
Hurdle take-off	1854	90	20.6
Standing take-off	833	34	24.5
All	2687	124	21.7

There is a smaller average difference in take-offs with hurdle step than those standing, with an average difference of 21.7 mm.

Average COM displacement on hurdle take-offs was 1606 mm and on back take-offs was 931 mm (calculated as the difference between COM height at take-of and the maximum height of the best-fit curve). Average displacement for take-offs with hurdle step was 1606mm and for backward standing take-offs was 931 mm. Average take-off velocity for take-offs with hurdle was 5.61 m/s and for standing backward take-offs was 4.27 m/s, both values calculated using Equation 5.4.

Take-off velocity can be calculated assuming a mean error of 20.6 mm COM displacement on take-offs with hurdle step and 24.5 mm, with results shown in Table 5-14.

*Table 5-14. The effect of flight-path and maximum height error on calculated take-off velocity.*

<b>Take-off</b>	<b>Mean COM displacement (mm)</b>	<b>Take-off velocity (m/s)</b>	<b>COM displacement including error (mm)</b>	<b>Take-off velocity including error (m/s)</b>	<b>Difference (m/s)</b>
Hurdle	1606.0	5.61	1626.6	5.64	0.03
Standing	931.0	4.27	955.5	4.33	0.06

These results show that the error in COM positioning, based on selecting the best BSM according to the process described earlier is 0.03 m/s and 0.06 m/s in hurdle and standing take-offs, respectively.

#### 5.7.6 Discussion

Different body-segment models will be identified as ‘best’ for each diver, depending on the dive performed and the method selected to determine the optimum model. It is



therefore necessary to choose dives with care and consider multiple repetitions of skills to determine the model that best represents the diver.

If the model selected as 'best' is used for all dives performed by the diver (even when it would not be rated as best when assessing that skill) then there will be consistent feedback which will reflect change in performance.

The calculation of the best-fit curve negates the need for a smoothing function on the marker-data and will be used to calculate performance data (take-off velocity, maximum height, horizontal displacement) supplementing data derived from point-reconstruction (including hurdle-length, joint angles, maximum springboard deflection, speed of rotation).

## 5.8 Summary

Section 2.7 concluded that a stick-figure should be used to represent a diver's body and that it was likely that one body-segment model (BSM) would not accurately represent a range of divers.

A method has been described which represents a diver as a stick figure and has shown how a BSM can attribute mass and COM-position to each segment for the calculation of COM for the whole body.

The position of each landmark has been defined and it has been shown that accurate COM calculation is most affected by lack of precision when locating segment-ends for upper-leg and trunk.

A range of BSM have been described, each reflecting a different age, sex or race of population, with some models being enhancements of older examples. As divers in Great Britain's World Class Programme (and around the world) are of different age, sex, state of physical maturation and body-composition, it follows that divers would be best-matched to different models. A method has been described that matches a diver to a model from the literature, combining an objective approach (considering RMSE, comparability of metrics) with a subjective assessment of the closeness of the COM path to a parabola for each dive and BSM. A 'best' model representing a diver is

required to calculate kinematic data with greatest accuracy, therefore reflecting changes in performance with most reliability.

As more athletes are matched to a 'best' BSM, some models will likely prove to be most frequently representative of 'best' for diving. Assuming there are a small number of models representing the cohort of divers who win World and Olympic medals, there is potential for adding an additional metric when identifying talent in new athletes – whether their morphology matches that of the best divers in the world. Adding formal identification of an ideal body-type, in addition to an 'expert-eye' assessment from selectors may better-match athletes to each discipline (springboard, platform, an ideal synchro partner) and enhance the development of that diver.

In summary, to identify the best BSM to represent a diver, the following process should be followed:

- Use the tool to determine the 'best' model using all methods of evaluation
- If different models are reported as 'best' a similar number of times, or multiple models have similar levels of error (between take-off velocity measures or RMSE compared to a best-fit parabola), the user should subjectively examine the COM-trace for each potential model and choose the model which shows the flight path closest to a parabola at key points in the dive (around take-off and the point of maximum height)

Errors:

- Mean error in take-off velocity of 0.03 m/s from the camera calibration process
- Mean error of 0.03 m/s and 0.06 m/s in hurdle step and standing take-offs, respectively.

## 6 Markers

### 6.1 Introduction

The previous chapter described the need for segment-ends to be identified in order that a body-segment model can be implemented to locate the diver's COM at any point in the skill. Manual digitisation of images is a method for locating these landmarks but comes with a cost of time and intra-user variation in the identified position of each landmark.

A method which mitigates these constraints is to use markers; tape fixed to the diver both consistently locates landmarks at (or near) segment ends and can facilitate automated tracking, accelerating the process and providing kinematic feedback in seconds. Divers use tape for both support and proprioception in the course of normal training and find it unobtrusive and are able to wear it without a negative impact on training.

Successful implementation of a marker system reduces an image to a plain background with only blobs (collections of pixels representing features of interest) in the foreground, as shown in Figure 6-1.

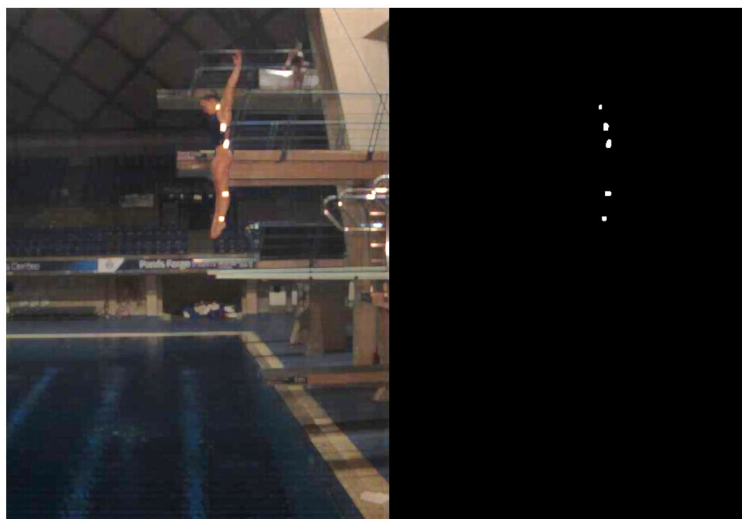


Figure 6-1. Markers facilitate the creation of a stick-figure from blobs to represent the diver.

This aim of this chapter is to identify a suitable method of creating and attaching tape markers to a diver such that marker locations can be used to calculate COM-position with a known level of comparability to the position calculated using manual digitisation.

The chapter will identify the tape most suited to providing effective markers and will describe a method for fixing markers to divers for the duration of a training session. It will describe a flexible method for dressing the environment to maximise the success of automated tracking.

A method for extracting marker information from the image will be described, following which an experiment will be conducted to assess the performance of an automated marker-tracking system.

## 6.2 A study to identify a suitable tape for markers

### 6.2.1 Introduction

Section 2.6 concluded that the most appropriate way to automatically track motion was through passive markers and that tape was a potential source of markers. This was supported by the understanding that divers wear tape as part of day-to-day training and could be worn comfortably during training.

A study was conducted to identify a suitable tape for use as a marker.

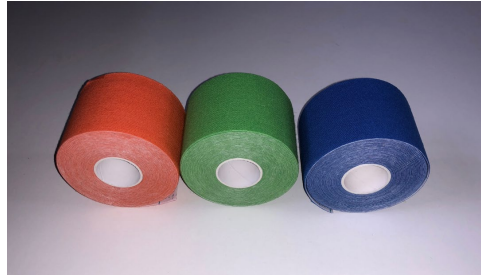
### 6.2.2 Method

A study was conducted with the aim of removing all background data from an image and leaving only desired foreground features ('blobs', or collections of pixels representing data of interest, in this case the tape marker) visible in white in a binary image.

Varieties of three types of tape were used:

- Red, green and blue Kinesiotape tape (Figure 6-2). This tape is commonly used by divers in training and competition for support and proprioception and is familiar and comfortable for the athletes. The colours were selected for their

match to the colour channels in an RGB image, and have greatest distance from each other in HSV space, increasing their potential for being separated from the background following colour-based image processing.



*Figure 6-2. Coloured tape was used in a trial based on the potential for colour-based image processing.*

- Black tape and white tape (Figure 6-3). The high-contrast colours were selected to optimise the effect of a thresholding filter during image processing, more effectively isolating the markers in the image.



*Figure 6-3. High-contrast tape was trialled with the aim of isolating markers using contrast-based image-processing.*

- Retro-reflective tape (tape containing a layer of glass beads, Figure 6-4). Although not used by divers in normal training, reflective markers were considered in combination with additional directed lighting and low exposure during filming, for their ability to produce a high-contrast reflection that could be separated from background data.

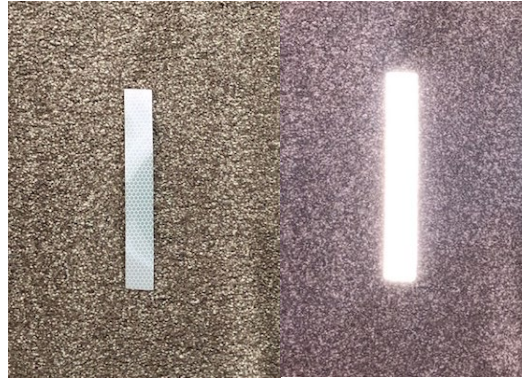


Figure 6-4. Retro-reflective tape (left) produces a bright reflection when a light is shined on it (right).

Markers (lengths of tape approximately 5 centimetres in length) of each type of tape were fixed to the divers and image-processing techniques were performed on captured images with the aim of removing background data and leaving only the markers in the image. A series of image-processing filters were applied to the images:

### Manipulation of colour levels

Changing the level of red, blue and green in the image as appropriate to the colour of the marker, aiming to leave markers a different brightness to the rest of the image (Figure 6-5).

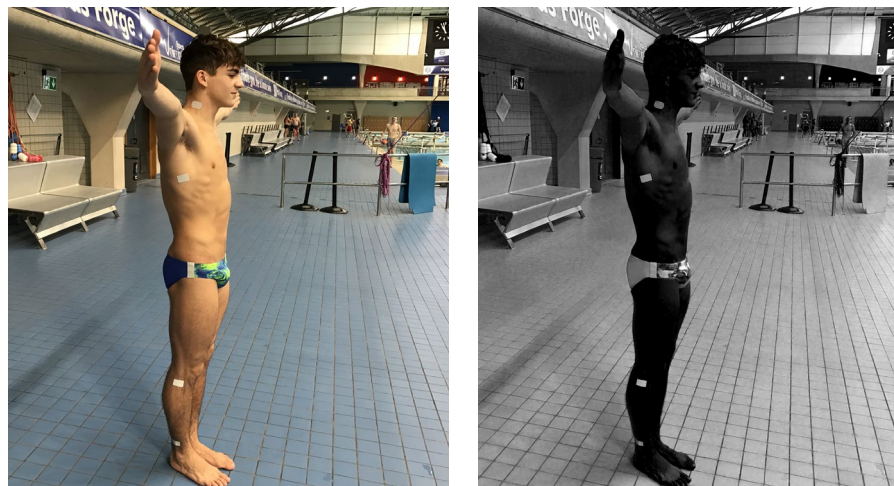


Figure 6-5. An example of manipulation of colour levels via image processing. Removal of Red and Green and an increase in Blue increases the brightness of pixels containing higher quantities of Blue. Unlit reflective markers are visible on landmark locations on the diver.

## Conversion to grayscale and contrast thresholding

Reducing a 24-bit colour image to an 8-bit grayscale image allows a thresholding function to be applied to the image. All pixels over a threshold value are converted to white and pixels below that value are converted to black.



Figure 6-6. A thresholding filter turns all pixels black or white depending on their brightness compared to a threshold value

## Inversion

An inversion filter (Figure 6-7) transposes brightness values along a range from 0 (black) to 255 (white) in the image. This filter would turn black markers (for example using the black tape) into white – required for counting and classifying markers in subsequent processing.



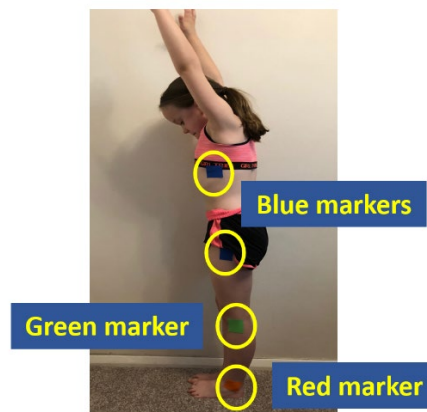
Figure 6-7. An inversion function turns dark pixels light and vice versa.

Following image-processing, subjective qualitative assessment of the images was used to identify the most suitable tape.

### 6.2.3 Results

#### **Coloured tape**

Kinesiotape tape can be easily attached to the diver (Figure 6-8), its flexibility overcoming the challenge of maintaining adhesion to varying contours of the limb to which it is fixed.



*Figure 6-8. Coloured markers attached to a diver's ankle, leg and rib.*

Tape was attached to a diver; images were collected in unaltered ambient lighting. Figure 6-9 shows the effect of colour manipulation to isolate the markers of each colour in turn.



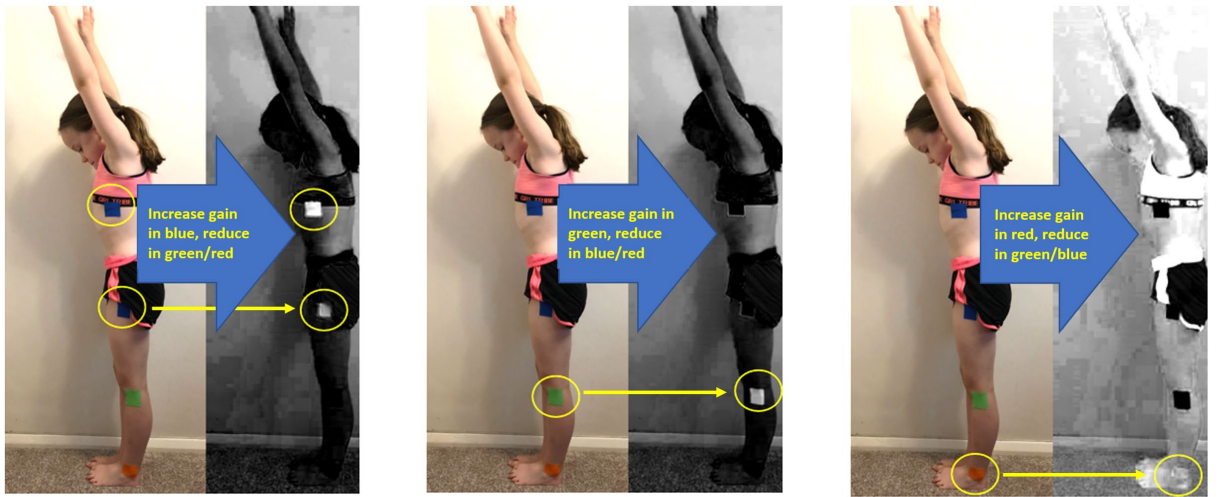


Figure 6-9. Colour manipulation to enhance blue markers (left), green markers (centre) and red markers (right).

Blue and green markers were more identifiable in the image following colour removal whereas the red (ankle) marker had little contrast difference to the rest of the foot.

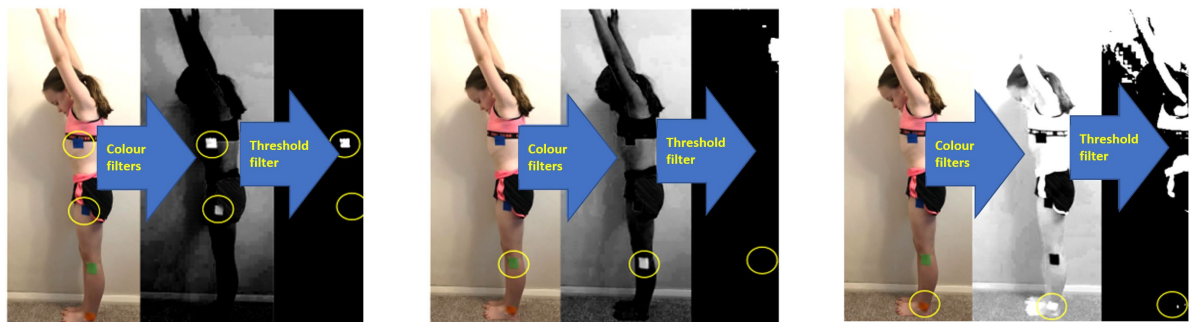


Figure 6-10 shows the results of conversion to grayscale and then application of a thresholding function in a further effort to separate background from blobs.

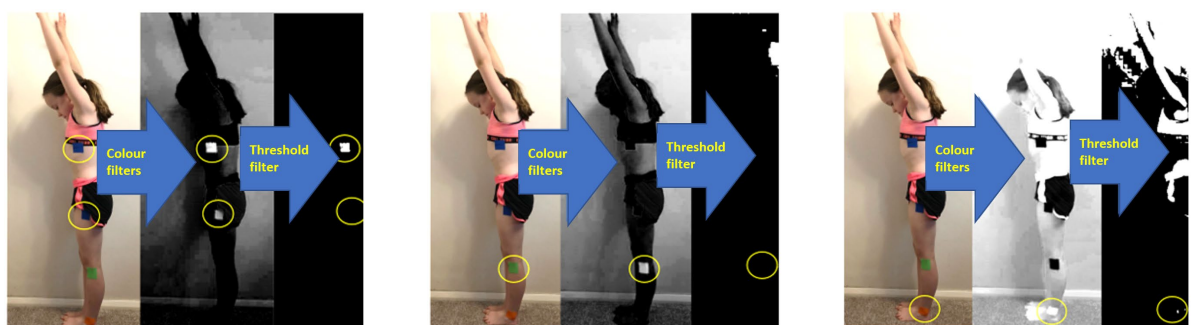


Figure 6-10. Application of a grayscale and contrast threshold function following colour manipulation to isolate blue (left), green (centre) and red (right) markers in the image.

Lighting was similar in the test environment (from above) as in the training environment and an assumption was made that results would be consistent in either space. There were no circumstances where image processing removed all background and consistently left only blobs as foreground data (although blue markers were processed with more success than red or green). For these reasons, a more consistently successful solution was sought, and coloured tape was rejected as a solution.

### **Black and white tape**

Images of an athlete were captured, again in ambient lighting similar to a training setting, wearing high-contrast markers in black and white (Figure 6-11).



*Figure 6-11. Black and white zinc oxide tape was used to make markers. The high contrast was selected to maximise the effect of contrast-threshold image-processing.*

As with the coloured tape, the zinc oxide tape of both colours could be fixed to any part of the body. Colour levels were subjectively manipulated and a grayscale and threshold function was applied to separate blob from background (Figure 6-12) When black tape was used, an inversion function was included in the processing series to achieve the aim of a white blob on a black background.

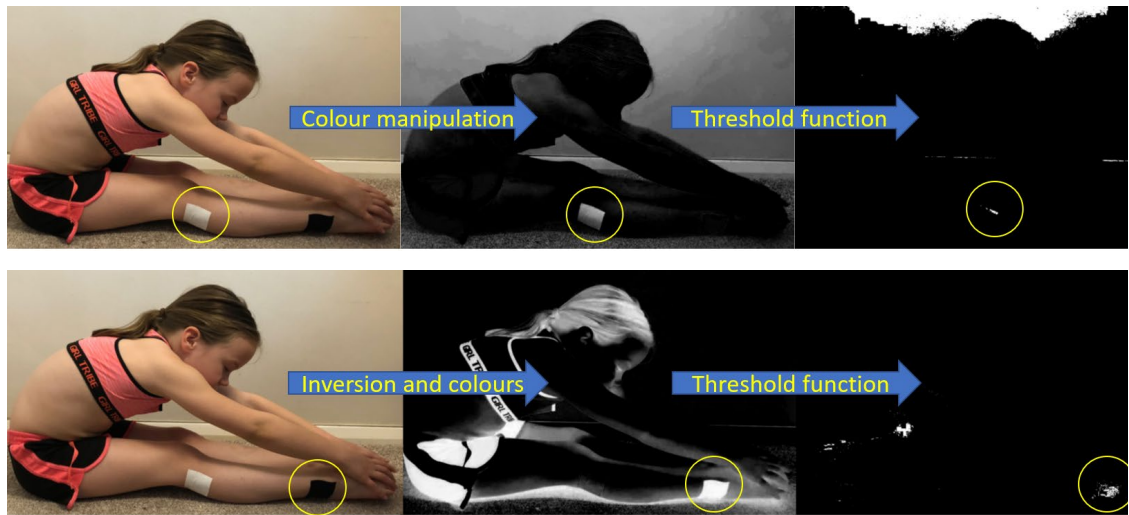


Figure 6-12. Image processing to isolate a white marker (top) and a black marker (bottom) in an image.

As with coloured markers, it was not possible to isolate the desired blob in the image. Additional features (clothing, reflection, shadow) left pixels of a similar brightness to the marker and were subsequently left in the image following processing. Figure 6-13 shows a view of the diving pool as the same processing filters are applied.

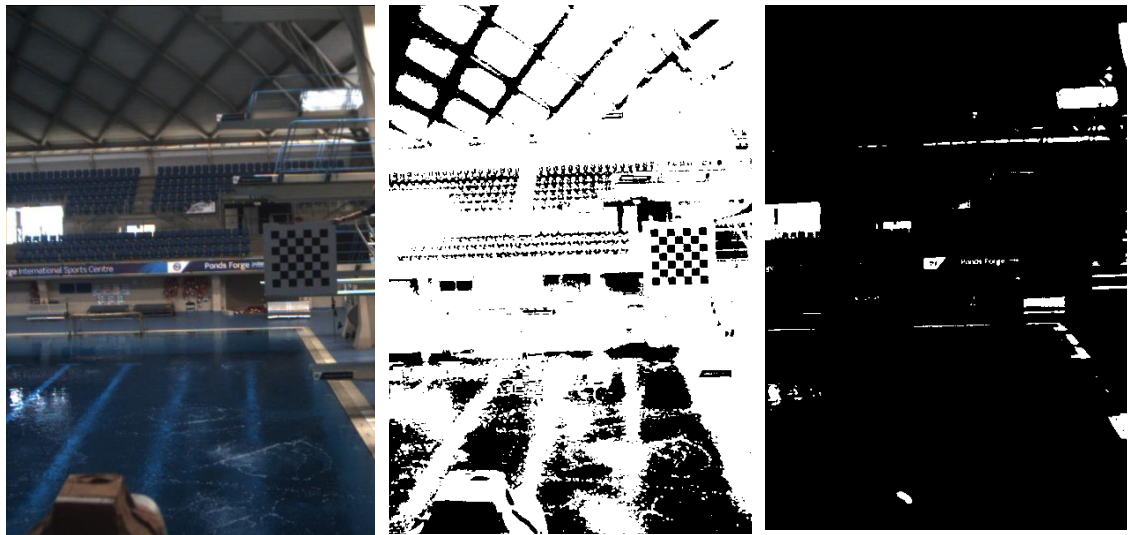


Figure 6-13. The view of the training environment with successive stages image-processing applied.

There are areas of high reflection and darkness in the image that remain after processing as evident in the test environment. For this reason, it was concluded that

black and white markers could not be isolated as blobs and therefore were discounted from further consideration as a solution.

### Retro-reflective tape

Retro-reflective tape was attached to lower-limb landmarks Figure 6-14. The subject was filmed in both ambient light and with additional lighting in the same direction as the camera.



Figure 6-14. Retro-reflective tape is used to create markers and can be used with and without additional lighting.

The effects of colour-level manipulation on lit and unlit retro-reflective markers are shown in Figure 6-15.

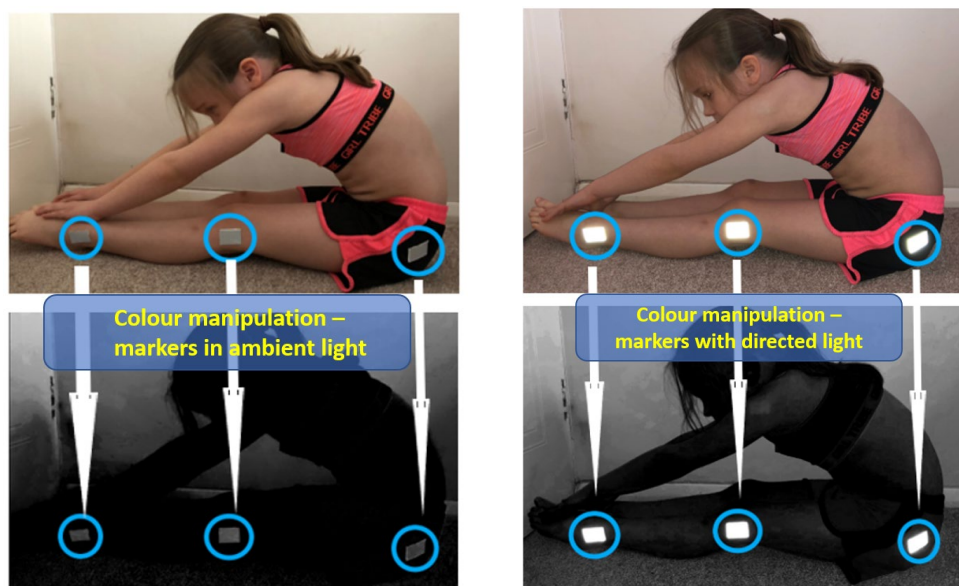


Figure 6-15. Colour removal is used to isolate the reflective markers in the image. Unlit (no directed lighting) markers are shown left, lit markers right.

Figure 6-16 and Figure 6-17 show the effect of the process of colour removal followed by the application of grayscale and threshold filters. When unlit markers are used, as with black and white markers, the markers are lost before the background artefacts and consequently can't produce the target image.

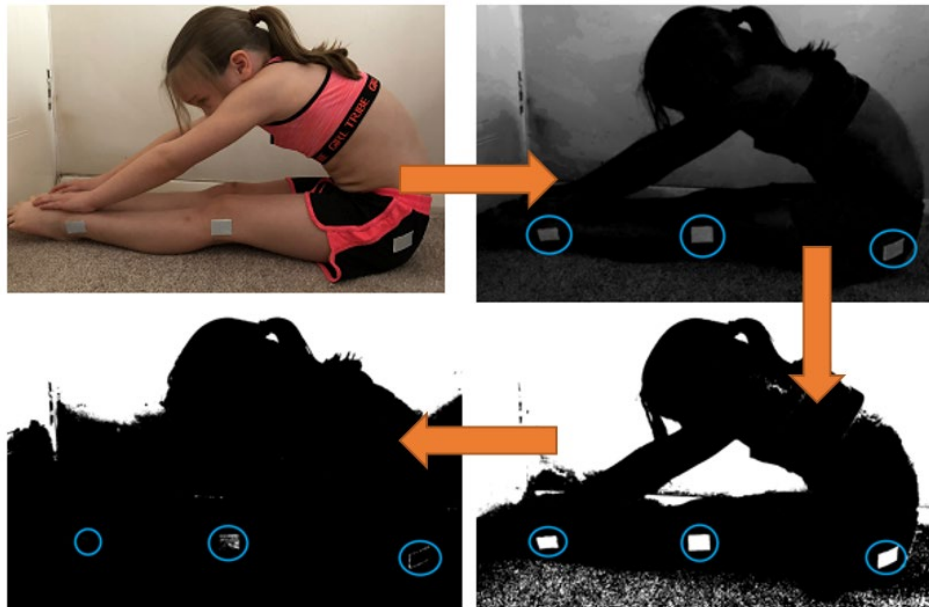


Figure 6-16. Colour removal and thresholding use to isolate reflective (but unlit) markers.

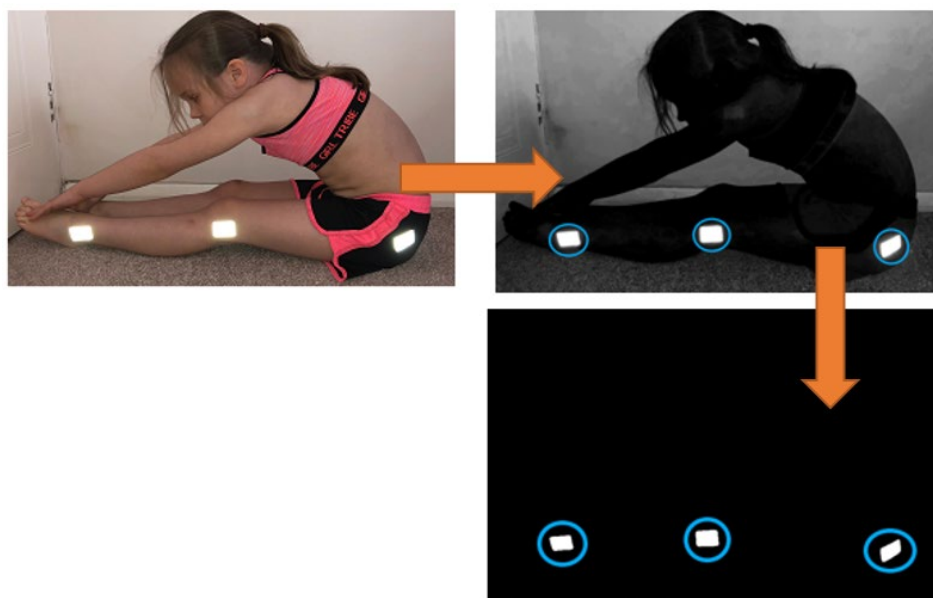


Figure 6-17. Colour removal and thresholding used to isolate lit retro-reflective markers.

When lit markers are used, image processing techniques produce the desired outcome – blobs remain as the only foreground data in the image (Figure 6-17, bottom-right). For optimal results, markers should be lit.

#### 6.2.4 Discussion

Although all the tape used in the trial satisfied the requirements of comfort and adhesion, image processing techniques could not consistently separate markers of coloured tape from the rest of the image. Retro-reflective tape, when lit, satisfied all needs and is therefore chosen as a suitable method for producing markers. As it is not as adhesive or flexible as Kinesiotape or zinc oxide tape, consideration should be made to ensure it lasts the duration of a training session and that the environment is lit to maximise its reflective qualities.

### 6.3 Application of markers

Retro-reflective tape is more rigid than zinc-oxide and Kinesiotape and the edges are sharper. A method of application was required that ensured that the markers (Figure 6-18) stayed attached to the diver for the duration of a session and were comfortable to wear during training.



*Figure 6-18. A retro-reflective marker. Edges are trimmed to ensure the divers' comfort.*

A series of observations were conducted following different methods of fixing the marker to the skin:

- Applying the marker directly to the skin

- Applying the marker after spraying the skin with pre-tape adhesive (Figure 6-19, left)
- Adhesive plus leukotape covering the edge of the marker (Figure 6-20)
- Covering the marker in Opsite Flexifix (surgical tape used for waterproof cover of wound and stitches, Figure 6-19, right)



Figure 6-19. Both spray adhesive and surgical tape were used to lengthen the time for which markers stuck to the skin.



Figure 6-20. Leukotape was used to increase adhesion time.

### 6.3.1 Method

Following the application of the markers to a group for divers, five training sessions were observed to identify the number of dives that could be completed before markers fell off in the water. These results were compared to the number of dives in a typical training session to assess the most suitable solution.

### 6.3.2 Results

The results of the observations are shown in Table 6-1.

*Table 6-1. A range of strategies were used to fix markers to the divers. The success of each strategy was measured by the number of dives completed before markers became detached.*

<b>Strategy to fix markers on skin</b>	<b>Lowest number of dives before marker detached</b>
Retro-reflective tape only	4
Retro-reflective tape plus spray adhesive	6
Tape, adhesive spray, leukotape bordering marker	13
Retro-reflective marker covered by surgical tape	Markers didn't detach through a session

A typical training session would consist of 40-80 skills, depending on the difficulty and the height from which they're performed. These numbers provide a benchmark against which the duration of adhesion can be compared. The solution that met the needs of the session was tape covered by surgical tape.

### 6.3.3 Discussion

Either method that left the marker uncovered resulted in their loss from the body during the session. The first marker to fall off was most frequently the ankle, followed by then knee. This is influenced by both the diver grasping the ankles in the tuck shape and closing the arms around the side of the knees when adopting a closed pike creates a friction that can remove the markers, also that the small circumference of the lower leg creates a greater curve around which the inflexible marker is fixed, limiting the time it stays attached to the limb.

Although the use of a tape border kept the markers in place longer, the available marker surface is reduced, the application time was greater, and the resources required (the leukotape as well as the reflective tape) were greater, for little additional benefit.



Markers covered with surgical tape stayed in place consistently throughout the session. The surgical tape is clear, flexible and designed to provide a waterproof seal on the skin. Divers were happy to train wearing these markers and expressed no restriction of movement, discomfort or distraction. This is the method of marker application identified as suitable.

## 6.4 Lighting the scene

### 6.4.1 Introduction

Directed lighting is required to maximise the effect of reflective markers. The design and specification of a method for lighting the scene must take several factors into account. Restrictions on electrical devices near water (Team, 2017) require that devices must remain in defined zones – demarked by distance from water – based on the voltage used. A stipulation that lights will be mounted in the spectator balcony (at a distance greater than 3.5 metres) ensures that this condition will be met.

Springboards are generally 10-13 metres away from the camera and lights used should illuminate retro-reflective markers at these distances. 400-Watt halogen lights (Figure 6-21) were used to light the training environment.



*Figure 6-21. 400w Halogen lights were used to illuminate the scene.*

Lights should be mounted at an appropriate height such that the camera can pick up reflections through the divers' flight path. The ideal theoretical configuration is shown in Figure 6-22 – where lighting provides reflection throughout the flightpath, regardless of the flightpath's height and distance. Practical considerations require a

more economical solution - providing enough illumination to gather marker reflections through the parts of the dive from which performance metrics may be calculated.

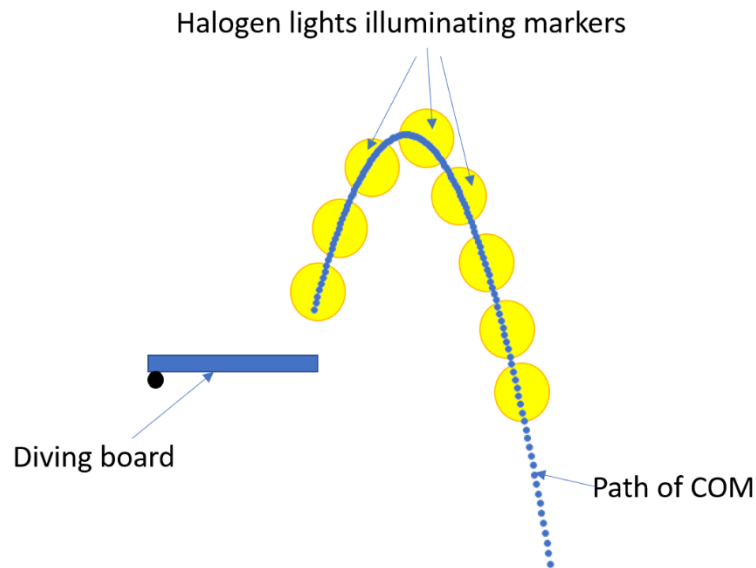


Figure 6-22. A theoretically ideal (but impractical) lighting configuration, with halogen lights illuminating the whole flight path of the diver.

Handrails in the spectator balcony provide mounting points for lights (Figure 6-23). The length of the handrails allows lights to cover the horizontal range of the dive and the tiered seating provides handrails at different heights to allow lighting of the vertical range of the dive. British High-Performance Centres (London, Leeds, Plymouth, Sheffield) all match this specification.

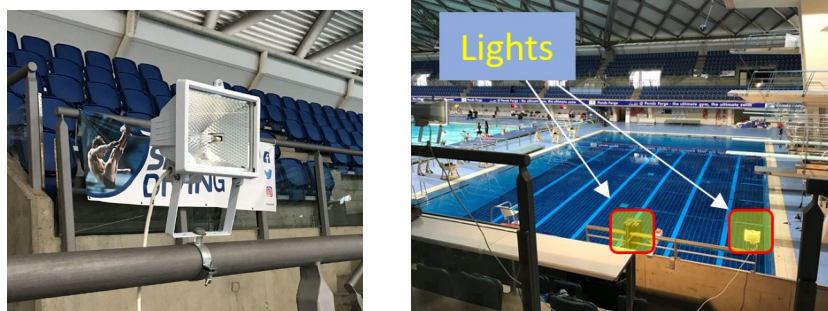


Figure 6-23. Halogen lights are mounted on handrails to ensure illumination from a range of heights.

## 6.4.2 Method

The spectator balcony provides a range of mounting points for lights and the best position for those lights must be identified for optimal marker reflection and to create the potential for motion tracking.

Between two and four lights were mounted in a range of positions during divers' training. The divers were filmed; the resulting images were subjectively assessed to identify the brightest reflections and therefore the best arrangement of lights. The arrangements tested are shown in Figure 6-24.

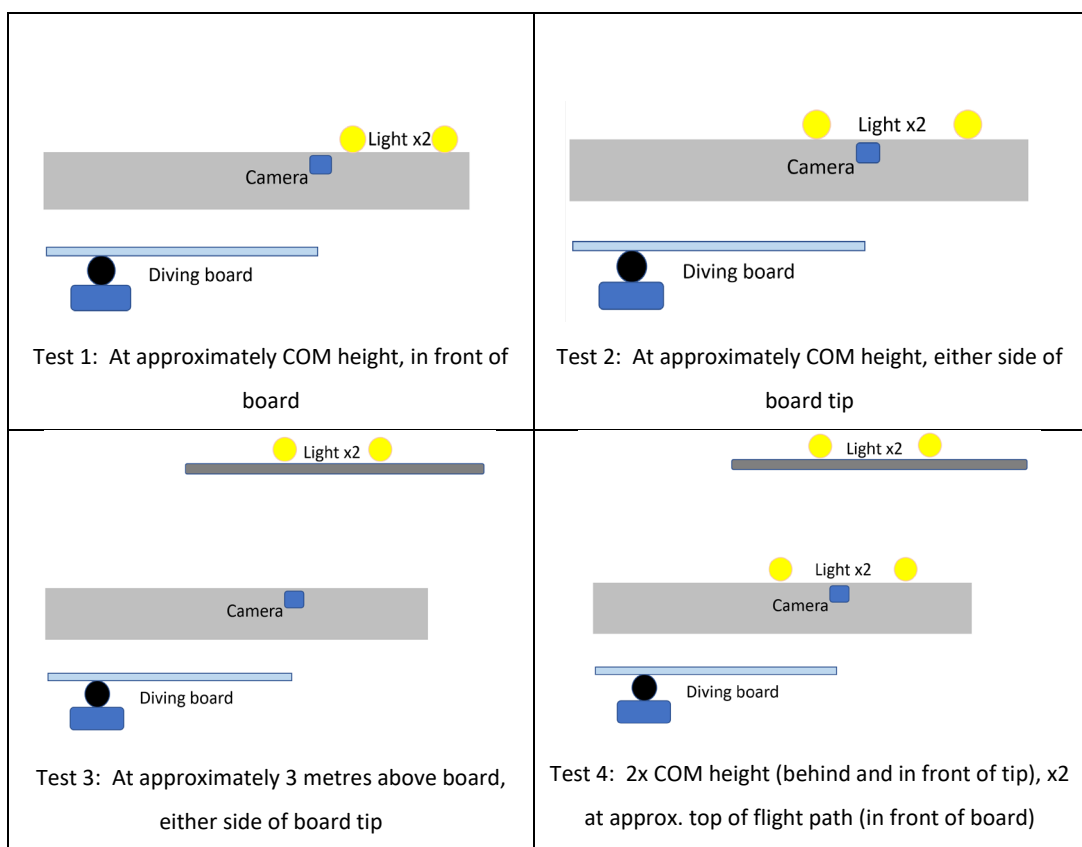


Figure 6-24. Lighting configurations used in filming tests.

## 6.4.3 Results

Two lights (Tests 1 and 2 above) proved insufficient despite their position. When they were in front of the board, detail in the hurdle-step (in the 1-1.5 metres before the end of the board) was lost. When they were only at COM level, detail towards the top of the divers' flight path was lost. In all circumstances, markers reflected less brightly

when covered in surgical tape (Figure 6-25, right). Images with reflections of lower brightness could not be processed to isolate markers.



*Figure 6-25. A two-light setup (left) producing reflections on uncovered markers (right) which were not bright enough for effective image-processing.*

With the addition of two more lights, all markers were visible for more of the flight path (Figure 6-26) and could be isolated using colour removal, grayscale and thresholding filters. The diver's technique before the point of take-off (i.e. the hurdle step) could be observed, allowing understanding of the relationship between hurdle-height, board deflection and take-off velocity (as measured by Miller (Miller et al., 2002)). Two lights close to the peak-height achieved by the divers increased the number of frames in which all markers were visible around the top of the flight path. This is important to correctly identify the best body-segment model (Section 5.7) with which to represent the diver.

Successive trials showed suitable effect when lights were positioned in approximately the same place – the lack of precision required in positioning increases the number of pools for which this configuration is suitable, considering the small differences in handrail positioning from pool to pool.



Figure 6-26. Top – markers visible on the diver in flight. Bottom – markers isolated in the image using image-processing techniques.

#### 6.4.4 Discussion

While brightness of reflection increases with the number of lights used, suitable reflections for image processing and marker isolation can be achieved with four lights (Figure 6-27), two at approximately the height of the COM at take-off, two at approximately the maximum height of the divers' flight path.



Figure 6-27. The required arrangement of environmental lighting.

## 6.5 A study into the effect on COM of segment-end approximation using retro-reflective tape markers

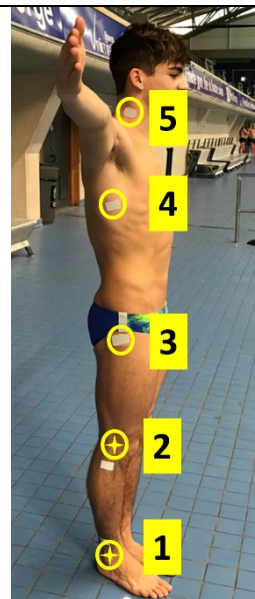
### 6.5.1 Introduction

Markers are, in most cases, attached to the diver on the same landmarks as those used for manual digitisation. There are, however, two cases where the landmark digitised to represent a segment-end cannot be the site of a retro-reflective marker. In the case of the ankle marker, the shape of the protruding medial malleolus does not allow the adhesion of a marker (which requires a greater flat surface-area for successful attachment). The skin covering the knee joint-centre continually stretches over repeated take-offs and acquisition of tuck shapes; markers stuck in this position are loosened by continual change of the knee-angle and so are positioned as close to the physical landmark as possible.

The definitions of both the segment-end landmarks and the point of application of reflective tape is shown in Table 6-2. The effect of inaccurate digitisation on the body's COM was investigated in Section 5.6. The effect on the variation of COM-position due to the different position of markers compared to landmarks was calculated to understand the error introduced by this limitation.

*Table 6-2. Segment-end landmarks and retro-reflective markers do not always occupy the same position on the body due to limb shape or skin-stretch.*

Marker	Manual digitisation landmark	Retro-reflective marker position
1. Ankle	Ankle joint-centre (lateral malleolus)	Fibula, directly above lateral malleolus
2. Knee	Knee joint-centre (lateral condyle)	Directly below head of fibula
3. Hip	Hip joint-centre (greater trochanter)	Greater trochanter
4. Ribs	Level with body of sternum	Approximately level with body of sternum
5. Neck	Chin-neck intersect	Level with spinous process of C7
Hip, ribs and neck landmark positions can be exactly covered with retro-reflective markers. Ankle and knee landmarks cannot.		



### 6.5.2 Method

A male and female diver were filmed performing forward dive and back dive in the tucked, piked and straight position. Both divers wore retroreflective markers to locate landmarks on the body. The model selected as best for each diver (Chen and Nikolova-female respectively) using the method defined in Section 5.7 was used to calculate COM-position in each frame.

Each dive was manually digitised twice to determine COM-position during the dive. Neck, ribs and hip landmarks were digitised in the centre of each corresponding marker. For the first digitisation of each dive, knee (lateral malleolus) and ankle (head of fibula) landmarks were located by eye using joint angle and shadow to guide the user.

For the second series of manual digitisations, knee and ankle landmarks were located as the centre point of their respective markers (Figure 6-28).

The resulting flight paths were compared and RMSE was calculated. The difference in COM-position in each frame of the dive using both methods was calculated and greatest difference in each dive recorded for comparison. Smaller RMSE values and smaller differences between COM-positions reflect flight paths that were closer and less affected by the difference in knee and ankle landmark location. Results are shown in Table 6-3.

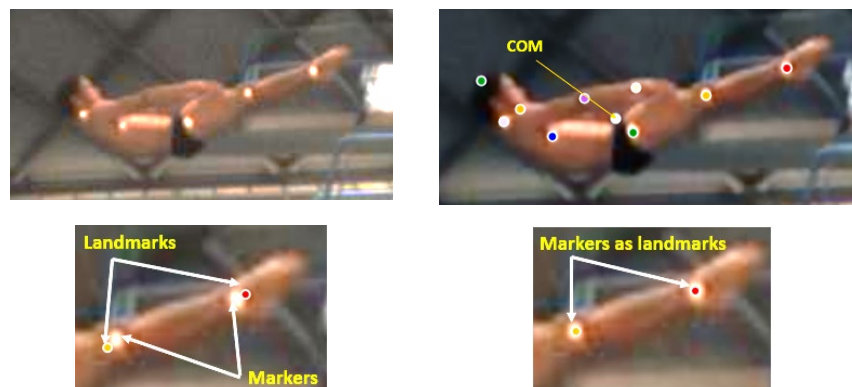


Figure 6-28. Top-left – a diver in flight. Top-right, digitised landmarks shown. Bottom-left – anatomical landmarks on lower leg digitised. Bottom-right – retro-reflective marker-centres digitised. Lower leg markers are close to, but not on the desired anatomical locations due to the shape and movement of bone and joint.

### 6.5.3 Results

Results of the investigation are shown in Table 6-3. Each dive is represented by a dive number as follows:

- 101a – forward dive, straight
- 101b – forward dive, piked
- 101c – forward dive with tuck
- 201a – back dive, straight
- 201b – back dive, piked
- 201c – back dive with tuck

Table 6-3. Comparisons of COM calculation using manual digitisation via observed and marker-based landmarks.

Diver and dive	RMSE (x) (mm)	RMSE (y) (mm)	Maximum distance between COM-position in each digitisation (mm)
Diver 1 - 201a	2.6	2.8	6.5
Diver 2 - 101a	3.1	1.7	5.3
Diver 1 – 201b	2.1	3	6.3
Diver 2 – 101b	1.8	3.5	5.8
Diver 1 – 201c	1.6	3.4	6.7
Diver 2 – 101c	2.8	3.7	7.1

The effect of skin-stretch (the skin moving over the bone beneath and not remaining constantly over the bony landmark) affects COM calculation more as a greater number of joints are bent. In straight shapes (dives 101a and 201a, above) where the hip and knee joint remain extended, COM consistency and vertical displacement of COM showed least difference. Dives tucked (101c and 201c, above) show greatest maximum difference between visual and marker location of leg landmarks.

The RMSE values in both axes showed less than 4 mm variance and the greatest distance between COM location using both methods was approximately 7 mm.

### 6.5.4 Discussion

There is some consequence to the calculation of COM when markers are not placed directly over lateral malleolus and lateral condyle. The effect of the largest RMSE



value in  $y$  (affecting maximum height, COM displacement and take-off velocity) using the method described in Section 5.7.5, is approximately 0.005 m/s when calculating take-off velocity from COM displacement and the benefits of comfort and duration (markers stay in place for a whole training session) outweigh the drawback. Retro-reflective markers should be attached to divers as described in Section 6.5.1.

## 6.6 A study into the comparability of COM-position using six and three-segment models to represent the diver.

### 6.6.1 Introduction

Retro-reflective markers are unsuitable for use on the diver's head and arms. The landmark representing the top of the head is, in most cases, covered by hair. The rotation of the shoulder inhibits the visibility of the segment end. The rotation of the upper and lower arm during skill execution would (for a retro-reflective marker to locate the elbow joint-centre) require a tape marker to be wound around the circumference of the limb to be visible in all positions. During trials this was both uncomfortable for the diver and restrictive (the flexion of biceps required to grab the legs in a tuck or pike shape resulted in discomfort as the elbow marker inhibited the bunching of the muscle). Wrapping a reflective marker around the wrist was both practical and comfortable but added little extra information as to the position of the arm segments without the shoulder or elbow marker. Furthermore, the wrist marker passed close to the hip marker during an arm swing and close to the ankle and knee markers in tuck and pike shapes respectively. Although a stereo calibration of the scene would have provided enough depth information to differentiate the wrist and leg/hip markers, this is not possible in a one-camera system. Consequently, the risk of misidentification of markers in an automated system supports unmarked upper limbs.

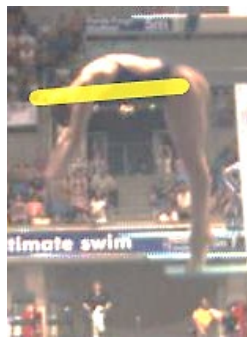
A three-segment model is implemented to create the potential for automated tracking. The head and arm segments are combined with the trunk creating a single upper-body segment linked to upper leg and lower leg segments. This approach assumes that the difference in the location of the COM is small and consequently has a minimal effect on the calculation of take-off velocity, compared to calculating the effect on COM-location from the position of each segment.

The difference in location and rate of change of COM when calculating take-off velocity using a three-segment model compared to a six-segment model should be found in order to understand the error introduced into the system by this approach.

### 6.6.2 Method

An assumption is made as to the position of the head and arms for the calculation of mass distribution and COM location of the coalesced upper-body segment (head, upper arm and lower arm is combined with the mass of the trunk). Figure 6-29 shows divers at the point of take-off for dives in all rotating directions.

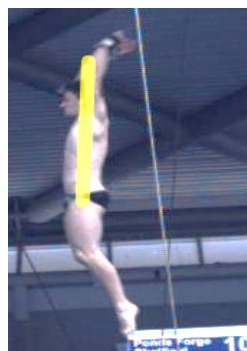
Forward rotation



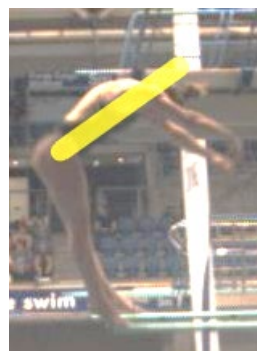
Backward rotation



Reverse rotation



Inward rotation



*Figure 6-29. Take-off shapes for dives rotating for different diving groups. The yellow line approximates a segment that goes from the hip landmark and extends through and beyond the neck marker.*

The accuracy of the three-segment model compared to the six-segment model must be at its greatest through and immediately after take-off, as these are the frames used to calculate take-off velocity and infer several performance metrics (maximum height,

trajectory, moment of inertia). In all groups, the head is closely aligned to the longitudinal trunk-midline (indicated by a yellow line in Figure 6-29, above). In back and reverse take-offs, the arms are also close to this line and are extended and above the shoulder in all poses. Although there are circumstances where the head and arms would be in a significantly different position to this pose, the take-off would be considered compromised to the extent that the coach would exclude it from analysis. For these reasons, a choice should be made between approximations of head and arm position that reflect diving posture (Figure 6-30).

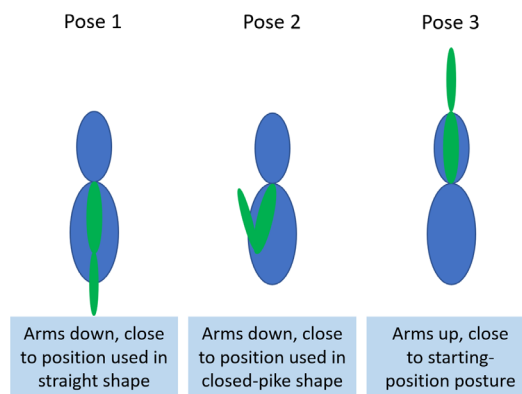


Figure 6-30. Head and arms can be assumed to be in one of a series of diving-specific postures for the purposes of merging upper-body segments for the three-segment model.

The take-off images shown in Figure 6-29 are closest to Pose 3 (above), with the arms extending above the head. This allows approximation to both forward and inward take-offs where the arms are in front of the hip-neck line and to back and reverse take-offs where the arms are behind that line.

To produce an approximation of the upper segment, a series of steps are followed. Initially, the head and upper arm are merged into a single segment where the new segment mass is the sum of head and arm mass and whose segment COM-position is calculated using Equation 6.1 (as described in Section 5.4.2) where  $COM_c$  is the combined segment:

$$COM_{cx} = (m_c m_1 COM_{1x}) + (m_c m_2 \left( 1 + \left( \frac{l_p}{COM_{2x} \times 100} \right) \right)) \quad [6.1]$$

$$COM_{cy} = (m_c m_1 COM_{1y}) + (m_c m_2 \left( 1 + \left( \frac{l_p}{COM_{2y} \times 100} \right) \right))$$

where  $m_1$  and  $m_2$  are the masses of the two segments (head and upper arm),  $COM_1$  and  $COM_2$  are the position of the COM of each segment and  $l_p$  is the length of the shorter segment (head) as a percentage of the longer segment (upper arm) length.

Relative segment lengths were determined using the average of segment data from the divers digitised (head, upper-arm and lower-arm lengths were calculated from the distances between digitised landmarks on the image). The resulting head/upper-arm segment is then merged with the lower-arm segment, resulting in new segment mass and a new COM for the segment. The third step is to combine the head/upper-arm/lower-arm segment with the trunk. This sequence is illustrated in Figure 6-31.

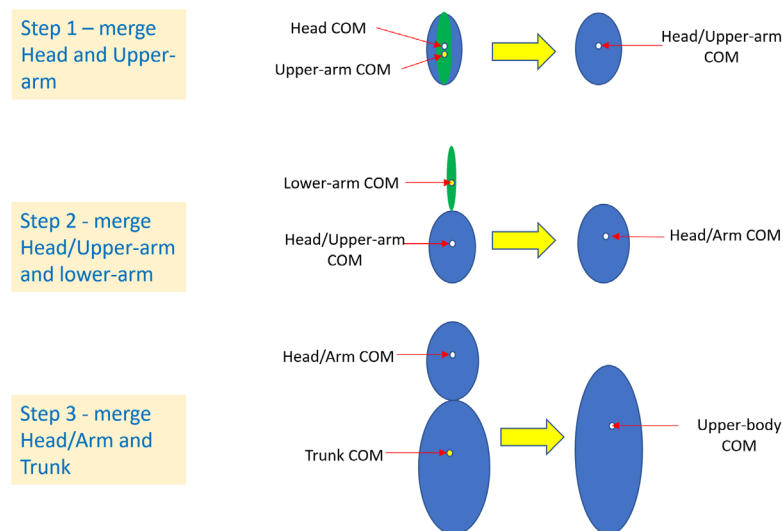


Figure 6-31. A process for coalescing Head, Upper-Arm, Lower-Arm and Trunk segments into an Upper-Body segment with re-calculated segment-COM position.

Typical last-contact frames were digitised to measure the difference in COM-position using a three and six segment model, as shown in Figure 6-32.

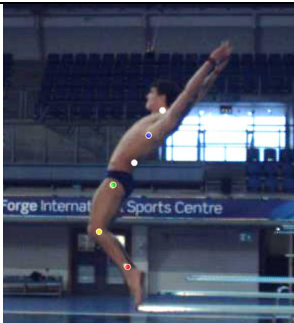
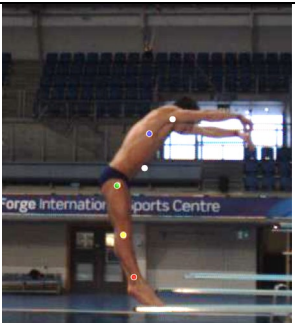
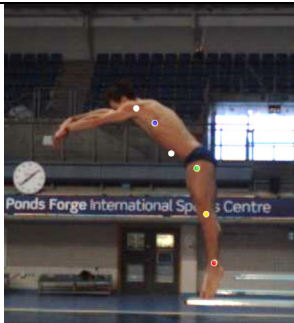
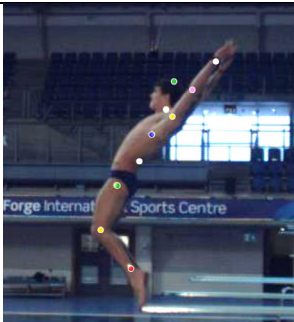

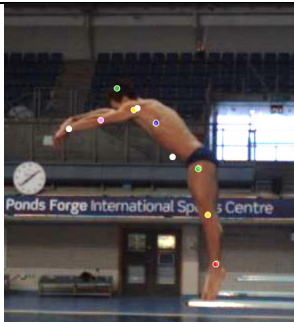
	Reverse	Inward	Forward
Three segment model	 COM (36,983)	 COM (-56,945)	 COM (102, 1054)
Six segment model	 COM (37, 981)	 COM (-56,927)	 COM (102, 1038)

Figure 6-32. COM position (shown in white), calculated using three and six segment models.

It can be seen that there is a negligible effect on the x-coordinate of COM, and a small effect (between 2 mm and 19 mm) on the y-coordinate of COM. The effect of this COM change on take-off velocity should then be established.

The dives used in 6.5.2 (dives by a range of divers covering all rotating groups) were re-digitised. The first digitisation implemented the 3-segment model described above to calculate COM-positions on frames around take-off. The second series of digitisations used all landmarks to create a 6-segment model as described in Chapter 5. The change in COM-position over time was used to determine take-off velocities in horizontal and vertical directions.

The velocities calculated for both body-segment models were then compared to calculate the inconsistency in dive-height (a key metric) inferred using both y-velocity values.

### 6.6.3 Results

The results of the study are shown in Table 6-4 and Table 6-5.

Table 6-4. Comparison of horizontal and vertical take-off velocity data calculated using a 3 and 6-segment model. Highlighted cells represent values of 0.1 m/s or greater.

Dive	3-segment		6-segment		difference	
	$v_x$ (m/s)	$v_y$ (m/s)	$v_x$ (m/s)	$v_y$ (m/s)	$v_x$ (m/s)	$v_y$ (m/s)
1	0.94	4.98	0.98	5.06	0.04	0.08
2	0.60	5.24	0.68	5.24	0.08	0.00
3	0.68	4.84	0.78	4.90	0.10	0.06
4	1.08	4.94	0.96	5.00	0.12	0.06
5	0.83	5.00	0.85	5.05	0.14	0.06
6	0.46	5.16	0.50	5.24	0.04	0.08
7	0.94	4.96	0.98	5.06	0.04	0.10
8	0.64	5.16	0.72	5.22	0.08	0.06
9	1.14	4.72	1.12	4.70	0.02	0.02
10	1.54	4.92	1.46	5.02	0.08	0.10
Mean					0.07	0.06
SD					0.04	0.03

Table 6-5. Displacement of COM between take-off and the top of the flight path based on initial velocities.

Dive	Displacement (mm)		Difference (mm)
	3-segment	6-segment	
1	1264	1305	41
2	1399.5	1399.5	0
3	1194	1223.8	29.8
4	1243.8	1274.2	30.4
5	1274.2	1299.8	25.6
6	1357.1	1399.5	42.4
7	1253.9	1305	51.1
8	1357.1	1388.8	31.7
9	1135.5	1125.9	9.6
10	1233.8	1284.4	50.6
		Mean	31.2
		SD	15.7

For most cases, take-off velocity calculated using the three and six-segment models were within 0.1 metres per second of each other and were different by no more than 0.1 metres per second when considering vertical velocity. This difference is the same

as the threshold level of accuracy for vertical velocity described in Miller's (2013) study inferring kinematic parameters from broadcast video.

There is greater inconsistency in  $x$  – reflecting that in forward and inward dives, it is likely that the arms are further from the 180° angle assumed during take-off. Some variation may have also have been introduced in the six-segment model during manual digitisation of the take-off frames; Section 5.6 identified that manual digitisation of landmarks (in this case head, shoulder, elbow and wrist, where retro-reflective markers are not present) risks inconsistency which may affect COM calculation in the frames from which velocity is calculated, although inconsistency in these digitisations were shown to have a limited effect.

These results show an average difference (with the six-segment model) of 31.2 mm, 2.4%. In these examples, the greatest difference in displacement is in Dive 7, where the difference in inferred COM displacement is 51.1 mm.

#### 6.6.4 Discussion

It is assumed that a more accurate COM calculation is obtained using a six-segment model considering the changing position of the head and arms. A three-segment model (which can be implemented using reflective markers) provides close agreement on measures of vertical velocity at take-off, COM displacement and shape of flight-path. This allows comparison of data generated between six and three segment models for these kinematic variables, although the difference in COM-position in each frame means that displacement relative to the tip of the board will have a greater difference between the two models.

### 6.7 Summary

Markers representing segment-ends provide the potential for both consistent location and an increase in processing speed with automated tracking.

Retro-reflective tape has been shown to be an effective resource from which markers can be produced and, when reinforced by Opsite Flexifix surgical tape, markers have

been shown to be secure for the duration of a training session. It has shown that optimum lighting conditions are achieved by the positioning of four halogen lights, two at approximately waist-height and two at a height of approximately the top of the flight path. Both pairs of lights should be separated horizontally by 1-1.5 metres for flight-path coverage. In this configuration, reflective markers can be tracked from the last step into the hurdle, through to the point at which the hands hit the water at entry.

It has been shown that positioning markers close to, but not on, the ankle joint-centre and knee joint-centre has a small effect (but no greater than the effect of error in point-reconstruction) on calculated COM location due to the relatively small mass of the lower-leg. This compromise allows uninterrupted training; when markers are placed directly on joint centres, the movement of the knee and ankle dislodged markers.

Marker-attachment is impractical on the head and arms. This limitation requires a three-segment model be used to represent the diver instead of the six-segment model achieved with manual digitisation. Key markers such as vertical take-off velocity show a close match between a three and six-segment model and the compromise in accuracy in performance data is balanced by the opportunity to produce real-time feedback in training via automated tracking.

Having created the potential for automated tracking with reflective markers, an algorithm for tracking with heuristics to manage occlusion (where a marker is obstructed and not visible) and correspondence (where a landmark must be identified from more than one foreground feature) should be developed.

Summary of approach:

- Use retroreflective tape for markers
- Fix markers to five defined sites on the body
- Cover markers with Opsite Flexifix tape
- Light the environment with halogen lights to maximise marker visibility

Errors:

- Mean error in take-off velocity of 0.03 m/s from the camera calibration process



- Mean error of 0.03 m/s and 0.06 m/s in hurdle step and standing take-offs, respectively
- Mean error of 0.06 m/s between measuring take-off velocity with 3-segment or 6-segment model.

## 7 Marker tracking

### 7.1 Introduction

It has been shown that a diver can be represented by a stick-figure and body-segment model describing the distribution of mass and segment mass-centres. Segments are defined by the position of segment-ends, whose location in each frame can be defined by the user with manual digitisation.

Manual digitisation of landmarks has limitations both in speed – an experienced user of the software can take up to seven minutes to digitise a dive – and the risk of both inter and intra-user inconsistency in digitisation accuracy. These limitations can be addressed with the implementation of an automated tracking process, using reflective markers as described in Chapter 6.

This aim of this chapter is to design and validate a method to track passive markers from which kinematic data is calculated. Tracking the flight path until the diver is approximately level with the board allows the computation of:

- Change in moment of inertia from take-off to tightest shape
- Change in angular velocity from take-off to tightest shape
- Rotational speed during somersaults in the flight phase
- Joint angles in the somersaulting shape
- Height at which each somersault is completed
- Height at which the diver opens from the shape
- Distance between closest landmark and diving board as the diver descends

These metrics were identified as matching and extending those calculated in related studies in the literature.

The method must track markers quickly enough that performance data can be shared with the diver and staff in the time taken for the diver to surface from the dive and receive feedback from the coach. Delayed video playback (presently used in high performance centres, where divers see a replay of their dive after each performance) are typically set to a twelve second to twenty second delay, therefore twelve seconds was selected as the limit to define 'quickly enough' for the tracking of markers.

Examples of marker tracking are shown in Figure 7-1.

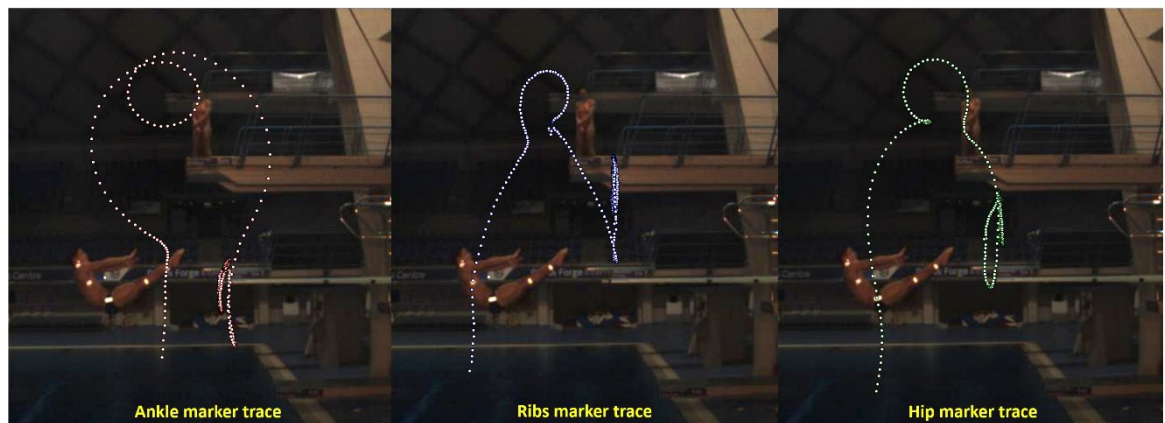


Figure 7-1. The paths of markers tracked through a dive.

The chapter describes the steps of image-processing required to automatically track motion and the methods designed to maximise efficiency and processing time. It defines methods to manage occlusion (where a landmark is not visible due to being blocked by a limb and so should have its position predicted) and correspondence (where more than one marker has the possibility of locating a single landmark).

It concludes with a study to measure the success of the tracking algorithm in a live training setting.

## 7.2 Methods

### 7.2.1 Introduction

Each frame of video must be processed with the aim of removing all background noise and leaving markers as the only foreground information in the image. This is achieved in both hardware (manipulation of camera settings) and in software, with the application of a series of image-processing filters; Aforge (2008) libraries were used as the source of these filters and for the blob counting and COM functions.

### 7.2.2 Camera exposure

The exposure setting on the camera defines the amount of time (in microseconds) light can be detected by the camera's sensor. A desirable exposure level is required that balances the ability for the diver and coach to see the athlete in the image while maximising the contrast between markers and background (Figure 7-2). Should this not be possible, a second camera could be used. This level should be subjectively selected by the user and may change depending on ambient lighting.

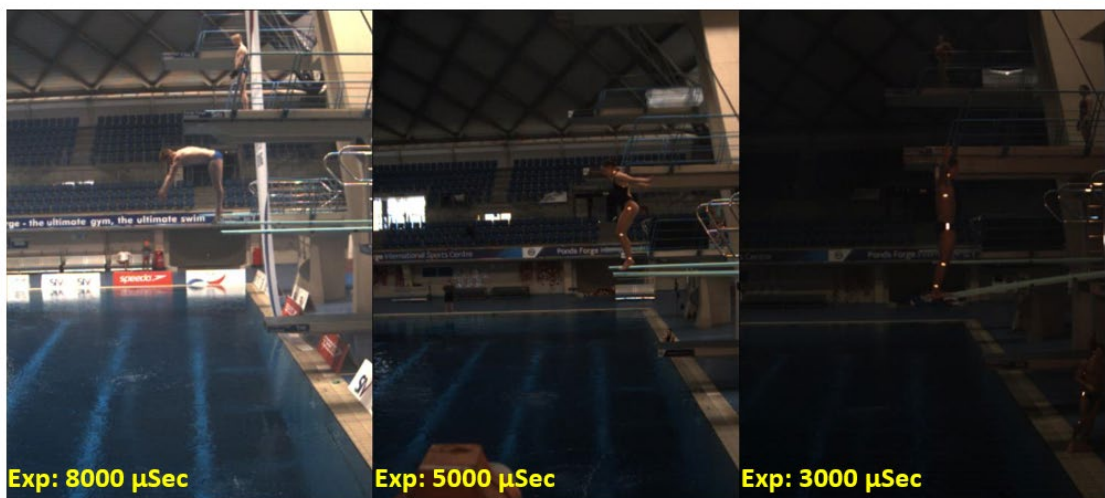


Figure 7-2. Reducing exposure time darkens the image and provides a different contrast between background and marker reflection.

### 7.2.3 Background subtraction

Extraneous noise in the image (reflections on the water, from handrails, lights etc.) has the potential to create error when locating and identifying reflective markers.

Background subtraction (Figure 7-3) is a process where pixel component-values (red, green and blue) from one image are subtracted from those from the corresponding pixel in another image.

To maximise the effect of background subtraction (by limiting the number of changes between foreground and background images), the background image is selected as the final image from the dive, when the diver is submerged. The process works to better effect when there are no other moving elements in the image (for example other divers) but this is not a critical condition as background athletes do not create high-

contrast noise in the image and their representation will be removed in further processing steps. Background subtraction is the first image processing filter used in the method.

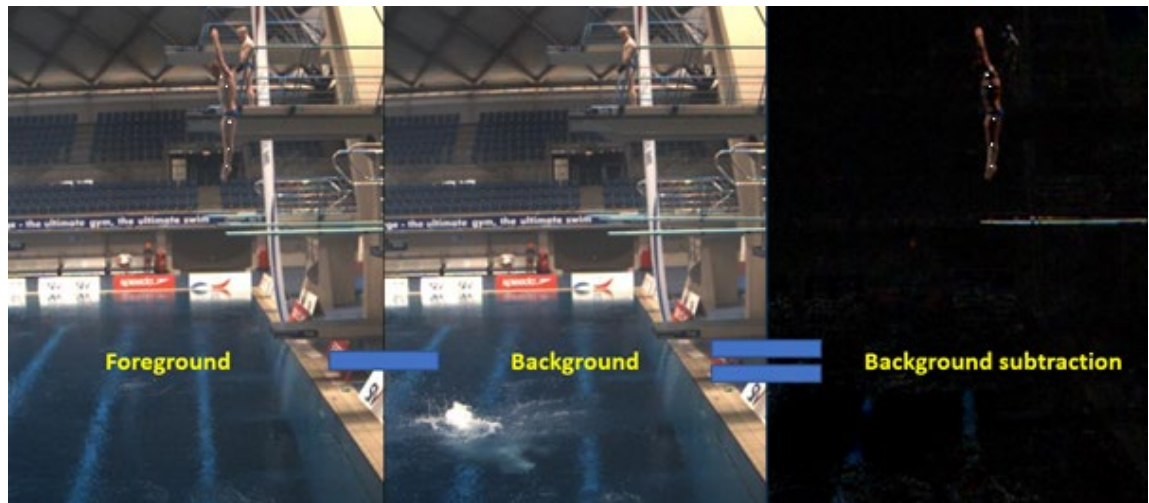


Figure 7-3. Background removal leaves the diver and minimal additional detail in the image for processing. Subsequent processing is required to isolate blobs as foreground detail.

#### 7.2.4 Conversion to grayscale

The Grayscale filter is used to convert a 24-bit RGB image into an 8-bit grayscale image (Figure 7-4). The luminance of each pixel (represented on a scale between black and white by a value between 0 and 255) is determined by applying weighting-coefficients to Red, Green and Blue components of the image. The Grayscale class in Aforge by default defines pixel luminance (L) as:

$$L = 0.2125L_R + 0.7514L_G + 0.0721L_B \quad [7-1]$$

where  $L_R$ ,  $L_G$  and  $L_B$  are the red, green and blue components of the pixel-colour (equation 7-1), respectively. The coefficients match those defined by the International Telecommunication Union (International Telecommunication Union, 2002) to derive luminance and reflect that human vision is most sensitive to green (the highest coefficient) and least to blue (the lowest coefficient).

The grayscale filter is the first software filter to be applied.

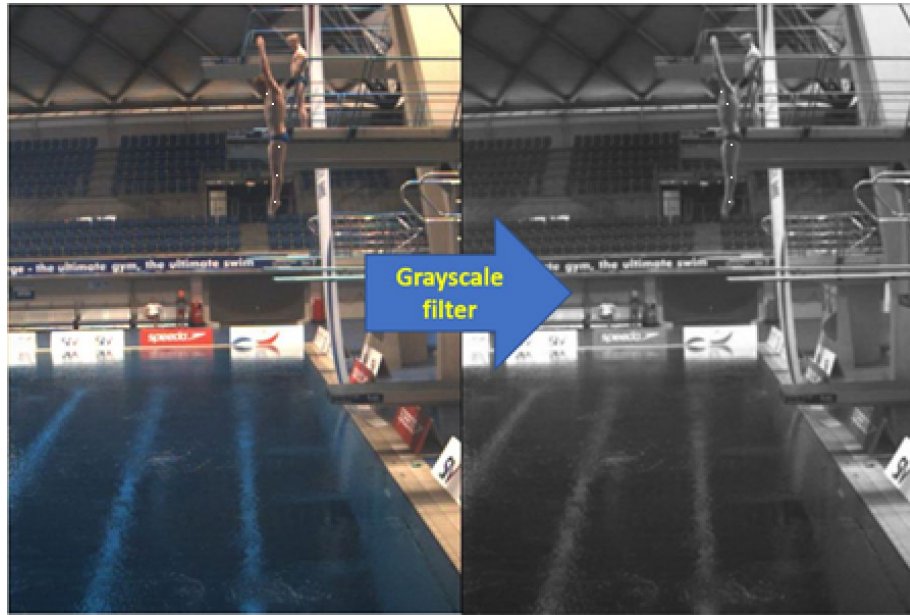


Figure 7-4. The grayscale filter converts a 24-bit RGB image to an 8-bit grayscale image.

### 7.2.5 Thresholding

A threshold filter converts a grayscale image to a binary image. A threshold value is used; pixels with a luminance below the threshold value are considered background and are represented in the binary image by black pixels. Pixels with a luminance at or above the threshold level are considered foreground detail and are coloured white. An example of a thresholding filter is shown in Figure 7-5.

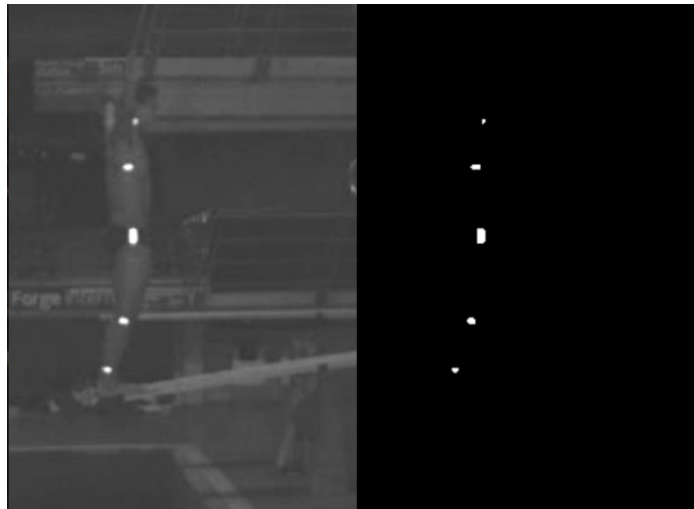


Figure 7-5. Background subtraction and a grayscale filter produces the image (left). A threshold filter leaves only blobs as foreground features.

A threshold value can be determined subjectively by the user or can be calculated with the implementation of an Otsu filter (Smith et al., 1979). Iterative examination of the effect of different threshold values allows the user to select a value to leave only marker reflections as foreground data. An Otsu filter calculates the optimum threshold level in an image, where optimal is defined as the lowest ‘within-class variance’ (where classes are defined as foreground and background based on the threshold value; variance in each class is calculated with pixel count weighted by the pixel count at each luminance level). An Otsu filter iterates through all possible threshold values and calculates variance of pixel-spread either side of the threshold value until the value with the lowest within-class variance is found.

The effect of thresholds selected by the user and calculated by an Otsu filter are shown in Figure 7-6.

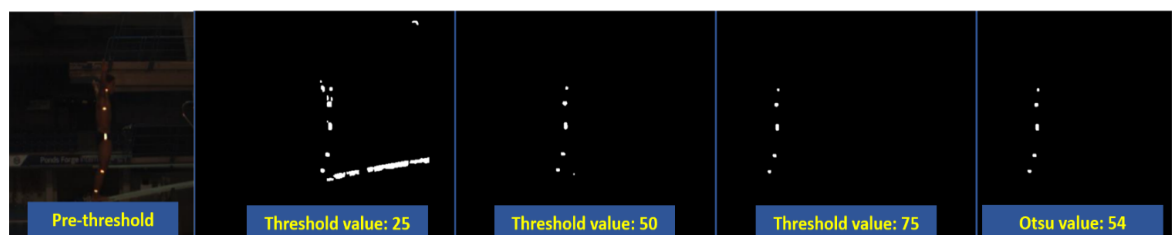


Figure 7-6. A thresholding function applied using manually-specified threshold values and a threshold value calculated using an Otsu filter. The Otsu filter effectively removes all features but blobs.

Experimentation showed that both manual selection and implementation of an Otsu filter effectively reduced the foreground pixels in the image to those representing the reflective markers. The use of the Otsu filter allowed the automation of the image processing series and was selected as the default method.

The use of this series of filters results in background (all detail except marker) removal as shown in Figure 7-7.

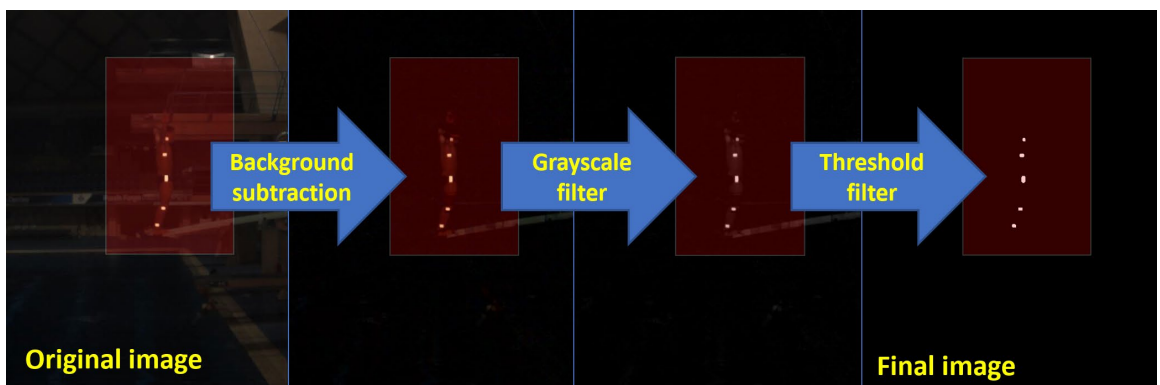


Figure 7-7. The series of processing filters reduces the image to markers against a black background as required.

Aforge orders groups of foreground pixels ('blobs') in ascending order of the y-coordinate of the blob-centre (Figure 7-8).

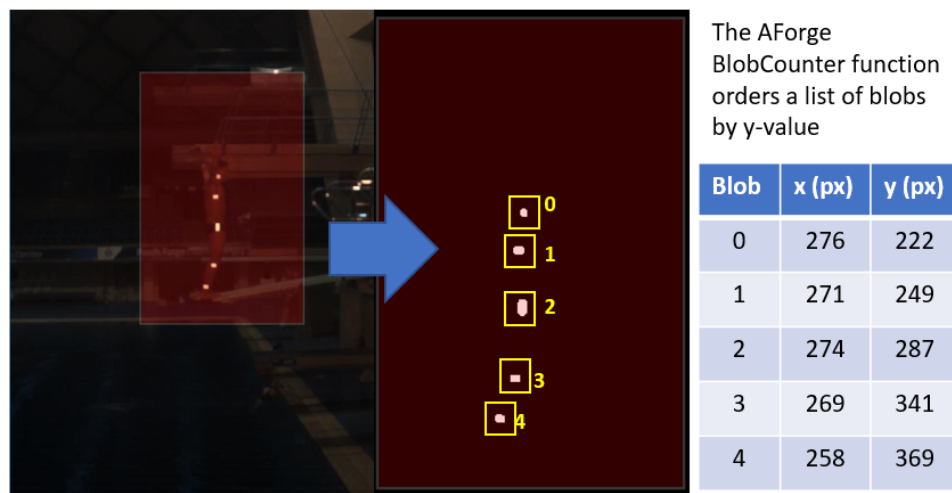


Figure 7-8. Markers reduced to a list of white-pixel groups ('blobs'). The red rectangle is the window defines the area to be searched for blobs and can be set by the user.



### 7.2.6 Starting frame and pose estimation

As described in Chapter 2, known starting conditions (pose and approximate location of the diver) support accurate marker identification. An assumption is made that divers will begin their skill upright with the ankle marker lowest in the image and the head marker highest, a consistent feature of all springboard dives. Using this assumption, the list of blobs can be attributed to landmarks in the following order: neck, ribs, hip, knee, ankle (Figure 7-9).

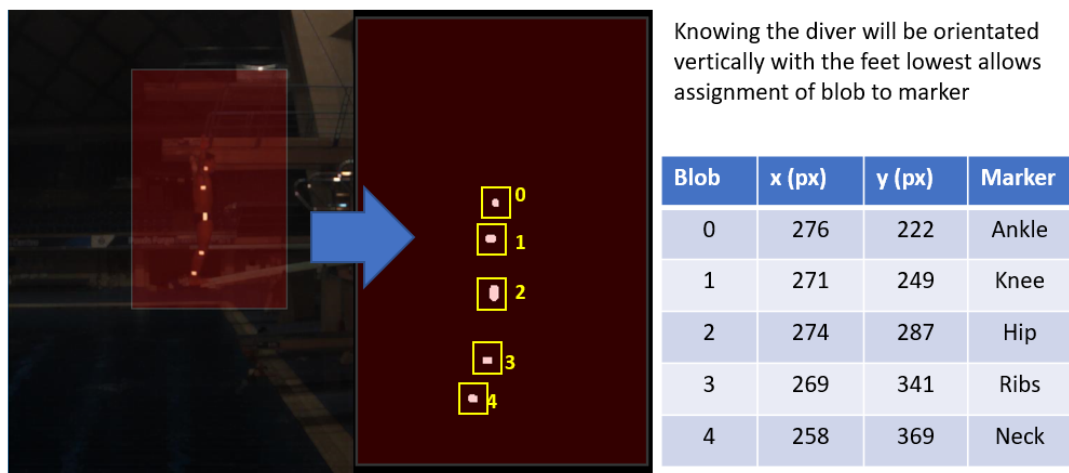


Figure 7-9. Knowing the initial pose of the diver allows the identification of landmark by ranking blob-height.

This attribution only holds if the expected number of blobs is detected in the image. If one marker is occluded there is no way to identify the missing marker. For this reason, the method iterates from the first frame until five markers are located (Figure 7-10), this frame is designated the starting frame.

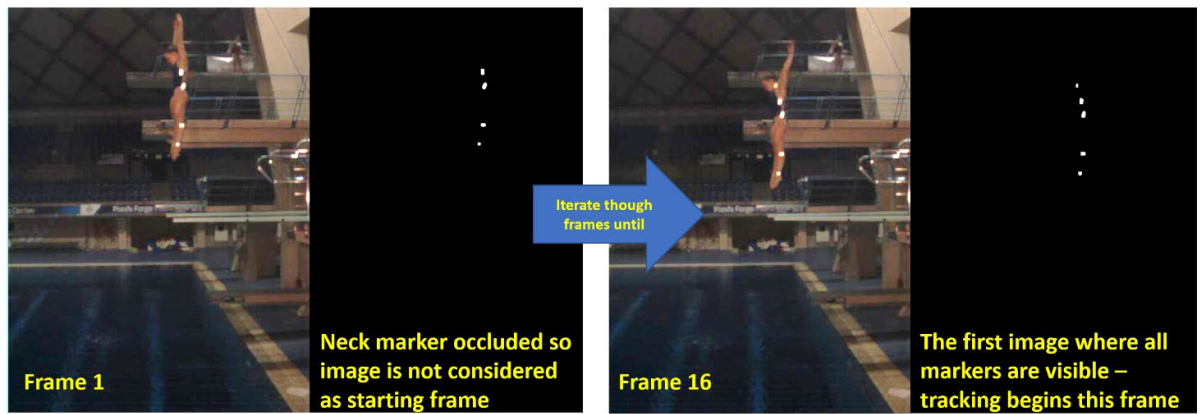


Figure 7-10. Each image is processed until five markers are detected in the image; this frame is designated the 'start of tracking' frame'.

### 7.2.7 Tracking movement

Processing all frames in the sequence using the method described above has limitations in both logic (safe assumptions) and speed. As the diver moves from the starting pose and subsequently rotates by more than 90 degrees, assumptions about the vertical order of markers no longer hold and heuristics are required to identify landmarks from markers.

The chosen method for tracking markers uses the assumption that a marker can only move by a limited number of pixels between frames – limited by the speed of movement of the human body, limb-length, resolution (488 x 656 px) and the framerate of the video (80 Hz). Markers with greater distance from the centre of mass have the capacity to move by a larger distance compared to markers close to the COM.

Crop-windows are defined as areas of image surrounding each marker. The optimum dimensions of the crop window maximise the probability of the marker staying within the crop window in the next frame and minimises the probability of another marker encroaching into the same area of the image. A marker in frame  $n+1$  will be searched for in the crop-window surrounding the marker in frame  $n$  (Figure 7-11).

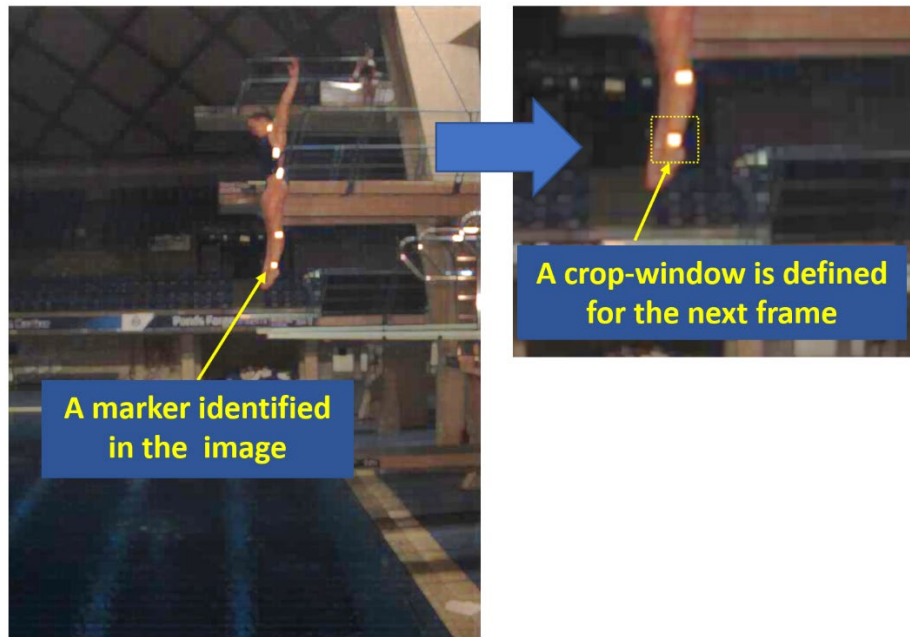


Figure 7-11. Crop-windows are created to reduce image-processing time and to simplify the assignment of landmarks to markers.

When landmarks have been identified in frame  $n$ , a window of pixels is defined around each with the expectation that in frame  $n+1$  the marker will still be visible. Assuming a marker is visible in that window, it is assumed to be the same landmark as in frame  $n$ . The crop-window is redefined for each marker and the process is repeated in frame  $n+2$ . This process is shown in Figure 7-12.

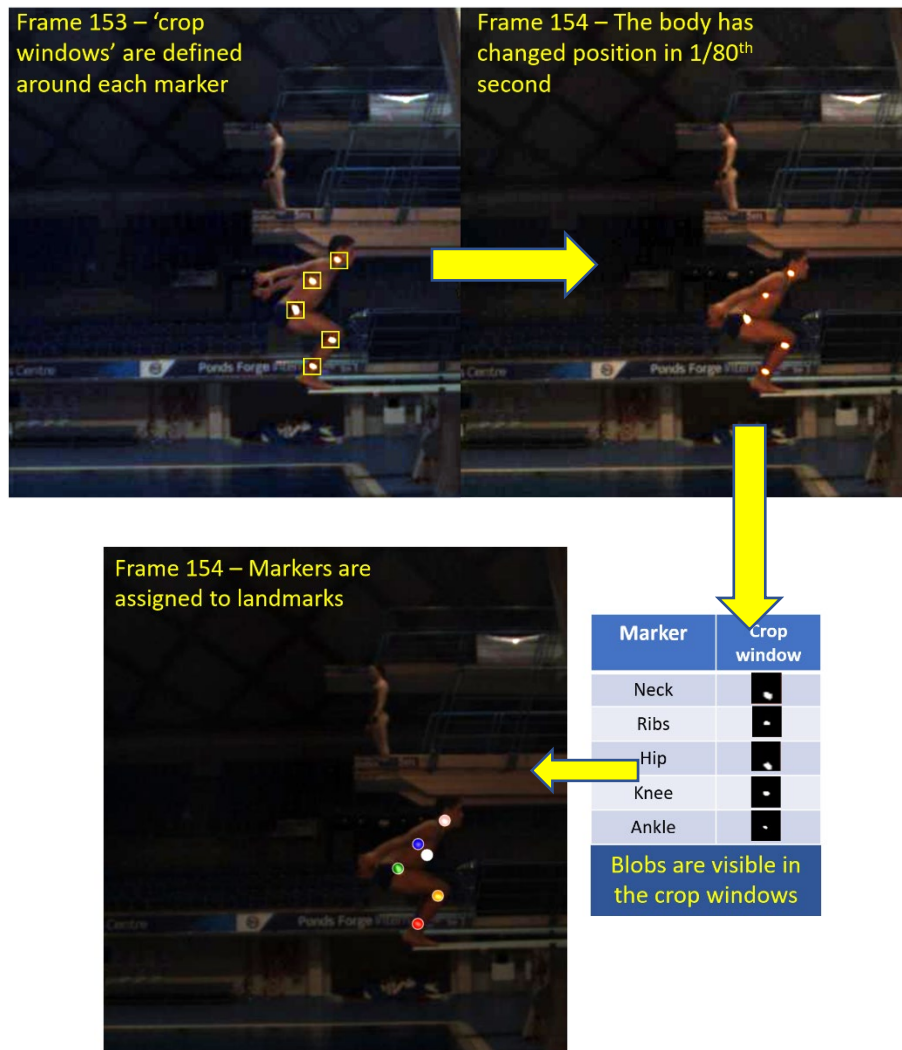


Figure 7-12. A crop-window is created around each landmark – this window reduces the area in the successive frame in which the corresponding marker is searched. The white circle below the ribs is the calculated position of COM.

### 7.2.8 Correspondence

This method of marker assignment requires adaptation under the condition of correspondence. Should two markers occupy the same crop window (Figure 7-13), a calculation is made to determine landmark identification.

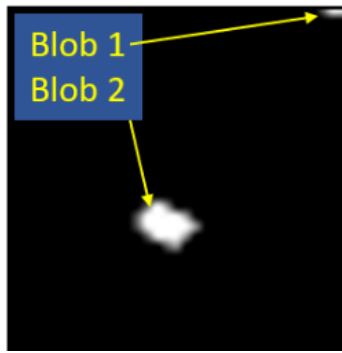


Figure 7-13. Elements of two markers may appear as blobs in one crop window. This requires a method for identifying the correct blob/marker which represents the landmark.

Three methods were considered for blob-selection.

1. A selection based on area (number of pixels in each blob). It was assumed that any other marker visible in the crop-window would encroach by only a few pixels, and the desired marker would appear as full-size and a therefore a larger area. Experimentation showed occasions when markers produced a smaller blob (likely due to the orientation of the segment with respect to the lighting and the camera) than the incorrect one, resulting in, for example, the knee being mistaken for the ankle. Consequently, this method was discounted.
2. To calculate segment lengths using an adjacent marker from the previous frame and both the markers visible in the crop window. The assumption was that even when accounting for the translation of the known marker from one frame to the next, the correct marker would have a segment-length closer to that calculated in the starting frame than the other. Trials showed that this was an unsafe assumption. For example, in a tight tuck shape, the hip and ankle markers could be a similar distance from the knee marker and be misidentified for any (or a combination of) the following reasons:
  - a. The size of the blobs could vary due to orientation to lighting and influence the landmark position (determined by COM of the blob) and therefore segment length.
  - b. Segment length calculation is influenced by the calibration parameters and reconstructions made in different parts of the image.
  - c. The anatomy of the diver could lead to segments of similar lengths.

For these reasons, this method was discounted.

3. Experimentation with dives from all sampled athletes showed that the most consistently accurate method (in terms of the number of correctly-assigned blobs to landmarks) was to calculate the distance of each visible marker from the centre of the crop-window, with the nearer marker selected as representing the desired landmark. The assumption was that the landmark would not change position in  $1/80^{\text{th}}$  second so much than an incorrect marker would be detected close to the desired landmark's last-frame location. This method resulted in correct match between marker and landmark in all trials and was therefore implemented in the automated tracking process.

#### 7.2.9 Occlusion and landmark prediction

When swinging the arms or transitioning into or out of a tuck or pike shape, body-markers are likely to be occluded by the arms. In this instance, a landmark location must be predicted, otherwise a COM location cannot be calculated, and a crop-window can't be defined to seek the marker in the next frame. At points in the dive, prediction may be required should a marker fail to produce a reflection bright enough to remain as a blob following image processing.

A method of prediction was designed that assumed that joint angles would not significantly change between one frame and the next and that segment lengths were known (segment lengths could be calculated in any frame where both markers were visible).

The markers required for landmark prediction are listed in Table 7-1.

Table 7-1. Each landmark can be predicted if a pair of markers have been detected in the image.

Missing landmark	Markers required for prediction	Joint
Ankle	Knee and Hip	Knee
Knee	Hip and Ribs	Hip
Hip	Ankle and Knee or Ribs and Neck	Knee or Rib
Ribs	Hip and Knee	Hip

Landmark-location prediction is only used when the required adjacent markers were located due to their visibility in the appropriate crop-marker (and were therefore ‘found’ as opposed to ‘predicted’), a decision was made to not predict landmarks using other predictions.

Figure 7-14 shows an example of a marker becoming occluded by the path of the arms as a tuck shape is adopted.

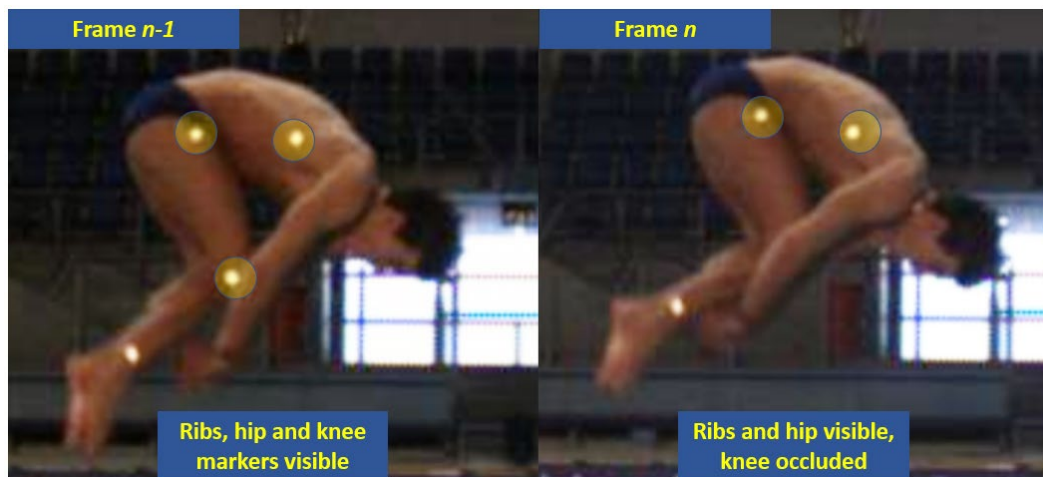


Figure 7-14. A marker can become occluded between one frame and the next, requiring a prediction of position.

Prediction of the knee-marker location requires the calculation of segment lengths (hip to ribs and hip to knee) in frame  $n-1$  with the size of the interior angle at the hip (Figure 7-15).

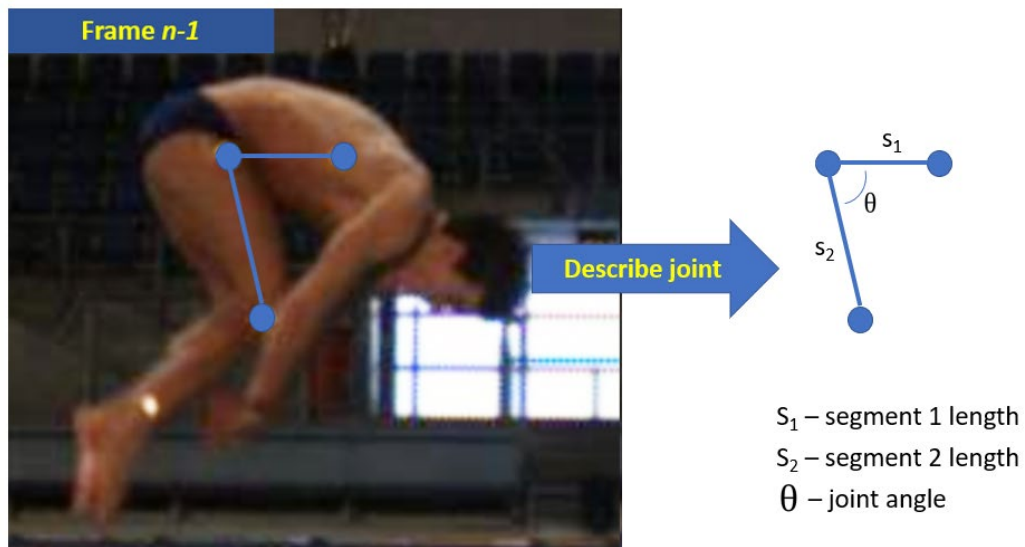


Figure 7-15. Segment lengths and interior angle are required for marker prediction.

The predicted marker location is then calculated with the same distance from (in this example) the hip marker in frame  $n$  with the same interior angle. Two positions are calculated with an interior angle of  $\theta$ , rotated in opposite directions (calculation of the interior joint angle does not identify the direction of rotation between each segment) as shown in Figure 7-16.

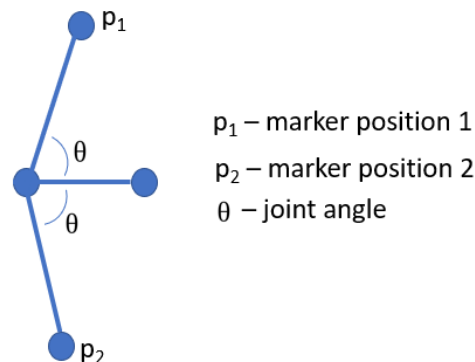


Figure 7-16. Two locations are calculated as potential marker positions

A test to find the location closer to that of the marker in frame  $n-1$  identifies the correct potential position (in the example above,  $P_2$ ). The predicted position is shown in Figure 7-17. A successfully predicted marker will be re-identified when it is no longer occluded in subsequent frames.



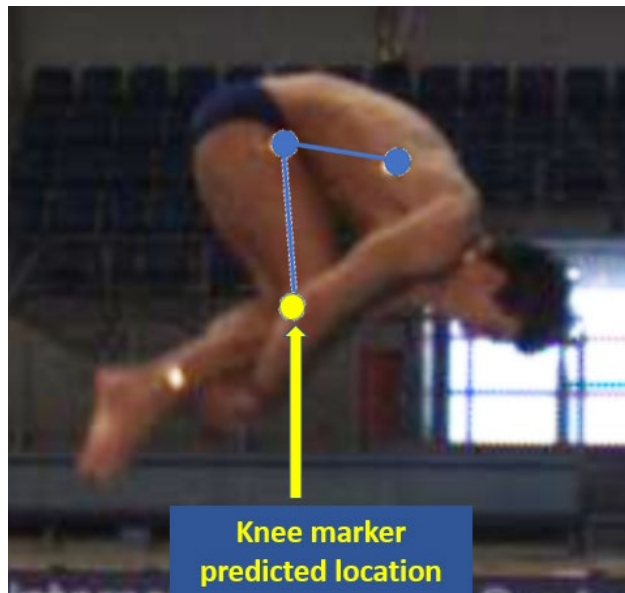


Figure 7-17. Marker location is predicted for the calculation of COM and kinematics.

#### 7.2.10 Tracking termination

Tracking is terminated when one of the following conditions is met:

1. The last frame of the video has been processed.
2. The landmark-prediction function cannot be used due to the lack of 'known' adjacent markers in the image.
3. One marker has been predicted over a threshold number of successive frames. Repeated predictions without detection limits the tracking accuracy. For this reason, a maximum number of successive predictions for each marker results in tracking ending.

Although tracking the whole dive is advantageous, many performance variables can be calculated with a small number of frames. Should markers be accurately tracked between frame  $n_{T-2}$  to frame  $n_{T+2}$  where  $n_T$  is the point of take-off, analysis of the COM-position in these frames allows estimation of:

- Take-off velocity
- Trajectory of COM
- Maximum height attained
- Distance of COM from board as diver passes the board during descent
- Flight time

These data provide comparative metrics to those found in existing studies and inform elements of What It Takes to Win. A greater amount of performance data can be inferred with landmarks tracked over more frames. Tracking the flight path until the diver is approximately level with the board allows the computation of metrics described in the introduction to this chapter and provide more sensitive analysis of the whole dive and reflect information required to answer performance questions raised by multi-disciplinary teams in British Diving.

### 7.3 Examples

Figure 7-18 shows key frames with tracked markers illustrated.

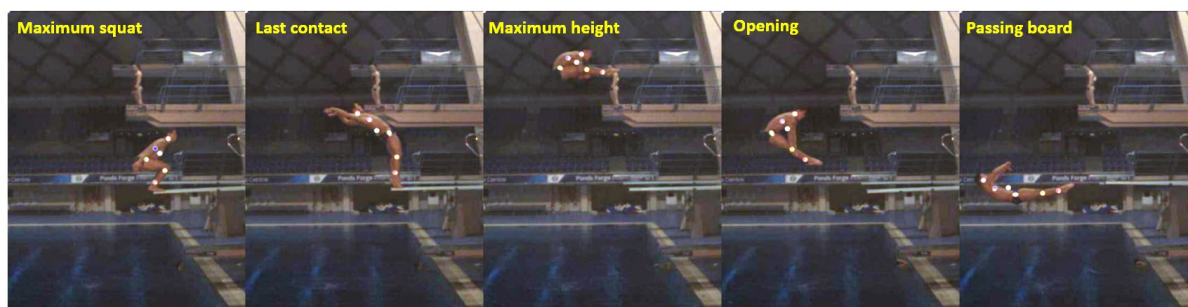


Figure 7-18. Key frames in a dive showing tracked markers.

*Maximum squat* is a key-frame due to empirical observation of the relationship between a deep squat and the take-off velocity, and height subsequently attained by the diver. The *Last contact* key frame provides data about the lean at take-off – an influence on the height and distance attained and the speed with which the diver can adopt a tight shape during rotation. *Maximum height* is important as a measure of virtuosity and the ability to earn high scores from judges. The *Passing the Board* key-frame quantifies COM distance to assess distance (and safety, if the value is low) to enhance judge score.

Figure 7-19 shows the traces of specific markers through the dive.

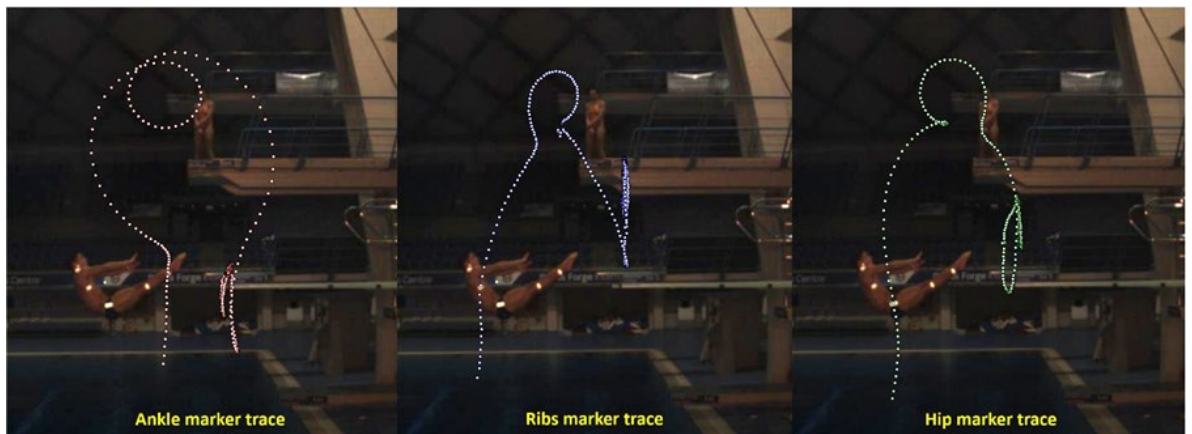


Figure 7-19. The dots show the position of specific landmarks in all frames of automated tracking.

## 7.4 A study to assess the performance of the automated tracking process

### 7.4.1 Introduction

The effect of the tracking function was tested on a series of dives captured in a training session.

Automated tracking is defined in this study with increasing levels of success as follows:

- Unsuccessful – landmarks cannot be tracked during take-off
- Moderately successful – landmarks are accurately tracked during take-off and up to 0.05 seconds of flight. From these data, a minimum set of performance data can be estimated (take-off velocity, maximum displacement and height, horizontal distance from the board and flight time)
- Successful – landmarks are accurately tracked beyond the top of the flight path. A best-fit curve can be fitted around these points giving greater accuracy to the data described in the point above, allows calculation of the best body-segment model to represent the diver and provides key frames from which somersault speed can be calculated.
- Perfect – all markers are tracked accurately in all frames. These data allow all performance metrics defined in Chapter 9 to be calculated.

#### 7.4.2 Method

Two divers performed a total of 26 dives (Table 7-2). The skills performed reflected 10 unique skills covering 4 groups. The automated marker-tracking process was implemented for each dive. The algorithm tracked until it met a stopping condition as follows:

- Too few markers were found to predict those missing (Table 7-1 defines the markers required to make a prediction of a single missing landmark)
- A marker had been predicted for a threshold number of frames, indicating a lack of accuracy in COM-position over time.

The level of success of the tracking algorithm was subsequently assessed.

#### 7.4.3 Results

The results of the study are shown in Table 7-2, below. An example of a COM-trace from automated tracking is shown in Figure 7-20. Images showing the COM-path for each skill are shown in Appendix A.

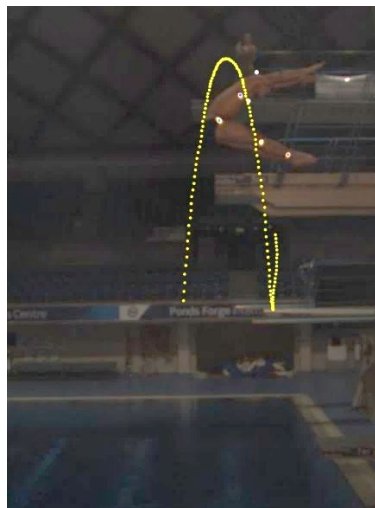


Figure 7-20. The path of the COM during take-off and flight calculated with automated tracking.

Table 7-2. The results of running the automated tracking method on a range of dives. The maximum number of frames in one video was 400. 'Post-TOF?' refers to frames after the top of the flight path. Highlighted rows indicate dives in which some success-measures were not achieved.

Time	Dive	Description	Flight tracked (s)	Take-off tracked?	Post-TOF tracked?	Max deflection	Max squat	#Frames tracked	Tracking summary
11:02:43	020b	Back pike roll	0.63	Yes	Yes	n/a	n/a	331	Successful
11:05:46	200b	Back jump, piked	1.11	Yes	Yes	Yes	Yes	289	Successful
11:07:05	200b	Back jump, piked	1.16	Yes	Yes	Yes	Yes	290	Successful
11:08:43	201b	Back dive, piked	1.18	Yes	Yes	Yes	Yes	278	Successful
11:10:16	201b	Back dive, piked	1.19	Yes	Yes	Yes	Yes	293	Successful
11:11:39	201b	Back dive, piked	1.15	Yes	Yes	Yes	Yes	274	Successful
11:13:17	201b	Back dive, piked	1.20	Yes	Yes	Yes	Yes	272	Successful
11:14:45	205b	Back 2.5s/s, piked	0.89	Yes	Yes	Yes	Yes	265	Successful
11:16:52	205b	Back 2.5s/s, piked	0.95	Yes	Yes	Yes	Yes	251	Successful
11:18:39	205b	Back 2.5s/s, piked	0.98	Yes	Yes	Yes	Yes	277	Successful
11:20:41	205b	Back 2.5s/s, piked	0.86	Yes	Yes	Yes	Yes	262	Successful
11:22:43	205b	Back 2.5s/s, piked	0.94	Yes	Yes	Yes	Yes	261	Successful
11:24:39	403b	Inward 1.5s/s, piked	0.51	Yes	No	Yes	Yes	237	Moderate
11:25:55	403b	Inward 1.5s/s, piked	1.10	Yes	Yes	Yes	Yes	284	Successful
11:27:05	403b	Inward 1.5s/s, piked	1.09	Yes	Yes	Yes	Yes	284	Successful
11:28:48	403b	Inward 1.5s/s, piked	0.40	Yes	No	Yes	Yes	220	Moderate
11:36:49	407c	Inward 3.5s/s with tuck	0.07	Yes	Yes	Yes	Yes	254	Successful
11:38:55	407c	Inward 3.5s/s with tuck	0.24	Yes	No	Yes	Yes	238	Moderate
11:41:39	407c	Inward 3.5s/s with tuck	0.36	Yes	No	Yes	Yes	245	Moderate
11:03:41	100a	Forward jump, straight	0.69	Yes	Yes	Yes	Yes	109	Successful
11:06:24	100a	Forward jump, straight	0.41	Yes	No	Yes	Yes	154	Moderate
11:07:55	103b	Forward 1.5s/s, piked	1.15	Yes	Yes	Yes	Yes	143	Successful
11:12:18	5132d	Forward 1.5s/s, 1 twist, free	0.18	Yes	No	Yes	Yes	60	Moderate
11:20:05	5152b	Forward 2.5s/s, 1 twist, piked	0.58	Yes	Yes	Yes	Yes	92	Successful
11:31:46	107b	Forward 3.5s/s, piked	0.55	Yes	Yes	Yes	Yes	109	Successful
11:33:34	107b	Forward 3.5s/s, piked	0.63	Yes	Yes	Yes	Yes	176	Successful

Dives in a range of groups with a range of complexity could be tracked. In general, easier dives (with fewer changes in body shape and less rotation) were tracked for longer. No dives were tracked perfectly, with markers in all frames to the point of entry tracked.

100% of dives were tracked to at least a moderate level of success – tracking past take-off and allowing the calculation of flight path parameters based on change of COM-position during take-off. 77% of dives were tracked to a standard defined as successful – providing COM reconstructions over enough of the flight path that a parabola could be estimated from which performance data could be calculated. In all dives, all markers in the frames of maximum squat and maximum deflection were correctly identified, providing the opportunity to calculate performance data linked to flight and rotation parameters.

Inward-rotating skills were tracked with the least success. In some instances, the diver obstructed the view of the knee marker for so long that the algorithm exceeded the number of acceptable predictions of a single marker. In the case of 407c (inward 3.5

somersaults), the high degree of angular momentum contributed to markers being 'lost' as the diver achieved great angular velocity.

Some skills (5132d, forward 1.5 somersaults with 1 twist) rate as 'moderately' successful although the algorithm tracked the skill for as long as possible. When the diver initiates the twist, the body begins to rotate around the longitudinal axis. After approximately 90° of twist rotation has occurred, markers cannot be in view. The algorithm is therefore limited in potential for some twisting dives. For other twisting dives (see 5152b, forward 2.5 somersaults with one twist, above) the twist is performed in the second somersault, during the descent from the top of the flight path. For these skills, 'successful' tracking can be achieved despite the longitudinal rotation.

Visual inspection of the marker-traces revealed that the marker needing prediction with greatest frequency was the neck marker. The arms should be overhead and covering the ears in forward and inward take-offs and should be above the head and covering the ears during preparation for entry and entry. These conditions required frequent prediction of the neck marker, with a large crop-window allowing the marker to be re-acquired when visible.

The rib marker needed frequent prediction due to its occlusion during an armswing and when attaining a tuck or pike shape. These conditions had a smaller impact due to the rib marker not being used to calculate COM, but it was nevertheless important to re-acquire the marker accurately in order to predict the neck marker later in the dive.

#### 7.4.4 Discussion

It was shown that dives with a variety of performer, shape, direction of rotation or difficulty (and speed of rotation) could be automatically tracked. Most dives could be tracked until the descent phase (dropping from the top of the flight path). The amount of marker data captured to that point can be used to estimate many flight parameters as well as take-off parameters (such as board deflection, speed of leg-extension and change in trunk angle) before the flight phase.

The most common landmark to need prediction was the neck, owing to correct technique placing the arms straight and above the head (therefore occluding the neck marker) for periods of take-off and entry.

Dives were never tracked until entry and submersion; lighting was positioned to capture movement above and around the level of the board and marker reflections were less bright between heights of 0m and 1.5m. As the arms were generally in the entry position close to the water (with the neck occluded), if either rib or hip marker were not identified, the prediction cannot be made and tracking ends.

The feedback cycle allows approximately twelve to twenty seconds (with twelve seconds defined as a threshold value for tracking) between entry and video replay; the diver must decelerate under the water, surface and get feedback from the coach before watching the replay. All videos were tracked in less than this time, ensuring that the provision of performance data in training does not have a detrimental effect on training rate.

Without 'perfect' tracking accuracy and considering the limitations of a three-segment model to represent the body and the possibility of COM-error due to marker prediction, automated tracking is not proposed as an optimal method from which to calculate performance data. It is, however, a method to produce data quickly which can give an indication to the coach of the objective performance of a dive (and compare to other repetitions) in that, or previous, training sessions. Should a metric (board deflection, velocity, height etc.) change when measured with automated tracking, the difference can (subject to the size of the change) be accepted as a real difference in performance. Over time, results from automated tracking and manual digitisation can be compared to give an indication of the link between data from each.

## 7.5 Summary

Limitations of manual digitisation were identified as the time cost to produce performance data and the risk of digitising error compromising the accuracy of COM-reconstruction. A proposed solution was the design and implementation of an automated marker-tracking algorithm.

Image processing, pose-estimation and heuristics to manage occlusion and correspondence have been considered and methods proposed to overcome challenges in marker recognition and tracking.

An automated process has been implemented and has been shown to track dives performed by a range of divers in different shapes, directions and of differing complexity with a quantifiable degree of success.

'Moderate success', defined as tracking the diver past take-off for long enough for many of the metrics presented in comparable studies in diving (Section 2.5, Figure 2-7 and Figure 2-8) to be calculated, was achieved in 100% of dives analysed. 'Success', defined as markers being tracked until the COM of the diver had passed the peak of the flight path – where metrics are calculated with greater accuracy – was achieved in 77% of the dives analysed.

Analysis of the success of the tracking algorithm indicates that it provides a unique solution to the calculation of performance metrics in a training environment, although manual digitisation will (with an inherent time cost) produce data with greater accuracy due to the larger number of segments in the model representing the diver.



## 8 'diveTracker' software tool

### 8.1 Introduction

Analysis of video data and production of feedback to the user is typically achieved using a software tool. Off-the-shelf software tools exist to perform this task and were considered for use in the study. Chapter 2.9 concluded that there were no existing tools that supported all the following features:

- Planar calibration
- Constant streaming from a machine vision camera
- Support for multiple body-segment models

Methods have been described to calculate performance metrics for dives with greater processing speed and accuracy than has been shown in the literature. Chapters 3 and 4 described the implementation of a planar calibration method to reconstruct world coordinates with a high level of accuracy from any part of the image. Chapter 5 showed the need to represent the body with a range of body-segment models with a process to select the optimal model for each diver. Chapters 6 and 7 described a method for landmark tracking via an automated marker tracking process. With no software tool on the market to implement these methods, a gap in practice therefore exists – a method for calculating performance characteristics of dives and communicating these data to the diver and support team in an accurate and time-efficient manner.

The diveTracker tool (Figure 8-1) was developed by the author to support the user to analyse dives and produce kinematic data using the methods listed above. The aim of this chapter is to describe the tool, the new practice undertaken by the World Class Programme and its members, the kinematic data generated from it, and the use of these data.

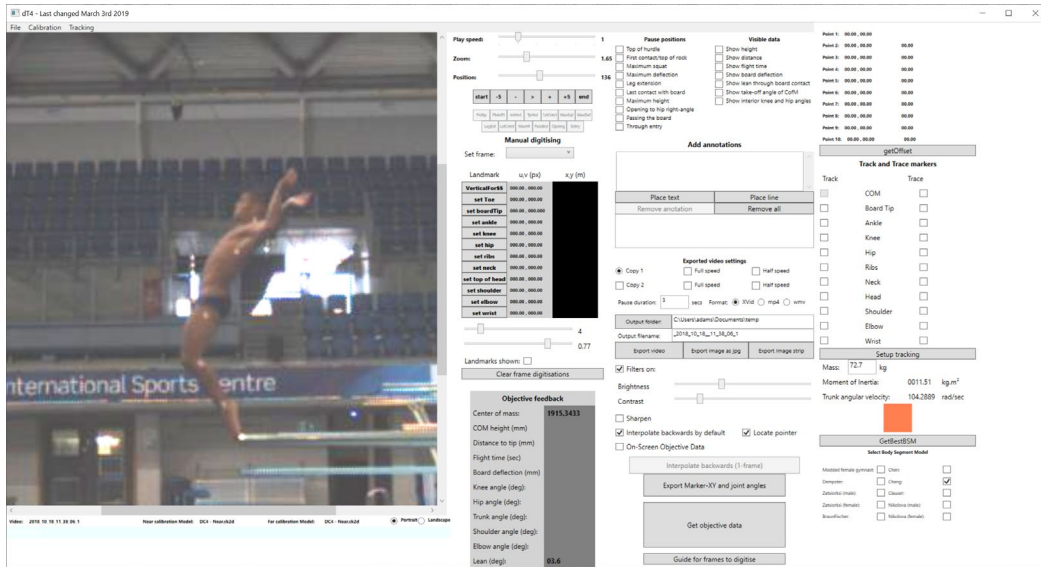


Figure 8-1. The diveTracker tool implements the methods used to produce kinematic data describing diving performance.

## 8.2 Implementation of methods

### 8.2.1 Calibration files

Chapters 3 and 4 described a method for calibrating a view of a diving scene in order to reconstruct world coordinates with greatest accuracy. Calibration files generated in Check2D are selected by the user to reconstruct world-coordinates from points in the image (Figure 8-2).

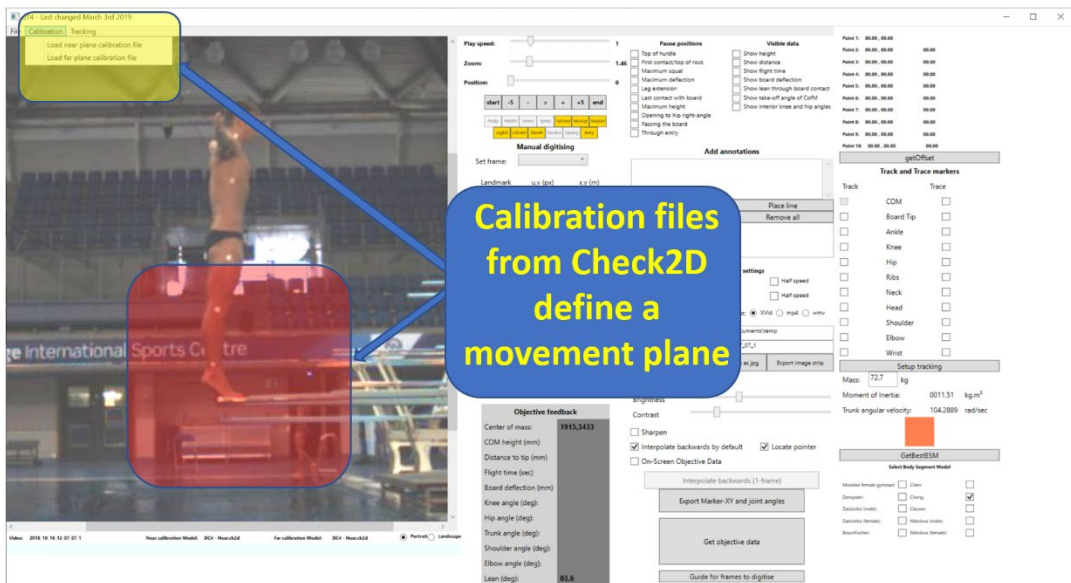


Figure 8-2. Calibration files selected to represent movement planes on all boards in the scene. The red box illustrates the plane in which the diver will perform a skill.

## 8.2.2 Landmarks

Landmarks of interest (representing segment ends and the tip of the diving board) are defined in the tool. Manual digitisation of these landmarks (or automatic tracking of markers) produces screen and world coordinates (Figure 8-3). In some circumstances, landmarks facilitate the measurement of segment positions and joint angles. In others, landmarks define key points of the dive (for example the smallest  $y$ -value of the board-tip coordinate defines the point of maximum deflection).

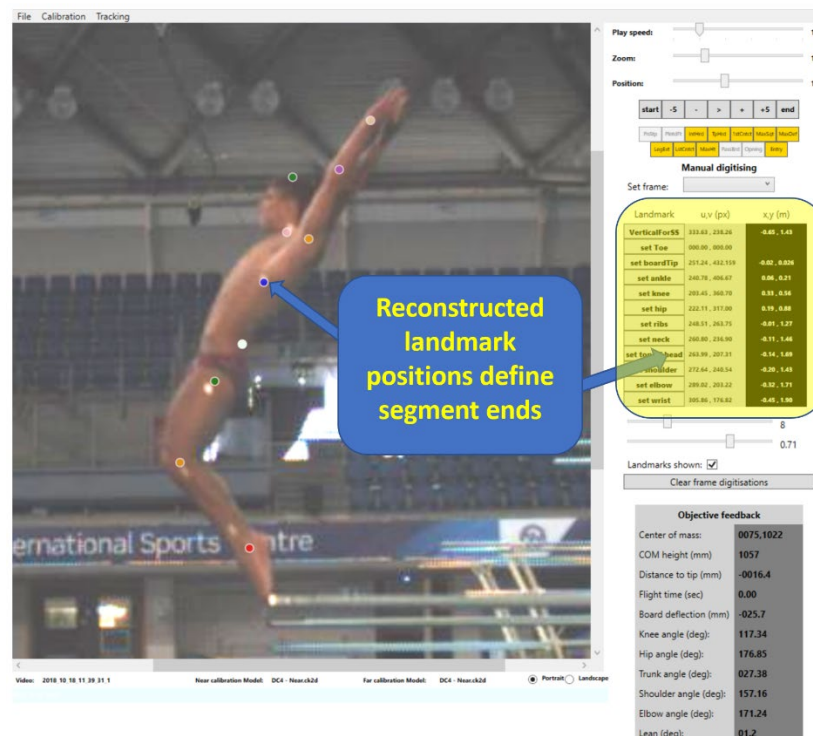


Figure 8-3. Segments are defined by landmarks digitised by the user or from automated marker tracking. The panel highlighted yellow displays the  $(u,v)$  and  $(x,y)$  coordinates of each landmark digitised.

Efficiency and speed of manual digitisation is enhanced by the tool constraining the number of landmarks required, providing a guide for consistently locating landmarks (via 'tooltips' – text that appears when the user hovers over the digitisation button of each landmark) and automatically assigning mouse-clicks to landmarks in sequence (from board-tip to wrist).

### 8.2.3 Body segment models

Models defined in Chapter 4 are available for selection by the user. The best model, defined as the model which results in COM-positions during the flight of the dive most closely fitting a parabola, can be calculated from within the tool (Figure 8-4).

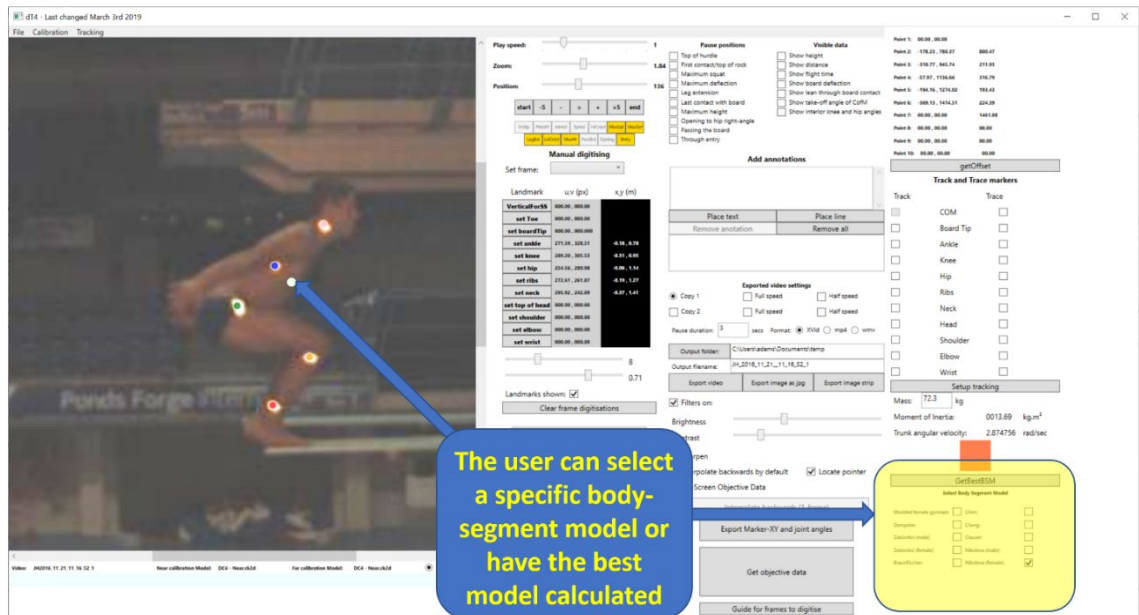


Figure 8-4. The most appropriate model for the diver can be calculated or manually selected by the user. The panel highlighted in yellow contains the range of models from which a choice can be made.

A limitation of existing tools and research is the assumption that all subjects can be accurately reflected by a single body-segment model. It has been shown that the individual morphology of divers leads to a variety of height, mass and mass distribution. The ability of diveTracker to match a model to a diver gives a closer estimation of the change in COM through a dive and provides more accurate data to the diver, coach and support team, giving better data from which to make decisions.

### 8.2.4 Automated marker tracking

Automated marker tracking reduces the time taken to track landmarks through a dive from approximately seven minutes per dive to under five seconds per dive. Although there is a reduction of accuracy (a mean difference of 2.4% when comparing maximum displacement and mean difference of 0.06 metres per second) when calculating the

position of the COM due to the implementation of a three segment model compared to the six segment model used in manual digitisation, the ability in diveTracker to provide close-to instant feedback to the user – with consistent data that can be compared to that of manual digitisation at a future point – gives an opportunity to provide objective feedback for divers that does not exist with any other tool.

Controls are available for the user to automatically or manually select components of an image-processing sequence. Contrast threshold value and the area of image containing the end of the board and the diver can be easily set and this maximises the speed and accuracy of the tracking algorithm (Figure 8-5).

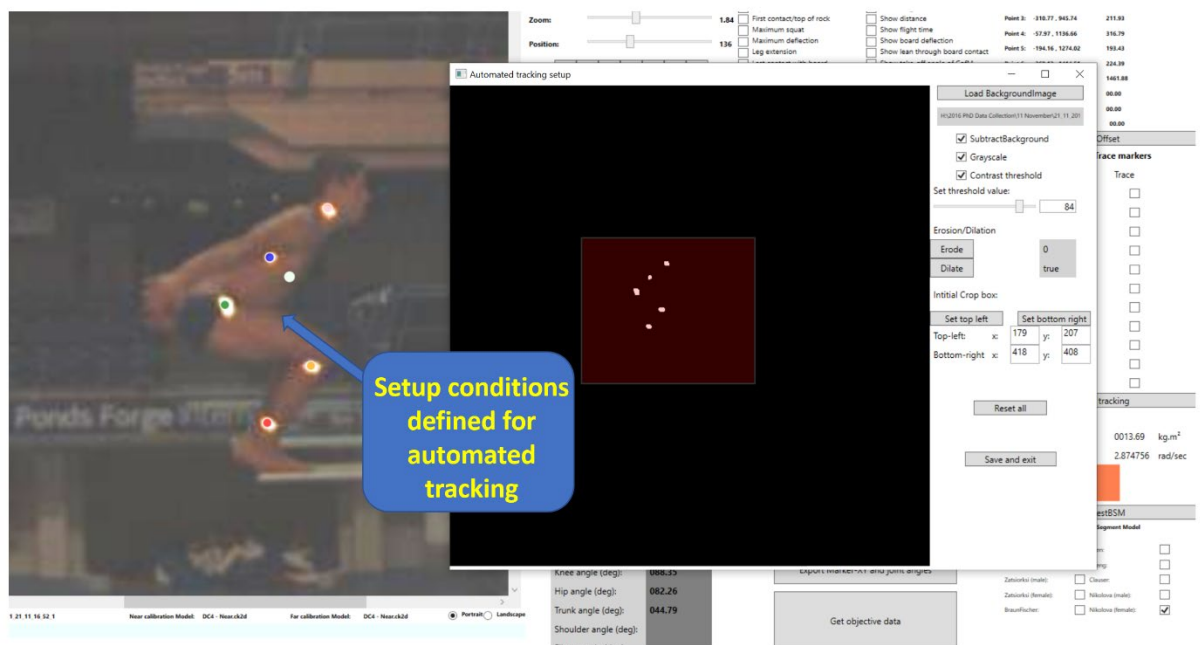


Figure 8-5. Automated tracking can be set-up by the user to optimise the performance of the algorithm. The white dots in the red square show the result of the image-processing algorithm, reducing the image of the diver to the markers designating each landmark.

The increase in processing speed creates a unique environment where data is available between repetitions of a skill and can be presented with no slowdown in training; the additional data available to the diver and coach adds to the subjective opinion of the coach and the ‘feeling’ achieved by the diver. The kinematic effect of making a change based on a coaching point can be assessed immediately, enhancing the understanding of what works for an individual diver.

## 8.2.5 Key-frames

Specific points of the take-off and flight – and the body’s transition between them – are commonly used by coaches for qualitative analysis. Presenting the diver’s posture to the athlete and team with associated kinematic feedback provides additional insight for decision-making about coaching points, and shows progression towards an ideal position over time. The performance data relates the preferred postures to overall improved performance or validates a different approach for the individual should the textbook technical model lead to reduced performance.

The user interface of diveTracker was designed to align use of the tool to the areas of focus described in the British Diving Single System ('BDSS', Evangulov et al., 2016) technical manual (Section 2.3.3). The interface uses buttons that, when clicked, allow the coach or analyst to skip directly to a position of importance ('key-frames' when referring to positions in the video). Key-frame buttons are shown in Figure 8-6.

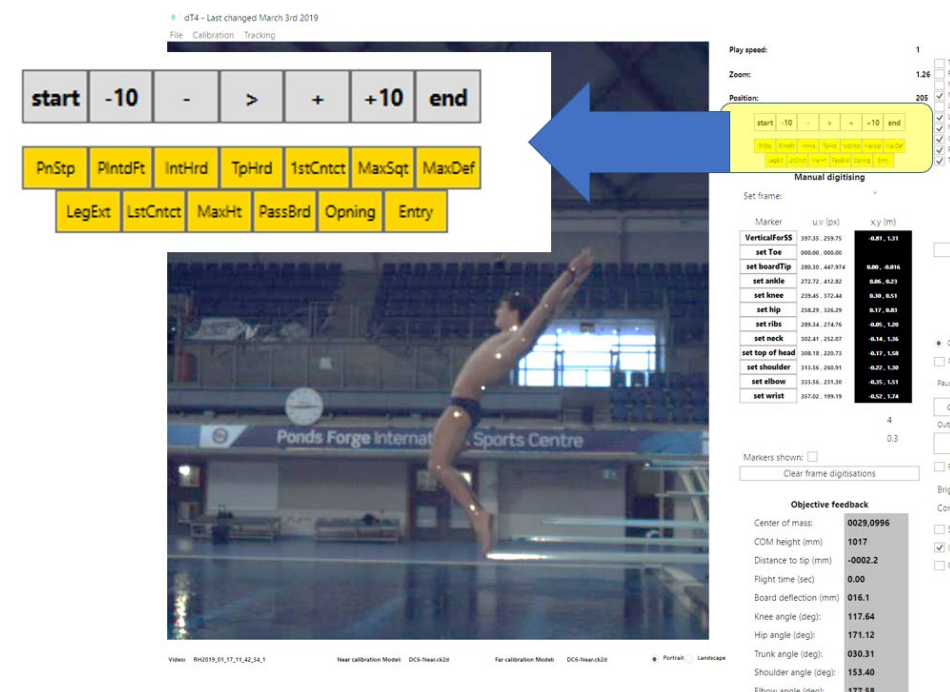


Figure 8-6. Key-frame buttons select points of interest in the dive, consistent with the British Diving Single System technical resource.

Key-frames referenced in the BDSS and used in diveTracker are listed in Table 8-1.

*Table 8-1. Positions of interest in a take-off and dive.*

<b>Position</b>	<b>Description</b>
Penultimate step	The point before the last step in the hurdle-approach; used to assess posture and to measure the length of the last step
Planted foot	The end of the last step and preparation for the hurdle; used to assess posture and measure last-step length
Into hurdle	The last frame showing contact of the drive leg into the hurdle-step; used to assess posture and calculate length of hurdle step
Top of hurdle	The highest point of the hurdle step; used to assess body-shape before descent to the end of the board
First contact/top of rock	The touch-down from the hurdle-step in forward and reverse dives and the highest point before the squat in back and inward dives; used to calculate distance from the end of the board and the height of the COM before the squat and drive-down
Maximum squat	The point at which the internal knee angle is smallest; used to calculate duration of impulse and change in knee angle through drive-down into the board
Maximum deflection	The position at which the board-tip is maximally depressed; used as an indicator of efficiency of drive-down and influence on take-off velocity
Leg extension	The point at which the legs have driven straight before leaving the board; used to assess posture, calculate impulse-time and to compare timing of leg-stretch to that of leaving the springboard
Last contact	The last point at which the feet are touching the board. This is considered the point of take-off
Maximum height	The point at which the COM is maximally displaced. A key indicator of performance
Opening	The point at which the body has opened from its somersaulting shape to a hip angle of 90°. This position defines the amount of 'drop' or time to prepare for entry available to the diver
Passing board	The point at which the COM is the same height as the board; used to measure distance
Entry	The point at which the diver breaks the surface of the water; used to calculate distance from the springboard and body-angle

### 8.3 Output from tool

Output was designed to meet the varying needs within the team and to facilitate both qualitative and quantitative analysis.

#### 8.3.1 Key frame images and image-strips

Key frames may be selected by the user to show the posture of the diver in positions of interest (Figure 8-7). This provides focus during qualitative analysis and allows comparison of the diver to desired postures as defined in the BDSS.

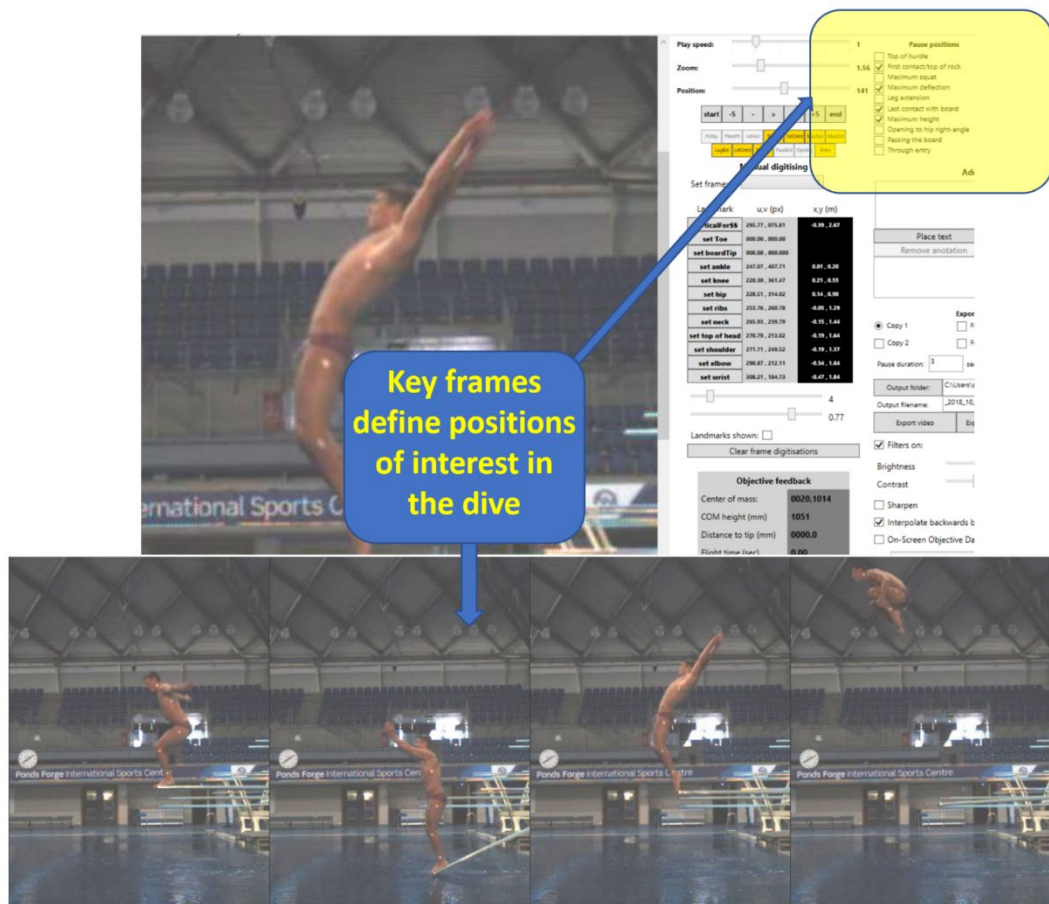


Figure 8-7. The yellow-highlighted control allows the user to show the posture of the diver in the positions of interest defined in Table 8-1. This provides an opportunity to subjectively compare to ideal positions defined in the Single System technical manual used by the British Diving WCP.

A series of images from key-frames can be output as an image-strip (Figure 8-8) for inclusion in reports and to provide context to numerical data during analysis by the team.





Figure 8-8. Image-strips are a stitched sequence of images, selected by the user, showing posture (and kinematic data) at key points in the dive. The yellow highlighted box presents the key-frames available for inclusion in the image strip.

### 8.3.2 Annotated replay

Relevant performance information can be superimposed on the image, adjacent to the diver, through the replay of the dive (Figure 8-9). Text annotations can be added by the user on any frame, adding a text commentary to the image and data shown. Video is a medium commonly used by team members for communication of progress and as such diveTracker produces annotated videos which can be paused at key-frames which can be viewed on the range of devices used by the coaching and support team.

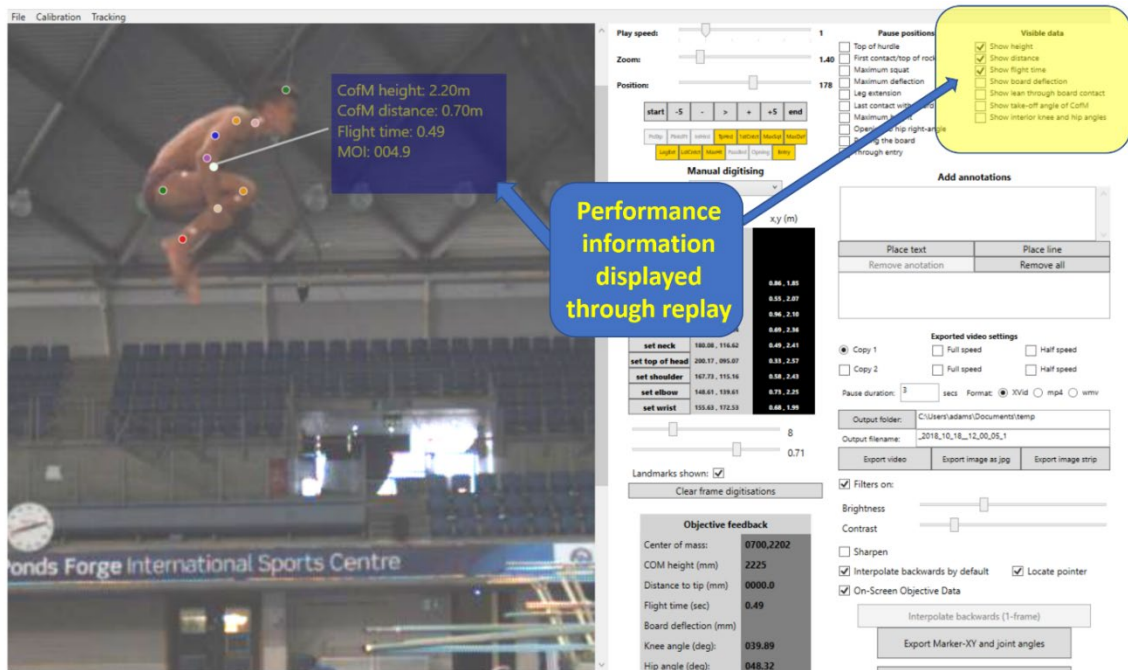


Figure 8-9. Performance data superimposed on image during playback and review. The yellow-highlighted box offers kinematic data, selectable by the user, for display alongside the image of the diver.

### 8.3.3 Key performance information

Standard performance data is produced for each dive. Data included in the output is defined in Table 8-2. These data include data produced in academic articles (Chapter 2.5) for comparison and additional parameters for further analysis. Sample output is shown in Appendix B. Tracking of these data over time allow progress to be quantified and analysis made of specific interventions from the coaching and performance support team to improve the quality of performance.

These data can also be used to assess the suitability of skill progression – comparison of take-off velocity, rotational speed and opening height of a lead-up (1 metre) skill to corresponding values in a more complex optional (3 metre) skill informs decision-making for when to learn a new dive and when to hold back if standards are not being met.

Table 8-2. Performance data produced for each dive. These data are calculated to increase insight and understanding of the influences on other kinematic variables, for example comparing the knee angle at maximum squat and the speed at which the legs extended to board deflection and take-off velocity.

Element/key-position of dive	Data produced
Hurdle step	Last step length, speed of last step, height of hurdle, length of hurdle, landing velocity
First contact	Segment and joint angles (shoulder, elbow, trunk, hip, knee), lean
Maximum squat	Segment and joint angles (shoulder, elbow, trunk, hip, knee). Change in COM height from first contact. Change in shoulder angle (reflecting arm-swing)
Maximum deflection	Segment and joint angles (shoulder, elbow, trunk, hip, knee). Lean. Board deflection. Change in arm position due to arm swing. Percentage of total impulse time to this point
Leg extension	Segment and joint angles (shoulder, elbow, trunk, hip, knee). Lean. Change in arm position due to arm swing. Percentage of total impulse time to this point
Last contact	Segment and joint angles (shoulder, elbow, trunk, hip, knee). Lean. Change in arm position due to arm swing. Take-off velocity.
Flight	COM trajectory at take-off. Maximum height and COM displacement. Speed of each somersault. Change in moment of inertia between take-off and tightest shape with time taken to reduce accordingly. Opening height.
Entry	Distance of COM at the body's first contact with the water

#### 8.3.4 Marker positions and joint angles

A .csv file showing landmark positions, joint angles and COM-position at each frame of video is produced for each dive. This feature adds value to the analysis process by creating the potential for further kinematic analysis to answer performance questions not answered by other presentation of data in the tool. Sample output is shown in Appendix C.

## 8.4 Developing understanding of World Class performance

In addition to the use of the system in high-performance centres, the diveTracker system is used at national and international events to conduct performance analysis of individual divers in competition (for comparison to both training and previous competition) and also to develop understanding of What It Takes to Win kinematic parameters by the analysis of performance characteristics of a world class cohort of divers in high-level (e.g. World Series) competition. These data, not available to the sport prior to the deployment of the tool, contribute proprietary knowledge of the kinematic demands of elite diving and informs the creation of more specific technical goals for divers in the WCP. The Programme believes that focusing training to the achievement of objective targets in addition to subjective goals increases the speed of development and probability of success in World and Olympic competition.

## 8.5 Summary

A software tool is required to measure performance metrics from video data. A camera calibration coupled with an appropriately representative body-segment model produces measurement with greatest accuracy. Section 2.9 identified the lack of an existing tool that implemented these methods.

In response to this gap that prevented British Diving collecting longitudinal training-based performance data about its athlete cohort, the diveTracker tool was developed by the author to facilitate analysis of dives and to measure kinematic parameters with more accuracy than in existing studies in the sport. Its user interface was designed to be specific to diving and its capacity to automatically track a diver and produce data quickly enough to fit into the coaching feedback cycle facilitates new practice, combining subjective coaching points with objective performance analysis, a unique performance advantage to the British Diving World Class Programme.

Users' need for data to be presented in a range of formats is made by output as numeric, graphic, video or spreadsheet data. The system's portability and flexibility facilitate objective measurement of progress in divers at training and in competition

and can be used to create new knowledge of performance of the hardest dives in the world performed by the best divers in the world.

## 9 What It Takes to Win – kinematic performance data

### 9.1 Introduction

What It Takes to Win (WITTW) was described in Chapter 2 as a model created by British Diving which defines performance indicators in multiple criteria as the standard which divers should achieve or surpass in order to maximise their probability of achieving medals in World and Olympic diving competition.

The criterion describing the performance of each dive in the WITTW model has, to date, been based on average judge score over all the performances of that dive in the current season. While indicative of the quality in which each dive is held in the eyes of a judging panel, there has historically been no quantitative measurement of the kinematic characteristics of high-scoring dives by competitors achieving World and Olympic medals, or by divers in the British Diving World Class Programme (WCP).

It was recognised that without clearly defined kinematic performance indicators at which to focus diver's development, the achievement of world class performance relies on an innate understanding by the athlete and support team of what is 'good enough' when refining existing dives or when enhancing preparatory ('lead-up') skills before attempting a new, greater-difficulty dive. There was an identified risk of sub-optimal development of talented divers without this understanding and experience.

The aim of this chapter is to mitigate the identified risk and generate new knowledge. Performance data was calculated using the diveTracker system and by analysis of competition broadcast footage. These data add to the overall knowledge base contained in British Diving's WITTW model and provides an additional set of standards by which divers progress and potential can be measured and tracked – enhancing the WCP's likelihood of achieving its Olympic aspirations.

## 9.2 Method

### 9.2.1 Athletes

Divers were filmed (when access was available the competition) or observed performing over a series of competitions from 2015 to 2019. Dives selected for analysis met two criteria:

- The diver had won an Olympic, a World Championships or World Cup medal
- The dive had achieved a rating of ‘very good’ by at least one judge (earning a score between 8.5 and 10)

Divers achieving the first criterion are listed in Table 9-1.

*Table 9-1. Divers meeting the standard required for WITTW analysis had won medals in World and/or Olympic competition.*

Male		Female	
Name	Nationality	Name	Nationality
Cao Yuan	China	Shi Tiangmao	China
Xie Siyi	China	Wang Han	China
Evgeny Kuznetsov	Russia	He Zi	Canada
Ilya Zakharov	Russia	Jennifer Abel	Canada
Patrick Hausding	Germany	Pamela Ware	Canada
Rommel Pacheco	Mexico	Madison Keeney	Australia
Jack Laugher	Great Britain		

Ethical approval was sought and granted to capture and analyse diving footage. British divers on the World Class Programme give consent for their performances to be captured and analysed when accepting their place on the WCP. When filming took place at World Series competition, details of the study were provided to team representatives prior to the technical meeting (a meeting where event rules and procedures are defined for all teams) with an invitation to opt-out of the process; no requests were made to exclude athletes.

### 9.2.2 Competitions

When analysis was performed at the event, camera calibrations were performed before each session of filming and the diveTracker system was used to produce performance data. When performances could not be captured at the event, broadcast footage was used to determine kinematic data using flight time and frame count - methods used by Miller (2013) and Sanders (R. Sanders et al., 2000-2002).

The events from which performance data were calculated are listed in Table 9-2.

*Table 9-2. Diving competitions from which kinematic analyses were made. Semi-finals and finals were used for analysis (as Semi-finals aren't run at National Championships, the Preliminary round was used).*

Competition	Country	Source
2019 World Championships final	Korea	FINA footage
2019 World Championships semi-final	Korea	FINA footage
2018 World Cup final	China	FINA footage
2018 World Cup semi-final	China	FINA footage
2017 World Championships final	Hungary	FINA footage
2017 World Championships semi-final	Hungary	FINA footage
2018 National Championships	Great Britain	diveTracker
2017 National Championships	Great Britain	diveTracker
2019 World Series	Great Britain	diveTracker
2015 World Series	Great Britain	diveTracker

### 9.2.3 Performance metrics

Data that could be produced using the diveTracker system and estimated from a broadcast video stream was calculated as follows:

**Flight time.** Calculated using the frame count between the point of last contact and the point at which the body first touched the water. Lower frame-rates used in broadcast video (30 Hz compared to 80 Hz in diveTracker) created circumstances



where precise marking of key-frames as impossible. An estimation process was used to mark key-positions when necessary (Figure 9-1).

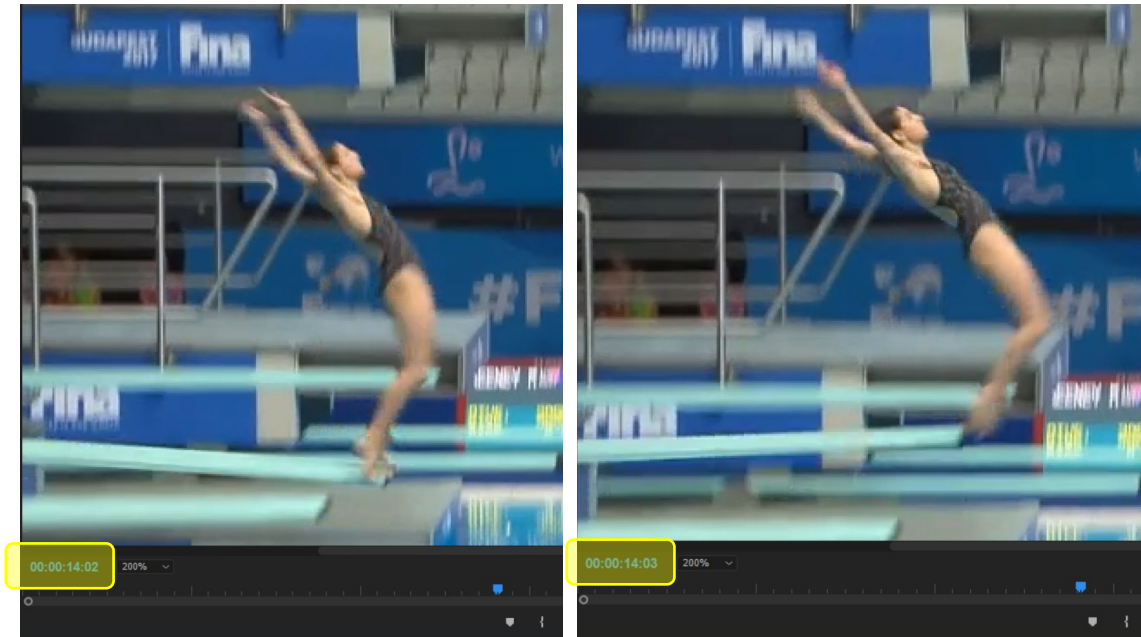


Figure 9-1. 30 Hz video could imprecisely identify key frames – in this example, the point of last contact (where the springboard is level) is not visible. Noting the time-stamps (highlighted in yellow), an intermediate position (in this example, 00:00:14:02.5) was used as the estimate of the timing of the desired position. This process was also used for start/end of somersault and entry frames.

**Take-off (vertical) velocity.** Calculated by rate of change of COM in diveTracker during take-off, and inferred from flight time on broadcast video using equation of motion 9.1 as follows:

$$s = ut + \frac{1}{2}at^2 \quad [9.1]$$

when rearranged, gives:

$$u = \frac{s - \frac{1}{2}at^2}{t}$$

where  $u$  is initial velocity,  $s$  is the overall displacement (-3000 mm in a springboard competition),  $a$  is acceleration due to gravity and  $t$  is the flight time estimated earlier.

**COM displacement.** Measured as the peak of the best-fit curve of COM-positions in diveTracker and estimated (when using broadcast video) using take-off velocity and equation of motion 9.3

$$v^2 = u^2 + 2as \quad [9.1]$$

When rearranged, gives:

$$s = \frac{v^2 - u^2}{2a}$$

where  $s$  is displacement,  $u$  is starting velocity,  $v$  is finishing velocity and  $a$  is acceleration due to gravity.

**Somersault speed.** Somersault speed (revolutions per second) is determined using a frame-count between two positions. For the first somersault, it is measured as the difference between the point of last-contact and the point at which the trunk has rotated to vertical. For subsequent somersaults, the speed is calculated using the time to get from a vertical trunk position to the same position on the next somersault. Frames defining the start and end of each somersault were marked manually to maintain consistency of measurement between video sources.

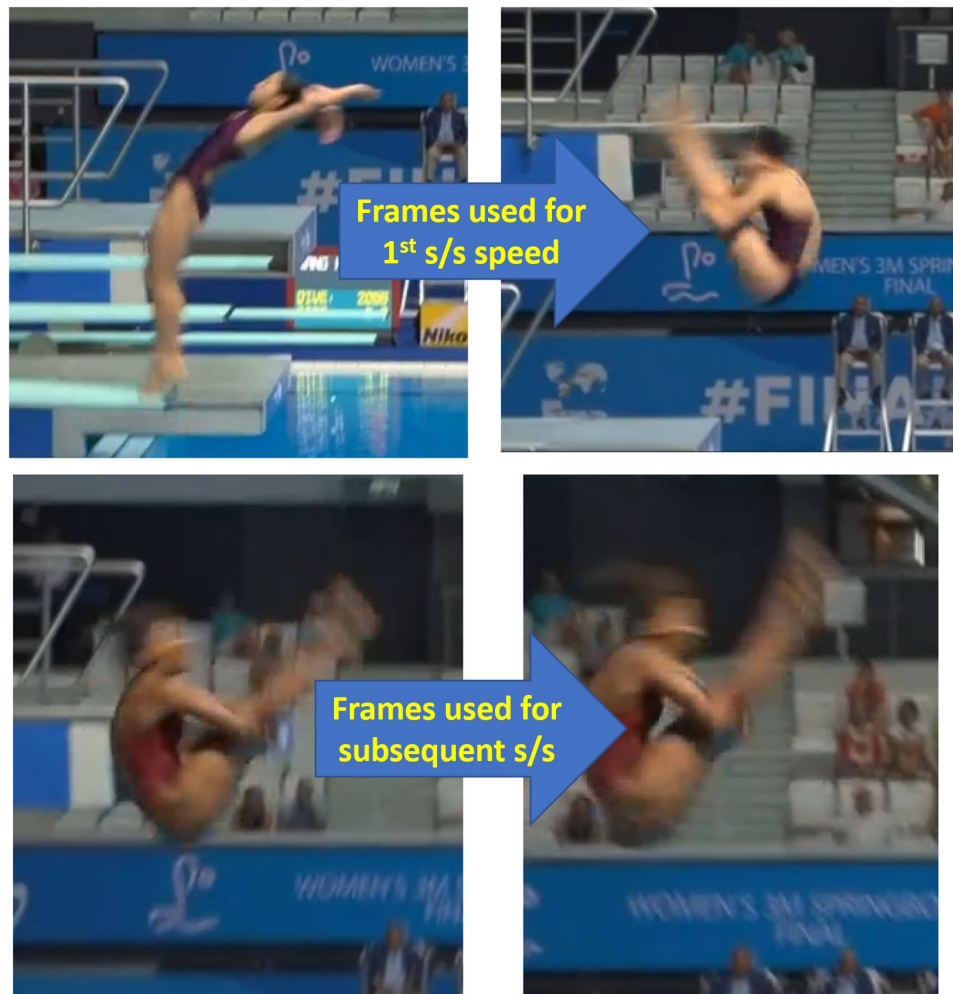
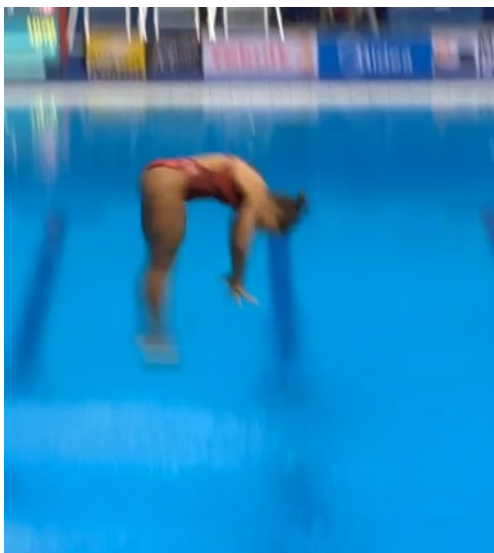


Figure 9-2. A vertical trunk position is used to mark the end of each somersault (s/s). For the first somersault, the take-off frame is used as the body does not leave the board with a vertical trunk on skills with rotation.

The speed of the final somersault is not calculated. A more skilled diver will open from the tight somersaulting shape during the final somersault, slowing down the rotation. A low final somersault speed could be due to this effect or due to the slow rotation of an unskilled diver and consequently does not provide helpful insight.

**Twist speed.** The method for calculating twist speed is the same as for somersault speed. The first twist of a forward-twisting dive is not calculated as the twist occurs during the straightening of the body and doesn't reflect optimum conditions for twisting quickly.

**Opening time.** The ‘opening’ of the dive is defined in WITTW as the point where the hip-angle of the diver has opened to 90° in preparation for entry. This is measured using hip-angle in diveTracker and is estimated in broadcast video as shown in Figure 9-3.



*Figure 9-3. The diver opening from a tight somersaulting shape to a right angle defines the point where the ‘drop’ (the preparation for entry) begins.*

**Opening height.** Measured using the COM-position in diveTracker and estimated using broadcast video using Equation 9.1 with  $u$ ,  $a$  and  $t$  known.

**Drop.** Defined in WITTW as the time between opening from the shape (Figure 9.3, where the hip angle as reached 90°) to the point of entry.

### 9.3 Results

The results of the study are shown in Table 9-4, Table 9-6, Table 9-6 and Table 9-5. Dive numbers are explained below the data tables.

Table 9-3. Women's 3 m Data collection metrics separated by method of collection. More samples of broadcast video were sampled than from the diveTracker tool.

Dive and metrics	Data collection method	
	DiveTracker	FINA footage
<b>107b (Forward 3.5 somersaults, piked)</b>		
Samples	4	10
	Mean (SD)	Mean (SD)
Flight time (s)	1.48 (0.02)	1.48 (0.03)
Vertical velocity at take-off (m/s)	5.25 (1.48)	5.21 (0.21)
Displacement (mm)	1404 (75.8)	1383 (109.1)
Somersault 1 speed (s/s per sec)	3.05 (0.23)	3.02 (0.21)
Somersault 2 speed (s/s per sec)	2.65 (0.15)	2.63 (0.08)
Opening time (s)		1.31 (0.03)
Opening height (mm)		1431 (254.4)
Drop (s)		0.017 (0.03)
<b>205b (Back 2.5 somersaults, piked)</b>		
Samples	4	9
	Mean (SD)	Mean (SD)
Flight time (s)	1.36 (0.01)	1.33 (0.02)
Vertical velocity at take-off (m/s)	4.46 (0.07)	4.27 (0.16)
Displacement (mm)	1016 (29.71)	929 (71.65)
Somersault 1 speed (s/s per sec)	1.66 (0.07)	1.63 (0.06)
Opening time (s)		103 (0.06)
Opening height (mm)		2149 (501.1)
Drop (s)		0.3 (0.08)
<b>305b (Reverse 2.5 somersaults, piked)</b>		
Samples	4	6
	Mean (SD)	Mean (SD)
Flight time (s)	1.51 (0.05)	1.47 (0.04)
Vertical velocity at take-off (m/s)	5.42 (0.32)	5.16 (0.24)
Displacement (mm)	1501 (175.2)	1359 (129.0)
Somersault 1 speed (s/s per sec)	1.47 (0.06)	1.51 (0.05)
Opening time (s)		1.07 (0.02)
Opening height (mm)		2884 (254.6)
Drop (s)		0.4 (0.04)
<b>405b (Inward 2.5 somersaults, piked)</b>		
Samples	4	8
	Mean (SD)	Mean (SD)
Flight time (s)	1.27 (0.04)	1.29 (0.07)
Vertical velocity at take-off (m/s)	3.87 (0.25)	3.96 (0.48)
Displacement (mm)	765 (101.4)	812 (216.6)
Somersault 1 speed (s/s per sec)	2.69 (0.29)	2.53 (0.42)
Opening time (s)		1.08 (0.04)
Opening height (mm)		1544 (559.9)
Drop (s)		0.20 (0.08)
<b>5152b (Forward 2.5 somersaults, 1 twist, piked)</b>		
Samples	2	6
	Mean (SD)	Mean (SD)
Flight time (s)	1.49 (0.06)	1.46 (0.04)
Vertical velocity at take-off (m/s)	5.29 (0.38)	5.13 (0.25)
Displacement (mm)	1434 (202.6)	1344 (131.4)
Somersault 1 speed (s/s per sec)	2.67 (0.06)	3.09 (0.59)
Opening time (s)		1.21 (0.04)
Opening height (mm)		2011 (219.7)
Drop (s)		0.25 (0.03)
<b>5154b (Forward 2.5 somersaults, 2 twists, piked)</b>		
Samples	0	5
	Mean (SD)	Mean (SD)
Flight time (s)		1.49 (0.01)
Vertical velocity at take-off (m/s)		5.29 (0.08)
Displacement (mm)		1429 (42.6)
Somersault 1 speed (s/s per sec)		2.95 (0.12)
Twist 2 speed		2.71 (0.18)
Opening time (s)		1.39 (0.02)
Opening height (mm)		847 (221.2)
Drop (s)		0.1 (0.03)

Table 9-4. WITTW Performance indicators – Women’s 3 m springboard. Dive numbers are described below the data tables

	Women's 3m performance indicators - mean (SD)					
	107b	205b	305b	405b	5152b	5154b
Flight time (s)	1.48 (0.03)	1.34 (0.03)	1.49 (0.05)	1.28 (0.06)	1.47 (0.05)	1.49 (0.01)
Take-off vertical velocity (m/s)	5.21 (0.16)	4.33 (0.17)	5.26 (0.30)	3.93 (0.42)	5.17 (0.30)	5.29 (0.08)
COM displacement (mm)	1389 (95)	956 (74)	1416 (165)	796 (188)	1366 (157)	1429 (43)
Somersault 1 speed (s/s per sec)	3.03 (0.20)	1.64 (0.07)	2.59 (0.39)	2.59 (0.39)	2.98 (0.54)	3.00 (0.0)
Somersault 2 speed (s/s per sec)	2.64 (0.10)					
Somersault 3 speed (s/s per sec)						
Twist 1 speed (twists/sec)						
Twist 2 speed (twists/sec)						2.72 (0.18)
Twist 3 speed (twists/sec)						
Opening time (s)	1.31 (0.03)	1.03 (0.06)	1.07 (0.02)	1.08 (0.04)	1.21 (0.04)	2011 (720)
Opening height (mm)	1431 (241)	2149 (501)	2884 (255)	1544 (560)	2011 (220)	847 (221)
Drop (s)	0.17 (0.03)	0.30 (0.07)	0.40 (0.04)	0.20 (0.08)	0.25 (0.03)	0.10 (0.03)

	Women's 3m performance indicators - maximum values					
	107b	205b	305b	405b	5152b	5154b
Flight time (s)	1.53	1.37	1.57	1.47	1.55	1.5
Take-off vertical velocity (m/s)	5.54	4.53	5.79	5.17	5.67	5.36
COM displacement (mm)	1566	1046	1709	1362	1637	1463
Somersault 1 speed (s/s per sec)	3.33	1.76	1.57	3.15	4.29	3.15
Somersault 2 speed (s/s per sec)	2.86					
Somersault 3 speed (s/s per sec)						
Twist 1 speed (twists/sec)						
Twist 2 speed (twists/sec)						3.03
Twist 3 speed (twists/sec)						
Opening time (s)	1.35	1.2	1.1	1.15	1.3	1.43
Opening height (mm)	2033	2601	3218	2862	2344	1052
Drop (s)	0.25	0.37	0.45	0.39	0.3	0.012

Dive number	Dive Description
107b	Forward 3.5 somersaults, piked
205b	Back 2.5 somersaults, piked
305b	Reverse 2.5 somersaults, piked
405b	Inward 2.5 somersaults, piked
5152b	Forward 2.5 somersaults, 1 twist, piked
5154b	Forward 2.5 somersaults, 2 twists, piked

Table 9-5. Men's 3 m data collection metrics separated by method of collection. More samples of broadcast video were sampled than from the diveTracker tool.

Dive and metrics	Data collection method		Dive and metrics	Data collection method	
	DiveTracker	FINA footage		DiveTracker	FINA footage
<b>109c (Forward 4.5 somersaults with tuck)</b>			<b>5154b (Forward 2.5 somersaults with 2 twists, piked)</b>		
Samples	3	17	Samples	2	12
	Mean (SD)	Mean (SD)		Mean (SD)	Mean (SD)
Fight time (s)	1.64 (0.04)	1.64 (0.04)	Fight time (s)	1.67 (0.07)	1.60 (0.04)
Vertical velocity at take-off (m/s)	6.19 (0.25)	6.23 (0.27)	Vertical velocity at take-off (m/s)	6.36 (0.39)	5.96 (0.27)
COM displacement (mm)	1958 (158.3)	1985 (170.9)	COM displacement (mm)	2071 (252.5)	1815 (163.9)
Somersault 1 speed (s/s per sec)	2.71 (0.03)	2.75 (0.23)	Somersault 1 speed (s/s per sec)		2.87 (0.23)
Somersault 3 speed (s/s per sec)	3.13 (0.21)	3.18 (0.20)	Twist 2 speed (twists per sec)		2.99 (0.34)
Somersault 3 speed (s/s per sec)	3.34 (0.16)	3.21 (0.19)	Opening time (s)		1.37 (0.05)
Opening time (s)		1.47 (0.07)	Opening height (mm)		1993 (347)
Opening height (mm)		1534 (337.7)	Drop (s)		0.23 (0.05)
Drop (s)		0.17 (0.04)			
<b>207c (Back 3.5 somersaults with tuck)</b>			<b>5156b (Forward 2.5 somersaults with 3 twists, piked)</b>		
Samples	6	11	Samples	2	9
	Mean (SD)	Mean (SD)		Mean (SD)	Mean (SD)
Fight time (s)	1.49 (0.02)	1.50 (0.02)	Fight time (s)	1.66 (0.02)	1.61 (0.03)
Vertical velocity at take-off (m/s)	5.29 (0.15)	5.32 (0.13)	Vertical velocity at take-off (m/s)	6.31 (0.14)	6.02 (0.20)
COM displacement (mm)	1430 (82.7)	1445 (70.0)	COM displacement (mm)	2033 (90.7)	1849 (123.3)
Somersault 1 speed (s/s per sec)	2.17 (0.41)	2.01 (0.07)	Twist 2 speed (twists per sec)	3.13 (0.63)	3.44 (0.30)
Somersault 2 speed (s/s per sec)	3.15 (0.13)	3.20 (0.17)	Twist 3 speed (twists per sec)	2.72 (0.00)	3.30 (0.26)
Opening time (s)		1.18 (0.05)	Opening time (s)		1.47 (0.04)
Opening height (mm)		2454 (370.2)	Opening height (mm)		1271 (380.5)
Drop (s)		0.32 (0.06)	Drop (s)		0.14 (0.04)
<b>307c (Reverse 3.5 somersaults with tuck)</b>			<b>5337d (Reverse 1.5 somersaults with 3.5 twists, free)</b>		
Samples	6	14	Samples	0	5
	Mean (SD)	Mean (SD)		Mean (SD)	Mean (SD)
Fight time (s)	1.66 (0.02)	1.64 (0.02)	Fight time (s)		1.63 (0.02)
Vertical velocity at take-off (m/s)	6.33 (0.15)	6.18 (0.14)	Vertical velocity at take-off (m/s)		6.18 (0.12)
COM displacement (mm)	2046 (94.9)	1950 (88.5)	COM displacement (mm)		1946 (78.0)
Somersault 1 speed (s/s per sec)	1.82 (0.08)	1.88 (0.12)	Twist 1 speed (twists per sec)		2.11 (0.24)
Somersault 2 speed (s/s per sec)	3.15 (0.22)	3.02 (0.06)	Twist 2 speed (twists per sec)		3.58 (0.21)
Opening time (s)		1.22 (0.06)	Twist 3 speed (twists per sec)		3.60 (0.28)
Opening height (mm)		3248 (320)	Opening time (s)		1.49 (0.05)
Drop (s)		0.42 (0.05)	Opening height (mm)		1317 (549)
			Drop (s)		0.15 (0.06)
<b>407c (Inward 3.5 somersaults with tuck)</b>					
Samples	4	10			
	Mean (SD)	Mean (SD)			
Fight time (s)	1.44 (0.03)	1.42 (0.02)			
Vertical velocity at take-off (m/s)	4.99 (0.19)	4.83 (0.10)			
COM displacement (mm)	1273 (94.8)	1183 (50.8)			
Somersault 1 speed (s/s per sec)	2.51 (0.21)	2.5 (0.22)			
Somersault 2 speed (s/s per sec)	3.17 (0.20)	3.10 (0.22)			
Opening time (s)		1.25 (0.03)			
Opening height (mm)		1340 (322)			
Drop (s)		0.16 (0.04)			
<b>407b (Inward 3.5 somersaults, piked)</b>					
Samples	0	4			
	Mean (SD)	Mean (SD)			
Fight time (s)		1.37 (0.03)			
Vertical velocity at take-off (m/s)		4.53 (0.22)			
COM displacement (mm)		1048 (102.0)			
Somersault 1 speed (s/s per sec)		3.04 (0.19)			
Somersault 2 speed (s/s per sec)		3.05 (0.12)			
Opening time (s)		1.21 (0.04)			
Opening height (mm)		1295 (270)			
Drop (s)		0.16 (0.04)			

Table 9-6. WITTW performance indicators – Men’s 3 m springboard. Dive numbers are explained below the data tables.

Men's 3m performance indicators - mean (SD)								
	109c	207c	307c	407c	407b	5154b	5156b	5337d
Flight time (s)	1.64 (0.04)	1.49 (0.02)	1.64 (0.03)	1.42 (0.02)	1.37 (0.03)	1.61 (0.05)	1.62 (0.04)	1.63 (0.02)
Take-off vertical velocity (m/s)	6.23 (0.27)	5.31 (0.14)	6.23 (0.16)	4.87 (0.15)	4.53 (0.22)	6.02 (0.32)	6.07 (0.22)	6.18 (0.12)
COM displacement (mm)	1981 (169)	1440 (75)	1979 (101)	1212 (77)	1048 (102)	1852 (200)	1882 (138)	1946 (78)
Somersault 1 speed (s/s per sec)	2.74 (0.23)	2.06 (0.26)	1.86 (0.11)	2.47 (0.14)	3.04 (0.19)	2.87 (0.23)		
Somersault 2 speed (s/s per sec)	3.17 (0.20)	3.18 (0.16)	3.06 (0.21)	3.12 (0.20)	3.05 (0.12)			
Somersault 3 speed (s/s per sec)	3.23 (0.19)							
Twist 1 speed (twists/sec)								2.11 (0.04)
Twist 2 speed (twists/sec)						2.99 (0.34)	3.39 (0.04)	3.58 (0.21)
Twist 3 speed (twists/sec)							3.19 (0.32)	3.60 (0.28)
Opening time (s)	1.47 (0.07)	1.18 (0.05)	1.22 (0.06)	1.25 (0.03)	1.21 (0.04)	1.37 (0.05)	1.47 (0.04)	1.49 (0.05)
Opening height (mm)	1534 (338)	2455 (370)	3248 (320)	1340 (322)	1295 (270)	1993 (347)	1271 (380)	1317 (549)
Drop (s)	0.17 (0.04)	0.32 (0.06)	0.42 (0.05)	0.16 (0.04)	0.16 (0.04)	0.23 (0.05)	0.14 (0.04)	0.15 (0.06)

Men's 3m performance indicators - maximum values								
	109c	207c	307c	407c	407b	5154b	5156b	5337d
Flight time (s)	1.73	1.53	1.7	1.47	1.42	1.73	1.68	1.66
Take-off vertical velocity (m/s)	6.75	5.54	6.57	5.17	4.85	6.75	6.45	6.33
COM displacement (mm)	2323	1566	2203	1362	1200	2323	2123	2046
Somersault 1 speed (s/s per sec)	3.15	3.03	2.07	2.72	3.15	3.33		
Somersault 2 speed (s/s per sec)	3.75	3.52	3.33	3.52	3.15			
Somersault 3 speed (s/s per sec)	3.55							
Twist 1 speed (twists/sec)							3.75	2.31
Twist 2 speed (twists/sec)						3.75	3.75	3.75
Twist 3 speed (twists/sec)								3.75
Opening time (s)	1.58	1.25	1.33	1.33	1.27	1.43	1.52	1.55
Opening height (mm)	2453	2987	3729	1836	1661	2774	2020	2171
Drop (s)	0.3	0.4	0.5	0.23	0.21	0.33	0.23	0.25

Dive number	Dive Description
109c	Forward 4.5 somersaults with tuck
207c	Back 3.5 somersaults with tuck
307c	Reverse 3.5 somersaults with tuck
407c	Inward 3.5 somersaults with tuck
5154b	Forward 2.5 somersaults, 2 twists, piked
5156b	Forward 2.5 somersaults, 3 twists, piked
5337d	Reverse 1.5 somersaults, 3.5 twists, free

### 9.3.1 Comparison of results using different data collection measures

For 7 out of 11 dive numbers, diveTracker measured an average take-off velocity higher than from FINA video footage, consequently maximum COM displacement and flight time have higher mean values. This could be due to the implicit estimation of parameter inference from take-off and entry frames or could be due to dives being performed better at events captured and analysed using the diveTracker tool. As National Championships are analysed using this method (and is of a generally lower standard than World Class events), this is, however, unlikely.



There is more similarity in values calculated for somersault and twist speed – this is to be expected as they are directly calculated by start and end frames, not inferred from take-off and entry frames (and an assumption of COM location in both frames).

A future investigation should be made to compare values for dives captured with the diveTracker system using both the system functions and Miller’s estimations to evaluate the similarity of metrics.

### 9.3.2 Flight time

Mean flight time in dives with a hurdle step (107b, 305b, 307c, 5152b, 5154b, 5156b, 1337d) are consistent in both Women’s diving (1.47 – 1.49 seconds) and Men’s (1.61 – 1.64 seconds). While published performance data does not exist from recent years (an identified gap in knowledge in diving kinematics), development in world class diving shows the increase in flight time from contemporary divers compared to historical studies as shown in Table 9-7 and Table 9-8.

*Table 9-7. Comparison of flight times for male divers performing dives from different groups between the 1999 World Championships and 2015-2019 WITTW values.*

	Forward	Back	Reverse
1999 World Championships, from Sanders (2000-2003)	1.48s (107b)	1.38s (205b)	1.51s (305b)
2015-2019 WITTW average	1.64s (109c)	1.49s (207c)	1.64s (307c)

*Table 9-8. Comparison of flight times for female divers performing dives from different groups between the 1999 World Championships and 2015-2019 WITTW values.*

	Forward	Back	Reverse
1999 World Championships, from Sanders (2000-2003)	1.35s (105b)	1.29s (205b)	1.40s (305c)
2015-2019 WITTW average	1.48s (107b)	1.34s (205b)	1.49s (305b)

Despite the same design and performance characteristics of the Duraflex Springboard in this time period, male divers have not only increase flight time by at a minimum of 0.1 seconds, they have also increased the number of somersaults performed by one in

each direction. Results are comparable in dives of the same group (for example 107b and 109c) due to the flight and rotation direction being the same. Female divers have similarly increased flight time in all groups and increased difficulty (due to adopting a slower-rotating pike shape) in forward and reverse groups.

### 9.3.3 Take-off velocity

Comparative data representing take-off velocity for male dives from 1996 and WITTW data are presented in Table 9-9.

*Table 9-9. Mean take off (vertical) velocity in optional dives performed by divers in the 1996 Olympic games and 2015-2019 WITTW values.*

	Forward	Back	Reverse	Inwards
1996 Olympic Games, from Miller (Zatsiorsky, 2000, p345)	5.44 m/s (107b)	4.64 m/s (205b)	5.8 m/s (307c)	4.7 m/s (407c)
2015-2019 WITTW average	6.23 m/s (109c)	5.31 m/s (207c)	6.57 m/s (307c)	4.87 m/s (407c)

Miller does not provide comparative data for female divers but increase in vertical take-off velocity is evident in all groups, including those where additional somersaults are also performed. Although a similar increase in velocity is shown in dives with hurdle (approximately 0.8 m/s), a significant difference in increase in take-off velocity is shown for standing dives (approximately 0.2 m/s for inwards but 0.7 m/s for back). This may be due to divers not having to produce full effort to complete back 2.5 somersaults piked (205b) compared to that required to complete inward 3.5 somersaults with tuck (407c) in 1996 – whereas by the time back 3.5 somersaults is used (and necessary to keep up with the competition), more effort is required to complete that dive.

### 9.3.4 Somersault speed and opening height

Fast somersault rotation is necessary both to complete dives of high difficulty and to allow the diver to open as high above the water as possible to prepare for a splash-less

and high-scoring entry. Both male and female divers can produce rotational speed of over 3 somersaults (1080°) per second. In general, divers increase angular velocity as the amount of rotation increases, reflecting the time it takes to close into the tightest shape they make.

In order to identify factors influencing a high opening, metrics from a minimum of ten samples of each dive performed by male and female divers had correlation calculations performed; these data are shown in Table 9-10 and Table 9-11.

Table 9-10. Correlation ( $r^2$ ) between kinematic metrics in the dataset of men's dives.

	Forward	Back	Reverse	Inward
Samples	20	17	20	14
Take-off vertical velocity and opening height	-0.04	0.52	0.19	0.64
1 <sup>st</sup> s/s speed and last s/s speed	0.14	-0.26	-0.76	0.24
1 <sup>st</sup> s/s speed and opening height	-0.73	0.67	0.68	0.38
Last s/s speed and opening height	0.11	0.42	0.58	0.68

Table 9-11. Correlations ( $r^2$ ) between kinematic metrics in the dataset of women's dives. Only the forward group has 3.5 somersaults and therefore has more than one somersault's speed measured.

	Forward	Back	Reverse	Inward
Samples	14	13	10	12
Take-off vertical velocity and opening height	0.51	0.62	0.88	0.89
1 <sup>st</sup> s/s speed and opening height	0.38	-0.71	-0.19	-0.71
Last s/s speed and opening height	-0.57	n/a	n/a	n/a

The lack of strong positive correlation between the speed of the first somersault and the last measured in each group (calculated as -0.76 to 0.24 depending on the group of dive measured) indicates that efforts to increase first somersault speed by either increasing lean or by greater trunk inclination at take-off compromises the speed of

subsequent somersaults – most likely due to being less able to adopt a shape with low moment of inertia (and correspondingly high angular velocity).

The groups that show strong correlation between both take-off velocity and opening height in men's diving are the reverse and inward groups. For women there is a higher correlation in all groups – perhaps due to the different shape (all female dives are performed piked whereas all males performed dives in the tuck position).

Backward-rotating group (back and reverse) for men have a moderate correlation between the fastest spinning, later somersaults and opening height. There is no correlation for males or females in forward and inward dives.

#### 9.3.5 Drop and preparation for entry

Divers can prepare a clean entry (required to earn 'very good' scores from judges and measured as 'drop' in the earlier tables) in as little as 0.1 seconds, with the greatest mean drop time for males and females (of 0.4 seconds) shown in reverse dives.

Development of difficulty in reverse optionals is therefore likely to occur in reverse-rotating dives next – evidenced by one female diver performing 307c in 2019 (although not to the 'very good' standard required for inclusion in this study) and a large number of male divers performing 305b (reverse 2.5 somersaults piked, a lead-up skill for 307b – reverse 3.5 somersaults piked) in 1 metre competition to a high standard.

## 9.4 Discussion

There is commonality in key performance metrics describing world class dives, most notably flight time and opening time. Measures of angular velocity through flight and the height at which divers open and prepare for entry have greater variability.

Strong correlation does not exist between key metrics and opening height, suggesting that maximising opening height appears to be based on individual divers optimising their physical characteristics (for example take-off speed, flight path, speed into a tight shape or a combination of these). Understanding the strengths of a diver allows

bespoke interventions for physical and technical development and increases the probability of achieving height, speed of rotation and a high opening.

## 9.5 Summary

A gap in knowledge in world diving was identified; kinematic data describing the performance of very good dives by World and Olympic medallists had not been calculated to define What It Takes to Win (WITTW) or published, and was not available to the World Class Programme.

A study was conducted to calculate these data, combining methods to derive metrics both when filming and analysis could be performed at an event and when estimations could be made only from broadcast video. The error in the system used to define WITTW parameters compares favourably with that implied by related studies and so, reinforced by the absence of published data over the last four Olympic cycles, these data represent contemporary best knowledge of world class performance metrics.

A comparison between the last published data and the data produced by the study described the change in performance of world class divers over fifteen to twenty years; continuing to calculate performance data through subsequent years could inform predictions of standards required in Olympic cycles to come.

These data serve as benchmarks; comparison of performance metrics of British divers on the World Class programme for take-off velocity, rotation speed and opening height allows understanding of strengths and weaknesses, provides focus for development, and informs readiness to perform new dives.

## 10 The effect of preparatory-phase training

### 10.1 Introduction

A study was designed to show the implementation of the methods described in earlier chapters; the study chosen was one designed to support a coach and team at an important time of the season.

British Diving defines the *Preparatory Phase* of training as the period from the start of September to the end of December each year. It is followed by *Competition Phase 1* (January to the end of April) and *Competition Phase 2* (May until the end of the major event of the season – usually concluding by the first week in August).

World Class Programme divers use the preparatory phase to build physical qualities and to develop technical excellence and consistency so that, by the time Competition Phase 1 begins, a competition list of higher quality and/or difficulty can be used at Grands Prix and World Series events. Successful completion of Competition Phase 1 optimally prepares the diver for the major event of the year (World Cup, World Championships or the Olympic Games) and the achievement of personal and WCP targets. There is, therefore, a competitive advantage from a well-planned and reviewed training programme at this critical time in the season.

Analysis of training, competition performances and a gap-analysis of the diver and What It Takes to Win standards inform goals in technical and physical development. While physical development can be objectively measured by profiling and regular testing and technical competence can be subjectively assessed by an experienced coach, a knowledge gap has existed; objective measurement of the change in diving performance as physical development takes place has not been practical.

A study was conducted between September 2018 and January 2019 to produce new knowledge:

- The change in technical performance
- The progression towards WITTW technical standards

- The opportunity to assess the impact of interventions designed and implemented by practitioners to support the achievement of agreed goals

Ethical approval was sought and granted for the application of markers to divers, their image being captured, and performance data being calculated from video images. The observed and filmed training sessions were led by the coach using practice consistent with the risk-assessment agreed with the facility (Appendix D).

This chapter presents methods, results and discussion of how these data informed future planning for the divers in the study, and the value added to the programme by use of the diveTracker system.

### 10.1.1 Training programme

Divers who were fully available for domestic training followed the training programme described in Table 10-1. This programme was modified when injury, camp-attendance or education precluded the completion of normal training.

*Table 10-1. The training programme followed by the divers in the study. An 'x' indicates a component of training that would be completed in the day.*

	Monday	Tuesday	Wednesday	Thursday	Friday	Saturday	Sunday
Acrobatics	x	x	x	x	x	x	
Gymnastics	x				x		
Pool Session 1	x	x	x	x	x	x	
Pool Session 2	x	x		x	x		
Strength and Conditioning (S&C)		x			x		
Soft-tissue therapy			x				
Physiotherapy	x		x				

The focus of pre-season training from a physical perspective is to build capability and to increase tolerance to training (supported by physiotherapy). Technical training aims to perfect:

- Entries (the ability to go through the water without producing any splash – a requirement for good judge scores in competition)
- Required dives (simple dives with either 0.5 or 1.5 somersaults, used to refine take-off technique)
- Skill-chains (dives of progressive difficulty that are linked by direction of rotation, used to refine vision and opening-sequence in preparation for entry)
- Lead-ups (complex skills from the 1 metre springboard in preparation for high difficulty ‘optional’ dives from 3 metres)

The most difficult, highest-intensity work in the pool is programmed for Monday and Thursday, allowing effective recovery from S&C training on Tuesday and Friday. Wednesday and Saturday are low intensity days to support recovery for the next half-week training block.

## 10.2 Methods

### 10.2.1 Profiling and agreement of goals

Divers returned to pre-season training between August 10<sup>th</sup> and 24<sup>th</sup> 2018. Individual start dates varied dependant on the timing of the end of the previous season, with each athlete competing at different events at the end of the 2017-2018 season.

The season officially began on September 3<sup>rd</sup> with start-of-season profiling taking place for the Sheffield divers on September 12<sup>th</sup>. Profiling is conducted to establish a baseline measure of fitness and performance and can be used to identify areas of potential weakness compared to other athletes in the cohort.

Each diver’s annual review and goal-setting meeting took place on the same day. Performance goals were established and agreed for each diver as shown in Table 10-2.



Table 10-2. Performance goals agreed between diver, coach and diving's Senior Leadership team at annual review (21/9/2018).

Diver	Performance goals
Diver 1	Increase physical capacity as measured by strength profiling Increase DD in two groups by changing forward 3 ½ somersaults (107b) and reverse 2 ½ somersaults (305b) to the pike shape and improve scoring potential of back 2 ½ somersaults, piked (205b)
Diver 2	Return to full-time training (following long-term injury) and develop physical capacity as measured by strength profiling Develop capacity to regularly train and compete forward 4 ½ somersaults with tuck, reverse 3 ½ somersaults with tuck and inward 3 ½ somersaults with tuck (109c, 307c and 407c respectively) and learn and compete back 3 ½ somersaults with tuck (207c) in 2018 season
Diver 3	Increase DD by learning and competing 307c and 407c in 2018 season
Diver 4	Improve quality and competition performance in 307c Explore potential to learn and compete 207c Improve quality of 407c ready for 2018 season

Physical profiling data for each diver is presented in Appendix B, with relevant strength testing baseline results shown, in Table 10-3 – to be compared to results measured at the end of the training phase. All tests were selected based on validity, repeatability, and specificity to the demands of the sport and were agreed by the Chief Medical Officer, Head Physiotherapist, High-Performance Centre S&C coaches in the World Class Programme. The testing protocol was endorsed by the English Institute of Sport Athlete Health team. All profiled athletes consented (as part of their Athlete Agreement with British Diving and UK Sport) to performance data being shared with the Sports Science and Medicine team, of which the author is Head. Data was collected by British Diving and English Institute of Sport staff and shared securely, via password-protected portable storage, with the author.

Table 10-3. Selected profiling results for Sheffield divers relevant to agreed preparatory-phase goals. All testing was performed on ForceDecks force plates and the English Institute of Sport, Sheffield.

Test	Diver 1	Diver 2	Diver 3	Diver 4
Countermovement jump (cm)	37.2	53.2	51.6	47.7
Single-leg countermovement jump – right leg (cm)	19.1	31.3	28.2	26.3
Single-leg countermovement jump – left leg (cm)	18.5	29.2	30.9	27.2
Drop jump height (cm)	36.8	46.8	49.1	41.2
Isometric squat – peak vertical force (N)	2876	3032	4237	4331
Isometric calf-raise – peak vertical force (N)	2237	2843	3229	3339

#### 10.2.2 Dives measured in the study

The preparatory phase of training limits the complexity of dives to lead-up skills. These dives are performed from a lower board (1 metre) and with fewer somersaults than their 3 metre equivalents, as described in

Table 10-4.

Table 10-4. Optional dives with their equivalent lead-up skills. The time of the season dictated that lead-up skills would be measured and compared to World Class optional dives in the same group.

Optional	Lead-ups
109c (forward 4.5 somersaults with tuck, 3 m)	107c (forward 3.5 somersaults with tuck, 1 m)
205b (backward 2.5 somersaults piked, 3 m)	203b, 204b (back 1.5 and back double somersaults, piked, 1 m)
207c (backward 3.5 somersaults with tuck, 3 m)	205c, 206c (back 2.5 and back triple somersaults with tuck, 1 m)
305b (reverse 2.5 somersaults piked, 3 m)	303b, 304b (reverse 1.5 and reverse double somersaults, piked, 1 m)
307c (reverse 3.5 somersaults with tuck, 3 m)	305c, 306c (reverse 2.5 and reverse triple somersaults with tuck, 1 m)
407c (inward 3.5 somersaults with tuck, 3 m)	405c, (inward 2.5 somersaults with tuck, 1 m)

To ensure the natural delivery of preparatory-phase training and to minimise any distraction caused by the study, no effort was made to influence the selection of skills in the training programme each day. Divers were filmed as they carried out their normal work and numbers of each skill were agreed by coach and diver with no consideration of the needs of the study. In addition to technical training, divers undertook S&C training twice per week as defined in Table 10-1.

### 10.2.3 Selection of divers

Four divers (1 female, 3 male) were selected to be tracked through the study. The divers comprised the World Class athlete-cohort training in the Sheffield Performance Centre. All divers were over 18 years old at the start of the study and gave informed consent (Appendix D) to having markers applied to them and being filmed, analysed and their performance data discussed in this study. The study was granted ethical approval. Membership of the World Class Programme (WCP) was considered the standard for inclusion due to the recognition that the athletes were on-track to contest medals in the 2020 or 2024 Olympic Games. Furthermore, non-WCP athletes do not have access to a performance support team.

### 10.2.4 Environment

Ponds Forge International Sports Centre was used for filming and the Centre management gave permission for filming to take place (Appendix D). A single camera was positioned to create an approximately perpendicular view of the 1 metre springboards from which the divers train. Although a view close to perpendicular to the board gives a view to the diver and coach that is most familiar, the planar calibration process is unaffected by any difference between the camera position and a true perpendicular placement. A planar calibration of camera and scene was performed according to the process described in Chapters 3 and 4 and the scene was lit with four halogen lights as described in Chapter 6.4.

For the purposes of automated tracking, divers had markers applied to landmarks on each side of their body as described in Chapter 6. Application of markers took place before warm-up and no further changes were required to their normal training routine.

Filming took place during training sessions which were written, organised and coached as they would be on a normal training day with no alterations made due to the filming of the divers. Divers performed skills without a cue from the author and worked at the speed they would in an un-observed session.

#### 10.2.5 Production of kinematic data

The diveTracker tool was used to digitise dives and to calculate kinematic metrics as described in Chapter 7. Automatic marker tracking was used to give quick feedback to athletes and coach and was supplemented by manual digitisation to give greatest accuracy in analysis through the implementation of a six-segment body-segment model. The body segment model selected for each diver was established using the process described in Section 5.7. The number of dives measured for each diver varied depending on the dive performed and is shown in Table 10-8 to Table 10-15.

### 10.3 Results

#### 10.3.1 Changes in strength measured in profiling sessions

Pre-study profiling was conducted in September 2018. Post-intervention force-plate testing was conducted on February 5<sup>th</sup>, 2019. The date was selected to reflect changes that had been made through the preparatory-phase of training and to allow the divers to present in 'peak' condition – two days after the British Winter National Championships. Force-plate tests were the same as those conducted at the start of the training phase in September.

All tests were repeated three times with the highest (jumping tests) or greatest-force (isometric tests) result being recorded. Changes achieved are described in Table 10-5.

Table 10-5. Change in jump-testing results pre and post intervention.

Test	Change (%)				
	Diver 1	Diver 2	Diver 3	Diver 4	Average
Countermovement jump	5.1	12.9	14.3	-2.8	7.4
Single-leg countermovement jump R	4.1	5.4	18	0.7	7.1
Single-leg countermovement jump L	9.1	7.1	7.1	-12.3	2.8
Drop jump	22.2	23.9	16.9	16.2	19.8
Isometric squat – peak vertical force	-2.5	8.8	-15.3	17.9	2.2
Isometric calf-raise – peak vertical force	48.1	27.4	27.9	-23.6	20

These data show increase in performance in 75 percent of tests. The test in which the athletes showed greatest average improvement was drop-jump (and was one of only two tests where all divers showed an increase post-intervention). Only one diver increased scores in all tests and Diver 4 showed reduced performance in half the tests performed.

The strength programme applied to each diver was specific with regard to the load managed by the athlete but was general across the cohort in terms of exercises chosen and numbers of sets and repetitions performed. Each athlete responded differently to the training dose applied; this may be explained by one or more of the following factors:

- Each diver may have been differently fatigued at the point of testing in September and February although steps were taken to reduce this risk with rest days before both assessment days
- Differences in chronological and training age imply different amounts of headroom (capacity for improvement) – Divers 3 and 4 had been training for more years than Divers 1 and 2
- Physiological adaptation to load is individual; athletes respond in different ways to the training programme applied (Borresen & Lambert, 2009)

Understanding the adaptations made by each athlete, combined with the impact of those changes on diving performance informs future interventions by the S&C coach (and the performance nutritionist who supports fuelling and recovery).

### 10.3.2 Performance metrics – data tables

Performance metrics were calculated for each diver performing dives classified by dive numbers described in Table 10-6.

*Table 10-6. Description of dives classified by dive number (defined by FINA).*

Dive number(s)	Description of dive
100a	Forward jump, straight – the simplest forward-facing skill
200a	Back jump, straight – the simplest backward-facing skill
105, 107	Forward 2.5 somersaults and forward 3.5 somersaults respectively. The diver performs a hurdle step and takes off facing forwards and rotates forwards by the designated number of somersaults.
203, 204, 205	Back 1.5 somersaults, double somersault and 2.5 somersaults respectively. The diver faces backwards and rotates backwards by the designated number of somersaults.
302, 303, 304, 305, 306	Reverse somersault, 1.5 somersault, double somersault, 2.5 somersault and triple somersault, respectively. The diver performs a hurdle step and takes off facing forwards and rotates backwards by the designated number of somersaults.
403, 405	Inward 1.5 somersaults and 2.5 somersaults respectively. The diver faces backwards and rotates forwards by the designated number of somersaults.

Testing dates were as shown in Table 10-7. All results are shown in Appendix B.

Table 10-7. Dates of data collection.

<b>Data Collection</b>	<b>Date</b>
Session 1	6/9/2018
Session 2	13/9/2018
Session 3	18/10/2018
Session 4	22/11/2018
Session 5	17/1/2019

### 10.3.3 Board deflection

#### **Introduction**

One target set by the coach and S&C coach for pre-season was to increase board deflection (the distance the board-tip is displaced during the leg-drive during take-off).

#### **Method**

A camera, calibrated and positioned as described in earlier chapters, filmed training on five occasions during the preparatory phase of training. Each captured dive was manually digitised, and the COM of the diver was calculated by selecting the most appropriate body-segment model as described in Chapter 5.

Mean values for each session of data collection, for four groups of skills, for each diver are shown in Figure 10-1 to 10-4 and Tables 10-8 to 10-11.

## Results

### Diver 1

Table 10-8 – Mean board deflection values – Diver 1.

Diver 1	06/09/2018		13/09/2018		18/10/2018		22/11/2019		17/01/2019	
	Samples	Mean (mm)	Samples	Mean (mm)	Samples	Mean (mm)	Samples	Mean (mm)	Samples	Mean (mm)
100a			3	741	5	786			1	810
200a			3	622			1	573	1	595
Back skill chain (203b, 204b)			3	651			6	587	3	598
Reverse skill chain (303, 304b)							5	813	4	827

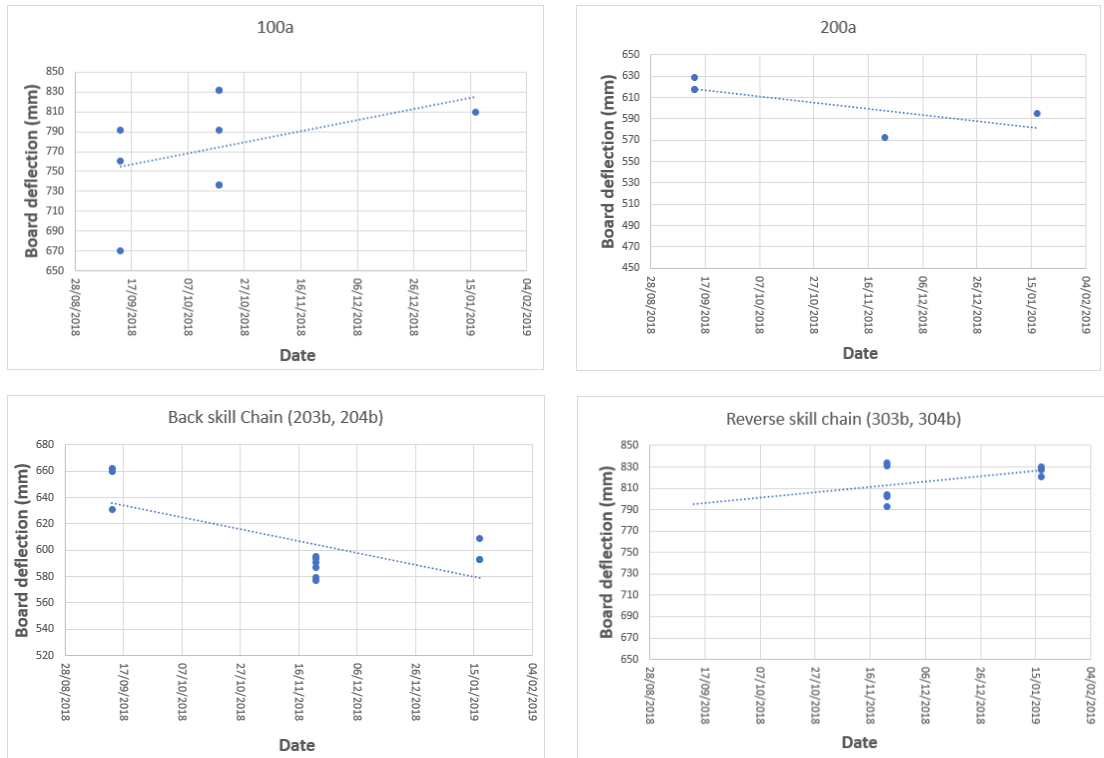


Figure 10-1 – Board deflection with trendline (dotted) – Diver 1.

Diver 1 increased board deflection on skills with a hurdle step (forward jump and reverse skill chain) but decreased deflection on back-facing take-offs (back jump and back skill chain) over the training phase. This raises the possibility of the S&C intervention having a greater effect on the movement into or out of the hurdle step, or increasing trunk stability and being able to benefit from the hurdle step to a greater degree by the end of preparatory phase.



## Diver 2

Table 10-9 – Mean board deflection values – Diver 2.

	06/09/2018		13/09/2018		18/10/2018		22/11/2019		17/01/2019	
	Samples	Mean (mm)	Samples	Mean (mm)	Samples	Mean (mm)	Samples	Mean (mm)	Samples	Mean (mm)
Diver 2										
100a	3	882					2	864	1	897
200a	3	752			3	745	3	734	1	768
Back skill chain (205c, 206c)					3	782	5	757	1	778
Reverse skill chain (305c, 306c)					3	938	6	912	1	966

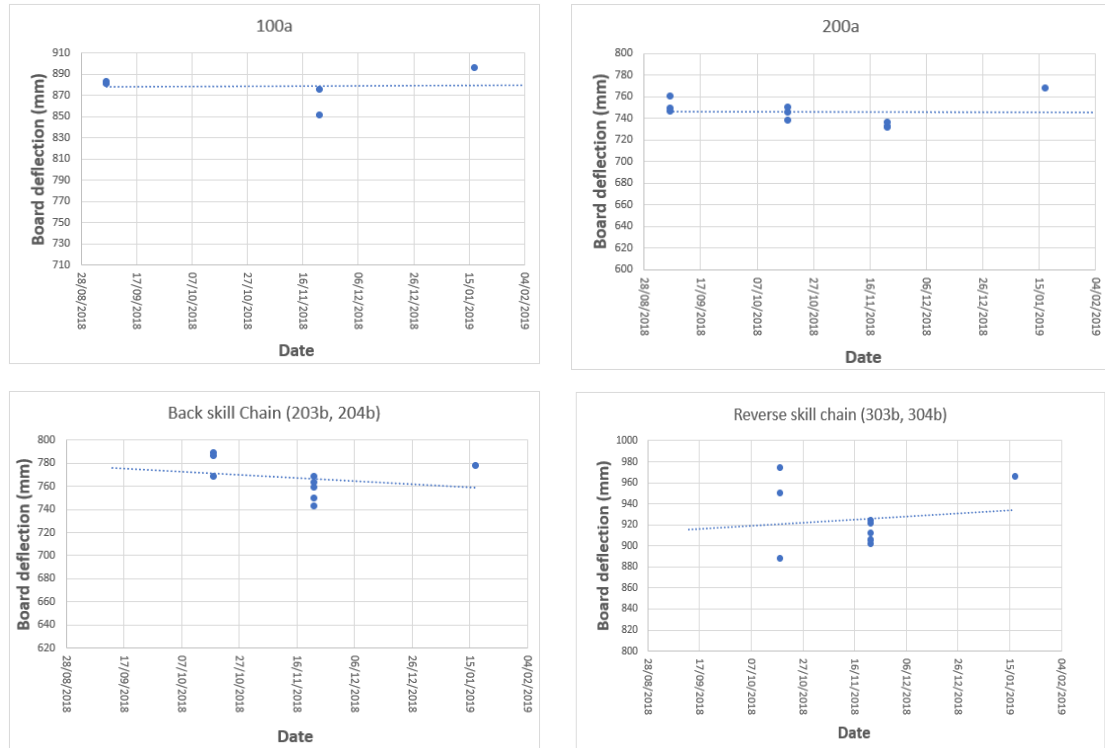


Figure 10-2 – Board deflection with trendline (dotted) – Diver 2.

Diver 2 showed little development of board deflection over preparatory phase. The trend for jumps with no rotation (100a and 200a) showed negligible change over time. The final sample in the phase on rotating skill chains (back and reverse) showed greater deflection than the middle-of-phase samples and the lower samples from the first test, but was no higher than the best sample from the first data collection. This implies that either the diver was focusing on different technical aspects, or that the S&C intervention did not improve physicality through the training phase.

### Diver 3

Table 10-10 – Mean board deflection values – Diver 3.

	06/09/2018		13/09/2018		18/10/2018		22/11/2019		17/01/2019	
	Data collection 1		Data collection 2		Data collection 3		Data collection 4		Data collection 5	
Diver 3	Samples	Mean (mm)	Samples	Mean (mm)	Samples	Mean (mm)	Samples	Mean (mm)	Samples	Mean (mm)
100a	3	935			1	1011			1	946
200a	3	711			2	780			1	747
Reverse skill chain (304c, 305c)	3	974			4	1010			3	1004
Inward skill chain (403, 405c)					3	780			5	764

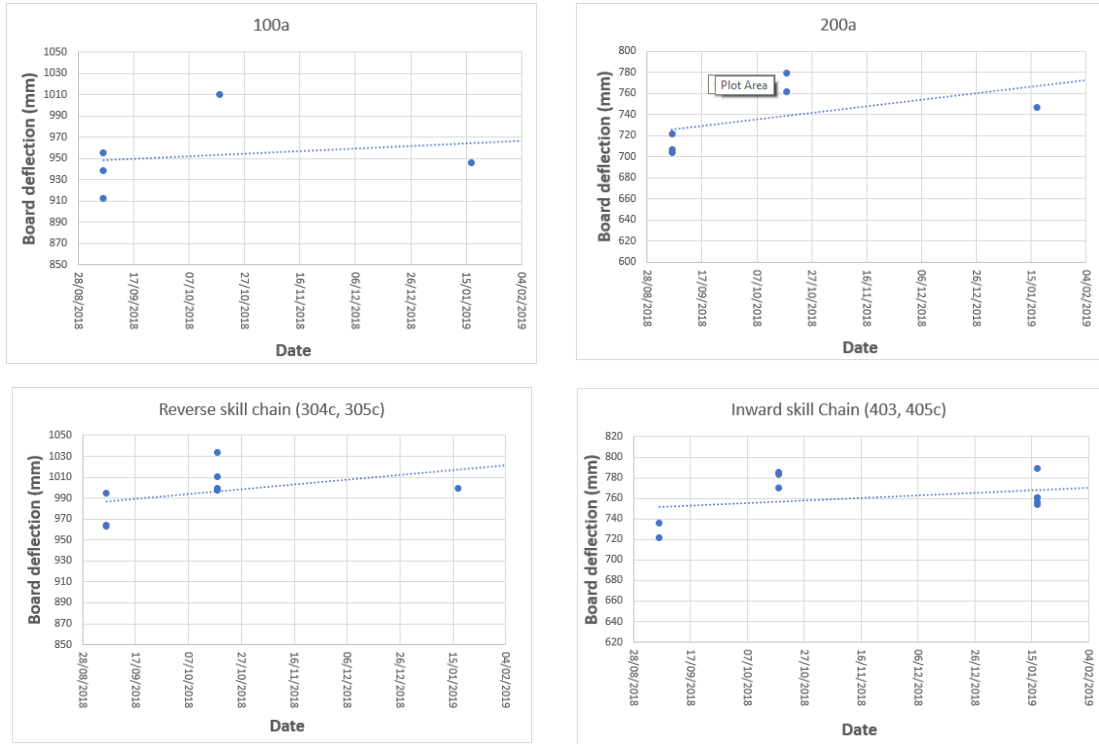


Figure 10-3 – Board deflection with trendline (dotted) – Diver 3.

The trendline in all groups shows improvement in deflection for Diver 3. In most cases, the samples in the second and third data collection sessions were all higher than those at the start of the testing phase. This suggests that the S&C programme achieved the desired effect.

## Diver 4

Table 10-11 – Mean board deflection values – Diver 4.

Diver 4	06/09/2018		13/09/2018		18/10/2018		22/11/2019		17/01/2019	
	Samples	Mean (mm)	Samples	Mean (mm)	Samples	Mean (mm)	Samples	Mean (mm)	Samples	Mean (mm)
100a	3	917	3	916	3	954			1	891
200a	2	739	3	775	3	776			1	730
Reverse skill chain (305c, 306c)	3	917	2	963	4	997			3	959
Back skill chain (203,204,205c)	4	738	5	795	5	792				

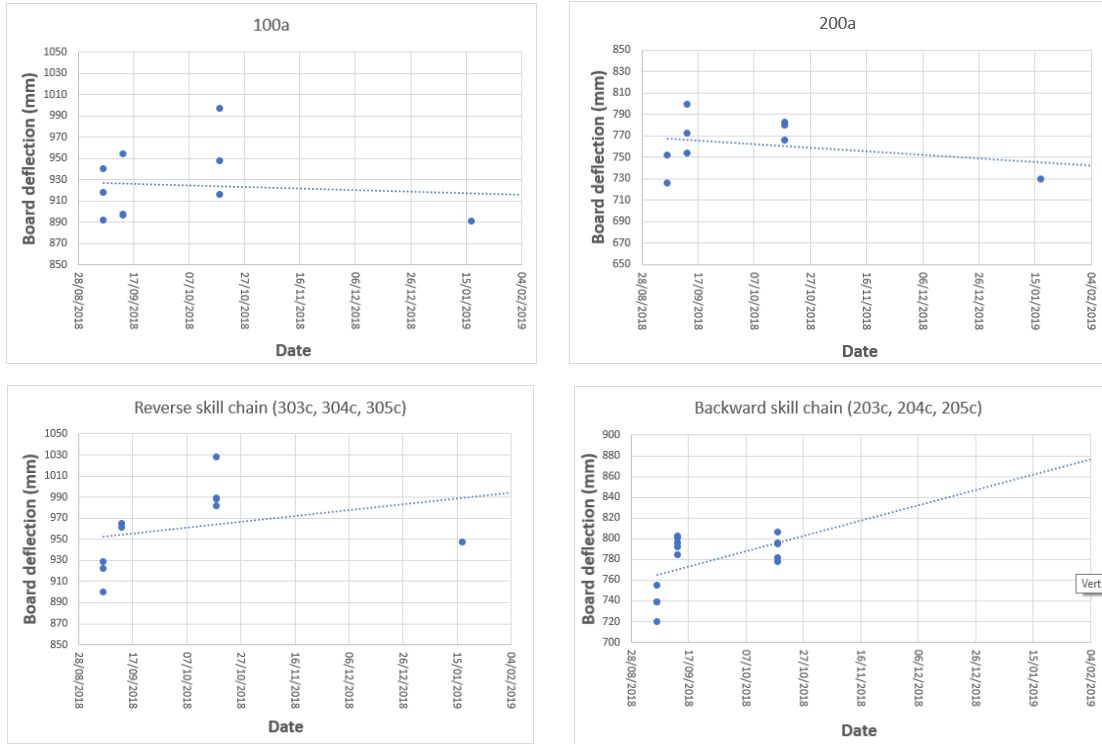


Figure 10-4 – Board deflection with trendline (dotted) – Diver 4.

The results of Diver 4 show a less clear effect of S&C on board deflection than for Diver 3. Although positive trendlines are seen in back and reverse rotating groups, the final sample in the reverse testing was lower than the best sample in the first data collection. Although the best sample in the forward jump (100a) was in the second data collection (showing improvement from the first test), the final (single) sample.

## Discussion

The results found would have greater reliability if there had been more samples, particularly in the final session of data collection, although the testing followed the objectives described earlier – that the coach’s training programme was not influenced or affected by the testing process.

The presented data, however, does not show that a planned S&C intervention, where organisation and exercise selection is consistent across the athlete cohort, consistently improves board deflection in training – although a clear improvement can be seen for some athletes in some groups. A subsequent study with more data samples and a more individualised approach to strength training would therefore be appropriate.

#### 10.3.4 Vertical take-off velocity

##### **Introduction**

The second stated aim was to increase take-off velocity as a result of S&C and technical training throughout the preparatory phase.

##### **Method**

The same dives (captured and digitised according to the method described earlier). Take-off velocity was calculated from the COM data describing the best-fit parabola from COM positions throughout the dive, as described in Section 5.7 (using the height of the peak of the parabola and the time taken to achieve that vertical displacement).

Results are shown in Tables 10-12 to 10-15 and Figures 10-5 to 10-8.

## Results

### Diver 1

Table 10-12 – Mean take-off vertical velocity values – Diver 1.

Diver 1	06/09/2018		13/09/2018		18/10/2018		22/11/2019		17/01/2019	
	Samples	Mean (mm)	Samples	Mean (m/s)	Samples	Mean (m/s)	Samples	Mean (m/s)	Samples	Mean (m/s)
100a			3	4.9	5	5.5			1	5.0
200a			3	3.7			1	4.2	1	4.1
Back skill chain (203b, 204b)			3	3.8			6	4.1	3	4.0
Reverse skill chain (303, 304b)							5	4.9	4	4.7

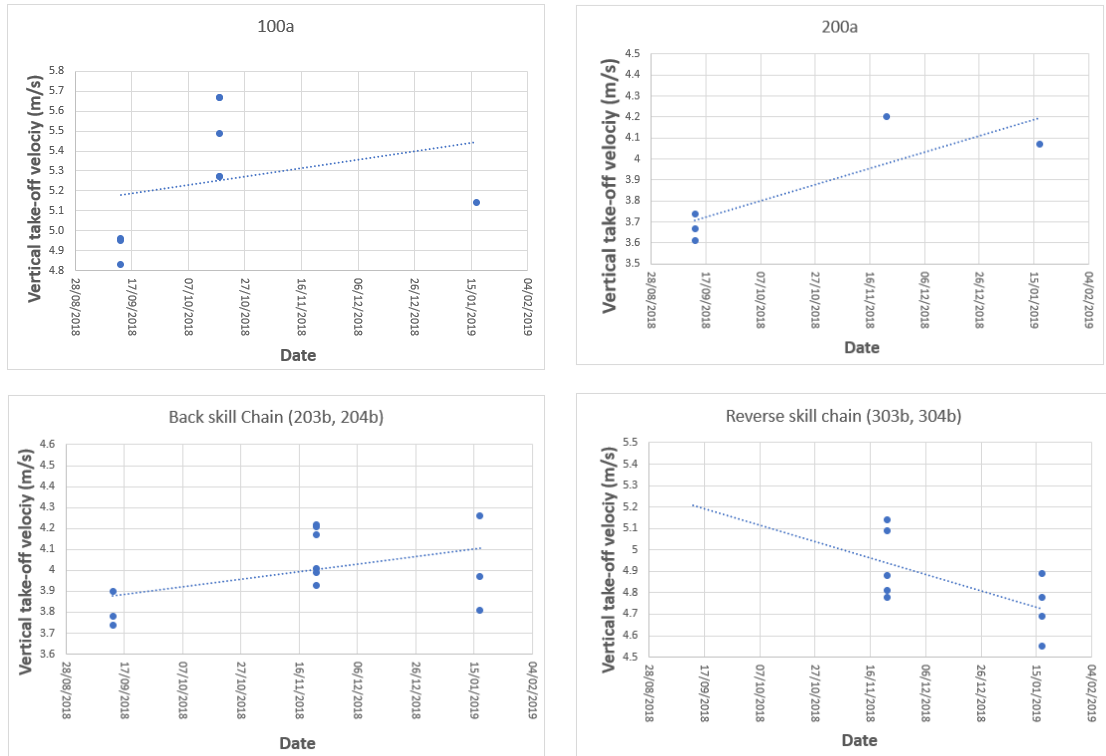


Figure 10-5 – Vertical take-off velocity with trendline (dotted) – Diver 1.

Diver 1 showed a trend of improvement in take-off velocity (both in mean values and trend using all samples) in three out of four groups, with a clear downward trajectory for the reverse skill chain. These data suggest that there was a clearer relationship between training (both S&C and technical) and the development of take-off velocity, compared to the development of board deflection.

## Diver 2

Table 10-13 – Mean take-off vertical velocity values – Diver 2.

	06/09/2018		13/09/2018		18/10/2018		22/11/2019		17/01/2019	
	Data collection 1		Data collection 2		Data collection 3		Data collection 4		Data collection 5	
Diver 2	Samples	Mean (m/s)	Samples	Mean (m/s)	Samples	Mean (m/s)	Samples	Mean (m/s)	Samples	Mean (m/s)
100a	3	5.38			2	6.03	2	6.30	1	6.15
200a	3	4.95			3	4.92	3	5.30	1	5.07
Back skill chain (205c, 206c)					3	5.18	5	5.33	1	5.28
Reverse skill chain (305c, 306c)					3	6.24	6	6.15	1	5.96

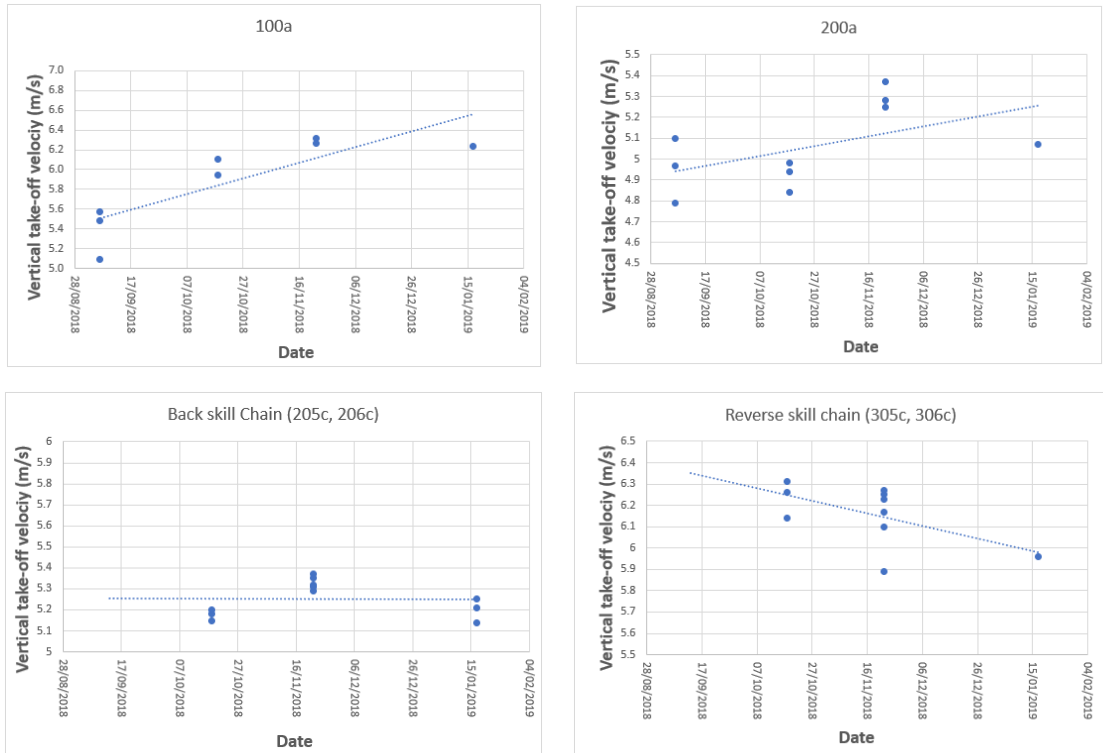


Figure 10-6 – Vertical take-off velocity with trendline (dotted) – Diver 2.

Diver 2 showed an improvement through the preparatory phase on jumps (100a and 200a) with some improvement in the back skill chain (albeit with a fairly level trendline) despite limited change in board deflection (Figure 10-3), but a reduction in take-off velocity (both in mean and in high/low values) in the reverse group (as shown by Diver 1).

### Diver 3

Table 10-14 – Mean take-off vertical velocity values – Diver 3.

Diver 3	06/09/2018		13/09/2018		18/10/2018		22/11/2019		17/01/2019	
	Samples	Mean (m/s)	Samples	Mean (m/s)	Samples	Mean (m/s)	Samples	Mean (m/s)	Samples	Mean (m/s)
100a	3	5.93			1	6.1			1	5.14
200a	3	5.16			2	4.8			1	4.52
Reverse skill chain (304c, 305c)	3	5.86			4	5.9			3	5.83
Inward Skill chain (403c, 405c)	2	4.45			3	4.56			5	4.65

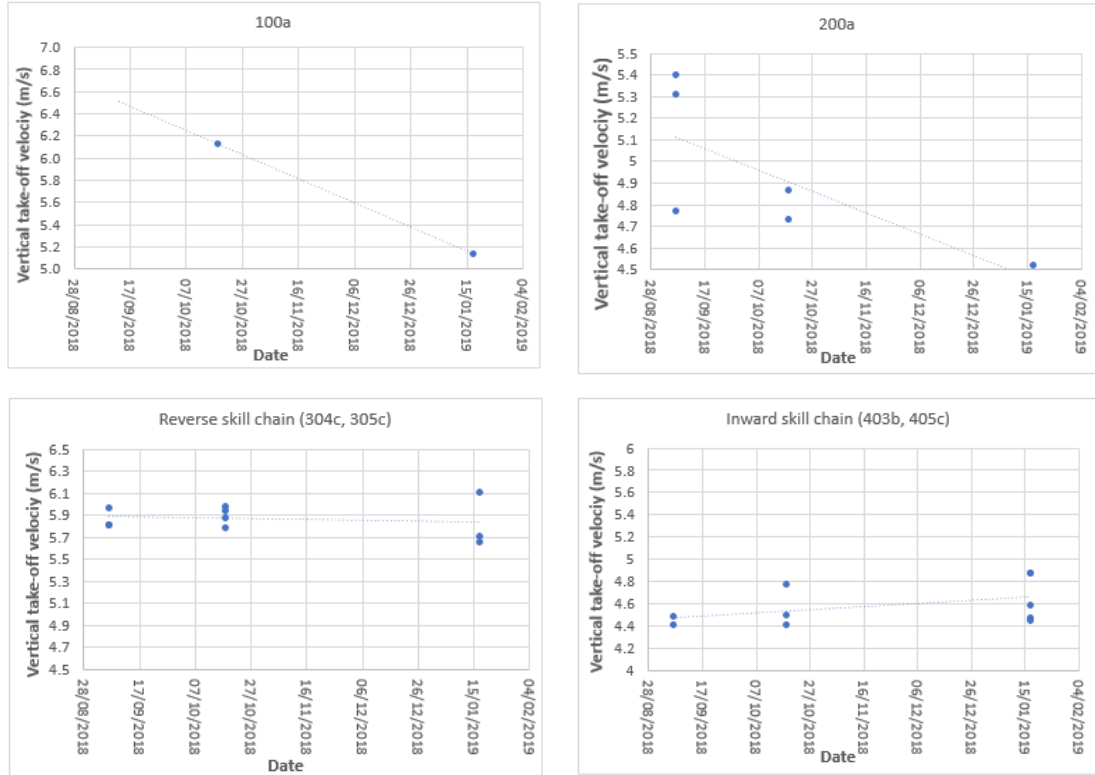


Figure 10-7 – Vertical take-off velocity with trendline (dotted) – Diver 3.

Diver 3 was unable to show an increase in take-off velocity over the preparatory phase in three groups out of four, although the maximum velocity measured in the reverse skill chain increased over each data collection, where the lowest measures result in a trendline with a negative gradient. Diver 3 was the athlete with an increase in board deflection shown in the most groups of all the divers measured – challenging the relationship between board deflection and take-off velocity. A small number of samples in the jumping skills limits the reliability of the trendlines for 100a and 200a.

## Diver 4

Table 10-15 – Mean take-off vertical velocity values – Diver 4.

Diver 4	06/09/2018		13/09/2018		18/10/2018		22/11/2019		17/01/2019	
	Samples	Mean (m/s)	Samples	Mean (m/s)	Samples	Mean (m/s)	Samples	Mean (m/s)	Samples	Mean (m/s)
100a	3	5.98	3	5.30	3	5.78			1	5.78
200a	2	4.63	4	4.09	3	4.6			1	4.69
Reverse skill chain (305c, 306c)	3	5.61	2	5.37	7	5.72			3	5.6
Back skill chain (203,204,205c)	4	4.43	5	4.3	5	4.71				

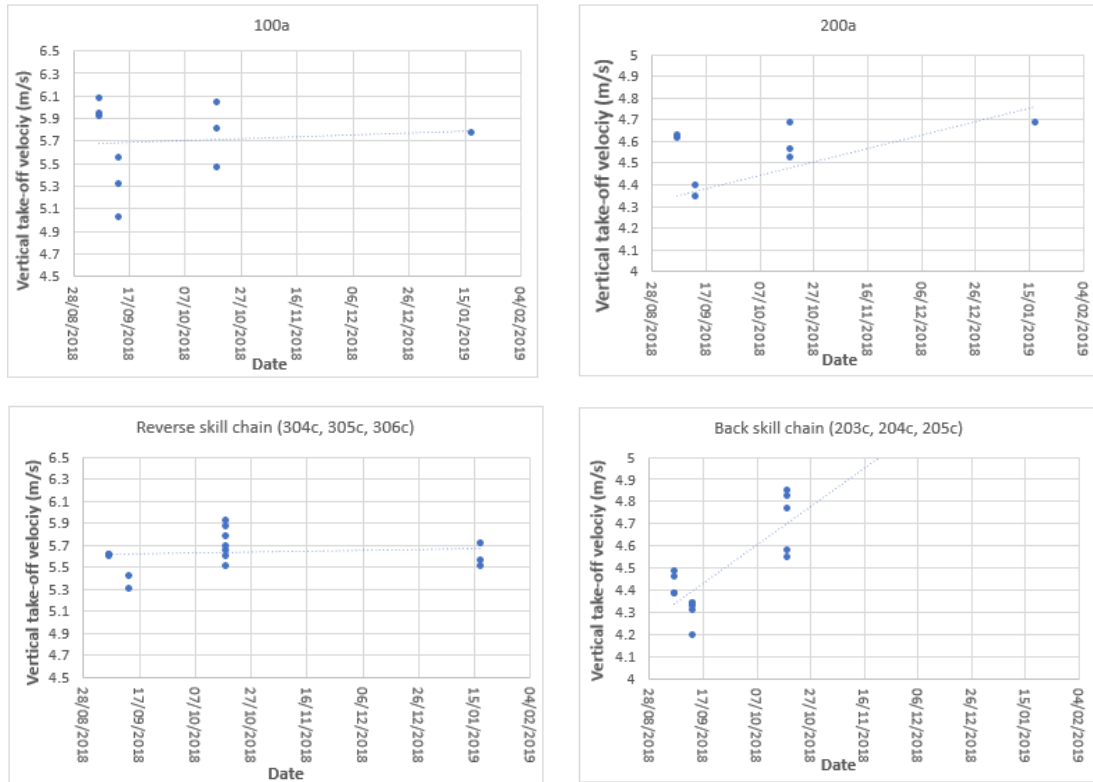


Figure 10-8 – Vertical take-off velocity with trendline (dotted) – Diver 4.

Diver 4 showed greatest improvement in standing take-offs (200a and the back skill chain) where the trendline showed improvement and mean/maximum values were greater at the end of testing than at the start. Forward jumps showed a positive trendline, however the single sample at the end of testing was approximately the same as the mean values from the other testing days. Mean and maximum values for the reverse skill chain indicate a small development in take-off velocity through the preparatory phase. As with the other divers, improvement of maximum deflection and take-off velocity were not always linked, casting doubt on the hypothesis that increased deflection leads to increased take-off velocity.



## Discussion

The same limitations as found with the maximum deflection analysis apply to these results – there are a small number of samples, and a further study with more samples (and more divers) would allow stronger conclusions to be drawn. Nevertheless, the rate of improvement, and the groups in which improvement, or decline, is shown varies across the diver cohort. It can also be concluded that a similar organisation of strength and conditioning, albeit with different load for different divers, does not produce a consistent performance change in a range of divers. This supports a hypothesis that an individualised approach to strength planning, with a greater understanding of each diver’s physical qualities, may produce a more beneficial effect.

These data also show that a commonly held belief – that greater board deflection leads to greater take-off velocity – is overly simplistic and does not apply in a great number of cases.

### 10.3.5 Relationship between board deflection and vertical take-off velocity

Although the goal set by the technical coach was to increase board-deflection on take-off with the aim of increasing vertical take-off velocity and correspondingly increasing COM displacement and flight-time, the data shows little evidence that one is dependent on the other.

The relationship between metrics is shown in Table 10-16.

*Table 10-16. The relationship between change in board-deflection and vertical take-off velocity. A blue, upward arrow indicates positive change in a metric (measured by the gradient of trendline). A red, downward arrow indicates negative change in a metric (measured by the gradient of the trendline). Shaded pairs of arrows indicate a mismatch between direction of change in metrics.*

Skill	Diver 1		Diver 2		Diver 3		Diver 4	
	Deflection	Vertical velocity	Deflection	Vertical velocity	Deflection	Vertical velocity	Deflection	Vertical velocity
Fwd jump	↗	↗	↗	↗	↗	↘	↘	↗
Back jump	↘	↗	↗	↗	↗	↘	↘	↗
Back	↘	↗	↗	↘				
Reverse	↘	↗	↗	↘	↗	↗	↗	↗
Inwards					↗	↗	↗	↗

In nine out of sixteen instances (indicated by shaded cells), the direction of change in board-deflection is not matched by the direction of change in vertical take-off velocity. The divers achieved the first goal (of increased board deflection) 69% of the time, and the second goal (to increase take-off velocity) 75% of the time. The expected relationship between increase in both deflection and take-off velocity was, however, only shown 44% of the time.

## 10.4 A study investigating influential components for take-off performance

### **Introduction**

It was therefore appropriate to consider the effect of other variables on maximum take-off velocity to identify the components of take-off that influence the dependent variable of vertical take-off velocity. This was achieved by performing a series of regression analyses.

### **Method**

The regression tool in Microsoft Excel was used to perform a series of regression analysis operations on performance data calculated throughout the preparatory phase (and used in Section 3-4). Analyses were carried out using whole-cohort data to identify group trends, and on individual diver's data to describe individual difference. In all cases, two jumping skills were used for analysis – 100a (forward jump with a hurdle step) and 200a (back jump).

### **Results**

In addition to the summary results presented in this section, detailed results are contained in Appendix G.

#### 10.4.1 Hurdle step and forward jump (100a)

An analysis was carried out to determine the relationship between the dependent variable of vertical take-off velocity and the independent variable of maximum board deflection is shown in Table 10-17.

Table 10-17. Regression analysis of the dependent variable 'vertical take-off velocity' and the independent variable 'board deflection'. Significance was set at  $p < 0.05$ .

Dataset	R-Square	p
All divers	0.33	0.00
Diver 1	0.47	0.06
Diver 2	0.01	0.86
Diver 3	0.34	0.42
Diver 4	0.31	0.12

The dataset for the whole cohort shows a weak relationship and considering all divers' data individually, Diver 1 showed the strongest relationship – although the r-square value stays below 0.5 and is therefore still a weak relationship. Results for Divers 2,3 and 4 have a p-value too high to have confidence in their result.

The effect of the combination of maximum deflection and the amount of remaining leg extension during recoil was calculated and shown in Table 10-18. When multiple independent variables were used, the adjusted R-Square value was used to avoid the feature of R-Square increasing as more independent variables are used.

Table 10-18. Regression analysis of the dependent variable 'vertical take-off velocity' and the independent variables 'maximum board deflection' and '% impulse after maximum deflection'. Significance was set at  $p < 0.05$ .

Dataset	Adjusted R-Square	p
All divers	0.28	0.00
Diver 1	0.49	0.07
Diver 2	-0.36	0.82
Diver 3	-0.46	0.69
Diver 4	0.49	0.05

Results for all divers, Diver 1 and Diver 3 have a p-value low enough to indicate reliability and these values show a weak relationship between variables. This indicates that the extent to which the legs are extended by maximum deflection has little influence on take-off velocity.

A higher hurdle step is sought by coaches to increase potential energy and landing velocity. S&C coaches typically build the divers' ability to deep-squat (minimising the internal knee angle) under load in order to develop leg strength. The effect of these variables is shown in Table 10-19.

*Table 10-19. Regression analysis of the dependent variable 'vertical take-off velocity' and the independent variables '1<sup>st</sup> contact landing velocity' and '1<sup>st</sup> contact knee angle'. Significance was set at  $p < 0.05$ .*

Dataset	Adjusted R-Square	p
All divers	0.35	0.00
Diver 1	0.26	0.19
Diver 2	0.96	0.00
Diver 3	0.12	0.54
Diver 4	0.42	0.07

The p-values in these results indicate that adjusted R-square values for all divers, Diver 2 and Diver 4 are the most reliable. These results show that, although landing speed and knee angle are not shown to be well related to take-off velocity, Diver 2 shows a strong relationship between variables.

The divers' posture at first contact is specifically coached to meet technical criteria to minimise unhelpful trunk movement leading to a misdirected resultant force on the body. For this reason, knee and trunk angle were used as independent variables. Results are shown in Table 10-20.

Table 10-20. Regression analysis of the dependent variable 'vertical take-off velocity' and the independent variables 'trunk angle at 1<sup>st</sup> contact' and '1<sup>st</sup> contact knee angle'. Significance was set at  $p < 0.05$ .

Dataset	Adjusted R-Square	p
All divers	0.38	0.00
Diver 1	0.40	0.11
Diver 2	0.42	0.14
Diver 3	0.71	0.30
Diver 4	0.42	0.07

These results show that, although the relationship between variables is generally weak, there is an indication of a strong relationship for Diver 3, with an adjusted R-square value of 0.71. The p-value associated with this result is high, however, and suggests that more data is required to have more confidence in the result.

#### 10.4.2 Back jump 200a

The relationship between deflection and take-off velocity is shown in Table 10-21.

Table 10-21. Regression analysis of the dependent variable 'vertical take-off velocity' and the independent variable 'board deflection'. Significance was set at  $p < 0.05$ .

Dataset	R-Square	p
All divers	0.12	0.06
Diver 1	0.83	0.08
Diver 2	0.28	0.17
Diver 3	0.66	0.09
Diver 4	0.35	0.12

Across the whole cohort, there is a weak relationship between maximum deflection and take-off velocity, although for Diver 1 and Diver 3 there is a stronger relationship. R-square values of 0.83 and 0.66 suggest a link, although the p value for both datasets is higher than 0.05.

*A fast armswing is considered by coaches to be important in an effective take-off. A more complete armswing (by maximum deflection) reduces the action-reaction effect where the arms lift and retard the movement of the body*

during recoil. For this reason, the speed of armswing to maximum deflection is added as an additional independent variable. Results are shown in

Table 10-22.

Table 10-22. Regression analysis of the dependent variable 'vertical take-off velocity' and the independent variables 'speed of armswing to maximum deflection' and 'maximum deflection'. Significance was set at  $p < 0.05$ .

Dataset	Adjusted R-Square	p
All divers	0.06	0.15
Diver 1	0.70	0.31
Diver 2	0.52	0.06
Diver 3	0.39	0.30
Diver 4	0.24	0.21

There are no p-values that indicate significance, but there is a high range of adjusted R-square values showing a greater relationship between variables for Diver 1 than others.

As with forward take-offs, S&C coaches develop strength from a deep squat to build the ability to produce force during take-off. Knee angle and the extent to which legs are driven straight by maximum deflection are used as independent variables; results are shown in Table 10-23.

Table 10-23. Regression analysis of the dependent variable 'vertical take-off velocity' and the independent variables '% impulse by maximum deflection' and 'maximum deflection'. Significance was set at  $p < 0.05$ .

Dataset	Adjusted R-Square	p
All divers	0.44	0.00
Diver 1	0.79	0.26
Diver 2	0.33	0.15
Diver 3	0.93	0.03
Diver 4	-0.26	0.77

There are limited measures that have a reliable p-value, but for those that do, the variables have a strong relationship for Diver 3. There is also a strong relationship for Diver 1, albeit with a high p-value that limits the confidence of the result.

## **Discussion**

The study described in this section is not intended to be an exhaustive investigation into key relationships between variables, and it is recognised that greater confidence would be implied by the results with more samples. The study shows, however, that there are relationships between independent and dependent variables that exist for some divers and not others in a cohort.

For example, the highest take-off velocities achieved in a forward jump with hurdle occurred for Diver 2 when first contact (the point at which the diver lands on the end of the board following the hurdle step) velocity was highest and the knees were most bent before driving into the board. For Diver 1, the timing of the leg extension was an influence in take-off velocity and Diver 4 gained their best take-off speed with an upright posture during the drive phase into the springboard.

Back jumps showed a similar range of influential variables. For Diver 1, maximum deflection and speed of armswing were key variables (matching the expectations of coach and S&C coach) whereas speed and extent of leg drive by maximum deflection showed a close relationship for Diver 3.

Comparing the results of Table 10-5 (development of S&C performance measured by profiling) to these results shows little relationship to the gains made in S&C and the gains made in diving.

It is furthermore an unsafe assumption that developing similar qualities in divers to improve key metrics across a cohort will lead to a consistent and optimal development of performance in a team of divers. This study shows that a more individualised analysis can be carried out using the diveTracker system to learn about divers' individual strengths and development areas and provide data leading to a more effective, bespoke physical and technical training intervention.

## **10.5 Performance metrics and WITTW values**

### **Introduction**

Comparison of divers' performance metrics to those of the world's best allow strengths and development areas to be identified. An investigation was carried out to compare the cohort involved in the study to WITTW standards.

## Method

Mean take-off velocities and rotation speed for each diver were compared to WITTW standards in each group, as defined by the study detailed in Chapter 9. Results are shown in Table 10-24 and Table 10-25; the comparison serves a gap-analysis of that metric. As divers were in pre-season training, their skills were lead-up skills of the dives shown in international competition, performing from 2 metres lower (on a 1 m springboard) and completing one fewer somersault in each dive.

## Results

*Table 10-24. The gap between mean vertical take-off velocity achieved by Divers 1-4 in training (of lead-up skills) and the average corresponding WITTW standards. The highlighted cell reflects where the diver exceeded the corresponding WITTW standard. All units are metres per second.*

Group \ Diver	1	2	3	4
Forward	0.45	0.44	0.94	
Back	0.38	0.16		0.65
Reverse	0.29	0.12	0.55	0.64
Inward		-0.02	0.10	0.63

*Table 10-25. The gap between somersault speed (revs, or 'somersaults per second') by Divers 1-4 in each group of lead-ups and the corresponding WITTW standard. Highlighted cells show where WITTW standards have been exceeded. All units are somersaults per second.*

Group \ Diver	1	2	3	4
Forward		-0.03		0.31
Back	0.26	0.21		0.57
Reverse	0.29	0.15	0.56	0.48
Inward	0.12	-0.16	0.43	0.45



The greatest gaps in performance were shown by Diver 3 (gaps between approximately 0.2 to 0.9 metres per second) and Diver 4 (approximately 0.6 to 0.7 metres per second). Diver 1 showed gaps of approximately 0.3 to 0.4 metres per second, showing that they were closer to WITTW standards. Diver 2 was closest to WITTW standards, having greater take-off velocity in the inward group, and having gaps of approximately 0.1 to 0.4 metres per second in other groups. Section 4.3 concluded potential error in calculation of vertical take-off velocity of up to 0.06 metres per second. The highlighted value belonging to Diver 2 is within that error range; accordingly, there must be the recognition that – although close to the WITTW target – the actual take-off velocity could be slightly lower.

Section 10.3.3 and Section 10.3.4 showed that Diver 1 and Diver 2 made the greatest percentage change in take-off velocity. The assumption of starting from a lower level is supported in the case of Diver 1 due to the high gap to WITTW standard in all groups. Divers 3 and 4 made a smaller percentage gain and remain (in most groups) greater than 0.5 metres per second from the WITTW standard for each dive. This implies that the physical and technical programmes may need re-evaluation to stimulate greater change in the athlete or reflect athletes closer to their physical peak with less headroom to improve.

Diver 2 showed rotation speed closest to WITTW standards, exceeding the target in the forward group and showing a difference of between approximately 0.1 to 0.2 somersaults per second in the other groups (between 5% and 7% speed of rotation). Diver 3 and Diver 4 showed differences of between approximately 0.4 to 0.6 and 0.3 to 0.7 somersaults per second respectively.

While the difference for Diver 1 in absolute terms is small (approximately 0.2 to 0.3 somersaults per second), her dives are performed in the slower-rotating pike position. These differences are between 8% and 15% of the target speed. Divers 3 and 4 show a difference of up to 18% spin speed.

A fast-rotating diver can, as shown by the WITTW tables (Table 9-3 to Table 9-6) create an equally high opening with lower take-off velocity than others. The results above show that Diver 2 is closest to WITTW standards in both take-off velocity and speed of rotation, indicating the potential for a high opening from each dive. Divers 1,3 and 4

show greater gaps that need to be closed by technical and performance-science interventions.

## 10.6 Discussion

Although all divers completed an S&C intervention, results showed individual adaptation both in terms of physical characteristics (measured in post-Preparatory Phase force plate testing) and in diving performance. Some divers made measurable progress in S&C but either limited gains or losses in diving performance markers. This raises questions as follows:

- Does the applied S&C intervention have the correct content? If only small gains are made in performance, and some of these gains can be accounted for by good technical coaching, the S&C programme should be reviewed for specificity
- If only small gains in S&C are made, but require approximately 3 hours of training each week, would the diver gain more by doing less S&C and either diving or resting more? If a threshold level of strength has been achieved for that diver, modification of the components of total load might have a greater performance effect

A conclusion can be drawn that, due to the range of effect following similar S&C programmes and similarly organised technical training programmes, each diver may benefit from more individualisation of components of load. The effects of this variation could then be measured by the diveTracker system to corroborate or challenge plans.

The lack of strong correlation between any single independent variable (measured in this study) and take-off velocity is intuitively understandable; different physical and technical capabilities between divers suggests that it is reasonable that a desired outcome is achieved by maximising the strengths of the individual.

Variation in technical attributes between divers suggests that there might be a collection of independent variables that influences dependent variables such as take-off velocity. For example, speed of rotation may be influenced by:

- Vertical take-off velocity

- Amount of lean (potentially inhibiting the adoption of a tight shape in flight)
- Change in trunk and arm posture during recoil (producing rotation by transfer of momentum)
- Change in moment of inertia (MOI) of the body between take-off and the adoption of the tightest shape
- Size of interior joint angles in the body during the flight-phase when MOI is smallest

An investigation could be conducted to identify a list of such influences, with the assumption being that strong capability in enough of these variables would produce high performance. All the kinematic parameters required to determine these data are calculated by the diveTracker tool and the automated tracking feature would allow a statistically significant number of dives to be analysed in a time-efficient manner.

Having determined the key factors that each diver uses to produce height and rotation efficiently and beautifully (to achieve high judge scores), the multi-disciplinary team is better equipped to design interventions to reduce weaknesses and enhance strengths.

## 10.7 Summary

Kinematic data has historically been produced by either filming competitions or by constructing a contrived training situation to observe a specific skill or movement (Section 2.5). This has the consequence of not necessarily reflecting normal performance (due to competition pressure) or adversely affecting the training programme of an elite diver by interrupting training to measure variables of academic interest. There have been no studies of dives performed in a natural training environment and no description of longitudinal change.

This chapter has shown that by implementing methods described in earlier chapters, performance data can be measured and change tracked over time with minimal impact (only the time taken to apply reflective markers to a diver) on the delivery of a diving training programme. Change in capability of a team of divers has been quantified and compared to standards met by their world class competition.

The British World Class Diving programme can now collect performance data on an athlete and use these to assess progress with more objective accuracy and validate or support the development of training interventions designed to produce a specific output.

The study has served to challenge an existing belief about performance, namely that increased take-off velocity is a predictable consequence of greater board deflection during take-off. It has also shown that there is not a direct relationship between improvement in certain physical tests (that are considered to be most specifically related to good diving by experts in the WCP) and improvement in diving performance.

Data analysis has suggested that divers have individual responses to training load and produce their best dives (by comparison of key indicators to WITTW data) by exploiting different strengths and technical attributes. The study has shown that the diveTracker system produces appropriate kinematic data to enhance understanding of these attributes, potentially enhancing the planning process so that more individualised interventions are applied to athletes in the search for greater performance. This tool and process is unique in Diving.

## 11 Summary and next steps

### 11.1 Introduction

This study has demonstrated that the calculation objective measurements in a sport which is inherently difficult to quantitatively analyse can be achieved. It has been shown that a single camera mounted in a training or competition environment, set up and operated by a single user, generates objective performance data that informs a diver, coach and multidisciplinary team. This study has proved that accurate and useful data can be derived from both a permanent installation and a simple, temporary setup, allowing implementation in a variety of centres, from smaller pools to designated World Class facilities, in both training and competition.

### 11.2 New process

Chapter 3 and Chapter 4 specified a method for performing a camera calibration that allows diving to be filmed using a single camera. The method supports flexibility in camera situation and lens setting, corrects for lens distortion and provides more accurate reconstructions from positions, including those close to the edge of the image, than achieved using linear calibration as implemented in historic studies in diving.

The diveTracker tool, specifically created to provide objective feedback to divers and their support team, facilitates the sharing of performance data which is more accurate (when considering the impact of greater reconstruction accuracy, higher frame rate of captured footage and the ability to identify the body segment model from a selection that best reflects the morphology of the diver) than in previous published studies.

Automated tracking can be achieved using a three-segment model defined by a small number (5) of reflective markers fixed to the diver. Performance metrics derived from this process closely match those achieved by manual digitisation and the utilisation of a six-segment body-segment model. The speed with which kinematic data can be returned to the diver and coach exceeds any comparable studies in the sport.

The variety of means with which performance data can be communicated within the team (numerical, pictorial and video) embeds the data collected into the day-to-day feedback cycle using hardware and reporting methods established in the team and informs and refines the decision-making within the multi-disciplinary support team.

### 11.3 New knowledge

A study into the kinematic parameters exhibited by world class divers has produced a collection of metrics describing contemporary springboard diving for males and females. It has described take-off velocity, flight time, speed of rotation, opening height and drop time required to achieve scores of 8.5 ('very good' as defined in FINA's rules of judging) or above. These data are now contained in British Diving's What It Takes to Win (WITTW) model as benchmark standards of performance to be achieved and surpassed by divers on the World Class Programme (WCP).

Performance data for WCP athletes is now collected in training and competition and longitudinal tracking of these metrics indicates progress towards these standards and informs the Programme and stakeholders of the development of the diver.

### 11.4 New practice

Divers and coaches can use the diveTracker system to get performance data in training and understand the effect of coaching points in an objective manner to support standard subjective assessment and feedback.

Kinematic data are now included in the multi-disciplinary planning process.

Performance questions can now be framed in terms of kinematic standards and athlete plans can be developed and implemented to address them. This has modified the process where goals were set in the context of the individual discipline (for example, a previous goal might be to demonstrate greater potential for producing force by increased a 3-repetition maximum load for back squat, where now the goal can be to increase the rate of leg-extension with the aim of achieving a defined take-off velocity).

WCP divers' performances from National Championships are now analysed and the resulting data used in performance reviews to inform understanding of the progress made, and remaining gap to World Class since the last review (Appendix E).

Programme divers' data is, as a result of this study, presented as part of the regular reporting to stakeholders to inform and to provide evidence when making an argument for selection to (or continued membership of) the WCP (Appendix E).

Data generated by both the diveTracker system and the study into WITTW kinematic benchmarks has influenced thinking about physical and technical development of divers. The historic question "how strong is strong enough?" has changed to "what variables are required to be excellent to perform at a world class level?" indicating an evolving understanding of the effect of ancillary components of load.

### 11.5 Benefits to the diver

The new knowledge derived from this study creates specific benefits to the diver:

- A quantitative gap analysis of performance characteristics between their dives and those defining WITTW supports identification of development areas and progress towards performance goals
- An understanding of the key influencing variables for each diver when performing a skill informs an individualised approach to physical and technical development
- A greater understanding of the effect of interventions (for example Strength and Conditioning) on diving performance allows more individualised programming
- An ability to compare training load and modulation with change in performance supports a more informed approach to planning load in each training cycle
- Performance markers from training inform return-to-training progression from injury and provide insight into progression back to 'full fitness' and 'readiness to compete'.

## 11.6 Future development

### 11.6.1 Longitudinal tracking and prediction of WITTW kinematic parameters

Annual updates of WITTW parameters can be achieved using the diveTracker system. This brings the benefits of maintaining a record of contemporary standards and understanding the rate of change of take-off and flight metrics as dives are replaced by higher-difficulty equivalents. It has been shown in Chapter 9 that take-off velocity has increased as has list-difficulty since 1990. The lack of data available between the Atlanta and London Olympic cycles limits understanding of rate of change (although progression of difficulty can be tracked through competition results, the kinematic measures cannot); a greater understanding of the development of performance characteristics ahead of increase in difficulty will help the WCP predict the required difficulty in future Olympic Games and both select and prepare potential talents accordingly.

Longitudinal analysis of Pathway athletes (those in the early stages of their career, progressing to senior world class standards) in an early-specialisation sport such as diving could give greater understanding of the effect of physical maturation. It is anecdotally and empirically understood that once-established technique become inconsistent as growth accelerates, and risk-management strategies are implemented to mitigate the risk of injury during growth spurts. Measuring rate of change in segment-length during video analysis and change in consistency in take-off performance could inform training programmes with the aim of maximising performance gains and minimising risk to the diver.

### 11.6.2 Identification of critical take-off parameters

Chapter 10 introduced the idea of multiple critical variables in the performance of an optimal take-off. The data generated in this study is of a size to limit the value of a statistical evaluation and prevents a trustworthy multiple-regression analysis to identify the critical independent variables that have greatest effect on take-off velocity. A further study analysing a greater number of dives by a larger sample size of divers might allow for the identification of such parameters; a coach and support team designing a training programme to maximise specific competencies already considered



strengths by the diver could realise the physical and technical potential of the athlete to a greater effect than by current practice.

### 11.6.3 Projects

Performance questions raised by coaches of individual divers could be studied with the results adding to the knowledge within the WCP for the benefit of all participants and a competitive advantage for British Diving. Examples of questions raised include:

- How to measure readiness to undertake specific diving training following strength and conditioning, acrobatic training or travel. Understanding how quickly a diver progresses from a state of fatigue to a state of readiness would inform programming of technical training
- The effect of taking off from a sub-optimal position (i.e. not from the tip of the diving board) and the intra-user consistency of take-offs on dives of different complexity. This would inform the amount of training required to produce a take-off that is stable 'enough' and could build confidence in divers who are only confident to attack the dive when they feel an 'ideal' hurdle and otherwise baulk (stop and restart) at the point of take-off
- The difference in kinematic parameters calculated in lead-up skills and optional skills when trained in the same session. Understanding typical change in take-off and flight parameters when difficulty (and stress) is added by performing the more difficult skill from a higher board would inform when to progress to maximise the value of training (training a dive poorly compromises the reinforcement of correct technique)
- The difference in kinematic parameters during performances under pressure (due to competition or to the performance of a new skill) compared to those performed in relaxed circumstances. Once understood, the effect of pressure-training (where task, environment and consequence is manipulated to increase stress on the diver to prepare them for the competition field of play) and performance-psychology interventions (to refine competition routine, minimise distraction and maintain a suitable arousal level) could be measured to maximise the probability of success in competition.

The data required to answer these performance questions are all produced with the diveTracker system.

#### 11.6.4 Enhance automated marker tracking

The automated tracking algorithm could be developed to manage fast forward and inward rotating skills. As 407c (inward 3.5 somersaults) was not consistently successfully tracked, 109c (forward 4.5 somersaults, a standard dive for male springboard divers) is likely to be similarly challenging.

Functionality could be extended to prompt the user to manually digitise any landmarks when prediction has failed, to then restart the tracking process. This would increase successful processing of markers in frames subsequent to that identified as a stopping point.

Segment lengths could be used to identify the diver and, for divers with similar limb lengths, historic performance data (average height of hurdle, depth of squat at first contact etc.) could be used to differentiate individuals. Once the diver has been identified, KPI could be stored in a database for longitudinal analysis and comparison.

#### 11.6.5 Extend the tool to analyse platform diving

The system developed for this study would require little modification to support the analysis of platform diving. The plane in which the diver performs would need to be determined since the diver can take-off from any point along the 3-metre width of the platform. The tracking algorithm would be adapted to change the assumption of starting position (as dives from the armstand group begin with the hands on the platform and the body inverted).

There would also need to be a study into an optimal camera view such that a flight path of a considerably greater length could be tracked, while maintaining the pixel-resolution of the diver's image to reconstruct landmarks with enough accuracy to produce meaningful kinematic data.

## 11.7 Summary

Section 1.3 stated that diving is hard to measure and made an argument in support of that assertion. The diveTracker system, developed to provide objective feedback to divers and coaches from the analysis of springboard dives, uses techniques in camera calibration, body-segment modelling, image-processing and performance analysis to meet that challenge.

This study has demonstrated a method for calculating performance data from springboard dives and has quantified metrics describing world class performance of dives of the highest difficulty. It has created proprietary knowledge for British Diving's World Class Programme, extending its understanding of What It Takes to Win and creating a base from which to individualise training programmes and measure progress.

An analysis of athletes from British Diving's World Class Programme has measured development in performance to support the subjective assessment of coach and support team. Data have been used to re-evaluate critical components of performance and a competitive advantage over international teams.

## References

- Abdel-Aziz, Y. I., & Karara, H. M. (1971). Direct linear transformation from comparator coordinates into object space coordinates in close range photogrammetry. *Proceedings of the Symposium on Close Range Photogrammetry. Falls Church (VA): American Society of Photogrammetry*, 1–18.
- BOA. (2016). *Team GB - About Diving*. <https://www.teamgb.com/summer-sports/diving>
- Borelli, G. (1680). *De Motu Animalium*.
- Borresen, J., & Lambert, M. I. (2009). The Quantification of Training Load , Effect on Performance. *Sports Medicine*, 39(9), 779–795.  
<https://doi.org/10.2165/11317780-000000000-00000>
- Bouget, J.-Y. (2015). *Matlab Camera Calibration Toolbox*.  
[http://www.vision.caltech.edu/bougetj/calib\\_doc/htmls/example.html](http://www.vision.caltech.edu/bougetj/calib_doc/htmls/example.html)
- Boutros, N., Shortis, M. R., & Harvey, E. S. (2015). A comparison of calibration methods and system configurations of underwater stereo-video systems for applications in marine ecology. *Limnology and Oceanography: Methods*, 13, 224–236.  
<https://doi.org/10.1002/lom3.10020>
- Braune, W., & Fischer, O. (1889). Human Factors: The Journal of Human Factors and Ergonomics Society. *Treat. of the Math.-Phys. Class of the Royal Acad. of Sc. of Saxony*, 26.
- Camera calibration with OpenCV*. (2017).  
[http://docs.opencv.org/2.4/doc/tutorials/calib3d/camera\\_calibration/camera\\_calibration.html](http://docs.opencv.org/2.4/doc/tutorials/calib3d/camera_calibration/camera_calibration.html)
- Chan, C. K., Loh, W. P., & Rahim, I. A. (2016). Human motion classification using 2D stick-model matching regression coefficients. *Applied Mathematics and Computation*, 283, 70–89. <https://doi.org/10.1016/j.amc.2016.02.032>

- Chen, S. C., Hsieh, H. J., Lu, T. W., & Tseng, C. H. (2011). A method for estimating subject-specific body segment inertial parameters in human movement analysis. *Gait and Posture*, 33(4), 695–700. <https://doi.org/10.1016/j.gaitpost.2011.03.004>
- Cheng, C., Chen, H., Chen, C., Lee, C., & Chen, C. (2000). *Segmental inertial properties of Chinese adults determined from magnetic resonance imaging*. 15.
- Cheng, K. B., & Hubbard, M. (2005). Optimal compliant-surface jumping: A multi-segment model of springboard standing jumps. *Journal of Biomechanics*, 38(9), 1822–1829. <https://doi.org/10.1016/j.jbiomech.2004.08.023>
- Cheng, K. B., & Hubbard, M. (2008). Role of arms in somersaulting from compliant surfaces: A simulation study of springboard standing dives. *Human Movement Science*, 27(1), 80–95. <https://doi.org/10.1016/j.humov.2007.05.004>
- Clauser, C. (1969). *Weight, volume and centre of mass of segments of the human body*.
- Cormie, P., McGuigan, M. R., & Newton, R. U. (2011). *Developing Maximal Neuromuscular*. 41(2), 125–146.
- CSER. (2013). *Check2D - camera calibration tool for 2D kinematic analysis*. [www.check2d.co.uk](http://www.check2d.co.uk)
- Dallas, G., Paradisis, G., Kirialanis, P., Mellos, V., Argitaki, P., & Smirniotou, A. (2015). The acute effects of different training loads of whole body vibration on flexibility and explosive strength of lower limbs in divers. *Biology of Sport*, 32(3), 235–241. <https://doi.org/10.5604/20831862.1163373>
- Dapena, J. (1981). Simulation of modified human airborne movements. *Journal of Biomechanics*, 14(2), 81–89. [https://doi.org/10.1016/0021-9290\(81\)90167-6](https://doi.org/10.1016/0021-9290(81)90167-6)
- Dartfish. (1999). *Dartfish*.
- Dempster, W. (1955). *Space requirements of the seated operator*.
- Diving, E. I. of S. (2018). *PDMS - Athlete Summary*. <https://pdms.eis2win.co.uk/sports/11/aer-summary>
- Driscoll, H., Gaviria, S., & Goodwill, S. (2014). Analysing splash in competitive diving. *Procedia Engineering*, 72(Fina 2010), 26–31.

<https://doi.org/10.1016/j.proeng.2014.06.008>

Duggal, M. (2014). Hawk Eye Technology. *Journal of Global Research Computer Science & Technology, 1*(11), 30–36.

Duraflex. (2016). *Springboard Definition*. [www.duraflexinternational.com](http://www.duraflexinternational.com)

EIS. (2018a). *What we do*. <https://www.eis2win.co.uk/what-we-do/>

EIS. (2018b). *What we do*.

Eltoukhy, M., Asfour, S., Thompson, C., & Latta, L. (2012). Evaluation of the Performance of Digital Video Analysis of Human Motion: Dartfish Tracking System. *International Journal of ...*, 3(3), 1–6.  
[http://www.ijser.org/researchpaper/Evaluation\\_of\\_the\\_Performance\\_of\\_Digital\\_Video\\_Analysis\\_of\\_Human\\_Motion.pdf](http://www.ijser.org/researchpaper/Evaluation_of_the_Performance_of_Digital_Video_Analysis_of_Human_Motion.pdf)

Evangulov, A., Sotheran, A., & Bellan, J. (2016). *British Diving Single System*.

Fina. (2010). *Diving officials manual* (Issue January).

FINA (Federation Internationale de Natation). (2017). *Fina Swimming Rules 2015 - 2017. September 2015*, 1–18.

Frohlich, C. (1980). The Physics of Somersaulting and Twisting. *Scientific American*, 242(3), 155–164. <https://doi.org/10.1038/scientificamerican0380-154>

Gibson, O. (2012, July). London 2012: how Team GB's fortunes turned around after disaster in Atlanta. *The Guardian*.  
<https://www.theguardian.com/sport/2012/jul/24/london-2012-team-gb-atlanta>

Golden, D. (1981). Kinematics of increasing rotation in springboard diving. *Proceedings of the 1981 United States Diving Sports Science Seminar*, 55–81.

Goodwill, S. (2013). *Check2D software - Background and Case Study - Technical Report C2D1* (Issue January). [www.check2d.co.uk](http://www.check2d.co.uk)

Haake, S., Goodwill, S., Heller, B., Schoraha, D., & Gomez, J. (2010). Dynamic modeling of a springboard during a 3 m dive. *Procedia Engineering*, 2(2), 3299–3304.  
<https://doi.org/10.1016/j.proeng.2010.04.148>

Haering, D., Huchez, A., Barbier, F., & Holvoe, P. (2017). *Identification of the*

*contribution of contact and aerial biomechanical parameters in acrobatic performance.*

Hall, S. J. (2012). *Basic Biomechanics* (6th Ed). McGraw-Hill.

Harless, E. (1860). The static moments of the component masses of the human body. *The Math.-Phys. Royal Bavarian Acad. of Sci.*, 8(1,2), 69–96, 257–294.

Hatze, H. (1988). High-precision three-dimensional photogrammetric calibration and object space reconstruction using a modified DLT-approach. *Journal of Biomechanics*, 21(7), 533–538. [https://doi.org/10.1016/0021-9290\(88\)90216-3](https://doi.org/10.1016/0021-9290(88)90216-3)

*Hawk-Eye Innovations*. (2015). [www.hawkeyeinnovations.co.uk](http://www.hawkeyeinnovations.co.uk)

Hebbelinck, M., & Ross, W. D. (1974). Kinanthropometry and biomechanics. *Biomechanics IV. International Series on Sports Sciences*, 535–552.

Hogan, K., & Norton, K. (2000). The 'Price' of olympic gold. *Journal of Science and Medicine in Sport*, 3(2), 203–218. [https://doi.org/10.1016/S1440-2440\(00\)80082-1](https://doi.org/10.1016/S1440-2440(00)80082-1)

Hraski, Z. (2015). Functional relationships between kinematic and kinetic parameters of backward somersaults. *7th International Conference on Kinesiology*, 146–149.

Huber, J. (1987). Increasing vertical jump through plyometrics. *NSCA Journal - Volume 9 #1*, 36.

Huber, J. (1990). Upper body strength and conditioning for divers. *National Strength and Conditioning Association Journal Vol 12, #6*, 26–28.

International Telecommunication Union. (2002). Parameter values for the HDTV standards for production and international programme exchange BT Series Broadcasting service. *Recommendation ITU-R BT.709-5, 5*, 1–32. [http://www.itu.int/dms\\_pubrec/itu-r/rec/bt/R-REC-BT.709-5-200204-!!!PDF-E.pdf](http://www.itu.int/dms_pubrec/itu-r/rec/bt/R-REC-BT.709-5-200204-!!!PDF-E.pdf)

Kolahi, A., Hoviattalab, M., Rezaeian, T., Alizadeh, M., Bostan, M., & Mokhtarzadeh, H. (2007). Design of a marker-based human motion tracking system. *Biomedical Signal Processing and Control*, 2(1), 59–67. <https://doi.org/10.1016/j.bspc.2007.02.001>

- Kong, P. (2005). *Computer simulation of the takeoff in springboard diving*.
- Kong, P. W., Yeadon, M. ., & King, M. A. (2006). Modelling the muscle activation in springboard diving takeoffs. *Journal of Biomechanics*, 39(Suppl 1), 2006.
- Koschorreck, J., & Mombaur, K. (2012). Modeling and optimal control of human platform diving with somersaults and twists. *Optimization and Engineering*, 13(1), 29–56. <https://doi.org/10.1007/s11081-011-9169-8>
- Kwon, Y. H. (1996). Effects of the method of body segment parameter estimation on airborne angular momentum. *Journal of Applied Biomechanics*, 12(4), 413–430. <https://doi.org/10.1123/jab.12.4.413>
- Liu, W. (2013). The Skills of Springboard Diving. *1st International Conference on Diving Biomechanics*.
- Maffiuletti, N. A., Dugnani, S., Folz, M., Pierno, D., & Mauro, F. (2002). Effect of combined electrostimulation and plyometric training on vertical jump height. *Med. Sci. Sports Exerc*, 34(10), 1638–1644. <https://doi.org/10.1249/01.MSS.0000031481.28915.56>
- Makaruk, H., & Porter, J. M. (2014a). Focus of Attention for Strength and Conditioning Training. *Strength and Conditioning Journal*, 36(1), 16–22. <https://doi.org/10.1519/SSC.0000000000000008>
- Makaruk, H., & Porter, J. M. (2014b). Focus of Attention for Strength and Conditioning Training. *Strength and Conditioning Journal*, 36(1), 16–22. <https://doi.org/10.1519/SSC.0000000000000008>
- Maletsky, L. P., Sun, J., & Morton, N. A. (2007). Accuracy of an optical active-marker system to track the relative motion of rigid bodies. *Journal of Biomechanics*, 40(3), 682–685. <https://doi.org/10.1016/j.jbiomech.2006.01.017>
- Miller, D. I., & Sprigings, E. J. (2001). Factors influencing the performance of springboard dives of increasing difficulty. *Journal of Applied Biomechanics*, 17(3), 217–231.
- Miller, Doris I. (2013). Teaming Up to Enhance Diving Performance. In T. Kothe & O. Stoll (Eds.), *1st Symposium for Researchers in Diving* (pp. 44–52). Feldhaus.



- Miller, Doris I, Zecevic, A., & Taylor, G. W. (2002). Hurdle preflight in springboard diving: a case of diminishing returns. *Research Quarterly for Exercise and Sport*, 73(2), 134–145. <http://www.ncbi.nlm.nih.gov/pubmed/12092888>
- Nikolova, G. S., & Toshev, Y. E. (2007). Estimation of male and female body segment parameters of the Bulgarian population using a 16-segmental mathematical model. *Journal of Biomechanics*, 40(16), 3700–3707. <https://doi.org/10.1016/j.jbiomech.2007.06.016>
- Organisation, K. (2009). *Kinovea - Measuring distances*.
- Organisation, T. K. (2009). *{Kinovea} A microscope for your videos*. <https://www.kinovea.org/help/en/120.html>
- Panjkota, A., Stancic, I., & Grujic Supuk, T. (2013). Design, development and evaluation of optical motion-tracking system based on active white light markers. *IET Science, Measurement & Technology*, 7(4), 206–214. <https://doi.org/10.1049/iet-smt.2012.0157>
- Pay up, pay up and win the game. (2006). *The Economist*, 8487, 35.
- Peterson, M. D., Rhea, M. R., & Alvar, B. A. (2004). *Maximising strength development in athletes: a meta-analysis to determine the dose-response relationship*. 18(2), 377–382. <https://doi.org/10.1519/R-12842.1>
- Phasespace. (2017). *Phasespace - State of the art motion-capture*. [www.phasespace.com/applications/sports-medical/](http://www.phasespace.com/applications/sports-medical/)
- Polhemus. (2010). *G4 Wireless Electromagnetic Tracker*. [https://polhemus.com/\\_assets/img/G4\\_Brochure.pdf](https://polhemus.com/_assets/img/G4_Brochure.pdf)
- Qian, J., Zhang, S., & Jun, H. (2005). Theoretical analyses of splash formation of competitive diving. *ISBS 2005*, 339–341.
- Quintic Consultancy Ltd. (n.d.-a). *Quintic*. Retrieved July 11, 2017, from <http://www.quinticsports.com/>
- Quintic Consultancy Ltd. (n.d.-b). *Quintic biomechanics*. Retrieved July 11, 2017, from <http://www.quinticsports.com/quintic-biomechanics/>

- Robertson, W. (2015). *Repository of body segment parameter models*.  
<https://github.com/wspr/body-segment-param>
- Salvi, J., Armangué, X., & Batlle, J. (2002). A comparative review of camera calibrating methods with accuracy evaluation. *Pattern Recognition*, 35(7), 1617–1635.  
[https://doi.org/10.1016/S0031-3203\(01\)00126-1](https://doi.org/10.1016/S0031-3203(01)00126-1)
- Sanders, R., & Gibson, B. (2003). Technique and Timing in Women’s Backward Two and One Half Somersault Tuck (205C) and the Men’s Backward Two and One Half Somersault Pike (205B) 3m Springboard Dives ROSS. *Sports Biomechanics*, 2(1), 73–84. <https://doi.org/10.1080/14763140308522809>
- Sanders, R., Gibson, B., & Prassas, S. (2002). Technique and Timing in the Women’s Reverse Two and One Half Somersault Tuck (305C) and the Men’s Reverse Two and One Half Somersault Pike (305B) 3m Springboard Dives ROSS. *Sports Biomechanics*, 1(2), 193–212. <https://doi.org/10.1080/14763140208522797>
- Sanders, R. H., & Gibson, B. J. (2000). Technique and timing in the womens forward two and one half somersault pike and mens three and one half somersault pike 3m springboard dives. *Journal of Science and Medicine in Sport / Sports Medicine Australia*, 3(4), 434–448. <http://www.ncbi.nlm.nih.gov/pubmed/11235008>
- Sayyah, M., King, M. A., & Yeadon, M. . (2016). Factors influencing variation in dive height in 1m springboard diving. *34th International Conference on Biomechanics in Sport*.
- Siegel, I. M. (1985). On the Centre of Gravity of the Human Body as Related to the Equipment of the German Infantry Soldier. *JAMA*, 254(1), 121–122.  
<https://doi.org/10.1001/jama.1985.03360010131042>
- Smith, P., Reid, D. B., Environment, C., Palo, L., Alto, P., & Smith, P. L. (1979). *Otsu1975*. 20(1), 62–66.
- Song, L. M., Wang, M. P., Lu, L., & Jing Huan, H. (2007). High precision camera calibration in vision measurement. *Optics and Laser Technology*, 39(7), 1413–1420. <https://doi.org/10.1016/j.optlastec.2006.10.006>
- Sotheran, A, Ryan, T., Evangulov, A., Bellan, J., & White, K. (2016). *TOKYO 2020*

*OLYMPIC CYCLE PERFORMANCE STRATEGY- DIVING WORLD CLASS PROGRAMME*  
*UK Sport Draft Tokyo Submission.*

Sotheran, Adam. (2017). *What it takes to win – Competition starts Women 's 3m Springboard Women 's 10m platform Men 's 3m Springboard.*

SPATA. (2013). *Indoor Pool Climate Control Controlling the indoor pool environment.*

Sturm, P. F., & Maybank, S. J. (2015). On plane-based camera calibration: A general algorithm, singularities, applications. *Proceedings. 1999 IEEE Computer Society Conference on Computer Vision and Pattern Recognition (Cat. No PR00149), 1*, 432–437. <https://doi.org/10.1109/CVPR.1999.786974>

Suliman, C., Puiu, D., & Moldoveanu, F. (2009). Single Camera Calibration in 3D Vision. *Vasa, 32(2)*, 69–72.  
<http://medcontent.metapress.com/index/A65RM03P4874243N.pdf>

Sultvedt, S. M., & Hinrichs, R. N. (2005). The Effect Of A Hurdle Preflight Approach On Takeoff Velocities In Springboard Diving. *Medicine & Science in Sports & Exercise, 37.5*, 124–125.

Supej, M. (2010). 3D measurements of alpine skiing with an inertial sensor motion capture suit and GNSS RTK system. *Journal of Sports Sciences, 28(7)*, 759–769.  
<https://doi.org/10.1080/02640411003716934>

Team, S. E. F. (2017). *Swim England Safety Guidance The Use of Electrical Equipment and Appliances near Swimming Pools.*

Technologies, A. V. (n.d.). *Prosilica GC660 datasheet.*  
[https://www.alliedvision.com/en/products/cameras/detail/Prosilica GC/660.html](https://www.alliedvision.com/en/products/cameras/detail/Prosilica%20GC/660.html)

Tong, W., & Dullin, H. R. (2017). A new twisting somersault - 513xd. *Journal of Nonlinear Science - ArXiv:1612.06455v2, 3*, 1–26.

UKSport. (2012). *Battle against illness and injury.*  
<http://www.uk sport.gov.uk/news/2012/07/25/battle-against-injury-and-illness>

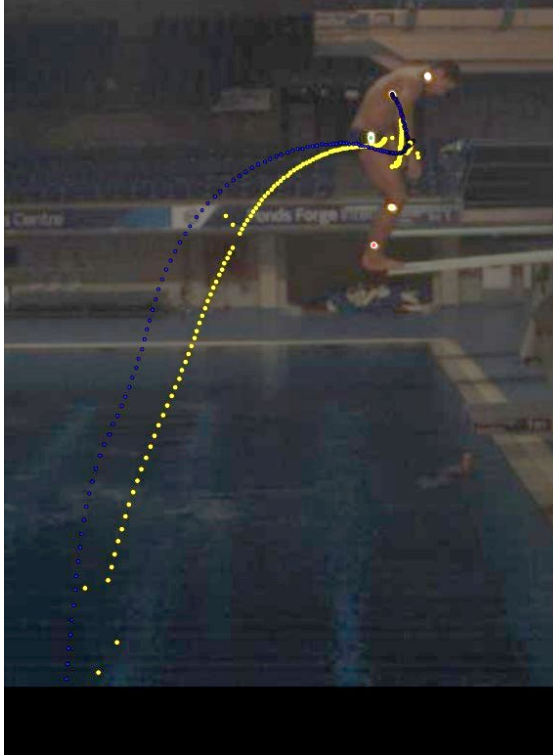
UKSport. (2017). *Diving 2017-2020 funding.*  
<http://www.uk sport.gov.uk/sports/olympic/diving>

- Walker, C., Sinclair, P., Graham, K., & Cobley, S. (2016). The validation and application of Inertial Measurement Units to springboard diving. *Sports Biomechanics*, 3141(February), 1–16. <https://doi.org/10.1080/14763141.2016.1246596>
- Wong, J. D., Bobbert, M. F., Van Soest, A. J., Gribble, P. L., & Kistemaker, D. A. (2016). Optimizing the distribution of leg muscles for vertical jumping. *PLoS ONE*, 11(2), 1–16. <https://doi.org/10.1371/journal.pone.0150019>
- Xcitex. (1999). *ProAnalyst*. <http://www.xcitex.com/athletic-performance-sports-applications-motion-analysis-software.php>
- Yeadon, M. R. (2000). Aerial movement. *Biomechanics in Sport*, 273–283.
- Yeadon, Maurice R., Kong, P. W., & King, M. A. (2006). Parameter determination for a computer simulation model of a diver and a springboard. *Journal of Applied Biomechanics*, 22(3), 167–176.
- Zatsiorsky, V. M. (2000). Biomechanics in Sport: Performance Enhancement and Injury Prevention. In *the Encyclopedia of Sports Medicine: Vol. IX*. <https://doi.org/10.1002/9780470693797.ch11>
- Zatsiorsky, V. M. (2002). *Kinetics of Human Motion*. Human Kinetics 2002.
- Zhang, Z. (2000). A flexible new technique for camera calibration. *IEEE Transactions on Pattern Analysis and Machine Intelligence*, 22(11), 1330–1334. <https://doi.org/10.1109/34.888718>
- Zhang, Z. (2002). A Flexible New Technique for Camera Calibration (Technical Report). *IEEE Transactions on Pattern Analysis and Machine Intelligence*, 22(11), 1330–1334. <https://doi.org/10.1109/34.888718>

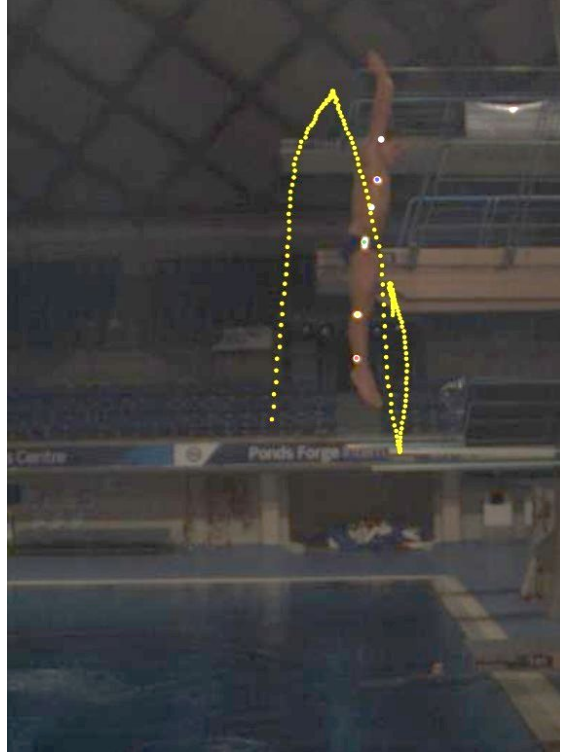
## Appendices

Appendix A - Automated marker tracking examples

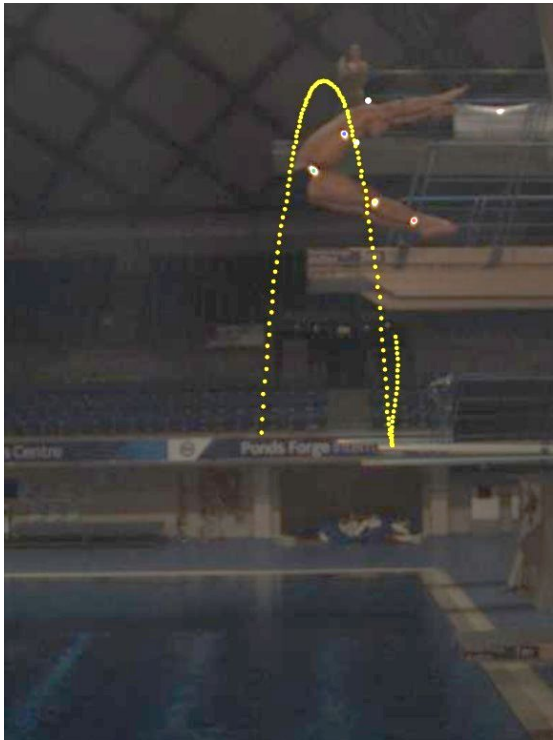
JH\_2016\_11\_21\_11\_02\_43\_1



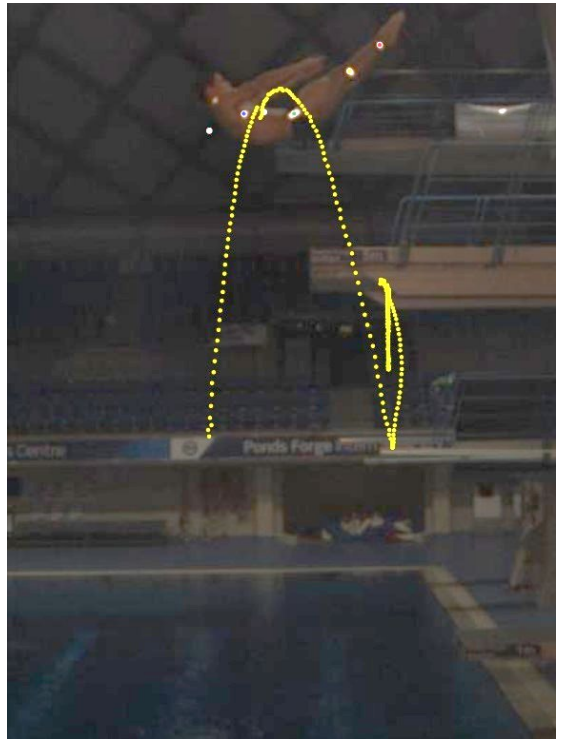
JH\_2016\_11\_21\_11\_02\_43\_1



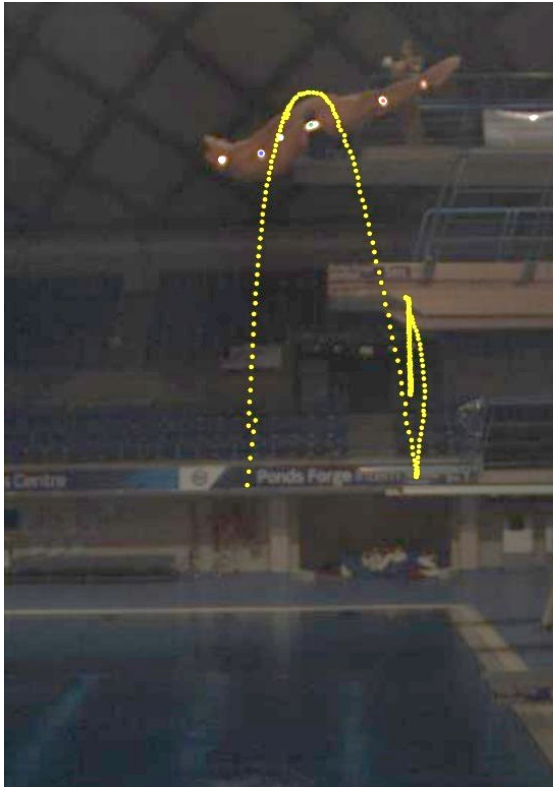
JH\_2016\_11\_21\_11\_07\_05\_1



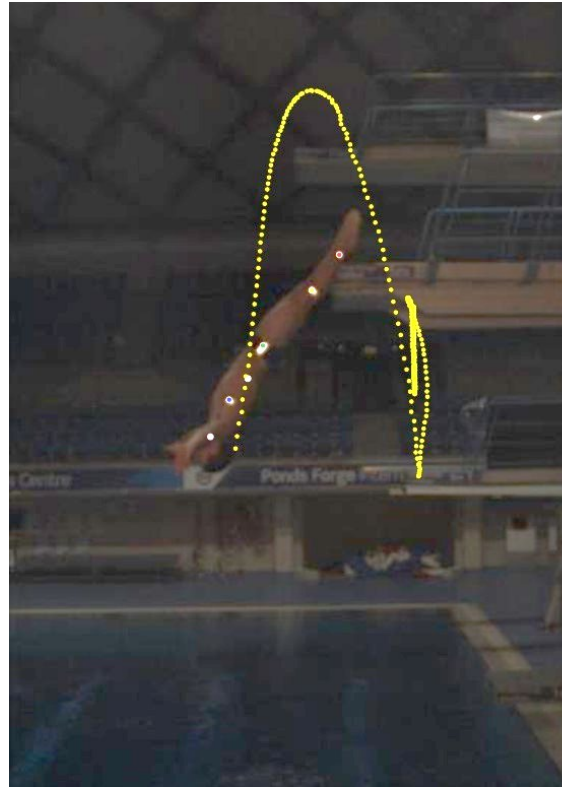
JH\_2016\_11\_21\_11\_08\_43\_1



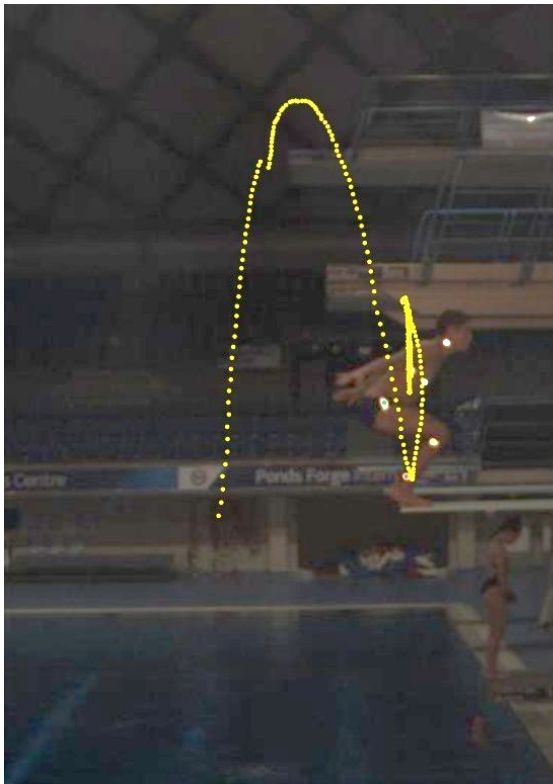
JH\_2016\_11\_21\_\_11\_10\_16\_1



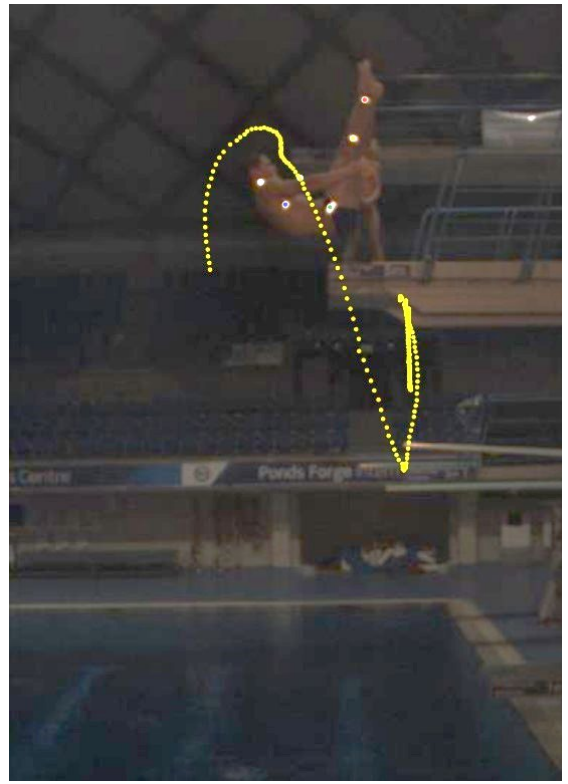
JH\_2016\_11\_21\_\_11\_11\_39\_1



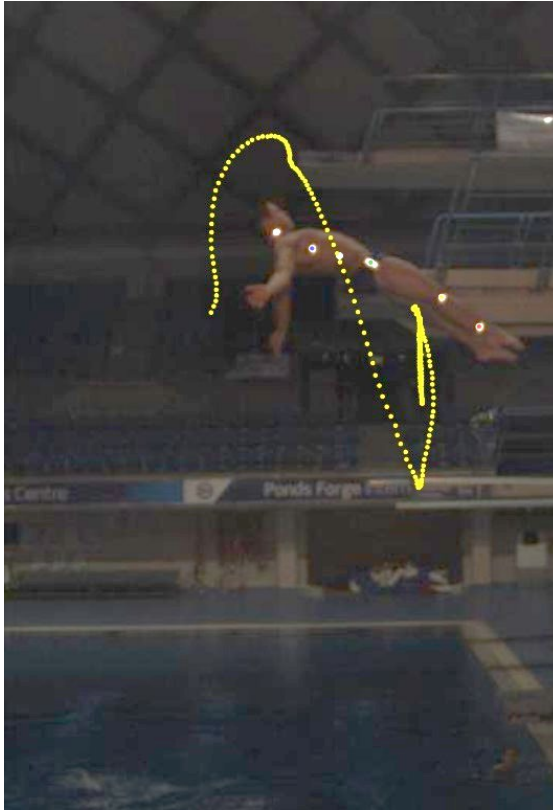
JH\_2016\_11\_21\_\_11\_13\_17\_1



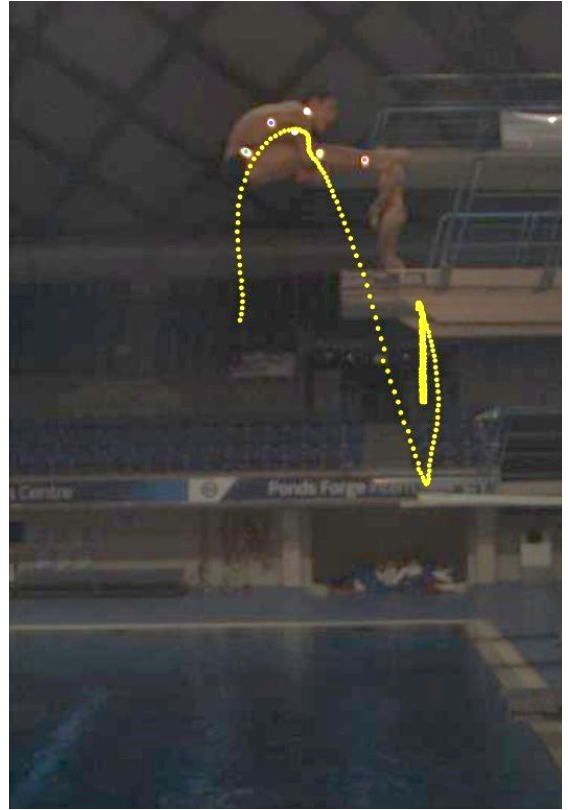
JH\_2016\_11\_21\_\_11\_14\_45\_1



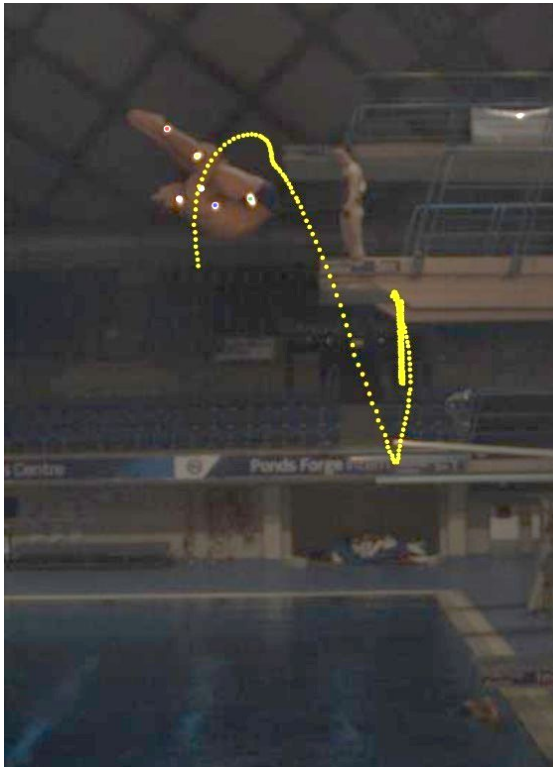
JH\_2016\_11\_21\_11\_16\_52\_1



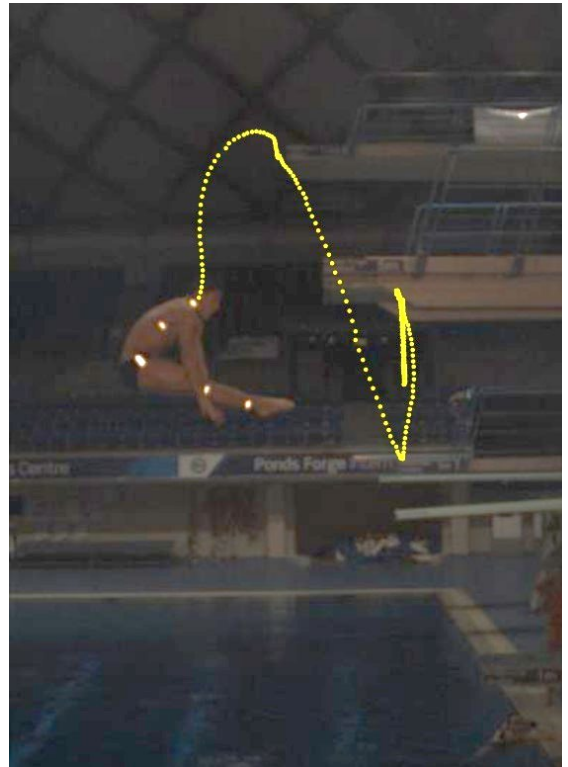
JH\_2016\_11\_21\_11\_18\_39\_1



JH\_2016\_11\_21\_11\_20\_41\_1

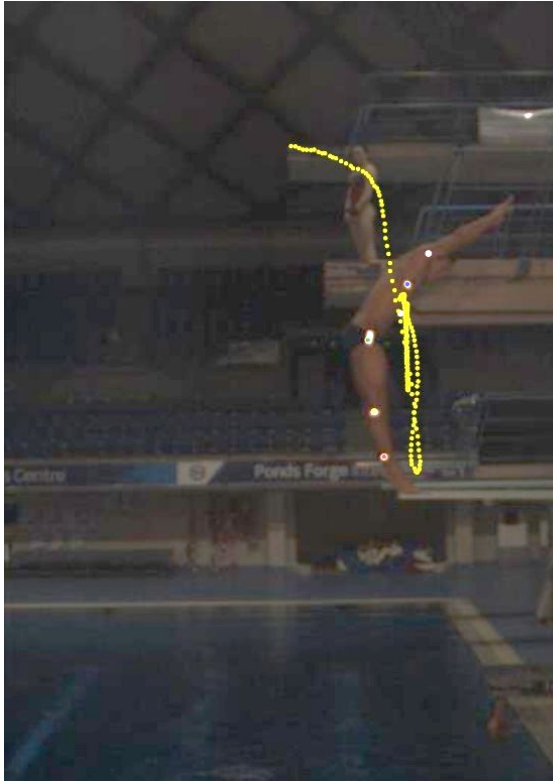


JH\_2016\_11\_21\_11\_22\_43\_1

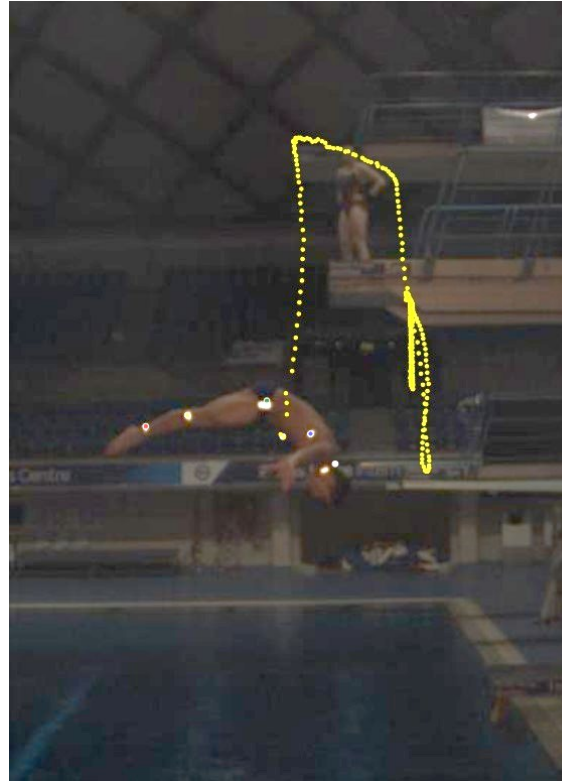




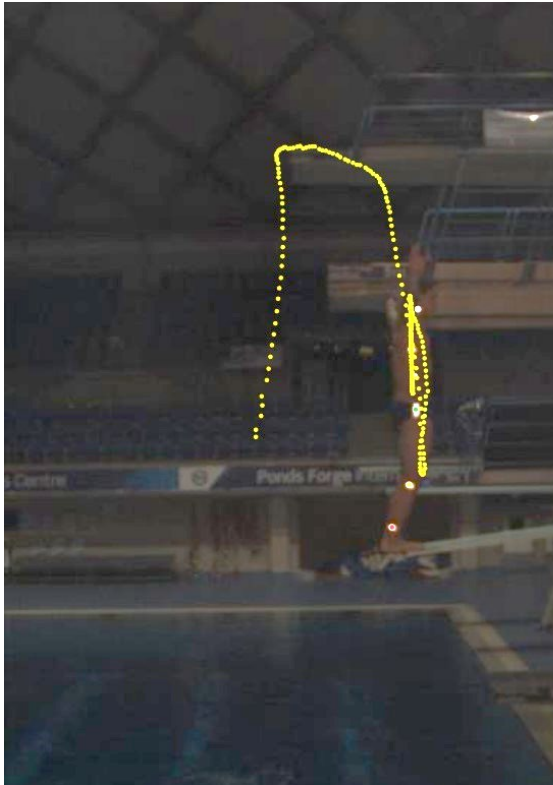
JH\_2016\_11\_21\_11\_24\_39\_1



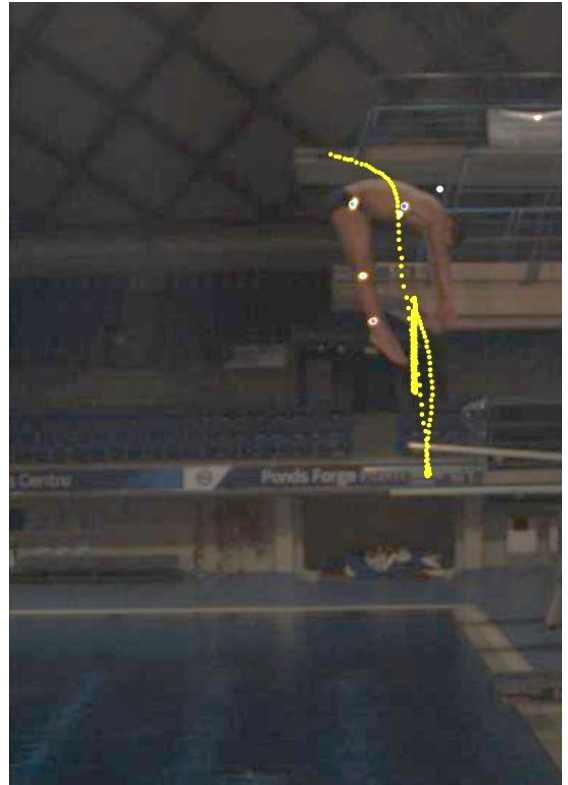
JH\_2016\_11\_21\_11\_25\_55\_1



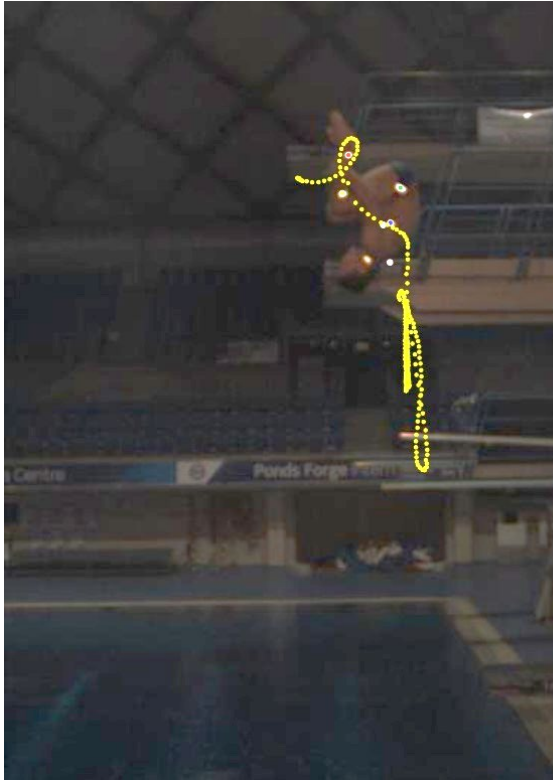
JH\_2016\_11\_21\_11\_27\_05\_1



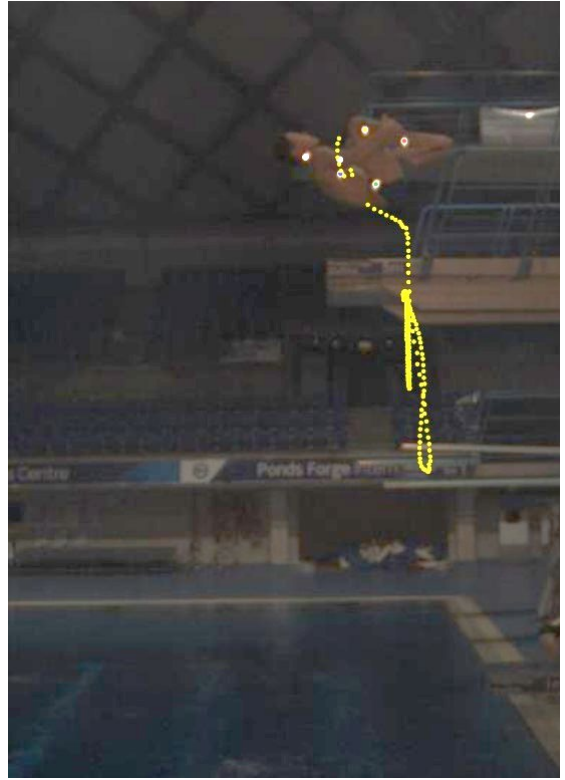
JH\_2016\_11\_21\_11\_28\_48\_1



JH\_2016\_11\_21\_\_11\_36\_49\_1



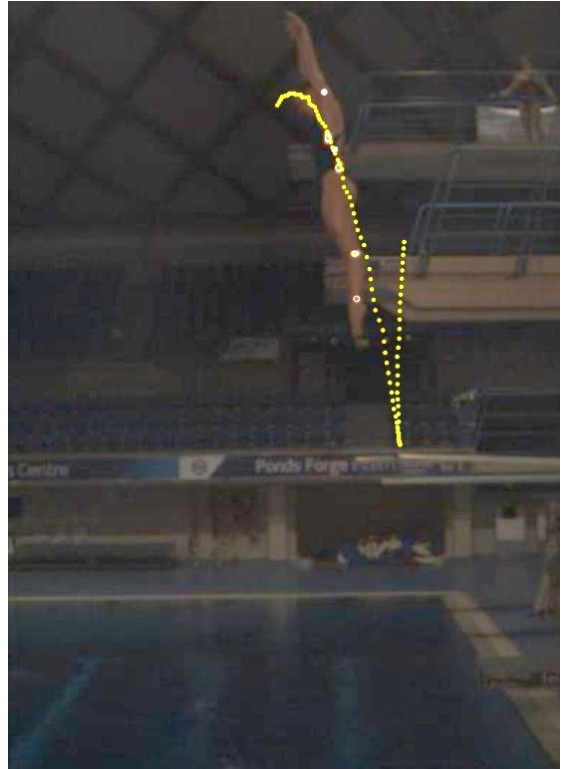
JH\_2016\_11\_21\_\_11\_38\_55\_1



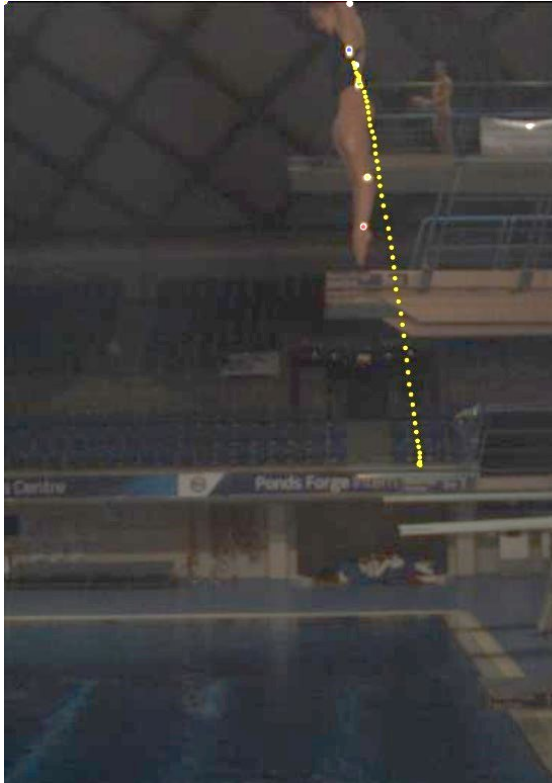
JH\_2016\_11\_21\_\_11\_41\_39\_1



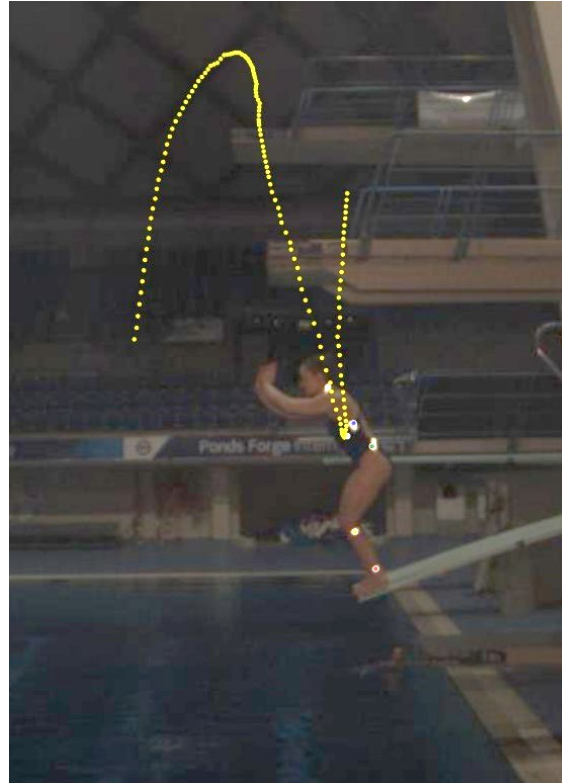
MF\_2016\_11\_21\_\_11\_03\_41\_1



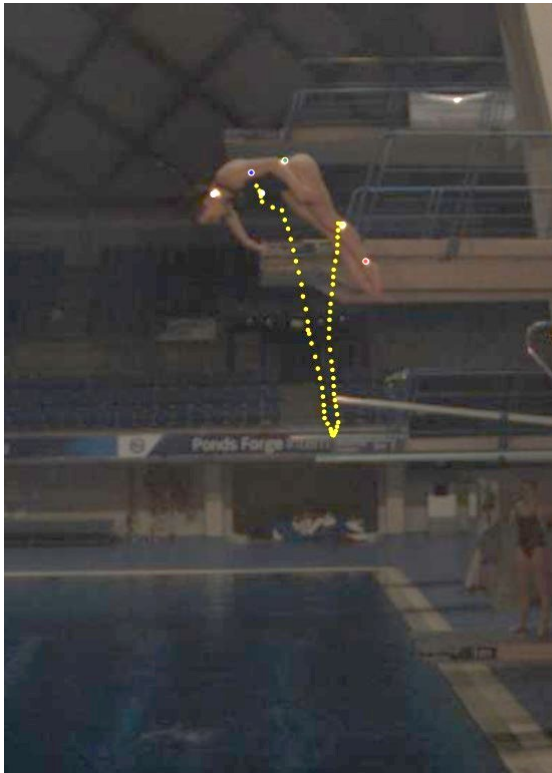
MF\_2016\_11\_21\_11\_06\_24\_1



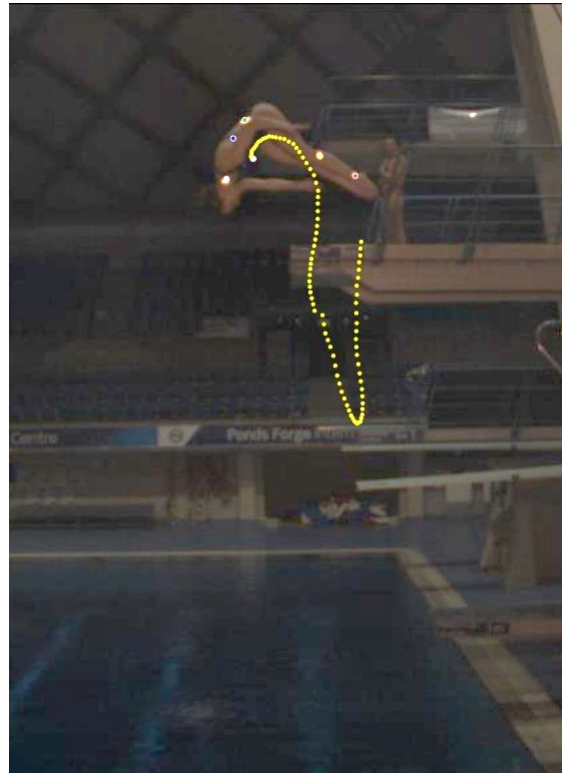
MF\_2016\_11\_21\_11\_07\_55\_1



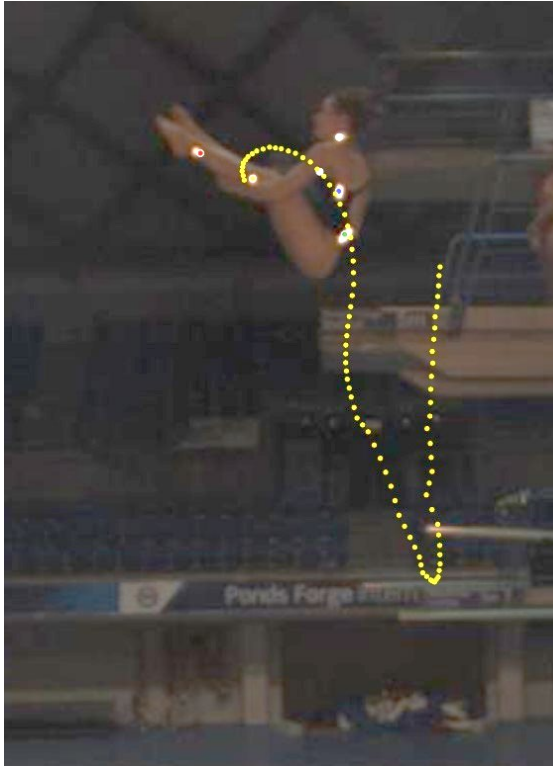
MF\_2016\_11\_21\_11\_12\_18\_1



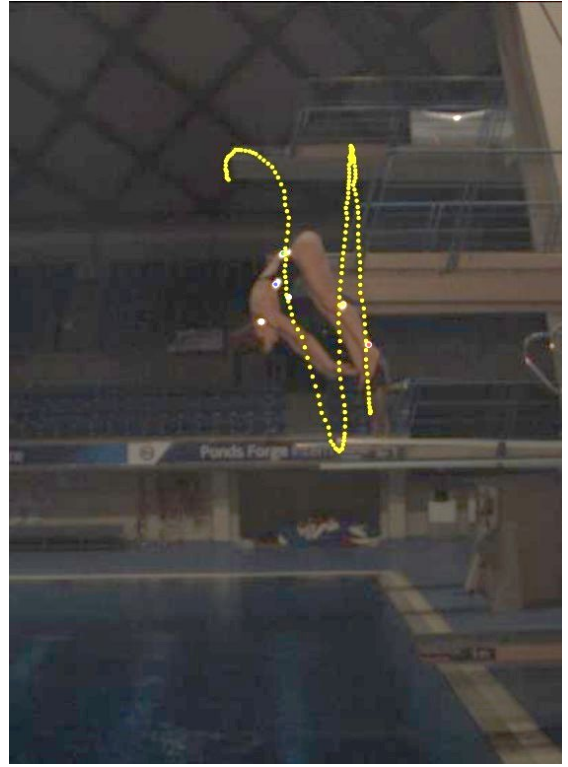
MF\_2016\_11\_21\_11\_20\_05\_1



MF\_2016\_11\_21\_11\_31\_46\_1



MF\_2016\_11\_21\_11\_33\_45\_1



# Appendix B - Athlete data

## Diver 1

### Diver 1 – September 2018 Profiling results

KEY	
	injured
	> 1SD
	< 1SD

All results were compared to mean of:

- All funded divers
- All divers of the same sex
- All divers in the same discipline (springboard or platform)
- All divers in the same discipline of the same sex

#### Diver 1

	ANTHROPOMETRICS			STRENGTH									
	Height	Weight	Skinfolds	Grip arm by side		Grip arm overhead		Elbow extension		Hip abduction		Hip external rotation	
	Left	Right		Left	Right	Left	Right	Left	Right	Left	Right	Left	Right
WC mean	168.0	62.5	69.3	38.2	39.4	36	36.9	52.2	54.2	51.2	51.9	41.8	40.8
stdev	5.9	9.0	22.9	11.2	11	9.2	9.6	12.6	13.2	12.5	10.4	12.1	11.4
Diver 1	163.0	62.1	79.7	32.9	39.0	32.8	35.5	50.8	55.7	35.4	41.4	39.6	38.1
Female mean	164.3	57.7	82.3	30.2	31.5	29.5	29.8	43.1	44	45.2	47	34.4	34.1
stdev	5.3	8.3	20.7	5.8	6.4	5	5.7	6.6	9	7.9	9	5.5	5.6
Diver 1	163.0	62.1	79.7	32.9	39.0	32.8	35.5	50.8	55.7	35.4	41.4	39.6	38.1
Spring mean	168.2	66.2	69.5	41.9	43.6	38.6	40.7	58.0	60.8	55.0	56.1	47.2	46.8
stdev	5.9	8.6	24.6	11.5	10.9	9.8	10.0	10.9	11.4	15.0	9.9	13.6	12.3
Diver 1	163.0	62.1	79.7	32.9	39.0	32.8	35.5	50.8	55.7	35.4	41.4	39.6	38.1
Fem spr mean	163.8	60.3	86.6	31.267	33.85	30.55	31.9	48.233	50.48	43.5167	48.8	35.633	36.417
stdev	6.1	9.7	21.1	7.3856	7.7807	6.2734	7.094	3.0781	8.86239	6.54933	7.37482	6.1559	6.271
Diver 1	163.0	62.1	79.7	32.9	39.0	32.8	35.5	50.8	55.7	35.4	41.4	39.6	38.1

	RANGE OF MOTION															
	Shoulder ER		Shoulder IR		Straight leg raise		Thomas test		Lumbar locked thoracic		Knee to wall		Lat length against wall		Combined elevation	
	Left	Right	Left	Right	Left	Right	Left	Right	Left	Right	Left	Right	Trial 1	Trial 2	Trial 1	Trial 2
WC mean	61.8	66.0	46.3	40.9	119.4	118.3	below	below	52.7	46.7	12.6	12.4	0.2	0.2	27.1	28.6
stdev	13.9	17.9	8.5	8.3	12.1	11.2	below	below	13.9	12.7	2.9	2.6	1.1	1.1	8.6	9.1
Diver 1	50.0	57.0	38.0	39.0	124.0	130.0	below	below	50.0	52.0	10.0	12.0	0.0	0.0	43.0	42.0
Female mean	63.9	66.8	50.1	44.2	127.8	126.2	below	below	52.2	47.8	13.2	12.9	0.0	0.0	27.7	29.7
stdev	14.6	17.1	7.9	7.7	9.0	9.6	below	below	16.2	14.7	2.6	2.2	0.0	0.0	10.2	11.8
Diver 1	50.0	57.0	38.0	39.0	124.0	130.0	below	below	50.0	52.0	10.0	12.0	0.0	0.0	43.0	42.0
Spring mean	66.8	70.6	44.8	40.2	122.5	121.2	below	below	55.5	47.6	14.4	14.2	0.4	0.4	25.5	26.5
stdev	16.0	17.2	9.3	8.1	11.9	11.4	below	below	10.2	12.8	2.1	1.8	1.5	1.5	5.6	6.1
Diver 1	50.0	57.0	38.0	39.0	124.0	130.0	below	below	50.0	52.0	10.0	12.0	0.0	0.0	43.0	42.0
Fem spr mean	59.7	60.2	51.2	45.8	123.7	123.0	below	below	46.7	46.3	11.3	11.3	0.0	0.0	31.1	34.1
stdev	8.0	12.9	7.1	7.9	8.7	11.4	below	below	19.7	17.0	1.3	0.9	0.0	0.0	13.0	14.8
Diver 1	50.0	57.0	38.0	39.0	124.0	130.0	below	below	50.0	52.0	10.0	12.0	0.0	0.0	43.0	42.0

	WORK CAPACITY								STRENGTH AND POWER							
	SL squat to box - 30 reps		Calf raise off step - 30 reps		Side plank - 120 seconds		Prone hold - 120 seconds	Supine hold - 60 seconds	Peak force (N)		Time to peak force (s)					
	Left	Right	Left	Right	Left	Right			ISO back squat	ISO calf raise	ISO back squat	ISO calf raise	R	L	R	L
WC mean	29	30	23	23	106	107	115	58	2969.64	2441.98	2.44	2.86	2.94	2.72		
stdev	5	0	6	6	23	23	13	5	854.80	543.36	1.03	1.64	0.55	0.67		
Diver 1	30.0	30.0	30.0	30.0	120.0	120.0	120.0	60.0	2876.0	2237.0	2.9	2.9	2.9	2.2		
Female mean	29	30	22	22	101	103	115	57	2363.76	2186.72	2.36	3.09	2.94	2.71		
stdev	3	0	6	5	27	26	12	8	692.85	581.03	1.18	2.35	0.70	0.81		
Diver 1	30.0	30.0	30.0	30.0	120.0	120.0	120.0	60.0	2876.0	2237.0	2.9	2.9	2.9	2.2		
Spring mean	30	30	25	25	105	103	114	58	3151.55	2645.55	2.21	2.40	2.82	2.62		
stdev	0	0	6	6	25	27	13	6	951.14	615.20	0.88	1.02	0.47	0.78		
Diver 1	30.0	30.0	30.0	30.0	120.0	120.0	120.0	60.0	2876.0	2237.0	2.9	2.9	2.9	2.2		
Fem spr mean	30	30	24	24	98	95	110	56	2447.25	2293.00	1.81	2.08	2.68	2.40		
stdev	0	0	5	6	31	34	16	9	951.53	868.45	1.10	1.53	0.75	1.13		
Diver 1	30.0	30.0	30.0	30.0	120.0	120.0	120.0	60.0	2876.0	2237.0	2.9	2.9	2.9	2.2		

STRENGTH AND POWER ASSESSMENT - JUMPS																								
	Peak force (s)				Jump height (cm)				Av. Peak velocity (m/s)				Flight time (m/s)				Rate of force development			Time to peak propulsive force			Movement start to peak force	RSI flight/contact time
	SLCMJ		DJ		SLCMJ		DJ		SLCMJ		DJ		SLCMJ		DJ		SLCMJ		DJ		CMJ	DJ		
	CMJ	R			L	CMJ			R	L			CMJ	R			L	CMJ					R	L
WC mean	0.71	0.78	0.80	0.08	41.27	23.65	22.84	38.69	2.80	2.14	2.09	2.77	576.36	436.15	427.45	544.52	42362.16	713.08	22675.00	195.08	216.00	3.96	0.68	2.45
stdev	0.15	0.14	0.17	0.05	10.07	4.68	5.91	8.40	0.35	0.22	0.23	0.41	68.69	44.07	55.46	96.55	148708.90	5612.29	62826.23	100.17	131.84	6.25	0.16	0.84
Diver 1	0.7	0.5	0.6	0.2	37.5	15.0	13.7	36.9	2.7	1.7	1.8	2.8	551.0	347.0	346.0	548.0	151866.0	-17600.0	7367.0	25.0	27.0	2.0	0.7	1.3
Female mean	0.76	0.73	0.81	0.07	33.89	19.22	16.40	32.09	2.61	1.98	1.86	2.49	523.17	394.40	366.00	482.58	67435.00	-1354.80	4090.25	213.80	238.25	3.83	0.70	2.31
stdev	0.16	0.14	0.21	0.04	6.92	3.63	2.38	4.90	0.37	0.28	0.16	0.40	47.31	37.19	21.40	102.21	110090.87	9190.91	2327.00	132.37	185.27	6.97	0.16	0.58
Diver 1	0.7	0.5	0.6	0.2	37.5	15.0	13.7	36.9	2.7	1.7	1.8	2.8	551.0	347.0	346.0	548.0	151866.0	-17600.0	7367.0	25.0	27.0	2.0	0.7	1.3
Spring mean	0.66	0.78	0.80	0.08	46.20	23.65	22.84	41.55	2.92	2.14	2.09	2.92	607.92	436.15	427.45	579.46	41940.08	713.08	22675.00	195.08	216.00	2.54	0.65	2.51
stdev	0.15	0.14	0.17	0.06	7.31	4.68	5.91	6.03	0.24	0.22	0.23	0.21	49.15	44.07	55.46	43.39	183472.91	5612.29	62826.23	100.17	131.84	3.73	0.18	0.98
Diver 1	0.7	0.5	0.6	0.2	37.5	15.0	13.7	36.9	2.7	1.7	1.8	2.8	551.0	347.0	346.0	548.0	151866.0	-17600.0	7367.0	25.0	27.0	2.0	0.7	1.3
Fem spr mean	0.73	0.73	0.81	0.08	38.72	19.22	16.40	35.14	2.67	1.98	1.86	2.70	555.00	394.40	366.00	533.40	117974.00	-1354.80	4090.25	213.80	238.25	1.80	0.68	2.31
stdev	0.20	0.14	0.21	0.06	4.29	3.63	2.38	3.77	0.15	0.28	0.16	0.14	21.62	37.19	21.40	29.02	155898.11	9190.91	2327.00	132.37	185.27	3.03	0.23	0.73
Diver 1	0.7	0.5	0.6	0.2	37.5	15.0	13.7	36.9	2.7	1.7	1.8	2.8	551.0	347.0	346.0	548.0	151866.0	-17600.0	7367.0	25.0	27.0	2.0	0.7	1.3

## Diver 1 – Results from filming and digitisation

### Forward facing dives with hurdle

Dive	Test 1	Test 2	Test 3	Change (%)
<b>100a</b>				
Mean board deflection (mm)	741.0	792.0	810.9	9.43
Maximum board deflection (mm)	791.9	792.0	810.9	2.40
Mean resultant take-off velocity (m/s)	4.99	5.63	5.17	12.91
Maximum resultant take-off velocity (m/s)	5.04	5.63	5.17	11.88
Mean vertical take-off velocity (m/s)	4.75	5.30	4.98	11.58
Maximum vertical velocity (m/s)	4.80	5.49	4.98	14.37
Mean vertical displacement (mm)	1229.9	1531.2	1348.5	24.50
Maximum vertical displacement (mm)	1252.8	1638.7	1348.5	30.80
<b>302/303/304b</b>				
Mean board deflection (mm)	835.2	812.8	827.7	-0.89
Maximum board deflection (mm)	841.1	833.4	827.8	-0.92
Mean resultant take-off velocity (m/s)	4.89	5.19	5.06	6.27
Maximum resultant take-off velocity (m/s)	5.04	5.35	5.11	6.23
Mean vertical take-off velocity (m/s)	4.61	4.78	4.68	3.65
Maximum vertical velocity (m/s)	4.74	4.97	4.73	4.96
Mean vertical displacement (mm)	1158.3	1244.4	1192.8	7.44
Maximum vertical displacement (mm)	1222.0	1346.2	1219.6	10.16
<b>104/5142</b>				
Mean board deflection (mm)			825.3	n/a
Maximum board deflection (mm)			829.9	n/a
Mean resultant take-off velocity (m/s)			4.77	n/a
Maximum resultant take-off velocity (m/s)			4.88	n/a
Mean vertical take-off velocity (m/s)			4.47	n/a
Maximum vertical velocity (m/s)			4.53	n/a
Mean vertical displacement (mm)			1087.4	n/a
Maximum vertical displacement (mm)			1119.4	n/a

### Back facing dives, dives

<b>Dive</b>	<b>Test 1</b>	<b>Test 2</b>	<b>Test 3</b>	<b>Change (%)</b>
<b>200a</b>				
Mean board deflection (mm)	621.4	573.4	595.2	-4.22
Maximum board deflection (mm)	628.6	573.4	595.2	-5.31
Mean resultant take-off velocity (m/s)	3.96	4.27	4.13	7.93
Maximum resultant take-off velocity (m/s)	4.12	4.27	4.13	3.64
Mean vertical take-off velocity (m/s)	3.55	4.06	3.93	14.44
Maximum vertical velocity (m/s)	3.61	4.06	4.18	15.64
Mean vertical displacement (mm)	686.8	899.5	843.3	30.98
Maximum vertical displacement (mm)	711.4	899.5	951.4	33.74
<b>201b</b>				
Mean board deflection (mm)		593.3		
Maximum board deflection (mm)		609.0		
Mean resultant take-off velocity (m/s)		4.13		
Maximum resultant take-off velocity (m/s)		4.36		
Mean vertical take-off velocity (m/s)		3.87		
Maximum vertical velocity (m/s)		4.12		
Mean vertical displacement (mm)		813.9		
Maximum vertical displacement (mm)		923.7		
<b>203b/204b</b>				
Mean board deflection (mm)	651.2	654.6	598.2	0.52
Maximum board deflection (mm)	662.2	595.0	609.0	-8.03
Mean resultant take-off velocity (m/s)	3.92	4.21	4.14	7.59
Maximum resultant take-off velocity (m/s)	3.97	4.36	4.36	9.95
Mean vertical take-off velocity (m/s)	3.68	3.95	3.89	7.42
Maximum vertical velocity (m/s)	3.77	4.08	4.12	9.19
Mean vertical displacement (mm)	738.1	851.7	822.7	15.39
Maximum vertical displacement (mm)	774.7	906.3	923.7	19.23

Key performance indicators – all dives - Diver 1. Dives coded as ‘date\_time\_dive-number’.

Any performance indicators which cannot be calculated are represented by ‘999’

Key Performance Indicators	_2018_09_13_11_04_59_100a	_2018_09_13_1_06_03_100a	_2018_09_13_1_07_26_100a	yh_2018_11_22_10_53_41_100a	yh_2018_11_22_10_54_40_100a	yh_2018_11_22_10_53_41_100a	yh_2018_11_22_10_54_40_100a	yh301_2018_11_2_2_11_22_57_1	yh_2019_01_17_1_1_46_49_100a
<b>Best model: 6</b>									
<b>Last step</b>									
Last step length (mm):									694.1
Last step speed - x (m/s):									0.7
Last step speed - y (m/s):									-3.5
Last step speed - resultant (m/s):	0	0	3.7	0	0.00	0	0.00	0.00	3.6
<b>Hurdle step</b>									
Into hurdle speed - x (m/s):	-0.3	-0.1	0	0.3	0.10	0.3	0.10	0.10	0
Into hurdle speed - y (m/s):	3.2	3.8	3.4	4.3	4.00	4.3	4.00	4.00	3.2
Hurdle height (mm):	1677.1	1725.8	1731.6	1970.3	1.90	1970.3	1.90	2082.90	1799.1
Hurdle displacement - measured (mm):	654.3	687.1	705.8	993.4	961.70	993.4	961.70	1067.80	818.6
Hurdle displacement - calculated (mm):	532.6	736.9	594.4	927.1	803.10	927.1	803.10	803.60	519.1
Difference (%):	18.6	7.2	15.8	6.7	16.50	6.7	16.50	24.70	36.6
Hurdle length (mm):				4.4	144.10	4.4	144.10	101.80	159.6
Velocity - x (m/s):	0.3	0	0.2	-0.4	-0.10	-0.4	-0.10	0.00	-0.1
Velocity - y (m/s):	-3.8	-3.9	-4.3	-4.7	-4.60	-4.7	-4.60	-4.60	-4.7
Distance from tip (mm):	36.1	35.7	95	148.5	25.70	148.5	25.70	28.40	418.5
<b>First contact</b>									
Knee angle (deg):	111.6	111.8	109.7	119.4	107.10	119.4	107.10	120.60	116.3
Hip angle (deg):	105.5	95.7	99.4	106.4	90.90	106.4	90.90	100.00	95.9
Trunk angle (deg):	28.8	38.7	33.5	34.6	41.80	34.6	41.80	40.30	38
Shoulder angle (deg):	40.8	14.4	38.7	54.1	28.90	54.1	28.90	48.00	7.1
Elbow angle (deg):	153.4	153.4	155.7	158.4	165.80	158.4	165.80	163.00	157.2
Lean angle (deg):	0.1	1.1	0.5	1.6	1.50	1.6	1.50	1.20	49.4
Landing velocity - x (m/s):	0.29	-0.01	0.18	-0.4	-0.12	-0.4	-0.12	0.00	-0.06
Landing velocity - y (m/s):	-3.85	-3.91	-4.32	-4.67	-4.60	-4.67	-4.60	-4.60	-4.67
Landing velocity - resultant (m/s):	3.856401	3.912774	4.321375	4.686209	4.61	4.686209	4.61	0.00	4.667753
<b>Max Squat</b>									
Knee angle (deg):	102.8	100.5	109.8	113.8	107.10	113.8	107.10	117.20	105
Hip angle (deg):	89.4	85	92.5	102	90.90	102	90.90	92.90	81.3
Trunk angle (deg):	37.7	42.4	39.4	36.7	41.80	36.7	41.80	44.20	45.2
Shoulder angle (deg):	15	6.7	18.3	42.9	28.90	42.9	28.90	43.50	2.8
Elbow angle (deg):	163	164.1	158.6	168.9	165.80	168.9	165.80	163.30	168.9
Arm speed from 1st contact (rad/sec):	7.7	7.85	12.43	7.57	7.57	7.57	7.57	12.21	1.24
Lean angle (deg):	0.2	2.8	0.3	2.9	1.50	2.9	1.50	0.50	56.3
Change in CoM (mm):	1036.2	1102.8	1071.1	1305.5	1251.90	1305.5	1251.90	1501.80	1210.3
<b>Maximum deflection</b>									
Knee angle (deg):	129	128.9	136.9	143	136.00	143	136.00	140.20	132.3
Knee extension (deg):	17.3	17.1	27.2	23.7	28.90	23.7	28.90	19.60	16
Impulse (percent of total time):	54.8	54.8	59.3	51.6	58.10	51.6	58.10	62.50	63
Hip angle (deg):	133.4	139.1	134.8	148.6	144.90	148.6	144.90	148.50	140.6
Trunk angle (deg):	20.6	18.5	19.3	17.3	16.70	17.3	16.70	14.80	17
Shoulder angle (deg):	70.5	70.1	91	76.6	86.30	76.6	86.30	107.40	90.9
Elbow angle (deg):	178.8	176.1	175.7	176.5	177.00	176.5	177.00	134.30	178.4
Lean angle (deg):	8.8	10.7	4.4	10.2	10.20	10.2	10.20	9.60	8.8
Arm speed from 1st contact (deg/sec):	7.7	7.85	12.43	7.57	7.57	7.57	7.57	12.21	1.24
Board deflection (mm):	791.9	669.9	761.3	736	831.80	736	831.80	792.00	810.9
<b>Leg Extension</b>									
Knee angle (deg):	172.8	175.6	176	175.3	176.40	175.3	176.40	171.50	171.6
Hip angle (deg):	178.5	177.8	176.1	177.7	176.30	177.7	176.30	171.70	179.5
Trunk angle (deg):	6.5	3.7	3.3	6.7	3.80	6.7	3.80	1.30	3.7
Shoulder angle (deg):	109	116.4	107.3	131.5	110.60	131.5	110.60	136.00	111.2
Elbow angle (deg):	168.9	177.5	171.8	172.3	171.80	172.3	171.80	103.70	172.5
Lean angle (deg):	9.6	8.8	9.5	11	9.40	11	9.40	11.30	49.4
Arm speed from maxSquat (rad/sec):	7.95	8.9	9.25	7.13	8.13	7.13	8.13	7.62	10.49
Impulse time since max deflection (%):	45.2	45.2	40.7	48.4	41.90	48.4	41.90	37.50	37
<b>Last contact</b>									
Knee angle (deg):	178.1	176.2	179.4	180	179.40	180	179.40	164.70	176.5
Hip angle (deg):	178.5	179.2	179	177.8	174.30	177.8	174.30	161.50	174.9
Trunk angle (deg):	6.1	7.1	4.9	7.5	2.00	7.5	2.00	10.90	2.5
Shoulder angle (deg):	119.5	124.5	134.6	137.9	145.70	137.9	145.70	162.90	146.5
Elbow angle (deg):	167.6	163.3	166.2	174.6	170.50	174.6	170.50	89.80	168.4
Lean angle (deg):	7.2	7.3	6.5	9.6	8.10	9.6	8.10	8.40	43.6
Impulse time (s):	0.4	0.4	0.3	0.4	0.40	0.4	0.40	0.30	0.3
Velocity - x (m/s):	0.93	0.46	0.82	1.16	1.02	1.16	1.02	1.27	0.57
Velocity - y (m/s):	5.13	5	5.18	4.89	5.31	4.89	5.31	5.21	5.38
Velocity - y from bfCurve (m/s):	4.95	4.96	4.83	5.27	5.67	5.27	5.67	5.49	5.14
Difference (%):	3.61	0.8	7.3	7.26	0.94	7.26	0.94	0.95	4.66
Resultant velocity (m/s):	5.04	5.036606	4.90	5.40	5.76	5.40	5.76	5.63	5.17
Rotation of trunk (rad/sec):	1.03	0.97	0.96	1.02	0.69	1.02	0.69	1.08	0.78
<b>Flight Characteristics</b>									
CoM trajectory (deg):	10.3	5.3	9	13.3	10.90	13.3	10.90	13.70	6
Max CoM height (mm):	2394.6	2383.5	2308.5	2463.4	2715.10	2463.4	2715.10	2511.20	2475.9
Max CoM height from bfCurve (mm):	2372.8	2377.3	2299.5	2474.5	2721.30	2474.5	2721.30	2511.30	2476
Difference (%):	0.92	0.26	0.39	0.45	0.23	0.45	0.23	0.00	0
Measured displacement (mm):	1331.8	1309.6	1250.1	1386.7	1612.20	1386.7	1612.20	1507.80	1438.9
Displacement using curve (mm):	1248.7	1252.8	188.2	1416.5	1638.70	1416.5	1638.70	1538.40	1348.5
Difference (%):	6.2	4.3	5	2.1	1.62	2.1	1.62	2.00	6.3
Time to minimum MOI (s):	0.48	0.48	0.46	0	0.00	0	0.00	0.00	0.5
Reduction in MOI (%):	5.75	6.64	6.92	0	0.00	0	0.00	0.00	4.24
Somersault 1 speed (sf/sec):	0	0	0	0	0.00	0	0.00	0.00	0
Somersault 2 speed (sf/sec):	0	0	0	0	0.00	0	0.00	0.00	0
Somersault 3 speed (sf/sec):	0	0	0	0	0.00	0	0.00	0.00	0
Somersault 4 speed (sf/sec):	0	0	0	0	0.00	0	0.00	0.00	0
Opening height (mm):									
Entry distance (mm):	0	0	803.2	0	1123.80	0	1123.80	0.00	0



Key Performance Indicators Best model: 6	2018_09_13_11_27_10_30tb	yh301_2018_11_22_11_24_02_30tb	yh301_2018_11_22_11_26_05_30tb	2018_09_13_11_29_58_30tb	2018_09_13_11_31_23_30tb	yh303_2018_11_22_11_27_34_30tb	yh303_2018_11_22_11_30_49_30tb	yh303_2018_11_22_1_32_27_30tb
	<b>Last step</b>							
Last step length (mm):								
Last step speed - x (m/s):	0.6			0.3	0.7			
Last step speed - y (m/s):	-2.8			-3.3	-3.1			
Last step speed - resultant (m/s):	2.9	0.00	0.00	3.3	3.2	0.00	0.00	0.00
<b>Hurdle step</b>								
Into hurdle speed - x (m/s):	0.1	0.10		0.3	-0.2	0.10	0.00	0.30
Into hurdle speed - y (m/s):	3	3.70		3.3	3.4	4.00	4.50	4.50
Hurdle height (mm):	1686.3	1950.00	2019.40	1684.2	1700.2	1989.50	1990.10	2063.20
Hurdle displacement - measured (mm):	668.5	950.00		620.9	705.5	990.20	985.30	1042.10
Hurdle displacement - calculated (mm):	465	689.00	50866510.00	555.1	583.7	823.20	1011.50	1037.30
Difference (%):	30.4	27.50	5091643.00	10.6	17.3	16.90	2.70	0.50
Hurdle length (mm):		120.50		170.5	36.1	111.30	189.70	119.90
Velocity - x (m/s):	0.4	0.00	-0.10	0.4	0	-0.50	0.00	0.10
Velocity - y (m/s):	-4.3	-4.20	-4.90	-4.3	-3.7	-5.20		-4.80
Distance from tip (mm):	72.4	18.20	55.40	23.8	147.6	41.10	22.70	10.60
<b>First contact</b>								
Knee angle (deg):	106.7	118.20	121.70	111.3	110.9	115.30	113.90	116.10
Hip angle (deg):	85.4	97.10	102.50	89.1	101.9	89.40	91.80	94.90
Trunk angle (deg):	40.2	38.60	35.50	39.4	32.1	42.60	40.80	41.90
Shoulder angle (deg):	36.5	52.60	66.30	37.5	63.8	33.90	42.40	43.70
Elbow angle (deg):	160.4	145.60	155.90	164.7	163.3	166.30	161.60	165.70
Lean angle (deg):	1.2	0.20	1.10	1.2	0.5	2.40	1.80	1.10
Landing velocity - x (m/s):	0.41	0.00	-0.09	0.4	-0.04	-0.48	0.00	0.08
Landing velocity - y (m/s):	-4.26	-4.22	-4.93	-4.28	-3.68	-5.18		-4.79
Landing velocity - resultant (m/s):	4.278509	4.22	4.93	4.298009	3.680341	5.21	0.00	4.79
<b>Max Squat</b>								
Knee angle (deg):	106.7	109.10	118.70	110	107.5	115.30	113.90	109.50
Hip angle (deg):	85.4	90.10	99.90	86.2	91.7	89.40	91.80	89.70
Trunk angle (deg):	40.2	41.80	39.30	43.7	39.9	42.60	40.80	45.10
Shoulder angle (deg):	36.5	45.70	44.70	24.4	31.9	33.90	42.40	32.80
Elbow angle (deg):	160.4	153.90	154.30	162	159.6	166.30	161.60	159.70
Arm speed from 1st contact (rad/sec):		12.23	13.76	10.67	12.34			10.24
Lean angle (deg):	1.2	2.10	1.60	0.3	0.9	2.40	1.80	3.50
Change in COM (mm):	983.5	1293.30	1342.50	1084.6	1051	1989.50	1269.70	1456.40
<b>Maximum deflection</b>								
Knee angle (deg):	133.7	133.10	136.90	138.7	133.7	141.50	141.00	137.00
Knee extension (deg):	26.9	14.90	15.20	27.4	22.8	26.20	27.10	20.80
Impulse (percent of total time):	60	62.10	68.00	65.4	61.5	68.00	69.20	66.70
Hip angle (deg):	136.7	140.10	143.30	152	141.1	149.80	154.90	141.60
Trunk angle (deg):	20.3	19.90	17.50	9.8	16.1	14.80	11.30	21.60
Shoulder angle (deg):	99.3	106.50	103.70	109.6	98	108.30	99.00	90.80
Elbow angle (deg):	142.1	139.00	138.00	139.1	138.4	128.00	122.60	129.50
Lean angle (deg):	7.7	10.80	9.00	8.1	7.7	8.80	10.10	10.90
Arm speed from 1st contact (deg/sec):		12.23	13.76	10.67	12.34			10.24
Board deflection (mm)	814.8	781.00		841.1	829.2	804.40	830.50	833.40
<b>Leg Extension</b>								
Knee angle (deg):	172.1	170.20	171.80	176.1	169.9	163.50	173.50	157.90
Hip angle (deg):	168.8	175.70	172.30	164.9	167.3	171.90	162.20	174.70
Trunk angle (deg):	4	3.40	1.80	5.3	4.7	2.60	7.70	2.90
Shoulder angle (deg):	147.9	141.90	120.80	132.7	133.6	131.70	133.70	116.50
Elbow angle (deg):	72.6	99.70	96.10	58.2	45.6	67.20	64.10	52.60
Lean angle (deg):	9.3	11.50	11.70	8	9.4	10.60	8.90	11.00
Arm speed from maxSquat (rad/sec):	4.69	5.28	6.62	6.46	5.66	5.97	5.61	8.38
Impulse time since max deflection (%):	40	37.90	32.00	34.6	38.5	32.00	30.80	33.30
<b>Last contact</b>								
Knee angle (deg):	172.3	171.50	166.90	152.8	151.1	129.20	134.60	122.30
Hip angle (deg):	163.8	170.60	161.10	158.1	148.8	149.70	152.80	159.00
Trunk angle (deg):	9.6	0.80	10.50	24.6	32.6	38.60	35.40	35.10
Shoulder angle (deg):	173.6	164.60	173.00	165.7	168.9	174.50	160.30	168.00
Elbow angle (deg):	94.5	82.40	96.70	95	126	85.00	114.80	90.50
Lean angle (deg):	5.8	9.00	9.40	2.2	3	4.70	3.30	3.90
Impulse time (s):	0.4	0.40	0.30	0.3	0.3	0.30	0.30	0.30
Velocity - x (m/s):	0.85	1.28	1.29	1.17	0.98	1.69	1.49	1.56
Velocity - y (m/s):	5.08	5.56	5.05	4.79	4.57	4.67	4.98	5.12
Velocity - y from bfCurve (m/s):	4.82	5.69	5.52	4.9	4.63	4.88	5.14	5.09
Difference (%):	5.33	0.98	0.91	2.15	1.35	0.96	0.97	1.01
Resulant velocity (m/s):	4.89	5.83	5.67	5.04	4.73	5.16	5.35	5.32
Rotation of trunk (rad/sec):	1.13	0.80	1.15	1.37	2	2.19	1.86	2.40
<b>Flight Characteristics</b>								
CofM trajectory (deg):	9.5	13.00	14.30	13.7	12	19.90	16.60	17.00
Max CofM height (mm):	2343.2	2612.20	2436.10	2220.2	2164.3		2270.40	2235.20
Max CofM height from bfCurve (mm):	2310.1	2635.60	2227.30	2214.8	2135.3	2126.70	2257.20	2227.30
Difference (%):	1.43	0.89	9.38	0.25	1.36	53.03	0.59	0.36
Measured displacement (mm):	1265.1	1581.40	1432.40	1233.1	1163.4		1334.30	1325.20
Displacement using curve (mm):	1183.6	1648.40	1552.30	1222	1094.5	1214.50	1346.20	1319.40
Difference (%):	6.4	4.20	8.40	0.9	5.9	21.60	0.90	0.40
Time to minimum MOI (s):	0.49		0.40	0.45	0.41		0.46	0.45
Reduction in MOI (%):	56		49.72	59.63	59.11		52.37	52.05
Somersault 1 speed (ss/sec):	0	0.00	0.00	0	0	0.00	0.00	0.00
Somersault 2 speed (ss/sec):	0	0.00	0.00	0	0	0.00	0.00	0.00
Somersault 3 speed (ss/sec):	0	0.00	0.00	0	0	0.00	0.00	0.00
Somersault 4 speed (ss/sec):	0	0.00	0.00	0	0	0.00	0.00	0.00
Opening height (mm):								
Entry distance (mm):	0	0.00	0.00	0	0	0.00	0.00	0.00

Key Performance Indicators	yh303_2018_11_22_11_34_53_304b	yh304_2018_11_22_11_41_25_304b	YH_2019_01_17_11_12_52_303b	YH_2019_01_17_11_15_31_304b	YH_2019_01_17_11_02_04_104b	YH_2019_01_17_11_03_21_5142b
<b>Best model: 6</b>						
<b>Last step</b>						
Last step length (mm):	0.00			896.9	890.9	874.3
Last step speed - x (m/s):				1.1	0.9	0.7
Last step speed - y (m/s):				-3	-3.3	-3.2
Last step speed - resultant (m/s):	0.00	0	0	3.2	3.4	3.3
<b>Hurdle step</b>						
Into hurdle speed - x (m/s):	0.20	0	-0.2	-0.1	-0.2	0.1
Into hurdle speed - y (m/s):	3.80	4	4	3.6	3	3.6
Hurdle height (mm):	2029.30	2072.9	1831.7	1854.7	1844.2	1862.2
Hurdle displacement - measured (mm):	983.50	1016.7	823.6	853.2	854.4	805.5
Hurdle displacement - calculated (mm):	720.10	822.4	817.8	653.3	445.7	673.2
Difference (%):	26.80	19.1	0.7	23.4	47.8	16.4
Hurdle length (mm):		174.1	121.4		8.7	77.8
Velocity - x (m/s):	-0.20	-0.1	-0.3	0	-0.1	0.2
Velocity - y (m/s):	-4.90	-4.7	-4.4	-4.4	-4.7	-4.2
Distance from tip (mm):	6.20	21.8	2.6	1.2	97.4	18.7
<b>First contact</b>						
Knee angle (deg):	117.40	113.5	110	104.8	110.4	102.2
Hip angle (deg):	96.00	95.4	82	87	89.7	85.9
Trunk angle (deg):	38.80	38.4	46	41	46.2	44.7
Shoulder angle (deg):	45.90	49.3	40.9	47.8	44.3	28.3
Elbow angle (deg):	156.70	157.7	152.7	159.4	159.4	159.3
Lean angle (deg):	1.30	1.6	0.6	0.3	4.1	5.7
Landing velocity - x (m/s):	-0.16	-0.12	-0.34	-0.03	-0.14	0.16
Landing velocity - y (m/s):	-4.90	-4.68	-4.45	-4.42	-4.69	-4.19
Landing velocity - resultant (m/s):	4.90	4.68	4.46	4.424682	4.70	4.194741
<b>Max Squat</b>						
Knee angle (deg):	115.80	113.5	108.1	104.8	110.4	102.2
Hip angle (deg):	95.50	95.4	74.2	87	89.7	85.9
Trunk angle (deg):	39.90	38.4	52.5	41	46.2	44.7
Shoulder angle (deg):	37.00	49.3	36	47.8	44.3	28.3
Elbow angle (deg):	158.10	157.7	164.5	159.4	159.4	159.3
Arm speed from 1st contact (rad/sec):	11.47		10.53			
Lean angle (deg):	0.20	1.6	0.6	0.3	4.1	5.7
Change in COM (mm):	1398.00	1342.2	1178.6	1111.5	1075.7	1145.1
<b>Maximum deflection</b>						
Knee angle (deg):	143.10	129.2	135.3	135.3	135.6	139.9
Knee extension (deg):	25.70	15.7	25.3	30.5	25.2	37.7
Impulse (percent of total time):	77.30	68	69.2	73.1	60.7	60
Hip angle (deg):	159.30	140.6	148.3	147.1	149.6	148.5
Trunk angle (deg):	9.50	16.2	12.7	13.5	19.1	24.1
Shoulder angle (deg):	110.80	97.4	99.2	117.1	131.4	147
Elbow angle (deg):	132.80	137.9	139.9	132.4	101.4	104.7
Lean angle (deg):	10.40	8.5	9.4	9.8	16.9	18.4
Arm speed from 1st contact (deg/sec):	11.47		10.53			
Board deflection (mm):	793.10	802.4	827.8	827.6	820.7	829.9
<b>Leg Extension</b>						
Knee angle (deg):	162.50	157.5	161.4	163.7	167	163.1
Hip angle (deg):	172.60	170.8	167.7	172.6	140.8	126
Trunk angle (deg):	2.10	7.8	6.6	2.8	45.7	57.1
Shoulder angle (deg):	134.10	130.5	137	129.5	159.5	140.7
Elbow angle (deg):	76.20	52.9	66.2	44.4	149.5	175.6
Lean angle (deg):	11.30	8.5	10.3	9.2	22	24.7
Arm speed from maxSquat (rad/sec):	7.78	5.01	5.84	6.11	7.13	9.16
Impulse time since max deflection (%):	22.70	32	30.8	26.9	39.3	40
<b>Last contact</b>						
Knee angle (deg):	112.80	127.1	128.2	117.9	178.6	178.2
Hip angle (deg):	158.10	144.1	154.5	153.3	112.7	109.4
Trunk angle (deg):	40.00	48.4	37.5	42.9	75.4	79.5
Shoulder angle (deg):	167.90	171.6	166	157.7	129.8	127.7
Elbow angle (deg):	73.20	105.9	68.8	58	164.6	165.8
Lean angle (deg):	3.60	1.4	0.7	0.8	25.2	27.4
Impulse time (s):	0.30	0.3	0.3	0.3	0.4	0.4
Velocity - x (m/s):	1.67	1.55	1.47	1.49	1.35	1.03
Velocity - y (m/s):	4.68	4.63	4.66	4.75	4.71	4.7
Velocity - y from bfCurve (m/s):	4.81	4.78	4.78	4.89	4.69	4.55
Difference (%):	0.97	0.97	0.97	0.97	1.01	3.36
Resultant velocity (m/s):	5.09	5.03	5.00	5.11	4.88	4.67
Rotation of trunk (rad/sec):	2.16	2.65	2.06	2.25	3.88	4.26
<b>Flight Characteristics</b>						
CoFM trajectory (deg):	19.60	18.5	17.5	17.4	16	12.3
Max CoFM height (mm):	1991.00	2045.6	2082.6	1987.5	1913.7	1887.6
Max CoFM height from bfCurve (mm):	1989.40	2060.9	2063.3	2063.3	1950.4	1879.6
Difference (%):	0.08	0.74	0.93	3.67	1.88	0.43
Measured displacement (mm):	1162.30	1164.2	1209.7	1126.1	1043.6	1079.6
Displacement using curve (mm):	1178.90	1163.1	1165.9	1219.6	1119.4	1055.3
Difference (%):	1.40	0.1	3.6	8.3	7.3	2.3
Time to minimum MOI (s):	0.43	0.43	0.41	0.39	0.48	0.44
Reduction in MOI (%):	48.13	50.93	54.51	50	51.26	45.64
Somersault 1 speed (sst/sec):	0.00	1.45	0	1.45	0	0
Somersault 2 speed (sst/sec):	0.00	0	0	0	0	0
Somersault 3 speed (sst/sec):	0.00	0	0	0	0	0
Somersault 4 speed (sst/sec):	0.00	0	0	0	0	0
Opening height (mm):						
Entry distance (mm):	0.00	0	0	0	1138.2	0

Key Performance Indicators	2018_09_13_1	2018_09_13_1	2018_09_13_1	yh_2018_11_22_	YH_2019_01_17_	2018_09_13_	yh_2018_11_22_	yh201_2018_11_22_
	1_01_15_200a	1_02_30_200a	11_03_33_200a	_10_52_37_200a	_11_47_25_200a	11_10_13_201b	10_57_37_201b	_10_59_28_201b
<b>Best model: 6</b>								
<b>First contact</b>								
Knee angle (deg):	90.2	176	172.8	177.3	168.3	178.2	174.4	999
Hip angle (deg):	91.8	176.6	176.8	176.4	168.1	179.7	170.5	999
Trunk angle (deg):	32.9	0.2	0.5	2.5	6	2.1	3.7	999
Shoulder angle (deg):	72.3	159	160	153.1	167.1	156.4	149.1	999
Elbow angle (deg):	163.9	167.1	164.5	163.2	162.4	160	161.7	999
Lean angle (deg):	10.9	0.3	1.3	1.8	20.8	0.7	0.2	999
Landing velocity - x (m/s):	0.36	0	0	0	0	0	0	0
Landing velocity - y (m/s):	-1.92	999	999	999	999	999	999	999
Landing velocity - resultant (m/s):	1.954375	0	0	0	0	0	0	0
<b>Max Squat</b>								
Knee angle (deg):	77.1	82.8	82.6	84	83	82.2	86.8	83.2
Hip angle (deg):	77.3	80.3	81.2	999	80.6	73.2	76.8	75.4
Trunk angle (deg):	41.1	41.1	41	999	39.6	44.1	42.3	42.2
Shoulder angle (deg):	30.5	46.9	33.9	999	50.6	44.1	76	72.7
Elbow angle (deg):	158.1	165.1	164	999	159.9	164.5	167.3	161.8
Arm speed from 1st contact (rad/sec):	7.11	4.58	4.57	38.37	4.95	2.97	2.71	44.11
Lean angle (deg):	13.1	4.2	4.5	999	28.8	3.6	1.5	3.9
Change in COM (mm):	205.6	411	449.4	-729.2	380	453	367.9	3730.5
<b>Maximum deflection</b>								
Knee angle (deg):	124.8	134.7	122.8	123.4	123.4	119.8	114.6	119.8
Knee extension (deg):	34.7	-41.3	-50	-53.9	-45	-58.4	-59.7	-879.2
Impulse (percent of total time):	52.9	61.8	55.9	61.8	64.7	61.3	64.7	61.1
Hip angle (deg):	128.4	137.6	123.7	138.6	127.9	122.1	121.9	131.2
Trunk angle (deg):	13.9	13.4	18.3	9.5	14.3	16	15	11.8
Shoulder angle (deg):	75.8	76.4	75.3	97.1	93.3	107.6	108.3	116.9
Elbow angle (deg):	176.9	173.8	171.7	176.6	176.7	170.7	169.3	167.3
Lean angle (deg):	0.5	1.4	2	3.7	1.6	1	0.5	2.7
Arm speed from 1st contact (deg/sec):	7.11	4.58	4.57	38.37	4.95	2.97	2.71	44.11
Board deflection (mm):	618	628.6	617.6	573.4	595.2	613.1	566	569.2
<b>Leg Extension</b>								
Knee angle (deg):	177.3	176.4	174	175.2	177.7	175.2	175.5	174.5
Hip angle (deg):	175.1	177.5	173.4	178	177.9	167.2	168.8	167.6
Trunk angle (deg):	10.2	3.2	0.9	1.8	0.4	15.9	13.1	11.6
Shoulder angle (deg):	138.4	117.1	119.8	131.4	137.6	132.1	153.3	146.9
Elbow angle (deg):	169.3	174.5	168.9	159.2	168.4	161.2	161.7	152.3
Lean angle (deg):	5.5	2	0.1	0.3	22.7	2.6	1.7	0.5
Arm speed from maxSquat (rad/sec):	5.87	5.86	6.33	-32.4	5.25	4.41	2.69	2.56
Impulse time since max deflection (%):	47.1	38.2	44.1	38.2	35.3	38.7	35.3	38.9
<b>Last contact</b>								
Knee angle (deg):	169.8	168.8	174.1	172.3	171.9	175.5	178.8	179.6
Hip angle (deg):	178.1	178.3	176.6	178.6	175.2	176.2	172.8	165.2
Trunk angle (deg):	3.4	4.2	1.4	0.6	7.3	14.2	13.8	16.5
Shoulder angle (deg):	142.5	146.9	139.4	151.6	153.8	173.6	179.6	163.5
Elbow angle (deg):	165.3	164.6	165.8	167.5	166.2	146.6	151.9	145.7
Lean angle (deg):	4.6	0.7	2.2	2.8	24	13.4	8.9	4.9
Impulse time (s):	0.4	0.4	0.4	0.4	0.4	0.4	0.4	0.5
Velocity - x (m/s):	0.69	0.39	0.46	0.77	0.71	1.02	0.78	0.71
Velocity - y (m/s):	4.06	4.09	3.87	4.08	3.64	4.01	4.04	4.23
Velocity - y from bfCurve (m/s):	3.67	3.74	3.61	4.2	4.07	2.92	4.35	999
Difference (%):	10.76	9.61	7.38	2.92	10.52	37.23	7.1	99.6
Resulant velocity (m/s):	4.12	4.11	3.64	4.27	4.13	3.09	4.42	999.00
Rotation of trunk (rad/sec):	0.66	0.61	0.71	0.37	0.76	1.11	1.01	0.99
<b>Flight Characteristics</b>								
CofM trajectory (deg):	9.6	5.5	6.8	10.7	11	14.2	10.9	9.5
Max CofM height (mm):	1822	1847.3	1811.8	1904.7	1863.2	1898.6	1952.8	1986.4
Max CofM height from bfCurve (mm):	1794.9	1824.5	1774.8	1918.3	1846.2	2299.5	1969.1	2017
Difference (%):	1.51	1.25	2.08	0.71	0.92	17.43	0.99	1.5
Measured displacement (mm):	780.3	778.9	746.1	881.3	838.6	849.3	913.7	942.8
Displacement using curve (mm):	685.5	711.4	663.4	899.5	843.3	435.1	962.9	0
Difference (%):	12.2	8.7	11.1	2.1	0.6	48.8	5.1	#DIV/0!
Time to minimum MOI (s):	0.4	0.38	0.39	0.01	0.28	0.39	0.4	0.44
Reduction in MOI (%):	6.48	5.57	4.76	0	2.93	57.19	55.7	51.36
Somersault 1 speed (ss/sec):	0	0	0	0	0	0	0	0
Somersault 2 speed (ss/sec):	0	0	0	0	0	0	0	0
Somersault 3 speed (ss/sec):	0	0	0	0	0	0	0	0
Somersault 4 speed (ss/sec):	0	0	0	0	0	0	0	0
Opening height (mm):	999	999	999	999	999	999	999	999
Entry distance (mm):	556.8	367	0	0	0	0	0	0

Key Performance Indicators	yh201_2018_11_22_11_00_44_201b	yh201_2018_11_22_11_02_00_201b	2018_09_13_11_21_14_203b	2018_09_13_11_22_49_203b	2018_09_13_1_24_23_203b	yh203_2018_11_22_11_04_07_203b	yh203_2018_11_22_11_05_30_203b	yh203_2018_11_22_11_07_21_203b
<b>Best model: 6</b>								
<b>First contact</b>								
Knee angle (deg):	999	999	176.6	177.6	174.2	999	171.4	171.2
Hip angle (deg):	999	999	178.2	172	175	999	167.8	167.9
Trunk angle (deg):	999	999	2.6	2.8	0.2	999	3.7	2.3
Shoulder angle (deg):	999	999	152.6	170.1	158.2	999	159.9	166.1
Elbow angle (deg):	999	999	158.3	166.6	157.3	999	165.7	166.2
Lean angle (deg):	999	999	1.6	1	0.1	999	0.8	1.5
Landing velocity - x (m/s):	0	0	0	0	0	0	0	0
Landing velocity - y (m/s):	999	999	999	999	999	999	999	999
Landing velocity - resultant (m/s):	0	0	0	0	0	0	0	0
<b>Max Squat</b>								
Knee angle (deg):	83.5	84	81.3	79.2	77.9	86.3	84.1	88.8
Hip angle (deg):	71.1	73.3	71.3	71.6	75.1	71.7	69.8	78.9
Trunk angle (deg):	46	44.1	43.7	41.9	38.7	45.3	44.3	38.1
Shoulder angle (deg):	91.4	62.7	41.1	51.4	46.9	53.4	78.9	67
Elbow angle (deg):	167	157.1	158.2	160.8	169.6	153	165.4	156.9
Arm speed from 1st contact (rad/sec):	12.4	11.37	3.32	3.79	3.91	15.52	2.87	3.62
Lean angle (deg):	2.2	3.2	2.5	2.1	2.7	1.2	0.2	0.7
Change in COM (mm):	999	999	463.8	430.8	495.3	999	420.2	430.9
<b>Maximum deflection</b>								
Knee angle (deg):	116.7	119	125.3	123	115.7	120.6	123.7	125.9
Knee extension (deg):	-882.3	-880	-51.4	-54.6	-58.5	-878.4	-47.6	-45.2
Impulse (percent of total time):	65.7	61.3	65.5	68.8	57.6	63.3	66.7	71
Hip angle (deg):	124.7	117.4	132.1	133.8	123.7	130.8	137.1	134.8
Trunk angle (deg):	16.1	20.7	8.9	7.9	9.9	7.2	3.2	5.1
Shoulder angle (deg):	111.7	93	129	114.4	107	113.7	107.8	140
Elbow angle (deg):	168.8	164.1	160.5	154.3	170.3	156.7	162.5	159.7
Lean angle (deg):	1.4	0	2.8	1.2	2	3.5	2.7	6
Arm speed from 1st contact (deg/sec):	12.4	11.37	3.32	3.79	3.91	15.52	2.87	3.62
Board deflection (mm):	565.1	554	662.2	660.3	631.2	576.7	591.4	587
<b>Leg Extension</b>								
Knee angle (deg):	175.6	176.2	175.3	172.2	164.8	173.8	174	171.2
Hip angle (deg):	167.4	171.5	157.9	160.7	154.5	157.6	159.9	159.4
Trunk angle (deg):	14.5	9.6	26.3	23.2	35.7	27.6	24.8	28.5
Shoulder angle (deg):	153.8	139	158.4	152.2	166.2	156.2	151.8	153.9
Elbow angle (deg):	165.9	160.6	120.7	104.4	126.9	138.2	138.3	131.5
Lean angle (deg):	1.5	18.4	7.1	5.1	9.1	7.6	6.3	9
Arm speed from maxSquat (rad/sec):	2.63	3.98	5.28	4.14	5.34	4.68	3.4	4.52
Impulse time since max deflection (%):	34.3	38.7	34.5	31.3	42.4	36.7	33.3	29
<b>Last contact</b>								
Knee angle (deg):	177	179.9	163.9	157.1	158.5	164.5	163.6	164.7
Hip angle (deg):	177.3	176.4	145.2	143.7	148.5	150.3	147	146.5
Trunk angle (deg):	10.3	11.5	51.9	55.5	52	44.4	47.2	48.2
Shoulder angle (deg):	177.4	178.4	161.4	171.3	163.9	160.8	168.2	156.3
Elbow angle (deg):	160.9	149.1	179	176.2	158	167.9	153	165.3
Lean angle (deg):	9.5	9	18.8	16.9	18.2	16.7	15.8	17.3
Impulse time (s):	0.4	0.4	0.4	0.4	0.4	0.4	0.4	0.4
Velocity - x (m/s):	0.95	0.92	0.99	0.74	1	0.95	1.08	0.89
Velocity - y (m/s):	4.32	4.19	4.08	3.82	3.89	4.28	4.15	3.91
Velocity - y from bfCurve (m/s):	4.3	4.32	3.78	3.9	3.74	4.17	4.22	4.21
Difference (%):	0.5	3.07	8.07	2.08	3.97	2.6	1.7	7.1
Resulant velocity (m/s):	4.40	4.42	3.91	3.97	3.87	4.28	4.36	4.30
Rotation of trunk (rad/sec):	0.9	1.18	2.36	2.27	2.33	2	1.9	2.01
<b>Flight Characteristics</b>								
CofM trajectory (deg):	12.5	12.4	13.6	11	14.4	12.5	14.5	12.8
Max CofM height (mm):	1963.6	1946.7	1778.3	1805.2	1767.1	1808.2	1811.4	1811.1
Max CofM height from bfCurve (mm):	1964.8	1962.2	1747.8	1806.3	1727.5	1814.2	1809.4	1807
Difference (%):	1	0.79	1.74	0.06	2.29	0.33	0.11	0.23
Measured displacement (mm):	917.4	920.9	813	818.6	816.7	875.1	885.7	893.1
Displacement using curve (mm):	942.3	951.4	727.1	774.7	712.4	884.2	906.3	901.9
Difference (%):	2.6	3.3	10.6	5.4	12.8	1	2.3	1
Time to minimum MOI (s):	0.43	0.43	0.35	0.36	0.38	0.35	0.39	0.39
Reduction in MOI (%):	54.49	54.21	58.34	55.9	58.05	53.09	55.34	55.8
Somersault 1 speed (ss/sec):	0	0	1.51	1.51	1.45	0	0	0
Somersault 2 speed (ss/sec):	0	0	0	0	0	0	0	0
Somersault 3 speed (ss/sec):	0	0	0	0	0	0	0	0
Somersault 4 speed (ss/sec):	0	0	0	0	0	0	0	0
Opening height (mm):	999	999	1521.5	1478.7	1390.4	999	999	999
Entry distance (mm):	0	0	0	0	0	0	0	0

Key Performance Indicators	yh204_2018_11_22_11_09_23_204b	yh204_2018_11_22_11_11_10_204b	yh204_2018_11_22_11_13_21_204b	YH_2019_01_17_11_35_46_203b	YH_2019_01_17_1_1_37_17_204b	YH_2019_01_17_11_38_12_204b
<b>Best model: 6</b>						
<b>First contact</b>						
Knee angle (deg):	170.8	171.4	169.5	169.9	171.1	171.7
Hip angle (deg):	172.8	172.9	167.9	169.5	168.1	170.5
Trunk angle (deg):	0	0.5	2.6	4.4	4.5	2.9
Shoulder angle (deg):	165.9	165.3	161.4	167.1	166.2	161.3
Elbow angle (deg):	163.5	164.1	167.7	163.5	166.7	161.5
Lean angle (deg):	0.2	0	0.9	1.5	0.3	0.3
Landing velocity - x (m/s):	0	0	0	0	0	0
Landing velocity - y (m/s):	999	999	999	999	999	999
Landing velocity - resultant (m/s):	0	0	0	0	0	0
<b>Max Squat</b>						
Knee angle (deg):	86	86.2	87.3	82.1	86.2	83.2
Hip angle (deg):	75.4	76.1	71.3	68.9	68.3	74.4
Trunk angle (deg):	39.8	38.5	42.8	43.8	46.7	38.8
Shoulder angle (deg):	77.4	45.3	78.5	34.3	53.2	61.5
Elbow angle (deg):	159.6	156.4	165.9	158.5	159.9	159.6
Arm speed from 1st contact (rad/sec):	3.56	3.85	3.5	4.48	3.65	3.54
Lean angle (deg):	0.8	0.6	1.4	2.1	0.5	0.7
Change in COM (mm):	409.6	501.4	416.8	510.6	498.3	440.1
<b>Maximum deflection</b>						
Knee angle (deg):	130.5	129.5	123.5	119.3	121.5	121.7
Knee extension (deg):	-40.3	-41.9	-46	-50.6	-49.6	-50.1
Impulse (percent of total time):	73.3	67.9	70	64.3	70.4	69
Hip angle (deg):	143	140.4	138.1	128	128.8	132.1
Trunk angle (deg):	0.6	2.2	2.1	8.3	6.3	3
Shoulder angle (deg):	126.5	119.3	104.8	134.1	130.9	124
Elbow angle (deg):	153.7	162	152.5	167.2	153.5	163.9
Lean angle (deg):	6	5.7	4.9	1.5	5.5	5.1
Arm speed from 1st contact (deg/sec):	3.56	3.85	3.5	4.48	3.65	3.54
Board deflection (mm)	594.9	594	578.6	593.2	609	592.5
<b>Leg Extension</b>						
Knee angle (deg):	172.9	170	163.9	165.8	163.4	163.1
Hip angle (deg):	161.2	156.7	161.3	165.8	174.1	168.9
Trunk angle (deg):	26.5	32	30.5	22.7	19.9	25.4
Shoulder angle (deg):	153.4	155.2	152.9	156.1	134.4	164.4
Elbow angle (deg):	122.9	129.4	135.6	127	128	125.2
Lean angle (deg):	9.3	10	9.1	6.4	8.7	9.5
Arm speed from maxSquat (rad/sec):	4.45	5.76	4.07	5.53	4.54	4.45
Impulse time since max deflection (%):	26.7	32.1	30	35.7	29.6	31
<b>Last contact</b>						
Knee angle (deg):	156.6	158.1	151.5	154.2	153.8	148.3
Hip angle (deg):	148.2	143.2	148.3	147.7	149.5	154.6
Trunk angle (deg):	53.8	57.2	57.1	51.4	52.6	53.7
Shoulder angle (deg):	156.6	150	154.3	164.3	147	169.6
Elbow angle (deg):	167.1	141.2	153.7	152.4	144.7	158.7
Lean angle (deg):	20.8	20.8	22.1	16.3	19.6	21.7
Impulse time (s):	0.4	0.4	0.4	0.4	0.3	0.4
Velocity - x (m/s):	0.81	1.17	1.15	0.95	1.01	1.04
Velocity - y (m/s):	3.93	3.84	3.72	4.01	3.99	3.63
Velocity - y from bfCurve (m/s):	4.01	3.99	3.93	4.26	3.97	3.81
Difference (%):	0.98	0.96	0.95	0.94	1	0.95
Resulant velocity (m/s):	4.09	4.16	4.09	4.36	4.10	3.95
Rotation of trunk (rad/sec):	2.05	2.44	2.23	2.45	2.42	2.2
<b>Flight Characteristics</b>						
CofM trajectory (deg):	11.6	16.9	17.1	13.3	14.2	16
Max CofM height (mm):	1758.1	1683.1	1687.9	1778.8	1701.1	1703.1
Max CofM height from bfCurve (mm):	1751.5	1681.9	1688.5	2063.3	2063.3	2063.3
Difference (%):	0.38	0.07	0.04	13.79	17.55	17.46
Measured displacement (mm):	844.3	803.2	779.8	837.9	814.2	805.5
Displacement using curve (mm):	818.6	811.6	787.4	923.7	805.3	739.2
Difference (%):	3	1	1	10.2	1.1	8.2
Time to minimum MOI (s):	0.39	0.38	0.34	0.39	0.39	0.38
Reduction in MOI (%):	51.28	49.93	51.11	54.72	52.66	51.64
Somersault 1 speed (ss/sec):	0	1.51	1.54	0	1.54	0
Somersault 2 speed (ss/sec):	0	0	0	0	0	0
Somersault 3 speed (ss/sec):	0	0	0	0	0	0
Somersault 4 speed (ss/sec):	0	0	0	0	0	0
Opening height (mm):	999	356.7	393.6	1463.8	999	999
Entry distance (mm):	0	0	0	1458.9	0	0

## Diver 2

### Diver 2 – September 2018 Profiling results

<div style="border: 1px solid black; padding: 5px;"> <p style="text-align: center;"><b>KEY</b></p> <div style="display: flex; justify-content: space-around;"> <div style="width: 20px; height: 20px; background-color: red; margin-bottom: 2px;"></div> <span>injured</span> </div> <div style="display: flex; justify-content: space-around;"> <div style="width: 20px; height: 20px; background-color: lightblue; margin-bottom: 2px;"></div> <span>&gt; 1SD</span> </div> <div style="display: flex; justify-content: space-around;"> <div style="width: 20px; height: 20px; background-color: lightpink; margin-bottom: 2px;"></div> <span>&lt; 1SD</span> </div> </div>	<p>All results were compared to mean of:</p> <ul style="list-style-type: none"> <li>• All funded divers</li> <li>• All divers of the same sex</li> <li>• All divers in the same discipline (springboard or platform)</li> <li>• All divers in the same discipline of the same sex</li> </ul>
---	--

#### Diver 2

ANTHROPOMETRICS				STRENGTH									
				Grip arm by side		Grip arm overhead		Elbow extension		Hip abduction		Hip external rotation	
				Left	Right	Left	Right	Left	Right	Left	Right	Left	Right
WC mean	168.0	62.5	69.3	38.2	39.4	36	36.9	52.2	54.2	51.2	51.9	41.8	40.8
stdev	5.9	9.0	22.9	11.2	11	9.2	9.6	12.6	13.2	12.5	10.4	12.1	11.4
Diver 2	165	69.4	60.6	60.8	61.1	56.7	54.8	76.6	78.7	61.6	67.8	61.3	56.2
Male mean	171.1	67.0	57.2	46.7	46.7	42.0	43.0	60.9	63.0	56.9	56.4	48.8	47.1
stdev	4.4	7.4	18.2	7.8	8.8	7.8	7.7	10.6	9.2	13.3	9.4	12.4	11.5
Diver 2	165	69.4	60.6	60.8	61.1	56.7	54.8	76.6	78.7	61.6	67.8	61.3	56.2
Spring mean	168.2	66.2	69.5	41.9	43.6	38.6	40.7	58.0	60.8	55.0	56.1	47.2	46.8
stdev	5.9	8.6	24.6	11.5	10.9	9.8	10.0	10.9	11.4	15.0	9.9	13.6	12.3
Diver 2	165	69.4	60.6	60.8	61.1	56.7	54.8	76.6	78.7	61.6	67.8	61.3	56.2
Male spr mean	171.0	70.6	56.7	49.9	50.9	44.6	46.2	65.2	67.2	63.7	61.6	55.8	53.6
stdev	3.9	4.4	19.2	6.2	5.8	7.4	7.2	8.5	7.5	13.7	8.0	10.9	9.8
Diver 2	165	69.4	60.6	60.8	61.1	56.7	54.8	76.6	78.7	61.6	67.8	61.3	56.2

RANGE OF MOTION																
Shoulder ER		Shoulder IR		Straight leg raise		Thomas test		Lumbar locked thoracic		Knee to wall		Lat length against wall		Combined elevation		
Left	Right	Left	Right	Left	Right	Left	Right	Left	Right	Left	Right	Trial 1	Trial 2	Trial 1	Trial 2	
WC mean	61.8	66.0	46.3	40.9	119.4	118.3	below	below	52.7	46.7	12.6	12.4	0.2	0.2	27.1	28.6
stdev	13.9	17.9	8.5	8.3	12.1	11.2	below	below	13.9	12.7	2.9	2.6	1.1	1.1	8.6	9.1
Diver 2	65	98	52	33	130	126	above	above	36	32	13	11.5	0	0	17	20
Male mean	59.8	65.3	42.9	37.9	111.5	111.1	below	below	53.3	45.7	12.1	11.8	0.4	0.4	26.6	27.6
stdev	13.7	18.6	7.5	7.7	8.5	7.8	below	below	12.3	11.6	3.0	2.7	1.5	1.5	6.9	5.8
Diver 2	65	98	52	33	130	126	above	above	36	32	13	11.5	0	0	17	20
Spring mean	66.8	70.6	44.8	40.2	122.5	121.2	below	below	55.5	47.6	14.4	14.2	0.4	0.4	25.5	26.5
stdev	16.0	17.2	9.3	8.1	11.9	11.4	below	below	10.2	12.8	2.1	1.8	1.5	1.5	5.6	6.1
Diver 2	65	98	52	33	130	126	above	above	36	32	13	11.5	0	0	17	20
Male spr mean	55.3	63.0	45.3	38.4	111.0	110.1	above	above	52.8	45.5	10.8	10.3	0.0	0.0	26.8	28.0
stdev	11.9	20.9	7.2	7.9	10.9	7.9	above	above	15.3	11.5	3.0	2.3	0.0	0.0	8.7	7.1
Diver 2	65	98	52	33	130	126	above	above	36	32	13	11.5	0	0	17	20

WORK CAPACITY							
SL squat to box - 30 reps		Calf raise off step - 30 reps		Side plank - 120 seconds		Prone hold - 120 seconds	Supine hold - 60 seconds
Left	Right	Left	Right	Left	Right		
WC mean	29	30	23	23	106	107	115
stdev	5	0	6	6	23	23	13
Diver 2	30	30	30	30	120	120	60
Male mean	28	30	24	25	110	110	115
stdev	6	0	6	5	19	21	14
Diver 2	30	30	30	30	120	120	60
Spring mean	30	30	25	25	105	103	114
stdev	0	0	6	6	25	27	13
Diver 2	30	30	30	30	120	120	60
Male spr mean	30	30	26	26	110	108	116
stdev	0	0	6	6	21	23	9
Diver 2	30	30	30	30	120	120	60

STRENGTH AND POWER							
Peak force (N)				Time to peak force (s)			
ISO back squat		ISO calf raise		R		L	
WC mean	2969.64	2441.98	2.44	2.86	2.94	2.72	
stdev	854.80	543.36	1.03	1.64	0.55	0.67	
Diver 2	3032	2843	3.35	3.35	3.1	3.1	
Male mean	3465.36	2650.82	2.51	2.67	2.93	2.73	
stdev	635.28	429.26	0.94	0.80	0.44	0.57	
Diver 2	3032	2843	3.35	3.35	3.1	3.1	
Spring mean	3151.55	2645.55	2.21	2.40	2.82	2.62	
stdev	951.14	615.20	0.88	1.02	0.47	0.78	
Diver 2	3032	2843	3.35	3.35	3.1	3.1	
Male spr mean	3554.00	2847.00	2.44	2.58	2.90	2.74	
stdev	731.72	351.39	0.71	0.68	0.26	0.57	
Diver 2	3032	2843	3.35	3.35	3.1	3.1	

STRENGTH AND POWER ASSESSMENT - JUMPS																										
Peak force (s)				Jump height (cm)				Av. Peak velocity (m/s)				Flight time (m/s)				Rate of force development				Time to peak propulsive force				Movement start to peak force		RSI flight/contact time
CMJ		SLCMJ		CMJ		SLCMJ		CMJ		SLCMJ		CMJ		SLCMJ		CMJ		SLCMJ		CMJ		SLCMJ		CMJ	DJ	
R	L	R	L	R	L	R	L	R	L	R	L	R	L	R	L	R	L	R	L	R	L	R	L			
WC mean	0.71	0.78	0.80	0.08	41.27	23.65	22.84	38.69	2.80	2.14	2.09	2.77	576.36	436.15	427.45	544.52	42362.16	713.08	22675.00	195.08	216.00	3.96	0.68	2.45		
stdev	0.15	0.14	0.17	0.05	10.07	4.68	5.91	8.40	0.35	0.22	0.23	0.41	68.69	44.07	55.46	96.55	148708.90	5612.29	62826.23	100.17	131.84	6.25	0.16	0.84		
Diver 2	0.56	0.61	0.71	0.1	53.2	31.3	29.2	46.6	3.08	2.43	2.35	3.11	655	501	486	618	455791	1350	570	96	160	7	0.55	2.17		
Male mean	0.65	0.82	0.79	0.09	48.09	26.41	26.51	44.78	2.98	2.24	2.22	3.03	625.46	462.25	462.57	601.69	19218.00	2005.50	33294.86	183.38	203.29	4.08	0.66	2.58		
stdev	0.14	0.14	0.17	0.06	7.35	2.71	3.46	5.94	0.22	0.11	0.13	0.19	44.07	22.69	30.69	41.10	178632.97	873.36	78829.00	82.35	106.25	5.79	0.17	1.03		
Diver 2	0.56	0.61	0.71	0.1	53.2	31.3	29.2	46.6	3.08	2.43	2.35	3.11	655	501	486	618	455791	1350	570	96	160	7	0.55	2.17		
Spring mean	0.66	0.78	0.80	0.08	46.20	23.65	22.84	41.55	2.92	2.14	2.09	2.92	607.92	436.15	427.45	579.46	41940.08	713.08	22675.00	195.08	216.00	2.54	0.65	2.51		
stdev	0.15	0.14	0.17	0.06	7.31	4.68	5.91	6.03	0.24	0.22	0.23	0.21	49.15	44.07	55.46	43.39	183472.91	5612.29	62826.23	100.17	131.84	3.73	0.18	0.98		
Diver 2	0.56	0.61	0.71	0.1	53.2	31.3	29.2	46.6	3.08	2.43	2.35	3.11	655	501	486	618	455791	1350	570	96	160	7	0.55	2.17		
Male spr mean	0.6113	0.8163	0.7914	0.0813	50.875	26.413	26.514	45.55	3.0775	2.235	2.22	3.06375	641	462.25	462.57	608.25	5581.125	2005.5	33294.86	183.375	203.29	3	0.63125	2.635		
stdev	0.1043	0.1369	0.1661	0.0694	4.0199	2.7053	3.4638	2.5568	0.104	0.1052	0.1334	0.08314	24.9571	22.6889	30.686	16.816	192635.45	873.358	78829	82.3459	106.25	4.2426	0.1631334	1.1357188		
Diver 2	0.56	0.61	0.71	0.1	53.2	31.3	29.2	46.6	3.08	2.43	2.35	3.11	655	501	486	618	455791	1350	570	96	160	7	0.55	2.17		

## Diver 2 – results of filming and digitisation

### Forward facing dives with hurdle

Dive	Test 1	Test 2	Test 3	Test 4	Change (%)
<b>100a</b>					
Mean board deflection (mm)	882.3	920.8	864.0	896.8	4.36
Maximum board deflection (mm)	883.5		875.8	896.8	1.51
Mean resultant take-off velocity (m/s)	5.44	6.03	6.33	6.67	22.55
Maximum resultant take-off velocity (m/s)	5.79	6.11	5.79	6.67	15.20
Mean vertical take-off velocity (m/s)	5.21	5.83	6.09	6.04	16.93
Maximum vertical velocity (m/s)	5.39	5.91	6.12	6.04	13.48
Mean vertical displacement (mm)	1477.6	1852.6	2020.2	1985.9	36.72
Maximum vertical displacement (mm)	1582.1	1905.5	2037.5	1985.9	28.78
<b>303c</b>					
Mean board deflection (mm)		922.9	896.4		
Maximum board deflection (mm)		967.3	926.3		
Mean resultant take-off velocity (m/s)		6.15	6.42		
Maximum resultant take-off velocity (m/s)		6.28	6.35		
Mean vertical take-off velocity (m/s)		5.82	6.07		
Maximum vertical velocity (m/s)		5.91	6.17		
Mean vertical displacement (mm)		1847.9	2007.3		
Maximum vertical displacement (mm)		1903.6	2075.5		
<b>305c/306c</b>					
Mean board deflection (mm)		937.7	911.8	966.1	3.90
Maximum board deflection (mm)		974.6	924.4	966.1	0.01
Mean resultant take-off velocity (m/s)		6.39	6.34	6.09	-0.82
Maximum resultant take-off velocity (m/s)		6.46	6.40	6.09	-0.92
Mean vertical take-off velocity (m/s)		6.03	5.95	5.76	3.6
Maximum vertical velocity (m/s)		6.11	6.07	5.76	3.40
Mean vertical displacement (mm)		1983.6	1930.6	1809.7	-2.67
Maximum vertical displacement (mm)		2031.9	2004.7	1809.7	-1.34
<b>107c</b>					
Mean board deflection (mm)				931.3	
Maximum board deflection (mm)				931.3	
Mean resultant take-off velocity (m/s)				6.09	
Maximum resultant take-off velocity (m/s)				6.20	
Mean vertical take-off velocity (m/s)				5.79	
Maximum vertical velocity (m/s)				5.86	
Mean vertical displacement (mm)				1828.0	
Maximum vertical displacement (mm)				1871.5	

Back facing dives, standing

Dive	Test 1	Test 2	Test 3	Test 4	Change (%)
<b>200a</b>					
Mean board deflection (mm)	755.1	745.3	733.9	768.0	1.72
Maximum board deflection (mm)	760.6	750.9	737.0	768.0	0.97
Mean resultant take-off velocity (m/s)	4.87	5.03	5.28	5.29	8.59
Maximum resultant take-off velocity (m/s)	5.06	5.21	5.28	5.05	4.35
Mean vertical take-off velocity (m/s)	4.79	4.76	5.13	4.90	6.91
Maximum vertical velocity (m/s)	4.94	4.82	5.19	4.90	5.16
Mean vertical displacement (mm)	1251.8	1234.5	1430.9	1308.6	14.30
Maximum vertical displacement (mm)	1327.3	1263.8	1467.8	1308.6	10.59
<b>203c/204c</b>					
Mean board deflection (mm)		773.5	770.5		
Maximum board deflection (mm)		780.3	796.9		
Mean resultant take-off velocity (m/s)		5.38	5.52		
Maximum resultant take-off velocity (m/s)		5.50	5.59		
Mean vertical take-off velocity (m/s)		4.94	5.02		
Maximum vertical velocity (m/s)		5.07	5.16		
Mean vertical displacement (mm)		1330.5	1374.9		
Maximum vertical displacement (mm)		1402.1	1452.9		
<b>205c/206c</b>					
Mean board deflection (mm)		777.5	757.0	783.6	0.79
Maximum board deflection (mm)		786.3	769.1	796.9	1.35
Mean resultant take-off velocity (m/s)		5.32	5.38	5.24	1.17
Maximum resultant take-off velocity (m/s)		5.39	5.50	5.51	2.23
Mean vertical take-off velocity (m/s)		5.01	5.15	5.10	4.25
Maximum vertical velocity (m/s)		5.03	5.20	5.31	4.73
Mean vertical displacement (mm)		1365.1	1446.2	1417.8	5.95
Maximum vertical displacement (mm)		1376.1	1471.0	1536.4	11.65
<b>405c</b>					
Mean board deflection (mm)			760.2	793.4	4.36
Maximum board deflection (mm)			763.2	795.7	4.26
Mean resultant take-off velocity (m/s)			5.16	4.95	-4.23
Maximum resultant take-off velocity (m/s)			5.36	5.01	-6.53
Mean vertical take-off velocity (m/s)			4.89	4.60	-6.00
Maximum vertical velocity (m/s)			4.93	4.63	-6.11
Mean vertical displacement (mm)			1304.9	1153.0	-11.64
Maximum vertical displacement (mm)			1322.9	1166.3	-11.84



Key performance indicators – all dives - Diver 2. Dives coded as ‘date\_time\_dive-number’.

Any performance indicators which cannot be calculated are represented by ‘999’

Key Performance Indicators	2018_09_06_11_34_30_100a	2018_09_06_11_35_49_100a	2018_09_06_1_1_36_46_100a	2018_10_18_11_15_11_100a	2018_10_18_1_1_16_01_100a	2018_11_22_1_0_49_34_100a	1h_2018_11_22_1_0_50_39_100a	JH_2019_01_17_11_01_06_100a
<b>Best model: 9</b>								
<b>Last step</b>								
Last step length (mm):	1101.5	1455.4	999	999	999	999	999	1424.3
Last step speed - x (m/s):	1.6	2.3	999	999	999	999	999	1.6
Last step speed - y (m/s):	-1.9	-1.7	999	999	999	999	999	-2.2
Last step speed - resultant (m/s):	2.5	2.9	0	0	0	0	0	2.7
<b>Hurdle step</b>								
Into hurdle speed - x (m/s):	0.1	0.1	999	999	999	0	0.6	-0.2
Into hurdle speed - y (m/s):	3.5	3	999	999	999	0	4.3	3.7
Hurdle height (mm):	1787.6	1785.3	999	999	999	4434.5	1901.5	1883
Hurdle displacement - measured (mm):	766.9	711	999	999	999	0	846.7	803.5
Hurdle displacement - calculated (mm):	631.6	450.7	999	999	999	0	936.7	696.8
Difference (%):	17.6	36.6	999	999	999	NaN	10.6	13.3
Hurdle length (mm):	166.2	307.1	999	999	999	224.3	999	182
Velocity - x (m/s):	0	0.5	0.2	0	0	0.1	0.2	0.6
Velocity - y (m/s):	-4.1	-3.4	-3.8	999	999	-4.3	-4.4	-4.3
Distance from tip (mm):	210.7	27.8	33.5	999	999	35.2	7.3	49.1
<b>First contact</b>								
Knee angle (deg):	110.3	103.1	106.4	103	105	94.7	95.8	92.2
Hip angle (deg):	115.4	96.9	84.9	178.7	999	78.7	79.3	80.2
Trunk angle (deg):	14.8	27.2	36.1	6.7	999	37	35.2	33.6
Shoulder angle (deg):	136.4	124	38.5	92.2	999	30.5	31.2	22.1
Elbow angle (deg):	178.8	176.7	150.9	173.4	999	165.1	166.5	170.7
Lean angle (deg):	7.5	0.4	1.1	6.5	999	1.7	0.3	1.2
Landing velocity - x (m/s):	-0.05	0.55	0.2	0	0	0.09	0.19	0.6
Landing velocity - y (m/s):	-4.1	-3.4	-3.76	999	999	-4.31	-4.43	-4.32
Landing velocity - resultant (m/s):	4.10	3.44	3.76	0.00	0.00	4.31	4.43	4.36
<b>Max Squat</b>								
Knee angle (deg):	85.8	87.4	92.6	179.5	999	82.1	86.8	84.3
Hip angle (deg):	84.9	76.9	77.1	178.7	999	72.2	81.1	80.2
Trunk angle (deg):	27.9	34.8	38.9	6.7	999	36.8	34.1	29.6
Shoulder angle (deg):	23.3	15.8	11.8	92.2	999	7.8	4.2	11.5
Elbow angle (deg):	175.7	171.1	173.9	173.4	999	177.5	174.8	173.6
Arm speed from 1st contact (rad/sec):	15.99	19.64	12.75	999	999	9.7	10.71	7.92
Lean angle (deg):	15.1	2.6	1.2	6.5	999	2.7	5	2.3
Change in COM (mm):	1268.3	1251.1	220	999	999	3976.7	1379.2	1358.2
<b>Maximum deflection</b>								
Knee angle (deg):	120.6	110	116.8	179.5	999	110	118.9	113.2
Change in knee angle	34.8	22.6	24.2	0	0	27.9	32.1	28.9
Knee extension (deg):	10.3	6.9	10.4	0	0	15.2	23.2	21
Impulse (percent of total time):	48.4	53.1	53.1	999	999	51.7	54.8	53.1
Hip angle (deg):	138.4	129.5	129.7	178.7	999	131.5	139.9	131.1
Trunk angle (deg):	12.8	15.9	17.1	6.7	999	14.8	12.4	15
Shoulder angle (deg):	39.3	29.9	24.9	92.2	999	61.2	50.1	92.3
Elbow angle (deg):	176.4	173.5	179.9	173.4	999	169.5	178.1	178.5
Lean angle (deg):	9.8	10.9	9.4	6.5	999	11.2	12.1	10.4
Arm speed from 1st contact (deg/sec):	15.99	19.64	12.75	999	999	9.7	10.71	7.92
Board deflection (mm):	883.5	882	881.4	999	999	852	875.9	896.8
<b>Leg Extension</b>								
Knee angle (deg):	177.1	176.2	176	179.5	173.2	176.5	176.2	176.9
Hip angle (deg):	177.1	179	179.3	178.7	172.4	177.3	177.9	177.8
Trunk angle (deg):	7.2	2.8	3.7	6.7	6.2	7.4	5.2	6.2
Change in trunk angle since max def	5.6	13.1	13.4	0	992.8	7.4	7.2	8.8
Shoulder angle (deg):	67.3	70.7	70.5	92.2	98.7	110.3	95.9	117.2
Elbow angle (deg):	177.8	179.6	177	173.4	178	174.8	179.4	173.5
Lean angle (deg):	17	7	6.6	6.5	5	8.1	6.6	7.1
Arm speed from maxSquat (rad/sec):	11.12	10.62	11.05	999	999	11.23	10.18	8.68
Impulse time since max deflection (%):	51.6	46.9	46.9	47	49	48.3	45.2	46.9
<b>Last contact</b>								
Knee angle (deg):	179.6	179.6	177	179.5	178.9	177.1	178.2	178.3
Hip angle (deg):	179.4	179.5	174.9	178.7	173.6	179.8	176.2	176.7
Trunk angle (deg):	5.7	4.4	6.5	6.7	6.2	7.4	6.3	8.4
Shoulder angle (deg):	81.7	74.2	79.9	92.2	98.4	123.5	122.6	130.8
Elbow angle (deg):	178	174.7	176.5	173.4	175.6	175.6	178.6	172.7
Lean angle (deg):	16	6.2	5.5	6.5	3.2	7.4	6.3	6.3
Impulse time (s):	0.4	0.4	0.4	999	999	0.4	0.4	0.4
Velocity - x (m/s):	0.83	0.9	0.72	999	0.73	0.74	0.65	0.85
Velocity - y (m/s):	5.73	5.7	5.7	999	6.17	6.22	6.31	6.62
Velocity - y from bfCurve (m/s):	5.48	5.09	5.57	5.94	6.11	6.27	6.32	6.24
Difference (%):	4.6	11.85	2.24	16712.56	0.89	0.76	0.27	6.01
Resulant velocity (m/s):	5.54	5.17	5.62	999.02	6.15	6.31	6.35	6.30
Rotation of trunk (rad/sec):	0.72	0.77	0.87	999	999	0.91	0.72	0.93
<b>Flight Characteristics</b>								
CofM trajectory (deg):	8.2	9	7.2	999	6.8	6.8	5.9	7.3
Max CofM height (mm):	2658.3	2727.1	2692.3	2834.2	2980.2	3060.5	3094.1	3018.9
Max CofM height from bfCurve (mm):	2653.6	2653.6	2653.6	2821.7	2978.7	3061.2	3087.9	3017.8
Difference (%):	0.18	2.77	1.46	0.44	0.05	0.02	0.2	0.04
Measured displacement (mm):	1551.1	1647	1595.5	1761.8	1889.4	2007.8	2025.3	1981.6
Displacement using curve (mm):	1529.4	1321.3	1582.1	1799.6	1905.5	2002.9	2037.5	1985.9
Difference (%):	1.4	19.8	0.8	2.1	0.9	0.2	0.6	0.2
Time to minimum MOI (s):	0	0	0	0	0.01	0	0	0.64
Reduction in MOI (%):	0	0	0	0	1.42	0	0	5.86
Somersault 1 speed (sst/sec):	0	0	0	0	0	0	0	0
Somersault 2 speed (sst/sec):	0	0	0	0	0	0	0	0
Somersault 3 speed (sst/sec):	0	0	0	0	0	0	0	0
Somersault 4 speed (sst/sec):	0	0	0	0	0	0	0	0
Opening height (mm):	999	999	999	999	999	999	999	999
Entry distance (mm):	0	0	0	0	0	0	0	0

Key Performance Indicators	_2018_10_18_11_22_18_303c	_2018_10_18_11_23_25_303c	_2018_10_18_11_25_12_303c	jh303_2018_11_22_11_14_12_303c	jh303_2018_11_22_11_15_45_303c	_2018_10_18_11_33_17_306c	_2018_10_18_11_34_46_306c	_2018_10_18_11_36_18_306c
	<b>Best model: 9</b>							
<b>Last step</b>								
Last step length (mm):	999	999	999	999	999	999	999	999
Last step speed - x (m/s):	999	999	999	999	999	999	999	999
Last step speed - y (m/s):	999	999	999	999	999	999	999	999
Last step speed - resultant (m/s):	0	0	0	0	0	0	0	0
<b>Hurdle step</b>								
Into hurdle speed - x (m/s):	0.3	0.5	0.3	0.3	0	-0.1	0.1	0.2
Into hurdle speed - y (m/s):	3.4	3.9	4.2	3.9	4.3	3.7	4.1	3.2
Hurdle height (mm):	1820.3	1883.5	1846.2	1825.1	1942.7	1884.7	1896.8	1879.9
Hurdle displacement - measured (mm):	749.8	829.3	774.5	756.4	872	836.3	823.7	822.5
Hurdle displacement - calculated (mm):	590.4	789.8	917.8	789.6	956.4	706.3	839.9	535
Difference (%):	21.3	4.8	18.5	4.4	9.7	15.5	2	35
Hurdle length (mm):	999	305.1	999	284	248.9	230.7	167.8	297.8
Velocity - x (m/s):	0.1	0.2	0	0.2	0.6	-0.1	0.4	0.2
Velocity - y (m/s):	-4.3	-4	-4.5	-3.6	-4.8	-4.8	-4.3	-4.5
Distance from tip (mm):	5.6	13.5	50.1	11.7	14.7	11.1	61	27.4
<b>First contact</b>								
Knee angle (deg):	100.6	87.7	90.4	92.2	91.8	90.3	97.7	100.6
Hip angle (deg):	80.5	74.5	67.8	77.2	76.1	68	78.1	84
Trunk angle (deg):	31.1	35.9	40.2	32.9	38.1	41.6	36.2	29.4
Shoulder angle (deg):	49.4	28.7	26.9	48.7	19.8	19.5	43.5	48.7
Elbow angle (deg):	167.5	170.4	167	173.2	178.4	176.6	179.8	178.5
Lean angle (deg):	5	0.3	1.7	1.2	3	1.7	1.9	4.2
Landing velocity - x (m/s):	0.12	0.22	0	0.16	0.6	-0.15	0.42	0.2
Landing velocity - y (m/s):	-4.26	-4.04	-4.52	-3.58	-4.82	-4.76	-4.28	-4.5
Landing velocity - resultant (m/s):	4.27	4.05	4.52	3.58	4.86	4.76	4.30	4.51
<b>Max Squat</b>								
Knee angle (deg):	85.4	82.6	88.2	84.4	90.8	89.8	87.5	86.8
Hip angle (deg):	70.6	82.2	68.6	72.3	81.3	80.5	66.2	67
Trunk angle (deg):	32.2	27.5	36.4	34	34.5	28	41.3	37.9
Shoulder angle (deg):	10.7	1.8	11.3	8.8	9.1	23.2	20	20
Elbow angle (deg):	178.5	177.3	175.2	174	180	179.2	177.3	175.8
Arm speed from 1st contact (rad/sec):	10.32	11.32	8.41	10.98	12.18	12.66	8.97	9.74
Lean angle (deg):	2.8	4.9	1.8	0	4.1	1	1.1	2.6
Change in COM (mm):	1298.4	1348.2	1234.7	1284.4	1350.8	1413.9	1317.2	1302.9
<b>Maximum deflection</b>								
Knee angle (deg):	117.6	135.3	121.8	110.5	126.7	124.6	115.8	129.2
Change in knee angle	32.2	52.7	33.6	26.1	35.9	34.8	28.3	42.4
Knee extension (deg):	17	47.5	31.4	18.2	34.9	34.3	18.1	28.6
Impulse (percent of total time):	59.3	70.8	62.1	58.1	66.7	61.5	58.1	66.7
Hip angle (deg):	124.6	140.3	129.5	123.9	136.7	133.2	130.3	134.7
Trunk angle (deg):	16.4	19.9	21.3	16.6	18.4	17.9	16.3	18.3
Shoulder angle (deg):	113	133.5	122.2	130.5	139.5	152.5	127.2	140.4
Elbow angle (deg):	106.6	113.1	106.3	107.2	110.6	120.9	98.9	101.6
Lean angle (deg):	6.2	11.4	9.8	9.1	12.2	9.4	8.8	8.7
Arm speed from 1st contact (deg/sec):	10.32	11.32	8.41	10.98	12.18	12.66	8.97	9.74
Board deflection (mm):	906.4	967.3	895.1	866.4	926.3	950	888.4	974.6
<b>Leg Extension</b>								
Knee angle (deg):	175.6	177.1	177.1	164.6	178.2	175.1	173.9	176.9
Hip angle (deg):	179.8	177.8	176.1	177.5	179.6	177.5	167.5	179
Trunk angle (deg):	6.5	9.5	3.6	3.8	7.6	3.6	5.7	6.9
Change in trunk angle since max def	9.9	10.4	17.7	12.8	10.8	14.3	10.6	11.4
Shoulder angle (deg):	161	157.8	164.1	176.4	149.4	175.4	164.4	161.2
Elbow angle (deg):	173.6	124.2	175.2	173.5	112.8	171.5	151.6	158
Lean angle (deg):	6.5	10	7.3	6.8	8.2	6.3	4.2	6.5
Arm speed from maxSquat (rad/sec):	7.4	8.87	6.44	5.96	7.68	9	6.62	6.69
Impulse time since max deflection (%):	40.7	29.2	37.9	41.9	33.3	38.5	41.9	33.3
<b>Last contact</b>								
Knee angle (deg):	136.1	146.1	140	150.4	152.1	137.6	146.6	132
Hip angle (deg):	174.6	178.5	177.1	172.7	178.6	176	171.3	173.1
Trunk angle (deg):	17.1	8.6	12.2	11.9	7	15.1	17.9	10.7
Shoulder angle (deg):	176.4	173.8	171.1	178.9	156.2	168.8	178.9	170.4
Elbow angle (deg):	151.4	146.7	170	172	179.8	153	159	141.6
Lean angle (deg):	4	5.6	4.1	4.7	3.9	2.9	0.2	1.9
Impulse time (s):	0.3	0.3	0.4	0.4	0.3	0.3	0.4	0.3
Velocity - x (m/s):	1.22	1.44	1.12	1.51	1.17	1.58	1.17	1.37
Velocity - y (m/s):	5.99	6.01	5.91	5.9	6.13	6.02	5.99	6.08
Velocity - y from bfCurve (m/s):	5.91	6.11	6.04	6.17	6.38	6.26	6.14	6.31
Difference (%):	1.33	1.73	2.02	4.31	3.86	3.8	2.38	3.76
Resulant velocity (m/s):	6.03	6.28	6.14	6.35	6.49	6.46	6.25	6.46
Rotation of trunk (rad/sec):	1.34	1.14	1.3	1.1	0.99	1.4	1.36	1.16
<b>Flight Characteristics</b>								
CofM trajectory (deg):	11.5	13.5	10.8	14.3	10.8	14.7	11	12.7
Max CofM height (mm):	2836.2	2948	2875.9	2880.5	3104.5	2975.9	2877.3	3020.7
Max CofM height from bfCurve (mm):	2842.2	2960.5	2882.5	2880.9	3102.7	2960.9	2878.1	3006.5
Difference (%):	0.21	0.42	0.23	0.01	0.06	0.51	0.03	0.47
Measured displacement (mm):	1797.5	1904.5	1833.4	1896.4	2037.2	2004.1	1915.8	2051.4
Displacement using curve (mm):	1782.7	1903.6	1857.4	1939	2075.5	1998.1	1920.7	2031.9
Difference (%):	0.8	0	1.3	2.2	1.9	0.3	0.3	1
Time to minimum MOI (s):	0.36	0.38	0.46	0.53	0.46	0.6	0.58	0.6
Reduction in MOI (%):	64.38	65.31	65.22	63.95	64.76	66.63	66.03	65.68
Somersault 1 speed (s/s):	1.36	0	0	0	0	1.7	1.63	1.7
Somersault 2 speed (s/s):	0	0	0	0	0	2.76	2.76	2.86
Somersault 3 speed (s/s):	0	0	0	0	0	0	0	0
Somersault 4 speed (s/s):	0	0	0	0	0	0	0	0
Opening height (mm):	999	999	999	999	999	999	999	999
Entry distance (mm):	0	0	0	0	0	0	0	0

Key Performance Indicators	jh305_2018_11_22__	jh305_2018_11_22__	jh305_2018_11_22__	jh306_2018_11_22__	jh306_2018_11_22__	jh306_2018_11_22__	JH_2019_01_17__	JH_2019_01_17__	JH_2019_01_17__
	11_19_03_305c	11_23_25_305c	11_26_35_305c	_11_30_10_306c	11_32_59_306c	_11_36_36_306c	_11_04_26_306c	_10_58_03_107c	11_00_05_107c
<b>Best model: 9</b>									
<b>Last step</b>									
Last step length (mm)	999	999	999	999	999	999	1428.1	1489.3	999
Last step speed - x (m/s)	999	999	999	999	999	999	2.3	2	999
Last step speed - y (m/s)	999	999	999	999	999	999	-2.1	-2.3	999
Last step speed - resultant (m/s)	0	0	0	0	0	0	3.1	3	0
<b>Hurdle step</b>									
Into hurdle speed - x (m/s)	999	-0.2	0.4	0.2	0.2	999	0.2	-0.1	999
Into hurdle speed - y (m/s)	999	3.2	4	4	4.1	999	4.1	3.6	999
Hurdle height (mm)	1965.7	1952.1	1945.4	999	1938.4	1965.1	1911.7	1884.2	999
Hurdle displacement - measured (mm)	999	889.4	875.9	999	852.6	866.4	813.8	822.3	999
Hurdle displacement - calculated (mm)	999	525.2	816.3	809.1	844.2	999	843.7	655.6	999
Difference (%)	999	40.9	6.8	19	1	999	3.7	20.3	999
Hurdle length (mm)	999	147	234.2	305.1	293.3	999	999	188.6	999
Velocity - x (m/s)	0.5	-0.2	0.1	0.1	0.4	0.2	0.3	-0.3	0
Velocity - y (m/s)	-4.5	-4.7	-4.7	-3.9	-4.4	-4.7	-4.8	-4.6	999
Distance from tip (mm)	24.3	58.9	3.2	36.3	18.2	9.5	10.2	417.4	999
<b>First contact</b>									
Knee angle (deg)	102.1	88.2	91.1	107.9	93.7	95.5	92.1	86.8	999
Hip angle (deg)	80.9	64.3	75.2	102.1	80.3	77.5	72.2	80.6	999
Trunk angle (deg)	34.3	43.2	36.9	24.2	34.3	36.9	37.7	30.5	999
Shoulder angle (deg)	26.1	15.9	34.7	0.6	35.8	19	20.8	19.2	999
Elbow angle (deg)	179.8	177.8	170.7	41.2	179.8	177.2	173.4	173.4	999
Lean angle (deg)	1.9	0	1.1	1.3	0.4	0.2	0.3	73.4	999
Landing velocity - x (m/s)	0.51	-0.18	0.13	0.12	0.41	0.21	0.26	-0.26	0
Landing velocity - y (m/s)	-4.47	-4.73	-4.73	-3.88	-4.35	-4.71	-4.76	-4.59	999
Landing velocity - resultant (m/s)	4.50	4.73	4.74	3.88	4.37	4.77	4.60	4.60	0.00
<b>Max Squat</b>									
Knee angle (deg)	92.4	88.2	93.1	92.4	80.1	93.2	89.8	86.8	999
Hip angle (deg)	75.7	64.3	75.6	93.7	68.3	78.9	80.8	80.6	999
Trunk angle (deg)	36.3	43.2	33.5	26.3	37.2	34.3	28.9	30.5	999
Shoulder angle (deg)	1.8	15.9	14.7	19	5	3	18.9	19.2	999
Elbow angle (deg)	175.4	177.8	166.5	136	174.6	173.8	178.8	173.4	999
Arm speed from 1st contact (rad/sec)	11.21	999	12.86	15.18	9.89	8.6	12.08	999	999
Lean angle (deg)	1	0	3.5	4.2	1.9	0.5	0.8	73.4	999
Change in CoM (mm)	1481.3	1244.3	1289.6	465.3	1373.1	1407.8	1411.1	1888.7	999
<b>Maximum deflection</b>									
Knee angle (deg)	113.4	127.1	131.1	133.2	109.9	129.6	122.2	116.8	999
Change in knee angle	21	38.9	48	50.8	29.8	36.4	33.4	30	0
Knee extension (deg)	11.3	38.8	40.1	25.3	16.2	34.2	30.1	29.9	0
Impulse (percent of total time)	57.1	74.1	66.7	60	62.1	68	59.3	56.3	999
Hip angle (deg)	119.4	137.9	136.8	136.5	120.2	142.5	133.5	143	999
Trunk angle (deg)	22.2	15.5	20.2	21.9	21.5	13.7	18	15.7	999
Shoulder angle (deg)	134	148.9	140	96	131.9	142.1	123.7	130.7	999
Elbow angle (deg)	108.9	103.9	106.6	90.3	107.5	114.9	102.7	87.3	999
Lean angle (deg)	8.8	10.2	10.8	11.6	9.8	9.2	10	15.7	999
Arm speed from 1st contact (deg/sec)	11.21	999	12.86	15.18	9.89	8.6	12.08	999	999
Board deflection (mm)	902	905.6	924.4	921.3	912	905.7	966.1	931.3	931.3
<b>Leg Extension</b>									
Knee angle (deg)	169.6	170.1	175.6	171.7	168.6	177.6	170.3	175.5	999
Hip angle (deg)	177.5	177.9	180	178.9	178.4	176	178	162.3	999
Trunk angle (deg)	0.9	7.5	5.9	8.3	2.9	3.2	4.1	26.3	999
Change in trunk angle since max def	21.3	8	14.3	13.6	18.6	10.5	13.9	-10.6	0
Shoulder angle (deg)	147.8	165.2	145.8	128.1	152.7	174.8	155.4	139.4	999
Elbow angle (deg)	160.7	119.8	139.4	131.3	163.1	132.8	152.3	174	999
Lean angle (deg)	5.8	9.8	6.8	10.5	4.9	6.8	5.2	71.3	999
Arm speed from maxSquat (rad/sec)	7.02	6.28	6.09	11.09	6.6	8.14	7.91	9.29	999
Impulse time since max deflection (%)	42.9	25.9	33.3	40	37.9	32	40.7	43.8	-899
<b>Last contact</b>									
Knee angle (deg)	135.5	131.7	144.4	126.3	139.9	135.4	130.5	178.4	176.7
Hip angle (deg)	177.2	175.6	170.9	175.0	168.8	176.4	179.9	135.9	128.4
Trunk angle (deg)	17.2	16.8	17.9	18	22.7	19.6	18.1	43.1	52.8
Shoulder angle (deg)	174	177.5	178.9	83.7	176.2	133.7	164.4	139	130.6
Elbow angle (deg)	149.9	145.4	157.8	43	146.6	173.8	158.3	174.2	177
Lean angle (deg)	2.1	5.1	2.2	5.2	0.6	1.4	0.3	83.7	19.6
Impulse time (s)	0.4	0.3	0.4	0.3	0.4	0.3	0.3	0.4	999
Velocity - x (m/s)	1.36	1.59	1.27	2.1	1.24	1.32	1.26	0.81	1.3
Velocity - y (m/s)	6.17	5.97	6.2	5.63	5.99	6.01	6.19	5.92	6.13
Velocity - y from bfCurve (m/s)	6.25	6.17	6.27	5.89	6.23	6.1	5.96	5.92	6.06
Difference (%)	1.2	3.31	1.14	4.48	3.96	1.42	3.92	0.07	1.1
Resultant velocity (m/s)	6.40	6.37	6.40	6.25	6.35	6.24	6.09	5.98	6.20
Rotation of trunk (rad/sec)	1.62	1.22	1.44	1.74	1.71	1.33	1.48	0.53	999
<b>Flight Characteristics</b>									
CoM trajectory (deg)	12.4	14.9	11.5	20.4	11.7	12.4	11.5	7.8	12
Max CoM height (mm)	3048.3	2964.4	3018.7	2715.6	2975.5	2893.1	2884.2	2789.9	2820.3
Max CoM height from bfCurve (mm)	3015.5	2937.7	2993.1	2697.4	2957.3	2890.3	2868.3	2800.4	2822
Difference (%)	1.02	0.91	0.86	0.68	0.62	0.45	0.55	0.38	0.66
Measured displacement (mm)	2005.8	1952.2	2021.5	1770.4	1997.2	1866.1	1907.6	1798.8	1871.5
Displacement using curve (mm)	1990.6	1943.4	2004.7	1768.9	1981	1894.8	1809.7	1784.4	1871.5
Difference (%)	0.8	0.5	0.8	0.1	0.8	1.5	5.1	0.8	0
Time to minimum MOI (s)	0.53	0.53	0.6	0.53	0.53	0.55	0.55	0.51	0.5
Reduction in MOI (%)	65.11	65.66	64.02	61.84	64.15	65.53	67.51	61.02	59.75
Somersault 1 speed (sf/sec)	1.7	1.67	1.7	1.78	1.74	1.78	1.74	2.5	2.58
Somersault 2 speed (sf/sec)	2.5	0	0	2.96	2.96	2.76	2.96	3.08	2.96
Somersault 3 speed (sf/sec)	0	0	0	0	0	0	1.95	3.2	3.2
Somersault 4 speed (sf/sec)	0	0	0	0	0	0	0	0	0
Opening height (mm)	0	999	999	999	999	999	1493.4	850	999
Entry distance (mm)	0	0	0	0	0	0	1618.9	0	0

Key Performance Indicators	_2018_09_06_	_2018_09_06_	_2018_09_06_	_2018_10_18_	_2018_10_18_	_2018_10_18_	ih_2018_11_22_	ih_2018_11_22_
	11_30_21_200a	11_40_48_200	11_42_15_200	11_18_16_200	11_19_23_20	11_20_36_20	10_53_17_200a	10_54_19_200a
<b>Best model: 9</b>								
<b>First contact</b>								
Knee angle (deg):	178.3	178.1	176.8	179.1	178.5	176	177.7	178.5
Hip angle (deg):	179.7	179.8	179.2	176.3	177.9	176.5	177.5	179.9
Trunk angle (deg):	0.8	1.4	0	3.5	1.2	1.7	0.5	1.1
Shoulder angle (deg):	160.3	154.4	168.6	145.8	149	150.2	160.6	148.8
Elbow angle (deg):	178	178.9	178.1	169.3	175.8	175.2	177	174
Lean angle (deg):	2.8	3.1	6.7	2.6	27.4	3.6	2.6	1.7
Landing velocity - x (m/s):	0	0	0	0	0	0	0	0
Landing velocity - y (m/s):	999	999	999	999	999	999	999	999
Landing velocity - resultant (m/s):	0	0	0	0	0	0	0	0
<b>Max Squat</b>								
Knee angle (deg):	67.5	65.4	66.5	68.6	63.3	62.9	68.6	68.7
Hip angle (deg):	60.2	66.2	68.4	70.9	59.4	57.1	67.1	62.4
Trunk angle (deg):	45.2	39.7	37	37.2	46.1	47.8	40.4	45.8
Shoulder angle (deg):	25.3	33.9	39.5	30.8	35.5	39	18.1	20.4
Elbow angle (deg):	179.1	177.3	179.8	176.9	178.6	178.1	178.6	174.2
Arm speed from 1st contact (rad/sec):	5.19	5.48	4.87	3.91	4.88	4.58	5.56	5.21
Lean angle (deg):	9	11.1	6.6	10.4	10.7	10.5	10.3	7.8
Change in CoM (mm):	631.7	543.2	529.3	554	576	541.9	658.1	650.6
<b>Maximum deflection</b>								
Knee angle (deg):	108.7	115.6	108.6	118.8	114.3	112.4	116.1	119
Knee extension (deg):	-69.6	-62.6	-68.2	-60.3	-64.1	-63.7	-61.5	-59.5
Impulse (percent of total time):	56.3	60	58.3	65.6	58.8	60	58.1	56.3
Hip angle (deg):	111	114.3	110.7	118	121	116.6	118.1	120.9
Trunk angle (deg):	19.6	21	18.3	20	17.2	17.8	18.2	16.9
Shoulder angle (deg):	108.8	136.4	128.6	123.3	134	141.8	147	126.3
Elbow angle (deg):	166.2	179	170.9	174.9	173.7	172.2	168.7	166.1
Lean angle (deg):	1.7	3.5	8.5	2.1	4.5	2.4	2.5	3.3
Arm speed from 1st contact (deg/sec):	5.19	5.48	4.87	3.91	4.88	4.58	5.56	5.21
Board deflection (mm)	749.5	760.6	999	738.6	746.3	750.9	731.7	732.9
<b>Leg Extension</b>								
Knee angle (deg):	177.2	177.5	176.2	175.9	172.5	177.4	176.2	174.7
Hip angle (deg):	173.5	179.2	171.2	177.8	177.3	177	177.7	174.9
Trunk angle (deg):	4	1.8	4.5	0.6	0.6	2.1	2.8	2.9
Shoulder angle (deg):	142.3	140.3	147	139	147.1	153.8	152.4	146.8
Elbow angle (deg):	167.7	171.9	175.8	178.5	179.6	168.9	164.5	167.1
Lean angle (deg):	1.7	3.3	7.6	1.9	28	2.2	3.1	2.4
Arm speed from maxSquat (rad/sec):	7.27	5.72	5.35	6.5	6.03	5.38	6.86	6.54
Impulse time since max deflection (%):	43.8	40	41.7	34.4	41.2	40	41.9	43.8
<b>Last contact</b>								
Knee angle (deg):	171.7	171.3	170.4	171.7	173.1	172	171.6	172.1
Hip angle (deg):	168.2	176	170.2	174.9	175	171.3	177.4	177.1
Trunk angle (deg):	8.5	4.6	8.2	6.4	5.9	8.5	3.6	3.4
Shoulder angle (deg):	154.4	159.2	146.3	144	150.9	151.2	157.9	157.9
Elbow angle (deg):	174.2	179	174.9	172.2	174.8	156.2	167.8	168.8
Lean angle (deg):	2.5	1.1	2.1	0.5	0.5	0.3	0.9	0.8
Impulse time (s):	0.4	0.4	0.5	0.4	0.4	0.4	0.4	0.4
Velocity - x (m/s):	0.59	0.57	0.5	0.59	0.38	0.62	0.81	0.77
Velocity - y (m/s):	4.7	4.79	5.03	5.17	4.83	4.99	5.22	5.01
Velocity - y from bfCurve (m/s):	4.97	5.1	4.79	4.94	4.84	4.98	5.37	5.25
Difference (%):	5.57	6.19	5.2	4.64	0.16	0.27	2.73	4.56
Resultant velocity (m/s):	4.73	4.82	5.06	5.21	4.85	5.03	5.28	5.07
Rotation of trunk (rad/sec):	1.03	0.87	0.9	0.92	0.79	0.92	0.82	0.75
<b>Flight Characteristics</b>								
CofM trajectory (deg):	7.2	6.8	5.7	6.5	4.5	7.1	8.8	8.7
Max CofM height (mm):	2168.5	2262.8	2234.6	2301.9	2397.2	2375.3	2457.8	2433.3
Max CofM height from bfCurve (mm):	2653.6	2653.6	2235.3	2309.8	2399.2	2373.1	2461.4	2431
Difference (%):	18.28	14.73	0.03	0.34	0.08	0.09	0.15	0.09
Measured displacement (mm):	1121.8	1183.5	1184.7	1241.8	1238.6	1313.8	1429.5	1384.4
Displacement using curve (mm):	1261.2	1327.3	1167	1245.8	1193.9	1263.8	1467.8	1403.9
Difference (%):	12.4	12.2	1.5	0.3	3.6	3.8	2.7	1.4
Time to minimum MCI (s):	0.43	0.51	0.5	999	0.49	999	0.03	0.03
Reduction in MCI (%):	6.1	8.45	7.35	999	19.66	999	0.89	3.68
Somersault 1 speed (ss/sec):	0	0	0	0	0	0	0	0
Somersault 2 speed (ss/sec):	0	0	0	0	0	0	0	0
Somersault 3 speed (ss/sec):	0	0	0	0	0	0	0	0
Somersault 4 speed (ss/sec):	0	0	0	0	0	0	0	0
Opening height (mm):	999	999	999	999	999	999	999	999
Entry distance (mm):	0	0	0	0	0	0	0	0

Key Performance Indicators	ih_2018_11_22_10_55_23_200a	JH_2019_01_17_11_08_44_200a	_2018_09_06_11_45_21_202	_2018_09_06_11_46_26_202c	_2018_10_18_11_39_15_203c	_2018_10_18_11_40_45_203c	_2018_10_18_11_41_48_203c	_2018_10_18_11_45_32_204
<b>Best model: 9</b>								
<b>First contact</b>								
Knee angle (deg):	178.9	179.6	179.5	178.6	179.6	176.8	176.7	179.6
Hip angle (deg):	175.4	177.9	178.2	179.1	179.3	178.7	175.2	177.7
Trunk angle (deg):	1.8	1.1	2.2	0	1.9	1.3	3.9	2.9
Shoulder angle (deg):	154.8	168.2	153.4	152.2	154.1	155.5	143.5	143.5
Elbow angle (deg):	175.5	177.3	173.9	178.8	174.8	173.5	167.7	167.8
Lean angle (deg):	3.1	2	2.1	2.3	2.9	2.5	3.2	2
Landing velocity - x (m/s):	0	0	0	0	0	0	0	0
Landing velocity - y (m/s):	999	999	999	999	999	999	999	999
Landing velocity - resultant (m/s):	0	0	0	0	0	0	0	0
<b>Max Squat</b>								
Knee angle (deg):	67.4	69.7	69.8	68.1	145.4	66.5	59.7	67.5
Hip angle (deg):	62.9	68	60.2	65.5	15	60.2	60.2	62.2
Trunk angle (deg):	44.6	39.9	43	40.1	42.8	41.5	40.3	40.7
Shoulder angle (deg):	10.7	19.5	22.4	38.7	999	33.1	18.9	23
Elbow angle (deg):	177.3	172.8	176.8	178.5	999	178.9	176.7	178.3
Arm speed from 1st contact (rad/sec):	5.19	5.12	4.68	4.28	37.73	4.22	4.65	4.32
Lean angle (deg):	10.5	9	7.6	8.9	999	7	10.2	9.8
Change in COM (mm):	691.7	506.5	571.5	523.8	120.9	533.2	603.3	586.6
<b>Maximum deflection</b>								
Knee angle (deg):	114.5	114.3	129.5	121.3	121.2	116.3	116.8	118.6
Knee extension (deg):	-64.4	-65.3	-50	-57.3	-58.4	-60.5	-59.9	-61
Impulse (percent of total time):	54.5	62.9	69	63.6	61.3	66.7	62.5	62.5
Hip angle (deg):	117.7	119.8	123.5	121.4	120.8	114.9	113.4	118.4
Trunk angle (deg):	18.5	15.8	16.8	15.7	13.9	16.3	18.4	16.4
Shoulder angle (deg):	156.1	156.6	136	122.8	152.2	145	162.1	147.8
Elbow angle (deg):	179.5	171.4	163.3	165.3	138.5	154.1	149.2	142.4
Lean angle (deg):	3.1	2.8	1.9	0.9	1.7	1.6	1.1	1.2
Arm speed from 1st contact (deg/sec):	5.19	5.12	4.68	4.28	37.73	4.22	4.65	4.32
Board deflection (mm)	737	768	999	999	778.9	768	772.2	774.4
<b>Leg Extension</b>								
Knee angle (deg):	177.6	178.2	176.1	176.1	174.4	175.9	172.4	174.2
Hip angle (deg):	178.3	177.3	176.4	175.9	170	175.4	172.9	168.8
Trunk angle (deg):	0.3	2.7	3.6	2.1	10.1	5.6	3.6	9.3
Shoulder angle (deg):	162.1	148.1	147	142.7	172.7	150.7	144.7	163.1
Elbow angle (deg):	166.5	163.7	163.9	165.9	164.5	152.1	154.9	160.5
Lean angle (deg):	1.3	2.4	4.2	3.3	5.6	4.8	2.5	4.7
Arm speed from maxSquat (rad/sec):	6.2	5.35	6.42	5.23	-36.02	4.64	5.07	5.88
Impulse time since max deflection (%):	45.5	37.1	31	36.4	38.7	33.3	37.5	37.5
<b>Last contact</b>								
Knee angle (deg):	175.7	175.1	176.4	177.2	176.7	176	176.7	167.2
Hip angle (deg):	173	169	163	169.7	166.5	165.3	161.9	167.8
Trunk angle (deg):	6.1	7.6	23.6	15.8	20.6	21.9	22.9	24.3
Shoulder angle (deg):	153.5	157.3	171	168.7	160.3	164.1	163.1	163.3
Elbow angle (deg):	163.8	169.8	175.7	171.8	161.9	166.2	171.1	178.5
Lean angle (deg):	0.1	1.1	13.4	10.2	11.6	12.1	10.1	12.2
Impulse time (s):	0.4	0.4	0.4	0.4	0.4	0.4	0.4	0.4
Velocity - x (m/s):	0.78	0.48	1.08	0.98	1.05	0.93	0.85	1.02
Velocity - y (m/s):	5.14	5.03	4.59	4.93	5.27	5.26	5.19	5.34
Velocity - y from bfCurve (m/s):	5.28	5.07	3.05	3.84	5.24	5.09	5.08	4.89
Difference (%):	2.66	0.76	50.37	28.42	0.48	3.37	2.21	9.17
Resultant velocity (m/s):	5.2	5.05	4.72	5.03	5.37	5.34	5.26	5.44
Rotation of trunk (rad/sec):	0.93	0.8	1.44	1.1	1.34	1.33	1.48	1.5
<b>Flight Characteristics</b>								
CofM trajectory (deg):	8.7	5.5	13.3	11.2	11.3	10	9.3	10.9
Max CofM height (mm):	2474	2387.4	2202.1	2271.7	2416.4	2387.3	2410.8	2448.6
Max CofM height from bfCurve (mm):	2464.5	2382.9	2653.6	2653.6	2415.6	2380	2418.7	2418.7
Difference (%):	0.38	0.19	17.02	14.39	0.03	0.31	0.33	1.23
Measured displacement (mm):	1415	1318.3	1216.9	1223.8	1417.1	1368.2	1355.9	1428.7
Displacement using curve (mm):	1420.9	1308.6	475.4	751	1402.1	1320.5	1315.5	1218.5
Difference (%):	0.4	0.7	60.9	38.6	1.1	3.5	3	14.7
Time to minimum MOI (s):	0	0.13	0.43	0.45	0.4	0.4	0.4	0.58
Reduction in MOI (%):	0	7.3	70.5	70.42	65.62	68.52	67.64	67.61
Somersault 1 speed (ss/sec):	0	0	0	0	0	0	0	1.67
Somersault 2 speed (ss/sec):	0	0	0	0	0	0	0	0
Somersault 3 speed (ss/sec):	0	0	0	0	0	0	0	0
Somersault 4 speed (ss/sec):	0	0	0	0	0	0	0	0
Opening height (mm):	999	999	999	999	999	999	999	999
Entry distance (mm):	0	0	0	0	0	0	0	0

Key Performance Indicators	2018_10_18	2018_10_18	jh_2018_11_22	jh203_2018_11_22	jh203_2018_11_22	2018_10_18	2018_10_18	2018_10_18
	11_46_52_204	11_48_55_204	10_56_46_203c	_10_58_13_203c	11_00_07_203c	11_45_32_204	11_46_52_204	11_48_55_204
<b>Best model: 9</b>								
<b>First contact</b>								
Knee angle (deg):	179.8	179.9	175.2	179	999	179.6	179.8	179.9
Hip angle (deg):	177.5	177.4	178.3	178.2	999	177.7	177.5	177.4
Trunk angle (deg):	0.5	3.3	4.1	0.4	999	2.9	0.5	3.3
Shoulder angle (deg):	166	149	142.8	152.5	999	143.5	166	149
Elbow angle (deg):	179.9	178.1	171.3	178	999	167.8	179.9	178.1
Lean angle (deg):	3	2.4	1.4	2.9	999	2	3	2.4
Landing velocity - x (m/s):	0	0	0	0	0	0	0	0
Landing velocity - y (m/s):	999	999	999	999	999	999	999	999
Landing velocity - resultant (m/s):	0	0	0	0	0	0	0	0
<b>Max Squat</b>								
Knee angle (deg):	61.7	65.3	68	71.2	67	67.5	61.7	65.3
Hip angle (deg):	58.7	62.4	62.1	56.2	65.5	62.2	58.7	62.4
Trunk angle (deg):	44.7	41.6	42	49.4	40.2	40.7	44.7	41.6
Shoulder angle (deg):	26.2	39.4	24	30.6	3.3	23	26.2	39.4
Elbow angle (deg):	179.9	172.6	177.9	179.9	179	178.3	179.9	172.6
Arm speed from 1st contact (rad/sec):	4.59	3.9	4.07	4.39	12.72	4.32	4.59	3.9
Lean angle (deg):	10.9	8.3	7	5.7	7.6	9.8	10.9	8.3
Change in CDM (mm):	605.4	550.1	1129.5	640.8	717.3	586.6	605.4	550.1
<b>Maximum deflection</b>								
Knee angle (deg):	113.9	120.2	114.4	117.9	124.4	118.6	113.9	120.2
Knee extension (deg):	-65.9	-59.7	-60.8	-61.1	-874.6	-61	-65.9	-59.7
Impulse (percent of total time):	59.4	65.6	60.6	61.3	58.6	62.5	59.4	65.6
Hip angle (deg):	114.3	116.5	111.6	116.8	121	118.4	114.3	116.5
Trunk angle (deg):	14.8	17.8	19.8	17.4	16.6	16.4	14.8	17.8
Shoulder angle (deg):	146.3	156.6	133	146.2	154.5	147.8	146.3	156.6
Elbow angle (deg):	136.4	142.5	150.5	137.5	135.7	142.4	136.4	142.5
Lean angle (deg):	2.2	1.8	1.6	1.9	1.8	1.2	2.2	1.8
Arm speed from 1st contact (deg/sec):	4.59	3.9	4.07	4.39	12.72	4.32	4.59	3.9
Board deflection (mm):	780.3	767	748.4	757.4	763.4	774.4	780.3	767
<b>Leg Extension</b>								
Knee angle (deg):	177.1	177.9	178.1	178.7	179.1	174.2	177.1	177.9
Hip angle (deg):	170.9	172.5	174.1	174.9	171.4	168.8	170.9	172.5
Trunk angle (deg):	12.8	7.7	6.8	7.6	9.2	9.3	12.8	7.7
Shoulder angle (deg):	170.4	147.4	148.6	160.4	163.6	163.1	170.4	147.4
Elbow angle (deg):	163.2	150.9	160.4	166.1	154.5	160.5	163.2	150.9
Lean angle (deg):	6.2	4.2	4.3	5.3	3.5	4.7	6.2	4.2
Arm speed from maxSquat (rad/sec):	6.38	5.34	5.04	5.53	7.68	5.88	6.38	5.34
Impulse time since max deflection (%):	40.6	34.4	39.4	38.7	41.4	37.5	40.6	34.4
<b>Last contact</b>								
Knee angle (deg):	166.6	167	175.3	179.2	179.5	167.2	166.6	167
Hip angle (deg):	161.9	167.3	167.8	164.8	162.9	167.8	161.9	167.3
Trunk angle (deg):	31.9	25.4	20.3	21.7	23	24.3	31.9	25.4
Shoulder angle (deg):	175.6	170.7	168.4	161	169.3	169.3	175.6	170.7
Elbow angle (deg):	177.2	167.5	175.5	163.2	170	178.5	177.2	167.5
Lean angle (deg):	15.2	13.3	11.7	12.4	11.4	12.2	15.2	13.3
Impulse time (s):	0.4	0.4	0.4	0.4	0.4	0.4	0.4	0.4
Velocity - x (m/s):	1.17	1.11	1.07	1.14	0.95	1.02	1.17	1.11
Velocity - y (m/s):	5.25	5.39	5.48	5.47	5.38	5.34	5.25	5.39
Velocity - y from bfCurve (m/s):	5.2	5.15	5.25	5.34	5.29	4.89	5.2	5.15
Difference (%):	1	4.74	4.48	2.51	1.73	9.17	1	4.74
Resultant velocity (m/s):	5.38	5.5	5.58	5.59	5.46	5.44	5.38	5.5
Rotation of trunk (rad/sec):	1.72	1.55	1.43	1.48	1.58	1.5	1.72	1.55
<b>Flight Characteristics</b>								
CofM trajectory (deg):	12.6	11.6	11	11.7	10	10.9	12.6	11.6
Max CofM height (mm):	2419.4	2400	999	2457.7	2477.3	2448.6	2419.4	2400
Max CofM height from bfCurve (mm):	2400.9	2393	2479	2456.4	2469.6	2418.7	2400.9	2393
Difference (%):	0.77	0.29	59.7	0.05	0.31	1.23	0.77	0.29
Measured displacement (mm):	1388.1	1384.3	999	1461.3	1452.3	1428.7	1388.1	1384.3
Displacement using curve (mm):	1376.6	1349.8	1402.8	1452.9	1425.4	1218.5	1376.6	1349.8
Difference (%):	0.8	2.5	40.4	0.6	1.8	14.7	0.8	2.5
Time to minimum MOI (s):	0.56	0.54	999	0.4	0.4	0.58	0.56	0.54
Reduction in MOI (%):	65.09	68.19	999	67.55	66.95	67.61	65.09	68.19
Somersault 1 speed (sst/sec):	1.67	1.67	0	0	0	1.67	1.67	1.67
Somersault 2 speed (sst/sec):	0	0	0	0	0	0	0	0
Somersault 3 speed (sst/sec):	0	0	0	0	0	0	0	0
Somersault 4 speed (sst/sec):	0	0	0	0	0	0	0	0
Opening height (mm):	999	999	999	999	2428.3	999	999	999
Entry distance (mm):	0	0	0	0	0	0	0	0

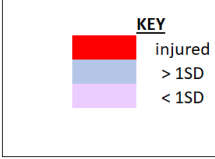
Key Performance Indicators	_2018_10_18_	_2018_10_18_	_2018_10_18_	jh203_2018_11_22_	jh205_2018_11_22_	jh205_2018_11_22_	jh206_2018_11_22_	jh206_2018_11_22_	JH_2019_01_17_
	11_50_37_206	11_52_36_206	11_54_33_206	11_01_29_205	_11_03_20_205c	_11_04_49_205c	11_08_28_206c	11_10_14_206c	11_10_12_205c
<b>Best model: 9</b>									
<b>First contact</b>									
Knee angle (deg):	173.1	179.5	178.9	177	179.4	178.3	177.5	179.2	175.3
Hip angle (deg):	179.9	179.9	178	174.5	179.3	178.7	176.9	179.5	177.2
Trunk angle (deg):	1.3	1.2	3.4	2.8	0	1.1	1	2.1	0.2
Shoulder angle (deg):	145.8	150.5	145.3	151.4	153.2	150.3	153.1	155.7	162.8
Elbow angle (deg):	170.4	168.2	167.2	171.5	167	172.5	174.6	170.6	179.3
Lean angle (deg):	3.2	3.1	3	1.9	0.8	1.1	1.9	2.9	1.7
Landing velocity - x (m/s):	0	0	0	0	0	0	0	0	0
Landing velocity - y (m/s):	999	999	999	999	999	999	999	999	999
Landing velocity - resultant (m/s):	0	0	0	0	0	0	0	0	0
<b>Max Squat</b>									
Knee angle (deg):	63.5	64.7	48.1	66.6	66.7	66	63	67.9	68.9
Hip angle (deg):	63.1	60.6	38.1	59.1	59.7	66.1	62.6	59.2	68.1
Trunk angle (deg):	39.2	40.8	11	42.4	45.6	35.7	40.7	42.3	35.3
Shoulder angle (deg):	23.4	25.8	16.6	14.2	24.1	5.6	13.5	8.2	1.2
Elbow angle (deg):	179.7	175.3	122.2	179.5	172.1	180	175.7	180	177.3
Arm speed from 1st contact (rad/sec):	4.74	4.52	1.82	5.35	4.77	5.13	5.38	5.3	5.87
Lean angle (deg):	10.9	9.8	25.1	7.3	6.8	10	7.2	6.5	6.8
Change in CoM (mm):	611.4	651.4	-1272.5	678.5	593.2	708.6	696.5	624.7	664.3
<b>Maximum deflection</b>									
Knee angle (deg):	120.9	121.4	118.7	116.7	119.4	116.1	120.9	118.9	112.3
Knee extension (deg):	-58.2	-58.1	-60.3	-60.3	-59.9	-62.2	-56.6	-60.2	-63
Impulse (percent of total time):	66.7	64.5	124	62.1	65.6	56.7	64.3	63.3	62.1
Hip angle (deg):	120.3	119.7	118.5	113	116.5	119.4	117.4	118.5	110.7
Trunk angle (deg):	15	15.4	15.9	17.5	18.2	14.1	17.6	17.2	16
Shoulder angle (deg):	141.3	149.9	142.8	152	149.5	140	167.7	155.3	155.9
Elbow angle (deg):	136	131.1	139	133.3	133.3	128.1	135.7	134	130.4
Lean angle (deg):	1.4	1.9	2	2.4	1.4	1.4	2.3	2.6	2.7
Arm speed from 1st contact (deg/sec):	4.74	4.52	1.82	5.35	4.77	5.13	5.38	5.3	5.87
Board deflection (mm)	789.6	768.6	786.3	769.1	759	749.7	764	743.3	778.2
<b>Leg Extension</b>									
Knee angle (deg):	178	178.9	177.2	179.6	179.1	176.8	179.8	178.3	176.8
Hip angle (deg):	177.9	174.6	167.3	176.1	179.8	173.3	178.9	177.6	177.5
Trunk angle (deg):	5.1	8.8	12.7	7.1	4.5	11.3	4.4	5.5	7.8
Shoulder angle (deg):	159.6	145.2	170.8	158	154.1	178	162.5	176.5	177.3
Elbow angle (deg):	163.9	146.8	178.8	163.8	151.4	171.4	163.1	176.3	169.4
Lean angle (deg):	3.8	5.9	6.4	5.1	5	6.2	5.1	5.9	5.1
Arm speed from maxSquat (rad/sec):	6.1	6.35	-5.32	7.1	5.7	7.78	7.47	7	7.55
Impulse time since max deflection (%):	33.3	35.5	-24	37.9	34.4	43.3	35.7	36.7	37.9
<b>Last contact</b>									
Knee angle (deg):	163.1	155.6	157.7	168.1	174.2	170.1	169.3	167.1	159.6
Hip angle (deg):	167.6	166.1	168	162.7	161.8	162.4	161.7	164.4	172.4
Trunk angle (deg):	25	34.1	30.2	28.4	25.9	28.8	30.8	29.4	27.8
Shoulder angle (deg):	178.9	161.7	169.1	178.5	165.2	176.3	165.9	165	165.9
Elbow angle (deg):	171.1	158.2	174.8	171.9	177	179.2	166.6	168	168.4
Lean angle (deg):	11.9	15.5	14.1	58.4	12.6	14.4	14.1	14.3	14.4
Impulse time (s):	0.4	0.4	-0.6	0.4	0.4	0.4	0.4	0.4	0.4
Velocity - x (m/s):	0.73	1.16	1.11	0.87	1.17	1.13	1.1	1.15	1.06
Velocity - y (m/s):	5.27	5.12	5.27	5.17	5.55	5.16	5.22	5.24	5.41
Velocity - y from bfCurve (m/s):	5.18	5.15	5.2	5.37	5.35	5.29	5.32	5.31	5.14
Difference (%):	1.83	0.75	1.46	3.69	3.79	2.45	1.8	1.24	5.2
Resultant velocity (m/s):	5.32	5.25	5.39	5.25	5.67	5.34	5.34	5.37	5.51
Rotation of trunk (rad/sec):	1.55	1.82	-1.46	1.78	1.58	1.66	1.88	1.76	1.65
<b>Flight Characteristics</b>									
CoM trajectory (deg):	7.8	12.8	11.9	9.5	11.9	12.4	11.9	12.4	11
Max CoM height (mm):	2425.2	2383	2380.7	2464	2506.9	2470.6	2451.7	2438.9	2364
Max CoM height from bfCurve (mm):	2381.6	2357.6	2353.1	2443.2	2481.9	2458.1	2435.3	2413.1	2347.7
Difference (%):	1.83	1.08	1.17	0.85	1.01	0.51	0.68	1.07	0.69
Measured displacement (mm):	1430.8	1357.5	1401.6	1473	1466.5	1419.2	1441.8	1442.4	1367
Displacement using curve (mm):	1367.7	1354	1376.1	1471	1456.8	1424.9	1441.9	1436.5	1347.1
Difference (%):	4.4	0.3	1.8	0.1	0.7	0.4	0.4	0.4	1.5
Time to minimum MOI (s):	0.56	0.53	0.54	0.54	0.54	0.55	0.55	0.56	0.53
Reduction in MOI (%):	64.54	63.73	63.37	67.39	67.27	67.59	66.46	67.7	66.6
Somersault 1 speed (sst/sec):	1.78	1.78	1.74	1.74	1.74	1.7	1.78	1.74	1.78
Somersault 2 speed (sst/sec):	2.86	3.08	3.08	2.67	2.67	2.86	2.86	2.96	0
Somersault 3 speed (sst/sec):	0	0	0	0	0	0	0	0	0
Somersault 4 speed (sst/sec):	0	0	0	0	0	0	0	0	0
Opening height (mm):	999	999	999	999	999	999	999	999	999
Entry distance (mm):	0	0	0	0	0	0	0	0	0

Key Performance Indicators	JH_2019_01_17_	JH_2019_01_17_	JH_2019_01_17_	jh405_2018_11_22_	jh405_2018_11_22_	jh405_2018_11_22_	JH_2019_01_17_	JH_2019_01_17_
	11_11_45_205c	_11_13_39_206c	11_15_09_206c	11_38_38_405c	_11_40_13_405c	11_44_16_405c	11_05_48_405c	11_07_23_405c
<b>Best model: 9</b>								
<b>First contact</b>								
Knee angle (deg):	179.4	175.1	179	178.2	177.6	999	177.7	177.4
Hip angle (deg):	178.9	174.7	179.5	177.6	178.5	999	179.7	175.4
Trunk angle (deg):	1.1	4	0.5	0.4	3.3	999	1	3.2
Shoulder angle (deg):	155	150.1	163.1	164.9	146.9	999	152.4	155.8
Elbow angle (deg):	174.8	173.1	175.8	176.5	174.7	999	175.4	178.5
Lean angle (deg):	1	0.5	1.8	3.6	3.5	999	2.4	3.1
Landing velocity - x (m/s):	0	0	0	0	0	0	0	0
Landing velocity - y (m/s):	999	999	999	999	999	999	999	999
Landing velocity - resultant (m/s):	0	0	0	0	0	0	0	0
<b>Max Squat</b>								
Knee angle (deg):	67.2	67	65.4	68.5	68.9	999	67.2	69.1
Hip angle (deg):	59.4	66.7	63.3	72.4	73.9	999	68.2	68.9
Trunk angle (deg):	42.6	35.9	41.7	38.1	38.7	999	39.5	39.2
Shoulder angle (deg):	8.9	15.9	18.4	24.3	25.3	999	26.2	1.5
Elbow angle (deg):	176.4	174.1	177.5	170.5	167.1	999	178.6	179.1
Arm speed from 1st contact (rad/sec):	5.12	4.73	5.07	6.87	6.44	999	6.6	5.91
Lean angle (deg):	6.7	7.4	8.6	11.9	13.8	999	11.8	10.9
Change in CDM (mm):	626.8	593.2	596.6	714.3	671.1	999	638.4	569.2
<b>Maximum deflection</b>								
Knee angle (deg):	117.5	123.9	126.7	122.9	118.9	111.5	118.6	125.6
Knee extension (deg):	-61.9	-51.3	-52.3	-55.3	-58.8	-887.5	-59.1	-51.7
Impulse (percent of total time):	61.3	67.7	66.7	53.3	56.3	999	54.5	58.8
Hip angle (deg):	117.6	121.4	126.5	128.5	133.9	122.5	125.8	133.5
Trunk angle (deg):	16.5	15.2	13.3	16.6	11.8	17	17.2	15.5
Shoulder angle (deg):	159.2	160.7	163.9	167.8	172.8	177.6	160.4	165.1
Elbow angle (deg):	135	132.4	135.5	99.7	86	103.7	90.1	89.8
Lean angle (deg):	1.1	3	1.2	5.5	6.8	6.2	5.5	6.8
Arm speed from 1st contact (deg/sec):	5.12	4.73	5.07	6.87	6.44	999	6.6	5.91
Board deflection (mm):	772.9	786.3	796.9	763.2	757.5	760	791.1	795.7
<b>Leg Extension</b>								
Knee angle (deg):	178.8	178.6	177.1	178.4	177.8	178.1	178.1	178.5
Hip angle (deg):	170.1	176.1	177.2	166.9	160.1	162	149.8	162.2
Trunk angle (deg):	11.7	5.8	4.6	12.6	19.2	16.6	22.9	17.1
Shoulder angle (deg):	161.4	153.4	154.1	153.5	170.5	164.6	159.3	152.2
Elbow angle (deg):	159.6	158.9	146.5	157.4	170.1	172.4	173.8	165
Lean angle (deg):	4.7	5.3	2.6	7.3	7	6.5	5.6	8.2
Arm speed from maxSquat (rad/sec):	6.61	6.36	6.53	9.28	8.41	999	8.98	7.5
Impulse time since max deflection (%):	38.7	32.3	33.3	46.7	43.8	-899	45.5	41.2
<b>Last contact</b>								
Knee angle (deg):	163.2	159.9	161.7	175.6	173.4	177.7	172.1	175.4
Hip angle (deg):	168.4	161.8	166.4	137.7	142.9	141.6	131	135.2
Trunk angle (deg):	27.3	34.3	28.2	33.8	31.7	30.5	39.8	37
Shoulder angle (deg):	179.4	163.9	169.8	147.3	152.2	145.6	138.4	147.1
Elbow angle (deg):	175.7	166.7	176.5	177.1	171.5	176.4	175.1	176.4
Lean angle (deg):	12.8	14.2	12.3	4.7	4.9	6	3.3	6.6
Impulse time (s):	0.4	0.4	0.4	0.4	0.4	999	0.4	0.4
Velocity - x (m/s):	0.95	0.76	0.68	0.82	0.92	0.87	0.98	0.56
Velocity - y (m/s):	5.31	4.94	5	4.92	5.06	5.29	4.78	4.98
Velocity - y from bfCurve (m/s):	5.25	5.21	5.49	5.03	5.09	5.06	4.73	4.78
Difference (%):	1.12	5.07	8.97	2.05	0.68	4.49	1.11	4.04
Resultant velocity (m/s):	5.39	5	5.04	4.99	5.14	5.36	4.88	5.01
Rotation of trunk (rad/sec):	1.65	1.77	1.53	2.07	1.73	999	2.21	1.93
<b>Flight Characteristics</b>								
CofM trajectory (deg):	10.2	8.8	7.7	9.4	10.4	9.3	11.6	6.5
Max CofM height (mm):	2386	2354.7	2406.6	2208.7	2236	2275.3	2079.2	2137
Max CofM height from bfCurve (mm):	2392.6	2348.1	2348.1	2205.1	2236.9	2271.7	2072.7	2127.1
Difference (%):	0.28	0.28	2.49	0.16	0.04	0.16	0.31	0.47
Measured displacement (mm):	1395.2	1331.8	1408.6	1265.7	1330.3	1298.3	1144.1	1194.5
Displacement using curve (mm):	1405.1	1382.4	1536.4	1287	1322.9	1304.9	1139.7	1166.3
Difference (%):	0.7	3.8	9.1	1.7	0.6	0.5	0.4	2.4
Time to minimum MOI (s):	0.5	0.55	0.55	0.48	0.45	0.48	0.44	0.48
Reduction in MOI (%):	63.34	67.26	66.6	64.16	63.51	64.54	61.6	62.98
Somersault 1 speed (sst/sec):	1.78	1.78	1.78	2.35	2.16	2.16	2.35	1.31
Somersault 2 speed (sst/sec):	80	3.08	3.08	0	0	0	2.96	0
Somersault 3 speed (sst/sec):	2.96	0	0	0	0	0	0	0
Somersault 4 speed (sst/sec):	80	0	0	0	0	0	0	0
Opening height (mm):	1441.3	999	999	999	999	999	845.1	864.7
Entry distance (mm):	0	0	0	0	0	0	0	0



## Diver 3

### Diver 3 – September 2018 Profiling results

 <p><b>KEY</b>  <span style="color: red;">■</span> injured  <span style="color: blue;">■</span> &gt; 1SD  <span style="color: purple;">■</span> &lt; 1SD</p>	<p>All results were compared to mean of:</p> <ul style="list-style-type: none"> <li>• All funded divers</li> <li>• All divers of the same sex</li> <li>• All divers in the same discipline (springboard or platform)</li> <li>• All divers in the same discipline of the same sex</li> </ul>
---	--

### Diver 3

ANTHROPOMETRICS				STRENGTH									
				Grip arm by side		Grip arm overhead		Elbow extension		Hip abduction		Hip external rotation	
	Height	Weight	Skinfolds	Left	Right	Left	Right	Left	Right	Left	Right	Left	Right
WC mean	168.0	62.5	69.3	38.2	39.4	36	36.9	52.2	54.2	51.2	51.9	41.8	40.8
stdev	5.9	9.0	22.9	11.2	11	9.2	9.6	12.6	13.2	12.5	10.4	12.1	11.4
Diver 3	174	72.7	39.4	53.8	53.8	50.2	51.3	76.5	75	72.2	63.7	70.6	73.2
Male mean	171.1	67.0	57.2	46.7	46.7	42.0	43.0	60.9	63.0	56.9	56.4	48.8	47.1
stdev	4.4	7.4	18.2	7.8	8.8	7.8	7.7	10.6	9.2	13.3	9.4	12.4	11.5
Diver 3	174	72.7	39.4	53.8	53.8	50.2	51.3	76.5	75	72.2	63.7	70.6	73.2
Spring mean	168.2	66.2	69.5	41.9	43.6	38.6	40.7	58.0	60.8	55.0	56.1	47.2	46.8
stdev	5.9	8.6	24.6	11.5	10.9	9.8	10.0	10.9	11.4	15.0	9.9	13.6	12.3
Diver 3	174	72.7	39.4	53.8	53.8	50.2	51.3	76.5	75	72.2	63.7	70.6	73.2
Male spr mean	171.0	70.6	56.7	49.9	50.9	44.6	46.2	65.2	67.2	63.7	61.6	55.8	53.6
stdev	3.9	4.4	19.2	6.2	5.8	7.4	7.2	8.5	7.5	13.7	8.0	10.9	9.8
Diver 3	174	72.7	39.4	53.8	53.8	50.2	51.3	76.5	75	72.2	63.7	70.6	73.2

RANGE OF MOTION																
	Shoulder ER		Shoulder IR		Straight leg raise		Thomas test		Lumbar locked thoracic		Knee to wall		Lat length against wall		Combined elevation	
	Left	Right	Left	Right	Left	Right	Left	Right	Left	Right	Left	Right	Trial 1	Trial 2	Trial 1	Trial 2
WC mean	61.8	66.0	46.3	40.9	119.4	118.3	below	below	52.7	46.7	12.6	12.4	0.2	0.2	27.1	28.6
stdev	13.9	17.9	8.5	8.3	12.1	11.2	below	below	13.9	12.7	2.9	2.6	1.1	1.1	8.6	9.1
Diver 3	39	39	46	37	116	112	above	above	60	60	6	7	0	0	37.5	38
Male mean	59.8	65.3	42.9	37.9	111.5	111.1	below	below	53.3	45.7	12.1	11.8	0.4	0.4	26.6	27.6
stdev	13.7	18.6	7.5	7.7	8.5	7.8	below	below	12.3	11.6	3.0	2.7	1.5	1.5	6.9	5.8
Diver 3	39	39	46	37	116	112	above	above	60	60	6	7	0	0	37.5	38
Spring mean	66.8	70.6	44.8	40.2	122.5	121.2	below	below	55.5	47.6	14.4	14.2	0.4	0.4	25.5	26.5
stdev	16.0	17.2	9.3	8.1	11.9	11.4	below	below	10.2	12.8	2.1	1.8	1.5	1.5	5.6	6.1
Diver 3	39	39	46	37	116	112	above	above	60	60	6	7	0	0	37.5	38
Male spr mean	55.3	63.0	45.3	38.4	111.0	110.1	above	above	52.8	45.5	10.8	10.3	0.0	0.0	26.8	28.0
stdev	11.9	20.9	7.2	7.9	10.9	7.9	above	above	15.3	11.5	3.0	2.3	0.0	0.0	8.7	7.1
Diver 3	39	39	46	37	116	112	above	above	60	60	6	7	0	0	37.5	38

WORK CAPACITY								
	SL squat to box - 30 reps		Calf raise off step - 30 reps		Side plank - 120 seconds		Prone hold - 120 seconds	Supine hold - 60 seconds
	Left	Right	Left	Right	Left	Right		
WC mean	29	30	23	23	106	107	115	58
stdev	5	0	6	6	23	23	13	5
Diver 3	30	30	30	30	120	120	120	60
Male mean	28	30	24	25	110	110	115	60
stdev	6	0	6	5	19	21	14	0
Diver 3	30	30	30	30	120	120	120	60
Spring mean	30	30	25	25	105	103	114	58
stdev	0	0	6	6	25	27	13	6
Diver 3	30	30	30	30	120	120	120	60
Male spr mean	30	30	26	26	110	108	116	60
stdev	0	0	6	6	21	23	9	0
Diver 3	30	30	30	30	120	120	120	60

STRENGTH AND POWER						
	Peak force (N)		Time to peak force (s)			
	ISO back squat	ISO calf raise	ISO back squat		ISO calf raise	
	R	L	R	L	R	L
WC mean	2969.64	2441.98	2.44	2.86	2.94	2.72
stdev	854.80	543.36	1.03	1.64	0.55	0.67
Diver 3	4237	3229	1.2	1.4	3.07	1.6
Male mean	3465.36	2650.82	2.51	2.67	2.93	2.73
stdev	635.28	429.26	0.94	0.80	0.44	0.57
Diver 3	4237	3229	1.2	1.4	3.07	1.6
Spring mean	3151.55	2645.55	2.21	2.40	2.82	2.62
stdev	951.14	615.20	0.88	1.02	0.47	0.78
Diver 3	4237	3229	1.2	1.4	3.07	1.6
Male spr mean	3554.00	2847.00	2.44	2.58	2.90	2.74
stdev	731.72	351.39	0.71	0.68	0.26	0.57
Diver 3	4237	3229	1.2	1.4	3.07	1.6

STRENGTH AND POWER ASSESSMENT - JUMPS																								
	Peak force (s)				Jump height (cm)				Av. Peak velocity (m/s)				Flight time (m/s)				Rate of force development			Time to peak propulsive force			Movement start to peak force	RSI flight/contact time
	SLCMJ		DJ		SLCMJ		DJ		SLCMJ		DJ		SLCMJ		DJ		SLCMJ			SLCMJ			CMJ	DJ
	CMJ	R	L		CMJ	R	L		CMJ	R	L		CMJ	R	L		CMJ	R	L	R	L	DJ	CMJ	DJ
WC mean	0.71	0.78	0.80	0.08	41.27	23.65	22.84	38.69	2.80	2.14	2.09	2.77	576.36	436.15	427.45	544.52	42362.16	713.08	22675.00	195.08	216.00	3.96	0.68	2.45
stdev	0.15	0.14	0.17	0.05	10.07	4.68	5.91	8.40	0.35	0.22	0.23	0.41	68.69	44.07	55.46	96.55	148708.90	5612.29	62826.23	100.17	131.84	6.25	0.16	0.84
Diver 3	0.62	0.97	1	0.01	51.6	28.2	30.9	49.5	3.01	2.32	2.38	3.18	642	479	499	633	-92730	804	6244	185	231	7	0.61	2.88
Male mean	0.65	0.82	0.79	0.09	48.09	26.41	26.51	44.78	2.98	2.24	2.22	3.03	625.46	462.25	462.57	601.69	19218.00	2005.50	33294.86	183.38	203.29	4.08	0.66	2.58
stdev	0.14	0.14	0.17	0.06	7.35	2.71	3.46	5.94	0.22	0.11	0.13	0.19	44.07	22.69	30.69	41.10	178632.97	873.36	78829.00	82.35	106.25	5.79	0.17	1.03
Diver 3	0.62	0.97	1	0.01	51.6	28.2	30.9	49.5	3.01	2.32	2.38	3.18	642	479	499	633	-92730	804	6244	185	231	7	0.61	2.88
Spring mean	0.66	0.78	0.80	0.08	46.20	23.65	22.84	41.55	2.92	2.14	2.09	2.92	607.92	436.15	427.45	579.46	41940.08	713.08	22675.00	195.08	216.00	2.54	0.65	2.51
stdev	0.15	0.14	0.17	0.06	7.31	4.68	5.91	6.03	0.24	0.22	0.23	0.21	49.15	44.07	55.46	43.39	183472.91	5612.29	62826.23	100.17	131.84	3.73	0.18	0.98
Diver 3	0.62	0.97	1	0.01	51.6	28.2	30.9	49.5	3.01	2.32	2.38	3.18	642	479	499	633	-92730	804	6244	185	231	7	0.61	2.88
Male spr mean	0.6113	0.8163	0.7914	0.0813	50.875	26.413	26.514	45.55	3.0775	2.235	2.22	3.06375	641	462.25	462.57	608.25	-5581.125	2005.5	33294.86	183.375	203.29	3	0.63125	2.635
stdev	0.1043	0.1369	0.1661	0.0694	4.0199	2.7053	3.4638	2.5568	0.104	0.1052	0.1334	0.08314	24.9571	22.6889	30.686	16.816	192635.45	873.358	78829	82.3459	106.25	4.2426	0.1631334	1.1357188
Diver 3	0.62	0.97	1	0.01	51.6	28.2	30.9	49.5	3.01	2.32	2.38	3.18	642	479	499	633	-92730	804	6244	185	231	7	0.61	2.88

Diver 3 – results of filming and digitisation

Forward facing dives with hurdle

Dive	Test 1	Test 2	Test 3	Change (%)
<b>100a</b>				
Mean board deflection (mm)	935.4	1010.5	946.4	8.03
Maximum board deflection (mm)	955.4	1010.5	946.4	5.77
Mean resultant take-off velocity (m/s)	5.85	5.87	5.94	1.54
Maximum resultant take-off velocity (m/s)	6.00	5.87	5.94	-1.00
Mean vertical take-off velocity (m/s)	5.75	5.93	4.97	3.09
Maximum vertical take-off velocity (m/s)	6.15	5.93	4.97	-3.57
Mean vertical displacement (mm)	1800.7	1913.6	1347.9	6.27
Maximum vertical displacement (mm)	2058.1	1913.6	1347.9	-7.02
<b>303c/304c</b>				
Mean board deflection (mm)	979.8	981.7	998.9	
Maximum board deflection (mm)	995.1	997.8	998.9	
Mean resultant take-off velocity (m/s)	5.87	5.80	5.85	
Maximum resultant take-off velocity (m/s)	6.22	5.99	5.85	
Mean vertical take-off velocity (m/s)	5.65	5.64	5.63	
Maximum vertical take-off velocity (m/s)	5.76	5.79	5.63	
Mean vertical displacement (mm)	1739.8	1733.8	1728.8	
Maximum vertical displacement (mm)	1807.5	1825.3	1728.8	
<b>305c</b>				
Mean board deflection (mm)		1014.6	1004.4	3.55
Maximum board deflection (mm)		1034.0	1033.7	3.91
Mean resultant take-off velocity (m/s)		5.74	5.95	1.45
Maximum resultant take-off velocity (m/s)		6.22	6.14	-1.30
Mean vertical take-off velocity (m/s)		5.68	5.64	0.43
Maximum vertical take-off velocity (m/s)		5.74	5.91	2.64
Mean vertical displacement (mm)		1754.8	1732.6	0.86
Maximum vertical displacement (mm)		1795.5	1904.3	5.36
<b>105b/5140b</b>				
Mean board deflection (mm)	960.0			
Maximum board deflection (mm)	975.0			
Mean resultant take-off velocity (m/s)	5.75			
Maximum resultant take-off velocity (m/s)	6.07			
Mean vertical take-off velocity (m/s)	5.29			
Maximum vertical take-off velocity (m/s)	5.43			
Mean vertical displacement (mm)	1526.6			
Maximum vertical displacement (mm)	1606.2			

Back facing dives, standing

Dive	Test 1	Test 2	Test 3	Change (%)
<b>200a</b>				
Mean board deflection (mm)	711.0	770.9	746.6	8.42
Maximum board deflection (mm)	721.4	779.6	746.6	8.07
Mean resultant take-off velocity (m/s)	4.67	4.63	4.95	6.00
Maximum resultant take-off velocity (m/s)	4.74	4.68	4.95	4.43
Mean vertical take-off velocity (m/s)	5.00	4.65	4.37	-7.02
Maximum vertical velocity (m/s)	5.22	4.72	4.37	-9.67
Mean vertical displacement (mm)	1360.8	1176.5	1041.8	-13.55
Maximum vertical displacement (mm)	1484.4	1211.1	1041.8	-18.41
<b>403c/403b</b>				
Mean board deflection (mm)	728.9		759.9	
Maximum board deflection (mm)	735.7		759.9	
Mean resultant take-off velocity (m/s)	4.29		4.62	
Maximum resultant take-off velocity (m/s)	4.40		4.62	
Mean vertical take-off velocity (m/s)	4.31		4.49	
Maximum vertical velocity (m/s)	4.35		4.49	
Mean vertical displacement (mm)	1011.3		1099.9	
Maximum vertical displacement (mm)	1029.4		1099.9	
<b>405c</b>				
Mean board deflection (mm)		779.6	763.9	6.96
Maximum board deflection (mm)		770.0	789.3	7.29
Mean resultant take-off velocity (m/s)		4.55	4.63	8.00
Maximum resultant take-off velocity (m/s)		4.65	4.80	9.09
Mean vertical take-off velocity (m/s)		4.77	4.51	4.59
Maximum vertical velocity (m/s)		4.88	4.72	8.55
Mean vertical displacement (mm)		1239.0	1106.1	9.38
Maximum vertical displacement (mm)		1695.5	1213.0	17.84

Key performance indicators – all dives - Diver 3. Dives coded as ‘date\_time\_dive-number’.

Any performance indicators which cannot be calculated are represented by ‘999’

Key Performance Indicators	2018_09_06_1 1_33_25_100a	2018_09_06_11 11_36_02_100a	2018_09_06_12 12_05_14_100a	2018_10_18_11 11_16_17_100a	JHsl_2019_01_17_11 11_29_35_100a	2018_09_06_12 12_08_49_303c	2018_09_06_12 12_10_44_303c	2018_09_06_12 12_13_38_304c	2018_09_06_12 12_15_07_304c
<b>Best model: 9</b>									
<b>Last step</b>									
Last step length (mm):	1363.7	999	999	999	1151.2	999	999	999	999
Last step speed - x (m/s):	1.1	1.4	999	999	1.2	0.1	999	999	999
Last step speed - y (m/s):	-2.7	-2.6	999	999	-2.7	3.3	999	999	999
Last step speed - resultant (m/s):	2.9	3	0	0	3	3.3	0	0	0
<b>Hurdle step</b>									
Into hurdle speed - x (m/s):	0.3	0.2	-0.2	0	-0.2	0.1	0.2	-0.2	-0.3
Into hurdle speed - y (m/s):	4.3	4	3.7	3.9	4.3	3.3	3.5	4.5	3.9
Hurdle height (mm):	2000.9	2048	2004.7	2024.1	2036.5	2028.4	2036.9	2036.8	2029.7
Hurdle displacement - measured (mm):	887.5	918.3	879	945.3	945.5	925.5	932.8	973.3	957.2
Hurdle displacement - calculated (mm):	955.2	831.7	700.4	756.6	922.2	568.7	606.8	1028.2	789.5
Difference (%):	7.6	9.4	20.3	20	2.5	38.6	34.9	5.6	17.5
Hurdle length (mm):	119	178.2	49.5	999	112.2	57.3	166.5	121.7	62.3
Velocity - x (m/s):	0.3	0	-0.1	0	0.1	-0.1	0	0	0.3
Velocity - y (m/s):	-4.1	-4.9	-4.8	-4.8	-4.5	-5.4	-5.4	-4.7	-5.3
Distance from tip (mm):	69.5	19.4	92	221.5	53.3	83.9	24.4	41	54.7
<b>First contact</b>									
Knee angle (deg):	104.9	95.5	98.7	95.9	101.8	98.6	95.2	101.6	97.6
Hip angle (deg):	89.1	85.4	80.6	71.9	80.5	73.9	86.7	76.8	80.2
Trunk angle (deg):	32.4	33.1	37.4	45.9	37.5	39.9	26.8	39.2	33.2
Shoulder angle (deg):	34.3	39.1	35.7	49.4	29.4	31.1	28.1	28.5	30.9
Elbow angle (deg):	177.9	177.3	173.6	177.3	178.3	178.6	179.9	179	172.9
Lean angle (deg):	0.9	0.7	2.2	21.5	3	1.2	3.4	1.4	0.4
Landing velocity - x (m/s):	0.35	-0.02	-0.07	0.05	0.09	-0.07	0.02	-0.05	0.33
Landing velocity - y (m/s):	-4.05	-4.89	-4.76	-4.78	-4.47	-5.35	-5.38	-4.73	-5.26
Landing velocity - resultant (m/s):	4.07	4.90	4.76	4.78	4.47	5.35	5.38	4.73	5.27
<b>Max Squat</b>									
Knee angle (deg):	100.6	90.8	98.7	94.8	100.9	98.1	91.5	98.3	88.8
Hip angle (deg):	89.6	82.1	80.6	76.7	79.1	82.5	91.1	79.9	74.7
Trunk angle (deg):	32.6	33.5	37.4	41.8	39.2	35	22.1	37.8	37.7
Shoulder angle (deg):	7.9	33.5	35.7	30.6	24.2	10.6	3.5	24.3	25
Elbow angle (deg):	179.9	178.6	173.6	174.8	177.4	174	179.9	172.6	172.5
Arm speed from 1st contact (rad/sec):	7.14	8.19	999	9.3	9.27	7.72	9.45	8.81	8.58
Lean angle (deg):	1.3	1.4	2.2	1.4	2.1	0	0	0.3	2.5
Change in COM (mm):	1314.1	1281.5	1207	2024.1	1278.8	1325	1368.4	1330.9	1342.9
<b>Maximum deflection</b>									
Knee angle (deg):	133.4	136.5	141.8	133.6	124.9	147.4	139.1	144.7	143
Knee extension (deg):	28.6	40.9	43.2	37.6	23.1	48.8	43.9	43.1	45.4
Impulse (percent of total time):	64.3	67.7	80	64.5	59.4	75	75	81.8	76
Hip angle (deg):	146.2	147.9	151.4	150.5	146.1	152.7	153.1	150.8	149.6
Trunk angle (deg):	11.6	14.1	11	13	8.8	13.1	9.3	12.8	14.4
Shoulder angle (deg):	130	108.2	135.4	110.2	118.8	130.4	145.1	139.5	125
Elbow angle (deg):	176.9	179.5	179.7	176.6	178.3	177.6	177.3	176.6	177.7
Lean angle (deg):	9.8	11.9	9.9	13.8	10.1	10	9.7	8.9	10.3
Arm speed from 1st contact (deg/sec):	7.14	8.19	999	9.3	9.27	7.72	9.45	8.81	8.58
Board deflection (mm)	938.3	912.5	955.4	1010.5	946.4	984	992.6	995.1	964.2
<b>Leg Extension</b>									
Knee angle (deg):	176.1	173	176.8	176.2	175.4	180	174.7	176	176.7
Hip angle (deg):	178.5	176	174.3	175.1	179.4	176.7	177.1	179.8	174.9
Trunk angle (deg):	6.1	3.5	5.9	6.6	3.5	5.1	4.4	6.1	4
Shoulder angle (deg):	131.3	122.2	135.7	131.8	138.4	145	137	140.9	134.9
Elbow angle (deg):	177.4	176.6	175.8	178.2	177.8	175.4	171.5	170.9	169.2
Lean angle (deg):	9.7	11.2	11.4	3.1	6.1	9.5	8.8	6	10
Arm speed from maxSquat (rad/sec):	9.41	8.38	9.11	7.98	6.83	10.62	10.33	16.81	9.14
Impulse time since max deflection (%):	35.7	32.3	20	35.5	40.6	25	25	18.2	24
<b>Last contact</b>									
Knee angle (deg):	173.4	179.1	128.8	175.9	178.3	139.1	126.2	133.1	123.9
Hip angle (deg):	177.3	179.8	176.2	176.9	178.9	176.2	175	176	176.8
Trunk angle (deg):	8.7	9.8	12.5	8.4	4.8	14.3	16	19.9	21.1
Shoulder angle (deg):	161.1	157.3	177	156.2	166.3	167.9	154	166.9	172.9
Elbow angle (deg):	177.9	177.4	172.5	173.7	176.1	174.9	170.2	178	177.3
Lean angle (deg):	9	10.2	1.9	9.2	5.3	4.7	1.6	0.9	2.8
Impulse time (s):	0.4	0.4	0.3	0.4	0.4	0.3	0.3	0.3	0.3
Velocity - x (m/s):	1.04	0.96	1.14	0.85	0.65	1.25	1.23	1.2	1.04
Velocity - y (m/s):	5.74	5.63	5.89	5.81	5.91	5.7	6.09	5.64	5.71
Velocity - y from bfCurve (m/s):	6.35	5.7	5.75	6.13	5.14	5.86	5.78	5.96	5.81
Difference (%):	0.9	0.99	2.4	5.22	14.9	2.57	5.42	5.22	1.7
Resulant velocity (m/s):	5.84	5.71	6	5.87	5.94	5.84	6.22	5.77	5.81
Rotation of trunk (rad/sec):	0.77	0.81	0.84	0.75	0.49	1.04	0.96	1.23	1.34
<b>Flight Characteristics</b>									
CofM trajectory (deg):	10.3	9.7	11	8.4	6.2	12.3	11.4	12	10.3
Max CofM height (mm):	3019.3	2817.5	2727.7	999	3094.4	2764.4	2768.1	2795.7	2746.7
Max CofM height from bfCurve (mm):	3131	3131	2748.5	3054.9	1871	2817.2	2790	2791.4	2750.9
Difference (%):	3.57	10.01	0.76	67.3	65.39	1.87	0.78	0.15	0.15
Measured displacement (mm):	1875.2	1679.6	1629.7	999	1959.9	1674.7	1701.2	1762.2	1723.6
Displacement using curve (mm):	2058.1	1658.4	1685.6	1913.6	1347.9	1747.3	1703	1807.5	1721.3
Difference (%):	9.8	1.3	3.4	91.6	31.2	4.3	0.1	2.6	0.1
Time to minimum MOI (s):	0.08	0.53	0.38	999	0.63	0.43	0.39	0.61	0.61
Reduction in MOI (%):	7.31	4.67	68.93	999	79.83	69.42	69.04	69.73	69.75
Somersault 1 speed (ss/sec):	0	0	0	0	0	0	0	0	0
Somersault 2 speed (ss/sec):	0	0	0	0	0	0	0	0	0
Somersault 3 speed (ss/sec):	0	0	0	0	0	0	0	0	0
Somersault 4 speed (ss/sec):	0	0	0	0	0	0	0	0	0
Opening height (mm):	999	999	999	999	999	999	999	999	999
Entry distance (mm):	0	1204	0	1173.1	0	0	0	1475.6	0

Key Performance Indicators	_2018_09_06_	_2018_10_18_	_2018_10_18_	_2018_10_18_	JHsl_2019_01_17_	_2018_10_18_	_2018_10_18_	_2018_10_18_	JHsl_2019_01_17_	JHsl_2019_01_17_
	12_16_58_304c	11_22_32_303c	11_25_48_303c	11_30_59_304c	11_31_48_303c	11_36_40_305c	11_40_25_305c	11_42_08_305c	11_33_44_305c	11_35_26_305c
<b>Best model: 9</b>										
<b>Last step</b>										
Last step length (mm):	999	999	999	999	999	999	999	999	999	1189.5
Last step speed - x (m/s):	999	0.1	999	999	1.2	999	999	999	1	0.8
Last step speed - y (m/s):	999	3.8	999	999	-2.8	999	999	999	-3.2	-3
Last step speed - resultant (m/s):	0	3.8	0	0	3	0	0	0	3.3	3.1
<b>Hurdle step</b>										
Into hurdle speed - x (m/s):	-0.1	0.1	-0.3	0.3	-0.3	0	-0.2	0.1	0.2	0.1
Into hurdle speed - y (m/s):	3.6	3.8	4.3	3.3	3.9	3.6	3.8	4.3	4	4.3
Hurdle height (mm):	2010.8	2012.4	2018.2	1997.8	2088.9	2045	1990.6	2011	2048	2066.4
Hurdle displacement - measured (mm):	930.8	897.2	966.1	917.9	1043.2	961.1	933.3	933.3	928.9	1024.7
Hurdle displacement - calculated (mm):	675.1	739.7	963.3	552.7	762.3	657.9	750.2	938.8	829.2	933.8
Difference (%):	27.5	17.6	0.3	39.8	26.9	31.5	19.6	0.6	10.7	8.9
Hurdle length (mm):	55.3	120.8	51.5	97.4	70.4	999	170	153.7	999	89.3
Velocity - x (m/s):	0.4	0.3	0	-0.5	-0.2	0	-0.2	0.1	-0.2	0.1
Velocity - y (m/s):	-4.9	-4.8	-5.1	-4.9	-5	-4.9	-4.6	-4.7	-5.2	-5
Distance from tip (mm):	65.9	25.4	70.7	92	124.4	41.9	27.2	23	24.2	20.1
<b>First contact</b>										
Knee angle (deg):	99	93.5	96.9	94.9	94.5	92.9	93	99.3	91.7	90.4
Hip angle (deg):	77.8	85.4	83.3	80.3	79	77.3	72.8	79.7	73.6	80.9
Trunk angle (deg):	36.8	29.4	32	31.6	37.7	32.2	35.9	37.1	39.2	33.6
Shoulder angle (deg):	35.7	33.2	34.9	36.4	16.9	34.5	44.6	49.4	26.5	16.2
Elbow angle (deg):	177.2	171.5	177.8	177.8	178.5	177.5	178.1	174.1	179.7	178.1
Lean angle (deg):	3.4	2.1	1.4	2.6	0.2	3.8	4.4	2.2	1.6	2
Landing velocity - x (m/s):	0.42	0.26	-0.02	-0.46	-0.2	-0.03	-0.2	0.14	-0.17	0.1
Landing velocity - y (m/s):	-4.92	-4.79	-5.09	-4.89	-5.02	-4.9	-4.61	-4.7	-5.16	-4.99
Landing velocity - resultant (m/s):	4.94	4.80	5.09	4.91	5.02	4.9	4.61	4.70	5.17	4.99
<b>Max Squat</b>										
Knee angle (deg):	92.5	92.4	96.9	94.9	94.5	92.9	93	92.7	91.7	90.4
Hip angle (deg):	78.5	87	83.3	80.3	79	77.3	72.8	79.7	73.6	80.9
Trunk angle (deg):	36.4	31.2	32	31.6	37.7	32.2	35.9	35.5	39.2	33.6
Shoulder angle (deg):	26.7	14.5	34.9	36.4	16.9	34.5	44.6	21.2	26.5	16.2
Elbow angle (deg):	178.3	178.1	177.8	177.8	178.5	177.5	178.1	179.3	179.7	178.1
Arm speed from 1st contact (rad/sec):	8.43	7.8	999	999	999	999	999	8.24	999	999
Lean angle (deg):	0.6	0.5	1.4	2.6	0.2	3.8	4.4	0.7	1.6	2
Change in COM (mm):	1281	1392.1	1238.2	1161.3	1297.7	1230.9	1175.6	1423.7	1282	1394.7
<b>Maximum deflection</b>										
Knee angle (deg):	138.8	142.6	130	132.7	142.6	143.2	133.4	127.6	146.2	150.2
Knee extension (deg):	39.8	49.1	33.1	37.8	48.1	50.3	40.4	28.3	54.5	59.8
Impulse (percent of total time):	73.1	72	71.4	75	76	80.8	75.9	68	80	82.6
Hip angle (deg):	149.3	158.7	145.5	148.9	155.3	156	145.7	142.2	154.3	155.6
Trunk angle (deg):	12.9	7.5	9.3	9.6	10.7	9.1	11.9	13.3	12.2	11.5
Shoulder angle (deg):	120.2	126.2	121.9	132.6	126.2	136.1	129.6	132.8	128.9	118.9
Elbow angle (deg):	178.9	175.7	177.5	177.9	176.9	172.7	177.8	175.8	172.9	173.4
Lean angle (deg):	10.2	10.2	8	9	11.9	8.9	8.8	10.2	8.8	8.7
Arm speed from 1st contact (deg/sec):	8.43	7.8	999	999	999	999	999	8.24	999	999
Board deflection (mm):	963.1	993.2	954.2	997.8	998.9	999	1010.7	1034	999.6	1033.7
<b>Leg Extension</b>										
Knee angle (deg):	175.7	178.7	173	175.3	176.3	173.9	173.8	176.9	175.6	177.7
Hip angle (deg):	173.3	170.2	176.1	172.6	174.6	178.9	173.7	172.7	174.8	179.4
Trunk angle (deg):	0.9	0.4	0.4	0.9	3.7	4.6	1	0.3	2.3	5.8
Shoulder angle (deg):	140.8	146.3	138.4	146.7	145.4	143.7	145.5	140.9	139.8	134.1
Elbow angle (deg):	170.2	175.6	176.1	179.3	178.1	170.5	179.5	176	159.5	168.1
Lean angle (deg):	8.9	8.4	6.7	8.5	11.1	8.9	7.8	7.2	8.9	8.2
Arm speed from maxSquat (rad/sec):	8.4	9.59	7.43	7.14	9.56	7.91	6.75	9.51	8.7	10.97
Impulse time since max deflection (%):	26.9	28	28.6	25	24	19.2	24.1	32	20	17.4
<b>Last contact</b>										
Knee angle (deg):	127.8	140.4	139.5	132.5	133.2	114.8	122.1	115.5	115.5	127.4
Hip angle (deg):	179.5	173.7	174.6	171.2	179.7	170.7	179.9	176.7	175.2	171.7
Trunk angle (deg):	17.7	17.7	18.9	22.7	11.7	20.9	24.1	25.5	22.5	16.2
Shoulder angle (deg):	158.8	174.2	169.9	163.4	166.7	170.9	175.4	168.8	161.6	169.1
Elbow angle (deg):	179.9	173.5	173	173.5	166	178.7	179.5	178.1	174.8	173.6
Lean angle (deg):	2.5	1.4	1	0.3	3.7	3.7	2.8	3.7	4.1	87.8
Impulse time (s):	0.3	0.3	0.4	0.4	0.3	0.3	0.4	0.3	0.3	0.3
Velocity - x (m/s):	1.15	1.19	1.25	1.38	1.42	1.36	1.14	1.34	1.22	1.25
Velocity - y (m/s):	5.59	5.87	5.42	5.67	5.67	5.59	5.88	5.61	5.75	6.02
Velocity - y from bfCurve (m/s):	5.81	5.83	5.67	5.98	5.82	5.78	5.59	5.94	5.66	6.11
Difference (%):	3.83	0.58	4.43	5.27	2.57	3.32	5.04	5.41	1.61	1.59
Resultant velocity (m/s):	5.7	5.99	5.57	5.83	5.85	5.75	5.7	5.77	5.87	6.14
Rotation of trunk (rad/sec):	1.15	0.95	1.01	1.16	0.84	1.07	1.26	1.51	1.28	1.04
<b>Flight Characteristics</b>										
CofM trajectory (deg):	11.6	11.5	13	13.6	14.1	13.7	11.6	13.4	12	11.7
Max CofM height (mm):	2720.8	2801.1	2672.7	2863.9	2774.4	2744.3	2785.4	2886.6	2715.7	2871.8
Max CofM height from bfCurve (mm):	2733.7	2817.6	2701.2	2849.9	2801	2726.4	2762.9	2873	2801	2886.8
Difference (%):	0.47	0.59	1.05	0.49	0.95	0.65	0.82	0.47	3.05	0.52
Measured displacement (mm):	1686.6	1741.2	1646.6	1804.4	1688.9	1699.9	1777.6	1818.4	1683.9	1884.3
Displacement using curve (mm):	1719.9	1734.9	1641.1	1825.3	1728.8	1704.7	1764.2	1795.5	1630.2	1904.3
Difference (%):	2	0.4	0.3	1.2	2.4	0.3	0.8	1.3	3.2	1.1
Time to minimum MOI (s):	0.63	0.41	0.38	0.63	0.5	0.59	0.6	0.61	0.55	0.64
Reduction in MOI (%):	69	68.93	67.47	69.57	69.22	68.13	68.52	68.86	67.62	80.62
Somersault 1 speed (ss/sec):	1.57	1.33	0	1.6	1.29	1.67	1.63	1.67	1.7	1.6
Somersault 2 speed (ss/sec):	0	0	0	0	0	2.5	2.5	2.5	2.42	2.58
Somersault 3 speed (ss/sec):	0	0	0	0	0	0	0	0	0	0
Somersault 4 speed (ss/sec):	0	0	0	0	0	0	0	0	0	0
Opening height (mm):	999	999	999	999	2724.4	999	999	999	1611.5	1826.2
Entry distance (mm):	0	1598.4	0	0	0	0	0	0	0	1236.1

Key Performance Indicators	JHsl_2019_01_17_	2018_09_06_	2018_09_06_1	2018_09_06_1	2018_09_06_1	2018_09_06_15_	2018_09_06_1	2018_09_06_	2018_09_06_
	11_37_02_305c	15_37_04_103b	5_40_15_5140b	5_42_24_5140b	5_46_32_5140b	48_20_105b	5_52_20_105b	15_54_09_105b	15_56_06_105b
<b>Best model: 9</b>									
<b>Last step</b>									
Last step length (mm):	1207.3	999	999	999	999	999	999	999	0
Last step speed - x (m/s):	1.3	999	999	999	999	999	999	999	999
Last step speed - y (m/s):	-2.8	999	999	999	999	999	999	999	999
Last step speed - resultant (m/s):	3.1	0	0	0	0	0	0	0	0
<b>Hurdle step</b>									
Into hurdle speed - x (m/s):	-0.3	0	2.1	1.8	0.2	2.3	-0.3	999	0.4
Into hurdle speed - y (m/s):	4.4	3.7	18	17.9	4	17.5	4.1	999	4.2
Hurdle height (mm):	2073.9	1990.6	2027.6	2029.9	2010.2	2051.9	2075.3	2037.6	2008.9
Hurdle displacement - measured (mm):	965.6	907.4	581	578.5	949.7	588.8	954.2	999	902.4
Hurdle displacement - calculated (mm):	967.1	707.6	16536.2	16329.7	821.7	15651.2	873.9	50866510	896.3
Difference (%):	0.2	22	2746.3	2722.6	13.5	2558	8.4	5091643	0.7
Hurdle length (mm):	50.9	31	0.3	45.4	55.5	96.1	70.2	999	98.5
Velocity - x (m/s):	0.4	-0.1	-0.2	-0.3	0.1	-0.2	0.3	0	0.2
Velocity - y (m/s):	-4.8	-4.6	-5.2	-5	-4.3	-5.2	-4.7	-4.6	-4.5
Distance from tip (mm):	12.7	74	156.4	72.8	96.4	65.8	56.3	126.5	63.7
<b>First contact</b>									
Knee angle (deg):	99.4	100.7	98.5	101.7	104	101.8	105.2	101.5	98.6
Hip angle (deg):	76.7	79.1	93	75.3	83.3	76.2	76.3	82	85.3
Trunk angle (deg):	39.5	38.2	27	43.6	38.3	42.8	45.2	39.8	30.3
Shoulder angle (deg):	41.7	0.8	8.4	3	10.1	11.3	2.1	4.9	5.9
Elbow angle (deg):	175.9	179.1	173.3	179.2	177.8	167.3	173.3	172.6	172.9
Lean angle (deg):	1.9	0.4	3.4	0.9	0.7	1.2	1.1	2.2	1.2
Landing velocity - x (m/s):	0.41	-0.15	-0.24	-0.32	0.06	-0.19	0.33	0	0.16
Landing velocity - y (m/s):	-4.8	-4.55	-5.25	-5.04	-4.28	-5.17	-4.72	-4.56	-4.48
Landing velocity - resultant (m/s):	4.81	4.56	5.25	5.05	4.28	5.17	4.73	4.56	4.49
<b>Max Squat</b>									
Knee angle (deg):	97.5	99	95.1	100.9	101	94.2	97.2	101.5	97.3
Hip angle (deg):	84.1	91.5	94.4	89	92.3	89.5	84.4	82	92.2
Trunk angle (deg):	35.3	28.9	28.5	34.5	31.8	29.5	35.2	39.8	25.7
Shoulder angle (deg):	18.4	17.5	39	24.2	27.2	14.3	18.2	4.9	29.6
Elbow angle (deg):	177.5	173.7	179.3	179	178.3	178.5	172.7	172.6	175.9
Arm speed from 1st contact (rad/sec):	11.76	9.87	10.9	12.37	14.46	10.16	9.85	999	10.19
Lean angle (deg):	1.1	3.4	7.4	4.9	4.6	6.2	5.7	2.2	2.5
Change in COM (mm):	1428.9	1274.8	1349.8	1345.9	1351.4	1345.2	1378	1268.2	1349.1
<b>Maximum deflection</b>									
Knee angle (deg):	135.1	138.6	128.6	128.8	125.4	140.4	134.6	124.6	129.7
Knee extension (deg):	35.7	37.9	30.1	27	21.4	38.6	29.4	23.1	31.1
Impulse (percent of total time):	66.7	65.5	60.7	60	54.8	67.9	63.3	52.9	60
Hip angle (deg):	148.6	157.4	152.1	150.8	146.8	161	153.9	145	150.9
Trunk angle (deg):	11.8	12.4	14.2	14	18.1	12.4	15.5	17.1	13.9
Shoulder angle (deg):	129	147.5	161.6	152.8	145	157.6	148	154.9	155.1
Elbow angle (deg):	167	107.4	97.7	105.4	107	109.8	108.8	107	110.3
Lean angle (deg):	9.9	15.5	19.2	18	19.6	18.7	17.9	18.3	16.9
Arm speed from 1st contact (deg/sec):	11.76	9.87	10.9	12.37	14.46	10.16	9.85	999	10.19
Board deflection (mm):	980	965.1	945.5	962.6	953.1	975	972.1	950.7	960.8
<b>Leg Extension</b>									
Knee angle (deg):	173.3	176.1	175.5	174.2	168.7	179.2	174.5	170	177
Hip angle (deg):	171.9	178.6	163.8	150.8	132.8	167.1	158.3	127.6	155.6
Trunk angle (deg):	0.3	12.1	27.2	35	47.7	24.8	29.3	53.6	31.5
Shoulder angle (deg):	154.3	163.5	161	160.3	161.6	161.3	166.6	141.8	161
Elbow angle (deg):	137	163.5	167.3	177.4	178	164.6	169.3	177.2	175.5
Lean angle (deg):	7.9	15.3	20.1	18.9	21.4	17.9	18.8	23.1	17
Arm speed from maxSquat (rad/sec):	7.02	7.66	10.68	9.76	10.79	8.91	9	9.77	9.38
Impulse time since max deflection (%):	33.3	34.5	39.3	40	45.2	32.1	36.7	47.1	40
<b>Last contact</b>									
Knee angle (deg):	107	177.7	178.7	176.8	170.8	172.1	178.5	168.5	179.9
Hip angle (deg):	173.6	152.4	123.5	109.9	106	106.9	121.7	121.8	114.1
Trunk angle (deg):	22.8	31.2	58.5	70.4	72.1	67	59.6	56.5	64.4
Shoulder angle (deg):	171.3	163.9	155.5	135.9	135.6	142.3	141.6	144.4	144.2
Elbow angle (deg):	176.1	177.6	172.2	179.5	179.9	179	177.6	178.4	174.7
Lean angle (deg):	0.6	13.4	21.3	87	25.3	19.2	21.8	23	18.2
Impulse time (s):	0.3	0.4	0.4	0.4	0.4	0.4	0.4	0.4	0.4
Velocity - x (m/s):	1.57	1.33	1.58	1.73	1.47	1.54	1.23	1.68	1.52
Velocity - y (m/s):	5.64	5.7	5.86	5.4	5.35	5.53	5.47	5.5	5.7
Velocity - y from bfCurve (m/s):	5.71	6.05	5.42	5.49	5.26	5.38	5.56	5.61	5.58
Difference (%):	1.29	5.77	8.21	1.68	1.62	2.61	1.51	2.06	2.2
Resultant velocity (m/s):	5.85	5.86	6.07	5.67	5.54	5.74	5.61	5.75	5.9
Rotation of trunk (rad/sec):	1.34	1.38	2.99	3.27	3.6	4.49	3.63	0.92	3.92
<b>Flight Characteristics</b>									
CofM trajectory (deg):	15.6	13.2	15.1	17.8	15.3	15.6	12.7	17	14.9
Max CofM height (mm):	2683.7	2777.8	2344.1	2402.4	2270.4	2357.4	2433.8	2320.9	2443.9
Max CofM height from bfCurve (mm):	2660.6	2794.9	2362.7	2416.8	2287.2	2358.4	2441.7	2348	2489.7
Difference (%):	0.87	0.61	0.79	0.59	0.73	0.04	0.32	1.15	1.84
Measured displacement (mm):	1699.6	1752.6	1470.4	1500.6	1412.1	1494.7	1584.8	1540.6	1534.6
Displacement using curve (mm):	1663.3	1867.5	1497.1	1536.1	1410.5	1477.9	1573.9	1606.2	1584.3
Difference (%):	2.1	6.6	1.8	2.4	0.1	1.1	0.7	4.3	3.2
Time to minimum MOI (s):	0.55	0.36	0.46	0.39	0.15	0.5	0.58	0.49	0.46
Reduction in MOI (%):	65.45	66.46	51.93	45.83	42.65	53.01	54.87	56.81	53.29
Somersault 1 speed (ss/sec):	1.7	1.45	0	2.58	0	2.42	2.42	2.42	2.42
Somersault 2 speed (ss/sec):	2.5	0	0	0	0	1.7	1.9	1.86	1.9
Somersault 3 speed (ss/sec):	0	0	0	0	0	0	0	0	0
Somersault 4 speed (ss/sec):	0	0	0	0	0	0	0	0	0
Opening height (mm):	999	999	999	999	999	999	0	2163.2	2259
Entry distance (mm):	0	0	1592.1	0	0	0	0	0	0

Key Performance Indicators	_2018_09_06_11_37_15_200a	_2018_09_06_1_38_32_200a	_2018_09_06_1_39_47_200a	_2018_10_18_1_18_36_200a	_2018_10_18_1_20_59_200a	JHsl_2019_01_17_11_28_41_200a	_2018_09_06_15_21_16_403b	_2018_09_06_15_23_02_403b	JHsl_2019_01_17_11_11_00_403c
	<b>Best model: 9</b>								
<b>First contact</b>									
Knee angle (deg):	177.9	175.4	179.1	173.6	178.9	178.6	176.7	999	177.2
Hip angle (deg):	175.3	172.1	175.3	179.8	173.4	176.4	179	999	179.5
Trunk angle (deg):	3.8	5.5	5	4	7.4	4.4	1.2	999	1.6
Shoulder angle (deg):	156.5	155.4	151.6	154.8	158.8	170.4	155.5	999	155.6
Elbow angle (deg):	168.7	174	177.9	170.2	176.5	176.1	172.1	999	178.6
Lean angle (deg):	1.9	2.4	2.6	2.2	2.4	2.9	16.6	999	1.9
Landing velocity - x (m/s):	0	0	0	0	0	0	0	0	0
Landing velocity - y (m/s):	999	999	999	999	999	999	999	999	999
Landing velocity - resultant (m/s):	0	0	0	0	0	0	0	0	0
<b>Max Squat</b>									
Knee angle (deg):	68.6	64.8	66	65.4	61.9	63.5	70	76.6	65.5
Hip angle (deg):	66.7	70	72.9	75.4	66.6	57.1	76	76.5	64.7
Trunk angle (deg):	41.7	37.2	34.7	32.1	38.7	47.5	30.6	36.2	42.3
Shoulder angle (deg):	4.4	1.7	12.6	10.3	19.6	6.5	34.8	35.2	34.5
Elbow angle (deg):	177.8	179.5	178.2	176.4	177	172.4	173.9	175.4	169.7
Arm speed from 1st contact (rad/sec):	6.49	6.16	6.2	5.36	5.96	5.95	6	15.32	6.25
Lean angle (deg):	9.6	14.3	12.7	14.4	12.6	11.8	25.2	11.3	12.8
Change in COM (mm):	483	502.6	529.7	506.8	574.3	504	456.4	999	502.1
<b>Maximum deflection</b>									
Knee angle (deg):	126.2	118.2	106.5	130.5	110.5	118.7	128.2	129.7	127.9
Knee extension (deg):	-51.7	-57.2	-72.6	-43.1	-68.5	-59.9	-48.5	-869.3	-49.3
Impulse (percent of total time):	60	54.1	54.1	60.6	55.9	61.1	58.3	54.1	58.8
Hip angle (deg):	134.5	125.7	124.8	135.9	121.9	127.6	143.9	142.8	142.2
Trunk angle (deg):	10.5	14.3	11.8	13.1	15.5	15.9	9.9	9.2	8.8
Shoulder angle (deg):	132.7	129.7	143.5	135.6	137.5	138.9	178.2	157.5	164.2
Elbow angle (deg):	176.5	173.3	175.6	170.1	172.3	176.1	62.7	77.1	83.6
Lean angle (deg):	2.8	3.6	5.4	4	4.8	5.6	7.6	5.8	6.6
Arm speed from 1st contact (deg/sec):	6.49	6.16	6.2	5.36	5.96	5.95	6	15.32	6.25
Board deflection (mm):	721.4	704.4	707.1	779.6	762.1	746.6	735.7	722.1	759.9
<b>Leg Extension</b>									
Knee angle (deg):	176.2	176.5	175	174.8	174.5	174.9	178.6	178.1	176.4
Hip angle (deg):	176.5	177.1	179.9	180	177.5	178	144.5	147.8	148.6
Trunk angle (deg):	3.8	3.1	1.5	1.3	2.6	2.5	26.3	24.9	25
Shoulder angle (deg):	155.2	161.1	151.4	154.5	162.9	162.9	179.9	179.9	178.6
Elbow angle (deg):	172.8	174.9	166	165.6	173	171.5	168.1	169.3	156
Lean angle (deg):	1.5	1.3	1.7	2.5	2.5	2.9	18.5	3.7	5.8
Arm speed from maxSquat (rad/sec):	5.57	5.27	5.15	6.39	5.89	5.39	7.01	6.52	6.33
Impulse time since max deflection (%):	40	45.9	45.9	39.4	44.1	38.9	41.7	45.9	41.2
<b>Last contact</b>									
Knee angle (deg):	178	172.6	172.9	174.8	173.4	170.4	176	173.8	172.1
Hip angle (deg):	177.5	179.3	179.8	173.8	179.2	178.9	133.5	132.7	127.1
Trunk angle (deg):	1.3	1.4	2.9	6.9	3.6	5.3	34.4	36.7	43.7
Shoulder angle (deg):	163.3	161.8	164.5	154.1	164.2	156.5	166.3	167.4	172.5
Elbow angle (deg):	171.8	173.6	175.2	166.1	171.8	177.7	168.6	171.8	150.1
Lean angle (deg):	1	0.8	0.1	0	0.2	0.8	19.6	2.7	4
Impulse time (s):	0.4	0.5	0.5	0.4	0.4	0.5	0.5	0.5	0.4
Velocity - x (m/s):	0.91	0.85	0.84	0.93	0.81	0.83	0.95	0.89	1.29
Velocity - y (m/s):	4.63	4.48	4.66	4.58	4.5	4.88	4.3	4.07	4.44
Velocity - y from bfCurve (m/s):	4.77	5.4	5.31	4.73	4.87	4.52	4.49	4.41	4.65
Difference (%):	0.97	16.91	12.19	3.17	7.62	7.83	4.33	7.81	4.43
Resulant velocity (m/s):	4.71	4.56	4.74	4.68	4.58	4.95	4.4	4.17	4.62
Rotation of trunk (rad/sec):	0.41	0.53	0.5	0.72	0.68	0.72	1.63	1.64	1.93
<b>Flight Characteristics</b>									
CofM trajectory (deg):	11.1	10.8	10.2	11.5	10.2	9.7	12.4	12.3	16.2
Max CofM height (mm):	2205.9	2201.5	2206.1	2219.5	2296.6	2299.5	1972.6	1929.1	2027.7
Max CofM height from bfCurve (mm):	2208.3	2320.6	2299.6	2214.3	2289.2	1871	1934.9	1906.2	1871
Difference (%):	0.11	5.13	4.06	0.23	0.32	22.9	1.95	1.2	8.38
Measured displacement (mm):	1124	1084.5	1064.4	1150	1207	1207	1060.1	999.3	1071.5
Displacement using curve (mm):	1160.7	1484.4	1437.2	1141.8	1211.1	1041.8	1029.4	993.1	1099.9
Difference (%):	3.3	36.9	35	0.7	0.3	13.7	2.9	0.6	2.6
Time to minimum MOI (s):	0.48	0.03	0.03	0.03	0	0.03	0.3	0.3	0.25
Reduction in MOI (%):	2.52	1.59	4.68	2.2	0	3.47	63.27	64.56	59.33
Somersault 1 speed (ss/sec):	0	0	0	0	0	0	0	0	2.16
Somersault 2 speed (ss/sec):	0	0	0	0	0	0	0	0	0
Somersault 3 speed (ss/sec):	0	0	0	0	0	0	0	0	0
Somersault 4 speed (ss/sec):	0	0	0	0	0	0	0	0	0
Opening height (mm):	999	999	999	999	999	999	999	999	1727.5
Entry distance (mm):	0	0	0	0	0	0	0	0	0

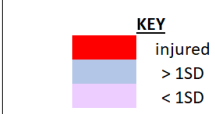


Key Performance Indicators	<u>2018_10_18_</u>	<u>2018_10_18_</u>						
	<u>12_05_06_40</u>	<u>12_07_07_40</u>	<u>2018_10_18_</u>	<u>JHs_2019_01_17_</u>	<u>JHs_2019_01_17_</u>	<u>JHs_2019_01_17_</u>	<u>JHs_2019_01_17_</u>	<u>JHs_2019_01_17_</u>
	5c	5c	12_08_35_405c	11_16_04_405c	11_18_00_405c	11_18_00_405c	11_12_39_45c	11_14_11_405c
<b>Best model: 9</b>								
<b>First contact</b>								
Knee angle (deg):	175.2	999	176.4	179.2	175.9	175.9	175.8	177.1
Hip angle (deg):	176.2	999	178.9	177.5	178.8	178.8	177.9	179
Trunk angle (deg):	5.6	999	3.3	4.8	2.6	2.6	3.9	1.7
Shoulder angle (deg):	160.6	999	158	158.7	169.4	169.4	157.7	165
Elbow angle (deg):	172.3	999	173	172.7	177.7	177.7	175.4	176
Lean angle (deg):	1.8	999	2.2	11.6	2.9	2.9	1.7	1.2
Landing velocity - x (m/s):	0	0	0	0	0	0	0	0
Landing velocity - y (m/s):	999	999	999	999	999	999	999	999
Landing velocity - resultant (m/s):	0	0	0	0	0	0	0	0
<b>Max Squat</b>								
Knee angle (deg):	65.8	66.8	68	63.3	63.8	63.8	63.5	66.1
Hip angle (deg):	67.8	69.1	65	68.9	67.4	67.4	73.6	66.3
Trunk angle (deg):	42.2	38.2	43.7	40.5	41.4	41.4	32.2	41.1
Shoulder angle (deg):	42.6	22.4	29.7	36.5	41	41	31.7	33.7
Elbow angle (deg):	177.7	168.8	174.3	172.9	175.8	175.8	169.6	177.7
Arm speed from 1st contact (rad/sec):	6.09	45.6	6.71	5.71	5.06	5.06	5.67	6.54
Lean angle (deg):	14.5	12.3	13.3	11.8	15.3	15.3	14	12.1
Change in COM (mm):	524.4	2769.9	479.5	557.7	515.8	515.8	516.7	501.4
<b>Maximum deflection</b>								
Knee angle (deg):	118.8	124.8	125.4	126.2	124.1	124.1	129.1	115.6
Knee extension (deg):	-56.4	-874.2	-51	-53	-51.8	-51.8	-46.7	-61.5
Impulse (percent of total time):	60	61.1	62.9	60.6	60.6	60.6	61.8	56.8
Hip angle (deg):	138.2	141	144.3	138.7	136.4	136.4	144.9	130.6
Trunk angle (deg):	11.2	11	9.8	12.8	15.8	15.8	9.6	14.7
Shoulder angle (deg):	174.8	171	178.8	170.4	167.8	167.8	173.9	170.6
Elbow angle (deg):	61.9	73	63.6	78.8	68.7	68.7	66.7	73.4
Lean angle (deg):	7.6	7.4	8.7	7.1	9.6	9.6	8.6	7.2
Arm speed from 1st contact (deg/sec):	6.09	45.6	6.71	5.71	5.06	5.06	5.67	6.54
Board deflection (mm):	783.7	770	785.1	789.3	760.7	760.7	755.4	753.6
<b>Leg Extension</b>								
Knee angle (deg):	179.7	178.8	178.9	175.5	174.7	174.7	177.7	177.5
Hip angle (deg):	142.4	136.4	145.2	145.9	142.8	142.8	140.9	127.7
Trunk angle (deg):	30.1	33	29.4	27.5	31.3	31.3	30.1	38.8
Shoulder angle (deg):	177.3	178.8	172.4	176.6	179.8	179.8	178.8	176.2
Elbow angle (deg):	148.5	139.7	151.9	124.1	131	131	134.4	135.9
Lean angle (deg):	5.7	3.7	8.1	8	10.4	10.4	6.3	4.5
Arm speed from maxSquat (rad/sec):	7.21	6.42	7.29	6.39	7.33	7.33	6.79	6.75
Impulse time since max deflection (%):	40	38.9	37.1	39.4	39.4	39.4	38.2	43.2
<b>Last contact</b>								
Knee angle (deg):	177.3	173.9	176.6	171.4	174.5	174.5	174.9	176.1
Hip angle (deg):	121.5	119.2	120.5	115.7	113.8	113.8	114.9	117.7
Trunk angle (deg):	46.7	48.8	50.2	55.5	58.3	58.3	52.3	49.4
Shoulder angle (deg):	164.9	173.7	176.4	154.6	150.6	150.6	154.7	166.6
Elbow angle (deg):	141.1	145.6	157.9	127.6	125.5	125.5	132.9	135.2
Lean angle (deg):	5.3	4.7	8.2	9.7	9.5	9.5	83.5	6.3
Impulse time (s):	0.4	0.5	0.4	0.4	0.4	0.4	0.4	0.5
Velocity - x (m/s):	0.88	1.23	0.91	1.36	1.3	1.3	1.32	1.18
Velocity - y (m/s):	4.57	4.32	4.41	4.24	4.57	4.57	4.61	4.23
Velocity - y from bfCurve (m/s):	5.77	4.41	4.5	4.47	4.88	4.88	4.45	4.59
Difference (%):	20.83	2.11	1.93	5.24	6.3	6.3	3.57	7.82
Resulant velocity (m/s):	4.65	4.49	4.5	4.45	4.75	4.75	4.8	4.39
Rotation of trunk (rad/sec):	2.13	2.14	2.21	2.51	2.8	2.8	2.28	2.29
<b>Flight Characteristics</b>								
CofM trajectory (deg):	10.9	15.9	11.7	17.8	15.9	15.9	16	15.5
Max CofM height (mm):	2045.5	1913.9	1946.2	1891.5	1939.2	1939.2	1884.4	1918.1
Max CofM height from bfCurve (mm):	2873	1910.8	1926.2	1871	1871	1871	1871	1871
Difference (%):	28.8	0.16	1.04	1.1	3.65	3.65	0.72	2.52
Measured displacement (mm):	1094.7	1002.1	1032.8	999.1	1015.8	1015.8	986.2	994.7
Displacement using curve (mm):	1095.5	991.2	1030.2	1020.5	1213	1213	1009.9	1074.3
Difference (%):	54.9	1.1	0.3	2.1	19.4	19.4	2.4	8
Time to minimum MOI (s):	0.41	0.4	0.19	0.41	0.16	0.16	0.15	0.18
Reduction in MOI (%):	55.19	55.58	57.56	59.72	55.21	55.21	53.27	56.2
Somersault 1 speed (ss/sec):	2.29	2.29	2.29	2.35	2.42	2.42	2.5	2.35
Somersault 2 speed (ss/sec):	2.67	2.67	2.58	2.67	0	2.76	2.67	2.67
Somersault 3 speed (ss/sec):	0	0	0	0	0	0	0	0
Somersault 4 speed (ss/sec):	0	0	0	0	0	0	0	0
Opening height (mm):	999	999	999	185.1	359.6	359.6	251.9	358.4
Entry distance (mm):	0	0	0	0	0	0	0	0

Key Performance Indicators	2018_09_06_	2018_09_06_	2018_09_06_	2018_09_06_	2018_09_06_	2018_09_06_
	11_42_31_201c	11_44_14_201c	11_45_43_201c	11_52_06_203c	11_53_37_203c	11_55_26_203c
<b>Best model: 9</b>						
<b>First contact</b>						
Knee angle (deg):	178.7	178.2	177.8	178.7	176.9	176.4
Hip angle (deg):	176.9	173.3	178.8	172.4	178.3	173.4
Trunk angle (deg):	3.4	5.8	2.6	6.5	2.6	6.1
Shoulder angle (deg):	159	163.5	167.2	153.7	165.8	157.4
Elbow angle (deg):	168.2	178.7	175.4	176.1	172	172.8
Lean angle (deg):	1.6	2.2	1.7	1.4	1.5	0.6
Landing velocity - x (m/s):	0	0	0	0	0	0
Landing velocity - y (m/s):	999	999	999	999	999	999
Landing velocity - resultant (m/s):	0	0	0	0	0	0
<b>Max Squat</b>						
Knee angle (deg):	63.6	65.6	66.9	68.9	63	66.2
Hip angle (deg):	67.3	66.2	66	65.6	64.9	67.4
Trunk angle (deg):	36.7	38.8	37.8	40.5	36.2	37.1
Shoulder angle (deg):	1.3	1.1	2.8	7.1	9	23.5
Elbow angle (deg):	179.1	178.1	174.4	171.3	175.9	171
Arm speed from 1st contact (rad/sec):	5.79	6.11	5.75	5.6	5.25	5.5
Lean angle (deg):	12.3	9.9	11.7	9.8	10	9.7
Change in COM (mm):	533.8	503.7	539.5	528.4	508.6	479.2
<b>Maximum deflection</b>						
Knee angle (deg):	120.7	114.7	131.4	128.5	132.4	127.5
Knee extension (deg):	-58	-63.5	-46.4	-50.3	-44.5	-48.8
Impulse (percent of total time):	62.5	63.6	67.7	75	75.9	68.8
Hip angle (deg):	121.6	124.3	134.8	138.1	138.7	136.1
Trunk angle (deg):	17.5	13.6	11.3	4.3	7.2	5.5
Shoulder angle (deg):	120.8	132.3	133.2	147.6	153.9	143.7
Elbow angle (deg):	174.1	180	178	178.3	177.8	177.3
Lean angle (deg):	4.6	3.4	1.7	1.2	0.1	0.2
Arm speed from 1st contact (deg/sec):	5.79	6.11	5.75	5.6	5.25	5.5
Board deflection (mm)	999	999	999	719.7	730.3	730
<b>Leg Extension</b>						
Knee angle (deg):	177.5	176.6	177.4	176.7	175.9	176.2
Hip angle (deg):	177.4	173.8	179.7	176.5	176.7	172.4
Trunk angle (deg):	3.1	6.2	2.3	8.3	2.2	11.9
Shoulder angle (deg):	153.6	153.1	152.3	155.3	163.6	153.8
Elbow angle (deg):	177.3	173.7	179.7	171.1	175.9	171.9
Lean angle (deg):	1.8	1.1	0.5	4.1	2.4	4.6
Arm speed from maxSquat (rad/sec):	6.71	6.19	6.8	6.72	6.32	5.44
Impulse time since max deflection (%):	37.5	36.4	32.3	25	24.1	31.3
<b>Last contact</b>						
Knee angle (deg):	177.3	179.2	178.6	147.1	155.3	156
Hip angle (deg):	178.7	175.8	177.7	170.6	175.7	170.7
Trunk angle (deg):	2	6.1	2.2	19.7	21.2	27.3
Shoulder angle (deg):	167.9	167.8	159	173.7	163.1	170.4
Elbow angle (deg):	174.1	173.1	176.5	157.8	145.3	169.2
Lean angle (deg):	2.4	4.1	4.9	14.6	9.6	12.3
Impulse time (s):	0.4	0.4	0.4	0.4	0.4	0.4
Velocity - x (m/s):	0.81	0.69	0.76	0.89	0.75	1.01
Velocity - y (m/s):	4.64	4.96	4.6	4.6	4.5	4.6
Velocity - y from bfCurve (m/s):	4.91	4.77	4.79	4.49	4.47	4.57
Difference (%):	5.55	4.1	4.11	2.52	0.72	0.46
Resultant velocity (m/s):	4.71	5.01	4.66	4.69	4.57	4.71
Rotation of trunk (rad/sec):	0.68	0.67	0.49	0.86	0.99	1.12
<b>Flight Characteristics</b>						
CofM trajectory (deg):	10	7.9	9.3	10.9	9.5	12.4
Max CofM height (mm):	2278.4	2278.4	2238.8	2093.9	2161.4	2115.9
Max CofM height from bfCurve (mm):	2320.6	2299.6	2278.7	2108.1	2179.4	2148.6
Difference (%):	1.82	0.92	1.75	0.67	0.83	1.52
Measured displacement (mm):	1172.1	1182.7	1184.3	1025.4	1071.4	1057.4
Displacement using curve (mm):	1228.5	1158.6	1170.9	1028.1	1019	1066.6
Difference (%):	4.8	2	1.1	0.3	4.9	0.9
Time to minimum MOI (s):	0.35	0.3	0.35	0.33	0.43	0.38
Reduction in MOI (%):	70.36	66.73	69.36	66.77	67.37	68.53
Somersault 1 speed (ss/sec):	0	0	0	0	0	0
Somersault 2 speed (ss/sec):	0	0	0	0	0	0
Somersault 3 speed (ss/sec):	0	0	0	0	0	0
Somersault 4 speed (ss/sec):	0	0	0	0	0	0
Opening height (mm):	2256.4	999	999	999	999	999
Entry distance (mm):	0	0	0	0	0	0

## Diver 4

### Diver 4 – September 2018 Profiling results

 <p><b>KEY</b>  <span style="color: red;">■</span> injured  <span style="color: blue;">■</span> &gt; 1SD  <span style="color: purple;">■</span> &lt; 1SD</p>	<p>All results were compared to mean of:</p> <ul style="list-style-type: none"> <li>• All funded divers</li> <li>• All divers of the same sex</li> <li>• All divers in the same discipline (springboard or platform)</li> <li>• All divers in the same discipline of the same sex</li> </ul>
---	--

### Diver 4

ANTHROPOMETRICS				STRENGTH									
	Height		Weight	Grip arm by side		Grip arm overhead		Elbow extension		Hip abduction		Hip external rotation	
	WC mean	stdev	Diver 4	Left	Right	Left	Right	Left	Right	Left	Right	Left	Right
WC mean	168.0	62.5	69.3	38.2	39.4	36	36.9	52.2	54.2	51.2	51.9	41.8	40.8
stdev	5.9	9.0	22.9	11.2	11	9.2	9.6	12.6	13.2	12.5	10.4	12.1	11.4
Diver 4	173	72.3	57	51.2	51.8	39.7	51.3	58.4	68.9	76.8	70.6	64.4	55.4
Male mean	171.1	67.0	57.2	46.7	46.7	42.0	43.0	60.9	63.0	56.9	56.4	48.8	47.1
stdev	4.4	7.4	18.2	7.8	8.8	7.8	7.7	10.6	9.2	13.3	9.4	12.4	11.5
Diver 4	173	72.3	57	51.2	51.8	39.7	51.3	58.4	68.9	76.8	70.6	64.4	55.4
Spring mean	168.2	66.2	69.5	41.9	43.6	38.6	40.7	58.0	60.8	55.0	56.1	47.2	46.8
stdev	5.9	8.6	24.6	11.5	10.9	9.8	10.0	10.9	11.4	15.0	9.9	13.6	12.3
Diver 4	173	72.3	57	51.2	51.8	39.7	51.3	58.4	68.9	76.8	70.6	64.4	55.4
Male spr mean	171.0	70.6	56.7	49.9	50.9	44.6	46.2	65.2	67.2	63.7	61.6	55.8	53.6
stdev	3.9	4.4	19.2	6.2	5.8	7.4	7.2	8.5	7.5	13.7	8.0	10.9	9.8
Diver 4	173	72.3	57	51.2	51.8	39.7	51.3	58.4	68.9	76.8	70.6	64.4	55.4

RANGE OF MOTION																
	Shoulder ER		Shoulder IR		Straight leg raise		Thomas test		Lumbar locked thoracic		Knee to wall		Lat length against wall		Combined elevation	
	Left	Right	Left	Right	Left	Right	Left	Right	Left	Right	Left	Right	Trial 1	Trial 2	Trial 1	Trial 2
WC mean	61.8	66.0	46.3	40.9	119.4	118.3	below	below	52.7	46.7	12.6	12.4	0.2	0.2	27.1	28.6
stdev	13.9	17.9	8.5	8.3	12.1	11.2	below	below	13.9	12.7	2.9	2.6	1.1	1.1	8.6	9.1
Diver 4	54	47	49	31	120	115	above	above	68	46	9	10.5	0	0	25	27
Male mean	59.8	65.3	42.9	37.9	111.5	111.1	below	below	53.3	45.7	12.1	11.8	0.4	0.4	26.6	27.6
stdev	13.7	18.6	7.5	7.7	8.5	7.8	below	below	12.3	11.6	3.0	2.7	1.5	1.5	6.9	5.8
Diver 4	54	47	49	31	120	115	above	above	68	46	9	10.5	0	0	25	27
Spring mean	66.8	70.6	44.8	40.2	122.5	121.2	below	below	55.5	47.6	14.4	14.2	0.4	0.4	25.5	26.5
stdev	16.0	17.2	9.3	8.1	11.9	11.4	below	below	10.2	12.8	2.1	1.8	1.5	1.5	5.6	6.1
Diver 4	54	47	49	31	120	115	above	above	68	46	9	10.5	0	0	25	27
Male spr mean	55.3	63.0	45.3	38.4	111.0	110.1	above	above	52.8	45.5	10.8	10.3	0.0	0.0	26.8	28.0
stdev	11.9	20.9	7.2	7.9	10.9	7.9	above	above	15.3	11.5	3.0	2.3	0.0	0.0	8.7	7.1
Diver 4	54	47	49	31	120	115	above	above	68	46	9	10.5	0	0	25	27

WORK CAPACITY								
	SL squat to box - 30 reps		Calf raise off step - 30 reps		Side plank - 120 seconds		Prone hold - 120 seconds	Supine hold - 60 seconds
	Left	Right	Left	Right	Left	Right		
WC mean	29	30	23	23	106	107	115	58
stdev	5	0	6	6	23	23	13	5
Diver 4	30	30	30	30	120	120	120	60
Male mean	28	30	24	25	110	110	115	60
stdev	6	0	6	5	19	21	14	0
Diver 4	30	30	30	30	120	120	120	60
Spring mean	30	30	25	25	105	103	114	58
stdev	0	0	6	6	25	27	13	6
Diver 4	30	30	30	30	120	120	120	60
Male spr mean	30	30	26	26	110	108	116	60
stdev	0	0	6	6	21	23	9	0
Diver 4	30	30	30	30	120	120	120	60

STRENGTH AND POWER						
	Peak force (N)		Time to peak force (s)			
	ISO back squat	ISO calf raise	ISO back squat		ISO calf raise	
			R	L	R	L
WC mean	2969.64	2441.98	2.44	2.86	2.94	2.72
stdev	854.80	543.36	1.03	1.64	0.55	0.67
Diver 4	4331	3339	2.09	2.13	2.9	2.8
Male mean	3465.36	2650.82	2.51	2.67	2.93	2.73
stdev	635.28	429.26	0.94	0.80	0.44	0.57
Diver 4	4331	3339	2.09	2.13	2.9	2.8
Spring mean	3151.55	2645.55	2.21	2.40	2.82	2.62
stdev	951.14	615.20	0.88	1.02	0.47	0.78
Diver 4	4331	3339	2.09	2.13	2.9	2.8
Male spr mean	3554.00	2847.00	2.44	2.58	2.90	2.74
stdev	731.72	351.39	0.71	0.68	0.26	0.57
Diver 4	4331	3339	2.09	2.13	2.9	2.8

STRENGTH AND POWER ASSESSMENT - JUMPS																									
Peak force (s)				Jump height (cm)				Av. Peak velocity (m/s)				Flight time (m/s)				Rate of force development			Time to peak propulsive force			Movement start to peak force		RSI flight/contact time	
CMJ	SLCMJ		DJ	CMJ	SLCMJ		DJ	CMJ	SLCMJ		DJ	CMJ	SLCMJ		DJ	CMJ	SLCMJ		R	L	DJ	CMJ	DJ		
	R	L			R	L			R	L			R	L			R	L							
WC mean	0.71	0.78	0.80	0.08	41.27	23.65	22.84	38.69	2.80	2.14	2.09	2.77	576.36	436.15	427.45	544.52	42362.16	713.08	22675.00	195.08	216.00	3.96	0.68	2.45	
stdev	0.15	0.14	0.17	0.05	10.07	4.68	5.91	8.40	0.35	0.22	0.23	0.41	68.69	44.07	55.46	96.55	148708.90	5612.29	62826.23	100.17	131.84	6.25	0.16	0.84	
Diver 4	0.54	0.7	0.79	0.03	47.7	26.3	27.5	41.4	2.95	2.21	2.27	2.91	622	462	473	580	-115244	2776	6156	231	255	0	0.52	4.39	
Male mean	0.65	0.82	0.79	0.09	48.09	26.41	26.51	44.78	2.98	2.24	2.22	3.03	625.46	462.25	462.57	601.69	19218.00	2005.50	33294.86	183.38	203.29	4.08	0.66	2.58	
stdev	0.14	0.14	0.17	0.06	7.35	2.71	3.46	5.94	0.22	0.11	0.13	0.19	44.07	22.69	30.69	41.10	178632.97	873.36	78829.00	82.35	106.25	5.79	0.17	1.03	
Diver 4	0.54	0.7	0.79	0.03	47.7	26.3	27.5	41.4	2.95	2.21	2.27	2.91	622	462	473	580	-115244	2776	6156	231	255	0	0.52	4.39	
Spring mean	0.66	0.78	0.80	0.08	46.20	23.65	22.84	41.55	2.92	2.14	2.09	2.92	607.92	436.15	427.45	579.46	41940.08	713.08	22675.00	195.08	216.00	2.54	0.65	2.51	
stdev	0.15	0.14	0.17	0.06	7.31	4.68	5.91	6.03	0.24	0.22	0.23	0.21	49.15	44.07	55.46	43.39	183472.91	5612.29	62826.23	100.17	131.84	3.73	0.18	0.98	
Diver 4	0.54	0.7	0.79	0.03	47.7	26.3	27.5	41.4	2.95	2.21	2.27	2.91	622	462	473	580	-115244	2776	6156	231	255	0	0.52	4.39	
Male spr mean	0.6113	0.8163	0.7914	0.0813	50.875	26.413	26.514	45.55	3.0775	2.235	2.22	3.06375	641	462.25	462.57	608.25	-5581.125	2005.5	33294.86	183.375	203.29	3	0.63125	2.635	
stdev	0.1043	0.1369	0.1661	0.0694	4.0199	2.7053	3.4638	2.5568	0.104	0.1052	0.1334	0.08314	24.9571	22.6889	30.686	16.816	192635.45	873.358	78829	82.3459	106.25	4.2426	0.1631334	1.1357188	
Diver 4	0.54	0.7	0.79	0.03	47.7	26.3	27.5	41.4	2.95	2.21	2.27	2.91	622	462	473	580	-115244	2776	6156	231	255	0	0.52	4.39	

Diver 4 – results of filming and digitisation

Forward facing dives with hurdle

Dive	Test 1	Test 2	Test 3	Test 4	Change (%)
<b>100a</b>					
Mean board deflection (mm)	917.0	916.3	954.1	890.8	4.04
Maximum board deflection (mm)	940.7	954.3	997.6	890.8	6.05
Mean resultant take-off velocity (m/s)	5.78	5.40	5.81	5.98	3.46
Maximum resultant take-off velocity (m/s)	5.89	5.72	6.03	5.98	2.38
Mean vertical take-off velocity (m/s)	5.79	5.14	5.47	5.59	-3.43
Maximum vertical velocity (m/s)	5.88	5.38	5.85	5.59	-0.48
Mean vertical displacement (mm)	1824.4	1437.7	1628.0	1701.3	-6.75
Maximum vertical displacement (mm)	1882.4	1577.6	1864.2	1701.3	-0.97
<b>303c/304c</b>					
Mean board deflection (mm)	917.2	963.1	996.8		8.67
Maximum board deflection (mm)	929.0	965.1	1028.1		10.67
Mean resultant take-off velocity (m/s)	5.66	5.61	5.78		1.97
Maximum resultant take-off velocity (m/s)	5.71	5.58	6.13		7.36
Mean vertical take-off velocity (m/s)	5.43	5.19	5.51		1.43
Maximum vertical velocity (m/s)	5.44	5.25	5.74		5.58
Mean vertical displacement (mm)	1605.2	1466.6	1651.4		2.88
Maximum vertical displacement (mm)	1609.1	1498.7	1793.7		11.47
<b>305c/306c</b>					
Mean board deflection (mm)	917.2		1022.7	958.8	11.50
Maximum board deflection (mm)	929.0		1059.8	967.1	14.08
Mean resultant take-off velocity (m/s)	5.66		5.96	5.85	5.18
Maximum resultant take-off velocity (m/s)	5.71		6.09	5.88	6.65
Mean vertical take-off velocity (m/s)	5.43		5.59	5.42	2.98
Maximum vertical velocity (m/s)	5.44		5.69	5.54	4.73
Mean vertical displacement (mm)	1605.2		1702.2	1600.4	6.04
Maximum vertical displacement (mm)	1609.1		1764.8	1669.2	9.68

Back facing dives, standing

Dive	Test 1	Test 2	Test 3	Test 4	Change (%)
<b>200a</b>					
Mean board deflection (mm)	739.1	775.3	776.2	729.5	5.02
Maximum board deflection (mm)	752.1	799.3	782.7	729.5	6.28
Mean resultant take-off velocity (m/s)	4.52	4.54	4.62	4.37	2.33
Maximum resultant take-off velocity (m/s)	4.59	4.73	4.73	4.37	3.05
Mean vertical take-off velocity (m/s)	4.47	3.97	4.37	4.54	1.42
Maximum vertical velocity (m/s)	4.48	4.25	4.53	4.54	1.28
Mean vertical displacement (mm)	1089.4	859.1	1041.0	1120.4	2.85
Maximum vertical displacement (mm)	1092.3	984.9	1120.1	1120.4	2.57
<b>203c/205c</b>					
Mean board deflection (mm)	738.4	795.2	787.0	794.5	7.70
Maximum board deflection (mm)	755.5	802.2	795.8	806.1	6.70
Mean resultant take-off velocity (m/s)	4.69	4.30	4.68	5.04	7.46
Maximum resultant take-off velocity (m/s)	4.84	4.71	4.71	5.09	5.17
Mean vertical take-off velocity (m/s)	4.29	4.16	4.41	4.66	8.75
Maximum vertical velocity (m/s)	4.34	4.20	4.43	4.69	8.20
Mean vertical displacement (mm)	1000.6	944.0	1060.5	1183.3	18.27
Maximum vertical displacement (mm)	1025.4	959.3	1067.5	1200.4	17.07
<b>403b/405c</b>					
Mean board deflection (mm)				806.6	
Maximum board deflection (mm)				860.6	
Mean resultant take-off velocity (m/s)				4.36	
Maximum resultant take-off velocity (m/s)				4.42	
Mean vertical take-off velocity (m/s)				4.2385	
Maximum vertical velocity (m/s)				4.312	
Mean vertical displacement (mm)				978.5	
Maximum vertical displacement (mm)				1012.7	

Key performance indicators – all dives - Diver 4. Dives coded as ‘date\_time\_dive-number’.

Any performance indicators which cannot be calculated are represented by ‘999’

Key Performance Indicators	_2018_09_06_11_34_05_100a	_2018_09_06_11_36_37_100a	_2018_09_06_15_39_39_100a	_2018_09_13_11_02_45_100a	_2018_09_13_11_03_52_100a	_2018_09_13_11_05_11_100a	_2018_10_18_11_15_53_100a	_2018_10_18_11_16_45_100a	_2018_10_18_11_17_54_100a
<b>Best model: 9</b>									
<b>Last step</b>									
Last step length (mm):	1039.2	891.2	999	999	999	999	999	999	999
Last step speed - x (m/s):	1.3	1	999	999	999	999	999	999	999
Last step speed - y (m/s):	-3	-2.9	999	999	999	999	999	999	999
Last step speed - resultant (m/s):	3.3	3.1	0	0	0	0	0	0	0
<b>Hurdle step</b>									
Into hurdle speed - x (m/s):	0.3	-0.2	999	999	-0.1	0.1	999	0.2	999
Into hurdle speed - y (m/s):	4.5	4.2	999	999	4	3.9	999	3.6	999
Hurdle height (mm):	2087.2	2124.9	2032.9	1879.5	1960.2	1928.3	1914.4	1935.2	2011.1
Hurdle displacement - measured (mm):	927.6	995.9	924.4	999	792.1	769.5	999	784.4	999
Hurdle displacement - calculated (mm):	1021.9	896.5	999	999	811.9	782	999	669	999
Difference (%):	10.2	10	999	999	2.5	1.6	999	14.7	999
Hurdle length (mm):	79.2	144	999	999	999	999	999	999	999
Velocity - x (m/s):	0.1	0	0.2	0.3	-0.3	0.2	0.3	0.2	0
Velocity - y (m/s):	-4.9	-4.7	-5.2	-3.9	-4.4	-4.4	-4.2	-4.5	999
Distance from tip (mm):	103.7	185.6	93.7	113.8	160.1	80.5	280.5	2.8	999
<b>First contact</b>									
Knee angle (deg):	105.1	107.7	112.3	128.6	107.5	111.1	115.1	104.6	101.4
Hip angle (deg):	91.9	94.3	94.3	121.5	94.6	99.1	114.7	92.9	999
Trunk angle (deg):	31.4	30.2	31.5	19	29.6	25.2	22	28.9	999
Shoulder angle (deg):	32.6	26.2	0.1	85.2	31.9	38.8	52.4	36.7	999
Elbow angle (deg):	162.3	174.2	123.8	156.7	160.6	150	162.9	163	999
Lean angle (deg):	1.4	2.1	0.7	1.6	1.4	3	73.3	0.9	999
Landing velocity - x (m/s):	0.05	0.01	0.2	0.3	-0.31	0.21	0.35	0.17	0
Landing velocity - y (m/s):	-4.89	-4.69	-5.18	-3.86	-4.39	-4.37	-4.17	-4.51	999
Landing velocity - resultant (m/s):	4.89	4.69	5.19	3.87	4.40	4.37	4.19	4.51	0.00
<b>Max Squat</b>									
Knee angle (deg):	97.4	100.1	103	111.3	102.7	108.6	99	99.1	99.4
Hip angle (deg):	89.5	98.8	84	98.5	92.1	92.2	102.1	86.1	999
Trunk angle (deg):	28.2	23.6	36.7	31.7	31.2	31.2	26.9	33.6	999
Shoulder angle (deg):	27.3	2.6	15.4	24.7	24.6	15.5	27	30.5	999
Elbow angle (deg):	174.7	172	168.4	175.9	175.3	173.2	175.1	154.8	999
Arm speed from 1st contact (rad/sec):	8.76	11.54	7.88	14.16	11.32	14.93	9.81	8.98	0
Lean angle (deg):	0.6	0.8	0	0.5	0.3	2.9	5.3	0.2	999
Change in COM (mm):	1496.6	1414.5	1337.2	1179	1205.1	1237.2	1151.9	1216.3	422.4
<b>Maximum deflection</b>									
Knee angle (deg):	122.1	128.7	127.9	131.8	123.7	128.7	135.8	131.8	999
Knee extension (deg):	17	21	15.6	3.2	16.2	17.6	20.8	27.2	897.6
Impulse (percent of total time):	51.7	59.3	60	53.1	52.9	56.3	61.8	58.8	58.6
Hip angle (deg):	128.4	142.1	142.7	140.3	138.7	143.2	148.7	147.7	999
Trunk angle (deg):	15.8	11.7	10.5	13.5	11	9.4	13.7	10	999
Shoulder angle (deg):	106.8	92.1	123.6	82.1	74	101.2	66.6	100.6	999
Elbow angle (deg):	178.4	176	172.9	170.7	177.7	179.5	176.2	177.2	999
Lean angle (deg):	5.9	8	8.7	6.3	6.8	6.9	12.2	9.8	999
Arm speed from 1st contact (deg/sec):	8.76	11.54	7.88	14.16	11.32	14.93	9.81	8.98	0
Board deflection (mm)	892.4	918	940.7	898	896.5	954.3	916.5	948.2	997.6
<b>Leg Extension</b>									
Knee angle (deg):	172.4	173	175.1	174.1	174.3	176.1	177.2	176.8	176
Hip angle (deg):	179.2	177	177.3	178.5	177.1	176.5	178.6	178.9	999
Trunk angle (deg):	2	1.9	3.1	4.4	0.8	0.2	6.2	5.2	999
Shoulder angle (deg):	124.4	115.8	133.5	91.4	102.4	114.6	93.1	119.5	999
Elbow angle (deg):	179.5	179.4	175.8	177.5	177.8	176	177.4	179.7	999
Lean angle (deg):	5.8	7.7	8.3	6.9	6.8	5.3	7.5	6.2	999
Arm speed from maxSquat (rad/sec):	9.87	10.43	8.42	9.07	8.07	8.45	8.68	7.1	-78.86
Impulse time since max deflection (%):	48.3	40.7	40	46.9	47.1	43.8	38.2	41.2	41.4
<b>Last contact</b>									
Knee angle (deg):	177.1	176.6	177.8	177.9	176.8	179.3	177.1	179	179.4
Hip angle (deg):	177.1	178.2	178.1	179.5	174	178.8	178.8	177.5	177.5
Trunk angle (deg):	6.7	5.2	6.3	6.1	1.4	2.8	8.1	6.2	7.1
Shoulder angle (deg):	135.4	141.8	138	118.3	121	131.3	113.6	136.7	137.8
Elbow angle (deg):	176.7	178.8	174.8	177.2	174.4	169.1	176.5	175.4	179.8
Lean angle (deg):	3.9	5.6	7.3	6.2	5.5	5	7	5.7	5.6
Impulse time (s):	0.4	0.3	0.4	0.4	0.4	0.4	0.4	0.4	0.4
Velocity - x (m/s):	0.73	0.95	0.87	0.67	0.67	0.8	0.89	0.76	0.8
Velocity - y (m/s):	5.62	5.82	5.71	5.09	5.3	5.66	5.77	5.52	5.98
Velocity - y from bFCurve (m/s):	5.92	6.08	5.95	5.03	5.32	5.56	5.47	5.82	6.05
Difference (%):	5.01	4.29	4.07	1.1	0.51	1.71	5.45	5.19	1.19
Resulant velocity (m/s):	5.67	5.89	5.78	5.13	5.34	5.72	5.84	5.57	6.03
Rotation of trunk (rad/sec):	0.9	0.67	0.62	0.72	0.45	0.46	0.74	0.58	37.97
<b>Flight Characteristics</b>									
CofM trajectory (deg):	7.4	9.2	8.7	7.5	7.2	8.1	8.8	7.8	7.7
Max CofM height (mm):	2853.1	2977.1	2948.1	2491.2	2601.3	2718	2659.3	2868.7	3044.3
Max CofM height from bFCurve (mm):	2856.6	2976.3	2943.5	2485.4	2596.7	2717.7	2621.2	2817.5	3022.5
Difference (%):	0.12	0.02	0.16	0.24	0.18	0.01	1.45	1.82	0.72
Measured displacement (mm):	1668.3	1825.8	1818.9	1292.9	1455.5	1589.1	1558.2	1741.1	1876.5
Displacement using curve (mm):	1783.5	1882.4	1807.4	1291.5	1444	1577.6	1527.4	1725.6	1864.2
Difference (%):	6.9	3.1	0.6	0.1	0.8	0.7	2	0.9	0.7
Time to minimum MOI (s):	999	999	0	0.5	0.54	0.58	0.56	0.6	0.61
Reduction in MOI (%):	999	999	0	3.95	4.65	8.1	78.63	80	80.84
Somersault 1 speed (ss/sec):	0	0	0	0	0	0	0	0	0
Somersault 2 speed (ss/sec):	0	0	0	0	0	0	0	0	0
Somersault 3 speed (ss/sec):	0	0	0	0	0	0	0	0	0
Somersault 4 speed (ss/sec):	0	0	0	0	0	0	0	0	0
Opening height (mm):	999	999	999	999	999	999	999	999	999
Entry distance (mm):	634.3	903.3	0	0	0	0	0	0	0

Key Performance Indicators	RH_2019_01_17_	2018_09_06_	2018_09_06_	2018_09_06_1	2018_09_13_	2018_09_13_	2018_10_18_	2018_10_18_	2018_10_18_
	_12_02_44_100a	12_13_00_303c	12_14_17_303c	2_17_45_303c	11_30_21_303c	11_31_45_303c	11_23_05_303c	11_24_28_303c	11_26_19_303c
<b>Best model: 9</b>									
<b>Last step</b>									
Last step length (mm):	980.1	999	999	999	999	999	999	999	999
Last step speed - x (m/s):	1.4	999	999	999	999	999	999	999	999
Last step speed - y (m/s):	-3.5	999	999	999	999	999	999	999	999
Last step speed - resultant (m/s):	3.8	0	0	0	0	0	0	0	0
<b>Hurdle step</b>									
Into hurdle speed - x (m/s):	0.1	-0.2	0.3	0.3	0.3	0.5	0.4	0.1	-0.1
Into hurdle speed - y (m/s):	4.3	3.7	3.9	4	3.5	3.9	3.8	3.8	4.1
Hurdle height (mm):	2057.6	2018.5	2046.7	1984.4	1907.9	1967.9	1961.3	2042.9	2075.3
Hurdle displacement - measured (mm):	896.8	883	915.4	847.7	776.9	818	819.6	931.5	948.9
Hurdle displacement - calculated (mm):	950.9	685.3	775.3	811.6	627.1	765.5	738.3	732.9	837.8
Difference (%):	6	22.4	15.3	4.3	19.3	6.4	9.9	21.3	11.7
Hurdle length (mm):	72.1	208.7	185.1	257.2	233.8	118.6	999	202.2	162.3
Velocity - x (m/s):	0.2	0.3	-0.2	0.2	0	0.1	0.5	0.2	0.4
Velocity - y (m/s):	-5	-4.8	-4.7	-4.4	-4.1	-4.9	-4.5	-4.4	-4.6
Distance from tip (mm):	81.4	116.9	141.8	97.7	5.4	169.8	26.5	29.4	57.7
<b>First contact</b>									
Knee angle (deg):	108.3	106.8	113.7	105.1	112.2	106.3	103.1	110.6	109.9
Hip angle (deg):	100.3	93	99.2	92.8	94.6	100.1	92.9	97.6	98.8
Trunk angle (deg):	28.5	30.4	28.5	28.9	30.2	25.3	30	31.4	27.8
Shoulder angle (deg):	25.1	27.7	42.8	27.4	36.7	13	47	64.1	30.8
Elbow angle (deg):	172.9	168.3	171.9	175	162.9	172.2	169.6	160.1	172
Lean angle (deg):	2.2	1.2	2.5	2.9	3	0.7	0.4	1	0.4
Landing velocity - x (m/s):	0.17	0.28	-0.22	0.19	0.03	0.06	0.51	0.22	0.44
Landing velocity - y (m/s):	-4.98	-4.77	-4.65	-4.4	-4.07	-4.9	-4.54	-4.37	-4.64
Landing velocity - resultant (m/s):	4.99	4.78	4.66	4.40	4.07	4.90	4.57	4.37	4.66
<b>Max Squat</b>									
Knee angle (deg):	105	106.8	102.8	102.3	102.6	106.3	103.1	95.4	102.1
Hip angle (deg):	96.5	93	89.5	88.6	87.9	100	92.9	85.8	93
Trunk angle (deg):	29.7	30.4	31.8	29.5	30.8	25.2	30	32	28.7
Shoulder angle (deg):	9.6	27.7	29.2	9.3	22.7	0.9	47	20	1
Elbow angle (deg):	172.8	168.3	171.8	171.4	175.9	173.9	169.6	177.2	169.9
Arm speed from 1st contact (rad/sec):	11.28	999	5.52	11.45	14.11	10.19	999	18.2	10.67
Lean angle (deg):	2.8	1.2	0.8	2.4	1.4	0.7	0.4	3.5	0.5
Change in COM (mm):	1382.8	1138.7	1212.7	1338.2	1145	1184.3	1131.3	1337.5	1451.1
<b>Maximum deflection</b>									
Knee angle (deg):	130.5	140.1	132.4	142.8	136.9	137.3	146.7	143	140.8
Knee extension (deg):	22.2	33.3	18.7	37.7	24.7	31	43.6	32.4	30.9
Impulse (percent of total time):	60	71.4	69	70.8	72.4	66.7	74.1	70.4	69.6
Hip angle (deg):	146.7	148.4	145.2	153.1	148.4	151.3	156.4	152.4	152.7
Trunk angle (deg):	11.4	11.8	11.1	9.3	10.1	7	9.4	12.4	10.5
Shoulder angle (deg):	108.8	119.3	104.7	122.7	141.2	121.3	94	112.1	124.5
Elbow angle (deg):	179.8	155.5	140.8	157.7	162.2	155.5	152.8	156.8	164.9
Lean angle (deg):	10.1	7.4	8.4	8	7.6	6.9	7.8	10.6	9.1
Arm speed from 1st contact (deg/sec):	11.28	999	5.52	11.45	14.11	10.19	999	18.2	10.67
Board deflection (mm)	890.8	922.7	929	900	965.1	961.1	982	1028.1	989.1
<b>Leg Extension</b>									
Knee angle (deg):	176.4	176.9	178.4	173.6	174.9	173.4	177	179.9	175
Hip angle (deg):	180	170	165.9	174.4	172.4	172.7	176.3	172	169.2
Trunk angle (deg):	5.5	0.8	3.3	0.9	2.6	0.6	5.4	3.3	1.5
Shoulder angle (deg):	126.7	120.3	118.2	124.2	120.3	125.3	111.3	114.7	133.7
Elbow angle (deg):	172.2	158.8	155.7	158.6	151.2	148	157.8	164.7	175.5
Lean angle (deg):	8	7.8	6.9	7.7	6.7	7.2	8.9	9.2	9.6
Arm speed from maxSquat (rad/sec):	8.57	7.61	7.18	10.97	7.88	9.22	7.64	9.17	11.71
Impulse time since max deflection (%):	40	28.6	31	29.2	27.6	33.3	25.9	29.6	30.4
<b>Last contact</b>									
Knee angle (deg):	177.4	138	146.9	150.9	141.7	145.6	132.1	145.1	131.2
Hip angle (deg):	179.7	173.4	160.7	163.3	169.6	168.5	165.7	164.4	174.7
Trunk angle (deg):	7.8	18.4	24.6	22.2	23.7	19.6	24.8	20.7	19.2
Shoulder angle (deg):	142.8	153.6	155	151.1	153.3	148.5	131.5	139.2	153.7
Elbow angle (deg):	177.1	170.1	165.5	165.4	170.2	164.6	172.9	163	178.7
Lean angle (deg):	7.4	3.9	3.1	2.2	0.7	2.2	3.7	3.9	2.6
Impulse time (s):	0.4	0.4	0.4	0.3	0.4	0.3	0.3	0.3	0.3
Velocity - x (m/s):	0.78	1.3	1.27	1.25	1.17	1.08	1.84	1.64	1.53
Velocity - y (m/s):	5.92	5.51	5.47	5.57	5.46	5.37	5.4	5.91	5.57
Velocity - y from bfCurve (m/s):	5.78	5.62	5.62	5.6	5.42	5.31	5.52	5.93	5.7
Difference (%):	2.54	1.93	2.62	0.53	0.63	1.15	2.13	0.4	2.23
Resulant velocity (m/s):	5.98	5.66	5.62	5.71	5.58	5.47	5.7	6.13	5.78
Rotation of trunk (rad/sec):	0.75	1.11	1.31	1.26	1.18	1	1.23	1.22	1.19
<b>Flight Characteristics</b>									
CofM trajectory (deg):	7.5	13.3	13	12.7	12.1	11.4	18.8	15.5	15.4
Max CofM height (mm):	2889.7	2618.1	2669.9	2608.7	2563.6	2502.4	2619.7	2835.3	2696.4
Max CofM height from bfCurve (mm):	2850.9	2632.2	2688.7	2628.2	2582.9	2514.3	2645.3	2842.8	2714.6
Difference (%):	1.36	0.53	0.7	0.74	0.75	0.47	0.97	0.26	0.67
Measured displacement (mm):	1752.7	1564.5	1567.1	1531.9	1464.8	1432.5	1531.6	1745.7	1616
Displacement using curve (mm):	1701.3	1607.7	1609.1	1598.8	1498.7	1434.5	1551.9	1793.7	1653.4
Difference (%):	2.9	2.8	2.7	4.4	2.3	0.1	1.3	2.7	2.3
Time to minimum MOI (s):	0.59	0.6	0.34	0.4	0.4	0.38	0.38	0.4	0.4
Reduction in MOI (%):	80.43	67.27	65.82	66.62	65.36	68.1	65.59	65.56	64.77
Somersault 1 speed (ss/sec):	0	0	0	0	0	0	0	0	0
Somersault 2 speed (ss/sec):	0	0	0	0	0	0	0	0	0
Somersault 3 speed (ss/sec):	0	0	0	0	0	0	0	0	0
Somersault 4 speed (ss/sec):	0	0	0	0	0	0	0	0	0
Opening height (mm):	999	999	999	999	999	999	999	999	999
Entry distance (mm):	0	0	0	0	0	0	0	0	0

Key Performance Indicators	_2018_10_18_11_34_33_304c	_2018_09_06_15_51_44_5140b	_2018_09_06_15_55_33_105b	_2018_09_06_15_56_56_105b	RH_2019_01_17_11_20_21_107c	RH_2019_01_17_11_23_00_107c	RH_2019_01_17_11_25_11_107c
<b>Best model: 9</b>							
<b>Last step</b>							
Last step length (mm):	999	999	999	999	974.2	1068.4	1096
Last step speed - x (m/s):	999	999	999	999	1.2	1.2	1.3
Last step speed - y (m/s):	999	999	999	999	-3.3	-3.2	-3.3
Last step speed - resultant (m/s):	0	0	0	0	3.5	3.4	3.6
<b>Hurdle step</b>							
Into hurdle speed - x (m/s):	999	0.1	0.2	-0.1	3.3	-0.2	0
Into hurdle speed - y (m/s):	999	4	3.7	3.9	16.3	3.7	4.1
Hurdle height (mm):	2026.9	2004.1	1904.9	1968.5	2086.2	2029.3	2096.4
Hurdle displacement - measured (mm):	999	871.6	766.6	866.1	668.8	907.4	943.6
Hurdle displacement - calculated (mm):	999	807.8	686.8	763.4	13477.6	707	874.4
Difference (%):	999	7.3	10.4	11.9	1915.3	22.1	7.3
Hurdle length (mm):	999	999	199.1	126.8	146.3	24.4	79.9
Velocity - x (m/s):	0	0.1	0.3	0	0.2	-0.6	0.4
Velocity - y (m/s):	999	-4.7	-4.2	-4.4	-5.1	-4.9	-5.3
Distance from tip (mm):	999	138.8	136.3	98.6	12.6	122.8	3.7
<b>First contact</b>							
Knee angle (deg):	109.3	110.3	101.9	109.1	104.9	99.1	94.2
Hip angle (deg):	999	94.3	93.1	93.4	102.8	92.5	93
Trunk angle (deg):	999	32.3	32.2	31.4	23	32.9	30.4
Shoulder angle (deg):	999	8.6	10.6	17.4	3.5	25.5	7.8
Elbow angle (deg):	999	179.1	177.3	174.6	177.7	175.5	179.2
Lean angle (deg):	999	1.1	3.1	0.2	3.2	6.1	7.1
Landing velocity - x (m/s):	0	0.13	0.26	0.05	0.24	-0.61	0.37
Landing velocity - y (m/s):	999	-4.7	-4.16	-4.43	-5.08	-4.91	-5.28
Landing velocity - resultant (m/s):	0.00	4.70	4.17	4.43	5.09	4.94	5.29
<b>Max Squat</b>							
Knee angle (deg):	94.3	96.9	94.7	100.1	96.3	99.1	91.1
Hip angle (deg):	999	92.5	84.9	86.3	101.4	92.5	92.6
Trunk angle (deg):	999	28.6	33	34.2	23	32.9	29.1
Shoulder angle (deg):	999	30	46	45.6	26	25.5	37.2
Elbow angle (deg):	999	176.6	173.3	166	179.4	175.5	177.7
Arm speed from 1st contact (rad/sec):	0	13.13	8.55	3.11	8.71	999	9.97
Lean angle (deg):	999	3.6	4	2	5.3	6.1	8.4
Change in COM (mm):	466.8	1342.2	1291.9	1362.6	1403	1310.1	1433.9
<b>Maximum deflection</b>							
Knee angle (deg):	999	127.2	131.1	126.5	117.9	128.5	134.7
Knee extension (deg):	889.7	16.9	29.1	17.3	13	29.4	40.5
Impulse (percent of total time):	70.8	51.6	50	51.6	54.5	54.8	60
Hip angle (deg):	999	144.3	147.6	143.5	141	148	153.2
Trunk angle (deg):	999	15.9	18.3	16.3	17.6	16.2	16.2
Shoulder angle (deg):	999	135.3	142.4	142.3	114.9	134.1	138.6
Elbow angle (deg):	999	104.1	104.5	101.6	100.7	101	101.4
Lean angle (deg):	999	15.4	16.4	14.9	17.7	17.2	18
Arm speed from 1st contact (deg/sec):	0	13.13	8.55	3.11	8.71	999	9.97
Board deflection (mm):	987.9	896.5	884.4	921	959.4	909.8	975
<b>Leg Extension</b>							
Knee angle (deg):	175.7	177.2	177.4	176.9	175.9	175.1	175.5
Hip angle (deg):	999	162.7	140.1	154.5	156.9	161.5	165.5
Trunk angle (deg):	999	26.8	45.8	32.3	30.5	29.6	25.9
Shoulder angle (deg):	999	144.8	111.6	135.1	138.1	133.9	139.1
Elbow angle (deg):	999	176.6	175.5	176.9	179.9	172.9	174.2
Lean angle (deg):	999	18.1	20.3	18.2	18.2	19.8	19.7
Arm speed from maxSquat (rad/sec):	-95.29	11.22	12.41	11.26	9.81	10.12	10.4
Impulse time since max deflection (%):	29.2	48.4	50	48.4	45.5	45.2	40
<b>Last contact</b>							
Knee angle (deg):	140	179.7	179.3	179.7	178.5	178.6	179
Hip angle (deg):	164.3	133.9	126.1	128.1	133.7	144.1	129.2
Trunk angle (deg):	26.3	49.3	59	54.6	50.2	45.4	55.6
Shoulder angle (deg):	148.2	126.7	115.7	117.9	120.5	124.9	124.1
Elbow angle (deg):	174.8	175.3	177.1	177.7	179.8	173.9	179.7
Lean angle (deg):	0	18.3	21.4	19.2	19.4	72.5	85.5
Impulse time (s):	0.3	0.4	0.4	0.4	0.4	0.4	0.4
Velocity - x (m/s):	1.64	1.32	1.27	1.04	0.95	1.45	1.35
Velocity - y (m/s):	5.24	5.41	5.13	5.57	6	5.87	6.09
Velocity - y from bfCurve (m/s):	5.61	5.38	5.13	5.34	6.08	5.72	5.94
Difference (%):	6.69	0.6	0.07	4.23	1.45	2.72	2.6
Resulant velocity (m/s):	5.49	5.57	5.29	5.66	6.07	6.05	6.24
Rotation of trunk (rad/sec):	39.77	2.6	3.16	2.81	2.39	0.12	3.06
<b>Flight Characteristics</b>							
CofM trajectory (deg):	17.4	13.7	13.9	10.5	9	13.9	12.5
Max CofM height (mm):	2622.9	2407.6	2247.9	2507.7	2820.5	2694.8	2743.9
Max CofM height from bfCurve (mm):	2603	2418.1	2266.6	2514.4	2860.2	2703	2748.3
Difference (%):	0.76	0.44	0.82	0.26	1.39	0.3	0.16
Measured displacement (mm):	1580.7	1422.2	1305	1493.7	1784.3	1663.2	1776.5
Displacement using curve (mm):	1606.7	1474.5	1343.4	1453.9	1886.5	1665.2	1795.7
Difference (%):	1.6	3.7	2.9	2.7	5.7	0.1	1.1
Time to minimum MOI (s):	0.56	0.49	0.48	0.59	0.49	0.53	0.49
Reduction in MOI (%):	66.05	57.77	55.21	56.02	63.84	63.64	64.2
Somersault 1 speed (ss/sec):	1.6	2.42	2.58	2.5	2.35	2.42	2.42
Somersault 2 speed (ss/sec):	0	0	1.95	2.16	2.86	2.86	2.86
Somersault 3 speed (ss/sec):	0	0	0	0	2.86	2.86	2.86
Somersault 4 speed (ss/sec):	0	0	0	0	0	0	0
Opening height (mm):	999	999	2076	2085.5	574.4	0	0
Entry distance (mm):	0	0	0	0	0	0	0



Key Performance Indicators	_2018_10_18_	_2018_10_18_	_2018_10_18_	RH_2019_01_17_	RH_2019_01_17_	RH_2019_01_17_
	11_39_31_306c	11_41_19_306c	11_43_26_306c	11_41_10_305c	11_42_34_305c	11_44_45_306c
<b>Best model: 9</b>						
<b>Last step</b>						
Last step length (mm):	999	999	999	1097.2	1085.4	1024.7
Last step speed - x (m/s):	999	999	999	1.3	1.4	0.8
Last step speed - y (m/s):	999	999	999	-2.9	-3	-2.9
Last step speed - resultant (m/s):	0	0	0	3.2	3.3	3
<b>Hurdle step</b>						
Into hurdle speed - x (m/s):	0	0.2	0.1	0.1	2.6	0.5
Into hurdle speed - y (m/s):	3.9	3.6	3.4	3.3	16.5	4
Hurdle height (mm):	2052	2006.7	2013.4	2056.2	2060.9	2064
Hurdle displacement - measured (mm):	913.9	898.2	910.4	909.6	626.2	926.6
Hurdle displacement - calculated (mm):	769.7	652.4	589.3	569.8	13948.7	805.5
Difference (%):	15.8	27.4	35.3	37.4	2127.4	13.1
Hurdle length (mm):	225.8	190.6	176.5	72.2	61.7	118.7
Velocity - x (m/s):	0.5	0.3	0.2	0	-0.3	0.2
Velocity - y (m/s):	-4.2	-4.4	-4.4	-4.5	-4.8	-4.5
Distance from tip (mm):	29.7	21.3	33	14.6	0.7	2.2
<b>First contact</b>						
Knee angle (deg):	103.6	108.7	104.2	101.5	106.8	106.7
Hip angle (deg):	97.4	93.9	99.2	89.6	97.6	95.9
Trunk angle (deg):	28.1	29.7	27.5	33.7	27.9	30.1
Shoulder angle (deg):	30.5	46.5	34.7	22.9	17.7	20.9
Elbow angle (deg):	170.2	170.3	172	168.1	174.2	175.5
Lean angle (deg):	1.4	0.9	2.3	1.2	0.3	1.8
Landing velocity - x (m/s):	0.51	0.35	0.24	-0.03	-0.26	0.24
Landing velocity - y (m/s):	-4.24	-4.36	-4.37	-4.5	-4.85	-4.49
Landing velocity - resultant (m/s):	4.27	4.38	4.38	4.50	4.85	4.50
<b>Max Squat</b>						
Knee angle (deg):	95.5	101.2	176.2	999	103.3	101.6
Hip angle (deg):	95.8	84.4	8.2	999	101.5	97
Trunk angle (deg):	23.9	34.7	43.1	999	22.3	24.6
Shoulder angle (deg):	0.1	30.7	999	999	24.8	18.3
Elbow angle (deg):	175.7	165	999	999	171	179.6
Arm speed from 1st contact (rad/sec):	8.59	12.13	327.52	656.44	9.23	12.16
Lean angle (deg):	2.8	0.4	999	999	1.9	1.6
Change in COM (mm):	1385	1242.9	836.4	-1165	1457.3	1486.2
<b>Maximum deflection</b>						
Knee angle (deg):	143.4	131.7	133.3	134.4	129.8	139.2
Knee extension (deg):	39.8	22.9	29.1	32.9	23	32.5
Impulse (percent of total time):	72	69	70.4	65.4	64	66.7
Hip angle (deg):	158.3	146.4	149	153.2	149.6	156.5
Trunk angle (deg):	9.3	9.8	12.4	9.2	7.9	8.5
Shoulder angle (deg):	126	123.5	119.8	110.9	123.8	110.4
Elbow angle (deg):	157.9	149.8	151.9	139.5	135.7	135.2
Lean angle (deg):	11	7.8	10.8	11	9.4	9.9
Arm speed from 1st contact (deg/sec):	8.59	12.13	327.52	656.44	9.23	12.16
Board deflection (mm)	1059.8	1009.3	999	947.2	962	967.1
<b>Leg Extension</b>						
Knee angle (deg):	175.7	178.4	176.8	175.1	175.9	174.6
Hip angle (deg):	168.8	160.1	169.8	160.3	162.6	163
Trunk angle (deg):	0.8	7.2	0.3	5.9	6	7
Shoulder angle (deg):	128	139.7	121.6	131.5	138.4	132.6
Elbow angle (deg):	158	155.7	156.8	132.9	142.6	134.2
Lean angle (deg):	9.4	6.5	8.4	9.5	8.2	7.9
Arm speed from maxSquat (rad/sec):	9.88	6.01	-40.82	-43.63	9.31	9.78
Impulse time since max deflection (%):	28	31	29.6	34.6	36	33.3
<b>Last contact</b>						
Knee angle (deg):	117.3	125.9	135.4	116.9	117.6	120.3
Hip angle (deg):	176.8	168.4	170.1	172.8	171.1	170.9
Trunk angle (deg):	27.4	31.2	24.1	29	30.3	33.1
Shoulder angle (deg):	157.2	151.5	156.3	151.9	153.4	157.9
Elbow angle (deg):	171.2	172.3	160.3	170.4	177.6	173.6
Lean angle (deg):	0.6	2	0.2	0.3	0.9	3.9
Impulse time (s):	0.3	0.4	0.3	0.3	0.3	0.3
Velocity - x (m/s):	1.64	1.41	1.26	1.54	1.64	1.36
Velocity - y (m/s):	5.69	5.93	5.72	5.62	5.64	5.67
Velocity - y from bfCurve (m/s):	5.88	5.66	5.79	5.52	5.57	5.72
Difference (%):	3.38	4.78	1.16	1.89	1.33	1
Resulant velocity (m/s):	5.92	6.09	5.86	5.83	5.88	5.83
Rotation of trunk (rad/sec):	1.38	1.51	1.38	1.52	1.57	1.71
<b>Flight Characteristics</b>						
CofM trajectory (deg):	16.1	13.4	12.4	15.3	16.2	13.5
Max CofM height (mm):	2816.2	2627.6	2705.1	2512.6	2570.4	2683.1
Max CofM height from bfCurve (mm):	2806.6	2620.7	2696.7	2536	2559	2688.9
Difference (%):	0.34	0.26	0.31	0.93	0.44	0.22
Measured displacement (mm):	1765.7	1627.1	1715.2	1536.8	1593.6	1649.7
Displacement using curve (mm):	1764.8	1632.2	1709.6	1551.4	1580.5	1669.2
Difference (%):	0.1	0.3	0.3	1	0.8	1.2
Time to minimum MOI (s):	0.58	0.56	0.59	0.51	0.54	0.56
Reduction in MOI (%):	67.71	66	65.82	64.75	64.82	66.3
Somersault 1 speed (ss/sec):	1.7	1.74	1.63	1.74	1.74	1.82
Somersault 2 speed (ss/sec):	2.58	2.67	2.67	2.58	2.58	80
Somersault 3 speed (ss/sec):	0	0	0	0	0	2.76
Somersault 4 speed (ss/sec):	0	0	0	0	0	80
Opening height (mm):	999	999	999	1534.3	0	584.1
Entry distance (mm):	0	0	0	0	0	0

Key Performance Indicators	2018_09_06	2018_09_06	2018_09_13	2018_09_13	2018_09_13	2018_10_18	2018_10_18	2018_10_18	RH_2019_01_17
	11_39_05_200a	11_40_31_200a	11_06_40_200a	11_07_49_200a	11_09_05_200a	11_19_01_200a	11_20_13_200a	11_21_32_200a	12_03_17_200a
<b>Best model: 9</b>									
<b>First contact</b>									
Knee angle (deg):	179	177.1	177.7	176.7	179.1	173.3	176.7	173.7	176.6
Hip angle (deg):	173.2	169.9	171.4	171.1	171.8	177.9	176.3	179.4	173.7
Trunk angle (deg):	5.5	7.8	7.4	5.8	7.4	6.4	5.6	5.2	6.9
Shoulder angle (deg):	150.7	154.6	153.2	155.6	156.1	152.9	148.4	153.4	154.1
Elbow angle (deg):	173.1	176	172.7	177.1	173.1	176	177	173.6	173.9
Lean angle (deg):	1.2	2.5	3.1	2.2	3	2.9	2.2	3.6	2.2
Landing velocity - x (m/s):	0	0	0	0	0	0	0	0	0
Landing velocity - y (m/s):	999	999	999	999	999	999	999	999	999
Landing velocity - resultant (m/s):	0	0	0	0	0	0	0	0	0
<b>Max Squat</b>									
Knee angle (deg):	72.1	69.2	72.7	69.3	67.9	74.6	66.7	71.6	74.9
Hip angle (deg):	68.8	68.2	76	77.1	70.9	999	66.7	72	62.4
Trunk angle (deg):	40.3	40.7	37.2	31	38.3	999	41.1	38.7	46.8
Shoulder angle (deg):	19.9	16.3	19.7	13.9	18.6	999	13.7	14.2	21.6
Elbow angle (deg):	177.5	178.9	175.5	172.1	176.7	999	171.9	174.3	163.2
Arm speed from 1st contact (rad/sec):	6.4	5.45	6.5	6.87	6.06	41.63	5.88	5.86	5.97
Lean angle (deg):	8.4	11.5	11.5	11.3	13.1	999	10.9	11.6	7.9
Change in COM (mm):	610.6	533.7	551	474.8	482.9	-471.6	494.6	503.6	431.2
<b>Maximum deflection</b>									
Knee angle (deg):	124.8	119.7	128.1	134.3	127	138.4	125.5	133.7	126.3
Knee extension (deg):	-54.2	-57.4	-49.7	-42.4	-52.1	-34.8	-51.2	-40	-50.3
Impulse (percent of total time):	63.3	63.6	57.1	63.9	64.7	67.7	61.8	66.7	63.6
Hip angle (deg):	119.3	115.2	125.4	129.1	123.9	129.2	121.8	131.8	116.4
Trunk angle (deg):	21.2	22.5	18.8	17.7	20.4	20.2	20.3	18.1	24.5
Shoulder angle (deg):	143.7	133.6	138.9	139.4	128.4	11.5	130.7	133.2	124.7
Elbow angle (deg):	172.7	174.3	178.1	172.4	171.6	6	169.6	173	178.1
Lean angle (deg):	1.6	3.7	4.1	2.8	4.8	2.6	4.5	4.6	3.6
Arm speed from 1st contact (deg/sec):	6.4	5.45	6.5	6.87	6.06	41.63	5.88	5.86	5.97
Board deflection (mm):	752.1	726	753.9	799.3	772.8	782.7	766.1	779.7	729.5
<b>Leg Extension</b>									
Knee angle (deg):	177.4	175.6	176.5	175	176.2	176.7	174.7	107.3	175.2
Hip angle (deg):	176.5	176.7	178.8	176.5	177.7	178.9	178	177.5	179.3
Trunk angle (deg):	1.9	2.2	1	2.4	4.2	2.1	1.8	3.8	1.4
Shoulder angle (deg):	147.1	142.1	154.5	148.7	152.5	156.9	149.2	148	137.4
Elbow angle (deg):	177	171.8	178.6	175.3	177.3	178.2	174	176.5	173.3
Lean angle (deg):	3.5	3.1	4.7	2.7	5.4	3.9	4.3	49.2	3.9
Arm speed from maxSquat (rad/sec):	8.37	6.81	6.68	6.07	6.43	-35.73	6.48	7.08	6.67
Impulse time since max deflection (%):	36.7	36.4	42.9	36.1	35.3	32.3	38.2	33.3	36.4
<b>Last contact</b>									
Knee angle (deg):	175	175.9	175.4	175.2	177	172.6	170.1	172.8	174.1
Hip angle (deg):	174.9	172.7	175.3	175.2	172.5	175.9	176.7	174.7	178
Trunk angle (deg):	5.1	6.5	4.9	4.3	8.5	8.1	6.5	8.8	4.9
Shoulder angle (deg):	155.4	147.7	153.1	151.6	150.7	150.9	150.7	141.4	159.1
Elbow angle (deg):	172.9	171.2	172.2	174.4	174	173.1	173.5	175	175.6
Lean angle (deg):	0.4	0.1	0.2	0.8	2.2	2.3	0.6	1.9	1.8
Impulse time (s):	0.4	0.4	0.4	0.5	0.4	0.4	0.4	0.4	0.4
Velocity - x (m/s):	0.66	0.76	0.51	0.62	0.38	0.57	0.54	0.53	0.52
Velocity - y (m/s):	4.54	4.38	4.23	4.6	4.71	4.65	4.41	4.7	4.33
Velocity - y from bfCurve (m/s):	4.62	4.63	4.35	3.51	4.4	4.57	4.53	4.69	4.69
Difference (%):	1.71	5.45	2.77	31.26	7.19	1.75	2.75	0.23	7.55
Resultant velocity (m/s):	4.59	4.44	4.26	4.64	4.73	4.69	4.44	4.73	4.37
Rotation of trunk (rad/sec):	0.92	0.96	0.81	0.71	0.96	0.96	0.89	0.92	0.98
<b>Flight Characteristics</b>									
CofM trajectory (deg):	8.2	9.8	6.9	7.6	4.6	7	7	6.5	6.9
Max CofM height (mm):	2226.3	2180	2072.5	2102.3	2124	2137.4	2169.7	2228.2	2170
Max CofM height from bfCurve (mm):	2220.6	2180.5	2071.8	2116.9	2116.9	2137.1	2172	2217	2158.2
Difference (%):	0.26	0.02	0.03	0.69	0.33	0.01	0.11	0.51	0.55
Measured displacement (mm):	1088.4	1065.1	969.2	1024.4	1033.9	1034.3	1052.3	1135.5	1110.4
Displacement using curve (mm):	1086.4	1092.3	965.6	626.7	984.9	1066.4	1047	1120.1	1120.4
Difference (%):	0.2	2.6	0.4	38.8	4.7	3.1	0.5	1.4	0.9
Time to minimum MOI (s):	0.03	0.03	0.44	0.43	0.38	0.41	0.49	0.48	0.19
Reduction in MOI (%):	0.59	2.24	21.46	9.77	7.86	2.7	7.19	3.69	1.6
Somersault 1 speed (ss/sec):	0	0	0	0	0	0	0	0	0
Somersault 2 speed (ss/sec):	0	0	0	0	0	0	0	0	0
Somersault 3 speed (ss/sec):	0	0	0	0	0	0	0	0	0
Somersault 4 speed (ss/sec):	0	0	0	0	0	0	0	0	0
Opening height (mm):	999	999	999	999	999	999	999	999	999
Entry distance (mm):	0	824.6	0	0	0	0	0	0	0

Key Performance Indicators	_2018_09_06_	_2018_09_06_	_2018_09_06_	_2018_09_06_	_2018_09_13_	_2018_09_13_	_2018_09_13_	_2018_09_06_	_2018_09_06_
	11_41_58_201c	11_43_34_201c	11_45_03_201c	11_46_44_201c	11_10_27_201c	11_11_52_201c	11_13_12_201c	11_54_30_203c	11_55_57_203c
<b>Best model: 9</b>									
<b>First contact</b>									
Knee angle (deg):	999	999	179.9	179.6	179	179.4	178.2	177.9	177.5
Hip angle (deg):	999	999	170.8	175.2	172.6	176.3	174.1	167.7	171.1
Trunk angle (deg):	999	999	7.7	5.1	8.6	5.6	6.5	7.5	5.6
Shoulder angle (deg):	999	999	150.3	152.3	150.5	155.1	149.5	157.6	158.4
Elbow angle (deg):	999	999	171	171.7	173.6	176.1	167.9	172.5	174.3
Lean angle (deg):	999	999	1.8	2.8	4.2	3.7	4.2	0.6	1.8
Landing velocity - x (m/s):	0	0	0	0	0	0	0	0	0
Landing velocity - y (m/s):	999	999	999	999	999	999	999	999	999
Landing velocity - resultant (m/s):	0	0	0	0	0	0	0	0	0
<b>Max Squat</b>									
Knee angle (deg):	72.9	70.4	74.9	74.5	74.4	72.8	73.5	77.6	76.8
Hip angle (deg):	71.5	60.9	71.2	67.4	70.7	67.4	64.2	64.6	73.7
Trunk angle (deg):	36.7	44.8	37.5	43.4	38.9	42.7	44.9	44.1	34.4
Shoulder angle (deg):	11.1	21.6	5.2	31.7	9.5	20.9	23.5	24.7	5
Elbow angle (deg):	179.6	179.2	175.1	168.3	172.9	168.9	176.5	176.2	178.3
Arm speed from 1st contact (rad/sec):	73.55	46.79	6.54	4.06	4.99	5.5	5.86	6.13	6.96
Lean angle (deg):	10.4	8.1	7.8	8	11.8	10.3	11.4	4.6	7
Change in COM (mm):	999	3463.6	569.5	424.2	527.9	511.7	490	492.2	530.6
<b>Maximum deflection</b>									
Knee angle (deg):	135	126.7	135.5	132.1	130.5	130.5	127.2	138.9	140.9
Knee extension (deg):	-864	-872.3	-44.4	-47.5	-48.5	-48.9	-50.9	-39	-36.6
Impulse (percent of total time):	72.4	66.7	74.1	71.9	72.4	65.6	66.7	75.9	70
Hip angle (deg):	129.6	121.8	131.1	126.6	125.3	125.4	123.7	137.4	138.4
Trunk angle (deg):	17.6	18.8	15	17.8	18.3	18.2	18.6	9	10.1
Shoulder angle (deg):	136.8	140.3	142	143.1	139.3	117.7	135	152.8	140
Elbow angle (deg):	170.1	168	163.7	171	174.6	160.1	170	165.6	163.4
Lean angle (deg):	1.2	1.6	0.5	1.7	2.6	3.1	3	3	1.7
Arm speed from 1st contact (deg/sec):	73.55	46.79	6.54	4.06	4.99	5.5	5.86	6.13	6.96
Board deflection (mm)	747.1	999	758.9	745	999	769.1	772.3	755.5	738.9
<b>Leg Extension</b>									
Knee angle (deg):	177.4	176.1	175.1	176.7	174.1	177.2	177.6	178.3	179.7
Hip angle (deg):	177.5	178.7	178.9	180	173.4	179.4	178.8	174.6	170.7
Trunk angle (deg):	0.2	1.7	1.8	0.9	3.2	0.6	0.1	7.8	10.7
Shoulder angle (deg):	145.5	153.5	147.8	146.9	138	156.1	147.9	151.5	155.5
Elbow angle (deg):	170.8	176.3	162.5	171.6	172.2	173.5	173	167.6	162.8
Lean angle (deg):	0.7	0.4	0.8	1.7	2.6	2.8	1.3	4.1	4.1
Arm speed from maxSquat (rad/sec):	7.58	5.96	8.31	5.61	7.88	6.81	6.53	6.62	6.54
Impulse time since max deflection (%):	27.6	33.3	25.9	28.1	27.6	34.4	33.3	24.1	30
<b>Last contact</b>									
Knee angle (deg):	175.6	175.2	174.9	175.4	174.7	175	171.8	165.8	163.4
Hip angle (deg):	178	178.4	173.5	179.9	178.1	176.4	179.3	160.4	162.9
Trunk angle (deg):	1.9	3	7.5	4.5	1.4	2.2	2.9	31.3	32.3
Shoulder angle (deg):	158.6	165	163	170.8	150.6	161	167.4	155.2	159.6
Elbow angle (deg):	174.8	178.1	175.4	178.5	170.6	175.2	179.4	171.4	170.8
Lean angle (deg):	6	6.9	5	6.7	4.8	3.7	5.8	12.7	14.1
Impulse time (s):	0.4	0.4	0.3	0.4	0.4	0.4	0.4	0.4	0.4
Velocity - x (m/s):	0.76	0.77	0	0.65	0.66	0.54	0.64	1.2	0.87
Velocity - y (m/s):	4.6	4.37	0	4.53	4.4	4.59	4.34	4.65	4.33
Velocity - y from bfCurve (m/s):	4.79	4.83	4.77	4.71	4.56	4.51	4.55	4.49	4.39
Difference (%):	3.94	9.44	100	3.82	3.39	1.8	4.5	3.65	1.39
Resulant velocity (m/s):	4.66	4.44	0	4.58	4.45	4.62	4.39	4.8	4.42
Rotation of trunk (rad/sec):	0.66	0.72	0.79	0.71	0.66	0.68	0.7	1.37	1.48
<b>Flight Characteristics</b>									
CofM trajectory (deg):	9.4	10	NaN	8.2	8.6	6.7	8.3	14.5	11.4
Max CofM height (mm):	2266.3	2279.3	2241.4	2261.4	2162	2145.8	2161.7	2045.1	2079.6
Max CofM height from bfCurve (mm):	2291.7	2296.3	2254.2	2290.8	2180.2	2156	2186.3	2050.7	2087.7
Difference (%):	1.11	0.74	0.57	1.29	0.83	0.47	1.12	0.27	0.39
Measured displacement (mm):	1134.8	1174.4	1160.1	1124.9	1047.8	1032.9	1044.5	1008.4	1012
Displacement using curve (mm):	1168.1	1187.7	1159.6	1132	1058.4	1035.4	1054.6	1025.4	982.4
Difference (%):	2.9	1.1	0	0.6	1	0.2	1	1.7	2.9
Time to minimum MOI (s):	0.33	0.34	0.25	0.29	0.38	999	0.38	0.4	0.34
Reduction in MOI (%):	72.04	72.46	70.3	69.29	71.66	999	68.55	65.84	66.53
Somersault 1 speed (ss/sec):	0	0	0	0	0	0	0	0	0
Somersault 2 speed (ss/sec):	0	0	0	0	0	0	0	0	0
Somersault 3 speed (ss/sec):	0	0	0	0	0	0	0	0	0
Somersault 4 speed (ss/sec):	0	0	0	0	0	0	0	0	0
Opening height (mm):	999	999	999	999	999	999	999	999	999
Entry distance (mm):	0	0	0	0	0	0	0	0	0

Key Performance Indicators	2018_09_06	2018_09_06	2018_09_13	2018_09_13	2018_09_13	2018_09_13	2018_09_13	2018_10_18	2018_10_18
	11_57_40_203c	12_01_25_203c	11_16_25_203c	11_17_48_203c	11_19_24_203c	11_24_39_204c	11_26_36_204c	11_50_11_203c	11_52_07_203c
<b>Best model: 9</b>									
<b>First contact</b>									
Knee angle (deg):	175.3	179.8	179.5	178.7	179.7	179.6	177.7	174.3	178.2
Hip angle (deg):	169.4	171.6	169.5	174.5	173.3	167.8	174.6	173.8	169.2
Trunk angle (deg):	8.7	7.1	7.8	6.2	6.5	9.7	5.2	6	8.6
Shoulder angle (deg):	146.5	141.5	158	149.6	157.9	155.2	149.2	154.4	152.7
Elbow angle (deg):	168.8	171.3	174.4	170.4	178	171.5	170.4	170.7	170
Lean angle (deg):	0.4	2.3	1.3	2.7	2.9	1.7	1.7	0.7	1
Landing velocity - x (m/s):	0	0	0	0	0	0	0	0	0
Landing velocity - y (m/s):	999	999	999	999	999	999	999	999	999
Landing velocity - resultant (m/s):	0	0	0	0	0	0	0	0	0
<b>Max Squat</b>									
Knee angle (deg):	73.1	75.1	75.5	74.3	71.9	71	74.7	71.4	81
Hip angle (deg):	64.7	67.3	68.8	68.7	72.6	65.1	73.2	71.2	77
Trunk angle (deg):	42.5	40.5	40.1	38.5	34.7	41.7	34.1	35.3	34.2
Shoulder angle (deg):	29.8	38.6	22.3	18.1	6.5	22.1	5.3	26.4	8.9
Elbow angle (deg):	170.8	172.2	178.5	171.4	174.5	173.3	170	173.5	175.7
Arm speed from 1st contact (rad/sec):	4.71	4.15	5.78	5.6	5.2	4.89	5.91	4.64	6.8
Lean angle (deg):	6.6	6.9	8.3	6.6	10	8.3	9.2	7.8	6.5
Change in COM (mm):	528.5	499	510.4	455	542.4	545.7	542.9	542.2	599.1
<b>Maximum deflection</b>									
Knee angle (deg):	137.6	128.5	142.2	138.1	135.6	132.3	139.2	138.1	141.5
Knee extension (deg):	-37.7	-51.3	-37.4	-40.5	-44.1	-47.2	-38.5	-36.2	-36.7
Impulse (percent of total time):	70	64.7	71	73.3	66.7	64.5	70	70	70.4
Hip angle (deg):	136.1	126.4	137.9	132.9	130.9	125.9	138.1	133.9	138.5
Trunk angle (deg):	9.3	13.7	11	14.4	14.1	14.6	9.2	12.5	10.7
Shoulder angle (deg):	149.4	116.9	153.7	149.1	146	130.9	158.6	147.3	164.7
Elbow angle (deg):	168.4	162.1	165.5	170.4	166.8	164.4	173.1	176.4	166.5
Lean angle (deg):	1.8	1.1	0.6	0.8	0.3	2.2	1.5	1	1.1
Arm speed from 1st contact (deg/sec):	4.71	4.15	5.78	5.6	5.2	4.89	5.91	4.64	6.8
Board deflection (mm):	739	720	796.4	792.3	802.2	784.4	800.6	778.1	795.8
<b>Leg Extension</b>									
Knee angle (deg):	179.3	177.3	173.6	177.9	179.7	176.4	179.5	176.5	176.3
Hip angle (deg):	171.8	174.8	168.8	179.2	172.4	174.7	171.5	172.1	170.8
Trunk angle (deg):	9.5	9.9	8.5	3.4	8.9	11.8	10	7.1	8.9
Shoulder angle (deg):	142	152.4	154	146	142.8	149.7	148.3	143.1	145.6
Elbow angle (deg):	167.3	172.3	174.8	168.4	168.2	168.9	174.2	166	166.9
Lean angle (deg):	3.6	4.5	2.8	2.4	3.1	5.6	3.9	3.6	3.5
Arm speed from maxSquat (rad/sec):	6.01	4.54	6.4	6.51	6.66	6.09	7.19	5.81	8.45
Impulse time since max deflection (%):	30	35.3	29	26.7	33.3	35.5	30	30	29.6
<b>Last contact</b>									
Knee angle (deg):	160.9	164.6	164	163.1	167.1	166.1	164.6	168.7	175.4
Hip angle (deg):	163.4	168.8	159.6	160.2	160.5	162.9	157.3	153.2	149
Trunk angle (deg):	32.9	26.3	30.2	32.4	29.5	31.6	34.7	32	33.2
Shoulder angle (deg):	161	147.8	144.7	158.3	154.2	148.4	150.3	154.5	157.3
Elbow angle (deg):	173.6	168.6	172.6	170.3	170.9	168.2	172.9	172.7	167
Lean angle (deg):	13.1	12	9.7	12	11.3	14.3	12.3	9.9	10.2
Impulse time (s):	0.4	0.4	0.4	0.4	0.4	0.4	0.4	0.4	0.3
Velocity - x (m/s):	1.12	0.95	0.74	1.08	0.92	0.94	0.81	0.58	1.06
Velocity - y (m/s):	4.71	4.6	4.58	4.58	4.49	4.52	4.59	4.6	4.59
Velocity - y from bfCurve (m/s):	4.46	4.39	4.34	4.31	4.34	4.2	4.33	4.58	4.55
Difference (%):	5.65	4.88	5.52	6.3	3.48	7.7	5.87	0.52	0.89
Resulant velocity (m/s):	4.84	4.7	4.64	4.71	4.58	4.62	4.66	4.64	4.71
Rotation of trunk (rad/sec):	1.44	1.33	1.4	1.55	1.52	1.61	1.53	1.55	1.61
<b>Flight Characteristics</b>									
CofM trajectory (deg):	13.3	11.7	9.2	13.2	11.5	11.8	10	7.2	13
Max CofM height (mm):	2092.3	2086.7	2033.8	2017.2	2045.7	1969.8	2008.5	2146.4	2105.8
Max CofM height from bfCurve (mm):	2093.2	2086.8	2032.3	2026.3	2060.5	1977.4	2016.3	2145.7	2107.5
Difference (%):	0.04	0.01	0.07	0.45	0.72	0.39	0.39	0.03	0.08
Measured displacement (mm):	1006.3	996.2	991.8	962.3	995.2	942.1	982.5	1102.7	1089.2
Displacement using curve (mm):	1012.2	982.3	959.3	946.4	957.9	899.1	957.1	1067.5	1053.4
Difference (%):	0.6	1.4	3.3	1.7	3.7	4.6	2.6	3.2	3.3
Time to minimum MOI (s):	0.34	0.38	0.41	0.34	0.34	0.38	0.38	0.38	0.38
Reduction in MOI (%):	67.98	67.75	65.75	66.16	67.99	65.67	65.73	66.37	66.28
Somersault 1 speed (ss/sec):	0	0	0	0	0	1.6	1.6	0	0
Somersault 2 speed (ss/sec):	0	0	0	0	0	0	0	0	0
Somersault 3 speed (ss/sec):	0	0	0	0	0	0	0	0	0
Somersault 4 speed (ss/sec):	0	0	0	0	0	0	0	0	0
Opening height (mm):	999	999	999	999	999	999	999	999	999
Entry distance (mm):	0	0	0	0	0	0	0	0	0

Key Performance Indicators	_2018_10_18_	_2018_10_18_	_2018_10_18_	_2018_09_06_	_2018_09_06_15	RH_2019_01_17_	RH_2019_01_17_
	12_00_05_205c	12_02_11_205c	12_06_11_205c	15_26_02_403b	_27_26_403b	10_59_56_405c	11_01_45_405c
<b>Best model: 9</b>							
<b>First contact</b>							
Knee angle (deg):	176.5	176	174.5	178.7	179.6	179.3	179.9
Hip angle (deg):	174.5	165	159.8	175	169.5	173.6	175.7
Trunk angle (deg):	4.7	9	11.5	5.3	8.4	7.4	3.9
Shoulder angle (deg):	156.1	151.4	148	151.3	149.8	154.7	153.4
Elbow angle (deg):	170	169.1	172.3	173	177.3	176.3	172.1
Lean angle (deg):	1.6	1.7	0.8	2.7	2.1	11.3	2.2
Landing velocity - x (m/s):	0	0	0	0	0	0	0
Landing velocity - y (m/s):	999	999	999	999	999	999	999
Landing velocity - resultant (m/s):	0	0	0	0	0	0	0
<b>Max Squat</b>							
Knee angle (deg):	76.9	74.2	80.1	76.9	75.6	74.5	74.5
Hip angle (deg):	73.6	77.2	76.1	76.6	69	76.9	73.2
Trunk angle (deg):	37	33.9	33.8	37.2	41.9	33.8	39.1
Shoulder angle (deg):	41.5	37.6	3.4	17.9	20.7	8.4	16.3
Elbow angle (deg):	177.8	180	175.4	168.5	174.9	177	178.2
Arm speed from 1st contact (rad/sec):	3.43	4.24	6.11	6.89	7.03	6.19	6.81
Lean angle (deg):	7.9	9.1	6.3	10.8	9.8	12.9	10.3
Change in COM (mm):	611.1	630.5	720.5	498.7	532.9	484.5	542.2
<b>Maximum deflection</b>							
Knee angle (deg):	139.3	127.8	134.4	135.9	133.4	134.3	134.4
Knee extension (deg):	-37.3	-48.1	-40.1	-42.7	-46.2	-45.1	-45.5
Impulse (percent of total time):	75	69	65.4	58.8	62.5	63.6	64.5
Hip angle (deg):	135.3	129.7	125.7	140	138.6	137.1	140.1
Trunk angle (deg):	9.9	9.8	14.6	15	14.4	16.3	15.1
Shoulder angle (deg):	155.1	148.2	146	160.4	160.7	166.3	162.4
Elbow angle (deg):	151.1	144	149.9	112	103.6	117.6	121.5
Lean angle (deg):	3.2	2.1	3.4	6.1	6	8	6.5
Arm speed from 1st contact (deg/sec):	3.43	4.24	6.11	6.89	7.03	6.19	6.81
Board deflection (mm)	795.3	782.2	806.1	752.8	763.1	860.6	752.6
<b>Leg Extension</b>							
Knee angle (deg):	178.7	178.7	177.5	177.8	177.5	178.3	176.8
Hip angle (deg):	173.6	164.7	175.5	155.6	160	164.3	170.8
Trunk angle (deg):	9.1	13.7	10.1	17.1	17	15	9.3
Shoulder angle (deg):	151.3	153	150.2	150.8	145.9	151.7	153.4
Elbow angle (deg):	141	147.5	142.3	175.6	177.5	177.9	177.9
Lean angle (deg):	4.9	4.9	5.4	4.2	5.3	8.4	6.4
Arm speed from maxSquat (rad/sec):	4.93	5.42	7.74	9.43	8.88	7.78	8.79
Impulse time since max deflection (%):	25	31	34.6	41.2	37.5	36.4	35.5
<b>Last contact</b>							
Knee angle (deg):	141.7	153.3	153.6	176.6	174.4	175.2	176.2
Hip angle (deg):	170.9	162.6	165.7	124.2	127.2	127.1	134.6
Trunk angle (deg):	36.4	35.6	34	41.8	39.7	39.1	36.2
Shoulder angle (deg):	157.5	157.8	153.4	123.9	134.2	118.6	123.5
Elbow angle (deg):	179.8	174.6	174.6	178.9	178.4	178.3	174.8
Lean angle (deg):	15.7	15.2	16.1	2.1	2.3	1.2	5.1
Impulse time (s):	0.4	0.4	0.3	0.4	0.4	0.4	0.4
Velocity - x (m/s):	1.06	1.08	0.98	1.11	0.66	0.88	0.81
Velocity - y (m/s):	4.98	4.91	4.9	3.93	4.15	4.21	4.35
Velocity - y from bfCurve (m/s):	4.77	4.83	4.85	4.02	4.13	4.3	4.46
Difference (%):	4.39	1.67	0.95	2.2	0.67	2.12	2.47
Resulant velocity (m/s):	5.09	5.03	5	4.08	4.21	4.3	4.42
Rotation of trunk (rad/sec):	1.66	1.67	1.88	2.09	1.99	1.98	1.94
<b>Flight Characteristics</b>							
CofM trajectory (deg):	12	12.4	11.4	15.7	9	11.8	10.5
Max CofM height (mm):	2207.6	2251.6	2239.1	1777.7	1826.6	1931.6	1974.3
Max CofM height from bfCurve (mm):	2204.6	2245.3	2237.8	1754.2	1800.9	1912	1949.3
Difference (%):	0.14	0.28	0.06	1.34	1.43	1.03	1.28
Measured displacement (mm):	1167.5	1220	1222.6	859	889.7	946.2	1024.3
Displacement using curve (mm):	1159.6	1190	1200.4	822.4	867.7	944.3	1012.7
Difference (%):	0.7	2.5	1.8	4.3	2.5	0.2	1.1
Time to minimum MOI (s):	0.53	0.5	0.54	0.3	0.28	0.39	0.44
Reduction in MOI (%):	67.08	66.28	67.74	58.81	61.61	61.69	63.32
Somersault 1 speed (ss/sec):	1.86	1.86	1.82	0	0	2.29	2.35
Somersault 2 speed (ss/sec):	2.67	2.58	2.58	0	0	2.67	2.67
Somersault 3 speed (ss/sec):	0	0	0	0	0	0	0
Somersault 4 speed (ss/sec):	0	0	0	0	0	0	0
Opening height (mm):	999	999	999	999	999	381.7	577.7
Entry distance (mm):	0	0	0	0	0	0	0

# Appendix C - CSV Output

Filename: c:\temp\RH\_2019\_01\_17\_11\_41\_10\_1\_obData.csv

First contact frame: 161  
Last contact frame: 198

Frame:	Board top(x):	Board top(y):	Angle(x):	Angle(y):	Knee(x):	Knee(y):	Hip(x):	Hip(y):	Ribs(x):	Ribs(y):	Ribs(z):	Neck(x):	Neck(y):	Neck(z):	Head(x):	Head(y):	Shoulder(x):	Shoulder(y):	Elbow(x):	Elbow(y):	Wrist(x):	Wrist(y):	COM(x):	COM(y):	Knee angle:	Hip angle:	Shoulder angle:	Neck angle:	Elbow angle:	Lean angle:	MOI:
196	0	0	-45.5	9.3	187.2	339.9	136.1	682	-27.7	1076	-116.7	1242.7	-179.7	1450.3	-162.5	1179.1	-273.9	1429.3	-405.5	1622.3	18.4	835.5	136.4	165.9	136.4	165.9	151.3	168.9	169.6	4.4	13
197	0	0	7	114.7	250.5	414.7	156.8	760.1	-29.8	1140.9	-113.7	1298.2	-172.3	1512.4	-156.4	1232.3	-277.4	1482.8	-426	1688.8	40.5	905.6	125.9	168.9	151.6	167	168.9	167	168.9	2.4	12.8
198	-20.5	64.4	219.8	309.3	499.8	176.3	831.4	-30.4	1201.7	-117.6	1355.5	-172.5	1573.6	-155.4	1192	-274.5	1536.3	-427.9	1744.4	59.8	975.8	116.9	172.8	151.9	164.2	170.4	164	170.4	0.4	12.6	
199	59.8	122.1	325.3	368.3	585.1	195.9	902.9	-30.9	1262.5	-121.5	1414.8	-171.6	1634.8	-154.5	1351.8	-271.6	1589.9	-429.8	1808.1	79.1	1046.1	108.2	176.2	151.8	162.7	170.2	3.4	12.5			
200	0	0	184.7	430.4	422.9	680.8	214.2	967.6	-30	1319.1	-132.3	1475.9	-180.3	1695	-158.8	1418.1	-262.3	1643.5	-413.2	1869.9	95.5	1116.6	100.5	178.7	152	159.4	169.7	7.5	12.4		
201	0	0	249.6	525.3	479.5	785.1	227.2	1007.7	-25.7	1360.4	-123.2	1518.1	-168	1726.5	-166	1483.2	-252.5	1714	-376.4	1907.5	117.1	1173.1	89.9	167.1	151.7	160.6	167.7	11.6	12.1		
202	0	0	314.8	620.6	536.3	889.7	240.2	1047.8	-21.5	1401.6	-114.2	1560.4	-155.8	1758.1	-173.2	1548.3	-242.6	1784.6	-339.6	1954.1	138.7	1229.7	78.7	154.5	150.3	161.5	166.6	16.1	11.9		
203	0	0	383.9	719.1	574.8	1006.7	258.6	1107.3	-22.8	1440.2	-119.6	1604.1	-163	1817.3	-162.5	1579.8	-208.6	1823.4	-289.1	2012.6	156.2	1295	74	147.8	145.7	160.8	167.9	21.6	11.5		
204	0	0	453.1	818	613.4	1124	277.1	1166.9	-24.2	1478.8	-125	1647.9	-170.2	1876.6	-151.9	1611.3	-174.5	1862.3	-238.5	2071.2	173.6	1360.4	69.7	141.3	140.9	160.3	168	27.7	11.1		
205	0	0	523.8	920.2	623.4	1244	300.7	1223.5	-16.6	1510.3	-130.4	1692.8	-183.1	1899.1	-140.8	1674.4	-136.4	1894	-170.2	2076.5	188.3	1424.2	69.3	134.2	141.6	162.7	168.2	33.2	10.6		
206	0	0	594.6	1022.7	633.5	1364.2	324.3	1280.2	-8.9	1541.8	-135.8	1737.6	-195.9	1921.6	-129.7	1737.6	-98.2	1925.8	-101.8	2081.9	203	1488.1	68.3	126.6	138.7	165.1	168.9	40.1	10.2		
207	0	0	668	1133.8	635.3	1480.7	351.1	1341	-3.3	1573.3	-127.4	1758	-215.5	1950.3	-119.5	1739.7	-59.3	1941.3	-22.7	2117.1	222.2	1543.8	69.2	120.5	128.6	165.5	172.9	47.3	9.6		
208	0	0	741.7	1245.3	637	1597.5	377.9	1402	2.3	1604.5	-118.9	1774.4	-195.1	1979	-109.3	1747.7	-20.2	1956.7	56.7	2152.5	241.4	1599.6	69.4	114.5	118.5	164.7	179.1	54.6	9.1		
209	0	0	783	1369.7	616.6	1689.9	400.7	1462.1	20.9	1633.2	-103.5	1783.6	-197.9	1996.4	-88.7	1760.1	28.1	1975.3	125.7	2168.2	256.5	1648.8	70.9	110.8	112.7	166.1	178.4	62.1	8.4		
210	0	0	824.4	1494.5	600.1	1782.5	423.5	1522.3	39.6	1641.5	-88.1	1792.8	-200.7	2013.8	-68	1778.5	76.4	1993.9	154.8	2184	271.6	1607.9	71.4	106.7	107.9	166.8	178.4	68.7	7.9		
211	0	0	839.5	1655.2	578.4	1867	447.4	1585.6	55.2	1660.9	-70.4	1819.4	-190.3	2025.1	-43.4	1792.8	113.8	2022.8	246.6	2206	285.8	1753	73.4	104.2	109.1	171.9	178.7	77.9	7.4		
212	0	0	854.6	1776.3	556.6	1951.6	471.4	1649.1	70.8	1680.3	-52.7	1846	-180	2036.5	-18.7	1807.1	151.2	2051.7	298.5	2228	300.1	1808.1	75.3	101.4	109.9	177	174.7	86.7	7		
213	0	0	843.3	1899.3	517.1	2033.1	495.5	1712.6	99.7	1697.6	-33.2	1853.2	-158.5	2044.7	9.2	1828.6	177	2062.1	336.2	2258.2	310.2	1855.5	71.6	96.1	109.4	172.4	176.7	94.2	6.5		
214	0	0	832	2022.6	477.7	2114.8	519.6	1776.4	128.6	1715	-13.7	1860.3	-137	2053	37.1	1850.1	202.9	2072.5	374	2288.5	320.4	1902.9	68.4	91.1	109.1	167.9	178.2	103.6	6.2		
215	0	0	795.3	2131.5	449.4	2170.5	543.8	1836.7	173.1	1744.2	14.1	1874.6	-117.4	2048.8	56.9	1860.8	229.6	2074.2	380.9	2308.2	333.1	1944.8	67.6	88.1	96.2	166.5	173.8	112	5.9		
216	0	0	758.5	2240.6	421	2226.2	568	1897.1	217.7	1773.4	42	1888.9	-97.9	2044.7	76.7	1871.4	256.3	2076	387.8	2370.2	345.7	1986.8	68.5	85.4	83.7	165.3	166.5	121.7	5.7		
217	0	0	712.2	2336.1	382.5	2250.2	579.9	1961.6	261	1796.1	81.1	1892.8	-74	2042.2	143.9	1902.9	291.4	2116.6	389	2373.7	356.7	2023.6	70.3	83.1	9	164.5	166.1	131.3	5.4		
218	0	0	667.4	2426.7	344	2274.2	591.7	2026.3	304.4	1813.7	120.2	1896.6	-50.1	2039.8	211.2	1924.5	326.5	2157.3	390.3	2427.3	367.7	2060.3	70.3	80.7	113.8	162.9	166.1	140.8	5.2		
219	0	0	614.1	2496.5	320.1	2286.8	619	2088.5	351.1	1853.3	156.6	1900.4	-24	2028.8	253	1892.2	346.9	2170	375.4	2441.8	388.5	2096.3	69.2	76.8	108.1	158.7	162.5	150.3	5		
220	0	0	560.7	2546.3	314.2	2299.4	645.5	2150.9	421.8	1891.9	213.1	1904.2	1.1	2018.7	294.9	1969.9	367.4	2182.8	360.6	2465.3	409.4	2120.3	68.8	73.4	102.9	154.5	160.1	160.4	5		
221	0	0	508.3	2594.5	300.3	2399.4	645.6	2209.5	480.6	1927.3	267.3	1909.3	40.3	1980.8	341.7	1980.1	392.3	2224.8	341.7	2435.3	423.6	2164.9	69.5	74.2	99.3	157.6	156.7	168.4	4.9		
222	0	0	455.9	2642.8	286.4	2399.3	645.8	2268.1	539.6	1962.8	321.5	1914.5	78.4	1941.8	388.6	1990.3	417.3	2269.3	322.8	2470.2	437.9	2127.5	68.6	75.8	94.4	160.8	149.1	172.8	4.9		
223	0	0	401.3	2646.2	291.6	2306.9	639.7	2333.2	586.4	2014.9	381	1929.7	137.7	1896.6	435.6	1995.6	435.6	2252.5	326.4	2538.8	456.2	2201.7	67.9	76.1	86.4	165.2	151.8	178.8	4.9		
224	0	0	346.8	2649.5	296.9	2314.6	633.6	2398.3	633.3	2067	440.6	1944.9	197.1	1851.4	537.9	2000.8	453.9	2318	329.9	2447.3	474.5	2231	67.7	76	70.1	168.6	151	163	4.9		
225	0	0	312.4	2641.5	312	2312.1	624.6	2448.1	670.2	2120.5	503	1967.8	283.2	1811.2	584.4	2038.9	477.1	2337.3	318.4	2608.8	497	2255.4	66.5	74.3	66.5	179.6	142.9	154.4	4.9		
226	0	0	278	2633.5	327.1	2309.7	615.6	2498	707.1	2174.1	565.6	1990.7	459.5	1770.9	631	2077.2	500.4	2356.6	306.9	2434.4	519.5	2280	65.6	72.6	63.2	168.1	136.8	154.6	5		
227	0	0	263.1	2616.5	346.2	2286.3	589.1	2532.3	714.2	2211.1	676.4	2021.7	599	1782.6	676.7	2103.4	525.2	2372.7	310.7	2317.2	537.4	2298.3	58.8	65.9	48.3	161.5	132	139.2	5		
228	0	0	248.2	2599.4	365.2	2263	562.5	2566.5	712.2	2248.2	687.3	2052.8	739	1794.4	722.4	2129.6	590.1	2388.9	316.4	2408.2	556.2	2316.7	52.3	59.4	33.1	158.8	128.2	132.6	5		
229	0	0	248.5	2566	407.5	2260.1	544.3	2587.3	748.7	2306.7	748.7	2306.7	857.4	1882.3	773.7	2184.9	570.2	2402.6	339.9	2387.5	580.6	2348.2	50	58.9	31.5	154.5	129.4	123.8	4.9		
230	0	0	246.9	2532.6	449.8	2257.2	526.1	2608.1	776.3	2353.3	810.6	2163.3	978.3	1970.5	825.1	2240.4	590.2	2416.3	365.3	2366.9	606	2368.8	43.8	58	31.9	149.2	130.9	114.4	4.9		
231	0	0	259.5	2494.2	497.5	2261.6	507.2	2602.7	791.9	2406.1	864.2	2217.6	1052.4	2076.7	865.1	2258.8	622	2442.6	407.4	2353.6	629.1	2388.6	47.3	57	25.4	147.8	122	105.9	4.9		
232	0	0	270.1	2455.7	545.2	2266	488.4	2549.3	807.6	2447.1	917.8	2272.1	1123.8	2183.4	905.2	2347.3	653.8	2468.9	449.6	2440.6	652.4	2390.5	45.6	55.1	20	145	121.8	97.1	4.9		
233	0	0	306.2	2402.9	601.6	2268.7	487.5	2587.9	820.6	2488.9	952.4	2332.1	1160.4	2315	940.7	2405.2	677.6	2485.3	513.1	2343.5	677.5	2426.3	46	53.8	18.1	134.5	122.4	86.5	4.7		
234	0	0	342.3	2350.1	658	2271.4	486.6	2578.6	838.6	2530.7	987	2392.3	1192.1	2447.1	976.3	2463.3	701.5	2501.8	576.8	2468.6	702.5	2445.1	46.9	53.1	17.5	122.7	120.6	75.3	4.7		
235	0	0	380.3	2301.4	722.7	2292	485.9	2548.2	824.5	2567.5	1000.3	2457.1	1212.1	2516	971.8	2529.3	714.5	2519.6	622.7	2317.9	721.1	2458.5	45.7	50.6	16.8	132.2	116.5	65.2	4.6		
236	0	0	426.5	2240.1	787.5	2312.5	485.3	2517.8	815.3	2604.3	1013.5	2522	1232.1	2585.1	967.3	2595.															

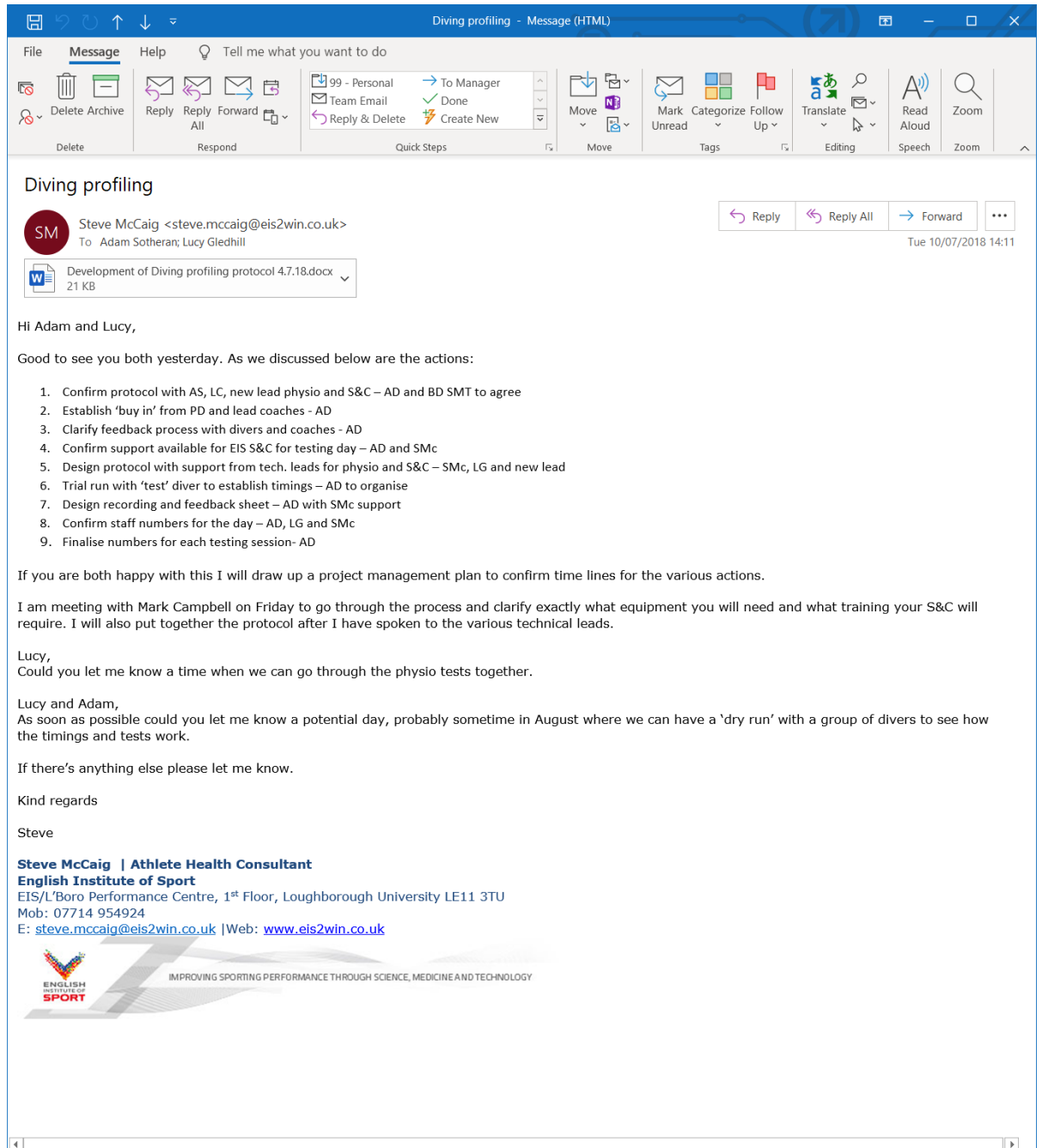
Filename: c:\temp\Hc\_2019\_01\_17\_11\_16\_04\_1\_ob\ObjData.csv

First count 162  
Last count 229

Frame:	Board (l):	Board (r):	Angle (l):	Angle (r):	Knee (l):	Knee (r):	Hip (l):	Hip (r):	Rib (l):	Rib (r):	Neck (l):	Neck (r):	Head (l):	Head (r):	Shoulder (l):	Shoulder (r):	Elbow (l):	Elbow (r):	Wrist (l):	Wrist (r):	COM (l):	COM (r):	Knee angle:	Hip angle:	Shoulder angle:	Neck angle:	Elbow angle:	Lean angle:	MDI:	COM y (m) offset:	MDI (smoothed):	
224	0	-232.4	-349.3	-215.1	195.7	-165.3	641.2	-470.7	1215.4	-643.2	1410.1	-780.2	1680.4	-674.1	1457.3	-906.9	1704.7	-843.9	1980.2	-47.9	618	175.4	144.5	177.8	166.5	123.9	7.6	13.6	2.9	3		
225	0	-216.2	-247.2	-164.7	282.7	-133.3	748.7	-458.7	1205.5	-647.4	1477.7	-799.2	1707.5	-696.3	1498.1	-851.5	1709.4	-943.7	2004.1	-29.2	618	175.4	144.1	178.5	140.1	171.7	123.5	7.3	13.3	17.2	2.1	
226	0	-203.5	-145	-114.2	368.9	-61.1	854.4	-466.7	1355.7	-651.7	1535.6	-818.2	1760.6	-722.5	1538	-899.6	1714.1	-1043.1	2027.9	-10.6	739.8	176.3	137.4	177.1	170.4	131.2	7	13.2	31.7	6.7		
227	0	65.9	-34.8	180.4	327.4	225.1	680.4	-56.2	1028.2	-246.5	1151.1	-363.3	1297.9	-271.1	1132.4	-477.3	1236.3	-563.9	1434.2	-2.6	787.1	169.8	133.8	179	161.4	140.5	4.8	12.8	466.3	8		
228	0	-171.2	72.9	-28.4	566.9	30.6	1066.8	-447.3	1483.2	-708.3	1627.5	-882.3	1821.4	-716.7	1593.5	-1054.6	1644.3	-1206.4	1873.6	12.6	839.7	170.6	124.3	166.1	160.8	131.7	7.7	12.4	530.6	9		
229	-296	2.4	-143.8	186.1	3.4	664.5	79.5	1171.6	-467.4	1540.3	-720.6	1671.7	-900.1	1865.4	-704.7	1631.3	-1092.1	1603.8	-1266.5	1796.6	27.9	892.4	171.5	115.5	155.1	160.3	128.2	8.5	12.2	658.3	9.7	
230	1063	2245.7	-110.6	290.4	13.8	791.6	115	1289.3	-412.6	1596.9	-702.7	1698.7	-904.1	1876.4	-692.2	1652.4	-1055.5	1544.1	-1281.6	1680.9	46.7	945.7	177.5	108.8	152.3	158	132.2	9.3	13	1375.2	10.2	
231	0	165.9	274.2	254.4	647.8	359.6	995	0.8	1190.1	-234.2	1253.9	-392	1379.3	-232	1215.9	-484.4	1090.8	-684.9	1159.5	65.6	999.1	176.3	101.5	147.3	156.9	134.9	7.9	10.5	883.8	10.4		
232	0	-25.3	491.4	35.1	1025.9	182.1	1520.8	-961.5	1731.4	-679	1745.2	-901.9	1882.1	-624.9	1710	-932.3	1451.9	-1221.6	1447	84.9	1047.6	169.9	94.6	144.5	151	140.9	12	9.8	906.9	10.4		
233	0	28.8	588.1	49.9	1133.1	213.8	1634.6	-353.3	1809.2	-673.1	1754.9	-895.7	1876.7	-570	1746.5	-945.6	1419.4	-1146.9	1332.4	104.3	1096.2	163.5	88.2	146.9	145.3	146.9	33.9	9.2	1017.9	10.3		
234	0	110.7	717.7	28.2	1241.4	223.6	1727.6	-360.4	1843.9	-659.8	1761.6	-903.3	1880.2	-573.2	1721.6	-742.4	1370.4	-989.4	1249.6	116.6	1135	149.1	79.3	145.4	138.8	141.6	19.3	8.4	1120.5	10.1		
235	0	194.9	847.8	10.4	1349.8	233.4	1820.8	-355.5	1878.7	-646.4	1758.4	-910.9	1883.6	-576.4	1696.6	-639	1321.3	-831.4	1170.5	128.9	1173.9	134.4	70.3	139.1	131.9	137.7	25.2	7.8	1213.5	9.7		
236	0	275.6	974.5	8.5	1437.9	231.5	1913.5	-333.5	1920	-607.1	1783.1	-900.8	1857.4	-537	1719.3	-488.2	1365.1	-643.9	1143.1	148.9	1219.1	125	65.5	126.7	139.3	137	30.4	7.2	1298.8	9.3		
237	0	356.7	1101.7	6.6	1526	229.6	2006.4	-311.4	1961.4	-567.8	1807.7	-890.6	1831.3	-497.5	1742.1	-336.7	1409	-455.5	1115.6	290.5	1542.3	63.8	52	82.7	141.6	142.2	112.6	5.2	1376.9	8.9		
238	0	561.1	896.2	278.9	1137.7	421.7	1490.2	33.9	1426.1	-127.4	1309	-353.6	1317	-53.3	1271.2	105.2	1068.5	78	865	185	1307.1	90.5	58.9	112.7	142	134.4	42.3	6.2	1457.6	8.5		
239	0	517.8	1465.7	53.8	1674	186.9	2190.5	-339.9	2002.3	-514.5	1810.1	-813.6	1777	-576.2	1781.9	-75.6	1576.3	-7.9	1303.2	201	1350.1	99.7	55.9	1149	138.4	138.5	55	6	1477.6	8		
240	0	561.7	1653.2	77.5	1744.4	179.4	2271.4	-324.1	2008.8	-472.1	1796.7	-768.2	1705.4	-338.2	1755.1	12.8	1865.3	220.1	1386.7	89.7	51.5	1023.5	142.2	136.6	155.2	5.7	267.2	5.7	267.2	5.7		
241	0	605.4	1841.4	101.2	1814.8	171.9	2353	-308.8	2015.3	-429.8	1783.3	-722.8	1633.2	-300.1	1808.3	101.6	1795.5	288.1	1618.4	239.3	1423.3	79.5	47.4	94.2	144.7	13.8	76.6	5.6	1604.2	7.2		
242	0	596.2	2027.8	132.7	1887.7	135.3	2425	-288.6	2054.8	-368.8	1793.7	-627.2	1630.2	-384.3	1917.2	384.3	1917.2	384.3	1917.2	384.3	1917.2	384.3	1917.2	384.3	1917.2	384.3	1917.2	384.3	1917.2	384.3	1917.2	384.3
243	0	601.2	2216.6	188.1	1958.2	94.4	2486.3	-254.2	2080.8	-298.7	1805.7	-534.1	1583.3	-154.9	1868.9	178.8	2042.4	440	1827.2	272.3	1504.1	68	50.8	88.7	142.8	142.7	100.3	5.2	1756.6	6.3		
244	0	606.2	2405.5	243.7	2028.9	53.6	2547.6	-219.7	2106.8	-228.5	1817.8	-540.8	1563.6	-72.1	1894.2	213.9	2151.6	495.8	2173.5	290.5	1542.3	63.9	52	82.7	141.6	142.2	112.6	5.2	1376.9	8.3		
245	0	558.5	2731.1	299.9	2153.1	51.1	2588.6	-194.9	2109.5	-165.8	1827.5	-317.2	1527.7	-99	1897.2	178.1	2338.7	474.1	2315	80.3	1501.1	64.8	56.8	62	147.4	143.3	124.4	5.4	1894.1	6.1		
246	0	484.1	2708.4	324.1	2247.9	-12.4	2595.4	-144	2065.7	-61.9	1835.3	-171.2	1532	11	1937.8	193.3	2303.7	452.4	2440.5	323.7	1603.7	63.3	58.1	74.5	140.7	142.6	137.6	5.3	2054.9	5.9		
247	0	529.3	2833.5	362.7	2352.9	-56.1	2612.7	-102	2319.4	-62.2	2359.3	-90.9	2003.8	-52.9	2463.3	235	2612.7	119.3	2833.5	362.7	1603.7	63.3	58.1	74.5	140.7	142.6	137.6	5.3	2054.9	5.9		
248	0	521.5	2091.1	550.2	1741.2	216.2	1895.7	244.8	1498.1	367.2	1333.3	357.2	1125.1	392.1	1453	414.2	1746.8	567.9	1896.1	354.6	1668.8	60.5	60.9	76.9	140.6	137.6	158.6	5.5	2072.5	5.7		
249	0	221.2	3033.9	361	2548.7	-10.1	2649.7	30.6	2110	193.9	1921.6	358	1616	255.5	2077.5	175	2477.5	337.8	2757.5	359.9	1697.7	62.5	61	70	167.8	138.5	170.4	5.7	1919.1	5.7		
250	0	130.5	3043.2	345.4	2619.2	-157.7	2614.3	103.4	2122.8	299.3	1981.7	504	1723.5	326.6	2142.2	179.3	2511	300.7	2808	377.5	1715	63.8	62.6	73	164.2	135.8	179.7	5.6	2069.9	5.7		
251	0	473.1	1101.7	173.7	2841.2	-10.5	2318.1	537.5	2550.6	405.1	2042	648.9	2863.7	398	2209	183.6	2544.6	263.6	2858.4	369.2	1732.3	63.8	64	75.7	161.6	133.2	169.2	5.2	2137.2	5.7		
252	0	-45.4	3033.4	319	2740.1	-192.1	2554.7	225.8	2200.2	479.8	2144.9	749.1	1986.4	441.6	2295	200.7	2572.9	212.2	2887.8	406.3	1759.4	58.7	60	72.8	161.6	137	158.9	5.5	2196.2	5.7		
253	0	-130.7	3014.3	308.2	2790.4	-209	2530.5	275.3	2265	554.8	2248.2	849.8	2118.1	488.5	2381.3	217.7	2601.2	160.8	2899.2	417.3	1786.4	53.7	55.4	68.4	163.7	140.3	147.9	5.4	2259.9	5.6		
254	0	-357.0	2817.2	169.7	2772.4	-239.1	2347.5	581	2729	561.9	3040	695.2	3207.5	456.2	2909.1	362.4	2709.3	17.4	2662	522.5	1776.6	46.5	43.8	61.5	163.9	150	5.9	4.8	2473.8	5.6		
255	0	-248.5	2901.6	238.9	2824.9	-160.8	2451.7	418.5	2373.9	689.4	2470.7	1006.6	2460.6	60.7	2545.5	252.2	2642.2	79	2878.6	451.9	1832.8	52.9	51.4	54.8	158.5	140.9	125.3	5.4	2348.9	5.5		
256	0	-271.8	2820.3	281	2833.5	-115.3	2411.5	470.3	2445.1	709.4	2583.8	40.2	2641	645.9	2637.3	259.7	2660.3	50	2863.1	462.8	1829.9	50.9	49.2	50.7	160.1	139.4	114	5.3	2391.4	5.5		
257	0	78.4	1972.4	430.6	2026.8	229.9	1697.5	659.2	1778.8	812.4	1900.3	1033.8	1977.2	773.3	1925.7	481.5	1905.5	309.7	2037.8	480.5	1856.4	49.7	47.9	48.1	160.8	138	105.9	5.3	2430.5	5.5		
258	0	-273.5	2647.1	173.7	2841.2	-10.5	2318.1	537.5	2550.6	405.1	2042	648.9	2863.7	398	2209	183.6	2544.6	263.6	2858.4	369.2	1732.3	63.8	64	75.7	161.6	133.2	169.2	5.2	2137.2	5.7		
259	0	-240.2	2555.9	161.2	2819.9	65.7	2286.2	554.8	2613.8	672.4	2893.5	400	3024	670.7	2817.4	510.1	2694.5	41	2762.8	500.2	1873.9	46.6	46.1	47.3	154.1	137.1	81.3	5.1	2372.2	5.4		
260	0	-206.8	2464.8	148.7	2798.5	142.1	2254.3	572.2	2677.1	633	2990.2	821	3232	715.4	2963.6	335.3	2709.6	-10.6	2720.1	510.4	1889.6	46.1	44.7	46.1	152.2	135.1	70.1	5.1	2429.3	5.3		
261	0	-142.3	2364.6	169.7	2772.4	-239.1	2347.5	581	2729	561.9	3040	695.2	3207.5	456.2	2909.1	362.4	2709.3	17.4	2662	522.5	1776.6	46.5	43.8	61.5	163.9	150	5.9	4.8	2473.8	5.6		
262	0	-77.8	2304.3	172.8	2772.4	-239.1	2347.5	581	2729	561.9	3040	695.2	3207.5	456.2	2909.1	362.4	2709.3	17.4	2662	522.5	1776.6	46.5	43.8	61.5	163.9	150	5.9	4.8	2473.8	5.6		
263	174	2711.																														

## Appendix D - Health and Safety documentation

### D.1 Health team involvement and support of profiling



**Diving profiling**

Steve McCaig <steve.mccaig@eis2win.co.uk>  
To Adam Sotheran; Lucy Gledhill

Development of Diving profiling protocol 4.7.18.docx  
21 KB

Hi Adam and Lucy,

Good to see you both yesterday. As we discussed below are the actions:

1. Confirm protocol with AS, LC, new lead physio and S&C – AD and BD SMT to agree
2. Establish 'buy in' from PD and lead coaches - AD
3. Clarify feedback process with divers and coaches - AD
4. Confirm support available for EIS S&C for testing day – AD and SMC
5. Design protocol with support from tech. leads for physio and S&C – SMC, LG and new lead
6. Trial run with 'test' diver to establish timings – AD to organise
7. Design recording and feedback sheet – AD with SMC support
8. Confirm staff numbers for the day – AD, LG and SMC
9. Finalise numbers for each testing session- AD

If you are both happy with this I will draw up a project management plan to confirm time lines for the various actions.

I am meeting with Mark Campbell on Friday to go through the process and clarify exactly what equipment you will need and what training your S&C will require. I will also put together the protocol after I have spoken to the various technical leads.

Lucy,  
Could you let me know a time when we can go through the physio tests together.


Lucy and Adam,  
As soon as possible could you let me know a potential day, probably sometime in August where we can have a 'dry run' with a group of divers to see how the timings and tests work.

If there's anything else please let me know.

Kind regards

Steve

**Steve McCaig | Athlete Health Consultant**  
**English Institute of Sport**  
EIS/L'Boro Performance Centre, 1<sup>st</sup> Floor, Loughborough University LE11 3TU  
Mob: 07714 954924  
E: [steve.mccaig@eis2win.co.uk](mailto:steve.mccaig@eis2win.co.uk) | Web: [www.eis2win.co.uk](http://www.eis2win.co.uk)



ENGLISH INSTITUTE OF SPORT

IMPROVING SPORTING PERFORMANCE THROUGH SCIENCE, MEDICINE AND TECHNOLOGY



## D.2 Risk assessment for diving squad pool training

Produced By Nikki Smith

Sheffield Diving Ltd - Diving Risk Assessment

### RISK ASSESSMENT - Diving Squad Session - Diving Pool, Ponds Forge I.S.C

HAZARD	RISK	PEOPLE AT RISK	CONTROL MEASURES	COMMENTS/ACTIONS	RESIDUAL RISK RATING L M H	SEVERITY RISK RATING L M H	INITIAL IF ALL IN PLACE
Deep water	<ul style="list-style-type: none"> <li>- Diver performs a bad dive (e.g. winding them) then they may struggle to swim to the side</li> <li>- Weak swimmers</li> </ul>	Staff, Participants, Volunteers	<ul style="list-style-type: none"> <li>• Participants must be able to swim competently in deep water without goggles</li> <li>• Staff hold an NPLQ or NRASTC qualification and are up to date with training guidelines</li> <li>• Ensure participants are medically fit to participate</li> </ul>	<p>Participants complete registration form with medical details / consent</p> <p>Incidents reported to the facility staff</p>	Medium	High	NS
Staff not appropriately qualified or trained to deliver session	<ul style="list-style-type: none"> <li>- Appropriate NGB, NPLQ or NRASTC qualifications not held</li> <li>- DBS clearance not obtained</li> <li>- Recommended training guidelines not adhered too</li> </ul>	Staff, Participants, Volunteers	<ul style="list-style-type: none"> <li>• Level 1 coaches and volunteers must work under supervision of a Level 2 coach</li> <li>• Lead coach must be Level 2 qualified or above and hold a NPLQ or NRASTC qualification</li> <li>• Coaches attendance at staff training recorded and monitored</li> <li>• A NPLQ qualified person will be on poolside during diving sessions</li> <li>• Staff holding NRASTC qualification to attend NPLQ training monthly</li> <li>• Lifeguard employed on sessions if the coach is not qualified or up to date with training</li> <li>• Session cancelled if associated risks are too great</li> </ul>	<p>If L2 coach is not present session cannot take place</p> <p>L2 coach can supervise max of 6 assistant teachers if not directly supervising a group and 2 if responsible for teaching group</p>	Medium	High	NS
Class size exceeds Swim England ratio guidelines	Amount of participants hinders staffs ability to supervise the session	Staff, Participants, Volunteers	<ul style="list-style-type: none"> <li>• Adhere to Swim England recommendations that coaches work to a 20:1 ratio (strictly poolside only)</li> <li>• Adhere to Swim England recommendations that coaches work to a 10:1 ratio for squad sessions.</li> <li>• Sheffield Diving works at a maximum of 12:1 for competitive squads. Participants ability and experience is risk assessed by coaches.</li> <li>• There is no legislation in place for appropriate ratios for a level 1 coach. A level one coach will adopt a 1:8 ratio. Level 1 coaches will be under the supervision of a level 2 coach.</li> </ul>	<ul style="list-style-type: none"> <li>• If ratio exceeds 1:12 then divers will be split into 2 groups and 1 group taken at a time. The session will not take place if there are no level 2 coach</li> <li>• See Safe Supervision document produced by Swim England for information about class ratios</li> </ul>	Low	Medium	NS



Signed:

Date: 1<sup>st</sup> April 2019 Review Date: 1<sup>st</sup> April 2020

Risk Assessment Carried Out By: Nikki Smith

Sheffield Diving Ltd - Diving Risk Assessment

Produced By Nikki Smith

	Slips, Trips & Falls	Staff, Participants, Volunteers	Mats to be used for jumping and gymnastics, floor exercises and activities Warm ups supervised by staff Area is not used if it is wet	Planned and structured session	Low	Medium	NS
Warm Up on poolside	Slips, Trips & Falls	Staff, Participants, Volunteers	<ul style="list-style-type: none"> <li>Mats to be used for jumping and gymnastics, floor exercises and activities</li> <li>Warm ups supervised by staff</li> <li>Area is not used if it is wet</li> </ul>		Low	Medium	NS
Warm Up on platform stairs, balcony e.g. stair runs	Collision, fall, trip or slip	Staff, Participants, Volunteers	<ul style="list-style-type: none"> <li>Participants instructed to wear suitable footwear</li> <li>Area not open to members of the public</li> <li>Activity is progressive, appropriate to the divers development and correct running and jumping technique reinforced</li> <li>Platform stairs are not used whilst divers are using the platforms and/or the area is wet</li> </ul>	Area is checked for objects and unsafe items are removed	Low	Medium	NS
Springboard	Fall, contact injury, lack of supervision	Participants	<ul style="list-style-type: none"> <li>Surface maintenance</li> <li>Regular inspection by staff (facility)</li> <li>Coach prevents inappropriate activity</li> <li>Coach ensures divers are watched in turn and only dive when instructed</li> <li>Healthy &amp; Safety regulations explained to all users</li> </ul>	Letting body to carry out regular checks	Low	Low	NS
Platform	Squad members diving from different areas of diving pit	Participants	<ul style="list-style-type: none"> <li>One board used at once in a session</li> <li>Coach ensures divers are watched in turn and only dive when instructed</li> <li>Appropriate use and safe teaching methods outlined by the Swim England</li> <li>Regular inspection by coaches and facility staff</li> <li>Healthy &amp; Safety regulations explained to all new users</li> </ul>	Letting body to carry out regular checks	Low	Medium	NS
Strains and Injuries during and after activity	Injury	Staff, Participants, Volunteers	<ul style="list-style-type: none"> <li>Recognised Coaching methods used</li> <li>Adequate Warm Up and Cool Down</li> <li>Coach check for injuries</li> <li>Participants wearing suitable clothing</li> <li>Access to Qualified First Aider, First Aid Kit &amp; phone</li> </ul>	Planned and structured coaching session	Low	Low	NS
Free Time	Collisions, slips, trips, lack of supervision	Participants	<ul style="list-style-type: none"> <li>Coach prevents inappropriate or dangerous activity</li> <li>Coach ensures divers are watched in turn and only dive when instructed</li> <li>Healthy &amp; Safety regulations explained to all users</li> </ul>		Low	Medium	Ns

Risk Assessment Carried Out By: Nikki Smith Date: 1<sup>st</sup> April 2019 Review Date: 1<sup>st</sup> April 2020

Signed:



Sheffield Diving Ltd - Diving Risk Assessment

Produced By Nikki Smith

Overhead rig	Structure of overhead rig could fail	Staff, Participants, Volunteers	<ul style="list-style-type: none"> <li>Regular checks by staff</li> <li>Regular maintenance checks organised by facility</li> <li>Safety inspection by facility staff</li> <li>Coach checks - replace as necessary</li> </ul>	Coaches to inform activity lead of any equipment faults. All faulty equipment removed or replaced	Low	Medium	NS
Harness / Rig work	Coaches become injured - back injury, slip on wet poolside, injury through use of overhead rig	Staff, Participants	<ul style="list-style-type: none"> <li>Coaches using rig have been trained by Adam Sotheran (Swim England/IOS Tutor)</li> <li>Coaches rig participants of an appropriate size</li> <li>Coaches ensure poolside area is dry before rigging</li> </ul>	Coaches to attend the Swim England/IOS dry & water harness when CPD's become available	Low	Medium	NS
Condition of pool side - Slippy, Wet, Cracked Tiles	Slips, Trips, Cuts & Falls	Staff, Participants, Volunteers	<ul style="list-style-type: none"> <li>Inspection of the floor surface to ensure it is safe for the session to take place</li> <li>Access to a qualified first aider, first aid kit and telephone</li> </ul>	Request letting body to clean or replace tiles if required	Low	Medium	NS
Obstructions: Slips, Trips & Falls (Benches, blocks, floor mats, chairs)	Slips, Trips & Falls	Staff, Participants, Volunteers	<ul style="list-style-type: none"> <li>Removal of any items to a safe distance from around the sides of the diving pit</li> <li>Mats piled away after use</li> <li>Access to a qualified first aider, first aid kit and telephone</li> </ul>	Request letting body to remove large items	Low	Low	NS
Supervision: - before, during and after a session	Unsupervised, lost children, interaction from strangers	Staff, Participants,	<ul style="list-style-type: none"> <li>Parents responsibility for children outside of designated training area</li> <li>Athletes do not go anywhere without coach</li> <li>Parent, participant &amp; coach code of conduct to be adhered to at all times</li> <li>Clear start and end times of session</li> <li>Emergency contact details available</li> <li>Controlled environment</li> </ul>	Ensure all parents and children are clear of where they need to be at certain times and their responsibilities	Medium	Medium	NS
Poolside blocks, steps to blocks and pool steps	Cuts, slips, falls	participants	<ul style="list-style-type: none"> <li>Inspection by staff and coaches each session</li> <li>Issues reported immediately to facility maintenance</li> </ul>		Low	Low	NS
Facility issues: - rescue equipment hard to find	Drowning	Participants	<ul style="list-style-type: none"> <li>Training - staff informed of rescue equipment location</li> <li>Staff attend staff training sessions</li> <li>Staff attend site specific training</li> </ul>	Staff kept informed Staff aware of facility NOP & EAP's	Low	high	NS

Risk Assessment Carried Out By: Nikki Smith

Date: 1<sup>st</sup> April 2019

Review Date: 1<sup>st</sup> April 2020

Signed:



	Dehydration	Staff, Participants, Volunteers	Regular breaks • Access to drinking water / working fountains	Planned and structured session	Low	Medium	NS
Heat Exhaustion		Participants, Volunteers					
Facility issues: - e.g. no access to alarms/radios	Drowning	Participants	<ul style="list-style-type: none"> <li>Communication - use of pool side phone on the other side of the pool</li> <li>Staff are aware of positioning of drowning alarms</li> <li>Staff to seek training on how to use radios</li> </ul>	Staff kept informed Staff aware of facility NOP & EAP's	Low	High	NS
Facility issues: - Lighting too dark or bright	Too dark / bright may be hard for divers to spot causing injury. Hard to check if the water is clear	Participants	<ul style="list-style-type: none"> <li>Ensure lighting is a correct level for diving squads</li> <li>Ensure TV lighting is altered after major events</li> </ul>	Communicate regularly with facility staff	Low	Medium	NS
Manual Handling	Back/knee injuries	Staff, Participants, Volunteers	<ul style="list-style-type: none"> <li>Suitable number of staff lifting equipment</li> <li>Suitable knowledge and training received if large and heavy items of equipment need to be moved</li> </ul>		Medium	Medium	NS
First Aid	Injury	Staff, Participants, Volunteers	<ul style="list-style-type: none"> <li>Access to a qualified first aider, first aid kit, telephone and alarm</li> <li>Coaches that hold an NPLQ qualification have emergency first aid training included in the qualification</li> </ul>	Ensure staff are appropriately qualified and renew certificates when needed	Low	Medium	NS
Emergency Exits	Injury	Staff, Participants, Volunteers	<ul style="list-style-type: none"> <li>Ensure emergency exits are unobstructed</li> <li>Ensure participants do not block the areas with mats or bags</li> <li>Ensure participants have access to space blankets and footwear if possible</li> </ul>	Staff to ensure that doors are accessible and unobstructed	Low	Medium	NS
Emergencies (Bomb threat, power cut, fires)	Injury or illness	Staff, Participants, Volunteers	<ul style="list-style-type: none"> <li>Follow the facilities EAP procedures (Emergency Action Plan)</li> <li>Ensure participants and staff know the EAP procedures</li> </ul>	Staff to remain in charge of their participants until picked up by parents	Low	Medium	NS
Child Welfare/ Safeguarding		Staff, Participants, Volunteers	<ul style="list-style-type: none"> <li>Ensure all staff have undertaken appropriate training around Safeguarding and Child Protection</li> </ul>	Ensure staff renew qualifications training and prior to expiry	Low	High	NS
Electrical equipment e.g. Plug Sockets, TV, cameras	Electric shock	Staff, Participants, Volunteers	<ul style="list-style-type: none"> <li>Ensure all poolside electrical equipment is stored safely</li> <li>Ensure all poolside electrical equipment is PAT tested</li> </ul>	Report any health and safety concerns to the facility staff	Low	High	NS



Sheffield Diving Ltd - Diving Risk Assessment

Produced By Nikki Smith

Hot Drinks	Scolds, burns	Staff, Participants, Volunteers	Staff do not walk around poolside with hot drinks	Report any health and safety concerns to the facility staff	Low	Medium	NS
The length of duty spells	Not maintaining the high levels of vigilance and concentration required	Participants Coach	<ul style="list-style-type: none"> <li>Staff do not walk around poolside with hot drinks</li> <li>Structured, controlled session</li> <li>Encourage staff to take a short break in between each session</li> <li>Assistant present when possible to allow the coach to take a break if required</li> </ul>	Advise staff to carry a drink at all times to avoid dehydration	Low	High	NS

Risk Assessment Carried Out By: Nikki Smith

Date: 1<sup>st</sup> April 2019

Review Date: 1<sup>st</sup> April 2020

Signed:



## D.3 Athlete letter of consent

15 Lindholme Gardens  
Owlthorpe  
Sheffield  
S20 6TD

March 30<sup>th</sup> 2016

Dear athlete,

### **Filming for PhD – September 2016-January 2017**

Thank you for agreeing to participate in the data-collection part of my PhD. Could you please sign the bottom of this letter to indicate your understanding of and consent to the details below:

- You are 18 years old or over
- You are prepared to be filmed approximately 8 times between September 2016 and the end of January 2017 in the diving pool at Ponds Forge International Sports Centre
- You are prepared to have reflective markers applied to either your skin (via the leukotape you usually use for joint support) or to your equipment (swimsuit/trunks/cap) before the filmed sessions (and to have the markers re-applied if necessary) as you have seen demonstrated
- You will be filmed using one camera and the scene will be lit by 4x halogen lights, all of which will be positioned in the Ponds Forge balcony
- The images captured will be used to infer biomechanical and kinematic performance information about your dive. The data will be available to you and/or your coach if you wish to see it
- The video data will be stored securely (a pass-key protected hard-drive) and will be securely deleted at the conclusion of the study
- At no point will you be asked to modify your technique or training programme; you will be filmed training as normal
- You are free to remove yourself from the study at any time
- My study has been given ethical approval by Sheffield Hallam University

If you have any questions about the study, please email ([adam.sotheran@swimming.org](mailto:adam.sotheran@swimming.org)), call (07766 660285) or see me at the pool during my normal work hours.

Thank you for your cooperation and help in my study.

Adam Sotheran.

---

**Study into real-time objective data collection contributing to the PhD study by Adam Sotheran.**

I (print name) \_\_\_\_\_ have read the parameters of the study as described above (and have been explained to me by Adam Sotheran), am compliant with its requirements and am happy to take part in the data-collection.

Signed \_\_\_\_\_

Date \_\_\_\_\_

## D.4 Letter of support from facility

[https://www.sheffieldinternationalvenues.co.uk/](#)

Sheffield International Venues  
Ponds Forge International Sports Centre  
Sheaf Street  
Sheffield  
S1 2BP  
0114 2233400

13<sup>th</sup> May 2016

Dear Sir/Madam,

Adam Sotheran

I am writing to confirm that Sheffield International Venues are happy for Adam to film in the diving pool as part of his PhD data-collection process.

We understand that he has worked with Sheffield Hallam University and the Sheffield Diving programme to ensure that all appropriate health and safety and child safeguarding processes will be followed.

Yours faithfully,

Ian Hamilton



## Appendix E - What It Takes to Win competencies

What It Takes to Win (WITTW) competencies are defined in eight areas. Competencies are rated by defined members of the World Class Programme and scored out of 10.

Gap analysis defines themes for the ensuing Individual Athlete Plan.

### Technical

#### Table ratings:

The WITTW summary table ratings are determined as follows:

Metric	Rated against	Rated by	A 10 is
Group 1-6	Closeness to BDSS standards, metrics derived from kinematic analysis and consistency in competition	Programme manager, technical coach, PA team	A dive (appropriate to place in pathway) which can consistently produce scores required for World/Olympic medal success
Acro	Ability to produce acrobatic work of a standard and quality to support and improve diving performance	Programme manager, <u>acro</u> coach, technical coach	TBC

### Tactical

#### Table ratings:

The WITTW summary table ratings are determined as follows:

Metric	Rated against	Rated by	A 10 is
Number of camps	Attendance at selected camps and a number matching that specified by international profiles and BD strategy	Programme manager, technical coach	Enough load, opportunity for physical, technical, environmental and behavioural development for Olympic success.
Number of comps	<u>A number of</u> starts matching international standards (considering the point in the athlete's career)	Programme manager, technical coach	Evidence of starts, progression, step up and score reflecting Olympic success
Camp/comp level	Athlete's profiled need for below/at/above level of competition	Programme manager, technical coach	The opportunity to build experiences to win, try new strategies and experience events at a level appropriate to point on pathway
List	Standards at athlete's level and consistency of performance in competition. At pathway level, this links to progress against skill progression charts (Table 1, Table 2)	Programme manager, technical coach	High quality performance and evidence of lead-up progression to meet the need of Olympic qualification and performance at targeted Games.

## Physical

### Table ratings:

The WITTW summary table ratings are determined as follows:

Metric	Rated against	Rated by	A 10 is
<b>Mobility</b>	Physical qualities required to minimise time loss, maximise effective training and performance of skills matching BDSS standards.	Local/Lead medical team, technical coach	Enough load, opportunity for physical, technical, environmental and behavioural development for Olympic success.
<b>Mental health</b>	The ability to manage the pressure of life, training and competition	Mental health working group, technical coach	Evidence of managing load with acceptable levels of emotional challenge, managing life and sport.
<b>CRY</b>	Cardiac Risk screen and any resulting actions	Local/Lead medical team	No risk of cardiac incident
<b>Strength</b>	The ability to tolerate a required training load, maximise performance characteristics to learn, train and compete skills appropriate to level in World Class pathway	Programme manager, S&C coach, technical coach	Able to train without modification and compete list of appropriate level and progression-skills of future necessary optionals.
<b>Respiratory</b>	Respiratory testing and resulting actions	Local/Lead medical team	No compromise to training, travel or competition due to respiratory ill-health

## Performance Nutrition

### Table ratings:

The WITTW summary table ratings are determined as follows:

Metric	Rated against	Rated by	A 10 is
General diet	A balanced meal plan that includes a variety of healthy foods from all food groups supporting performance nutrition strategies with optimal energy availability	Performance nutritionist, athlete	Demonstration of understanding and skills to plan and prepare meals that match the demands of training and competition
Body composition	What It Takes to Win-identified standards	Performance nutritionist	Male: 40-50mm Female: 50-60mm
Travel strategy	Adherence to agreed plans to promote health, energy availability and optimal time to normal training post-travel	Performance nutritionist, athlete, technical coach	Hydration: 250ml per hour + electrolytes Snack: High protein, balanced low sugar (limited chocolate etc) Implementation of individualised travel advice
Camp strategy	Behaviour facilitating the achievement of load and technical goals established for the camp	Performance nutritionist, athlete, technical coach	Adherence to behaviours (where possible) around timing, content and individual targets as described above
Competition strategy	Implementation of individualised fuelling/recovery plan.	Performance nutritionist, athlete	Evidence of following plan and adapting if necessary.

## Performance Psychology

### Table ratings:

The WITTW summary table ratings are determined as follows:

Metric	Rated against	Rated by	A 10 is
Managing pressure	Ability to use a strategy to adopt state leading to achievement of training/competition goals.	Performance psychologist, athlete, technical coach	Evidence of athlete knowing their typical pressure response and having key strategies to refocus and protect their performance
Emotional regulation	Ability to train/compete with appropriate control and behaviours regardless of circumstances.	Performance psychologist, athlete, technical coach	Athlete has managed thoughts and emotions to achieve desired behaviours; individual has regulated their physiology to be ready for performance
Competition plan	Reproduction of competition plan leading to achievement of competition goals	Performance psychologist, athlete, technical coach	a clear and consistent plan, able to execute it or achieve the purpose behind the behaviours regardless of circumstance or situation
Values	Ability to act in a manner that promotes and supports the best work of themselves and others.	Performance psychologist, athlete, technical coach	A clear set of values and behaviours as set by the athletes, staff and management that defines the agreed upon culture of the group.
Managing distraction	Ability to return to desired state following unexpected event, leading to successful performance	Performance psychologist, athlete, technical coach	Athlete recognises when they become distracted (both internal and external) and can refocus to perform skill.

## Performance Lifestyle

### Table ratings:

The WITTW summary table ratings are determined as follows:

Metric	Rated against	Rated by	A 10 is
<b>Engagement</b>	Willingness to actively engage and communicate with Performance Lifestyle Advisor and ability to understand role of PL and how to access support.	PL advisor & athlete	Athlete understands role of PL, proactively seeks support when necessary and regularly communicates with their advisor. Fully engages in initiatives and sessions run by the PL team.
<b>Independence</b>	Ability to balance commitments, manage various demands, independently organise themselves and demonstrate acquisition of key life skills with limited support required.	PL advisor, athlete, technical coach, programme manager	Athlete demonstrates excellent time-management, organisational and life-skills (cooking, cleaning, hygiene, finance and budget, food planning and shopping) allowing the athlete to attend training sessions on time with correct equipment and suitable preparation.
<b>Life after Sport</b>	Commitment to personal and professional development (PPD) such as education, work experience and career planning to maximise opportunities for post diving career.	Lifestyle advisor, athlete	Athlete has clear direction and commitment to PPD. Highly motivated and assertive with accessing/creating opportunities and does so with complete independence.
<b>Identity and Awareness</b>	Athlete able to articulate their interests and passions and think more broadly than only having an athletic identity.	Lifestyle advisor, athlete, technical coach, programme manager	Athlete regularly engages in something outside of diving to fulfil their interests and passions and to facilitate development of robust identity. Self-aware; conscious of own strengths & weaknesses.
<b>Relationships and Communication</b>	Ability to manage relationships and communicate effectively with athletes, coaches and support staff across the WCP.	Lifestyle advisor, athlete, technical coach, programme manager	Confidently communicates within performance programme and shows excellent ability to interview, speak in public and conduct themselves on social media. Develops relationships inside and outside of sport and actively maintains those through good communication.

## Experiential

### Table ratings:

The WITTW summary table ratings are determined as follows:

Metric	Rated against	Rated by	A 10 is
Funnel	Scores considered likely targets for World/Olympic success – the funnel is a projection based on season-average scores.	Performance analysis team, technical coach, programme manager	The lower-end of the funnel projects into the gold score-band
Score	The average season-best score achieved by World/Olympic medallists	Performance analysis team, technical coach, programme manager	Season <u>highscore</u> is in the gold score-band
Difficulty	The highest DD demonstrated each year by a World/Olympic medallist	Performance analysis team, technical coach, programme manager	Season-high DD is in the gold score-band
Variance	The average standard-deviation of scores achieved by World/Olympic medallists	Performance analysis team, technical coach, programme manager	Season standard deviation is under 20
Starts	The average number of competitive starts competed by World/Olympic medallists	Performance analysis team, technical coach, programme manager	Maintenance of current starts-per-season will lead to exceeding average 'Starts to first WC medal' by targeted Games
Progress	The average round-progress percentage shown by World/Olympic medallists	Performance analysis team, technical coach, programme manager	100% progress through rounds, 100% step-up
Vs Medal	The average score (as a percentage of major medal score) achieved in the season and at the diver's peak event	Performance analysis team, technical coach, programme manager	Peak scores > medal-winning score, % of best score at major event >90

## Daily Training Environment

### Table ratings:

The WITTW summary table ratings are determined as follows:

Metric	Rated against	Rated by	A 10 is
Pool	Standards detailed in Table 6	Programme manager, SSSM team, technical coach	Meets or exceeds standards
Dry	Standards detailed in Table 7 and Table 8	Programme manager, SSSM team, technical coach	Meets or exceeds standards
Time	Training hours completed in line with programme manager expectations	Programme manager, SSSM team, technical coach	Meets or exceeds standards
Team	Technical coaches, performance-support staff for medical, physical, acrobatic, PL, PN and PA with enough FTE to meet needs	Programme manager, SSSM team, technical coach	Meets or exceeds need
Space	Space for meetings, performance-support, storage of food, drink, supplements	Programme manager, SSSM team, technical coach	Meets or exceeds need

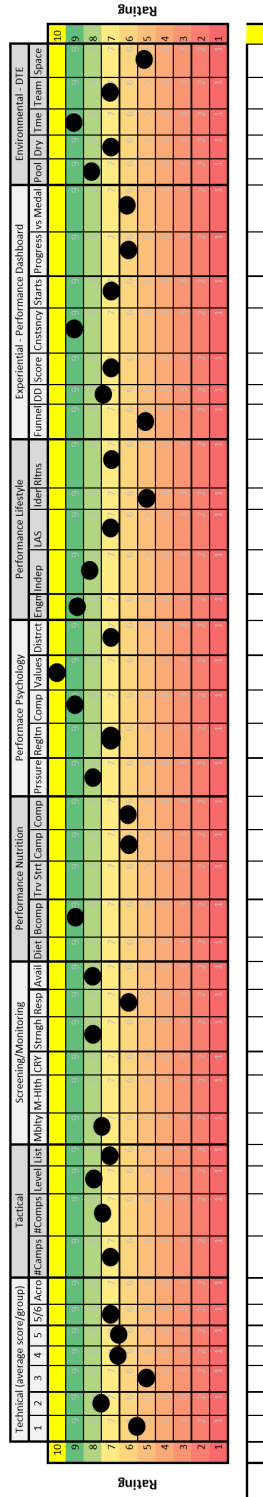


# Appendix F – Annual review feedback

Example of WITTW data and IAP presented to diver at Annual Review

## British Diving - SSSM and WITTW report

Name: Sheffield  
 Programme: Sheffield  
 Funding level: E



Rating by section	Overall rating
T: I: P: PN PS: PL: Exp: DTE	
Good choice to use 205b this season - and needs to increase DD to match ROW. Progress made with 109c and 307c.	
DD improvement on forward, consistently using 307c - similar other ops. Consistency on 109c and 307c should be improved.	
You did a good job to manage a hectic season and a large competition density. You could look at your training load and modulation to ensure you don't overtrain and peak at the times you want to	
Physio goals - 1. Increase capacity and strength in early-season 2. R Shoulder: Maintain >85deg lat rot and >45 deg med rot and >45 deg Horizontal add. S&C: increase strength through the mid-section, improved shoulder function and overhead range/strength.	
Figure out a way to increase support in other ways; LB's contract focuses on Podium athletes.	
continue to develop reset and self-reg strategies (i.e., non-emotional diving)	
1. Utilise skills for independent living. 2. Gain clarity around future career. 3. Develop communication skills inside and outside of programme	
Great job for increasing the number of starts and DD. Now you've increased exposure at world level, consistency and step up will help you get closer to the top end of finals	
Great pool, dryland could be equipped better (if there was more space). Team is committed and skilled - FTE is an issue, there isn't too much contact with some services	

## British Diving - SSSM and WITW report

### Update by section

Technical		Performance Psychology	
Forwards	Target v=6.2m/s . Need to measure and compare	Managing pressure	Strategies in place and can be used to greater effect
Back	Target v=5.3m/s for 207c. Currently v=4.7 m/s	Emotional regulation	A growth area
Reverse	Target v=6.2m/s for 207c. Currently v=5.7 m/s	Competition strategy	Well established
Inwards	Work shape for maximum spin speed	Behaviours and values	A high performing athlete in this area
Twist	Armswing by bottom of board for 5154b	Managing distraction	A development area
Twist	Narrow reach for 5337d		
Acro	More contact with RP to build acro qualities		
Tactical		Performance Lifestyle	
# Camps	Both Team A and Team B exposure	Engagement	attended all requested meetings and contributed considerably.
# Comps	A high number of starts last season - experience has built well	Independence	Independent, self-organised, punctual and highly capable.
Level	GPs, DWS, WCh and ECh - a great range	Life after sport	has considered variety of career plans and completed relevant CPD
List	New dives added this year - only one group is under	Identity and awareness	Activity outside of training is largely focused on coaching so does not offer separate focus/interest.
		Relationships and communication	Confident communicator and recently developed public speaking skills through AIP programme.
Physical		Experiential	
Mobility	Shoulder rotation is key marker for shoulder health and tends to drop in response to load.	Performance funnel	Trajectory for average score (and funnel) is downward
Mental Health	Profiling will start at an appropriate time in the next year	Difficulty	Increasing year on year and closing in on opposition
Cardiac risk	Not tested	Score	An upturn from last season - getting closer to 2017 PB
Strength	Weak post shoulder & reduced rotator cuff capacity	Consistency	Very consistent
Respiratory health	Nasal	Starts	An appropriately high number this season
Availability	15.25 days (5%) affected last season (Shoulder 14, Lumbar Spine 1.25)	Progress	Progress and step up are lower - and competitions have been harder
		versus medal	Markers are improving - need to reproduce best performances at times of greatest pressure
Performance Nutrition		Environmental	
Diet		Pool	Great pool, new springboards, all equipment there
Body composition	fine - in line with WITW targets	Dry	Well specced for space - lacks size and foam pit
Travel strategy		Time	Access is fine and meets needs
Camp plan	limited support	Team	A mix of EIS and contractors - FTE is comparatively low
Competition plan	limited support	Space	Treatment space is okay, meeting space is challenged



British Diving - SSSM and WITW report

Diver	Event	Dives	Nat Champs Jan 2019		DWS JPN-1 Mar 2019		DWS CHN-2 Mar 2019		GP CAN-2 Apr 2019		DWS CAN-3 Apr 2019		NatChamps May 2019		ECH UKR Aug 2019		Highest score	Lowest score	Average score	Range	
			Prelim	FINAL	Semi-F	FINAL	Semi-F	FINAL	Prelim	FINAL	Semi-F	FINAL	Prelim	FINAL	Prelim	FINAL					
		407C	35.70	71.40	69.70		76.50	68.00	61.20		73.10		69.70	71.40	61.20	66.30	76.50	35.70	65.84	-30.14 / 10.66	
		5337D	49.00	71.75	56.00		77.00	56.00	78.75		71.75		73.50	64.75	66.50	66.25	78.75	49.00	66.66	-17.66 / 12.09	
		107B/109C*		55.10	*		77.90	72.20	*					55.10	*	64.60	*	77.90	55.10	64.98	-9.88 / 12.92
	Men 3m	205B	67.50	72.00	63.00		67.50	67.50	61.50		67.50		67.50	72.00	63.00	72.00	61.50	67.50	61.50	67.36	-5.86 / 4.64
		307C	52.50	40.25	50.75		71.75	63.00	63.00		45.50		42.00	61.25	43.75	70.00	71.75	40.25	54.89	-14.64 / 16.86	
		5154B	76.50	78.20	76.50		71.40	73.10	79.90		66.30		71.40	78.20	66.30	73.10	79.90	66.30	73.72	-7.42 / 6.18	
	<b>Total</b>		<b>281.20</b>	<b>388.70</b>	<b>315.95</b>		<b>442.05</b>	<b>399.80</b>	<b>344.35</b>		<b>324.15</b>		<b>324.10</b>	<b>402.70</b>	<b>300.75</b>	<b>414.25</b>	<b>456.80</b>	<b>307.85</b>	<b>393.44</b>	<b>-85.59 / 63.36</b>	

Diver	Event	Dives	Nat Champs Jan 2018		GP GER Feb 2018		CWG AUS Apr 2018		GP CAN May 2018		GP ITA July 2018		Highest score	Lowest score	Average score	Range			
			Prelim	FINAL	Prelim	FINAL	Prelim	FINAL	Prelim	FINAL	Prelim	FINAL					Semi-F	FINAL	
		5337D	70.00	73.50	70.00	63.00	70.00	66.50	75.25	61.25	63.00	64.75	52.50	73.50	75.25	52.50	66.94	-14.44 / 8.31	
		107B	72.85	71.30	63.55	75.95	71.30	68.20	74.40	69.75	75.95	62.00	69.75	60.45	75.95	60.45	69.62	-9.17 / 6.33	
	Men 3m	305B/307C*	63.00	64.50	61.50	66.00	67.50	61.50	67.50	57.75	22.75	*	80.50	78.75	77.00	80.50	22.75	64.02	-41.27 / 16.48
		205B	49.50	61.50	60.00	64.50	70.50	66.00	64.50	70.50	63.00	63.00	55.50	72.00	72.00	49.50	63.38	-13.88 / 8.63	
		405B	67.50	67.50	63.00	63.00	64.50	70.50	64.50	73.50	66.00	66.00	67.50	72.00	73.50	63.00	67.25	-4.25 / 6.25	
		5154B	76.50	81.60	76.50	76.50	83.30	71.40	83.30	71.40	81.60	73.10	71.40	71.40	83.30	71.40	76.50	-5.10 / 6.80	
	<b>Total</b>		<b>399.35</b>	<b>419.90</b>	<b>394.55</b>	<b>408.95</b>	<b>427.10</b>	<b>404.10</b>	<b>432.45</b>	<b>395.15</b>	<b>379.80</b>	<b>409.35</b>	<b>395.40</b>	<b>426.35</b>	<b>460.50</b>	<b>319.60</b>	<b>407.70</b>	<b>-88.10 / 52.80</b>	

# British Diving - SSSM and WITW report


**WITW**

**Athlete Dashboard**


British Diving - 2018

GB diver: Average | 2nd page of ratings

**Gold target: 560** **Bronze target: 518**



vs. Average



Coach: Tom Owens

Programme: Sheffield

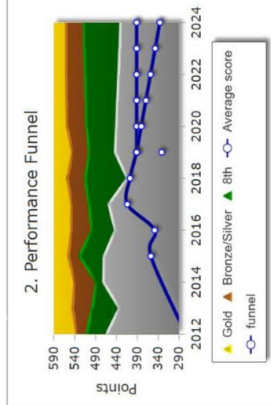
PB (Achieved): 452.9 (2017)

Age zone: 22(2020) 26(2024)

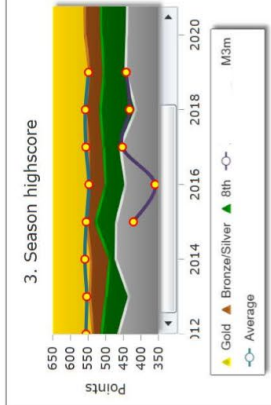
Last update: 09/08/2019

Last event: European Championships UKR - Aug


### 2. Performance Funnel



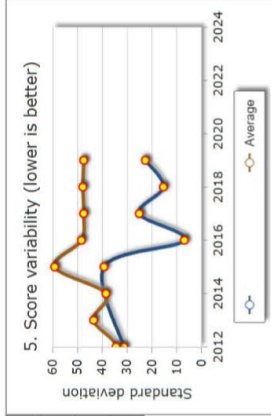
### 3. Season highscore



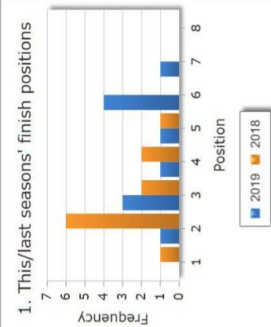
### 4. List difficulty



### 5. Score variability (lower is better)



### 1. This/last seasons' finish positions



### Breakdown of 2019 results

- % results in top 3: 33.3
- % results in top 8: 58.3
- % results below top 8: 08.3

### Change in highscore

Change required:	sw/yr	9.60
Change last year:	sw/yr	2.17
Average career change:	sw/yr	4.80
Ave change (last two yrs):	sw/yr	4.80

### Change in difficulty

Change required:	sw/yr	1.10
Change last year:	sw/yr	0.30
Average career change:	sw/yr	0.55
Ave change (last two yrs):	sw/yr	0.55

### Change in consistency

Change required:	sw/yr	7.29
Change last year:	sw/yr	-0.76
Average career change:	sw/yr	3.65
Ave change (last two yrs):	sw/yr	3.65

Update: GB

Update Comparison

Print

## British Diving - SSSM and WITW report

Comparison of performance data

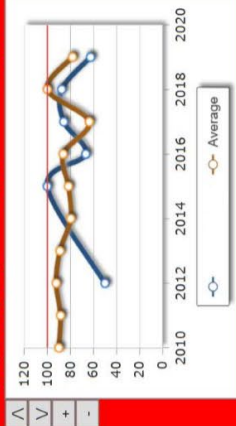
### 6. Competitive starts

	Ross Haslam	Average
total starts(career)	47	142.96
ave starts/year(quad)	10	10.00
most starts/year	12	12.50



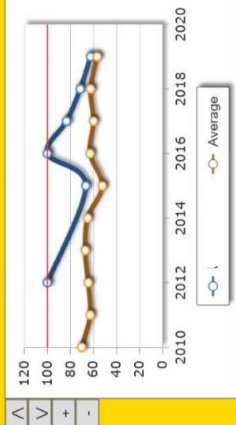
### 7. Progress through rounds

	Ross Haslam	Average
career progress (%)	75.86	83.16
last quad progress (%)	76.92	79.01
best progress in year (%)	100.00	100.00



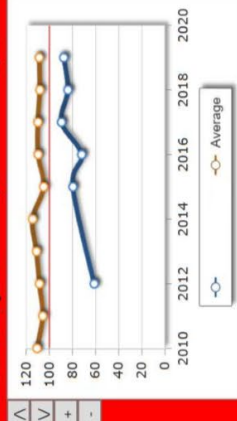
### 8. Step-up through rounds

	Ross Haslam	Average
career step-up (%)	74.07	63.34
last quad step-up (%)	73.91	60.70
best annual step-up (%)	100.00	75.00



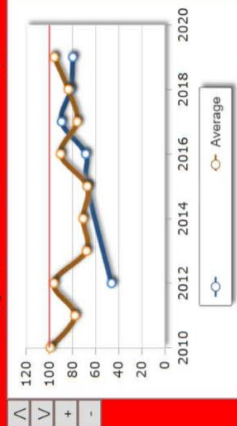
### 9. Season best vs major bronze-score

	Ross Haslam	Average
Highest % of medal:	89.52	116.85
Year achieved:	2017	2008
# times >=95% / years:	0 / 6	10 / 10



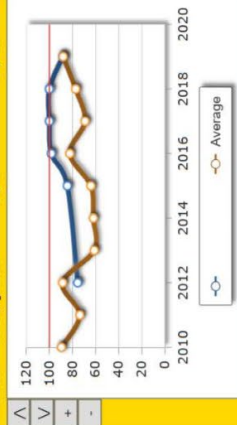
### 10. Peak event score vs major bronze score

	Ross Haslam	Average
Highest % of medal:	89.52	99.28
Year achieved:	2017	2010
# times >=95% / years:	0 / 6	3 / 10



### 11. Percent of season-best at major event

	Ross Haslam	Average
Highest % of season best achieved:	100.00	89.65
Year achieved:	2018	2010
# times >=95% / years:	3 / 6	0 / 15



### 12. Event history to first medal

Average number of starts to first World Class medal:	18
Smallest number of starts to first World Class medal:	03
Largest number of starts to first World Class medal:	42

## Appendix G – Results of regression analyses

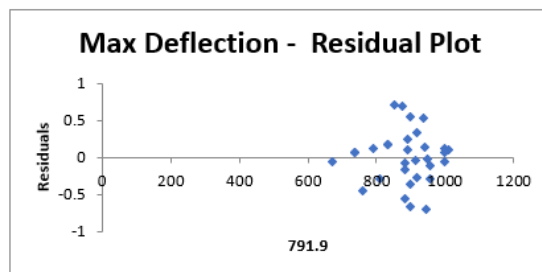
<b>100a</b>	Dependent variable:	Vertical take-off velocity
<b>All divers</b>	Independent variable:	Maximum board deflection

SUMMARY OUTPUT

<i>Regression Statistics</i>	
Multiple R	0.574514273
R Square	0.33006665
Adjusted R Square	0.3069655
Standard Error	0.360593992
Observations	31

ANOVA					
	<i>df</i>	<i>SS</i>	<i>MS</i>	<i>F</i>	<i>Significance F</i>
Regression	1	1.857825923	1.857825923	14.28788826	0.000724675
Residual	29	3.770812787	0.130028027		
Total	30	5.62863871			

	<i>Coefficients</i>	<i>Standard Error</i>	<i>t Stat</i>	<i>P-value</i>	<i>Lower 95%</i>	<i>Upper 95%</i>	<i>Lower 95.0%</i>	<i>Upper 95.0%</i>
Intercept	3.011524322	0.702889507	4.284491791	0.000183884	1.573953867	4.449094776	1.573953867	4.449094776
791.9	0.002987126	0.000790259	3.779932309	0.000724675	0.001370865	0.004603388	0.001370865	0.004603388



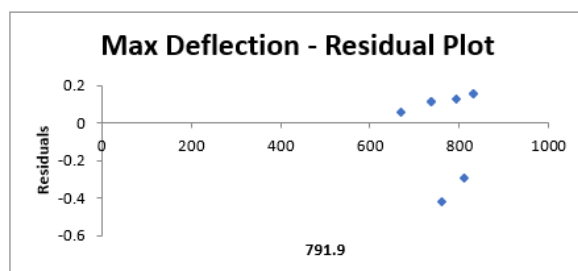
<b>100a</b>	Dependent variable:	Vertical take-off velocity
<b>Diver 1</b>	Independent variable:	Maximum board deflection

SUMMARY OUTPUT

<i>Regression Statistics</i>	
Multiple R	0.684738367
R Square	0.468866632
Adjusted R Square	0.380344404
Standard Error	0.24399923
Observations	8

ANOVA					
	<i>df</i>	<i>SS</i>	<i>MS</i>	<i>F</i>	<i>Significance F</i>
Regression	1	0.315336253	0.315336253	5.29659773	0.060980493
Residual	6	0.357213747	0.059535624		
Total	7	0.67255			

	<i>Coefficients</i>	<i>Standard Error</i>	<i>t Stat</i>	<i>P-value</i>	<i>Lower 95%</i>	<i>Upper 95%</i>	<i>Lower 95.0%</i>	<i>Upper 95.0%</i>
Intercept	2.380330614	1.266141449	1.879987908	0.109156848	-0.717805903	5.478467131	-0.717805903	5.478467131
791.9	0.003769609	0.001637939	2.301433842	0.060980493	-0.000238284	0.007777502	-0.000238284	0.007777502



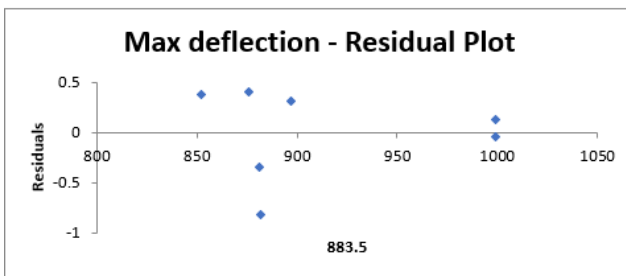
<b>100a</b>	Dependent variable:	Vertical take-off velocity
<b>Diver 2</b>	Independent variable:	Maximum board deflection

SUMMARY OUTPUT

Regression Statistics	
Multiple R	0.082099782
R Square	0.006740374
Adjusted R Square	-0.191911551
Standard Error	0.494584982
Observations	7

ANOVA					
	df	SS	MS	F	Significance F
Regression	1	0.008299904	0.008299904	0.033930576	0.861092332
Residual	5	1.223071524	0.244614305		
Total	6	1.231371429			

	Coefficients	Standard Error	t Stat	P-value	Lower 95%	Upper 95%	Lower 95.0%	Upper 95.0%	
Intercept	5.37530132	3.040370531	1.767975734	0.137305192	-2.440219941	13.19082258	-2.440219941	13.19082258	
	883.5	0.00061272	0.003326338	0.18420254	0.861092332	-0.007937904	0.009163344	-0.007937904	0.009163344



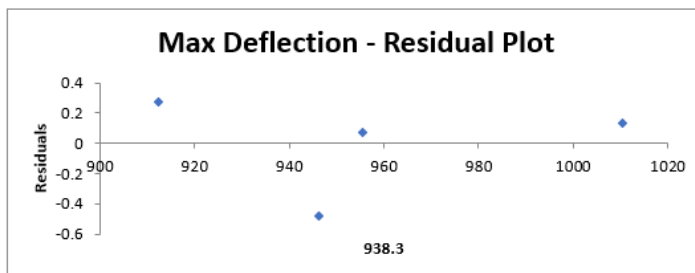
<b>100a</b>	Dependent variable:	Vertical take-off velocity
<b>Diver 3</b>	Independent variable:	Maximum board deflection

SUMMARY OUTPUT

Regression Statistics	
Multiple R	0.578904977
R Square	0.335130973
Adjusted R Square	0.002696459
Standard Error	0.407452815
Observations	4

ANOVA					
	df	SS	MS	F	Significance F
Regression	1	0.167364408	0.167364408	1.008111248	0.421095023
Residual	2	0.332035592	0.166017796		
Total	3	0.4994			

	Coefficients	Standard Error	t Stat	P-value	Lower 95%	Upper 95%	Lower 95.0%	Upper 95.0%	
Intercept	0.122690328	5.53865557	0.022151644	0.984338343	-23.70822118	23.95360184	-23.70822118	23.95360184	
	938.3	0.00581187	0.005788441	1.004047433	0.421095023	-0.019093783	0.030717522	-0.019093783	0.030717522



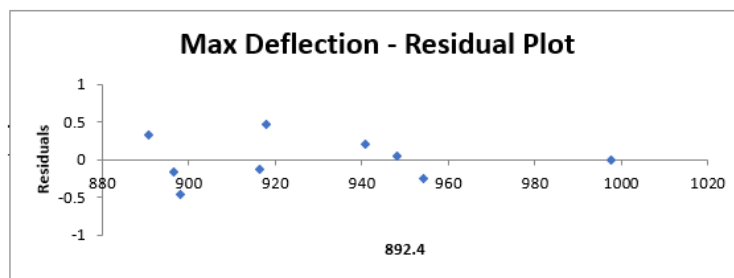
<b>100a</b>	Dependent variable:	Vertical take-off velocity
<b>Diver 4</b>	Independent variable:	Maximum board deflection

SUMMARY OUTPUT

Regression Statistics	
Multiple R	0.552879482
R Square	0.305675722
Adjusted R Square	0.206486539
Standard Error	0.316451258
Observations	9

ANOVA					
	df	SS	MS	F	Significance F
Regression	1	0.308610209	0.308610209	3.081744536	0.122606862
Residual	7	0.700989791	0.100141399		
Total	8	1.0096			

	Coefficients	Standard Error	t Stat	P-value	Lower 95%	Upper 95%	Lower 95.0%	Upper 95.0%	
Intercept	0.407773364	3.00133612	0.135863945	0.895753456	-6.689258813	7.504805541	-6.689258813	7.504805541	
	892.4	0.005668258	0.003228876	1.755489828	0.122606862	-0.001966819	0.013303336	-0.001966819	0.013303336



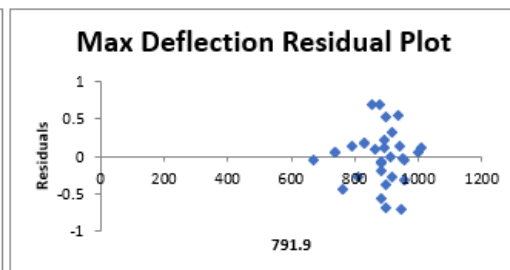
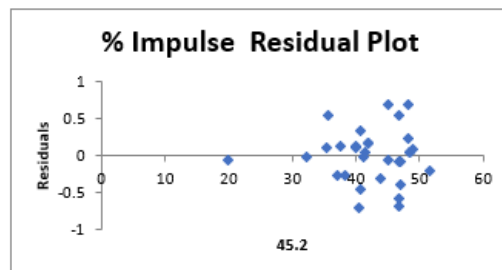
<b>100a</b>	Dependent variable:	Vertical take-off velocity
<b>All divers</b>	Independent variables:	Maximum board deflection % impulse after MD

SUMMARY OUTPUT

Regression Statistics	
Multiple R	0.575874828
R Square	0.331631818
Adjusted R Square	0.283891234
Standard Error	0.366547747
Observations	31

ANOVA					
	df	SS	MS	F	Significance F
Regression	2	1.866635688	0.933317844	6.946538716	0.003549938
Residual	28	3.762003021	0.134357251		
Total	30	5.62863871			

	Coefficients	Standard Error	t Stat	P-value	Lower 95%	Upper 95%	Lower 95.0%	Upper 95.0%	
Intercept	2.850160334	0.952686819	2.991707533	0.005733772	0.89866985	4.801650819	0.89866985	4.801650819	
	791.9	0.003036098	0.000825759	3.676736952	0.000992573	0.001344608	0.004727588	0.001344608	0.004727588
	45.2	0.002782613	0.010866788	0.25606583	0.799771959	-0.019476994	0.02504222	-0.019476994	0.02504222



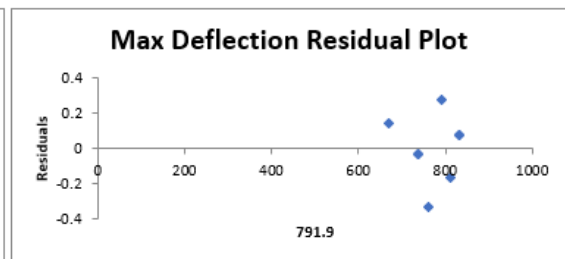
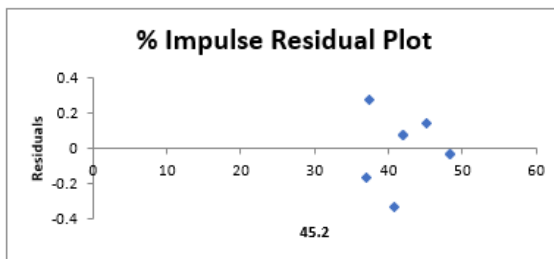
<b>100a</b>	Dependent variable:	Vertical take-off velocity
<b>Diver 1</b>	Independent variables:	Maximum board deflection % impulse after MD

SUMMARY OUTPUT

Regression Statistics	
Multiple R	0.797799608
R Square	0.636484215
Adjusted R Square	0.491077901
Standard Error	0.221125549
Observations	8

ANOVA					
	df	SS	MS	F	Significance F
Regression	2	0.428067459	0.214033729	4.377280443	0.07967245
Residual	5	0.244482541	0.048896508		
Total	7	0.67255			

	Coefficients	Standard Error	t Stat	P-value	Lower 95%	Upper 95%	Lower 95.0%	Upper 95.0%
Intercept	-0.525149954	2.231193494	-0.235367284	0.823259878	-6.260615421	5.210315514	-6.260615421	5.210315514
791.9	0.005521546	0.00188008	2.936867861	0.032373931	0.000688647	0.010354444	0.000688647	0.010354444
45.2	0.036466041	0.024016265	1.518389361	0.189376047	-0.025269733	0.098201814	-0.025269733	0.098201814



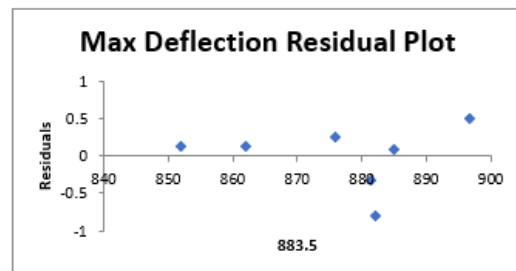
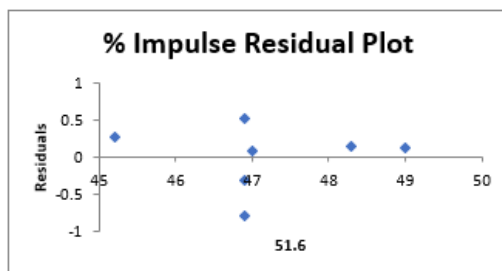
<b>100a</b>	Dependent variable:	Vertical take-off velocity
<b>Diver 2</b>	Independent variables:	Maximum board deflection % impulse after MD

SUMMARY OUTPUT

Regression Statistics	
Multiple R	0.301536085
R Square	0.090924011
Adjusted R Square	-0.363613984
Standard Error	0.529010917
Observations	7

ANOVA					
	df	SS	MS	F	Significance F
Regression	2	0.111961229	0.055980614	0.200036106	0.826419154
Residual	4	1.1194102	0.27985255		
Total	6	1.231371429			

	Coefficients	Standard Error	t Stat	P-value	Lower 95%	Upper 95%	Lower 95.0%	Upper 95.0%
Intercept	18.26074977	23.02809549	0.792976986	0.472172596	-45.67549324	82.19699277	-45.67549324	82.19699277
883.5	-0.010963517	0.017640137	-0.621509755	0.567932271	-0.059940388	0.038013354	-0.059940388	0.038013354
51.6	-0.057610466	0.219012001	-0.263047072	0.805507921	-0.665685264	0.550464333	-0.665685264	0.550464333



<b>100a</b>	Dependent variable:	Vertical take-off velocity
<b>Diver 3</b>	Independent variables:	Maximum board deflection % impulse after MD

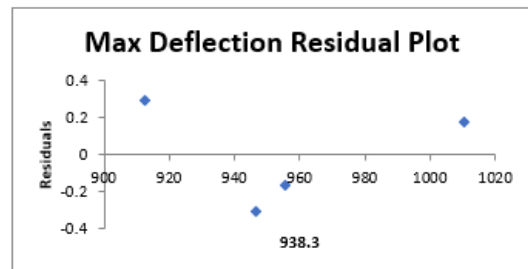
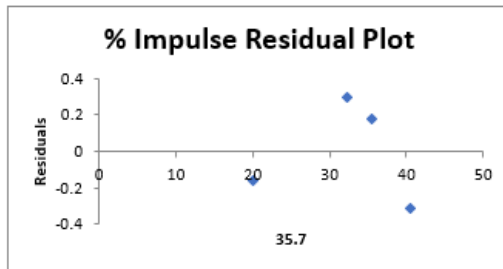
SUMMARY OUTPUT

Regression Statistics	
Multiple R	0.715994356
R Square	0.512647918
Adjusted R Square	-0.462056245
Standard Error	0.493339264
Observations	4

ANOVA

	df	SS	MS	F	Significance F
Regression	2	0.25601637	0.128008185	0.525952322	0.698106068
Residual	1	0.24338363	0.24338363		
Total	3	0.4994			

	Coefficients	Standard Error	t Stat	P-value	Lower 95%	Upper 95%	Lower 95.0%	Upper 95.0%
Intercept	0.366443819	6.71829249	0.054544189	0.965310465	-84.99755604	85.73044368	-84.99755604	85.73044368
	938.3	0.006218696	0.007040921	0.88322194	-0.083244684	0.095682076	-0.083244684	0.095682076
	35.7	-0.019712168	0.032661483	-0.60352949	0.654308669	-0.434715655	0.395291319	-0.434715655



<b>100a</b>	Dependent variable:	Vertical take-off velocity
<b>Diver 4</b>	Independent variables:	Maximum board deflection % impulse after MD

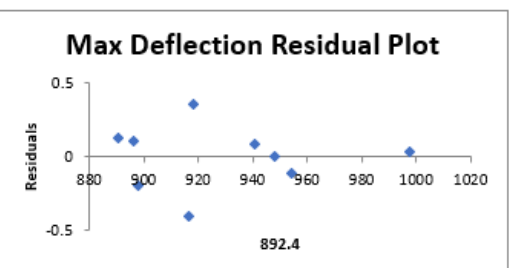
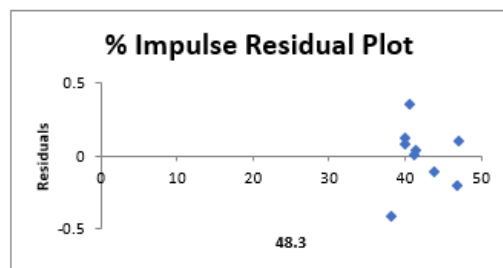
SUMMARY OUTPUT

Regression Statistics	
Multiple R	0.786151615
R Square	0.618034361
Adjusted R Square	0.490712481
Standard Error	0.253519397
Observations	9

ANOVA

	df	SS	MS	F	Significance F
Regression	2	0.623967491	0.311983745	4.854109621	0.055727927
Residual	6	0.385632509	0.064272085		
Total	8	1.0096			

	Coefficients	Standard Error	t Stat	P-value	Lower 95%	Upper 95%	Lower 95.0%	Upper 95.0%
Intercept	4.524122797	3.03888851	1.488742605	0.18712792	-2.911769512	11.96001511	-2.911769512	11.96001511
	892.4	0.004209908	0.002669226	1.577201867	-0.002321452	0.010741269	-0.002321452	0.010741269
	48.3	-0.06552719	0.029582257	-2.215084195	0.068660972	-0.137912366	0.006857985	-0.137912366





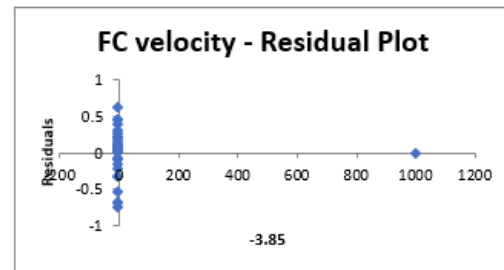
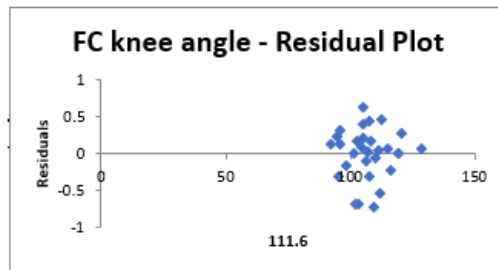
100a	Dependent variable:	Vertical take-off velocity
All divers	Independent variables:	First contact - velocity First contact - knee angle

SUMMARY OUTPUT

Regression Statistics	
Multiple R	0.629719843
R Square	0.39654708
Adjusted R Square	0.3534433
Standard Error	0.348292696
Observations	31

ANOVA					
	df	SS	MS	F	Significance F
Regression	2	2.232020247	1.116010123	9.199821467	0.000849195
Residual	28	3.396618463	0.121307802		
Total	30	5.62863871			

	Coefficients	Standard Error	t Stat	P-value	Lower 95%	Upper 95%	Lower 95.0%	Upper 95.0%
Intercept	9.021909133	0.819017853	11.01552194	1.09135E-11	7.344227113	10.69959115	7.344227113	10.69959115
111.6	-0.031471609	0.007611979	-4.13448426	0.000292699	-0.047064042	-0.015879176	-0.047064042	-0.015879176
-3.85	0.000218348	0.000355662	0.613920077	0.544224238	-0.000510192	0.000946888	-0.000510192	0.000946888



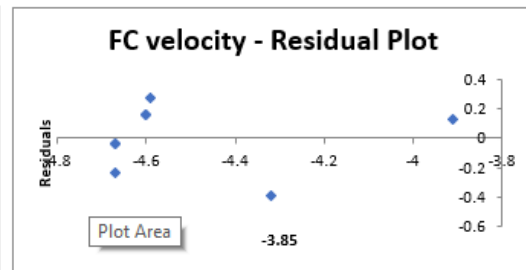
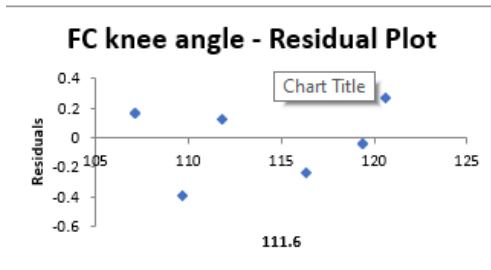
<b>100a</b>	Dependent variable:	Vertical take-off velocity
<b>Diver 1</b>	Independent variables:	First contact - velocity First contact - knee angle

SUMMARY OUTPUT

Regression Statistics	
Multiple R	0.689737535
R Square	0.475737868
Adjusted R Square	0.266033015
Standard Error	0.265553195
Observations	8

ANOVA					
	df	SS	MS	F	Significance F
Regression	2	0.319957503	0.159978751	2.268606859	0.199008316
Residual	5	0.352592497	0.070518499		
Total	7	0.67255			

	Coefficients	Standard Error	t Stat	P-value	Lower 95%	Upper 95%	Lower 95.0%	Upper 95.0%
Chart Area	3.912933187	2.292820718	1.706602333	0.148606542	-1.980950103	9.806816477	-1.980950103	9.806816477
	111.6	-0.020879516	0.018743698	-1.113948582	0.31596419	-0.069061727	0.027302694	0.027302694
	-3.85	-0.833364573	0.400140191	-2.082681499	0.091748786	-1.861957679	0.195228534	-1.861957679



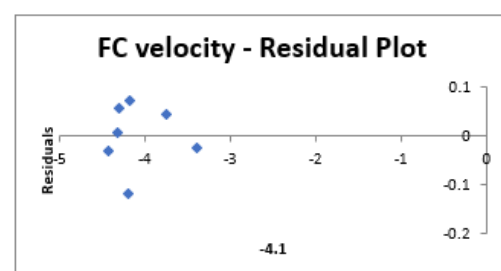
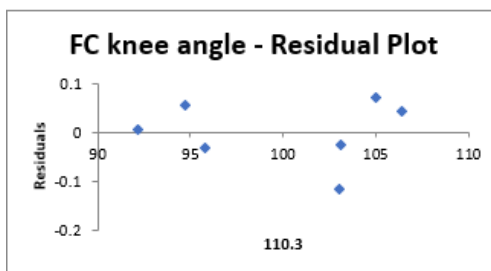
<b>100a</b>	Dependent variable:	Vertical take-off velocity
<b>Diver 2</b>	Independent variables:	First contact - velocity First contact - knee angle

SUMMARY OUTPUT

Regression Statistics	
Multiple R	0.989648503
R Square	0.97940416
Adjusted R Square	0.969106239
Standard Error	0.07962589
Observations	7

ANOVA					
	df	SS	MS	F	Significance F
Regression	2	1.206010299	0.60300515	95.10698638	0.000424189
Residual	4	0.02536113	0.006340282		
Total	6	1.231371429			

	Coefficients	Standard Error	t Stat	P-value	Lower 95%	Upper 95%	Lower 95.0%	Upper 95.0%
Intercept	1.460353106	1.082442998	1.349127028	0.248607228	-1.544990459	4.46569667	-1.544990459	4.46569667
	110.3	-0.003373485	0.007357187	-0.458529151	0.670379439	-0.023800311	0.017053341	-0.023800311
	-4.1	-1.177198262	0.112055339	-10.50550804	0.000464189	-1.488313759	-0.866082765	-1.488313759



100a	Dependent variable:	Vertical take-off velocity
Diver 3	Independent variables:	First contact - velocity First contact - knee angle

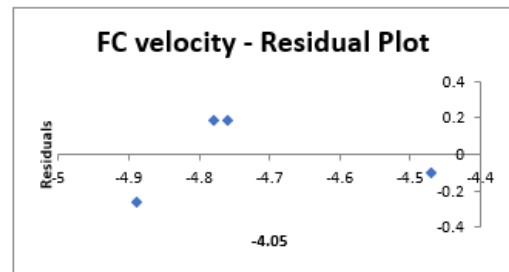
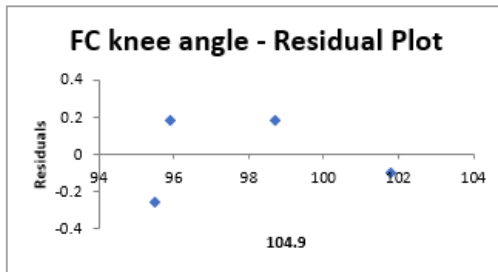
SUMMARY OUTPUT

Regression Statistics	
Multiple R	0.840573474
R Square	0.706563764
Adjusted R Square	0.119691293
Standard Error	0.382808119
Observations	4

ANOVA

	df	SS	MS	F	Significance F
Regression	2	0.352857944	0.176428972	1.203947704	0.54169755
Residual	1	0.146542056	0.146542056		
Total	3	0.4994			

	Coefficients	Standard Error	t Stat	P-value	Lower 95%	Upper 95%	Lower 95.0%	Upper 95.0%
Intercept	20.97280623	37.32504823	0.561896293	0.674094769	-453.2868984	495.2325108	-453.2868984	495.2325108
104.9	-0.138342679	0.216773726	-0.638189331	0.638382394	-2.892714024	2.616028665	-2.892714024	2.616028665
-4.05	0.367975078	3.52985539	0.104246502	0.933873465	-44.4830902	45.21904036	-44.4830902	45.21904036



100a	Dependent variable:	Vertical take-off velocity
Diver 4	Independent variables:	First contact - velocity First contact - knee angle

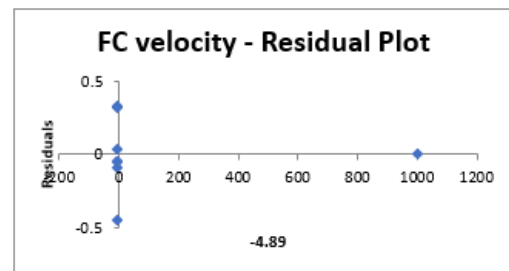
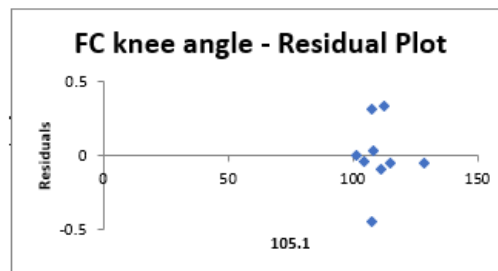
SUMMARY OUTPUT

Regression Statistics	
Multiple R	0.755535812
R Square	0.570834363
Adjusted R Square	0.427779151
Standard Error	0.268727131
Observations	9

ANOVA

	df	SS	MS	F	Significance F
Regression	2	0.576314373	0.288157187	3.990308036	0.079045076
Residual	6	0.433285627	0.072214271		
Total	8	1.0096			

	Coefficients	Standard Error	t Stat	P-value	Lower 95%	Upper 95%	Lower 95.0%	Upper 95.0%
Intercept	9.271421413	1.518255429	6.106628198	0.000879205	5.556384211	12.98645861	5.556384211	12.98645861
105.1	-0.032571522	0.013547528	-2.404240888	0.052987854	-0.06572113	0.000578086	-0.06572113	0.000578086
-4.89	8.09949E-05	0.000317344	0.255226968	0.807071366	-0.000695519	0.000857509	-0.000695519	0.000857509



100a	Dependent variable:	Vertical take-off velocity
All divers	Independent variables:	First contact - trunk angle First contact - knee angle

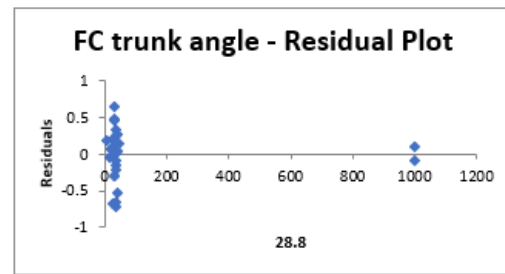
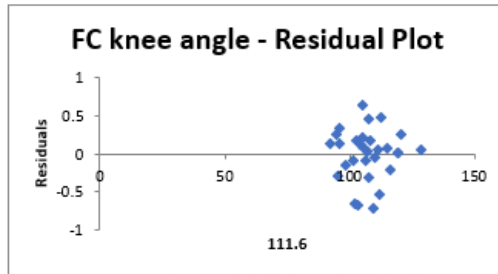
SUMMARY OUTPUT

Regression Statistics	
Multiple R	0.649419195
R Square	0.421745291
Adjusted R Square	0.380441383
Standard Error	0.340943378
Observations	31

ANOVA

	df	SS	MS	F	Significance F
Regression	2	2.373851872	1.186925936	10.21078426	0.000467378
Residual	28	3.254786838	0.116242387		
Total	30	5.62863871			

	Coefficients	Standard Error	t Stat	P-value	Lower 95%	Upper 95%	Lower 95.0%	Upper 95.0%
Intercept	8.927136954	0.804547508	11.09584812	9.23713E-12	7.279096093	10.57517781	7.279096093	10.57517781
111.6	-0.030820526	0.007456285	-4.13349646	0.000293479	-0.046094033	-0.015547019	-0.046094033	-0.015547019
28.8	0.000330049	0.000259836	1.270219894	0.214460546	-0.000202201	0.0008623	-0.000202201	0.0008623



100a	Dependent variable:	Vertical take-off velocity
Diver 1	Independent variables:	First contact - trunk angle First contact - knee angle

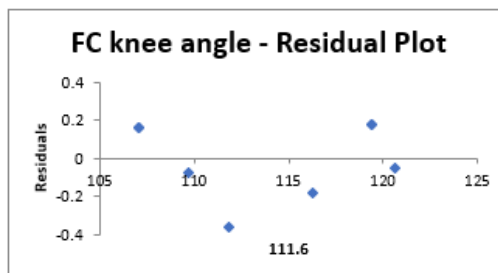
SUMMARY OUTPUT

Regression Statistics	
Multiple R	0.75755473
R Square	0.573889169
Adjusted R Square	0.403444837
Standard Error	0.239407953
Observations	8

ANOVA

	df	SS	MS	F	Significance F
Regression	2	0.385969161	0.19298458	3.367018204	0.118524036
Residual	5	0.286580839	0.057316168		
Total	7	0.67255			

	Coefficients	Standard Error	t Stat	P-value	Lower 95%	Upper 95%	Lower 95.0%	Upper 95.0%
Intercept	1.132296449	2.691065764	0.420761345	0.69140222	-5.785308322	8.04990122	-5.785308322	8.04990122
111.6	0.011097943	0.017595275	0.630734278	0.55591629	-0.034132151	0.056328037	-0.034132151	0.056328037
28.8	0.076251115	0.029934878	2.547233156	0.051438908	-0.00069894	0.153201169	-0.00069894	0.153201169



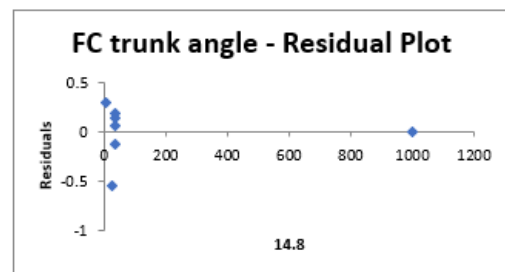
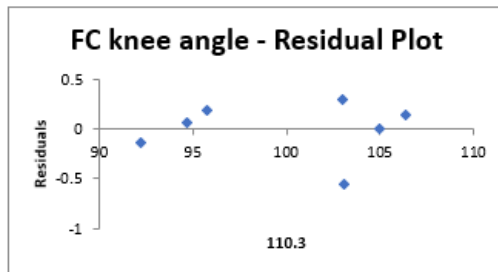
100a	Dependent variable:	Vertical take-off velocity
Diver 2	Independent variables:	First contact - trunk angle First contact - knee angle

SUMMARY OUTPUT

Regression Statistics	
Multiple R	0.784531416
R Square	0.615489543
Adjusted R Square	0.423234315
Standard Error	0.344047668
Observations	7

ANOVA					
	df	SS	MS	F	Significance F
Regression	2	0.757896238	0.378948119	3.201419014	0.147848291
Residual	4	0.47347519	0.118368798		
Total	6	1.231371429			

	Coefficients	Standard Error	t Stat	P-value	Lower 95%	Upper 95%	Lower 95.0%	Upper 95.0%
Intercept	12.46195985	2.666226886	4.674005769	0.009489958	5.05932726	19.86459243	5.05932726	19.86459243
	110.3	-0.066270189	0.026877409	-2.465646489	0.069269833	-0.14089384	0.008353462	-0.14089384
	14.8	0.000603224	0.000413724	1.458033341	0.218577116	-0.000545459	0.001751907	-0.000545459



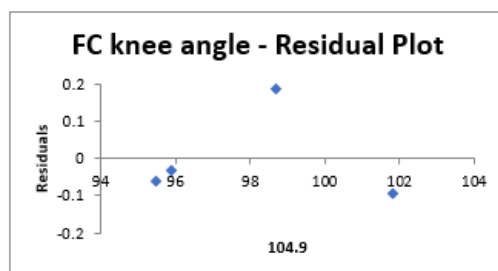
100a	Dependent variable:	Vertical take-off velocity
Diver 3	Independent variables:	First contact - trunk angle First contact - knee angle

SUMMARY OUTPUT

Regression Statistics	
Multiple R	0.950931147
R Square	0.904270046
Adjusted R Square	0.712810138
Standard Error	0.218649352
Observations	4

ANOVA					
	df	SS	MS	F	Significance F
Regression	2	0.451592461	0.225796231	4.723025601	0.309402576
Residual	1	0.047807539	0.047807539		
Total	3	0.4994			

	Coefficients	Standard Error	t Stat	P-value	Lower 95%	Upper 95%	Lower 95.0%	Upper 95.0%
Intercept	14.96015822	4.500177943	3.324348149	0.186020635	-42.22002408	72.14034052	-42.22002408	72.14034052
	104.9	-0.108257613	0.043660226	-2.479547686	0.244046544	-0.663013385	0.44649816	-0.663013385
	32.4	0.03447385	0.023797371	1.448641099	0.384637781	-0.267900423	0.336848123	-0.267900423



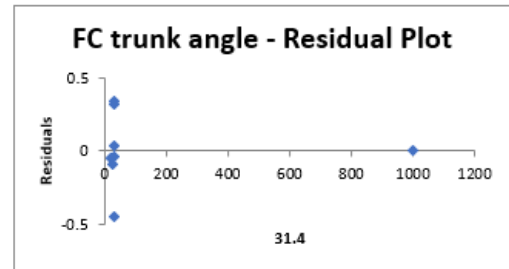
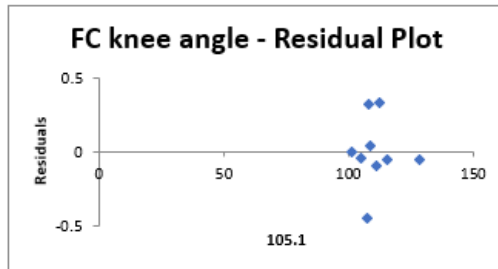
100a	Dependent variable:	Vertical take-off velocity
Diver 4	Independent variables:	First contact - trunk angle First contact - knee angle

SUMMARY OUTPUT

Regression Statistics	
Multiple R	0.755826778
R Square	0.571274119
Adjusted R Square	0.428365491
Standard Error	0.268589417
Observations	9

ANOVA					
	df	SS	MS	F	Significance F
Regression	2	0.57675835	0.288379175	3.997478179	0.078802339
Residual	6	0.43284165	0.072140275		
Total	8	1.0096			

	Coefficients	Standard Error	t Stat	P-value	Lower 95%	Upper 95%	Lower 95.0%	Upper 95.0%
Intercept	9.255310684	1.531277481	6.044176053	0.000928083	5.508409667	13.0022117	5.508409667	13.0022117
105.1	-0.032454911	0.013617361	-2.383348026	0.054518565	-0.065775394	0.000865572	-0.065775394	0.000865572
31.4	8.7955E-05	0.000329251	0.267136631	0.79830866	-0.000717693	0.000893603	-0.000717693	0.000893603



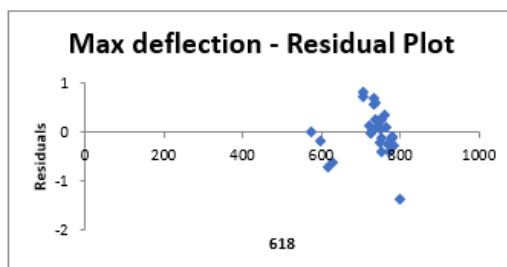
200a	Dependent variable:	Vertical take-off velocity
All divers	Independent variable:	Maximum board deflection

SUMMARY OUTPUT

Regression Statistics	
Multiple R	0.350338106
R Square	0.122736789
Adjusted R Square	0.088995896
Standard Error	0.480019631
Observations	28

ANOVA					
	df	SS	MS	F	Significance F
Regression	1	0.838177858	0.838177858	3.637627182	0.067592659
Residual	26	5.990889999	0.230418846		
Total	27	6.829067857			

	Coefficients	Standard Error	t Stat	P-value	Lower 95%	Upper 95%	Lower 95.0%	Upper 95.0%
Intercept	2.411429869	1.187107847	2.031348605	0.052558833	-0.028705258	4.851564996	-0.028705258	4.851564996
618	0.003099728	0.001625229	1.907256454	0.067592659	-0.000240978	0.006440434	-0.000240978	0.006440434



200a	Dependent variable:	Vertical take-off velocity
Diver 1	Independent variable:	Maximum board deflection

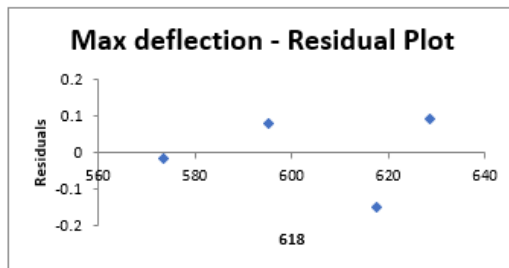
SUMMARY OUTPUT

Regression Statistics	
Multiple R	0.913767094
R Square	0.834970302
Adjusted R Square	0.752455452
Standard Error	0.13731221
Observations	4

ANOVA

	df	SS	MS	F	Significance F
Regression	1	0.190790714	0.190790714	10.11903082	0.086232906
Residual	2	0.037709286	0.018854643		
Total	3	0.2285			

	Coefficients	Standard Error	t Stat	P-value	Lower 95%	Upper 95%	Lower 95.0%	Upper 95.0%
Intercept	10.1141835	1.953140642	5.178420482	0.035326891	1.71049759	18.51786942	1.71049759	18.51786942
618	-0.010285214	0.003233284	-3.18104241	0.086232906	-0.024196912	0.003626485	-0.024196912	0.003626485



200a	Dependent variable:	Vertical take-off velocity
Diver 2	Independent variable:	Maximum board deflection

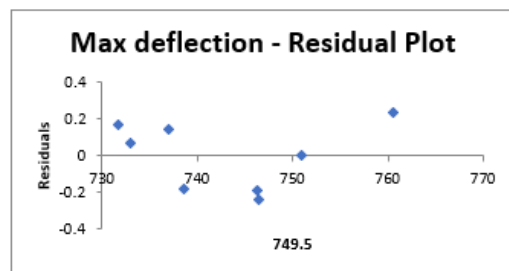
SUMMARY OUTPUT

Regression Statistics	
Multiple R	0.526787399
R Square	0.277504963
Adjusted R Square	0.157089124
Standard Error	0.197426194
Observations	8

ANOVA

	df	SS	MS	F	Significance F
Regression	1	0.089824888	0.089824888	2.304555319	0.17979351
Residual	6	0.233862612	0.038977102		
Total	7	0.3236875			

	Coefficients	Standard Error	t Stat	P-value	Lower 95%	Upper 95%	Lower 95.0%	Upper 95.0%
Intercept	13.60684696	5.624720628	2.419115163	0.051925602	-0.156348607	27.37004252	-0.156348607	27.37004252
749.5	-0.011490416	0.007569064	-1.51807619	0.17979351	-0.030011248	0.007030416	-0.030011248	0.007030416



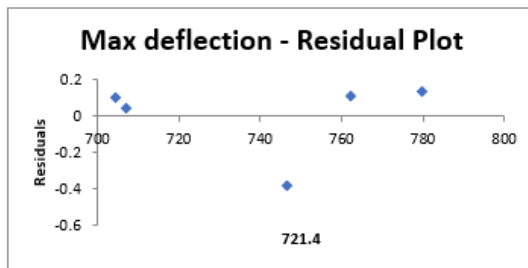
200a	Dependent variable:	Vertical take-off velocity
Diver 3	Independent variable:	Maximum board deflection

SUMMARY OUTPUT

Regression Statistics	
Multiple R	0.817266156
R Square	0.667923969
Adjusted R Square	0.557231959
Standard Error	0.251300628
Observations	5

ANOVA					
	df	SS	MS	F	Significance F
Regression	1	0.381063983	0.381063983	6.034075703	0.091155929
Residual	3	0.189456017	0.063152006		
Total	4	0.57052			

	Coefficients	Standard Error	t Stat	P-value	Lower 95%	Upper 95%	Lower 95.0%	Upper 95.0%	
Intercept	11.8135066	2.789842906	4.234470183	0.024104181	2.934981353	20.69203185	2.934981353	20.69203185	
	721.4	-0.009253888	0.003767201	-2.456435569	0.091155929	-0.021242804	0.002735029	-0.021242804	0.002735029



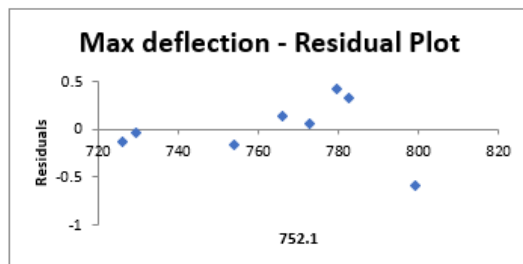
200a	Dependent variable:	Vertical take-off velocity
Diver 4	Independent variable:	Maximum board deflection

SUMMARY OUTPUT

Regression Statistics	
Multiple R	0.592632395
R Square	0.351213156
Adjusted R Square	0.243082015
Standard Error	0.338216768
Observations	8

ANOVA					
	df	SS	MS	F	Significance F
Regression	1	0.371544008	0.371544008	3.248029697	0.121576523
Residual	6	0.686343492	0.114390582		
Total	7	1.0578875			

	Coefficients	Standard Error	t Stat	P-value	Lower 95%	Upper 95%	Lower 95.0%	Upper 95.0%	
Intercept	11.24100837	3.785957393	2.969132297	0.024985578	1.977104356	20.50491238	1.977104356	20.50491238	
	752.1	-0.008929307	0.004954591	-1.802229091	0.121576523	-0.021052753	0.003194139	-0.021052753	0.003194139





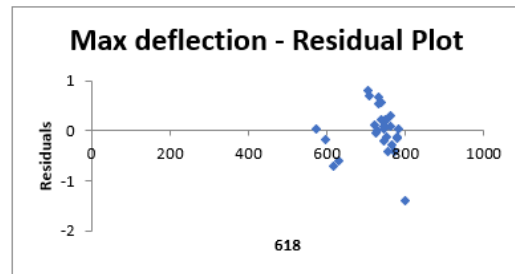
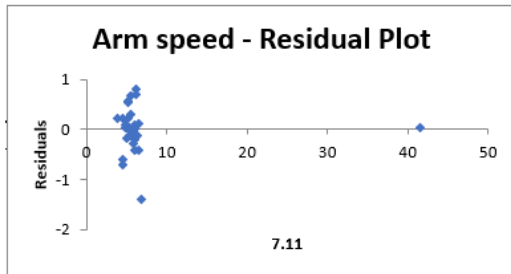
<b>200a</b>	Dependent variable:	Vertical take-off velocity
<b>All divers</b>	Independent variables:	Max deflection Arm speed to max def

SUMMARY OUTPUT

Regression Statistics	
Multiple R	0.371008208
R Square	0.137647091
Adjusted R Square	0.068658858
Standard Error	0.48534798
Observations	28

ANOVA					
	df	SS	MS	F	Significance F
Regression	2	0.940001323	0.470000661	1.995225638	0.15705903
Residual	25	5.889066534	0.235562661		
Total	27	6.829067857			

	Coefficients	Standard Error	t Stat	P-value	Lower 95%	Upper 95%	Lower 95.0%	Upper 95.0%
Intercept	2.292687585	1.213796997	1.888855873	0.070565886	-0.207174124	4.792549295	-0.207174124	4.792549295
618	0.00334889	0.001686403	1.985817977	0.058123789	-0.000124323	0.006822103	-0.000124323	0.006822103
7.11	-0.009190671	0.013979013	-0.65746208	0.516891953	-0.037980988	0.019599646	-0.037980988	0.019599646



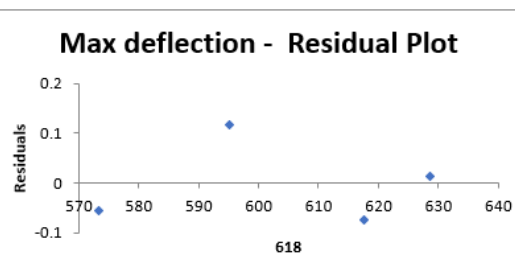
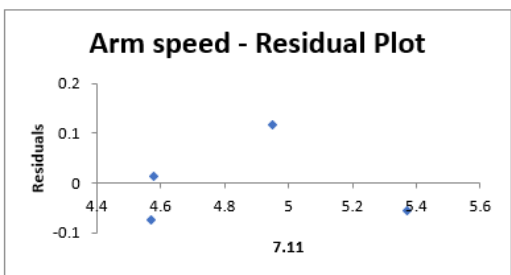
<b>200a</b>	Dependent variable:	Vertical take-off velocity
<b>Diver 1</b>	Independent variables:	Max deflection Arm speed to max def

SUMMARY OUTPUT

Regression Statistics	
Multiple R	0.948671835
R Square	0.89997825
Adjusted R Square	0.699934749
Standard Error	0.151178603
Observations	4

ANOVA					
	df	SS	MS	F	Significance F
Regression	2	0.20564503	0.102822515	4.498912722	0.316262154
Residual	1	0.02285497	0.02285497		
Total	3	0.2285			

	Coefficients	Standard Error	t Stat	P-value	Lower 95%	Upper 95%	Lower 95.0%	Upper 95.0%
Intercept	-2.046015843	15.23610122	-0.134287362	0.915018404	-195.6390374	191.5470057	-195.6390374	191.5470057
618	0.002843886	0.016669944	0.170599632	0.892428518	-0.208967836	0.214655608	-0.208967836	0.214655608
7.11	0.869884267	1.079010006	0.806187396	0.568051973	-12.84023778	14.58000631	-12.84023778	14.58000631



<b>200a Diver 2</b>	Dependent variable:	Vertical take-off velocity
	Independent variables:	Max deflection Arm speed to max def

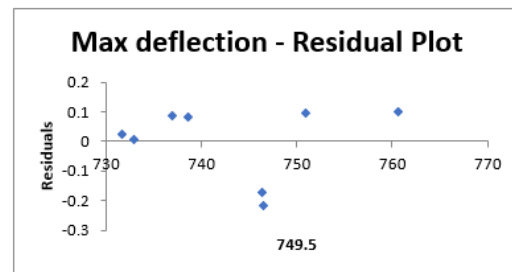
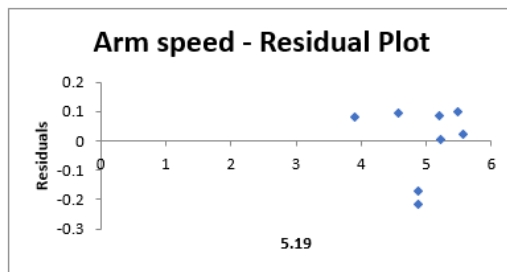
SUMMARY OUTPUT

Regression Statistics	
Multiple R	0.811517607
R Square	0.658560827
Adjusted R Square	0.521985158
Standard Error	0.148673866
Observations	8

ANOVA

	df	SS	MS	F	Significance F
Regression	2	0.213167908	0.106583954	4.821948379	0.068121369
Residual	5	0.110519592	0.022103918		
Total	7	0.3236875			

	Coefficients	Standard Error	t Stat	P-value	Lower 95%	Upper 95%	Lower 95.0%	Upper 95.0%
Intercept	12.24343382	4.274897209	2.864029991	0.035239853	1.2544607	23.23240693	1.2544607	23.23240693
749.5	-0.011310403	0.005700472	-1.984116855	0.104029199	-0.025963934	0.003343127	-0.025963934	0.003343127
5.19	0.247913841	0.104948955	2.362232572	0.064571865	-0.021866038	0.517693719	-0.021866038	0.517693719



<b>200a Diver 3</b>	Dependent variable:	Vertical take-off velocity
	Independent variables:	Max deflection Arm speed to max def

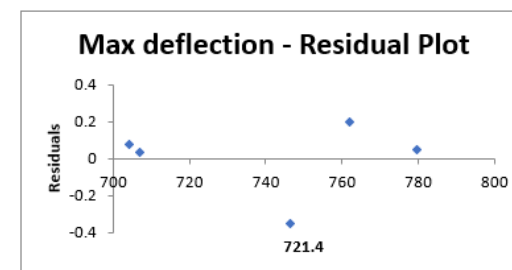
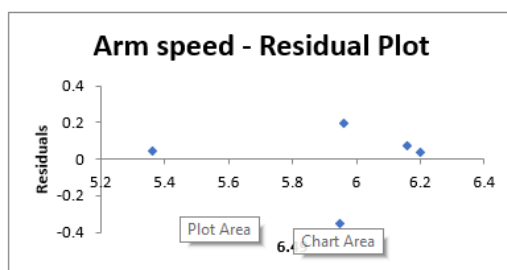
SUMMARY OUTPUT

Regression Statistics	
Multiple R	0.835542353
R Square	0.698131024
Adjusted R Square	0.396262048
Standard Error	0.293447004
Observations	5

ANOVA

	df	SS	MS	F	Significance F
Regression	2	0.398297712	0.199148856	2.312695507	0.301868976
Residual	2	0.172222288	0.086111144		
Total	4	0.57052			

	Coefficients	Standard Error	t Stat	P-value	Lower 95%	Upper 95%	Lower 95.0%	Upper 95.0%
Intercept	16.65575283	11.3035991	1.473491114	0.278530028	-31.97970869	65.29121434	-31.97970869	65.29121434
721.4	-0.012666932	0.008806633	-1.438339989	0.28693813	-0.050558813	0.02522495	-0.050558813	0.02522495
6.49	-0.390943304	0.873884084	-0.447362883	0.69839716	-4.150963044	3.369076437	-4.150963044	3.369076437



<b>200a</b>	Dependent variable:	Vertical take-off velocity
<b>Diver 4</b>	Independent variables:	Max deflection Arm speed to max def

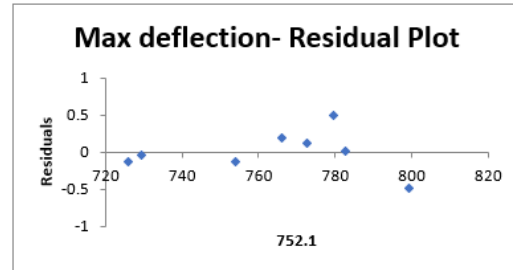
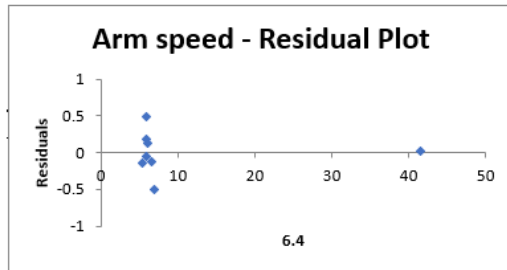
SUMMARY OUTPUT

Regression Statistics	
Multiple R	0.678718506
R Square	0.46065881
Adjusted R Square	0.244922334
Standard Error	0.337805359
Observations	8

ANOVA

	df	SS	MS	F	Significance F
Regression	2	0.487325197	0.243662598	2.135284761	0.213628393
Residual	5	0.570562303	0.114112461		
Total	7	1.0578875			

	Coefficients	Standard Error	t Stat	P-value	Lower 95%	Upper 95%	Lower 95.0%	Upper 95.0%
Intercept	12.40202271	3.953119086	3.137275262	0.025745304	2.240206598	22.56383883	2.240206598	22.56383883
	752.1	-0.010598124	0.005218534	-2.030862465	0.09800337	-0.024012793	0.002816544	-0.024012793
	6.4	0.010785549	0.010707542	1.007285234	0.36002828	-0.016739063	0.03831016	-0.016739063



<b>200a</b>	Dependent variable:	Vertical take-off velocity
<b>All divers</b>	Independent variables:	Max squat % impulse to max def

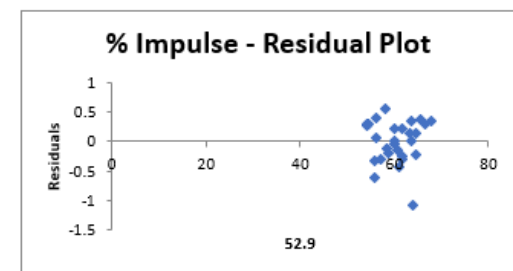
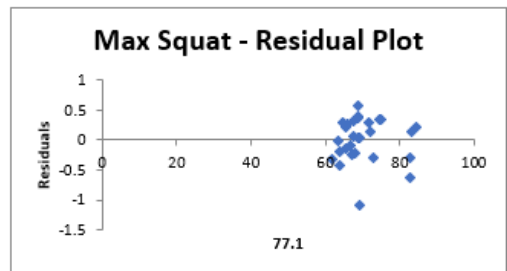
SUMMARY OUTPUT

Regression Statistics	
Multiple R	0.69773105
R Square	0.486828618
Adjusted R Square	0.445774908
Standard Error	0.374405245
Observations	28

ANOVA

	df	SS	MS	F	Significance F
Regression	2	3.32458567	1.662292835	11.85833417	0.000238935
Residual	25	3.504482187	0.140179287		
Total	27	6.829067857			

	Coefficients	Standard Error	t Stat	P-value	Lower 95%	Upper 95%	Lower 95.0%	Upper 95.0%
Intercept	9.779457013	1.20447382	8.119277355	1.79218E-08	7.298796744	12.26011728	7.298796744	12.26011728
	77.1	-0.046093115	0.011989714	-3.84438825	0.000738058	-0.070786394	-0.021399837	-0.070786394
	52.9	-0.031195198	0.0193507	-1.612096668	0.119495258	-0.07104871	0.008658313	-0.07104871



200a Diver 1	Dependent variable: Independent variables:	Vertical take-off velocity Max squat % impulse to max def
-----------------	---	---

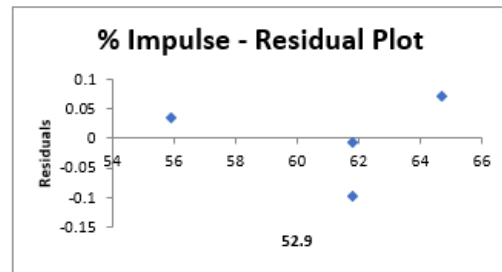
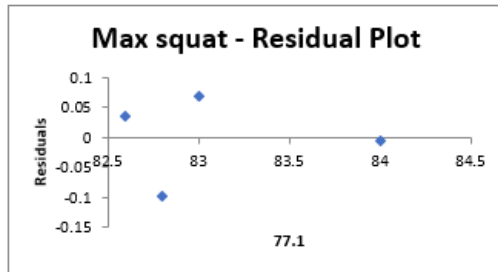
SUMMARY OUTPUT

Regression Statistics	
Multiple R	0.96439735
R Square	0.930062249
Adjusted R Square	0.790186747
Standard Error	0.126415094
Observations	4

ANOVA

	df	SS	MS	F	Significance F
Regression	2	0.212519224	0.106259612	6.649214747	0.264457465
Residual	1	0.015980776	0.015980776		
Total	3	0.2285			

		Coefficients	Standard Error	t Stat	P-value	Lower 95%	Upper 95%	Lower 95.0%	Upper 95.0%
Intercept		-23.60260235	10.14030693	-2.327602361	0.258329433	-152.4474183	105.2422136	-152.4474183	105.2422136
	77.1	0.305814643	0.127225685	2.403717789	0.250982173	-1.310740964	1.922370251	-1.310740964	1.922370251
	52.9	0.034306396	0.02140774	1.602523053	0.355164693	-0.237704725	0.306317518	-0.237704725	0.306317518



200a Diver 2	Dependent variable: Independent variables:	Vertical take-off velocity Max squat % impulse to max def
-----------------	---	---

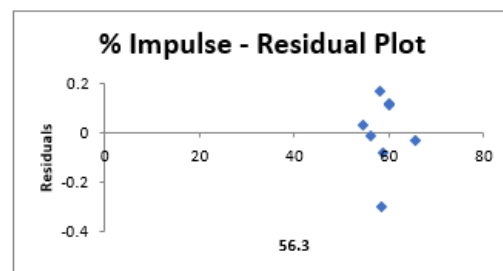
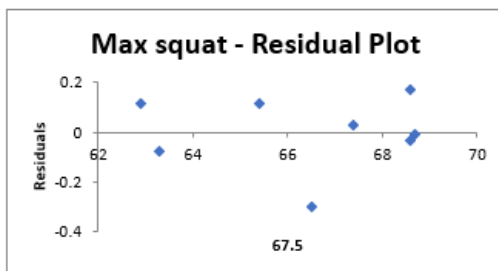
SUMMARY OUTPUT

Regression Statistics	
Multiple R	0.72286452
R Square	0.522533114
Adjusted R Square	0.33154636
Standard Error	0.175812436
Observations	8

ANOVA

	df	SS	MS	F	Significance F
Regression	2	0.169137437	0.084568719	2.735965205	0.157528139
Residual	5	0.154550063	0.030910013		
Total	7	0.3236875			

		Coefficients	Standard Error	t Stat	P-value	Lower 95%	Upper 95%	Lower 95.0%	Upper 95.0%
Intercept		3.613799187	2.267984984	1.593396434	0.171951725	-2.216241817	9.443840191	-2.216241817	9.443840191
	67.5	0.04902213	0.028234019	1.736278844	0.14302927	-0.023555726	0.121599986	-0.023555726	0.121599986
	56.3	-0.030557153	0.020395743	-1.498212312	0.194349371	-0.082986078	0.021871773	-0.082986078	0.021871773



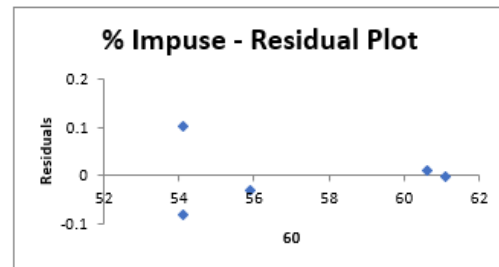
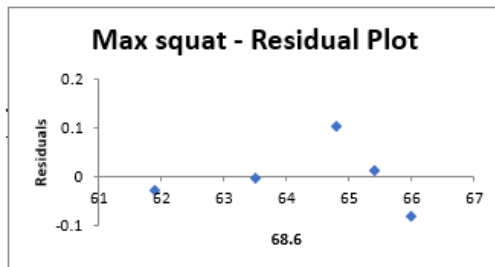
200a	Dependent variable:	Vertical take-off velocity
Diver 3	Independent variables:	Max squat % impulse to max def

SUMMARY OUTPUT

Regression Statistics	
Multiple R	0.984097999
R Square	0.968448871
Adjusted R Square	0.936897743
Standard Error	0.094869779
Observations	5

ANOVA					
	df	SS	MS	F	Significance F
Regression	2	0.55251945	0.276259725	30.69458724	0.031551129
Residual	2	0.01800055	0.009000275		
Total	4	0.57052			

	Coefficients	Standard Error	t Stat	P-value	Lower 95%	Upper 95%	Lower 95.0%	Upper 95.0%
Intercept	5.483694677	2.136478797	2.566697448	0.12414889	-3.708831653	14.67622101	-3.708831653	14.67622101
68.6	0.077522488	0.029208649	2.654093608	0.117467215	-0.048152185	0.203197161	-0.048152185	0.203197161
60	-0.096290083	0.013868951	-6.942852657	0.020121485	-0.155963362	-0.036616803	-0.155963362	-0.036616803



200a	Dependent variable:	Vertical take-off velocity
Diver 4	Independent variables:	Max squat % impulse to max def

SUMMARY OUTPUT

Regression Statistics	
Multiple R	0.312788692
R Square	0.097836766
Adjusted R Square	-0.263028528
Standard Error	0.43689523
Observations	8

ANOVA					
	df	SS	MS	F	Significance F
Regression	2	0.103500291	0.051750146	0.271117138	0.773059303
Residual	5	0.954387209	0.190877442		
Total	7	1.0578875			

	Coefficients	Standard Error	t Stat	P-value	Lower 95%	Upper 95%	Lower 95.0%	Upper 95.0%
Chart Area	1.034825919	4.716318549	0.219413915	0.835003631	-11.08885688	13.15850871	-11.08885688	13.15850871
72.1	0.034429276	0.054491311	0.631830568	0.555255024	-0.105645098	0.174503649	-0.105645098	0.174503649
horizontal (Value) Axis	0.014876127	0.051545639	0.288601076	0.784468616	-0.117626157	0.14737841	-0.117626157	0.14737841

